

AD 713034

FTD-MT-24-116-70

# FOREIGN TECHNOLOGY DIVISION



## THEORY OF ROCKET ENGINES

by

V. Ye. Alemasov, A. F. Dregalin,  
and A. F. Tishin



Reproduced by the  
CLEARINGHOUSE  
for Federal Scientific & Technical  
Information Springfield Va. 22151

Distribution of this document is  
unlimited. It may be released to  
the Clearinghouse, Department of  
Commerce, for sale to the general  
public.

OCT 27 1970

FTD-MT- 24-110-70

## EDITED MACHINE TRANSLATION

THEORY OF ROCKET ENGINES

By: V. Ye. Alemasov, A. F. Dregalin, and  
A. F. Tishin

English pages: 732

Source: Teoriya Raketnykh Dvigatelye, Moscow,  
1969, Izd-Vo "Mashinostroyeniye,"  
2nd Edition, pp. 1-547.

This document is a Systran machine aided  
translation, post-edited for technical  
accuracy by: Edwin P. Pentecost.

UR/0000-69-000-000

THIS TRANSLATION IS A RENDITION OF THE ORIGINAL FOREIGN TEXT WITHOUT ANY ANALYTICAL OR EDITORIAL COMMENT. STATEMENTS OR THEORIES ADVOCATED OR IMPLIED ARE THOSE OF THE SOURCE AND DO NOT NECESSARILY REFLECT THE POSITION OR OPINION OF THE FOREIGN TECHNOLOGY DIVISION.

PREPARED BY:

TRANSLATION DIVISION  
FOREIGN TECHNOLOGY DIVISION  
WP-AFB, OHIO.

FTD-MT- 24-110-70

A

Date 23 July 1970



## TABLE OF CONTENTS

U. S. Board on Geographic Names Transliteration System.....	x
Designations of the Trigonometric Functions.....	xi
Preface.....	xiii
Basic Abbreviations and Conventional Designations.....	xvii
Part I. Physical Principles and Basic Parameters.....	1
Chapter I. Introduction.....	2
1.1. Types of Rocket Engines.....	2
1.2. Chemical Rocket Engines.....	8
1.3. Utilization of Rocket Engines and Generators of the Working Medium.....	19
1.4. Brief Survey of the Development of Rocket Engines.....	27
Bibliography.....	39
Chapter II. Thrust of the Chamber and Engine.....	41
2.1. Thrust of a Chamber with a Laval Nozzle.....	41
2.2. Characteristic Modes of Operation of a Laval Nozzle.....	45
2.3. Thrust of Chamber in Modes with Breakaway of Flow Inside a Laval Nozzle.....	50
2.4. Chamber Thrust with Nozzles of Other Shapes.....	53
2.5. Thrust, Total Impulse, Power of Engine.....	55
Bibliography.....	57
Chapter III. Specific Parameters of the Chamber and Engine.....	58
3.1. Specific Thrust.....	58
3.2. Specific Impulse of Pressure in the Chamber.....	63
3.3. Thrust Coefficient.....	64
3.4. Specific Fuel Consumption.....	66
3.5. Specific Weight of the Engine.....	67

Bibliography.....	68
Chapter IV. Interconnection of Rocket, Engine, and Fuel Parameters.....	69
4.1. Connection between the Engine and Rocket Parameters.....	69
4.2. Effect of Fuel Characteristics on Rocket Characteristics.....	76
4.3. Rating the Efficiency of a Fuel.....	78
Bibliography.....	85
Part II. General Methods of Calculation.....	86
First Section. Theoretical Thermodynamic Characteristics.....	87
Chapter V. Composition and Total Enthalpy of Propellant.....	88
5.1. Equivalent Formula.....	88
5.2. Composition of Component.....	89
5.3. Composition of Bipropellant.....	90
5.4. Composition of Multipropellant.....	93
5.5. Density of Propellant.....	94
5.6. Total Enthalpy of Propellant.....	95
Bibliography.....	101
Chapter VI. Equilibrium Composition of Combustion Products.....	102
6.1. Preliminary Information.....	102
6.2. System of Equations for Determination of the Equilibrium Composition at $p$ , $T = \text{const}$ or $v$ , $T = \text{const}$ .....	103
6.3. Method of Solution of System of Equations.....	113
6.4. Calculation of Equilibrium Composition at $p$ , $T = \text{const}$ or $v$ , $T = \text{const}$ .....	116
6.5. Determination of Partial Derivatives of Equilibrium Composition.....	130
Bibliography.....	135

Chapter VII. Thermodynamic Properties and Properties of Transfer of Combustion Products.....	136
7.1. Thermodynamic Functions of the Mixture.....	136
7.2. Thermal Coefficients.....	140
7.3. Heat Capacity.....	141
7.4. Speed of Sound.....	145
7.5. Transfer Coefficients (Diffusion, Viscosity, Thermal Conductivity).....	148
7.6. Electrical Conductivity.....	157
7.7. Emissivities.....	162
Bibliography.....	169
Chapter VIII. Thermogas-Dynamic Calculation of Processes in a Chamber.....	172
8.1. Problems of Calculation and Basic Assumptions.....	172
8.2. Calculation of Combustion in an Isobaric Chamber.....	177
8.3. Calculation of Isentropic Equilibrium Expansion....	179
8.4. Calculation of Isentropic Frozen Expansion.....	187
8.5. Calculation of Combustion in Nonisobaric Cylindrical Chamber.....	189
8.6. Thermodynamic Calculation with the Aid of Diagrams and Nomograms.....	193
Bibliography.....	195
Chapter IX. Determination of Thermodynamic Characteristics...	197
9.1. Determination of Thermodynamic Characteristics in Terms of Data of Detailed Calculation.....	197
9.2. Determination of Thermodynamic Characteristics with Respect to Gas-Dynamic Relationships.....	199
9.3. Extrapolation and Interpolation of Thermodynamic Characteristics.....	205
Bibliography.....	219
Chapter X. Relationships of Thermodynamic Characteristics to Basic Factors.....	220

10.1.	General Information.....	220
10.2.	Relationships to Component Ratios of Propellant....	222
10.3	Relationships to Pressure in the Combustion Chamber.....	228
10.4.	Relationship to Degree of Pressure Decrease in the Nozzle or to Relative Nozzle Section Area.....	230
10.5.	Relationship to Relative Combustion Chamber Area...	233
10.6.	Relationship to Temperature or Enthalpy with Independent Heating.....	236
	Bibliography.....	239
	Second Section. Thermogas-Dynamics of Real Flows and Heat Exchange.....	240
Chapter XI.	Properties of Real Processes.....	241
11.1.	Basic Distinctions from Theoretical Schemes.....	241
11.2.	Nonadiabaticity of Processes.....	242
11.3.	Heterogeneity of Parameters and Incomplete Combustion.....	249
11.4.	Nonideality of Working Medium.....	256
11.5.	Chemical Nonequilibrium.....	262
	Bibliography.....	272
Chapter XII.	Single-Phase Flow in the Nozzle. Fundamentals of Profiling.....	274
12.1.	General Information.....	274
12.2.	Profiling the Subsonic Part of Round Nozzles.....	276
12.3.	Profiling of the Supersonic Part of Round Nozzles.....	279
12.4.	Fundamentals of Profiling Ring Nozzles.....	291
12.5.	Estimation of Pulse Losses in the Nozzle.....	296
12.6.	Some Principles of Selection of a Nozzle.....	305
	Bibliography.....	307
Chapter XIII.	Two-Phase Flow in a Nozzle.....	309
13.1	Basic Features.....	309



13.2.	Thermodynamic Estimation of Maximum Possible Losses.....	314
13.3.	Nonequilibrium Expansion of Two-Phase Flow.....	319
13.4.	Coagulation of Particles of Condensate in the Nozzle.....	327
13.5.	Nonequilibrium of the Crystallization Process of Condensate in the Nozzle.....	336
13.6.	Nonequilibrium of Condensation Process in the Nozzle.....	345
13.7.	Profiling of Nozzles for Two-Phase Combustion Products.....	346
	Bibliography.....	349
Chapter XIV.	Heat Output to Chamber Walls.....	351
14.1.	Preliminary Information.....	351
14.2.	Calculation of Convective Heat Exchange and Friction in the Boundary Layer of Reacting Gas (V. M. Iyevlev Method).....	359
14.3.	Utilization of Criterion Relations for Calculation of Convective Heat Exchange.....	371
14.4.	Calculation of Radiative Heat Exchange.....	374
14.5.	Distribution of Specific Heat Flows Along the Chamber Passage.....	376
	Bibliography.....	379
Chapter XV.	Liquid Rocket Fuels.....	380
15.1.	Requirements for Fuels.....	380
15.2.	Physicochemical Features of Components.....	384
15.3.	Kinetic Properties of Fuels.....	393
15.4.	The Leading Fuels Used.....	399
15.5.	Promising Propellants.....	402
15.6.	Promising Metalliferous Fuels.....	405
	Bibliography.....	410
Chapter XVI.	Processes of Fuel Conversion in the Combustion Chamber.....	412

16.1. Overall Picture of the Phenomena.....	412
16.2. Evaluating an Improvement of the Processes.....	414
16.3. Generalized Characteristics of the Processes.....	426
Bibliography.....	429
Chapter XVII. Processes of Gas Generation.....	430
17.1. General Information.....	430
17.2. Utilization of Unitary Fuel.....	433
17.3. Utilization of a Bipropellant.....	439
17.4. Obtaining Steam in the Coolant Passage of the Chamber.....	445
17.5. Thermodynamic Efficiency of the Various Methods of Gas Generation.....	447
Bibliography.....	449
Chapter XVIII. Calculation of the Basic Parameters of an Engine.....	450
18.1. Determination of Actual Specific Thrust and Second Fuel Expenditure in Seconds.....	450
18.2. Determination of the Chamber Size.....	452
18.3. Calculation of an Engine Without the Afterburning of the Generator Gas.....	456
18.4. Calculation of an Engine with Afterburning of the Generator Gas in the Basic Chamber.....	461
Bibliography.....	464
Chapter XIX. Characteristics and Thrust-Vector Control.....	465
19.1. Preliminary Information.....	465
19.2. Altitude Characteristic.....	468
19.3. Consumption Characteristics.....	471
19.4. Thrust-Vector Control.....	476
Bibliography.....	493
Chapter XX. Protection of the Chamber Wall.....	494
20.1. Basic Methods of Shielding the Wall.....	494
20.2. External Regenerative Cooling.....	495

20.3. Internal Cooling.....	520	Cha
20.4. Combined Systems of Wall Shielding.....	528	
Bibliography.....	530	
Chapter XXI. Selection of Optimum Parameters.....	531	
21.1. Criterion of the Selection of Optimum Parameters...	531	
21.2. Selection of the Fuel and the Excess Oxidizer Ratio.....	535	
21.3. Selection of Pressure in the Combustion Chamber....	538	Cha
21.4. Selection of Parameters of the Cross-Section of the Nozzles.....	542	
21.5. Trends in the Development of Liquid-Fuel Rocket Engine.....	547	
Bibliography.....	551	
Part IV. Rocket Engines on Solid Propellant.....	552	
Chapter XXII. Solid Rocket Propellants.....	553	Cha
22.1. Basic Requirements for Propellants.....	553	
22.2. Composition of Solid Propellants.....	555	
22.3. Mechanism of Combustion.....	560	
22.4. Dependence of Combustion Rate on Basic Factors.....	565	
22.5. Limits of Stable Combustion.....	574	
Bibliography.....	578	
Chapter XXIII. Interior Ballistics of a Chamber.....	579	Cha
23.1. Preliminary Information.....	579	
23.2. Pressure and Temperature in a Combustion Chamber.....	580	
23.3. Change in Parameters of Flow Along the Length of a Charge and in Time.....	592	
23.4. Interior Ballistics of Transitional Processes.....	605	
23.5. Geometry of Burning Out of Charge.....	610	
Bibliography.....	615	

Chapter XXIV. Bases for Calculation of Charge and Engine.....	616
24.1. Calculation of a Thrust Chamber with a Charge Which Burns on the Lateral Surfaces.....	616
24.2. Calculation of Thrust Chamber with a Charge Burning on the End.....	623
24.3. Calculation of Gas Generator.....	625
24.4. Selection of Igniter.....	628
Bibliography.....	631
Chapter XXV. Characteristics and Control of Thrust Vector....	632
25.1. Characteristics.....	632
25.2. Concepts Concerning Variance of Ballistic Parameters of an RDTT.....	633
25.3. Control of Thrust Vector.....	637
Bibliography.....	646
Chapter XXVI. Protecting the Walls of the Chamber.....	647
26.1. Means of Liquid-Less Heat Shielding.....	647
26.2. Accumulation of Heat in the Wall.....	649
26.3. The Use of Refractory Coatings.....	657
26.4. Use of Ablating Coatings.....	662
26.5. Radiation Cooling.....	669
Bibliography.....	672
Chapter XXVII. Selection of Optimum Parameters.....	674
27.1. Features in the Selection of Optimum Parameters of an RDTT.....	674
27.2. Selection of Propellant.....	679
27.3. Selection of Sizes of Charge and Combustion Chamber.....	683
27.4. Selection of Pressure in a Combustion Chamber.....	684
27.5. Selection of Nozzle Dimensions.....	686
27.6. Tendencies in the Development of RDTT.....	689
Bibliography.....	692



Part V. Combined Engines on Chemical Propellant.....	693
Chapter XXVIII. Hybrid Rocket Engines.....	694
28.1. General Information.....	694
28.2. Propellants for a GRD.....	696
28.3. Some Arrangements for a GRD.....	701
28.4. Operating Processes in a Combustion Chamber.....	703
Bibliography.....	710
Chapter XXIX. Combined Engines Which Use Surrounding Medium.....	712
29.1. General Information.....	712
29.2. Rocket-Ramjet Engines (RPD).....	713
29.3. Turbojet Engines.....	721
29.4. The Possibility of Using the Atmosphere of Other Planets.....	723
29.5. Hydorocket Engines.....	725
Bibliography.....	729
Bibliography to Entire Course.....	730
Appendix I.....	731
Appendix II.....	732

# U. S. BOARD ON GEOGRAPHIC NAMES TRANSLITERATION SYSTEM

Block	Italic	Transliteration	Block	Italic	Transliteration
А а	<i>А а</i>	A, a	Р р	<i>Р р</i>	R, r
Б б	<i>Б б</i>	B, b	С с	<i>С с</i>	S, s
В в	<i>В в</i>	V, v	Т т	<i>Т т</i>	T, t
Г г	<i>Г г</i>	G, g	У у	<i>У у</i>	U, u
Д д	<i>Д д</i>	D, d	Ф ф	<i>Ф ф</i>	F, f
Е е	<i>Е е</i>	Ye, ye; E, e*	Х х	<i>Х х</i>	Kh, kh
Ж ж	<i>Ж ж</i>	Zh, zh	Ц ц	<i>Ц ц</i>	Ts, ts
З з	<i>З з</i>	Z, z	Ч ч	<i>Ч ч</i>	Ch, ch
И и	<i>И и</i>	I, i	Ш ш	<i>Ш ш</i>	Sh, sh
Я я	<i>Я я</i>	Y, y	Щ щ	<i>Щ щ</i>	Shch, shch
К к	<i>К к</i>	K, k	Ъ ъ	<i>Ъ ъ</i>	"
Л л	<i>Л л</i>	L, l	Ы ы	<i>Ы ы</i>	Y, y
М м	<i>М м</i>	M, m	Ь ь	<i>Ь ь</i>	'
Н н	<i>Н н</i>	N, n	Э э	<i>Э э</i>	E, e
О о	<i>О о</i>	O, o	Ю ю	<i>Ю ю</i>	Yu, yu
П п	<i>П п</i>	P, p	Я я	<i>Я я</i>	Ya, ya

\* ye initially, after vowels, and after ъ, ы; e elsewhere.  
 When written as ѐ in Russian, transliterate as yѐ or ѐ.  
 The use of diacritical marks is preferred, but such marks  
 may be omitted when expediency dictates.

FOLLOWING ARE THE CORRESPONDING RUSSIAN AND ENGLISH  
DESIGNATIONS OF THE TRIGONOMETRIC FUNCTIONS

Russian	English
sin	sin
cos	cos
tg	tan
ctg	cot
sec	sec
cosec	csc
sh	sinh
ch	cosh
th	tanh
cth	coth
sch	sech
csch	csch
arc sin	$\sin^{-1}$
arc cos	$\cos^{-1}$
arc tg	$\tan^{-1}$
arc ctg	$\cot^{-1}$
arc sec	$\sec^{-1}$
arc cosec	$\csc^{-1}$
arc sh	$\sinh^{-1}$
arc ch	$\cosh^{-1}$
arc th	$\tanh^{-1}$
arc cth	$\coth^{-1}$
arc sch	$\operatorname{sech}^{-1}$
arc csch	$\operatorname{csch}^{-1}$
<hr/>	
rot	curl
lg	log

This book treats general questions of the theory and calculation of thermal rocket engines, describes processes of ZhRD and RDTT and considers their characteristics. The necessary information about liquid and solid fuels for RD is given.

In the 2nd considerably reworked edition, contemporary methods of thermogas-dynamic design of processes in RD with high-temperature working media have been more fully explained. Results published in recent years of theoretical and experimental investigations to determine thermophysical features of combustion products and characteristics of chemically nonequilibrium processes combustion and expansion are reflected. Considerable attention is given to questions of the specific character of two-phase flows and to schemes of heat shielding.

The book is intended for students of aviation institutes of technology and departments and may also be useful to engineers and graduate students, who specialize in rocket technology. Tables 36, illustrations 257, bibliography 178 names.



## PREFACE

The present, second publication of the textbook retains the systematical structure accepted earlier: the basic parameters and general methods of theory and design are stated in conformity with all types of thermal rocket engines (including nonchemical); questions specific for chemical rocket engines, which operate on various forms of fuel are considered.

In Part I of the book preliminary information is given about rocket engines, physical principles of the creation of thrust are stated, and basic engine parameters in their interconnection with characteristics of fuel and aircraft are considered.

Part II consists of two divisions. The first is dedicated to definition of theoretical thermodynamic characteristics. Its basis is design methods worked out by the authors, successfully checked, and now widely used. In comparison with the first publication, this division has been augmented: methods of determination of thermophysical features of combustion products, new variants of thermogas-dynamic calculation of ideal processes, and methods of extrapolation and interpolation of thermodynamic characteristics have been included in it. In the second division, rewritten, contemporary methods of calculation of imperfect and nonequilibrium processes, determinations of specific heat flows and shapings of nozzle are given.

Part III, dedicated to liquid rocket engines, has been completed with information on fuels, new schemes of organization of procedures, and means of liquid cooling and control of the thrust vector.

Part IV, in which solid-propellant rocket engines are considered, likewise contains new information on fuels, means of liquidless heat shielding, and control of thrust vector. The method of interior-ballistic engine design has been revised.

The distribution between Parts III and IV of material pertaining to means of heat shielding and control of the thrust vector is somewhat conditional. Part III describes means applicable predominantly for ZhRD, but some of them could be used even for RDTT. In Part IV are considered means suitable mainly for RDTT, although their utilization for ZhRD as well is not excluded.

In Part V combined engines running on chemical fuel are examined in greater detail than in the first publication.

In preparation of the 2nd publication of the book, the authors have taken into account opinions, remarks and wishes on the first publication. Digital and graphic illustrative material involved in systematical pursuits, borrowed from Russian and foreign literature or based on arbitrary data, has been renovated. Bibliography has been expanded and renovated.

The International System of Units (SI) is used in conclusions and a majority of formulas of the book. Departures are sometimes made from it in such cases:

1) with fulfillment of thermodynamic calculation of the composition of combustion products and of the processes in the chamber - in connection with the use of reference data not translated into the SI system;

2) in illustrative materials pertaining to thrust (kgf) and specific thrust (kgf·s/kg) for the purpose of free utilization and comparison of extensive data presented in traditional units.

The book has been revised by the author of the first publication together with his colleagues, who also prepared part of the new material. Chapters XI, XII, XIV, and XXIII were written by Candidate of Technical Sciences, Lecturer A. F. Dregalin; Chapters XIII, XV, and XVIII by Candidate of Technical Sciences A. P. Tishin.

In using this book it is recommended that reference be made to other literature sources. Among them it is possible to isolate textbooks, monographs, and reference books pertaining to the whole course or most of it (the list is given at the end of the book) and works more comprehensively illuminating separate themes, an enumeration of which is given at the end of each chapter.

The authors express their deep gratitude to corresponding members of the AN SSSR [Academy of Sciences of the USSR] A. P. Vanichev and V. M. Iyevlev, Doctor of Technical Sciences, Professor S. D. Grishin, and Candidate of Technical Sciences U. G. Pirumov for valuable remarks and recommendations expressed by them during the discussion and review of the prospectus and manuscript.

V. I. Vychenok (Chapter VII), Yu. M. Danilov (Chapter 11, § 12.2), Yu. N. Drozdov (§§ 19.4, 25.3), V. Ya. Klabukov (§ 7.7, Chapter XX), A. S. Lyashev (§ 11.5), N. I. Sitnitskaya, V. A. Khudyakov (Chapter IV), and A. S. Cherenkov (§ 7.6) took part in preparation of material to separate chapters and paragraphs of the book. Substantial aid in formulation of the book was rendered by R. A. Dobronravov, V. P. Ivshin, Yu. D. Krechetnikov, V. P. Mikheyeva, S. M. Potapov, V. P. Trinos, and A. Z. Khamidullin. The authors express their gratitude to all people.

Opinions, critical remarks and wishes should be directed to the Publishing House ("Mashinostroyeniye") (Moscow, K-51, Petrovka, 24).

[Translator's Note: divergences in superscript positioning will be noted throughout the document. They were entered in the translation just as they appeared in the original document.]



## BASIC ABBREVIATIONS AND CONVENTIONAL DESIGNATIONS

### Abbreviations

РД - RD - rocket engine;  
ГРД - GRD - hybrid rocket engine;  
ЖРД - ZhRD - liquid-propellant rocket engine;  
РДТТ - RDTT - solid-propellant rocket engine;  
ХРД - KhRD - chemical rocket engine;  
ЭРД - ERD - electrical rocket engine;  
ВРД - VRD - airbreathing jet engine;  
ПВРД - PVRD - ramjet engine;  
ТРД - TRD - turbojet engine;  
РПД - RPD - ramjet engine;

### Conventional Designations

$a$  - velocity of sound; coefficient of thermal conductivity;  
 $\alpha$  - excess oxidant ratio; heat-transfer coefficient;  
 $\alpha_p$  - coefficient isobaric of expansion;  
 $\beta_T$  - isothermal compression coefficient;  
 $\beta$  - specific impulse of pressure (consumption complex);

$C_p, c_p$  - molar and specific heat capacity at constant pressure;  
 $C_v, c_v$  - molar and specific heat capacity at constant volume;  
 $d$  - diameter;  
 $E$  - internal energy;  
 $\epsilon$  - relative expense of auxiliary fuel; Erosion ratio; emissivity factor;  
 $\xi$  - coefficient of loss of complete impulse;  
 $F$  - cross section area;  
 $f$  - relative area (geometrical degree of expansion);  
 $G$  - consumption of the working material per second; weight;  
 $g$  - weight fraction; acceleration of gravity;  
 $\eta$  - coefficient of dynamic viscosity;  
 $I$  - complete enthalpy;  
 $I_\Sigma$  - total impulse;  
 $K$  - equilibrium constant with respect to partial pressures;  
 $K_p$  - thrust coefficient (thrust complex);  
 $k$  - ratio of specific heat capacities;  
 $\kappa_0$  - weight stoichiometric coefficient of ratio of fuel components;  
 $\kappa$  - weight coefficient of ratio of fuel components;  
 $\kappa'_0$  - molar stoichiometric coefficient of ratio of fuel components;  
 $\kappa'$  - molar coefficient of ratio of fuel components;  
 $L$  - length; work;  
 $\Lambda$  - relative fuel content on craft;  
 $\lambda$  - reduced velocity; coefficient of thermal conductivity;  
 $M$  - Mach number;  
 $u$  - mass number of rocket;  
 $N$  - power;  
 $n$  - number of moles; mean index of isentrope;

$\nu$  - exponent in formula of combustion rate of solid fuel;  
 coefficient of kinematic viscosity;  
 $\Pi$  - perimeter;  
 $\pi$  - degree of lowering of pressure (degree of expansion);  
 $P$  - thrust;  
 $P_{yA}$  - specific thrust (specific or single impulse);  
 $p$  - pressure;  
 $\Delta p$  - pressure drop;  
 $Q$  - heat;  
 $q$  - specific heat flow;  
 $R_0$  - universal gas constant;  
 $R$  - specific gas constant;  
 $r$  - radius;  
 $\rho$  - density;  
 $S^0$  - standard molar entropy;  
 $S, s$  - molar and specific entropy;  
 $\sigma$  - electrical conductivity; coefficient of restitution of pressure;  
 $T$  - absolute temperature;  
 $t$  - temperature in  $^{\circ}\text{C}$ ;  
 $\tau$  - time; tangential stress;  
 $\tau_g$  - delay of fuel ignition (induction time);  
 $\tau_n$  - time fuel stays in combustion chamber;  
 $\tau_{np}$  - fuel conversion time;  
 $u$  - linear rate of combustion of solid fuel;  
 $V$  - flight speed; volume;  
 $v$  - specific volume;  
 $V_H$  - final velocity of flight;

$\phi$  - impulse coefficients;  
w - velocity of working body;  
x - mole fraction of gas component;  
z - weight fraction of condensed phase;  
 $\Omega$  - surface area.

#### Subscripts

ад - adiabatic;  
г - fuel;  
г - gas;  
дв - engine;  
ж - liquid;  
э - frozen, delays;  
h - at altitude;  
ид - ideal [perfect];  
кр - critical;  
к.с - combustion chamber;  
н - saturated;  
нр - nonequilibrium;  
ок - oxidant;  
опт - optimum;  
п - in a vacuum;  
р - equilibrium;  
с - nozzle;  
ст - wall, turbine;  
т - fuel;  
т - turbine;

t - theoretical;  
уд - specific;  
х - cold;  
э - equivalent;  
эк - experimental;  
эф - effective;  
z - condensed;  
\* - (superlinear) - pertains to parameters of stagnation flow.

#### Sections of Engine Chamber

l - beginning of heat supply;  
д - diaphragm (for RDTT) [retainer or grain support];  
к - exit from combustion chamber;  
кр - critical;  
с - nozzle exit.

P A R T I

PHYSICAL PRINCIPLES AND BASIC PARAMETERS

## CHAPTER I

### INTRODUCTION

This chapter gives preliminary information about a family of rocket engines, characteristic criteria and distinctive characteristics of their various types. The basic (PA) [RD - rocket engine] schemes, the history of their development and the range of contemporary utilization are briefly examined.

#### 1.1. Types of Rocket Engines

Rocket engines are jet [reactive] engines. The force necessary for motion is the thrust they create, converting a certain original (primary) energy into the kinetic energy of a jet stream. The magnitude of thrust is proportional to the velocity of the jet stream and its mass ejected in a unit of time.

The jet stream of rocket engines is formed from substances stored on the craft, but the environment is not used for this purpose. In this respect rocket engines differ from air-breathing jets and hydrojets, which create a jet stream, using the surrounding medium - air or water. The term (rocket) in explicit form does not reflect this distinction, but it is traditionally widely used.

The primary energy utilized in rocket engines can be chemical, nuclear, and solar energy. The source of chemical energy for RD is chemical rocket fuels - substances or sets of substances able to

release heat as a result of chemical reactions. The source of nuclear energy is nuclear rocket fuels - substances or sets of substances able to liberate energy as a result of nuclear fission of heavy elements, nuclear fusion of light elements or radioactive decay. The source of solar energy is the radiation of the sun.

In accordance with the type of primary energy utilized in an engine, chemical, nuclear, and solar rocket engines differ. The latter two types are frequently combined and given the name nonchemical RD.

In processes of conversion of primary energy into kinetic energy of the jet stream the working medium (working substance) of the rocket engine takes part. The jet stream is the final form of the working medium. Depending on the original form of the working medium, two characteristic cases can be distinguished.

Energy releasable by chemical rocket fuels is imparted to products of their reaction, which are the working medium of chemical RD. In other words, chemical rocket fuels are simultaneously also sources of energy and sources of working medium.

In nonchemical RD reaction products are rarely used as a working medium, inasmuch as their mass is negligible. In the vast majority of cases, a special working medium receiving energy from an independent source (a nuclear or radioisotope reactor or a concentrator of solar radiation) is used. The energy source and working medium are initially divided. Energy is supplied to the working medium only in the chamber - the energy converter.

Figure 1.1 shows the schematic diagram of a rocket engine running on chemical fuel and having an independent energy source.

An important criterion according to which rocket engines are classified is means of acceleration of working medium. For many engines this is thermal acceleration, i.e., conversion of heat into kinetic energy. Such engines are called thermal.



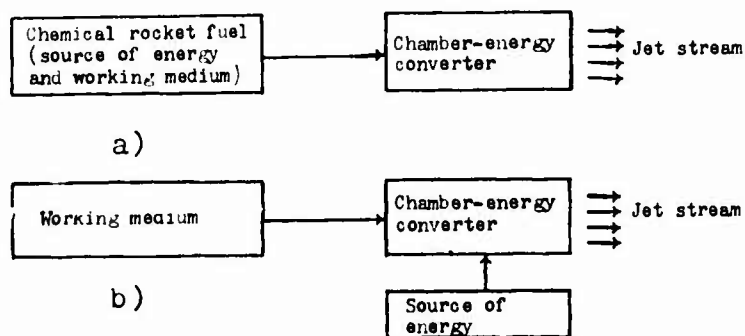


Fig. 1.1. Schematic diagrams of a rocket engine: a) running on chemical fuel; b) with an independent energy source.

The type of primary energy utilized in thermal RD can be various. As can be seen from Table 1.1, where characteristic parameters of various types of rocket engines are presented, thermal engines are all chemical RD and some are variants of nuclear and solar engines.

For processes of conversion of energy in thermal RD, two stages are characteristic. The first is communication of heat to the working medium either in the chamber where the chemical fuel reacts, or in the heat exchanger, which obtains energy from an independent source. In certain cases the working medium can be heated by intermediate (secondary) energy, for example, electrical energy (variant 8 in Table 1.1). The second stage is conversion of heat to kinetic energy, or thermal acceleration of the working medium carried out in the jet nozzle.

The jet stream leaving the nozzles of thermal RD consists of gaseous and, possibly, condensed products of combustion or heating. Sometimes it is a low-temperature plasma.

In a majority of thermal RD heat is supplied to the working medium at constant or almost constant pressure. Figure 1.2 shows the character of change in parameters of the working medium through the channel of such an engine.

Table 1.1. Characteristic parameters of rocket engines of various types.

Type of engine	Variant	Type of energy converter	Composition of jet stream	Exhaust velocity of jet stream $w$ m/s	Specific weight of engine $\gamma_{\Sigma}$ kg/kgf	Acceleration from thrust $a/g_0$
Thermal	1	Chemical reactor + nozzle	Products of combustion or decomposition	Up to $5 \cdot 10^3$	0,01	$1-100$
	2	Reactor with solid nuclear fuel + nozzle	Products of heating	$8,0 \cdot 10^3-1,2 \cdot 10^4$	0,1	$1-10$
	3	Reactor with liquid nuclear fuel + nozzle	The same	$1,2 \cdot 10^4-2,0 \cdot 10^4$	0,1	$1-10$
	4	Combined reactor (nuclear and chemical) + nozzle	Fragments of nuclei with combustion products	$5,0 \cdot 10^4$	0,1	$1-10$
	5	Reactor with gaseous nuclear fuel + nozzle	Products of heating	$2,0 \cdot 10^4-7,0 \cdot 10^4$	0,1	$1-10$
Electrical	6	Solar heater + nozzle	The same	$8,0 \cdot 10^3-1,2 \cdot 10^4$	$10^2$	$10-2$
	7	Radio-isotope heater + nozzle	The same	$8,0 \cdot 10^3-1,2 \cdot 10^4$	$10^3$	$10-3$
	8	Electro-arc heater + nozzle	Plasma	Up to $2,5 \cdot 10^4$	$2,5 \cdot 10^2-2,5 \cdot 10^3$	$4 \cdot 10-4 \cdot 10^4$
	9	Plasma generator + electrodynamic accelerator	The same	$5,0 \cdot 10^4-10^5$	$5 \cdot 10^2-10^4$	$2 \cdot 10-3 \cdot 10^4$
Sail system	10	Ionization chamber + electrostatic accelerator	The same	$5,0 \cdot 10^4-10^6$	$5 \cdot 10^2-10^5$	$2 \cdot 10-3 \cdot 10^5$
	11	Radio isotope sail	Alpha particles	$8,0 \cdot 10^6$	$2,5 \cdot 10^4$	$4 \cdot 10-5$
	12	Solar sail	Photons of solar radiation	$3,0 \cdot 10^8$	$5 \cdot 10^3$	$2 \cdot 10-4$

ve  
no  
de  
ma  
by  
  
re  
ma  
con  
of  
per  
ful  
(sp  
rel  
  
acce  
The  
prim  
into  
in a  
  
high  
bein

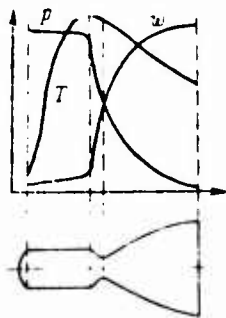


Fig. 1.2. Change in parameters along the channel a thermal rocket engine.

Thermal RD are included among engines with a limited exhaust velocity of jet stream. For chemical RD the limitations are the nature of the fuel and the maximum temperature permissible for the design materials; for RD with an independent energy source, the maximum temperature of heating of the working medium is also conditioned by the temperature permissible for the body.

As can be seen from Table 1.1, a majority of thermal RD have relatively low specific weight (the ratio of engine weight to the maximum thrust developable by it) and are able to impart to crafts considerable accelerations  $a$  in comparison with gravity on the surface of the earth  $g_0$ . For them large expense of mass of working medium per unit of thrust is characteristic. This determines the basic task fulfilled by such engines: acceleration of heavy crafts to high (space) velocities in circumplanetary and interplanetary flights with relatively short work of the engines.

A characteristic feature of electrical rocket engines is acceleration of the working medium with the aid of electrical energy. The latter can be obtained by means of various conversions of certain primary energy. Thus, for instance, nuclear energy can be converted into heat in a reactor-heat exchanger, then into mechanical energy in a turbomachine and into electrical energy in an electric generator.

Electrical acceleration of the working medium can guarantee very high exhaust velocities and, consequently, small expense of the mass being ejected per unit of thrust. Exhaust velocity can be regulated

over wide limits. The jet stream of an (ЭРД) [ERD - electrical rocket engine] is a neutral plasma. Table 1.1 gives the characteristic parameters of two basic types of ERD: electromagnetic (also called plasma or magnetohydrodynamic) and electrostatic (ionic). In the first of them (variant 9) the working medium, high-temperature plasma, is accelerated because of action of an electromagnetic field on it; in the second (variant 10) the working medium (usually alkaline metals) is ionized, and ions are accelerated in a strong electrostatic field. To get a neutral jet stream the beam of ions is neutralized with electrons.

As can be seen from Table 1.1, ERD have considerable specific weight and impart small accelerations to crafts. A limitation for them is the power of the electrical generator. An increase in this power is accompanied by a substantial weight increase.

Utilization of ERD as basic engines of aircrafts is possible after imparting orbital velocity to the aircraft with the aid of (ХРД) [KhRD - chemical rocket engine]. Long work of ERD can guarantee distant space flights and, possibly, achievement of escape velocity. The ERD can be used likewise as auxiliary engines, for example, for orientation of aircraft.

A special place is occupied by so-called sail systems, which have practically zero expense of mass. A radio isotope sail creates thrust owing to the reaction of a one-sided leakage of alpha particles during radioactive decay. The thrust created by the solar sail is caused by pressure of solar radiation on the reflective surface. Sail systems are engines of limited thrust. The magnitude of the latter is limited by the maximum area of the reflective surface. Characteristic parameters of sail systems are presented in Table 1.1. Their possible utilization is analogous to utilization of electrical RD but is even more limited.

Figure 1.3 presents for clearness, the same as Table 1.1, characteristic parameters of rocket engines of various types.

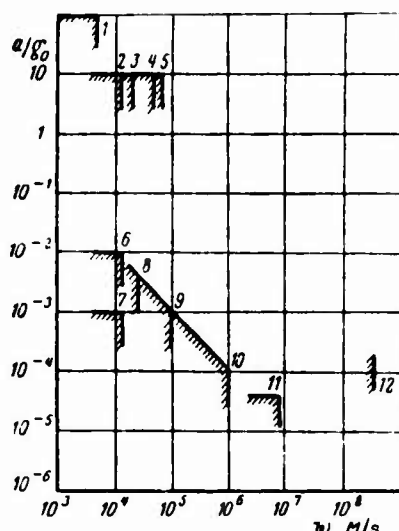


Fig. 1.3. Characteristic parameters of rocket engines of various types (Numeration according to Table 1.1).

## 1.2. Chemical Rocket Engines

Chemical rocket engines have been mastered best and are widely used. The variety of fulfilled and developed KhRD is caused first of all by differences in fuels used and schemes of organization of the working process.

### Fuels

Chemical rocket fuels are capable of exothermal (with liberation of heat) reactions. The main types of exothermal reactions are the following.

1. Combustion. Combustion (oxidation) is the main and most widely used means of obtaining heat. In a combustion reaction participation is necessary of fuels and oxidizing elements which can be in the composition of one or more substances which form fuel. Usually substances in which combustible elements prevail are called fuels, and substances in which oxidizing elements prevail oxidant.

2. Decomposition. Certain individual substances or mixtures and solutions of substances are capable of exothermal decomposition.

3. Recombination. The energy release of recombination (reunification) of atoms or radicals having free valence is quite considerable, and its utilization in rocket engines is promising. However, the means of industrial obtaining and conservation of free atoms and radicals in the condensed phase has not yet been found. Fuels on their base are hypothetical.

The basis of classification of chemical rocket fuels can be various criteria. One of the characteristic and general criteria is the original aggregate state of fuels. Classification by this criterion is given in Fig. 1.4.

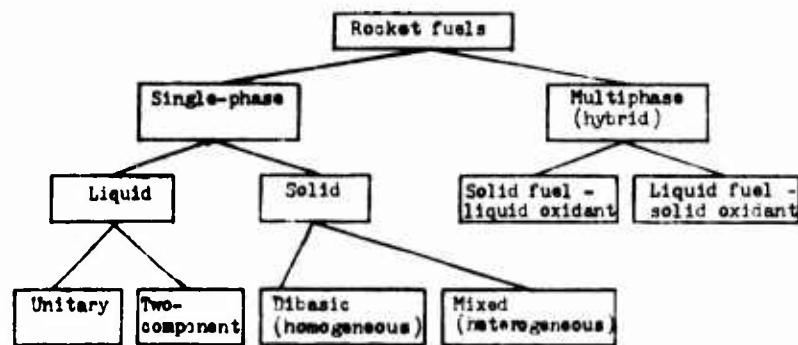


Fig. 1.4. Classification of chemical rocket fuels.

Single-phase fuel can be liquid or solid. Multiphase (hybrid) fuel is a combination of solid and liquid components.

The fuel or component in the solid state is usually placed directly into the combustion chamber of the engine, liquid fuel or component is kept in special vessels - tanks - whence it is gradually supplied to the engine.

Unitary liquid fuel is supplied to the engine in the form of one liquid. It can be an individual substance (single-component fuel), or a uniform mixture, or a solution of various substances. Two-component liquid fuel consists of two components individually stored and separately supplied to the engine - fuel and oxidant, which, in turn, can be individual substances or mixtures of substances. This fuel, also called fuel or separate supply, is a basic contemporary liquid rocket fuel. Utilization of multicomponent (usually not more than three components) of liquid and hybrid fuels is also possible.

Solid rocket propellants contain fuels and oxidizing elements and are unitary. There are two main classes of solid fuels. Dibasic (homogeneous) fuels are a solid solution of components. One of the bases of such a fuel is nitrocellulose; a second is a solvent of the nitroglycerine type and other substances. Mixed (heterogeneous) solid fuel is a mechanical mixture of fuel and oxidant.

The difference of terms must be emphasized in reference to fuels of rocket and air-breathing jet engines. A vehicle with an air-breathing jet engine carries in its tanks only one component of fuel. The oxidant necessary for combustion - oxygen - is not carried by the craft, but is taken in from the air of the atmosphere. Therefore, in the practice of air-breathing jet engines the idea "combustible" is identified with the idea "fuel." For rocket engines both fuel and oxidant are carried by the craft; expense of the one and the other diminishes the general fuel reserve, and, therefore, the ideas "combustible" and "fuel" are essentially different.

Detailed information on chemical rocket fuels is given in Chapters XV, XXII, and XXVIII.

#### Basic Schemes

Division of chemical RD into characteristic types is based on the classification of fuels used in them (Fig. 1.5). The types are:

- 1) liquid-propellant rocket engines ((ЖРД) [ZhRD]);
- 2) solid-propellant rocket engines ((РДТТ) [RDTT]);
- 3) hybrid rocket engines ((ГРД) [GRD]).

The most developed and extensive class of chemical rocket engines is ZhRD. Figure 1.5 shows the main varieties of ZhRD, distinguishing by type of fuels (unitary or separate supply), by means of fuel feed (displacer or pumping), by means of organization of the working process (with afterburning or without afterburning of generator gas). The most widespread combinations of these criteria are shown by double lines.

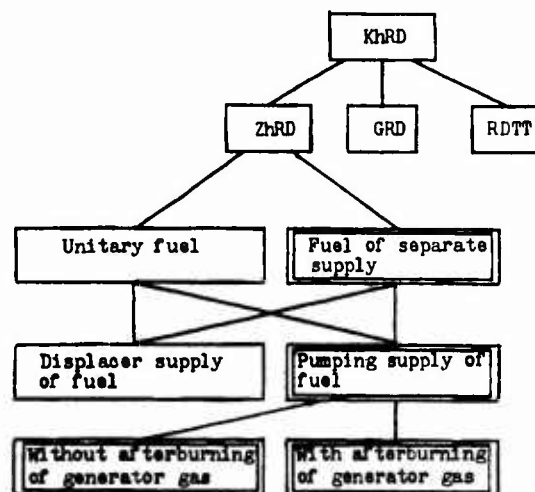


Fig. 1.5. Classification of chemical rocket engines.

The main unit of ZhRD is its chamber, which creates thrust. The chamber consists of a combustion chamber and nozzle, the construction of which usually represents one whole. The main part of the combustion chamber is its mixing head — a device for injection and mixing of fuel components. Elements of the mixing head are injectors of various types. Ignition of fuel is carried out by chemical,



pyrotechnic, and electrical means; frequently components of fuel will form a self-igniting fuel. The chamber of the ZhRD is usually cooled by one of the components of fuel passing prior to entering the combustion chamber through a cooling tract - the space between the inside or fire wall and the external or power jacket of the chamber, connected by various means. Figure 1.6 gives the diagram of a ZhRD chamber operating on two-component fuel.

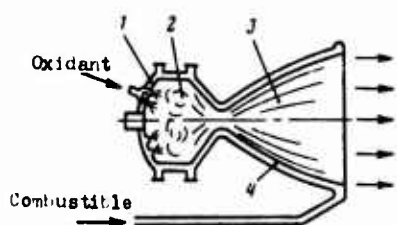


Fig. 1.6. Diagram of ZhRD chamber running on two-component fuel: 1 - mixing head; 2 - combustion chamber; 3 - nozzle; 4 - cooling tract

A liquid-propellant rocket engine consists of a chamber (or several chambers), systems of supply of fuel, systems of adjustment, auxiliary units, engine frames, etc. The system of adjustment of a ZhRD carries out automatic maintenance of or a programmed change in parameters of the working process to ensure a given value of thrust and relationships of components of fuel, and steady work of the ZhRD and also control of transient conditions (starting, stopping, etc.). The electrical, electronic, pneumatic, hydraulic, pyrotechnic, and mechanical devices in the system of automatic adjustment are usually called organs of automation.

A rocket engine installation with a ZhRD consists of one or more engines, fuel tanks, systems of supply and organs of automation, and systems of bracing.

Figure 1.7 gives the elementary diagram of an engine with a ZhRD having displacer fuel supply. With such a supply method, fuel components are forced out of the tanks with compressed and, possibly, hot gas. Gas of high pressure enters either from the pressure accumulation - balloon, in which it has been stored earlier, or from a gas generator - a unit in which hot gas is continuously owing to combustion

or decomposition of fuel or its components. In gas generators the main (the same as in the engine chamber) fuel or a special auxiliary fuel is used, including solid fuel. The temperature of the generator gas is limited by the heat resistance the design elements on which it acts. In order not to exceed permissible temperature, it is necessary to allow only incomplete fuel combustion, so that a considerable part of one of the components is ballast. If there is excess fuel, reducing generator gas is prepared; if there is excess oxidant oxidizing gas is prepared. In displacer supply of two-component fuel, there must be two gas generators: a reducing one for supercharging the fuel tank and an oxidizing one for an oxidant tank.

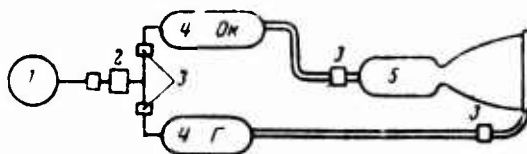


Fig. 1.7. Diagram of ZhRD with displacer fuel feed: 1 - pressure accumulator; 2 - reducer; 3 - organs of automation; 4 - fuel tank; 5 - engine chamber.

Designations: OK = Oxidant;  
F = Fuel.

A system of displacer supply also has reducers, maintaining assigned supply pressure, locking devices, and other organs of automation. In connection with high pressure in fuel tanks, the weight of the system is considerable, and, therefore, its use is limited to engines with low thrust and short operating time.

More widespread in ZhRD is a pumping supply of fuel. The drive of pumps is usually carried out from a gas turbine. Characteristic is a turbopump unit (THA) [TNA - turbopump], usually representing a general grouping of turbine and pumps. The turbine is run with gas or steam at high pressure and moderate temperature. The gas or stream is prepared either in a liquid gas generator, or in the cooling tract

of the chamber, where the coolant is evaporated (usually one of the components of fuel). To drive the turbine it is also possible to use gas removed from the main combustion chamber.

Figure 1.8 gives the diagram of a ZhRD with a turbopump supply of fuel without afterburning of generator gas. The latter after operation on the turbine is ejected into the surrounding medium through auxiliary nozzles, which are frequently steering nozzles. Generator gas consists of products of incomplete combustion, and it is expanded in the auxiliary nozzles less than in the nozzle of the main chamber. Therefore, the economy of utilization of fuel supplied to the gas generator is lower than the basic fuel. In a scheme without afterburning of generator gas, lowering of economy is additionally caused by the TNA drive.

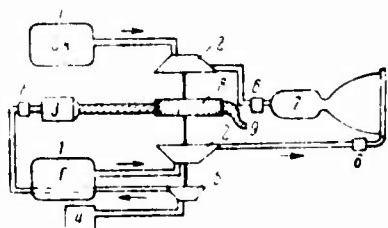


Fig. 1.8. Diagram of ZhRD with pumping fuel feed without afterburning of generator gas: 1 - tanks of basic fuel; 2 - pumps of fuel and oxidant; 3 - gas generator; 4 - tank of auxiliary fuel; 5 - pump of auxiliary fuel; 6 - organs of automation; 7 - engine chamber; 8 - turbine; 9 - exhaust of gas behind turbine.

Figure 1.9 gives the diagram of a ZhRD with afterburning of generator gas in the main chamber. Here generator gas, passing through the turbine, is sent to the combustion chamber. Through the gas generator they usually let pass the entire expense of one of the components and a small part of the expense of another, preparing either reducing or oxidizing gas. The remaining large part of the second component in the liquid phase enters the combustion chamber, where afterburning takes place. In contrast with an engine without afterburning, where both components are supplied to a combustion chamber in the liquid state (scheme of organization of the "liquid-liquid" type), in a ZhRD with afterburning, the combustion chamber operates on gas and liquid ("gas-liquid" scheme).

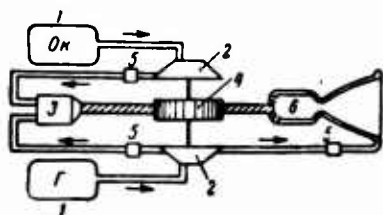


Fig. 1.9. Diagram of a ZhRD with pumping supply of fuel and afterburning of generator gas in main chamber (one gas generator): 1 - fuel tanks; 2 - pumps; 3 - gas generator; 4 - turbine; 5 - organs of automation; 6 - engine chamber.

The scheme with afterburning of generator gas in the main chamber is energetically more advantageous than the scheme without afterburning for the reason that in ZhRD with afterburning, all the fuel is used under optimum conditions, in which complete release of heat and its conversion into kinetic energy is ensured.

Figure 1.10 shows one additional variant of ZhRD with afterburning of generator gas. Here there are two turbines and two gas generators operating on them, one of which prepares reducing, and the other oxidizing gas. The chamber combustion is entered by two gaseous components which burn there ("gas-gas" scheme).

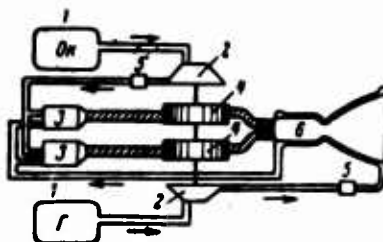


Fig. 1.10. Diagram of ZhRD with pumping supply of fuel and afterburning of generator gas in main chamber (of two gas generators): 1 - tanks of fuel; 2 - pumps; 3 - gas generators; 4 - turbines; 5 - organs of automation; 6 - engine chamber.

Figure 1.11 gives a simplified ZhRD, in which the turbine operates on hydrogen gasified and preheated in the cooling tract. The process in the combustion chamber is organized according to the "gas-liquid" diagram. A system of pumping fuel is more complex than a system of displacer supply, but under certain conditions is more advantageous in connection with less weight of fuel tanks not under high pressure.

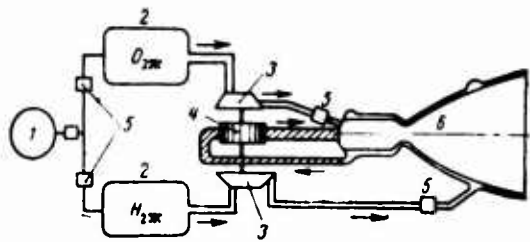


Fig. 1.11. The ZhRD with drive of turbine by gas, obtained in the cooling tract of the chamber: 1 - pressure accumulator; 2 - tanks of fuel; 3 - pumps; 4 - turbine; 5 - organs of automation; 6 - engine chamber.

A characteristic property of a solid-propellant rocket engine is the placing in the combustion chamber of a whole supply of fuel in the form of fuel charges of determined form. A fuel supply system is absent. Ignition of fuel is carried out by a special igniter. Combustion proceeds on the surfaces of charge not protected by armored coating. As a rule, a RDTT does not have liquid cooling. The system of adjustment in RDTT is called upon to solve the same problems as in ZhRD (excepting ratio control of fuel components), however, its possibilities are still considerably less than in ZhRD.

Figure 1.12 gives the elementary diagram of the RDTT.

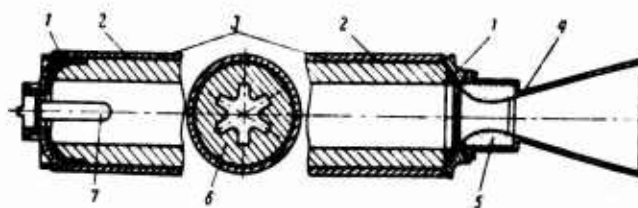


Figure 1.12. Solid-propellant rocket engine: 1 - armoring covering; 2 - housing; 3 - padding; 4 - nozzle; 5 - nozzle insert; 6 - fuel; 7 - igniter.

The schematic diagram of a hybrid rocket engine is shown in two variants in Fig. 1.13. As it appears, GRD combines elements of ZhRD and RDTT.

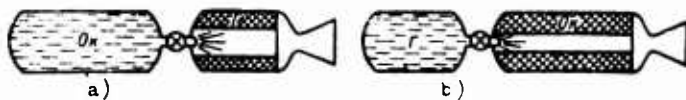


Fig. 1.13. Diagram of hybrid rocket engine: a) liquid oxidant - solid fuel; b) liquid fuel - solid oxidant.

### Characteristic Properties

The possibilities of chemical rocket engines are interesting to compare with the possibilities of highly developed and widely used air-breathing jet engines. From Fig. 1.14 it is evident that the possibilities of aircrafts with (BPA) [VRD - air-breathing jet engines] (to say nothing of engine-propeller units) are substantially limited by height and velocity of flight. Within the limits of relatively dense layers of atmosphere, the limitations are the aerodynamic supporting power of the wing and maximum permissible aerodynamic heating. At heights of more than 30-40 km utilization of VRD is practically excluded because of the low density of air necessary for engines.

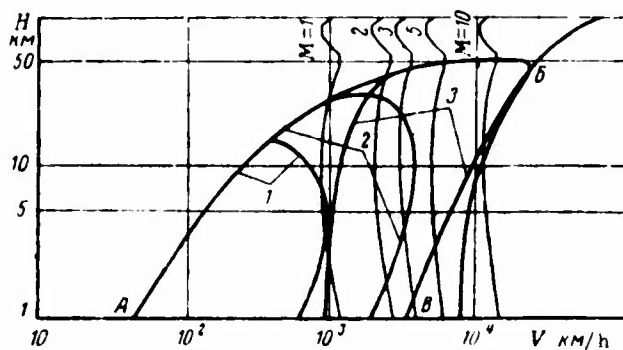


Fig. 1.14. Ranges of utilization of aircrafts with engines of various types: A5 - limit of carrying capability of wing; 5B - limit of permissible aerodynamic heating; 1 - aircrafts with a propeller-driven device; 2 - with (TPA) [TRD - turbojet engine]; 3 - with (PAPA) [PVRD - ramjet engine].

Utilization of chemical RD in the dense layers of the atmosphere separates the mentioned limitations, and beyond earth atmosphere rocket engines are singularly suitable. The main reason is the capability of a rocket engine to operate without utilization of surrounding medium.

Furthermore, a characteristic feature of chemical RD is extremely high concentration of generated power per unit weight and volume. This causes a high thrust-weight ratio of crafts (ratio of thrust to weight of craft) and high accelerations and flight speeds.

An important feature of chemical RD is the large expense of fuel per unit of thrust, which is explained by the need to transport and spend in the engine not only fuel but also oxidant. The time of work of the engine is limited by reserves of fuel on the craft and is relatively short.

The ZhRD are engines of high thermal intensity and more flow rate. High pressures and often unfavorable physical and chemical features of fuels even more than redouble position. In connection with this chemical RD have a relatively short service life, which for RDTT will be tens and hundreds of seconds, and for ZhRD minutes and hours.

With the generality of the characteristic criteria mentioned, various types of ZhRD have their peculiarities. Thus, during comparison of engines running on solid and liquid fuel, it is discovered that RDTT are simpler in design and operation, retain constant readiness for work for a long time, and are very reliable. At the same time they are inferior to ZhRD in effectiveness, that is caused by features of fuels, and have fewer possibilities of regulation of thrust, of repeated starting, etc.

In connection with such distinctions each type of engine has its most rational range of utilization and types of tasks executable by them.

### 1.3. Utilization of Rocket Engines and Generators of the Working Medium

#### Engines

Rocket engines are applied in battle and space rockets, aircraft, and certain underwater crafts (see Chapter XXIX).

Their utilization is widest and most effective on space rockets intended for launching automatic or piloted crafts and artificial satellites of planets. Engines of space rockets have the highest absolute and specific parameters and are structurally highly perfected and reliable. Examples are engines of the Soviet rocket-space systems "Vostok," "Voskhod," "Soyuz," "Proton," "Kosmos," "Zond," and others.

Engines of space are divided with respect to purpose in the following manner.

1. Main (carrier) engines, which provide acceleration of craft on the active section of flight. Main engines of space rockets are predominantly ZhRD — the predominating engine model in contemporary cosmonautics. The thrust of main engines reaches tens and hundreds of tons.

2. Auxiliary engines, to which belong steering (vernier) engines, serving for control of flight according to the assigned program; correcting engines, switched on in space flight to correct direction and velocity of the craft; braking engines, used for landing (leaving orbit and actually landing), and also for braking individual stages of multistage rockets during their separation. Steering, correcting and brake engines have relatively low thrust (up to hundreds of kgf). They are predominantly ZhRD and sometimes RDTT.



Also auxiliary engines are engines of systems of orientation and stabilization of aircraft, and also individual RD serving for movement and maneuvering of an astronaut in floating flight outside the cabin. Orientational, stabilizing and individual engines usually develop very low thrust (kilograms and grams), they are often called microrocket engines. Besides chemical RD, electrorocket engines are starting to be used as microrocket engines.

Figure 1.15a shows the Soviet three-stage rocket-carrier "Vostok," and Fig. 1.15b gives a look at the engines of its first and second stages. On the first stage there are 4 ZhRD RD-107, and on the second 1 ZhRD RD-108. The engines operate on liquid oxygen and kerosene. The RD-107 (Fig. 1.16) is a four-chamber engine with two steering rocking chambers. The engine thrust in a vacuum is 102 T.<sup>1</sup> The RD-108 (Fig. 1.17), in contrast with TD-107, has 4 steering chambers, other units of automation, and a frame. Its thrust in a vacuum is 96 T.

Figures 1.18 and 1.19 show the Russian ZhRD, RD-214, and RD-119, utilized on the "Kosmos" rocket-carrier. The four-chamber engine of the first stage RD-214 is first powerful serial rocket engine in the USSR running on high-boiling nitrogen-oxygen oxidant and the products of processing of kerosene as rule. Its thrust in a vacuum is 74T. A single-chamber engine of the second stage RD-119 operates on liquid oxygen and asymmetrical dimethylhydrazine and develops a thrust of 11 T in a vacuum. The engine has steering nozzles for control of flight with respect to pitch, course, and roll.

Figure 1.20 shows some American ZhRD, intended for spacecraft.

Chemical RD are widely used as engines of military pilotless rockets. Such crafts are usually divided into four groups, defining each of them by starting place and final target.

---

<sup>1</sup>More detailed information about the RD-107 and other engines mentioned below are given in Appendix I.



Fig. 1.15. Vostok rocket-carrier: a) general view; b) engines of the first and second stages.

of

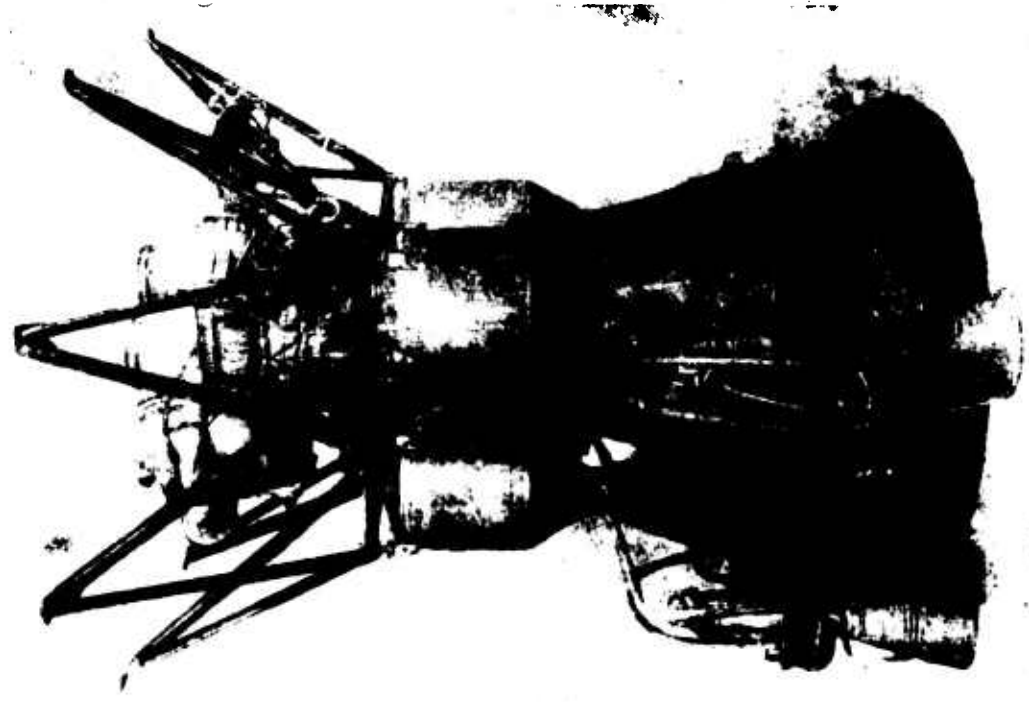


Fig. 1.16. ZHRD RD-108.

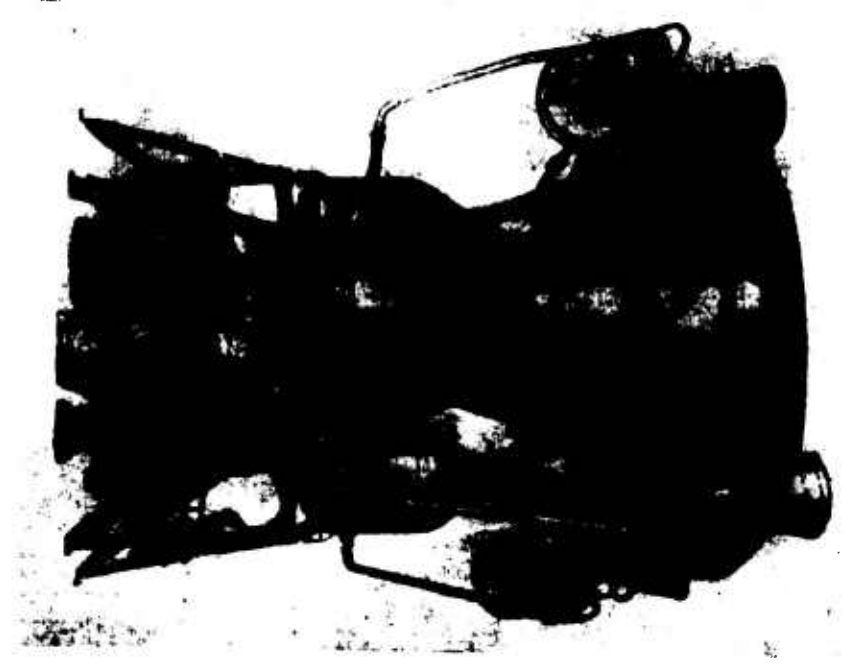


Fig. 1.17. ZHRD RD-108.

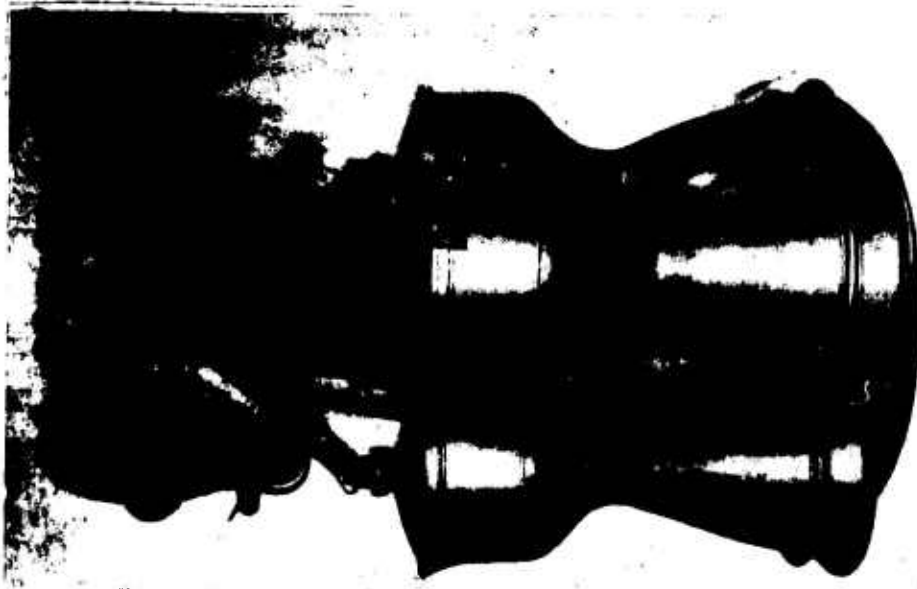


Fig. 1.18. ZHED RD-214.

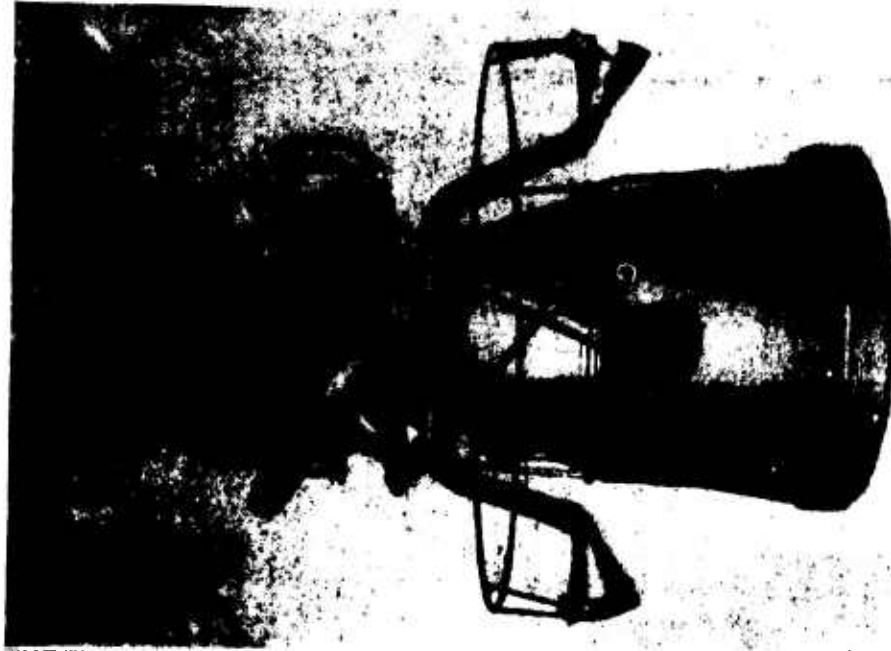


Fig. 1.19. ZHED RD-119.

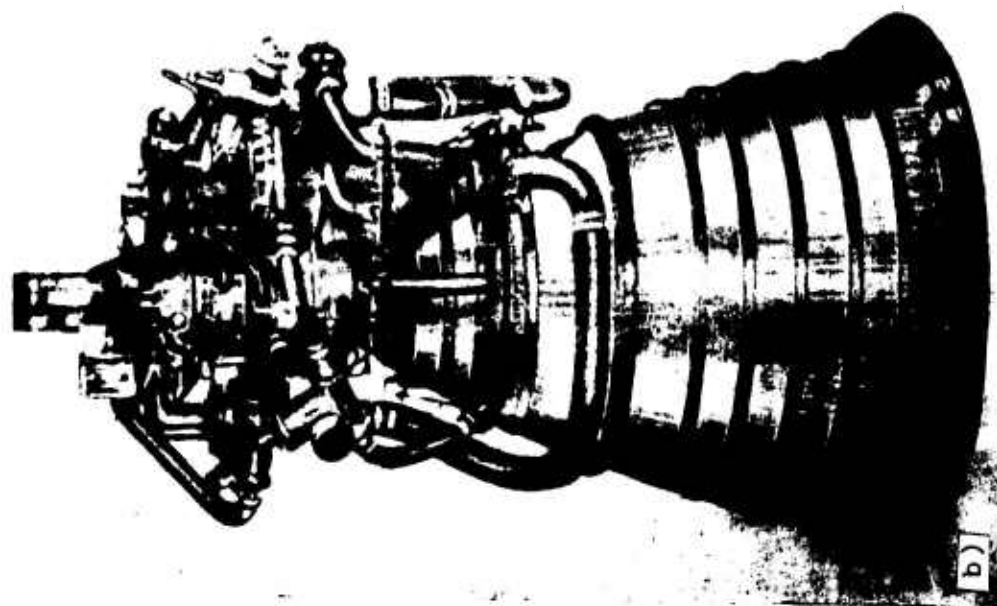
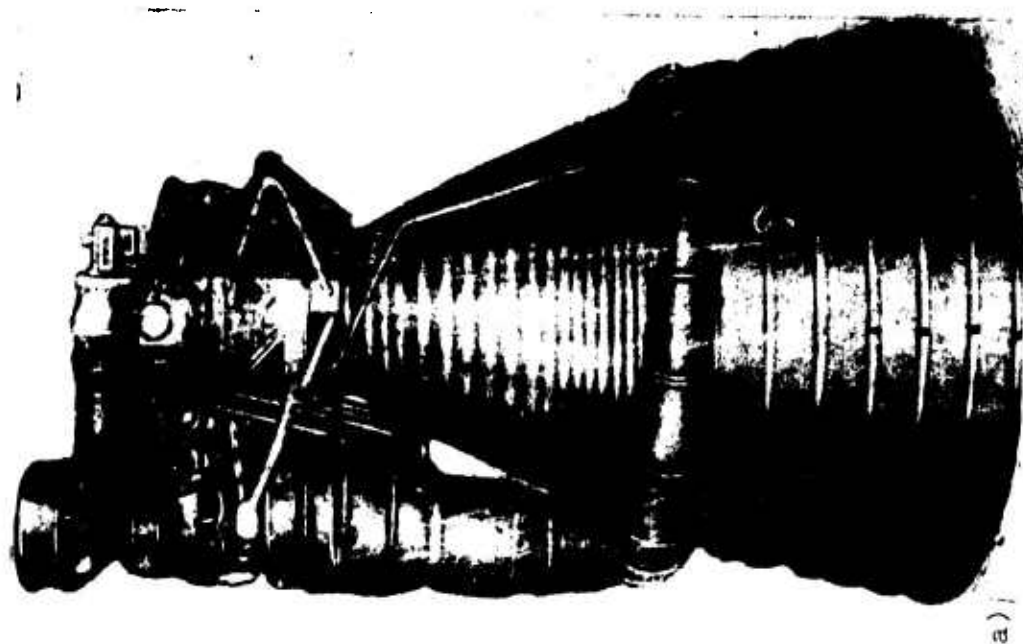


Fig. 1.20. American rocket engines: a) ZhRD F-1; b) ZhRD RL-103A-3.

Surface-to-surface missiles starting from earth and having a terrestrial target are usually ballistic missiles. The flight path of these rockets, excepting the initial section on which the rocket is accelerated by the engine, is the trajectory of a projectile. Ballistic missiles can be short-range, medium range, and long-range rockets. The possibilities of the latter, usually multi-stage, are very great. At present near the surface of the earth the distance of flight of ballistic rockets is unlimited. A very high velocity of flight permits covering huge distances in a short time. A hit accuracy of the rocket is high.

Winged rockets are also surface-to-surface missiles.

Surface-to-air missiles start from earth and must reach a certain air object. Anti-aircraft rockets are a means of anti-aircraft defense considerably more effective than usual artillery of the type. Antimissiles intended for interception of ballistic rockets belong here.

Air-to-surface missiles include ballistic missiles launched from aircraft carriers, and likewise aviation bombs and torpedoes equipped with engines. Utilization of a rocket engine provides great distance and accuracy in attacking ground targets.

Finally, air-to-air missiles are aviation rocket projectiles, both guided and unguided. Advantages of such a weapon are high fire power in the absence of recoil, simplicity and relatively small weight.

It must be noted that in a given classification the idea of surface as a place of launch on target of a rocket must be broadly construed in connection with the fact that it is possible to launch rockets from surface vessels or submarine, and it is equally possible to attack these ships with rockets.

Among engines of pilotless rockets RDTT are used in addition to ZhRD.

Chemical RD are sometimes used even on aircraft. In contrast with pilotless aircraft for single utilization, piloted aircraft are intended for repeated utilization with return to the airfield. Aircraft equipped with rocket engines possess high velocity, climbing rate and considerable altitude. They have, however, serious deficiencies. As a result of a large specific expense of fuel, flight of aircraft with a working engine is possible only for a very limited time. The radius of action of the aircraft in this case is small. The aircraft can be used either as a destroyer-interceptor for repulsion of bomb raids, or as experimental craft for investigations at supersonic velocities and great heights. According to communications of the foreign press, such aircraft have reached flight speeds of more than 6600 km/h and a height of 108 km.

It is possible to use a rocket engine on an aircraft simultaneously with an air-breathing jet engine. Combination of an RD and a turbojet or direct-flow VRD provides the aircraft with broad ranges of speed and heights with considerable time and radius of action. In this case the air-breathing jet engine with small specific fuel consumption is the main engine, and the RD is an accelerator of maneuvers switched on only for a brief increase of the flight velocity or altitude on a starting accelerator.

Of chemical rocket engines used for other purposes, let us note engines for underwater torpedoes and submarines (see Chapter XXIX). Such engines are not always purely rocket (autonomous) engines, because utilization of the surrounding medium - sea water is usually provided for their work.

Rocket engines are widely used to drive rocket carts (sleds) moving on a railway. The purpose of such devices is various kinds of testing of aviation and rocket technology connected with high velocities and considerable overloads.

## Generators of Working Medium

In recent years utilization of rocket chambers as generators of working medium with high energy parameters has considerably expanded. By burning chemical rocket fuels or heating various substances with the aid, for example, of electric power, workined media can be obtained with a high concentration of heat or kinetic energy. The chemical composition of such workined media, usually called low-temperature plasma in industry, and their temperature, pressure, and escape velocity can be regulated.

Low-temperature plasma is now used in various branches of technology: heat-power engine ring, chemistry, machine building, metallurgy, mining and others.

The problems of generation of low-temperature plasma and control of its parameters, research on features of working substances in conformity with aircraft engines and industrial devices have much in common.

### 1.4. Brief Survey of the Development of Rocket Engines

#### Rocket Engines on Solid Fuel

The oldest jet engine is the RDTT, known for several hundred years and previously called the powder rocket. Such rockets have been widely used since ancient times as flares, signal and combat rockets. In the Nighteenth Century in a number of countries of Europe there was formed, as a specific type of armament, rocket artillery distinguished for its lightness and maneuverability. Considerable successes in this field were also achieved by Russia. Foundations were laid in the epoch of Peter I, who took an active part in the work of the special "rocket institute." In the beginning of the Nighteenth Century active work was done in the field of battle rockets by General A. D. Zasyadko (1779-1873), who created new models



of rockets and light launch bays for them. A. D. Zasyadko was the initiator of wide introduction into the Russian army of that time of a new rocket weapon.

The original creator of Russian rocket artillery was the outstanding scientist-artilleryman General K. I. Konstantinov (1818-71). In the middle of the past century K. I. Konstantinov widely ran scientific tests the results of which were used in designs of new rockets. He was the organizer of mass mechanized and safe production of powder rockets. The works of K. I. Konstantinov allowed a considerable increase in the range and accuracy of rocket weaponry.

The Russian revolutionary and member of "Narodnaya Volya" N. I. Kibal'chich (1853-81) was the author of the first rocket in the world for manned flight. In his project created in 1881 before his execution, Kibal'chich described a powder engine, a program mode of combustion, means of control of flight by means of slanting the engine, etc.

The most valuable ideas of Kibal'chich were buried in the archives of the Tsar's police and became the property of scientists only after the Great October Socialist Revolution.

At the beginning of 1921 in Moscow on the initiative of N. I. Tikhomirov, the first Russian research and experimental-design laboratory on rocket technology was created. Relocated in 1927 to Leningrad it received the name gas-dynamic laboratory ((ГДЛ) [GDL]). In GDL in 1927-33 with the active creative participation of V. A. Artem'yev, B. S. Petropavlovsk, G. E. Langemak and others powder was created with nonvolatile solvent and gun-powder accelerators for launching aircraft and rocket projectiles for various purposes were developed. Subsequent development of these works became the basis of creation of rocket mortars ("Katyusha rocket launchers") effectively used in the great Fatherland War (WW II).

Work with RDTT was conducted between 1930-1950 in the USA under the leadership of T. von Karman and others.

At the present time in the USSR and abroad, numerous variants of unguided and guided projectiles with RDTT have been developed. Among them are solid-propellant rockets of very large sizes and long flying ranges, including intercontinental ballistic missiles.

### Liquid-Propellant Rocket Engines

Development of liquid-propellant rocket engine began at approximately the turn of the century. During this period the bases of the theory of reactive motion and mechanics of bodies of variable mass were formed. In the development of these questions the role of the outstanding Russian scientists N. E. Zhukovskiy (1847-1921), I. V. Meshcherskiy (1859-1935) and others has been considerable.

However, the greatest contribution to the development of problems of jet propulsion were the works of the famous Russian scientist K. E. Tsiolkovskiy (1857-1935), rightly considered the founder of contemporary cosmonautics and rocket technology. Having begun to take an interest in problems of jet propulsion in 1883, Tsiolkovskiy after long-standing strained work published in 1903 the work "Investigation of near-earth space with jet devices," which has gained a world-wide reputation. In this work Tsiolkovskiy derived the laws of motion of rockets as bodies of variable mass in space without weight as well as in the field of gravity, supported the possibility of utilization of rockets for interplanetary communications, determined efficiency, and investigated many other questions. For the first time in the world, Tsiolkovskiy proposed a new type of engine - the liquid-propellant rocket engine - developed bases of its theory, and showed the elements of its design. He examined and recommended the utilization of various fuels for ZhRD. Tsiolkovskiy offered the use of fuel components for regenerative cooling of the engine and expressed a number of other technical ideas. In subsequent years

Tsiolkovskiy published a series of works on important questions of the development of cosmonautics and rocket construction. Specifically, in 1929 the work "Space rocket trains" was published in which for the first time the theory of the specific type of component rockets was presented.

A considerable place in the works of Tsiolkovskiy was occupied by problems of interplanetary navigation and the prospect of their development. He developed routes of space flights, studied conditions of life and works of people in space, and foresaw the creation of artificial earth satellites, interplanetary stations, and settlements.

The first followers of Tsiolkovskiy in our country were the gifted scientists and inventors F. A. Tsander (1887-1933) and Yu. V. Kondratyuk (1897-1942).

F. A. Tsander even in his student years studied the works of Tsiolkovskiy and was interested in questions of space flights. In 1924 he presented his main idea - combination of a rocket with an aircraft for takeoff from earth and subsequent combustion of the metal part of the aircraft as fuel for the RD. Tsander performed theoretical investigations of various questions of air-breathing jet and rocket engines and began work on their practical realization.

Yu. V. Kondratyuk worked independently of Tsiolkovskiy. His main theoretical investigation "The conquest of interplanetary space" (1929) partly repeated and supplemented the works of Tsiolkovskiy; some problems found a new solution. Specifically, Yu. V. Kondratyuk offered as fuel for engines certain metals and their hydrogen compounds for example, boron hydride.

By the same means as Tsiolkovskiy, but later than him, scientists of foreign countries came to the idea of creation of liquid-propellant rockets.

Works dedicated to this problem were published by R. Esnaut-Pelterie in France (1913), R. Goddard in the USA (1919), and G. Obert in Germany (1923).

K. E. Tsiolkovskiy did not conduct experimental works on the creation of ZhRD. This problem was solved by his students and followers both in the USSR and abroad.

In the USA experimental work was started by R. Goddard (1882-1945), who proposed many different technical solutions in the field of creation of engines and rockets. In 1923 Goddard carried out the first launching of an experimental ZhRD running on liquid oxygen and gasoline, and in 1926 the first flight of an experimental liquid-propellant rocket.

In Germany bench tests of ZhRD were started by G. Obert in 1929, and flight tests of liquid-propellant rockets by I. Winkler since 1931. Since 1937 under the leadership of W. von Braun, the V-2 rocket, powerful for those times, was developed, the flight tests of which were started in 1942.

In the USSR experimental work on realization of the ideas of Tsiolkovskiy began 15 May 1929, when in the GDL in Leningrad the first experimental-design subdivision for development in electrical and ZhRD was created and approached practical activity.

In  
created  
operate  
300 kgf

In this subdivision a family of experimental ZhRD was created with thrust from 6 to 300 kgf operating on various low-boiling and high-boiling liquid oxidant with liquid fuels. The engines had the designation (OPM) [ORM - experimental rocket motor].

The first Soviet experimental ZhRD, ORM-1, (Fig. 1.21) was developed and built in 1930-31. The fuel of the engine was nitrogen tetroxide and toluene or liquid oxygen and gasoline. During a test on oxygen fuel ORM-1 developed thrust up to 20 kgf.

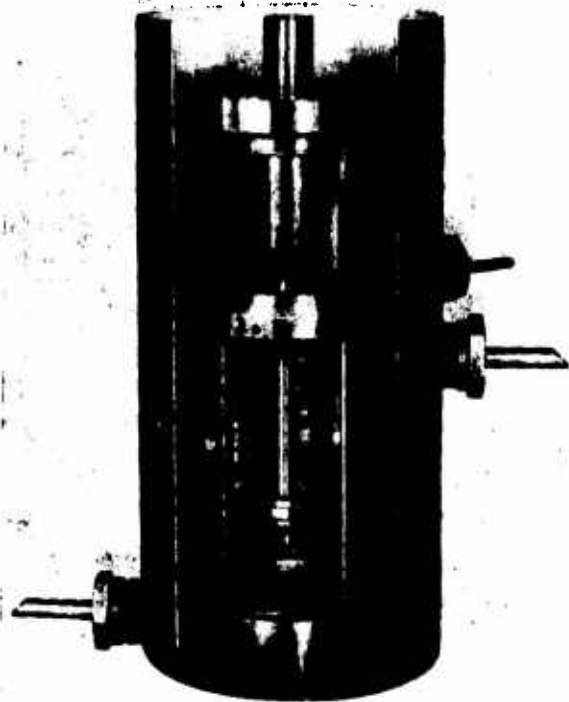


Fig. 1.21. The first Russian experimental ZhRD ORM-1, worked out at the GDL in 1930-31.

In the period 1930-33 a series of ZhRD from ORM-1 to ORM-52 was created in GDL. The most powerful was the ORM-52 (Fig. 1.22), which operated on nitric acid and kerosene. It developed thrust up to 250-300 kgf at a pressure in the combustion chamber of 20-25 bar.

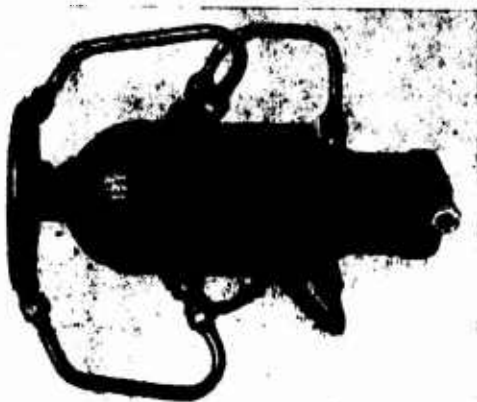


Fig. 1.22. ZhRD ORM-52.

In GDL many practical questions of creation of ZhRD were successfully solved for the first time. A mixture of nitric acid with nitrogen tetroxide, chloric acid, tetranitromethane, hydrogen peroxide, three-component fuel (oxygen, hydrogen and beryllium) and others was proposed for the first time in 1903 as components of rocket fuel. Ceramic heat insulation of combustion chambers with zirconium dioxide were created and systems of mixing components and ignition were mastered. Since 1931 there has been used pyrotechnic ignition (by gun-powder cartridge) and, chemical ignition proposed for the first time (with the use of self-igniting fuel). At the same time a profiled nozzle and a cardan suspension of the engine were proposed. In 1931-32 piston fuel pumps driven by gas removed from the combustion chamber of an RD were developed and tested, and in 1933, a design of a turbopump unit with centrifugal fuel pumps.

The problems of rocket technology which were attracting wide attention were worked out by many Soviet enthusiasts on social principles. Their unification was called Group for the Study of Jet Propulsion ((ГИПД) [GIRD]). Such public organizations at Osoaviakhim [Society for Assistance to the Defense, Aviation, and Chemical Construction of the USSR] were created in 1931 in Moscow (MosGIRD) and Leningrad (LenGIRD), and later in other cities. Among the organizers and active workers of MosGIRD were F. A. Tsander (its first leader), S. P. Korolev, V. P. Vetchinkin, M. K. Tikhonravov, H. A. Pobedonostsev and others. MosGIRD developed wide lecture and press propaganda, organized courses on the theory of jet propulsion and began work with the design of aviation ZhRD OR-2 (the Tsander project) for rocket aircraft RP-1. In 1932 in Moscow a scientific-research and experimental-design organization for development of rockets and engines, also named GIRD, was created. The basic personnel of MosGIRD entered this organization, and S. P. Korolev became its chief.

Engines developed at GIRD used liquid oxygen as oxidant and gasoline and ethyl alcohol as fuel. The first ZhRD of Tsander, OR-2, was tested 18 March 1933 on oxygen and gasoline; its subsequent modification (engine 02) operated on oxygen and ethyl alcohol.

Engine 09, intended for the first Soviet experimental liquid-propellant rocket "GIRD-09" (M. K. Tikhonravov project), was a hybrid rocket engine. The oxidant was liquid oxygen supplied to the chamber by the pressure of its own vapors, and the fuel was consolidated gasoline, which was placed in the combustion chamber. The first flight of the rocket "GIRD-09" occurred 17 August 1933, and on 25 November 1933 the GIRD rocket "GIRD-Kh" with a ZhRD operated on liquid oxygen and ethyl alcohol was launched.

At the end of 1933 in Moscow State Scientific Research Institute of the First Jet Propulsion (RNII) was created on the basis of GDL and GIRD. Specialists on ZhRD who had been at GDL developed in RNII in 1934-38 a series of experimental engines from ORM-52 to ORM-102 and a gas generator GG-1 that operated for several hours on nitric acid-kerosene fuel with water at a temperature of 580°C and a pressure of 25 bar. The engine ORM-65 (Fig. 1.23), officially tested in 1936, was the best engine of its time. The engine operated on nitric acid and kerosene, its thrust was regulated within the limits of 50-175 kgf, its launching was multiple, including automated launching. The ORM-65 was fire-tested on flight vehicles of S. P. Korolev design: winged rocket 212 (flying 1939) and the rocket-glider RP-318-1 (ground 1937-38). On 28 February 1940 the flier V. N. Fedorov completed the first flight on the rocket-glider RP-318-1 with engine ORM-65, which was a modification of the ORM-65.

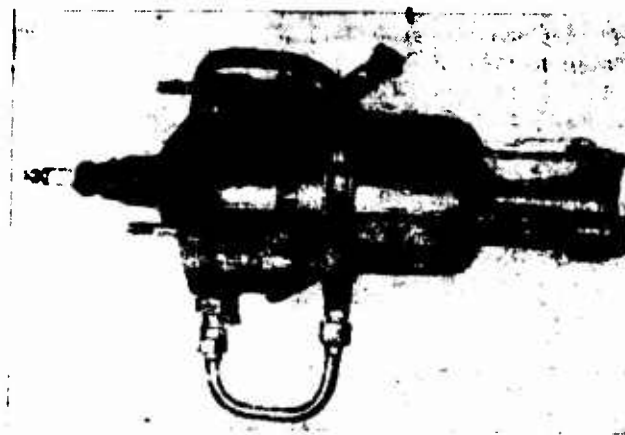


Fig. 1.23. ZhRD ORM-65.



In 1941-42 at the RNII the ZhRD D-1-A-1100 was developed which operated on nitric acid and kerosene and which developed a nominal thrust of 1100 kgf. The engine was destined for the first Soviet aircraft with a ZhRD. This aircraft, BI-1, was developed in the same years by A. Ya. Bereznyak and A. M. Isayev under the guidance of the chief designer V. F. Bolkhovitinov. On 15 May 1942 the flier G. Ya. Bakhchivangi completed the first flight on the BI-1.

The GDL, GIRD and RNII made a fundamental contribution to the development of rocket engineering in the USSR.

In 1939 the Experimental Design Office (OKB) on ZhRD was created. In the 1940's OKB developed a family of aviation ZhRD from RD-1 to RD-3 (Fig. 1.24). Auxiliary air-borne ZhRD with pumping supply of nitric acid-kerosene fuel, chemical ignition, an unlimited number of repeated, completely automated launchings, and adjustable thrust were put through numerous tests in 1943-46, including flight tests on the aircraft of V. M. Petlyakov, S. A. Lavochkin, A. S. Yakovlev, and P. O. Sukhou design.



Fig. 1.24. Airborne ZhRD (GDL-OKB): 1 - RD-1 with thrust of 300 kgf; 2 - RD-1Kh3 with thrust of 300 kgf with chemical ignition; 3 - modification RD-1Kh3; 4 - RD-2 with thrust of 600 kgf; 5 - RD-3 with thrust of 900 kgf; three-chamber with TNA (units are shown under the engines).



Post-war development of work on rocket-space technology was carried out at a rapid rate and led, beginning in 1949, to regular launchings of geophysical and meteorological rockets, and then to vehicles of another purpose.

The fruitful work of Soviet scientists, engineers, and workers was crowned on 4 October 1957 with a triumphant success - the first launching of an artificial earth satellite. This was followed by launchings of new satellites and space rockets, achievement of escape velocity, and flights of interplanetary automatic stations. The problem of accurate return of the rocket ship to earth was solved successfully.

The first manned flight into outer space on 12 April 1961 became a historical event. This flight was carried out by the flier-astronaut Yu. A. Gagarin on the space ship (Vostok). This flight marked the beginning of direct penetration of man beyond the earth atmosphere. The remarkable flights of the glorious pleiad of Soviet astronauts brought many new unprecedented achievements, including the first exit of man from a ship-satellite into open space.

The decisive factor in all these successes was the creation and improvement in the Soviet Union of multistage rockets, the characteristic features of which are enormous power of the engines and exclusively high accuracy of systems of adjustment and automatic control.

An outstanding contribution to the development of cosmonautics was made by academician S. P. Korolev (by 1906-66), the leading developer of the first powerful rocket-space systems. S. P. Korolev was actually a designer of rockets, space stations and ships. Rocket-space systems were developed by him together with the chief designers of engines, flight control systems, and other onboard systems, and the complex of ground launching equipment. Work was conducted in collaboration with Scientific Research Institutes of Industry and the Academy of Sciences of the USSR.

The OKB which evolved from GDL developed in 1954-57 ZhRD RD-107 and RD-108, which considerably exceeded in economy the analogous American ZhRD. In 1952-57 the RD-214 was developed, and in 1958-62 the RD-119, also having the highest economy in their classes. Powerful engines of this OKB were on all Russian rocket-carriers which put into orbit artificial satellites, of the Earth, Sun, Moon, automatic stations to the Moon, Venus, and Mars; and the piloted ships Vostok, Voskhod, and others.

The ZhRD of the multistage powerful rocket-carrier Proton, which began flights in 1965, have been made according to the most perfect scheme and are distinguished by high pressure in the combustion chamber, high quality of the working process, compactness, and reliability.

The development of rocket-space thematics gave life to new creative collectives headed by the chief designers of rockets, space ships, engines, control systems and launch systems. They created a number of remarkable intercontinental rockets, rocket-carriers, and space objects. The basic type of engine in all these systems is the ZhRD.

#### Electrical and Nuclear Rocket Engines

The possibility of utilization of electrical and nuclear energy in jets was shown with brilliant sagacity by K. E. Tsiolkovskiy as early as 1912. This possibility was discussed also in works of R. Goddard, G. Obert, Yu. V. Kondratyuk, and others.

The first theoretical work which treated of the principle of work of ERD of the electrothermal type and made the necessary calculations was the work "Metal as an explosive substance. Jet engine with high escape velocity," dated 10 April 1929. The work was approved, and the author was given the possibility of practically realizing it at GDL. In the period 1929-1933 the first ERD of the electrothermal type was developed and tested. In its chamber with the aid of powerful brief pulses of electrical current thin metallic wires (or a jet of

electrically conductive liquid) were exploded. The products of the explosion, which are gases of high temperature, were expanded in the jet nozzle, attaining high exhaust velocities.

No further research was done on ERD at GDL inasmuch as the main attention was focused on development of ZhRD, as it was more necessary at that time for practical utilization.

It is characteristic that works in the field of ERD of various schemes were activated in our country and abroad after exit of flight vehicles into space had been provided for with the aid of ZhRD. At present ERD are already used in spacecraft, mainly in orientation systems. In 1964 electrostatic (ion) RD were tested in flight on a ballistic trajectory (USA) as well as in the flight of the spaceship "Voskhod" (USSR). In the same year electromagnetic (plasma) RD were tested in the space flight of the Soviet robot space station "Zond-2." In 1965 on one of artificial earth satellites launched in the USA, an ERD of the electrothermal type was tested. The ERD are developed even for long work as main engines of vehicles which reached orbital velocity.

Nuclear rocket engines (RPD) [YaRD - nuclear rocket engine] are in the stage of active experimental investigations. Close to realization is a YaRD having a reactor with a solid active zone and using hydrogen as its working medium. Creation of YaRD with a so-called gas reactor [1] is promising. It is considered that YaRD will be fulfilled as engines of high thrust utilized for acceleration of space systems [6].

Effective combination on a rocket of chemical, nuclear and electrical rocket engines will expand possibilities in the study and conquest of space.

■  
■

In the 10 years since the moment of the first breakthrough into space, in the USSR alone more than 250 satellites weighing more

than 736 t (not considering weights of final stages of rockets) there have been put into orbits around the earth, sun, and moon, and 22 stations weighing more than 30 t have been accelerated to escape velocity. Some of them have been returned to earth. In the USA the "Apollo" program has successfully landed astronauts on the moon.

tek  
app  
roc

Utilization of artificial earth satellites of the meteorological, extra-long-range radio and television communication, navigation, geodesic, geophysical, astronomical and other type opens new wide possibilities for solution of problems of the national economy, and provides the most valuable scientific information. The rocket-nuclear power of the Soviet Union serves as a reliable stronghold of the conquests of socialism.

Ahead are new grandiose problems in the development of rocket-space technology and of its fundamental principle - rocket engines. Solution of these problems depends to a considerable extent on successes in the theory and practice of Russian rocket-engine design.

#### Bibliography

1. Bassard R., Delauer R., Yadernyye dvigateli dlya samoletov i raket (Nuclear engines for aircraft and rockets), Voenizdat, 1967.
2. Glushko V. P., Langemak G. E., Rakety, ikh ustroystvo i primeneniye (Rockets, their equipment and utilization), ONTI, 1935.
3. Grodzovskiy G. L., et al., Mekhanika kosmicheskogo poleta s maloy tyagoy (Mechanics of space flight with small thrust), izd-vo "Nauka," 1966.
4. Kondratyuk Yu. V., Zavoyevaniye mezhplanetnykh prostranstv (Conquest of interplanetary space), Oborongiz, 1947.
5. Korolev S. P., Raketnyy polet v stratosfere (Rocket flight in the stratosphere), Voenizdat, 1934.
6. Korliss U., Dvigateli dlya kosmicheskikh poletov (Engines for space flights), IL, 1962.
7. Petrovich G. V., Vestnik AN SSSR, 1965, No. 10; 1967, No. 10.

8. Feodos'yev V. I., Sinyarev G. B., Vvedeniye v raketnyyu tekhniku, (Introduction to rocket technology), Oborongiz, 1960.

9. Tsander P. A., Problema poleta pri pomoshchi reaktivnykh apparatov (The problem of jet-aided flight), Oborongiz, 1961.

10. Tsiolkovskiy K. E., Trudy po raketnoy tekhnike, (Works on rocket technology), izd-vo "Mashinostroyeniye," 1967.



## CHAPTER II

### THRUST OF THE CHAMBER AND ENGINE

The acceleration of the working medium necessary for creation of jet thrust can be obtained by means of various effects on a flow: geometrical, flow-rate, thermal, mechanical. Of them the easiest to realize is geometrical.

Obtaining thrust by using geometrical nozzles is considered below.

#### 2.1. Thrust of a Chamber with a Laval Nozzle

The thrust of the rocket-engine chamber is the resultant all forces applied to the chamber during its work, excepting the forces of weight and of reactions of supports. This means the thrust is determined by forces acting on the part of the gaseous working medium on the inside surface of the chamber, and by forces of the environment on its external surface.

Forces acting on the part of gas on the solid surface washed by it can be presented as normal and tangential: pressure  $p$  and tangent stress of friction  $\tau$ .

The real distribution of pressure over the external surface of the chamber depends on the arrangement of the chamber on the craft, and the aerodynamic form and velocity of craft. However, the pressure on the external surface of the chambers is assumed constant and equal to the barometric pressure of the unperturbed environment  $p_h$ .

In this instance the force of thrust of the chamber should be written down as the sum of integrals of forces of pressure on the external surface and the forces of pressure and tangential stresses on the internal surface:

$$\vec{P} = \int_{F_{\text{ext}}} p_h \vec{n} dF + \int_{F_{\text{int}}} \vec{T} dF. \quad (2.1)$$

Here  $p_h$  is the pressure of the surrounding medium;  $\vec{T}$  is the force acting on a unit of inside surface (the normal component of this force is the local pressure of the working medium, and the tangential component is the stress of friction).

It is easy to see that the first term of the right side of equation (2.1) is equal to

$$\int_{F_{\text{ext}}} \vec{p}_h dF = p_h \vec{F}_c. \quad (2.2)$$

For determination of the second member let us avail ourselves of the theorem of momentum, according to which the resultant of external forces acting on a certain gas volume is equal to the change per unit of time of the quantity of motion of the working medium which flowed through the surface bounding the isolated volume. Let us designate the control surface on the inside walls of chamber, as shown in Fig. 2.1 with a dotted line. The motion of the gas in the combustion chamber and nozzle will be considered one-dimensional, continuous, and steady.



Fig. 2.1. For derivation of the equation of thrust of a chamber.

The integral of forces of pressure and frictions acting on the isolated volume can be presented as the sum of two quantities: integrals of forces acting on the part of the control surface coinciding with the inside surface of the chamber and on the surface of out of the nozzle:

$$\int_{F_{\text{nozzle}}} \vec{f}_n dF = \int_{F_{\text{chamber}}} \vec{f}_n dF + \int_{F_c} p dF, \quad (2.3)$$

where  $\vec{f}_n$  is the force acting on the gas on the part of the inside surface of the chamber. It is obvious that

$$\vec{f}_n = -\vec{f}.$$

Analogously (2.2) can be written

$$\int_{F_c} p dF = \overline{p_c F_c}.$$

The isolated volume is entered by a working medium with a quantity of motion equal to zero (liquid or gas is supplied at a negligible rate), and through area  $F_c$  in a unit of time mass  $G$  flows out at a rate of  $w_c$ . In this way the per-second change in momentum is equal to  $G\vec{w}_c$ . According to the theorem of momentum

$$G\vec{w}_c = - \int_{F_{\text{chamber}}} \vec{f} dF + \overline{p_c F_c}. \quad (2.4)$$

Substituting equations (2.4) and (2.2) in expression (2.1), we obtain

$$\vec{P} = -G\vec{w}_c + \overline{p_c F_c} + \overline{p_h F_c}.$$

The positive direction is the direction of thrust. Then

$$P = Gw_c + p_c F_c - p_h F_c. \quad (2.5)$$



iding  
The obtained expression is the basic equation of chamber thrust with the assumptions made earlier relative to regularity and continuity of flow. Rejection of these assumptions somewhat changes the form of the equation and will be specially discussed subsequently.

3)  
The following characteristic cases of determination of chamber thrust are of interest.

1. Thrust in a vacuum, where  $p_h = 0$ ,

$$P_R = Gw_0 + p_c F_c. \quad (2.6)$$

As it appears, it is wholly defined by processes which proceed inside the chamber and is total impulse of flow.

2. Thrust at any height, where  $p_h \neq 0$ ,

$$P_h = P_R - p_h F_c. \quad (2.7)$$

ntity  
In formula (2.7) it is evident that the influence of the surrounding medium always diminishes chamber thrust.

3. Thrust in the condition of equality of pressures, where  $p_h = p_c$ :

$$P = Gw_c. \quad (2.8)$$

4)  
The absence in the last formula of the term  $p_h F_c$  does not mean that the influence of external pressure has disappeared. The result of such pressure as before is force  $p_h F_c$ . It has been excluded here simultaneously with the part of positive thrust created by the chamber ( $p_c F_c$ ).

Sometimes the formula of thrusts for all conditions is presented in the following manner:

$$P = Gw_{\infty}. \quad (2.9)$$

where  $w_{\text{eff}}$  is the so-called effective exhaust velocity.

The value of  $w_{\text{eff}}$  is determined from the following equation

$$Gw_{\text{eff}} = Gw_c + p_c F_c - p_h F_c$$

whence

$$w_{\text{eff}} = w_c + \frac{p_c - p_h}{G} F_c \quad (2.10)$$

or, using the continuity equation:

$$w_{\text{eff}} = w_c + \frac{p_c - p_h}{\rho_c w_c}, \quad (2.11)$$

where  $\rho_c$  is the density of gas leaving the nozzle.

Obviously, only at  $p_c = p_h$  does the arbitrary value of effective exhaust velocity coincide with the value of velocity in the output section of the nozzle  $w_c$ .

## 2.2. Characteristic Modes of Operation of a Laval Nozzle

The mode of operation of the nozzle is determined by the relationship of pressure on the cut-off of the nozzle and of the surrounding medium. Mentioned above was the mode of equality of these parameters  $p_c = p_h$ . The modes  $p_c > p_h$  and  $p_c < p_h$  are also possible.

Let us examine the physical picture of escape from the nozzle in various modes.

In modes of underexpansion the pressure at the cut-off of the nozzle  $p_c$  is greater than the pressure of the surrounding medium  $p_h$ . With escape from a flat nozzle in these modes, complete expansion of the jet behind the nozzle occurs, which is accompanied by a system

of lines of weak disturbance, but without jumps of condensation. Escape from an axisymmetrical nozzle in all modes of underexpansion is accompanied by appearance of jumps of condensation. Jumps have the form of surfaces of rotation with a curved generatrix. The form of separate sections of the jet is barrel-shaped.

Figure 2.2a, shows the spectrum of a jet behind a conical axisymmetrical nozzle when  $p_c > p_h$ . On the axis of the jet curved jumps AB and  $A_1B_1$  are closed by straight jump BB<sub>1</sub>. With an increase in the difference of pressures  $p_c - p_h$  the jump is moved aside from the cut of the nozzle. At small differences of pressure, curved jumps AB and  $A_1B_1$  are not closed by a straight line, but even in the mode of equality ( $p_c = p_h$ ) they continue to exist (Fig. 2.2b).

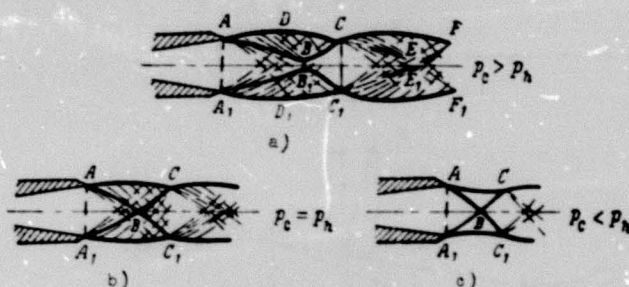


Fig. 2.2. Spectra of gas jet leaving conic expandable nozzle in various modes of its operation.

Modes of overexpansion, when  $p_c < p_h$ , are also accompanied by the system of curved jumps shown in Fig. 2.2c.

Comparison of the work of the nozzle in mode  $p_c = p_h$  and in mode  $p_c \neq p_h$ , all things being equal, is necessary for correct selection of parameters of a nozzle in designing. Qualitatively it can be done in the following manner.

Given that three variants of a nozzle are designed for the same rocket-engine chamber: 1)  $p_c = p_h$ ; 2)  $p_c < p_h$ ; 3)  $p_c > p_h$ .

If a conic nozzle is designed, then at a constant angle of the opening these nozzles will differ in length. In Fig. 2.3a the considered nozzles are limited lengthwise by sections 3-3, 1-1, and 2-2. Obviously, the longest of them will provide mode  $p_c < p_h$ , and the shortest mode  $p_c > p_h$ . If the average nozzle for  $p_c = p_h$  in a particular case, then the shorter nozzle will operate with under-expansion, and the longer one with overexpansion.

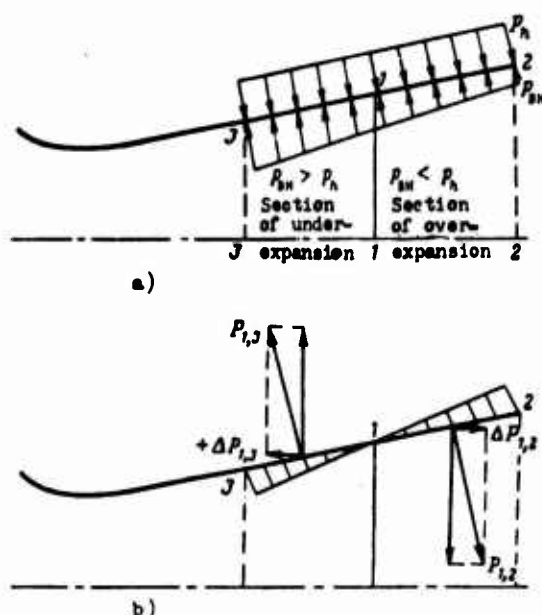


Fig. 2.3. For comparison of thrust in various modes of operation of a nozzle.

Let us compare the thrusts developed by these nozzles. As was noted, the thrust is the axial component of the resultant of forces of pressure on the external and internal chamber surfaces (for simplicity forces of friction are disregarded). Therefore, diagrams of pressures with respect to the contours of the chamber with various nozzles should be compared. These diagrams from the left of section 3-3 are identical; therefore, the distribution of pressures can be compared only in section 3-1-2.

In Fig. 2.3a it is evident that in the section of nozzle 1-2 external pressure everywhere exceeds internal pressure. The resulting diagram is shown in Fig. 2.3b. Let us replace this diagram with one resultant force and isolate in the latter the radial and axial components. The axial component  $\Delta P_{1,2}$  is opposite in direction to the direction of thrust; consequently, section 1-2 diminishes the total thrust. The thrust of a chamber with overexpansion is less than the thrust of a chamber operating in the mode  $p_c = p_h$  by the value  $\Delta P_{1,2}$ .

In nozzle section 1-3 internal pressure is greater than external pressure, and the resulting diagram, as can be seen from Fig. 2.3b, is positive. The resultant force  $P_{1,3}$  equivalent to it has axial component  $+\Delta P_{1,3}$ , coinciding in direction with thrust. Consequently, section 1-3 creates positive thrust. To pass from a nozzle, operating in mode  $p_c = p_h$  to the nozzle with underexpansion, we deprive ourselves of this section and in this way lose thrust. The thrust of the chamber with an underexpanding nozzle  $P_3$  is  $\Delta P_{1,3}$  less than thrust  $P_1$ . Thus modes of operations of nozzles differing from mode  $p_c = p_h$  lead to a lowering of chamber thrust.

Disturbances in the jet behind the nozzle cannot be shifted upstream on account of the supersonic jet velocity. However, in the boundary layer near the walls of the nozzle the velocity of flow is subsonic. This creates the possibility of influence of the external medium on the flow inside the nozzle. In modes of underexpansion this pressure is prevented by positive difference of pressures  $p_c - p_h > 0$ .

In modes of overexpansion the pressure  $p_h$  is greater than the pressure on the cut-off  $p_c$ . At a rather large positive difference  $p_h - p_c$  the boundary layer is detached from the wall of the nozzle as a result of restoration of pressure in the slanting jump of condensation. The surrounding medium is sucked into the region between the wall of the nozzle and the flow detaching itself. The greater the difference  $p_h - p_c$  (or the ratio  $p_h/p_c$ ), the nearer to the critical section the system of jumps is moved. The diagram of this movement is given in Fig. 2.4.

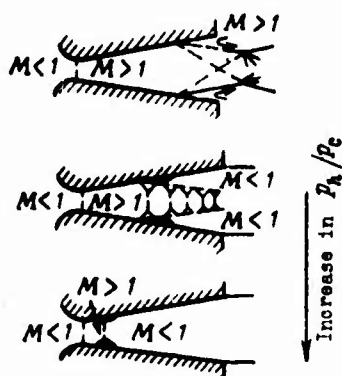


Fig. 2.4. Picture of movement of the system of condensation jumps inside a nozzle in the overexpansion mode.

In contrast with all the modes of underexpansion and of modes of overexpansion without entrance of jumps into the nozzle, the modes of overexpansion with jumps and detachment of flow inside nozzles lead to chambers in the spectra of flow not only beyond the nozzle, but also inside the expanding part of it. This is accompanied by a change of the diagram of internal pressure on the walls of the nozzle.

Figure 2.5 gives idealized diagrams of external and internal pressure on the walls of a nozzle operating with overexpansion. Up to the section in which detachment occurs the flow does not change. Therefore, the diagram of internal pressure in the section of nozzle prior to detachment of flow will be the same as in the corresponding section of a nozzle operating with the same original parameters without overexpansion. In section 2 when  $p_c < p_h$  there is detachment of flow from the wall. In section 2-c in the case of overexpansion without detachment of flow, internal pressure would be considerably lower than steady-state pressure of the surrounding medium after detachment. In this case the resulting influence of external and internal pressure in section 2-c would create a negative thrust component, i.e., it would diminish total thrust. In case of overexpansion with detachment of flow from the wall, in section 2-c the same influence acts from without and within. In this case the negative component of thrust does not appear. Consequently, overexpansion with detachment of flow at the same parameters on entering the nozzle provides a higher value of thrust in comparison with continuous overexpansion.

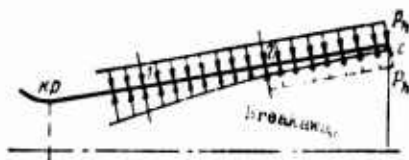


Fig. 2.5. Idealized diagrams of external and internal pressures on walls of nozzle without and with breakaway of flow from the wall

From what has been said it can be concluded that the expression (2.5) for calculation of chamber thrust is not universal, inasmuch as it does not consider phenomena connected with detachment of the flow. Therefore, it is expedient to divide modes of operation of the nozzle into modes of continuous flow and modes of flow with breakaway of flow inside the nozzle. Expression (2.5) is applicable only for modes of continuous flow. The thrust of the chamber in the nozzle of which the flow is detached from the wall is calculated somewhat differently.

### 2.3. Thrust of Chamber in Modes with Breakaway of Flow Inside a Laval Nozzle

The real picture of flow with breakaway is distinguished from idealized basically by the presence of a boundary layer about the wall of the nozzle. The physical model of flow with breakaway and the diagram of pressure on the wall of the nozzle are shown in Fig. 2.6.

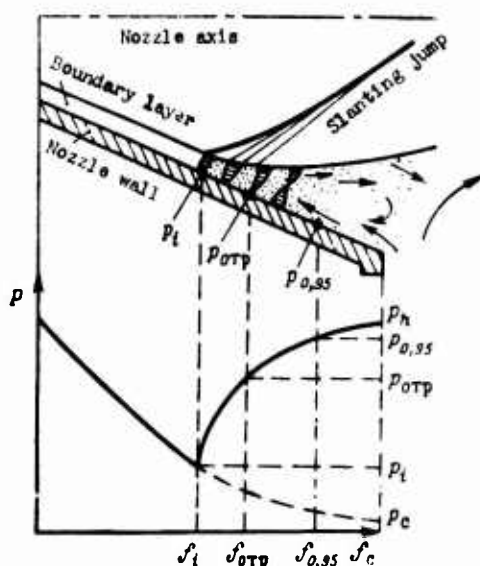


Fig. 2.6. Model of flow in nozzle with breakaway from the wall.

In section 1 at pressure  $p_1$  thickening of the boundary layer begins. This section is located somewhat upstream from the place of detachment of the flow. In the section from the place of thickening of the boundary layer to the place of flow detachment and downstream, there is a gradual pressure increase up to the pressure of the environment.

Theoretical research on phenomena of breakaway and, the more so, obtaining final calculation dependences on the basis of only theoretical prerequisites is difficult. Therefore in practice the results of experimental investigations are usually used in the form of empirical relationships or in the form of charts. Below is one of the possible means of calculation of thrust of a chamber with a conic nozzle in the mode of operation with detachment of the flow [3].

For the sake of simplicity of calculation the whole range of flow downstream from section 1 is divided into 2 subdomains:

a) the subdomain located between section 1 and the section where static pressure is 0.95 of external pressure  $p$ ; it embraces the zone of interaction of the slanting jump of condensation with the turbulent boundary layer;

b) the subdomain located downstream from the section where  $p = 0.95 p_h$ , to the cut of the nozzle.

The thrust of the chamber in the mode with breakaway from the wall is written thus:

$$P_{\text{отр}} = (Gw_1 + p_1 F_1) + \int_{F_1}^{F_{0.95}} p \cos(n, x) \cdot dF + \int_{F_{0.95}}^{F_c} p \cos(n, x) \cdot dF - p_h F_c. \quad (2.12)$$



Integrals entering here are calculated with empirical relationships obtained on the basis of experimental results of a number of works:

$$\int_{F_1}^{F_{0.95}} p \cos(n, x) \cdot dF \approx 0.55(p_1 + 0.95p_h)(F_{0.95} - F_1); \quad (2.13)$$

$$\int_{F_{0.95}}^{F_c} p \cos(n, x) \cdot dF \approx 0.975p_h(F_c - F_{0.95}). \quad (2.14)$$

Then

$$P_{\text{отр}} = (Gw_1 + p_1 F_1) + 0.55(p_1 + 0.95p_h)(F_{0.95} - F_1) - p_h(0.975F_{0.95} - 0.025F_c). \quad (2.15)$$

The unknowns in this expression are  $w_1$ ,  $p_1$ ,  $F_1$ , and  $F_{0.95}$ . They are found in the following manner.

For calculation of  $p_1$  it is possible to use the empirical dependence

$$p_1 = p_h \frac{2}{3} \left( \frac{p_k^*}{p_h} \right)^{-0.2}. \quad (2.16)$$

Figure 2.7 gives results of experimental investigations [3] of conic nozzles with various magnitudes of aperture half-angle of the supersonic part  $\alpha$  for a number of working bodies. The dependence curve (2.16) is plotted there.

As it appears, this curve rather well reflects the results of experiments over a wide range of relationships of pressures.

Area  $F_1$  and velocity  $w_1$  can be calculated with the aid of usual gasdynamic relationships, utilization of which will be explained subsequently. The area in section c, where  $p = 0.95 p_h$ , can be found from the equation

$$F_{0.95} = \frac{F_l - F_{kl}}{2.4} + F_l. \quad (2.17)$$

This equation just as equation (2.16) is obtained on the basis of a mathematical treatment of experimental results.

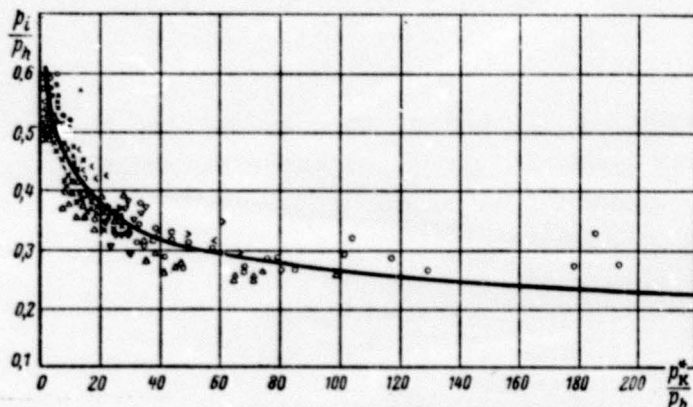


Fig. 2.7. For determination of parameters of breakaway with overexpansion.

In this way can be found all quantities which enter formula (2.15) for calculation of thrust of a chamber with a conic nozzle in which there is breakaway of flow.

Detachment of the flow in a profiled nozzle, as shown by results of experiments [4] appears at greater pressure ratios  $p_h/p_c$  than occurs in conic nozzles. The character of the dependence of pressure ratio at the point of breakaway on the ratio  $p_k^*/p_h$  is the same as for conic nozzles. Therefore, for a tentative estimate the curve of Fig. 2.7 can be used.

#### 2.4. Chamber Thrust with Nozzles of Other Shapes

In the usual round Laval nozzle the walls of the supersonic part are at a rather small angle to the direction of the thrust vector. Every elementary ring of the supersonic part of a nozzle with radius  $r$  and width of  $dS$  perceives a force

$$dR = 2\pi r p dS.$$

Part of this force is used for creation of thrust.

$$dP = 2\pi r p dS \sin \alpha.$$

Here  $\alpha$  is the angle of inclination of the wall of the nozzle to the axis. The relative magnitude of force useful to the usable portion is equal to  $\sin \alpha$ .

It is obvious that the characteristics of the nozzle can be improved if we increase the angle of slope of the wall of the supersonic part to the axis as much as possible. However, in this case the magnitude of pressure on the wall must be correct. This is achieved by turning the gas flow, which is realized in curved nozzles [2].

In the curved nozzle (Fig. 2.8) the flow of gas after passing the critical section will be inclined to the side wall ( $\kappa p-c$ ). The opposite wall of the nozzle ( $\kappa p'-c'$ ) will be acted on by decreased pressure. Under some conditions this wall can be generally removed. Then the enlarging part of the nozzle will turn into a curved channel open from one side. Such a channel is an element of a nozzle unit which can be used for creation of various types of nozzles of rocket engines. These elements can be placed on a circumference or on straight lines.

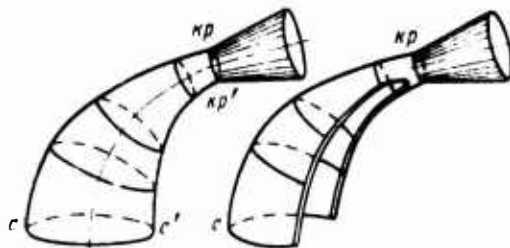


Fig. 2.8. Diagram of curved nozzles.

Figure 2.9 shows two cases of forming of a nozzle unit by rotation of element abcde around the axis. This type is called a ring nozzle. Basic principles of shaping of ring nozzles are considered in Chapter XII.

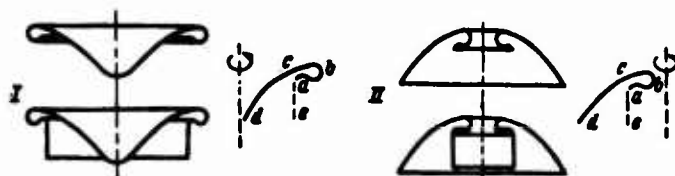


Fig. 2.9. Diagram of form of annular nozzles.

Elements of the surface of the nozzle creating thrust can be almost perpendicular to the direction of thrust. Therefore, with identical thrusts such nozzles can be considerably shorter than the usual round Laval nozzle. Another advantage of them is the possibility of self-regulation in the overexpansion mode. In these modes high atmospheric pressure tightens the boundary of the free enlarging jet; as a result static pressure on the wall of the nozzle increases, and the unfavorable effect of overexpansion of the flow is diminished.

The thrust of chambers with nozzles of this type is called on the basis of general definition (2.1).

## 2.5. Thrust, Total Impulse, Power of Engine

The engine can consist of several chambers; its thrust will be equal to the total thrust of all chambers.

In engines with a turbopump fuel supply, waste gas after the turbine can be ejected through a special output nozzle and create a certain thrust  $\Delta P$ .

With allowance for this the engine thrust is

$$P_{\text{th}} = \sum_{i=1}^n P_i \cos(x, X) + \Delta P. \quad (2.18)$$

Here  $n$  is the number of thrust chambers;  $x$  is the direction of the axis of the thrust chamber;  $X$  is the direction of the axis of the engine.

It is sometimes convenient to characterize the rocket engine by the quantity of total impulse — by the determined integral of thrust taken in the complete time of work:

$$I_z = \int_0^t P_{\text{th}} d\tau. \quad (2.19)$$

According to the value of thrust of the rocket engine  $P$  and the velocity  $V$  of the aircraft on which it is placed, the power being spent to move the aircraft forward can be defined. It is called thrust power:

$$N_P = P_{\text{th}} V. \quad (2.20)$$

Also used is determination of rocket-engine power from power of the jet:

$$N_w = G \frac{w_c^2}{2} = \frac{1}{2} P w_c. \quad (2.21)$$

Below are the relationships between units of measurement of thrust, total impulse and power in the technical system of units as well as in the international system of units (SI):

Parameter	Technical system of units	International system of units SI
$P$	$\text{kgf} \cdot \tau$	$h = \frac{\text{kg} \cdot \text{M}}{\text{s}^2} = \frac{1}{g_0} \text{kgf} = \frac{1}{9.80665} \text{kgf}$
$I_s$	$\text{kgf} \cdot \text{s}$	$\text{N} \cdot \text{s}$
$N_p$	$N_p = P_{\text{an}} V \frac{\text{kgf} \cdot \text{M}}{\text{s}}$ $N_p = \frac{P_{\text{an}} \cdot V}{75} \text{ hp}$	$\frac{\text{N} \cdot \text{m}}{\text{s}} = \frac{\text{J}}{\text{s}} = \text{W}$
$N_w$	$N_w = \frac{1}{2} P_{w_c} \frac{\text{kgf} \cdot \text{M}}{\text{s}}$ $N_w = \frac{P_{w_c}}{2.75} \text{ hp}$	$\frac{\text{N} \cdot \text{m}}{\text{s}} = \text{W}$

### Bibliography

1. Ginzburg I. P., Aerogazodinamika (Aerogas-dynamics), izd-vo "Vysshaya shkola," 1966.
2. Il'sen V., VRT, 1963, No. 3.
3. Kolt S., Bedel D., VRT, 1966, No. 3.
4. Roshke F. Dzh., Mess'yer N. F., "Raketnaya tekhnika," 1962, No. 10.

## CHAPTER III

### SPECIFIC PARAMETERS OF THE CHAMBER AND ENGINE

Such indices as thrust, total impulse, and thrust power are parameters which depend on absolute quantities of expense of fuel, time of action of engine, and flight velocity. Specific parameters are the relative quantities characterizing the effectiveness of the fuel used and the perfection of engine design.

This chapter considers basic specific parameters most widely utilized in the theory and design of engines.

#### 3.1. Specific Thrust

The most commonly used specific parameter of a rocket chamber and engine is specific thrust, i.e., thrust referred to mass flow rate of fuel per second:

$$P_{ya} = \frac{P}{G}. \quad (3.1)$$

It is obvious that specific thrust is a characteristic of economy. The higher the specific thrust, the less the fuel that must be spent to get the assigned thrust.

The specific thrust of the chamber is the thrust referred to mass flow rate per second of fuel being directly burned in the thrust chamber. In accordance with equations (2.6), (2.7), and (2.8) it can be written thus:

in a vacuum ( $p_h = 0$ )

$$P_{yA.n} = w_c + \frac{p_c F_c}{G}; \quad (3.2)$$

at any height, where  $p_h \neq 0$ :

$$P_{yA} = P_{yA.n} - \frac{p_h F_c}{G}; \quad (3.3)$$

in the mode of equality of pressures  $p_c = p_h$

$$P_{yA} = w_c. \quad (3.4)$$

It is evident also that

$$P_{yA} = P_{yA.n} - \frac{p_h}{q_c w_c}. \quad (3.5)$$

In the last expression two components of specific thrust are evident: that depending only on intrachamber processes ( $P_{yA.n}$ ) and that caused by pressure of the surrounding medium (quantity  $-\frac{p_h}{q_c w_c}$ ).

If we make use of the arbitrary magnitude of effective exhaust velocity, then

$$P_{yA} = w_{\text{eff}}. \quad (3.6)$$

For modes of overexpansion occupying a specific position, with detachment of the flow inside the nozzle, specific thrust is determined on the basis of expression (2.15) as

$$P_{yA.\text{отр}} = \frac{\bar{P}_{\text{отр}}}{G}. \quad (3.7)$$



In the SI system thrust  $P$  is expressed in newtons (N), flow rate per second  $G$  - in kg/s, and consequently,  $P_{y\Delta}$  - in N·s/kg. Because  $N = \text{kg} \cdot \text{m/s}^2$ , the dimension of  $P_{y\Delta}$  will be expressed in m/s.

Thus, in the SI system specific thrust has the dimension of velocity, and, as is evident from expression (3.6), it is numerically equal to effective exhaust velocity.

In technical literature the dimension of thrust is kgf, mass flow rate per second is kg/s, and, consequently, the dimension of  $P_{y\Delta}$  is kgf·s/kg. The dimension of  $P_{y\Delta}$  is frequently written in s. In such a treatment specific thrust shows that in a few seconds thrust of 1 kgf will be created by a chamber which expended 1 kg of fuel.

In the SI system the numerical value of specific thrust is  $g_0 = 9.80665$  times greater than in the technical system of units.

In (МРД) [ZhRD - liquid propellant rocket engine], besides the basic fuel burned in thrust chambers, auxiliary fuel can be used to drive the units of the system for supplying fuel and other systems. Therefore, in general thrust and the mass flow rate of engine fuel differ from thrust and the mass flow rate of the chamber, and consequently specific thrusts are different.

The specific thrust of the engine is defined as the ratio of engine draught to complete fuel expenditure, including the mass flow rate of basic fuel in all chambers  $\sum_{i=1}^n G_i$  and the mass flow rate of auxiliary fuel  $G_{\text{всп}}$ :

$$P_{y\Delta, \text{э}} = \frac{P_{\text{э}}}{\sum_{i=1}^n G_i + G_{\text{всп}}} \quad (3.8)$$

Introducing the idea of relative expense of auxiliary fuel

$$\epsilon = \frac{G_{\text{всп}}}{\sum_{i=1}^n G_i}, \quad (3.9)$$

we write

$$P_{\text{уд.дв}} = \frac{P_{\text{уд}}}{(1+\epsilon) \sum_{i=1}^n G_i}. \quad (3.10)$$

Obviously, specific engine thrust and specific chamber thrust are connected by the relationship

$$P_{\text{уд.дв}} < P_{\text{уд}}.$$

For ZhRD with afterburning of generator gas in the basic chamber  $\epsilon = 0$  and  $P_{\text{уд.дв}} = P_{\text{уд}}$ . For ZhRD with separate exhaust of generator gas  $\epsilon > 0$  and  $P_{\text{уд.дв}} < P_{\text{уд}}$ . The quantity  $\epsilon$  is determined by calculation of auxiliary systems, and in the stages of preliminary design they are taken according to statistical data.

In (РДТТ) [РДТТ - solid-propellant rocket engine], where there are no expenditures of auxiliary fuel, and the chamber and engine are identical, differences are not made between specific thrust of chamber and engine. However, for РДТТ other characteristics of specific thrust should be noted.

In contrast with ZhRD for РДТТ it is very difficult to determine instantaneous values of specific thrust, inasmuch as it is intricate to fix instantaneous values of fuel mass flow rate. In connection with this specific thrust of РДТТ is defined in interval of time  $\tau$  (for example, in the operating time of the engine), as an average value:

$$\bar{P}_{yA} = \frac{\int_0^{\tau} P d\tau}{\int_0^{\tau} G d\tau} \quad (3.11)$$

This quantity in practice of RDTT is usually called specific or single impulse (frequently it is designated  $I_{yA}$ ). Obviously, with thrust and specific thrust constant in time

$$\bar{P}_{yA} = P_{yA}$$

Having designated total fuel consumption for time  $\tau$

$$G_{\tau} = \int_0^{\tau} G d\tau \quad (3.12)$$

and using the idea of total impulse introduced earlier (2.19), we obtain the next expression for specific pulse:

$$\bar{P}_{yA} = \frac{I_{yA}}{G_{\tau}} \quad (3.13)$$

The range of specific thrust in a vacuum for contemporary ZhRD constitutes 300-450 kgf·s/kg or s (≈3000-4500 N·s/kg or m/s). The difference in range of values is caused by various fuels and conditions of utilization of fuel in the engine. The specific thrust of certain ZhRD are given in Appendix I.

The specific impulse of RDTT, as a rule, is lower than for ZhRD. Its values in a vacuum for contemporary engines reach 250-300 kgf·s/kg or s (≈2500-3000 N·s/kg or m/s). Different values within the limits of the range shown are caused by the same factors as for ZhRD. Appendix II gives the specific pulses of certain foreign RDTT.

Along with mass specific thrust, which is called specific thrust for short, the idea of volumetric specific thrust is sometimes used, i.e., thrust referred to the volumetric expenditure of fuel per second:

$$P_{y\lambda} = \frac{P}{V}. \quad (3.14)$$

Obviously, volumetric specific thrust is connected with specific thrust by the simple relationship

$$P_{y\lambda} = P_{y\lambda} Q_r, \quad (3.15)$$

where  $Q_r$  — is the density of fuel.

### 3.2. Specific Impulse of Pressure in the Chamber

The specific pressure impulse in the chamber (the consumption unit) is the quantity

$$I_{p_k} = \frac{p_{kp}^* F_{kp}}{G}, \quad (3.16)$$

where  $p_{kp}^*$  is the pressure of braked flow in the critical section of the nozzle.

The numerator of this expression is an unbalanced force generated because of the gas pressure on a section of the front wall of the combustion chamber with area  $F_{kp}$  (Fig. 3.1). Force  $p_{kp}^* F_{kp}$  is the part of thrust created by the chamber. Referred to the per second expenditure of fuel in the chamber, it obtains the dimension of specific thrust. In this way the specific pressure impulse in the chamber is a component of the specific chamber thrust.

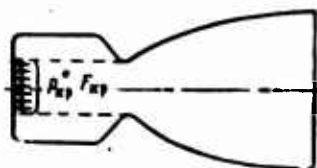


Fig. 3.1. Determination of thrust component  $p_{kp}^* F_{kp}$ .

In the ideal case, in the absence of irreversible phenomena in the subsonic part of the nozzle, the origin of force  $p_{\kappa p}^* F_{\kappa p}$  and its magnitude are not connected with the nozzle of the chamber and the conditions of its work. Such a force appears even in a combustion chamber with a simple aperture with area  $F_{\kappa p}$ , inasmuch as braking pressure, i.e.,

$$p_{\kappa}^* = p_{\kappa p}^*,$$

is constant, where  $p_{\kappa}^*$  is pressure of braked flow at the entrance to the nozzle.

This pertains to the component of specific thrust  $I_{p_{\kappa}}$ , which is its important feature.

For brevity we will subsequently call the consumption unit simply a unit, designating it  $\beta$ . When  $p_{\kappa}^* = p_{\kappa p}^*$ , the recording equivalent to expression (3.16), looks like this:

$$\beta = \frac{p_{\kappa}^* F_{\kappa p}}{G}. \quad (3.17)$$

The quantity  $\beta$  can be obtained by theoretical calculation, and also in experiment, inasmuch as all parameters entering it can be measured. A comparison of experimental values of  $\beta$  with theoretical ones can be used to estimate the degree of completion of processes in a section of combustion chamber.

### 3.3. Thrust Coefficient

Let us compare the thrust of chamber  $P$  and its component  $p_{\kappa}^* F_{\kappa p}$ . The relationship of these quantities is called thrust coefficient (thrust complex), designating  $K_p$ :

$$K_p = \frac{P}{p_{\kappa}^* F_{\kappa p}} \quad (3.18)$$

or, in the ideal case

$$K_p = \frac{P}{p_{kp} F_{kp}}.$$

As it appears, quantity  $K_p$  is unmeasurable and its physical meaning is clear: the thrust coefficient shows by how much chamber thrust exceeds the component acting on the front wall of the combustion chamber. It is obvious that the thrust coefficient can be defined as the ratio of the specific thrust of the chamber to its  $\beta$ :

$$K_p = \frac{P_{y1}}{\beta}. \quad (3.19)$$

The thrust coefficient is basically a nozzle characteristic. The relative contribution of the nozzle to the creation of specific thrust can be estimated by the quantity

$$\frac{P_{y1} - \beta}{P_{y1}} = 1 - \frac{1}{K_p}.$$

The greater  $K_p$ , the greater the role of the nozzle in the creation of specific thrust.

In contrast with complex  $\beta$ , determined uniquely, the thrust coefficient can take different values, depending on the dimensions of the nozzle and its mode of operation.

In accordance with the nomenclature of thrust the coefficients of thrust in a vacuum ( $p_h = 0$ ), in random nozzle mode ( $p_c \neq p_h$ ) and in the mode of equality of pressure ( $p_c = p_h$ ) differ.

Just as the magnitude of unit  $\beta$ , the magnitude of  $K_p$  can be determined theoretically and experimentally. A comparison of experimental values with the theoretical is useful for an analysis of completeness of processes in a real nozzle.

### 3.4. Specific Fuel Consumption

A characteristic of rocket-engine economy less commonly used than specific thrust is specific fuel consumption, i.e., the consumption of fuel necessary to obtain a unit of thrust in a unit of time. By definition, per second specific consumption of fuel is equal to

$$C_{ya} = \frac{G}{P} = \frac{1}{P_{ya}} \frac{\text{kg}}{\text{kgf} \cdot \text{s}}, \quad (3.20)$$

and the hourly, to

$$C_{ya} = \frac{3600}{P_{ya}} \frac{\text{kg}}{\text{kgf} \cdot \text{h}}, \quad (3.21)$$

As it appears, the amount of specific consumption of fuel is uniquely connected with the amount of specific thrust. This feature is characteristic only for rocket engines which do not use the environment.

In ZhRD, analogously to specific thrust, we distinguish specific consumption of fuel of the chamber and the engine.

When comparing the specific consumption of fuel of engines of various types, it is convenient to use specific fuel consumption per thrust power  $C_N$ . The quantity  $C_N$  is the relationship of the per second or hourly consumption of fuel to thrust power:

$$C_N = \frac{G}{N_p} \frac{\text{kg}}{\text{kW} \cdot \text{s}} \quad (3.22)$$

or

$$C_N = \frac{3600G}{N_p} \frac{\text{kg}}{\text{kW} \cdot \text{h}}. \quad (3.23)$$

It is also possible to evaluate fuel consumption per unit of jet power. Specific consumption in this case is determined thus:

$$C_{\bullet} = \frac{G}{N_{\bullet}} \frac{\text{kg}}{\text{kW} \cdot \text{s}} \quad (3.24)$$

or

$$C_{\bullet} = \frac{3600G}{N_{\bullet}} \frac{\text{kg}}{\text{kW} \cdot \text{h}}. \quad (3.25)$$

### 3.5. Specific Weight of the Engine

The specific weight of the engine is the ratio of engine weight in the working state (for a ZhRD filled with fuel components) to the thrust generated by it:

$$\gamma_{\text{дв}} = \frac{G_{\text{дв}}}{P_{\text{дв}}}. \quad (3.26)$$

For rocket engines of the first stage, weight pertains to thrust on earth; for the rest to thrust in a vacuum. The most commonly used dimension of specific weight of an engine is kg/T.

The quantity  $\gamma_{\text{дв}}$  to a known extent defines the design completeness of an engine. All things being equal, an engine with lower specific weight is preferred.

The specific weight of a ZhRD depends on the purpose and layout of the engine, the type of fuel being used and thrust. Figure 3.2 gives for orientation certain statistics on specific weight of ZhRD. The weight characteristics of ZhRD are considerably better than those of air-breathing jet engines.



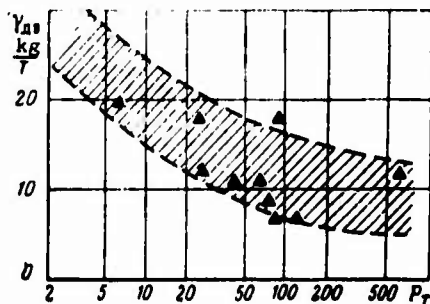


Fig. 3.2. Specific weight of some ZhRD.

Weight of RDTT is difficult to separate from the weight of the rocket on the whole. Therefore, usually the weight completeness of the whole rocket is usually evaluated. Indexes used in this case are considered in Chapters IV and XXVII.

#### Bibliography

1. "Aviatsiya i kosmonavtika," 1967, No. 12.
2. J. Spacecraft and Rockets, 1967, No. 12.
3. Space World, 1966, NN 3, 5.

## CHAPTER IV

### INTERCONNECTION OF ROCKET, ENGINE, AND FUEL PARAMETERS

This chapter considers the interconnection of the parameters of the rocket, the engine and the fuel used. The effect of engine indexes and of characteristics of fuel on the basic rocket parameters is evaluated.

#### 4.1. Connection Between the Engine and the Rocket Parameters

The most important parameters of a rocket are velocity, height and distance of flight with a definite payload. The determinant factor is the maximum velocity of rocket achieved by it at the moment of termination of the engine work (at the end of the powered flight segment).

The maximum increase in the velocity of the rocket during its flight outside the field of gravity and in the absence of aerodynamic resistance is determined by the Tsiolkovskiy formula:

$$\Delta V_{\max} = V_{\max} - V_0 = w_{\text{эф}} \ln \mu_k \quad (4.1)$$

where  $V_0$  is the initial velocity of the rocket;  $w_{\text{эф}}$  is effective exhaust velocity;  $\mu_k$  is the mass number of the rocket determined by the ratio of weights of the rocket at the moment of launching  $G_0$  and at the moment of termination of engine operation  $G_k$ :

$$\mu_k = G_0/G_k. \quad (4.2)$$

If the initial velocity of the rocket is zero, then equation (4.1) determines the so-called ideal (characteristic) velocity of the rocket

$$V_{ид} = w_{\phi} \ln \mu_k. \quad (4.3)$$

Since

$$w_{\phi} = P_{y\phi},$$

then

$$V_{ид} = P_{y\phi} \ln \mu_k. \quad (4.4)$$

In the presence of forces of gravity and of aerodynamic resistance, the velocity of the rocket at the end of powered flight will be less than ideal. This velocity is called final velocity; it is equal to

$$V_k = V_{ид} - \delta V_{з.г} - \delta V_{a.c.} \quad (4.5)$$

where  $\delta V_{з.г}$  denotes losses of velocity due to the earth's gravity;  $\delta V_{a.c.}$  denotes losses of velocity caused by the aerodynamic drag of the rocket.

For a multistage rocket the velocity of the last stage at the end of the powered segment is equal to the sum of  $\Delta V_k$  for each of the stages

(4.1)

$$V_k = \sum_{i=1}^n \Delta V_{ki},$$

moreover for the upper stages velocity losses caused by aerodynamic drag are insignificant and can be disregarded. Selection of rocket parameters which would provide maximum velocity  $V_k$  at assigned

launching weight or minimum launching weight at assigned final velocity  $V_k$  is in general very complex, and requires conducting joint ballistic and weight analysis. However, when the rocket parameters are known, the connection between the characteristics of the rocket stage and engine can easily be established. It is common both for a single-stage rocket and for a stage of multistage rocket.

Thus, the main factors which determine the value of ideal or final velocity, are specific thrust of engine and mass number of the rocket.

To illustrate the importance of an increase of  $P_{yA}$  let us give some examples. Figure 4.1 shows a change in the range of flight of a ballistic rocket with change in specific thrust of engine to  $1 \text{ kgf} \cdot \text{s/kg}$  ( $\frac{dL}{dP_{yA}}$ ). The effect of specific thrust increases with an increase in the range of flight. For an intercontinental ballistic missile with a flight range of 11,000 km and a specific thrust in a vacuum of 310  $\text{kgf} \cdot \text{s/kg}$ , increase in the range of flight with an increase of  $P_{yA}$  per unit is approximately 170 km, and with increase of  $P_{yA}$  1% it is more than 500 km. The effect of specific thrust is diminished with an increase of the absolute quantity of  $P_{yA}$ . With a fixed flying range  $L$ , an increase of  $P_{yA}$  allows increasing rocket payload.

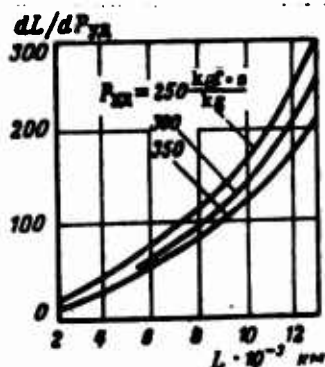


Fig. 4.1. Effect of change in specific thrust on flight range of a rocket.

For satellite launches rockets, an increase in the specific thrust means either an increase in altitude of orbit, or putting a greater payload into an assigned orbit. For the above rocket, a growth of specific thrust 1 kgf·s/kg leads to an increase of altitude of orbit from 550 to 600 km (i.e., almost 10%), or to an increase of payload of approximately 1.3%. At fixed distance (or height) or flight and weight of payload, an increase of  $P_{yA}$  provides a decrease of the take-off weight of the rocket.

The considerable effect of specific thrust on the characteristics of aircraft explains one of the basic trends of contemporary rocket-engine building - an increase of  $P_{yA}$ .

The relative effect of the mass number of the craft on ideal velocity can be established in the following manner. Let us record expression (4.4) in differential form:

$$dV_{IA} = \ln \mu_K dP_{yA} + P_{yA} \frac{d\mu_K}{\mu_K}.$$

Condition  $V_{IA} = \text{const}$  ( $dV_{IA} = 0$ ) corresponds to the equality of effects of specific thrust and mass number. In this case

$$\frac{d\mu_K}{\mu_K} = - \ln \mu_K \frac{dP_{yA}}{P_{yA}}. \quad (4.6)$$

Let relative change in specific thrust be 1% ( $dP_{yA}/P_{yA} = 0.01$ ), then the change in mass number equivalent to it will be

$$\frac{d\mu_K}{\mu_K} = -0.01 \ln \mu_K. \quad (4.7)$$

The minus sign shows that a decrease in specific thrust can be compensated by an increase in mass number, and vice versa.

Dependence (4.7) is given in Fig. 4.2. From it it follows only that at  $\mu_H < e$  ( $e$  is the base of natural logarithms) is the effect of mass number on ideal velocity more than the effect of specific thrust. When  $\mu_H > e$ , for 1% compensation of change in specific thrust a change in mass number of more than 1% is required.

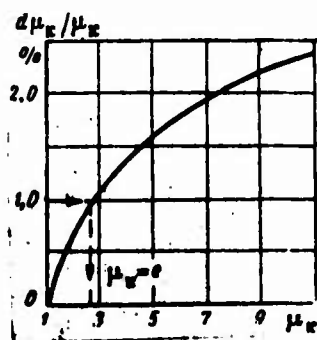


Fig. 4.2. Change in mass number of the craft, equivalent with respect to influence on ideal velocity to changing specific thrust 1%.

Figure 4.3 shows change in ideal velocity, depending on  $\mu_H$  at various values of specific thrust.

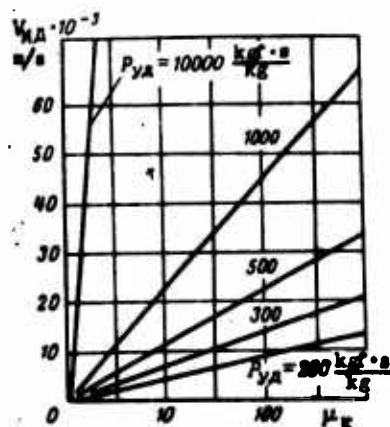


Fig. 4.3. Dependence of ideal velocity on mass number of the rocket at various values of  $P_{yA}$ .

The radical method of increasing mass number is by going to multistage systems. For an increase in the mass number of each stage, weight perfection of the design, including the engine, is necessary.

It is of interest to evaluate the effect of a change in weight of the engine on ideal velocity of craft.

Let us record the expression  $V_{ид} = P_{ya} \ln (G_0/G_k)$  in differential form for the case of constant fuel weight:

$$G_r = G_0 - G_k = \text{const.}$$

Then

$$\frac{dV_{ид}}{V_{ид}} = \frac{dP_{ya}}{P_{ya}} - \frac{dG_k}{G_k} \frac{G_0 - G_k}{G_0 \ln (G_0/G_k)}.$$

When  $V_{ид} = \text{const}$  we obtain

$$\frac{dG_k}{G_k} = \frac{G_0}{G_0 - G_k} \ln \frac{G_0}{G_k} \frac{dP_{ya}}{P_{ya}}$$

or

$$\frac{dG_k}{G_k} = \frac{\mu_k}{\mu_k - 1} \ln \mu_k \frac{dP_{ya}}{P_{ya}}. \quad (4.8)$$

Engine weight is part of the final weight of the craft; therefore,

$$dG_k = dG_{дв.}$$

Now expression (4.8) can be written thus:

$$\frac{dG_{дв.}}{G_{дв.}} = \frac{G_k}{G_{дв.}} \frac{\mu_k}{\mu_k - 1} \ln \mu_k \frac{dP_{ya}}{P_{ya}}. \quad (4.9)$$

Equation (4.9) determines the effect of a relative change of weight and specific thrust on ideal velocity. If the relative change in specific thrust is 1%, then the change in engine weight equivalent is equal to

$$\frac{dG_{\text{дв}}}{G_{\text{дв}}} = 0,01 \frac{G_{\text{к}}}{G_{\text{дв}}} \frac{\mu_{\text{к}}}{\mu_{\text{к}} - 1} \ln \mu_{\text{к}}. \quad (4.10)$$

Dependence (4.10) is given in Fig. 4.4. For the engine of the German V-2 rocket, the quantity  $dG_{\text{дв}}/G_{\text{дв}}$  is approximately 7.3% (point in Fig. 4.4). For contemporary practice, as a result of increased  $\mu_{\text{к}}$  and  $G_{\text{к}}/G_{\text{дв}}$ , this quantity can be evaluated at 10-15%. Consequently, reducing engine weight 10-15% in its effect on ideal velocity is equivalent to increasing specific thrust by 1%. The effect of engine weight is diminished with an increase of mass number  $\mu_{\text{к}}$ .

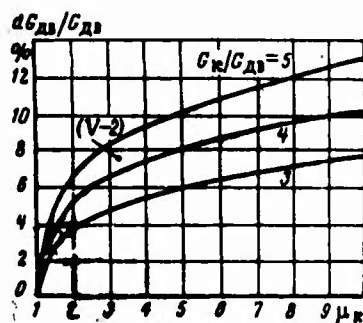


Fig. 4.4. A change in engine weight, equivalent in influence on ideal velocity to a 1% change in specific thrust.

Utilization of the weight equivalent of specific thrust is convenient during examination of the concrete design of the rocket and when selecting optimum engine parameters. Thus, if some measure is connected with an increase in specific thrust, and also with a simultaneous increase in engine weight, the expediency of such a measure can be evaluated on the basis of an equivalent. For example, the weight of an engine with a thrust of 100 t at a specific weight of 10 kg/t thrust is 1000 kg. At  $\mu_{\text{к}} = 5$  and a thrust-to-weight of ratio  $P/G_0 = 1.5$ , the weight equivalent of 1 kgf·s/kg of specific thrust at  $P_{\text{уд}} = 300$  kgf·s/kg is, according to formula (4.9), about 70 kg. If an increase in specific thrust of 1 kgf·s/kg is accompanied by a weight increase of 20 kg, then the effective increase is

$$\Delta P_{\text{уд}} = 1 - \frac{20}{70} \approx 0,7 \text{ kgf} \cdot \text{s/kg}.$$



#### 4.2. Effect of Fuel Characteristics on Rocket Characteristics

The most important characteristic of fuel is its specific thrust. It is possible to show, however, that not only it influences rocket characteristics.

Let us analyze the detailed relation between ideal velocity of craft, determined by expression (4.4), and fuel characteristics.

Let us convert the expression for  $\mu_k$ :

$$\mu_k = \frac{G_0}{G_k} = \frac{G_k + G_T}{G_k} = 1 + \frac{G_T}{G_k}. \quad (4.11)$$

The weight of propellant on the craft is

$$G_T = V_T \rho_T, \quad (4.12)$$

where  $V_T$  is volume of fuel;  $\rho_T$  is density of fuel.

Consequently:

$$\mu_k = 1 + \frac{V_T}{G_k} \rho_T \quad (4.13)$$

or

$$\mu_k = 1 + \sigma_k \rho_T, \quad (4.14)$$

where

$$\sigma_k = \frac{V_T}{G_k}. \quad (4.15)$$

The quantity  $\sigma_k$  characterizes the design perfection of the craft. The higher  $\sigma_k$ , the more fuel can be placed at the assigned final weight of the craft.

Now expression (4.4) ought to be written thus:

$$V_{\text{ид}} = P_{\text{yd}} \ln(1 + \sigma_{\text{к}} q_{\text{т}}). \quad (4.16)$$

As it appears, ideal velocity is a function of three parameters: specific thrust, fuel density, and coefficient  $\sigma_{\text{к}}$ . Thus, the second important characteristic of fuel is its density.

Obviously, an increase in  $\sigma_{\text{к}}$ , i.e., the increase in the relative content of fuel in the craft, always increases  $V_{\text{ид}}$ . However the rate of increase in  $V_{\text{ид}}$  with an increase in  $\sigma_{\text{к}}$  is unequal for various fuels. Of this one can be certain, having differentiated the equation (4.16) with respect to  $\sigma_{\text{к}}$ :

$$\frac{\partial V_{\text{ид}}}{\partial \sigma_{\text{к}}} = P_{\text{yd}} \frac{q_{\text{т}}}{1 + \sigma_{\text{к}} q_{\text{т}}}. \quad (4.17)$$

Expression (4.17) shows that with an increase in  $\sigma_{\text{к}}$  the effect of fuel density is diminished. The rate of increase of  $V_{\text{ид}}$  is more considerable for fuels which have high specific thrust. In connection with this, results of utilization of two fuels can be different at different  $\sigma_{\text{к}}$ . An example of dependence  $V_{\text{ид}} = f(\sigma_{\text{к}})$  for certain fuels is given in Fig. 4.5.

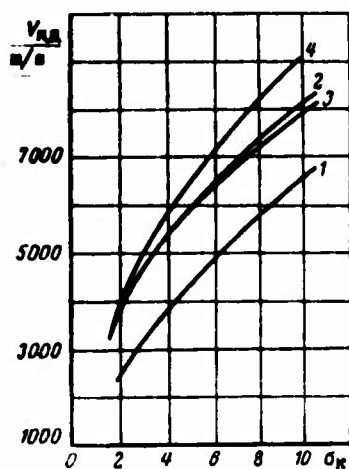


Fig. 4.5. The dependence of ideal velocity on coefficient  $\sigma_{\text{к}}$ : 1 - liquid oxygen + liquid hydrogen; 2 - liquid oxygen + kerosene; 3 -  $\text{N}_2\text{O}_4$  + asymmetrical dimethylhydrazine; 4 - liquid fluorine + liquid hydrogen.

#### 4.3. Rating the Efficiency of a Fuel

Having explained the fundamental effect of specific thrust and density of fuel on ideal velocity of craft, let us show how to compare the efficiency of various fuels, using  $V_{ид}$  as a criterion.

Two characteristic cases of rocket design are usually considered [3].

1. Final weight of apparatus  $G_H$  and volume of fuel  $V_T$  are considered.

In this case  $\sigma_H$  is also constant.

Let us write expression (4.16) in differential form:

$$dV_{ид} = \ln \frac{G_0}{G_K} dP_{y\lambda} + P_{y\lambda} \frac{G_K}{G_0} \frac{V_T}{G_K} dQ_T. \quad (4.18)$$

Maximum  $V_{ид}$  corresponds to condition  $dV_{ид} = 0$ . In this case, from expression (4.18) we obtain

$$\frac{dP_{y\lambda}}{P_{y\lambda}} + \frac{G_T/G_0}{\ln(G_0/G_K)} \frac{dQ_T}{Q_T} = 0. \quad (4.19)$$

The quantity  $G_T/G_0$  is the specific gravity of the fuel stored on the craft:

$$G_T/G_0 = \Lambda. \quad (4.20)$$

It is easy to find the connection between the number  $\mu_H$  and by the quantity  $\Lambda$ :

$$\mu_K = \frac{G_0}{G_K} = \frac{1}{1 - \Lambda}. \quad (4.21)$$

By substituting expression (4.21) in equation (4.19), we obtain

$$\frac{dP_{yA}}{P_{yA}} + \frac{\Lambda}{\ln \frac{1}{1-\Lambda}} \frac{dQ_T}{Q_T} = 0. \quad (4.22)$$

Having designated

$$\frac{\Lambda}{\ln \frac{1}{1-\Lambda}} = c, \quad (4.23)$$

Let us record

$$\frac{dP_{yA}}{P_{yA}} + c \frac{dQ_T}{Q_T} = 0 \quad (4.24)$$

or

$$d \ln P_{yA} + c d \ln Q_T = 0.$$

The quantity  $c$  entering this expression weakly changes with a change in  $Q_T$ . If it is assumed to be constant and equal to a certain average value in the considered range, then we can record this as a result of integration of the last expression:

$$P_{yA} Q_T^c = \text{const.} \quad (4.25)$$

Maximum  $V_{\text{нД}}$  corresponds to maximum product  $P_{yA} Q_T^c$  in which characteristic  $c$  is determined by formula (4.23).

The dependence of  $c$  on  $\Lambda$  is shown in Fig. 4.6. As it appears, with increase in  $\Lambda$  characteristic  $c$  is diminished. Thus, for instance, when  $\Lambda = 0.2$   $c \approx 0.9$  and for determination of maximum  $V_{\text{нД}}$  maximum of expression  $P_{yA} Q_T^{0.9}$  must be sought. When  $\Lambda = 0.8$   $c \approx 0.5$  and then the maximum magnitude of  $P_{yA} Q_T^{0.5}$  is found. A decrease in characteristic

$c$  means a decrease in the effect of fuel density on ideal velocity  $V_{ид}$ . At small  $\Lambda$ , characteristic for boosters and first stages of rockets, the effect of fuel density is commensurate with the effect of specific thrust. At  $\Lambda \rightarrow 0$   $c \rightarrow 1$ , which gives a basis in this instance for comparing the efficiency of various fuels with respect to the quantity  $P_{уд}Q_T$ , i.e., with respect to volumetric specific thrust. For rockets with low  $\Lambda$  (and, consequently, with low  $V_{ид}$ ) in case of limited volume of fuel  $V_T$  and final weight  $G_K$  heavy fuels are better.

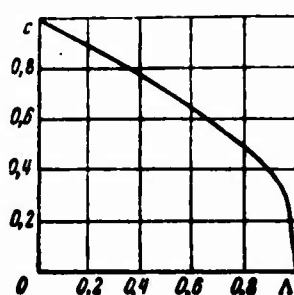


Fig. 4.6. Dependence of characteristic  $c$  on relative content of fuel.

As an example also illustrating the error from the assumption that  $c = \text{const}$ , accepted when obtaining expression (4.25), let us examine a selection of the optimum relationship of components of oxidant and fuel  $\kappa$  for fuel  $O_2 + H_2$ . Let us assume as constant the weight of design elements and the volume of the tanks, so that at a certain ratio of components  $\mu_K = 3.0$ . Figure 4.7 shows a change in  $Q_T$ ,  $\mu_K$ , and  $c$  from  $\kappa$ . Figure 4.8 shows a change in theoretical specific thrust of fuel, ideal velocity of rocket  $V_{ид}$  and product  $P_{уд}Q_T$  calculated for two cases:

for  $c$ , variable in accordance with Fig. 4.7 and constant  $c = 0.6$ . From an examination of the curve in Fig. 4.8, it is evident that the maximum ideal velocity is substantially displaced to the right in comparison with maximum  $V_{уд}$ . Its positions, found by  $V_{ид}$  and the product  $P_{уд}Q_T$  under the condition that  $c = \text{const}$  match, i.e., the error allowed in deriving formula (4.25) is small.

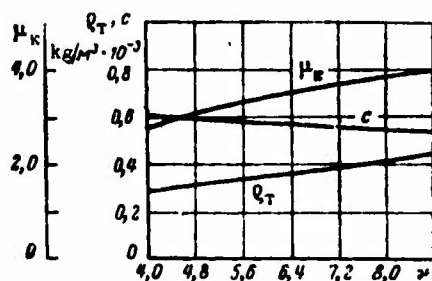


Fig. 4.7. Change of  $q_T$ ,  $\mu_k$  and characteristic  $c$ , depending upon the relationship between oxidant and fuel for fuel  $H_2 + O_2$ .

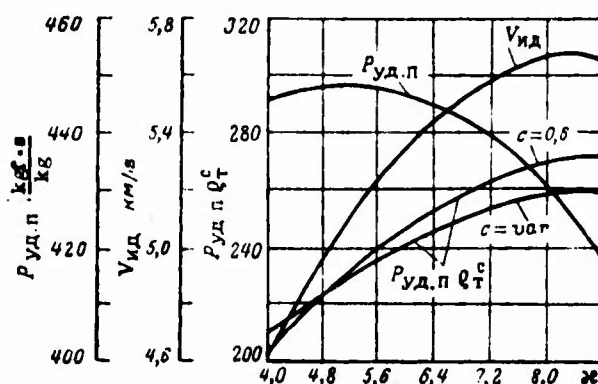


Fig. 4.8. A change of  $P_{уд.п}$ ,  $V_{ид}$  and magnitude of  $P_{уд.п} q_T^c$  when  $c = var$  on Fig. 4.7 as well as when  $c = 0.6$ , depending on  $\kappa$  for fuel  $H_2 + O_2$  ( $p_k/p_c = 30/0.1$ ).

2. The launch weight of craft  $G_0$  and part of the weight of the empty craft  $G_{k1}$  are considered assigned and constant.

Weight  $G_{k1}$  consists of weight of payload and weight of structure of craft, which does not depend on the type of fuel. The second part of the weight of the empty craft  $G_{k2}$  is considered proportional to the volume of fuel  $V_T$ , which in this instance is variable. Quantity  $G_{k2}$  can be written in the following manner:

$$G_{k2} = \frac{G_{k2}}{V_T} V_T.$$

Having designated

$$\frac{V_{\tau}}{G_{K2}} = \sigma_{K2},$$

we obtain

$$G_{K2} = \frac{G_{\tau}}{\sigma_{K2} Q_{\tau}}.$$

Since

$$Q_{\tau} = G_0 - G_K = G_0 - G_{K1} - G_{K2},$$

then

$$G_{K2} = \frac{G_0 - G_{K1} - G_{K2}}{\sigma_{K2} Q_{\tau}},$$

whence

$$G_{K2} = \frac{G_0 - G_{K1}}{1 + \sigma_{K2} Q_{\tau}}$$

or

$$G_{K2} = \frac{\frac{G_0 - G_{K1}}{\sigma_{K2} Q_{\tau}}}{1 + \frac{1}{\sigma_{K2} Q_{\tau}}}. \quad (4.26)$$

The value

$$\frac{1}{\sigma_{K2} Q_{\tau}} = \frac{G_{K2}}{G_{\tau}}$$

usually does not exceed 0.15 and can be disregarded. Then

$$G_{k2} \approx \frac{G_0 - G_{k1}}{a_{k2} Q_T}. \quad (4.27)$$

Let us determine the change of  $V_{нД}$ , caused by a change of fuel. Writing the differential of expression

$$V_{нД} = P_{YA} \ln \frac{G_0}{G_K}$$

considering  $G_0 = \text{const}$ , we obtain

$$dV_{нД} = \ln \frac{G_0}{G_K} dP_{YA} - P_{YA} \frac{dG_K}{G_K}. \quad (4.28)$$

If  $dV_{нД} = 0$ , then

$$\frac{dP_{YA}}{P_{YA}} = \frac{dG_K}{G_K \ln \frac{G_0}{G_K}}. \quad (4.29)$$

Since

$$G_K = G_{K1} + G_{K2} \quad \text{and} \quad G_{K1} = \text{const},$$

then

$$dG_K = dG_{K2}.$$

On the basis of expression (4.27) it is possible to write

$$dG_{K2} = - \frac{G_0 - G_{K1}}{a_{K2} Q_T} \frac{dQ_T}{Q_T} = - G_{K2} \frac{dQ_T}{Q_T}. \quad (4.30)$$



Substituting expression (4.30) in equality (4.29), we obtain

$$\frac{dP_{yA}}{P_{yA}} + \frac{\frac{G_{K2}}{G_K}}{\ln \frac{G_0}{G_K}} \frac{dQ_T}{Q_T} = 0. \quad (4.31)$$

By analogy with the previous variant (4.22), it may be concluded that dependence (4.31) answers the expression

$$P_{yA} Q_T^c = \text{const},$$

where

$$c = \frac{\frac{G_{K2}}{G_K}}{\ln \frac{G_0}{G_K}} = \frac{\frac{G_{K2}}{G_K}}{\ln \mu_K}. \quad (4.32)$$

Consequently, in this instance finding the maximum of  $V_{нд}$  boils down to a determination of the maximum of  $P_{yA} Q_T^c$ , but with a new value of characteristic  $c$ . The dependence (4.32), determining the value of  $c$ , is given in Fig. 4.9. For single-stage ballistic projectiles and the upper stages of rockets  $\mu_K \geq 5$ , and  $G_{K2}/G_K \leq 0.5$ ; in this case the values of  $c$  are small and less than in the preceding case. This means that if the volume of fuel is not limited, the effect of fuel density on  $V_{нд}$  is diminished. This explains the recommendations to use fuels, although light, with a high specific thrust, for example, liquid hydrogen with liquid oxygen.

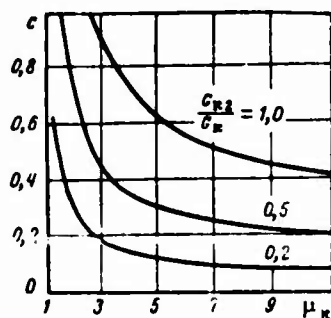


Fig. 4.9. Dependence of characteristic  $c$  on mass number and relative weight  $G_{K2}/G_K$ .

After determining characteristic  $c$  for any of the variants of design, the optimum fuel is selected, comparing the quantities of  $P_{\text{max}}$ , proportional to the values of  $V_{\text{нд}}$ . The maximum corresponds to the most effective fuel.

#### Bibliography

1. Glushko V. P., Zhidkoye toplivo dlya reaktivnykh dvigateley (Liquid fuel for jet engines), ch. I, VVIA, im. Zhukovskogo, 1936.
2. Issledovaniye raketnykh dvigateley na zhidkom toplive, (Investigation of liquid-propellant rocket engines), Collection of translations, izd-vo "Mir," 1964.
3. Henry I. G., J. of the British Interplanetary Society, 1960, No. 10.

P A R T    I I

GENERAL METHODS OF CALCULATION

FIRST SECTION

Theoretical Thermodynamic Characteristics

## CHAPTER V

### COMPOSITION AND TOTAL ENTHALPY OF PROPELLANT

In the chapter there is shown how to reduce data characterizing the composition and total enthalpy of propellant to the form applied in thermodynamic calculation. With known composition of propellant its density is determined.

#### 5.1. Equivalent Formula

Propellant can be monopropellant (monofuel), bipropellant and multipropellant. In all cases it is the most convenient to represent propellant by an equivalent formula, which is usually written on some conditional (equivalent) molecular weight  $\mu_g$ . If the propellant consists of  $m$  chemical elements, then its equivalent formula is written so:

$$A_{b_{1r}}^{(1)} A_{b_{2r}}^{(2)} A_{b_{3r}}^{(3)} \dots A_{b_{mr}}^{(m)} \quad (5.1)$$

[Translators note:  $r$  = propellant,  $e$  = equivalent]

where  $A^{(l)}$  - symbol of  $l$ -th chemical element;  $b_{lr}$  - quantity of atoms of  $l$ -th chemical element in the equivalent formula.

The molecular weight of propellant, specified by equivalent formula, is calculated so:

$$\mu_r = \sum_{l=1}^m \mu_l b_{lr} \quad (5.2)$$

where  $\mu_l$  - atomic weight of chemical element  $A^{(l)}$ .

## 5.2. Composition of Component

The propellant component can be an individual substance or a mixture of such substances. The composition of component is also rationally specified by equivalent formula of the type (5.1):

$$A_{b1k}^{(1)} A_{b2k}^{(2)} A_{b3k}^{(3)} \dots A_{bmk}^{(m)} \quad (5.3)$$

[Translators note:  $k$  = component.]

with molecular weight

$$\mu_k = \sum_{i=1}^m b_{ik} \mu_i. \quad (5.4)$$

Let us examine some characteristic cases of writing the equivalent formula of component.

1. Component - individual substance. In this instance the formula of component is usually known in the form (5.3), for example,  $C_2H_6N_2$ ,  $N_2H_4$ ,  $H_2$ ,  $O_2$ ,  $F_2$ , and the molecular weight is determined according to expression (5.4). Frequently the original formula leads to conditional molecular weight  $\mu_3$ . Then the numbers of atoms are found by formula

$$b_{i3} = \frac{b_{ik} \mu_k}{\mu_i}. \quad (5.5)$$

2. Component has been assigned by elementary weight composition. If  $g_i$  - weight fraction of  $i$ -th chemical element in the component, then the number of atoms of this element in the equivalent formula with molecular weight  $\mu_3$  comprises

$$b_{i3} = \frac{\mu_3 g_i}{\mu_i}. \quad (5.6)$$

3. Component - mixture of the several substances. In component  $r$  of substances:  $n$  substance is recorded by formula

$$A_{b1n}^{(1)} A_{b2n}^{(2)} \dots A_{bmn}^{(m)}$$

with molecular weight  $\mu_n$  and comprises weight fraction  $g_n$ .

The quantity of moles of  $n$ -th substance in the component

$$n_n = \frac{\mu_n g_n}{\mu_n} \quad (5.7)$$

Then the quantity of atoms of  $i$ -th chemical element in the component will be

$$b_{ik} = \sum_{n=1}^r b_{in} n_n \quad (5.8)$$

### 5.3. Composition of Bipropellant

Bipropellant is a characteristic type of liquid rocket propellant consisting of fuel and oxidizer.

#### Component Ratio, Excess Oxidant Ratio

Fuel and oxidizer of bipropellant are in a definite ratio. In order to guarantee thorough combustion of one mole of fuel, there is required  $\kappa_0'$  moles of oxidizer. The amount of  $\kappa_0'$  with dimension mole ox/mole  $r$  is called molar stoichiometric coefficient of the component ratios of propellant. Stoichiometric component ratios of propellant, expressed in units of weight,  $\kappa_0$  is called weight stoichiometric coefficient; dimension of  $\kappa_0$  - kg ox/kg  $r$ .  
[Translators note: ox = oxidizer,  $r$  = fuel.]

It is obvious that

$$\kappa_0 = \kappa_0' \frac{\mu_{ox}}{\mu_r} \quad (5.9)$$

In practice the component ratio in liquid propellant is selected most frequently not stoichiometric, but something different from it - real ( $\kappa'$  or  $\kappa$ ). The degree of difference of the real component ratio of propellant from stoichiometric is evaluated by excess oxidant ratio  $\alpha$ , which is determined by formula

$$\alpha = \frac{\kappa'}{\kappa_0} = \frac{\kappa}{\kappa_0}. \quad (5.10)$$

As can be seen,  $\alpha$  is a relative dimensionless quantity. With stoichiometric ratio of fuel and oxidizer coefficient  $\alpha$  is equal to one. With deficiency of oxidizer as opposed to its theoretically necessary quantity, which is frequently observed in liquid-fuel rocket engine propellants,  $\alpha < 1$ .

The magnitude of  $\alpha$  is usually assigned, therefore for determination of the real component ratio  $\kappa'$  it is required to find the value of magnitude  $\kappa_0'$ . The most convenient and common is determination of the molar stoichiometric coefficient  $\kappa_0'$  by formula

$$\kappa_0' = - \frac{\sum_{i=1}^n b_{ir} v_i}{\sum_{i=1}^n b_{iox} v_i} \frac{\text{mole ox}}{\text{mole r}}, \quad (5.11)$$

where  $v_i$  - valence of  $i$ -th chemical element;  $b_{ir}$ ,  $b_{iox}$  - number of atoms of  $i$ -th element.

In this case in accordance with formula (5.3) fuel and oxidizer must be recorded in the form:

$$A_{r1}^{(1)} A_{r2}^{(2)} A_{r3}^{(3)} \dots A_{rn}^{(n)},$$

$$A_{ox1}^{(1)} A_{ox2}^{(2)} A_{ox3}^{(3)} \dots A_{oxm}^{(m)}.$$

The numerator of expression (5.11) represents the algebraic sum of the highest valences in fuel, the denominator - in oxidizer, moreover the valences are taken with signs assigned to them. Listed below are valences of basic chemical elements, present in the composition of rocket propellants.



Element	H	Li	K	Na	Be	Mg	B	Al	C	Si	P	S	N	F	Cl	Br	O
Valence	1	1	1	1	2	2	3	3	4	4	5	4	0	-1	-1	-1	-2

With known values of  $\alpha$  and  $\kappa_0'$  it is possible to formulate the formula of conditional mole of bipropellant. The quantity of atoms of  $i$ -th chemical element in conditional mole is equal to

$$b_{i\tau} = b_{i\tau} + \alpha \kappa_0' b_{i\text{ок}}, \quad (5.12)$$

and molecular weight

$$\mu_\tau = \mu_\tau + \alpha \kappa_0' \mu_{\text{ок}}. \quad (5.13)$$

#### Excess Oxidizing Element Ratio

Excess oxidizing element ratio  $\alpha_3$  is used along with excess oxidant ratio and is the ratio of total quantity of oxidizing elements if propellant to their total stoichiometric quantity:

$$\alpha_3 = - \frac{\sum_r^{(-)}}{\sum_r^{(+)}} ,$$

where  $\sum_r^{(-)}$  - sum of products of  $b_{i\tau} v_i$  for elements with electronegative valence ( $v_i < 0$ ) in propellant;  $\sum_r^{(+)}$  - sum of products of  $b_{i\tau} v_i$  for elements with electropositive valence ( $v_i > 0$ ) in propellant.

For liquid-fuel rocket engine bipropellant with known values of  $\alpha$  and  $\kappa_0'$  the formula for  $\alpha_3$  can be represented in the form

$$\alpha_3 = - \frac{\sum_r^{(-)} + \alpha \kappa_0' \sum_{\text{ок}}^{(-)}}{\sum_r^{(+)} + \alpha \kappa_0' \sum_{\text{ок}}^{(+)}} , \quad (5.14)$$

where  $\sum_r^{(-)}$  - sum of products of  $b_{ir}v_i$  for oxidizing elements (with electronegative valence) in fuel;  $\sum_r^{(+)}$  - sum of products of  $b_{ir}v_i$  for combustible elements (with electropositive valence) in fuel. The meaning of sums of  $\sum_{ox}^{(-)}$ ,  $\sum_{ox}^{(+)}$  for oxidizer is analogous. For simplicity of writing expression (5.14) let us introduce designations

$$\alpha_{r,z} = \frac{\sum_r^{(+)} + \sum_r^{(-)}}{\sum_r^{(+)}}, \quad 0 \leq \alpha_{r,z} \leq 1, \quad (5.15)$$

$$\alpha_{ox,z} = \frac{\sum_{ox}^{(+)} + \sum_{ox}^{(-)}}{\sum_{ox}^{(+)}}, \quad 0 \leq \alpha_{ox,z} \leq 1, \quad (5.16)$$

[Translators note:  $r.z$  = combustible element,  $ox.z$  = oxidizing element.]

which represent the ratios of unreplaced (free) valences to the overall number of corresponding valences. With allowance for the introduced designations, formula (5.14) is reduced to

$$\alpha_z = \frac{\alpha_{r,z} + \alpha_{ox,z}(1 - \alpha_{r,z})}{\alpha_{ox,z} + \alpha_{r,z}(1 - \alpha_{ox,z})}. \quad (5.17)$$

Let us determine, for example, the value of  $\alpha_z$  for propellant  $B_2H_6 + H_2O_2$  with excess oxidant ratio  $\alpha = 0.5$ . In accordance with formulas (5.15) and (5.16)  $\alpha_{r,z} = 1.0$  and  $\alpha_{ox,z} = 0.5$ . By formula (5.17), we obtain  $\alpha_z = 0.66$ .

As can be seen, generally  $\alpha_z \neq \alpha$ ; these quantities coincide only when  $\alpha_{r,z} = \alpha_{ox,z} = 1.0$ .

#### 5.4. Composition of Multipropellant

If multipropellant (for example, solid) is specified by weight fractions of components, then the equivalent formula of such propellant is the same as for compound component [formulas (5.7) and (5.8)].

If the equivalent formulas of all components result in the same conditional molecular weight  $\mu_3$ , then

$$n_k = \frac{\mu_3 g_k}{\mu_3} = g_k$$

and the quantity of atoms of i-th chemical element in propellant will be

$$b_{ii} = \sum_{k=1}^i b_{ik} g_k \quad (5.18)$$

In this instance the molecular weight of propellant  $\mu_T$  is equal to conditional molecular weight  $\mu_3$ .

In case of liquid bipropellant, the molecular weight of which is assigned by formula (5.13),  $\mu_T \neq \mu_3$ , if even  $\mu_T = \mu_{OK} = \mu_3$ . This is directly evident from formula (5.13).

#### 5.5. Density of Propellant

With known composition of propellant it is easy to determine its density.

The average density of propellant  $\rho_T$ , consisting of n components with weight fractions  $g_n$ , can be determined having assumed the additivity of volumes of separate components:

$$\frac{1}{\rho_T} = \sum_{n=1}^n \frac{g_n}{\rho_n}$$

Hence the average density of propellant is equal to:

$$\rho_T = \frac{1}{\sum_{n=1}^n \frac{g_n}{\rho_n}} \quad (5.19)$$

where  $\rho_n$  - density of component n.

In case of liquid bipropellant the weight fractions of fuel and oxidizer will be:

$$g_r = \frac{1}{1 + \alpha x_0} \quad (5.20)$$

$$g_{ox} = \frac{\alpha x_0}{1 + \alpha x_0} \quad (5.21)$$

By substituting them in equation (5.19), we obtain a formula for the average density of liquid bipropellant:

$$\rho_r = \frac{1 + \alpha x_0}{\frac{1}{\rho_r} + \frac{\alpha x_0}{\rho_{ox}}} \text{ kg/m}^3, \quad (5.22)$$

where  $\rho_r$ ,  $\rho_{ox}$  - densities of fuel and oxidizer.

#### 5.6. Total Enthalpy of Propellant

##### System of Indicating Total Enthalpy

During thermodynamic investigation of the processes in a rocket engine along with physical heat content (enthalpy) of propellant its chemical energy must be considered. For this the idea of total enthalpy is used, the introduction of which is based on the following considerations.

The magnitudes of enthalpy of gases and solid substances at 0°K are not equal to zero and cannot be measured or computed. Therefore, theoretical calculations for gases, measurements of thermal capacity and heat of phase and polymorphic transformations for substances in condensed state permit finding only the difference of enthalpy of a substance at a given temperature as well as at any other (for example, 0°K):

$$H_T^0 - H_0^0 = \int_0^T C_p^0 dT + \sum \Delta H^{(i)}, \quad (5.23)$$

where  $\Delta H^{(i)}$  - heats of phase and polymorphic transformations.

Chemical energy, being dissipated or absorbed in the reaction, is the difference of energy levels of initial and final substances of the reaction. Usually several initial substances take part in the reaction and several products are obtained. Chemical energy, strictly speaking, pertains to the entire system of substances taking part in the reaction, however, it can be conditionally referred to one of them.

As the basis for determination of the numerical value of chemical energy there is the value of heat of formation  $\Delta H_{fT}$ . Heat of formation - this is the amount of heat which is dissipated ( $-\Delta H_{fT}$ ) or absorbed ( $+\Delta H_{fT}$ ) with the formation of a unit of mass of substance. If the reaction of formation of substance is carried out at constant pressure, and then the temperature of reaction products is brought to a certain temperature T, then on the basis of the law of conservation of energy it is possible to write

$$\Delta H_{fT} = X + [(H_T^0 - H_0^0)_{\text{prod}} - (H_T^0 - H_0^0)_{\text{ncx}}], \quad (5.24)$$

[Translators note: прод = product, нсх = initial.]

where X - chemical energy, the value of which is determined only by the structure of molecules or atoms of initial and final substances, and therefore it depends neither on the temperature, nor on pressure. It is obvious that when  $T = 0^\circ\text{K}$  the magnitude of  $X = \Delta H_{f0}$ .

Heat of formation  $\Delta H_{fT}$  is not unique until it is stipulated in which chemical (atomic, molecular) and phase (liquid, solid substance, gas) state the initial elements, used in the reaction of formation, have been taken.

It is convenient to determine the heat  $\Delta H_{fT}$  with formation of the substance from elements in standard state, i.e., in steady and most widespread natural state. Standard elements are gaseous  $\text{H}_2$ ,  $\text{O}_2$ ,  $\text{N}_2$ ,  $\text{F}_2$ ,  $\text{Cl}_2$  and others, hard carbon C ( $\beta$  - graphite) and metals.

Heat of formation of substances from standard elements, determined under standard conditions  $p = 1.02 \text{ bar}$  (1 atm),  $T_0 = 293.15^\circ\text{K}$ , is called the standard heat of formation and is designated  $\Delta H_{f,293.15}^0$ .

Usually it is accepted that the enthalpy of standard elements, their standard heat of formation and chemical energy when  $p = 1.02 \text{ bar}$  and  $T = 293.15^\circ\text{K}$  are equal to zero. In such a case the magnitude of  $(H_{293.15}^0 - H_0^0)_{\text{ex}}$  in formula (5.24) is equal to zero. Using this, equation (5.24) can be reduced to

$$\Delta H_{f,293}^0 + H_T^0 - H_{293}^0 = X + H_T^0 - H_0^0. \quad (5.25)$$

The sum of values of enthalpies  $(H_T^0 - H_0^0)$  and chemical energy of the substance is called total enthalpy  $I_T^0$ :

$$I_T^0 = \Delta H_{f,293}^0 + H_T^0 - H_{293}^0 \quad (5.26)$$

or, in accordance with equality (5.23),

$$I_T^0 = \Delta H_{f,293}^0 + \int_{293}^T C_p^0 dT + \sum \Delta H^{(i)}. \quad (5.27)$$

For liquid and solid substances, if their thermal capacity is taken constant:

$$H_T^0 - H_{293}^0 = C(T - 293) + \sum \Delta H^{(i)}. \quad (5.28)$$

Thus, total enthalpy of the substance according to formula (5.27) is equal to its heat of formation from standard elements at temperature  $T^\circ\text{K}$ .

Magnitudes of standard heats of formation<sup>1</sup>  $\Delta H_{f,293}^0$ , heats of phase and polymorphic transformations  $\Delta H^{(i)}$  and thermal capacities  $C$  of solid and liquid substances are determined experimentally. The thermal capacities of gases  $C_p^0$  are usually computed [2].

<sup>1</sup>In chemistry literature magnitudes of heats of formation  $\Delta H_{f,293}^0$  are sometimes allowed with sign opposite that accepted here.

The described system of indication of total enthalpy is presently generally accepted in our country. There are other systems which use another temperature zone reference and other substances in standard state.

If in various systems of indication there are used the same reliable data on thermodynamic functions  $I^0$ ,  $S^0$ ,  $C_p^0$  and heats of formation, then calculations with utilization of any of these systems must lead to identical results.

#### Total Enthalpy of Components

If the propellant component is an individual substance, or has been specified by elementary composition, then its total enthalpy is determined by formula (5.27). With supply of component into the chamber under standard conditions ( $T = 293.15^\circ\text{K}$ ) its total enthalpy in accordance with expression (5.27) is equal to the standard heat of formation.

For simplicity of writing subsequent formulas let us subsequently everywhere omit index T in the symbol of total enthalpy, designating the relationship to temperature.

Working formulas for enthalpy of component are written so:  
at temperature T

$$I_k = \Delta H_{f293}^0 + \int_{293}^T C_p^0 dT + \sum \Delta H^{(1)}; \quad (5.29)$$

at temperature T -  $293.15^\circ\text{K}$

$$I_k = \Delta H_{f293}^0, \quad (5.30)$$

where units of measurement of quantities are such:  $C_p^0$  kJ/kg·deg;  
 $I_k$ ,  $\Delta H_{f293}^0$  and  $\Delta H^{(1)}$  in kJ/kg.

If the component is a mixture of  $n$  different chemical compounds, assigned by weight fractions  $g_m$ , then its total weight enthalpy should be determined by formula:

$$I_k = \sum_{m=1}^n g_m I_m - \sum g_{m \text{ pacTB}} Q_{m \text{ pacTB}} \tag{5.31}$$

where  $I_m$  – total enthalpy of  $m$ -th substance in kJ/kg;  $g_{m \text{ pacTB}}$  – weight fraction of substance  $m$ , dissolving in compound component;  $Q_{m \text{ pacTB}}$  – heat of dissolution of 1 kg of substance in compound solvent in kJ/kg.

Value of total enthalpy of component per mole is determined so:

$$I_{\mu_k} = I_k \mu_k \text{ kJ/kmole.} \tag{5.32}$$

Magnitudes of enthalpy of certain components of rocket propellants are listed in Table 5.1.

Table 5.1. Total enthalpy of certain components of rocket propellants.

Component	Formula	I kJ/kg
Fuel		
Hydrogen	H <sub>2</sub>	–3828
Ammonia	NH <sub>3</sub>	–4180
Diethylamine	(C <sub>2</sub> H <sub>5</sub> ) <sub>2</sub> NH	–1725
Triethylamine	(C <sub>2</sub> H <sub>5</sub> ) <sub>3</sub> N	–610
Aniline	C <sub>6</sub> H <sub>5</sub> NH <sub>2</sub>	380
Hydrazine	N <sub>2</sub> H <sub>4</sub>	1573
Monomethylhydrazine	H <sub>2</sub> N – NHCH <sub>3</sub>	1222
Unsymmetrical Dimethylhydrazine	H <sub>2</sub> N – N (CH <sub>3</sub> ) <sub>2</sub>	774
Aerosine —50	50% H <sub>2</sub> N – N (CH <sub>3</sub> ) <sub>2</sub> + 50% N <sub>2</sub> H <sub>4</sub>	1173
Xylidine	C <sub>6</sub> H <sub>3</sub> (CH <sub>3</sub> ) <sub>2</sub> NH <sub>2</sub>	–291
Methyl alcohol	CH <sub>3</sub> OH	–7440
Ethyl alcohol	C <sub>2</sub> H <sub>5</sub> OH	–6025
Methane	CH <sub>4</sub>	–5439
Kerosene	C <sub>7.21</sub> H <sub>13.29</sub>	–1728
Diborane	B <sub>2</sub> H <sub>6</sub>	438
Pentaborane	B <sub>5</sub> H <sub>9</sub>	381
Aluminum	Al	0
Beryllium	Be	0
Lithium	Li	0
Aluminum hydride	AlH <sub>3</sub>	–380.7
Lithium hydride	LiH	–11380



Table 5.1 (Cont'd).

Component	Formula	I kJ/kg
Oxidizers		
Oxygen	O <sub>2</sub>	-398
Ozone	O <sub>3</sub>	2606
Fluorine	F <sub>2</sub>	-335
Chlorine trifluoride	ClF <sub>3</sub>	-2000
Nitrogen trifluoride	NF <sub>3</sub>	-2050
Perchloryl fluoride	FClO <sub>3</sub>	-398
Nitric acid	HNO <sub>3</sub>	-2753
Hydrogen peroxide	H <sub>2</sub> O <sub>2</sub>	-5530
Nitrogen tetroxide	N <sub>2</sub> O <sub>4</sub>	-209
Bromine pentafluoride	Br F <sub>5</sub>	-2625
Chloric acid	HClO <sub>4</sub>	-460
Fluoric oxide	OF <sub>2</sub>	222
Ammonium nitrate	NH <sub>4</sub> NO <sub>3</sub>	-4564
Ammonium perchlorate	NH <sub>4</sub> ClO <sub>4</sub>	-2520
Lithium perchlorate	Li ClO <sub>4</sub>	-3576
Nitronium perchlorate	NO <sub>2</sub> ClO <sub>4</sub>	230
Tetranitromethane	C (NO <sub>2</sub> ) <sub>4</sub>	189

Notes. 1. Data are listed for substances of 100% concentration.

2. Values of total enthalpy are given at  $t_{\text{кнп}}$  for low-boiling substances and at 293°K for the remaining.

### Total Enthalpy of Multipropellant

Total enthalpy of compound propellant, the composition of which includes several components, is calculated in accordance with formula (5.31).

Total enthalpy of one conditional mole of liquid bipropellant is determined by formula:

$$I_{\mu\tau} = I_{\mu r} + \alpha x'_0 I_{\mu ox} \quad \text{kJ/kmole} \quad (5.33)$$

where  $I_{\mu\tau}$ ,  $I_{\mu r}$ ,  $I_{\mu ox}$  - total enthalpies of 1 mole of propellant, fuel and oxidizer respectively in kJ/kmole.

If the total enthalpy on 1 kg of propellant must be determined, then we use obvious relationship

$$I_r = \frac{I_{\mu r}}{\mu_r} \text{ kJ/kg.} \quad (5.34)$$

For bipropellant the total enthalpy of one kg comprises

$$I_r = \frac{I_{\mu r} + \alpha x_0' \mu_{OK}}{\mu_r + \alpha x_0' \mu_{OK}}. \quad (5.35)$$

Between the total enthalpy of propellant and its calorific value there is a unique connection, namely:

$$H_H = I_{r, T=293} - I_{\text{prod, crop, } T=293} = (\Delta H_{f293}^0)_r - (\Delta H_{f293}^0)_{\text{prod, crop}}, \quad (5.36)$$

where  $(\Delta H_{f293}^0)_{\text{prod, crop}}$  - standard heat of combustion products.

Formula (5.36) can be applied for determination of the total enthalpy of propellant according to its calorific value. The value of the latter should be known at constant pressure and corresponding phase composition of combustion products.

#### Bibliography

1. Vanichev A. P., Termodinamicheskiy raschet goreniya i istecheniya v oblasti vysokikh temperatur (Thermodynamic calculation of combustion and outflow in the high-temperature range). BNT, 1947.
2. Gurvich L. V. et al., Termodinamicheskiye svoystva individual'nykh veshchestv (Thermodynamic properties of individual substances), Spravochnik, AN SSSR, 1962.
3. Termicheskiye konstanty veshchestv. Spravochnik (Thermal constants of substances, Reference book), AN SSSR, 1965.
4. Kit B., Evered D. S., Rocket Propellant Handbook, New York 1960.

CH A P T E R VI

EQUILIBRIUM COMPOSITION OF COMBUSTION PRODUCTS

In this chapter are examined methods of determination of the equilibrium composition of combustion products and its logarithmic partial derivatives. Temperature and pressure (or volume) of the mixture are assumed assigned.

As it is known, the state of the working medium in any section of the rocket engine chamber is determined by some values of temperature and pressure (volume). Their particular magnitudes are determined during thermodynamic calculation. Determination of equilibrium composition at assigned  $p$  and  $T$  (or  $v$ ) is the basis of such calculation.

6.1. Preliminary Information

The working medium, taking part in processes at high temperature, is generally a multicomponent mixture of gases and condensed (solid or liquid) substances. The mixture, consisting only of gases, is called homogenous, mixture of gases and condensed substances - heterogeneous. The gas components of the mixture are usually fully or partially dissociated and, possibly ionized.

As it is known, the intensity of dissociation and ionization is determined basically by the temperature and pressure. In the combustion chamber of a rocket engine operating on chemical fuel at pressure from one to hundreds of bar the temperature can be

within 2000-5000 'K. Under these conditions with considerable dissociation the ionization of combustion products of propellants, not containing easily ionized substances, is unessential. In nonchemical rocket engines a higher level of temperatures is possible, and consequently, noticeable ionization.

For determination of the composition of multicomponent reacting mixture generally it is necessary to know the mechanism and kinetics of proceeding reactions. If the rates of forward and reverse reaction are sufficiently great and identical, then the mixture can be considered being in chemical equilibrium. The composition of mixture, determined under the assumption of chemical equilibrium, is called equilibrium. It is usually characterized by numbers of moles of components of mixture  $n_q$  or by partial pressures (for ideal gases)  $p_q$ . There are used relative quantities: molar or weight fractions.

For calculation of equilibrium composition it is necessary to formulate and solve a system of equations of chemical equilibrium.

#### 6.2. System of Equations for Determination of the Equilibrium Composition at p, T = const or v, T = const

In the majority of practically interesting cases the equilibrium composition must be determined at constant (assigned) temperature and pressure or temperature and volume.

The chemical equilibrium is calculated usually with some simplifying assumptions. The necessity of their introduction is determined by requirements of sufficient simplicity of calculation and by the contemporary standard of knowledge about processes in reacting mixtures. Below are given basic assumptions, in most cases providing acceptable description of the processes at high temperature.

For homogenous dissociated mixture it is assumed that it consists of ideal components. Their thermodynamic functions  $I^0$ ,  $E^0$ ,  $S^0$  and, consequently, thermal capacity  $C_p^0$ ,  $C_v^0$  and constants of equilibrium  $K_p$  do not depend on pressure. Equation of state of ideal gas is applicable to separate gases and to the mixture on the whole.

During calculation of ionized working medium there is not considered the coulomb interaction of charged particles. Products of ionization are also considered ideal gases.

Finally, during calculation of heterogeneous mixture there is introduced the assumption about the presence of temperature equilibrium between condensate and gas ( $T_c = T_g$ ) and the presence of phase equilibrium, i.e., partial pressure of gas phase of condensed product is assumed equal to pressure of saturated vapor for this product and depends only on the temperature.

The latter simultaneously means that condensed products will not form solutions and alloys. The volume of condensed substances is neglected, their thermodynamic functions are considered depending only on the temperature.

The system of equations of chemical equilibrium at  $p$ ,  $T = \text{const}$  for a dissociated mixture consists of equations of dissociation, equations of conservation of substance and equations of Dalton law.

If the propellant consists of  $m$  chemical elements,  $m$  atomic and  $l$  molecular components can be present in products of reactions. The number  $l$  should include all the substance formed from  $m$  chemical elements, which has the necessary information (thermodynamic functions in the necessary temperature range).

Formula of  $j$ -th molecular component of the mixture can generally be written so:

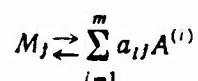
$$A_{a_{1j}}^{(1)} A_{a_{2j}}^{(2)} \dots A_{a_{ij}}^{(i)} \dots A_{a_{mj}}^{(m)},$$

where  $a_{ij}$  - number of atoms of  $i$ -th chemical element in component  $j$ .

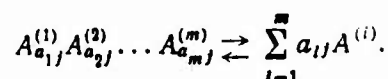
Let us now write equations of chemical equilibrium, beginning from the simplest case, when the products are a homogenous dissociated mixture.

#### Homogenous Dissociated Products

It is the simplest, most convenient and uniform to consider dissociation of all molecular components only into atoms. Dissociation of  $j$ -th molecular component should be written so:



or



If  $j = 1, 2, \dots, l$ , then these equations describe dissociation of all molecular components.

For the state of chemical equilibrium it is possible to write the equality of chemical potentials:

$$\varphi_j = \sum_i a_{ij} \varphi_i, \quad j=1, 2, 3, \dots, l. \quad (6.1)$$

According to determination of chemical potential

$$\varphi_j = \left( \frac{\partial Z}{\partial n_j} \right)_{p, T, n_q}, \quad q \neq j.$$

Here  $Z$  - thermodynamic potential of gas mixture, equal to

$$Z = \sum_q n_q Z_q,$$

where  $n_q$  - number of moles of  $q$ -th component in the mixture;  $q = l + m$  - overall number of components in the mixture.

Thus:

$$\varphi_j = \frac{\partial}{\partial n_j} \left( \sum_q n_q Z_q \right)_{p, T, n_q}, \quad q \neq j.$$

Consequently, for a mixture of ideal gases

$$\varphi_j = Z_j = I_j^0 - TS_j. \quad (6.2)$$

Now equation (6.1) can be written so:

$$I_j^0 - TS_j = \sum_i a_{ij} (I_i^0 - TS_i), \quad j=1, 2, 3, \dots, l.$$

Since

$$S_q = S_q^0 - R_0 \ln p_q,$$

where  $S_q^0$  - standard entropy;  $R_0$  - universal gas constant,

then

$$I_j^0 - T(S_j^0 - R_0 \ln p_j) = \sum_i a_{ij} [I_i^0 - T(S_i^0 - R_0 \ln p_i)].$$

After conversions we obtain

$$\ln p_j - \sum_i a_{ij} \ln p_i + \ln K_j = 0, \quad (6.3)$$

where  $p_1, p_j$  - partial pressures, and the magnitude of

$$\ln K_j = \frac{\sum_i a_{ij} S_i^0 - S_j^0}{R_0} - \frac{\sum_i a_{ij} I_i^0 - I_j^0}{R_0 T} = f(T) \quad (6.4)$$

is the logarithm of equilibrium constant with respect to partial pressures for the reaction of dissociation of j-th component to atoms.

Group of equations (6.3) in quantity  $l$  is the logarithmic form of equations of dissociation. The use of  $\ln p_q$  as unknowns makes it possible not to fear their disappearance during calculations for any values of determining parameters  $p$  and  $T$ , and also excludes the possibility of appearance of negative values of  $p_q$  in the process of calculation, not having physical meaning.

Equations of conservation of substance express the condition of equality of the quantity of atoms of  $i$ -th chemical element in propellant and in dissociated products. When writing these equations there is introduced magnitude  $M_i$  - number of moles of propellant, which is determined by the condition of equality of total the quantity of moles of  $N$  dissociated products to total pressure:

$$N = \sum_i n_i = \sum_i p_i = p. \quad (6.5)$$

Since for ideal gases there is valid relationship

$$x_i = \frac{p_i}{p} = \frac{n_i}{N},$$

the introduction of number  $M_i$  is responsible for equality

$$n_i = p_i. \quad (6.6)$$

Here  $N = \sum_i n_i$  - total number of moles of gaseous products in the mixture;  $p = \sum_i p_i$  - overall pressure of gas mixture.

After introduction of new unknown - magnitude  $M_i$  the equations of conservation of substance should be written so:

$$\sum_j a_{ij} n_j + n_i = M_i b_i, \quad i = 1, 2, 3, \dots, m; \quad j = 1, 2, 3, \dots, l.$$

The right side of the equation expresses the quantity of atoms of  $i$ -th element in the propellant (working medium), left - the quantity of atoms of this element in the products of dissociation.



Let us write the equations in logarithmic form:

$$\ln \left( \sum_i a_i \nu_i + a_i \right) - \ln M_i - \ln h_i = 0 \quad (6.7)$$

The quantity of equations of conservation of substance comprises  $m$ .

Equation of Dalton law has usual form:

$$\sum_i p_i = p$$

and in logarithmic form

$$\ln \sum_i p_i - \ln p = 0. \quad (6.8)$$

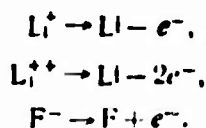
System of equations (6.3), (6.7), (6.8) describes the chemical equilibrium of homogenous dissociated mixture at fixed  $p$  and  $T$ . The system is closed, since for determination of  $l + m + 1$  unknowns ( $\ln p_i$  in quantity  $l + m$  and  $\ln M_i$ ) there are  $(l + m + 1)$  equations.

#### Homogenous Ionized Products

The algorithm of writing equations for products, in which besides dissociations reactions there proceed ionizations reactions, is practically unchanged.

Ionization reactions are written according to the scheme in which positive or negative ions are considered as molecular components, and atoms and electronic gas as atomic.

For example:



In this instance for each ionization reaction the equation can be written in the same form as for dissociation reaction (6.3). The expression of equilibrium constant for ionization reaction retains the form (6.4).

Equations of conservation of substance and Dalton law are written in usual form (6.7) and (6.8).

An additional specific equation for ionized mixture is the equation of conservation of charge (electroneutrality of the system). It has the form:

$$\sum_q a_{eq} n_q = 0, \quad q=1, 2, 3, \dots, l+m+1, \quad (6.9)$$

where  $a_{eq}$  - number of electrons acquired or lost by the component (multiplicity of ionization of component  $q$ ). For a neutral atom or molecule  $a_{eq} = 0$ , for positive ions  $a_{eq}$  - negative, for negative ions  $a_{eq}$  - positive.

For electronic gas  $q = l + m + 1$  and  $a_{eq} = 1$ . In case of single ionization, for example,  $a_{eq} = \pm 1$ .

Logarithmization of equation (6.9) is not performed in connection with the fact that values of  $\sum_q a_{eq} n_q$  can be negative until the solution is reached.

System of equations (6.3), (6.7), (6.8), (6.9) describes the chemical equilibrium of homogenous dissociated and ionized products of dissociation. In the system  $(l + m + 2)$  are unknowns, namely:  $l$  logarithms of partial pressures of molecules and ions,  $m + 1$  logarithms of partial pressures of atoms and electronic gas and logarithm of number  $M_T$ . There are so many equations that, consequently, the system is closed.

## Heterogeneous Dissociated Products

As was mentioned, with the presence of condensed components in the mixture their partial pressures are assumed equal to pressures of saturated vapor of condensed substances. The amount of pressure of saturated vapor can be found from the condition of equality of thermodynamic potential of the same substance in gas and condensed phases:

$$Z_{qz} = Z_{qs}$$

or

$$I_{qz}^0 - TS_{qz}^0 = I_{qs}^0 - T(S_{qs}^0 - R_0 \ln p_q^n),$$

whence

$$\ln p_q^n = \frac{S_{qs}^0 - S_{qz}^0}{R_0} - \frac{I_{qs}^0 - I_{qz}^0}{R_0 T}. \quad (6.10)$$

With earlier formulated assumptions the value of  $p_q^H$  for the given substance depends only on the temperature.

For simplicity let us assume that in the considered heterogeneous system substances  $r$  ( $j = r$ ;  $q = r$ ) and  $s$  ( $1 = s$ ,  $q = l + s$ ) are condensed. Partial pressures of these components can be written so:

$$p_{1-s} = p_s = p_s^n; \quad p_{j-r} = p_r = p_r^n.$$

At fixed temperature they are known.

Equations of dissociation (1-1) of uncondensed substances will preserve the earlier obtained form (6.3), in this case  $j \neq r$ .

In equations of conservation of substance the numbers of moles of condensed substances  $n_{rz}$  and  $n_{sz}$ , being new unknowns must be present. Equations will take the form:



$$\ln \left( \sum_i a_i n_i + n_l + a_l n_{rz} + \delta_{ls} n_{sz} \right) - \ln M_T - \ln b_{lT} = 0, \quad (6.11)$$

where  $\delta_{ls} = 1$  when  $l = s$ ;  $\delta_{ls} = 0$  when  $l \neq s$ .

Equation of Dalton law keeps the previous form (6.8).

It remains to write the equation of dissociation of gas phase of the condensed substance. By applying equation (6.3) to molecule  $i$ , we obtain:

$$\ln p_i - \sum_l a_{li} \ln p_l + \ln K_i = 0. \quad (6.12)$$

In equations (6.3), (6.8), (6.11), (6.12) the knowns at stated temperature are magnitudes  $\ln p_r^H$ ,  $\ln p_s^H$ , and also constants of equilibrium  $K_r$ ,  $K_s$ .

System of equations (6.3), (6.8), (6.11), (6.12) describes the chemical equilibrium of heterogeneous mixture. The unknowns in it are  $l+m-2$  of logarithms of partial pressures (excluding  $\ln p_r^H$  and  $\ln p_s^H$ ),  $\ln M_T$  and numbers of moles of condensed substances  $n_{rz}$  and  $n_{sz}$ , in all  $l+m+1$ . The number of equations comprise  $(l-1)+m+1+1$ , i.e., system is closed.

#### Equation of Constancy of Volume

In many instances the process in a dissociated system proceeds at constant volume or under conditions close to this. For description of the processes in reacting mixture at  $T$ ,  $v = \text{const}$  the equation of Dalton law should be substituted by an equation expressing condition of constancy of volume.

Let us assume the mass of propellant (working substance)  $M$  and volume  $V$ , in which the process proceeds, is specified. Density of reaction products comprises

$$\rho = \frac{M}{V}.$$

Let us now replace the condition of constancy of volume at assigned mass by the condition of constancy of density equivalent to it. If calculation is by  $M_1$  of moles of propellant, then the mass comprises  $\nu_1 M_1$  kg, and the volume, according to equation of state, when  $p = N$  is equal to  $R_0 T$ . Then

$$v = \frac{p_1 M_1}{R_0 T}$$

In logarithmic form it is possible to write:

$$\ln M_1 - \ln T + \ln D = 0, \quad (6.13)$$

where

$$D = \frac{p_1}{R_0 T}$$

Thus, the state of reacting system at assigned temperature and density is described by system of equations (6.3), (6.11), (6.12), (6.13).

Examination of the listed forms of writing equations of chemical equilibrium for dissociated and ionized, homogenous and heterogeneous mixtures shows that in all cases the form of writing is identical. If for initial we take recording of equations for a homogenous mixture, then the recording for other variants is a small modification of initial.

The considered method of writing equations provides an account of any quantity of dissociated and ionized gaseous products, and also atomic and molecular condensed substances (in this case their gaseous phase is considered).

From the general system of equations written for propellants (working media), containing all  $m$  atoms, it is easy to change to systems of equations for particular cases, when those separate from atoms are absent. For this, from the number of unknowns there are excluded the absent atomic products and those of molecular, whose composition includes these atoms. From the system of equations there

are excluded equations of dissociation, pertaining to excluded molecules, and equations of conservation of substance for absent atoms. The remaining equations retain their previous form.

### 6.3. Method of Solution of System of Equations

From a mathematical point of view the system of equations of chemical equilibrium is a system of nonlinear algebraic equations. In many instances, when the number of components of dissociated and ionized mixture being considered includes all possible components, for which the necessary information is available (thermodynamic functions in the necessary temperature range), the system can consist of several tens of equations. The complexity and work input of solution of such systems are widely known. At present the system of equations of chemical equilibrium is usually solved by an electronic computer. The most effective method of solving such systems is the Newton method.

For solution of the system of equations of form

$$f_k(x_q) = 0, \quad q, k = 1, 2, 3, \dots, n$$

each function  $f_k(x_q)$  is written through initial (approximate) values of roots  $x_q^0$  and corrections to them  $\Delta x_q$  and is decomposed into Taylor series according in powers not higher than the first:

$$f_k(x_q^0 + \Delta x_q) = f_k(x_q^0) + \sum_{q=1}^n \left( \frac{\partial f_k}{\partial x_q} \right)^0 \Delta x_q + \dots = 0.$$

Having designated

$$f_k(x_q^0) = b_k^{(0)},$$

we obtain

$$\sum_{q=1}^n \left( \frac{\partial f_k}{\partial x_q} \right)^0 \Delta x_q = -b_k^{(0)}.$$



The last expression is a writing of the system of equations, linear relative to unknowns-corrections  $\Delta x_q$ .

Thus, system of nonlinear algebraic equations relative to  $x_q$  is reduced to a system of linear equations relative to  $\Delta x_q$ . Its solution gives values of corrections  $\Delta x_q$ . To get values of unknowns  $x_q$  with the necessary accuracy there is necessary repeated successive finding of corrections  $\Delta x_q$  by solution of a system written in more general form:

$$\sum_{q=1}^n \left( \frac{\partial f_k}{\partial x_q} \right)^{(r-1)} \Delta x_q^{(r)} = -\delta_k^{(r-1)}, \quad (6.14)$$

where  $r$  - number of approximation ( $r = 1, 2, 3, \dots$ ).

Refinement of approximate values of unknowns is accomplished by formula:

$$x_q^{(r)} = x_q^{(r-1)} + \Delta x_q^{(r)}. \quad (6.15)$$

Approximations are continued until achievement of the specified accuracy, i.e., until satisfaction of condition

$$\sum_{k=1}^n |\delta_k| \leq \omega, \quad (6.16)$$

where  $|\delta_k|$  - modulus of value  $\delta_k$ ;  $\omega$  - small quantity assigned in advance.

To ensure convergence of successive approximations when it is not guaranteed by Newton method in usual form, a special method is applied. The method uses the following idea: convergence of successive approximations from arbitrary initial values of unknowns can be guaranteed if expansion of approximate solution into Taylor series is applied at partial intervals of the function.

Let us assume for some function  $f(x) = 0$  there is zero approximation

$$f(x^0) = y^{(0)}.$$

We will seek correction  $\Delta x_1$ , which does not turn the function to zero, but only reduces  $y^{(0)}$  to magnitude  $a$ :

$$f(x^0 + \Delta x_1) = y^{(0)} - a.$$

To this equation let us apply the Newton method. Decomposition into Taylor series gives

$$f(x^0) + \left(\frac{\partial f}{\partial x}\right)^0 \Delta x_1 = y^{(0)} - a.$$

Since

$$f(x^0) = y^{(0)},$$

then

$$\left(\frac{\partial f}{\partial x}\right)^0 \Delta x_1 = -a$$

and

$$\Delta x_1 = -\frac{a}{\left(\frac{\partial f}{\partial x}\right)^0}.$$

With utilization of the Newton method in usual form the correction comprised

$$\Delta x = -\frac{y^{(0)}}{\left(\frac{\partial f}{\partial x}\right)^0}.$$

Consequently:

$$\Delta x_1 = \frac{a}{y^{(0)}} \Delta x = \sigma \Delta x, \quad (6.17)$$

where  $\sigma$  - step coefficient  $0 < \sigma < 1$ .



With utilization of step coefficient  $\sigma$  the refinement of unknowns from approximation to approximation is produced by formula

$$x_q^{(n)} = x_q^{(n-1)} + \sigma \Delta x_q^{(n-1)}. \quad (6.18)$$

The introduction of step coefficient can slow down the convergence of the process of successive approximations, but in most cases guarantees it with arbitrary assignment of initial values of unknowns.

Determination of the magnitude of  $\sigma$  with solution of systems of equations of chemical equilibrium will be examined below.

#### 6.4. Calculation of Equilibrium Composition at p, T = const or v, T = const

##### Homogenous Mixture

For calculation of the equilibrium composition of homogenous dissociated mixture it is necessary to apply the Newton method to system of equations (6.3), (6.7), (6.8), in which the unknowns are  $\ln p_q$  and  $\ln M_r$ . This gives a system of linear equations:

$$\sum_q \left( \frac{\partial f_k}{\partial \ln p_q} \right) \Delta \ln p_q + \left( \frac{\partial f_k}{\partial \ln M_r} \right) \Delta \ln M_r = -b_k, \\ k=1, 2, 3, \dots, l+m+1$$

or

$$\sum_q \left( \frac{\partial f_k}{\partial \ln p_q} \right) \Delta_q + \left( \frac{\partial f_k}{\partial \ln M_r} \right) \Delta_M = -b_k,$$

where there are briefly designated:

$$\Delta_q = \Delta \ln p_q, \\ \Delta_M = \Delta \ln M_r.$$

Refinement of unknowns is by formulas:

$$\begin{aligned}\ln p_q^{(r)} &= \ln p_q^{(r-1)} + \Delta_q^{(r)}, \\ \ln M_i^{(r)} &= \ln M_i^{(r-1)} + \Delta_M^{(r)}.\end{aligned}$$

In further writing the numeration of approximations are omitted for simplicity.

Linearized equations take the following form.

Equations of dissociation:

$$\Delta_j - \sum_i a_{ij} \Delta_i = -\delta_j, \quad j=1, 2, 3, \dots, L, \quad (6.19)$$

where

$$\delta_j = \ln p_j - \sum_i a_{ij} \ln p_i + \ln K_j.$$

Equations of conservation of substance:

$$\sum_j a_{ij} n_j \Delta_j + n_i \Delta_i - B_i \Delta_M = -\delta_i B_i, \quad (6.20)$$

where

$$\begin{aligned}B_i &= \sum_j a_{ij} n_j + n_i; \\ \delta_i &= \ln B_i - \ln M_T - \ln b_i.\end{aligned}$$

Equation of Dalton law

$$\sum_q p_q \Delta_q = -\delta_p p_z, \quad (6.21)$$

where

$$\begin{aligned}p_z &= \sum_q p_q, \\ \delta_p &= \ln p_z - \ln p.\end{aligned}$$

If calculation is performed at assigned density (volume), then instead of equation of Dalton law there is used equation (6.13). Relative to corrections it is written, so:

$$\Delta_M = -\delta_0, \quad (6.22)$$

where

$$\delta_0 = \ln M_T - \ln T + \ln D.$$

Expressions (6.19), (6.20), (6.21) or (6.22) represent a system of equations, linear relative to corrections  $\Delta_q$  and  $\Delta_M$ .

Let us write down the augmented matrix of coefficients with corrections and absolute terms of equations (6.19), (6.20), (6.21). For simplification of the solution let us determine a definite sequence of arrangement of columns and lines of the matrix, namely:

Columns:

- 1) corrections pertaining to molecular products;
- 2) corrections pertaining to atomic products;
- 3) correction to number  $M_T$ ;
- 4) absolute terms of equations.

Lines:

- 1) equations of dissociation in the same sequence as molecular products in columns;
- 2) equations of conservation of substance in the same sequence as atomic products in columns;
- 3) equation of Dalton law.

Augmented matrix for calculation of the equilibrium composition of a homogenous dissociated mixture at  $p, T = \text{const}$  are listed on page 120.

As can be seen, this matrix can be broken down into cells in the following manner:

$$\begin{bmatrix} E & e_1 \\ e_2 & e_3 \end{bmatrix},$$

where  $E$  - unit matrix, order of which is equal to the quantity of molecular products. The presence of a unit matrix is governed by the sequence of arrangement of lines and columns of the matrix listed above and permits substantially simplifying the solution of the system of linear equations. By applying a compact scheme of the method of successive exclusion to the matrix, broken down into cells, there can be excluded unknowns pertaining to molecular components, having obtained matrix

$$[e_4] = [e_3] - [e_2][e_1].$$

Solution of the system of linear equations with matrix of coefficients  $[e_4]$  gives values of corrections  $\Delta_1$  and  $\Delta_m$ . Corrections pertaining to molecular components are determined on the basis of expression (6.19):

$$\Delta_j = \sum_i a_{ij} \Delta_i - b_j, \quad j = 1, 2, 3, \dots, l. \quad (6.23)$$

Let us illustrate the effectiveness of obtaining the unit matrix and exclusion of unknowns of corrections to molecular components thanks to this. During calculation of compound propellant, consisting, for example, of 8 atoms ( $m = 8$ ), in the combustion products there can be present about 100 molecular components ( $l = 100$ ). The total amount of unknowns  $l + m + 1 = 100 + 8 + 1 = 109$ ; for finding them generally a system of 109 equations must be solved. By the above-described conversion matrix  $[e_4]$  of only the 9th order in all can be obtained. Thus, instead of solving a system of 109 equations we solve a system of 9 equations, which many times reduces the time of solution and considerably simplifies it.

Matrix of coefficients of system of linear equations,  
homogenous mixture

$$\begin{array}{c} \text{Absolute Terms} \\ \text{[Composition } (\partial \ln f / \partial \ln T)_p \text{ } (\partial \ln f / \partial \ln p)_T \text{]} \end{array}$$

1	0	0	..	0	-a <sub>11</sub>	-a <sub>21</sub>	..	-a <sub>m1</sub>	0	-b <sub>1</sub>	-K <sub>1</sub> '	0
0	1	0	..	0	-a <sub>12</sub>	-a <sub>22</sub>	..	-a <sub>m2</sub>	0	-b <sub>2</sub>	-K <sub>2</sub> '	0
0	0	0	1	..	-a <sub>13</sub>	-a <sub>23</sub>	..	-a <sub>m3</sub>	0	-b <sub>3</sub>	-K <sub>3</sub> '	0
:	:	:	:	:	:	:	:	:	:	:	:	:
0	0	0	0	1	-a <sub>1n</sub>	-a <sub>2n</sub>	..	-a <sub>mn</sub>	0	-b <sub>n</sub>	-K <sub>n</sub> '	0
<hr/>												
a <sub>11</sub> n <sub>1</sub>	a <sub>12</sub> n <sub>2</sub>	a <sub>13</sub> n <sub>3</sub>	..	a <sub>1n</sub> n <sub>n</sub>	n <sub>A1</sub>	0	..	0	-b <sub>1</sub>	-b <sub>A1</sub>	b <sub>1</sub>	0
a <sub>21</sub> n <sub>1</sub>	a <sub>22</sub> n <sub>2</sub>	a <sub>23</sub> n <sub>3</sub>	..	a <sub>2n</sub> n <sub>n</sub>	0	n <sub>A2</sub>	..	0	-b <sub>2</sub>	-b <sub>A2</sub>	b <sub>2</sub>	0
:	:	:	:	:	:	:	:	:	:	:	:	:
a <sub>m1</sub> n <sub>1</sub>	a <sub>m2</sub> n <sub>2</sub>	a <sub>m3</sub> n <sub>3</sub>	..	a <sub>mn</sub> n <sub>n</sub>	0	0	..	n <sub>Am</sub>	-b <sub>m</sub>	-b <sub>Am</sub>	b <sub>m</sub>	0
p <sub>1</sub>	p <sub>2</sub>	p <sub>3</sub>	..	p <sub>n</sub>	p <sub>A1</sub>	p <sub>A2</sub>	..	p <sub>Am</sub>	0	-b <sub>p</sub>	p <sub>p</sub>	p <sub>p</sub>

After finding the corrections the unknowns are refined by formulas (6.15) or (6.18). For utilization of formula (6.18) the coefficient of step  $\sigma$  must be determined. General expression for it is written so:

$$\sigma = \frac{nc}{\sum_{k=1}^n |\delta_k|},$$

where  $n$  - number of equations of the system;  $c$  - some empirical quantity;  $|\delta_k|$  - moduli of errors in equations of the system.

In connection with the fact that errors for molecular products are expressed in equations of dissociation through errors of atomic, when determining  $\sigma$  one should take into account only the errors of equations of conservation of substance and Dalton law. In this case  $\sigma$  should be determined by formula

$$\sigma = \frac{(m+1)c}{|\delta_p| + \sum_i |\delta_i|}. \quad (6.24)$$

On the basis of mass calculations of chemical equilibrium of a wide range of propellants it is recommended to take  $c = 0.1-0.5$ .

The practice of mass calculations showed at the same time that the proposed algorithm of writing the system of equations and the logarithmic form of unknowns in many instances provides the solution of the system even when  $\sigma = 1$ . Values of  $\sigma < 1$ , determined by formula (6.24), are only sometimes applied.

Refinement of approximate values of unknowns is finished with achievement of the specified accuracy of solution. Estimation of the latter is by formula

$$\sum_j |\delta_j| + \sum_i |\delta_i| + |\delta_p| \leq \omega. \quad (6.25)$$

Usually it is sufficient to establish  $\omega = 10^{-4}$ .



For homogenous ionized mixture the equations of dissociation and ionization, written relative to corrections, have working form (6.19), equations of conservation of substance - form (6.20) and equations of Dalton law - form (6.21). In accordance with the Newton method let us convert the equation of electroneutrality (6.9), specific for ionized mixture. It takes the form:

$$\sum_q a_{eq} n_q \Delta_i = -\delta_{e-}, \quad q=1, 2, 3, \dots, l+m+1, \quad (6.26)$$

where

$$\delta_{e-} = \sum_q a_{eq} n_q.$$

Equations (6.19)-(6.21), (6.26) will form a system of equations, linear relative to corrections  $\Delta_q$  and  $\Delta_m$ . The technology of solution of this system is similar to that described above.

#### Heterogeneous Mixture

During calculation of the equilibrium composition of heterogeneous mixture to get a system of equations, linear relative to corrections, it is necessary to apply the Newton method to system of equations (6.3), (6.11), (6.8), (6.12).

By analogy with the previous, from equation (6.3) we obtain linearized equations of dissociation of uncondensed substances:

$$\Delta_j - \sum_i' a_{ij} \Delta_i = -\delta_j, \quad j=1, 2, 3, \dots, l, \quad j \neq r, \quad (6.27)$$

where

$$\delta_j = \ln p_j - \sum_i a_{ij} \ln p_i + \ln K_j.$$

The prime at the sign of the sum in equation (6.27) means that summation is not performed on condensed products. This is understandable since differentiation of known (constant at given temperature) quantities of partial pressure of saturated vapor of condensate gives zero.

From equation (6.11) we obtain linearized equations of conservation of substance:

$$\sum_j' a_{ij} n_j \Delta_j + (1 - \delta_{is}) n_i \Delta_i + \delta_{is} n_{ss} \Delta_{ss} + a_{ir} n_{rs} \Delta_{rs} - B_i \Delta_M = -\delta_i B_i, \quad (6.28)$$

where

$$B_i = \sum_j a_{ij} n_j + \delta_{is} n_{ss} + a_{ir} n_{rs} + n_i, \\ \delta_i = \ln B_i - \ln M_r - \ln b_{ir}.$$

Linearized equation of Dalton law is obtained from equation (6.8):

$$\sum_q' p_q \Delta_q = -\delta_p p_s, \quad (6.29)$$

where

$$p_s = \sum_q p_q, \\ \delta_p = \ln p_s - \ln p.$$

Finally, from relationship (6.12) we obtain linearized equation of dissociation of gas phase of condensed substance:

$$\sum_i' a_{ir} \Delta_i = \delta_r, \quad (6.30)$$

where

$$\delta_r = \ln p_r - \sum_i a_{ir} \ln p_i + \ln K_r.$$

In equations (6.28)-(6.30), as in subsequent equations, incomplete summation (prime at the sign of sums) has the same meaning as in equation (6.27). One should pay attention to the fact that when determining quantities  $\delta_j$ ,  $B_i$ ,  $\delta_i$ ,  $p_s$ ,  $\delta_p$ ,  $\delta_r$  summation is complete.



System of equations (6.27-6.30), linear relative to corrections, can be written in form of matrix of coefficients with unknowns. Augmented matrix for this case can be compiled, being guided by the following arrangement of columns and lines:

Columns:

- 1) corrections pertaining to molecular uncondensed products;
- 2) corrections pertaining to atomic products (including atoms of substances in condensed state at its usual place);
- 3) corrections pertaining to molecular condensed substances;
- 4) correction  $\Delta_m$  for number  $M_T$ ;
- 5) absolute terms of equations.

Lines:

- 1) equations of dissociation of molecules of uncondensed substances in the same order as molecular products in columns;
- 2) equations of conservation of substance in the same order as atomic products in columns;
- 3) equation of Dalton law;
- 4) equations of dissociation of gas phase of condensed substances.

As can be seen, the augmented matrix for calculation of the equilibrium composition of heterogeneous dissociated mixture at  $p, T = \text{const}$  is a modification of the original matrix for calculation of homogeneous dissociated mixture. In connection with this the methods of solution of system of linear equations, determination of corrections and improvements of unknowns are completely retained.

In case of calculation of the equilibrium composition at specified temperature and density the line of equation  $p = \text{const}$  in augmented matrices is replaced by line of equation  $\rho = \text{const}$  (6.22).

The augmented matrix for calculation of the equilibrium composition of heterogeneous mixture at  $p, T = \text{const}$  is represented on page 126 s,  $r = 2$ .

In connection with the fact that from approximation to approximation the composition of working medium changes, it is necessary after each approximation to check the possibility of appearance or disappearance of condensed phase. For this the following conditions are used:

for gaseous components -

$$\ln p_q > \ln p_q^u,$$

for condensed components -

$$\ln n_{qz} < \ln \psi,$$

where  $\psi$  - assigned small quantity.

If the first inequality is fulfilled, then  $q$ -th component should be considered as being in condensed state, its partial pressure is excluded from the number of unknowns, and  $n_{qz}$  is considered sought.

With fulfillment of the second inequality  $q$ -th component is considered being only in gas phase,  $n_{qz} = 0$ , and partial pressure is considered sought.

On calculation of heterogeneous systems there are imposed some limitations by rule of phases, which, as it is known, is written in the form

$$r = q - \Phi + 2 - R,$$

Matrix of coefficients of system of linear equations,  
heterogeneous mixture

Absolute terms									
[Composition $(\partial \ln f / \partial \ln T)_p (\partial \ln f / \partial \ln p)_T$ ]									
1	0	..	0	-a <sub>11</sub>	0	..	-a <sub>m1</sub>	0	-b <sub>1</sub>
0	1	..	0	-a <sub>12</sub>	0	..	-a <sub>m2</sub>	0	-b <sub>2</sub>
:	:	:	:	:	:	:	:	:	:
0	0	..	1	-a <sub>11</sub>	0	..	-a <sub>m1</sub>	0	-b <sub>1</sub>
<hr/>									
a <sub>11</sub> n <sub>1</sub> , a <sub>12</sub> n <sub>2</sub>	..		a <sub>11</sub> n <sub>1</sub>	n <sub>A1</sub>	0	..	0	a <sub>12</sub> n <sub>22</sub>	-b <sub>1</sub> , -b <sub>A1</sub> , b <sub>1</sub>
a <sub>21</sub> n <sub>1</sub> , a <sub>22</sub> n <sub>2</sub>	..		a <sub>21</sub> n <sub>1</sub>	0	n <sub>A22</sub>	..	0	a <sub>22</sub> n <sub>22</sub>	-b <sub>2</sub> , -b <sub>A2</sub> , b <sub>2</sub>
:	:	:	:	:	:	:	:	:	:
a <sub>m1</sub> n <sub>1</sub> , a <sub>m2</sub> n <sub>2</sub>	..		a <sub>m1</sub> n <sub>1</sub>	0	0	..	n <sub>A1</sub>	a <sub>m2</sub> n <sub>22</sub>	-b <sub>m</sub> , -b <sub>A1</sub> , b <sub>m</sub>
p <sub>1</sub> , p <sub>2</sub>	..		p <sub>1</sub>	p <sub>A1</sub>	0	..	p <sub>A1</sub>	0	-b <sub>p</sub> , p <sub>2</sub>
0	0	..	0	a <sub>12</sub>	0	..	a <sub>m2</sub>	0	b <sub>2</sub>

where  $r$  - quantity of thermodynamic degrees of freedom;  $\Phi$  - number of phases, i.e., number of parts of the system having uniform composition and separated by a physical boundary;  $R$  - number of independent chemical reactions in the system.

In our case the necessary thermodynamic degrees of freedom are  $p$  and  $T$ , i.e.,  $r = 2$ , the number of components  $q = 1 + m$ , number of independent chemical reactions  $R = 1$ . This governs equality

$$\Phi = m,$$

i.e., the number of phases should not exceed the numbers of chemical elements, from which the system has been formed. Since one of the phases is gaseous, the number of condensed phases  $\Phi_z$  (each product in condensed state will form a new phase) for case of independents  $p$  and  $T$  must not exceed numbers  $(m-1)$ :

$$\Phi_z \leq m - 1.$$

#### Sequence of Calculation

The system of equations of chemical equilibrium at assigned  $p$ ,  $T$  or  $v$ ,  $T$  has a physically obvious unique solution. Mathematical proof of the uniqueness of solution was given by Ya. B. Zel'dovich.

Calculation of the equilibrium composition of homogenous or heterogeneous mixture at assigned  $p$ ,  $T$  or  $v$ ,  $T$  is performed in the following order.

1. For all components of mixture being considered at a specified temperature according to reference data [4] there are found values of thermodynamic functions  $I_q^0$ ,  $S_q^0$ ,  $C_{p,q}^0$ , and for molecular components  $\ln K_q$ . For those substances, which at the given temperature can be in condensed state, there are determined  $I_{qz}^0$ ,  $S_{qz}^0$ ,  $C_{qz}^0$ ,  $p_{qz}^H$ .

2. Values of unknowns  $p_q$ ,  $M_T$  are assigned in zero approximation. With fulfillment of calculations on an electronic computer these quantities can be assigned randomly, for example, having taken them all equal to specified pressure. In zero approximation  $n_{qz}$  is considered equal to zero.

3. The quantities necessary for formation of augmented matrix are determined:  $\delta_j$ ,  $\delta_i$ ,  $\delta_p$ ,  $B_i$ ,  $p_\Sigma$ .

4. As a result of conversion of matrix according to a compact scheme the corrections to quantities  $\ln n_i$  and  $\ln M_T$  are found, and then by formula (6.23) - corrections to molecular products.

5. By formulas (6.15) or (6.18) we specify unknowns. Here is checked the possibility of appearance or disappearance of condensed phases, changing the system of equations depending on results of the check.

6. By formula (6.25) the accuracy of solutions is checked. If no solution is reached, calculation is repeated while using refined values of unknowns.

#### Relative Composition. Molecular Weight.

After the equilibrium composition (number of moles  $n_q$ ,  $n_{qz}$ , and number  $M_T$ ) has been determined with the necessary accuracy, it is possible to calculate a number of characteristic quantities of mixture in the state of equilibrium. Since calculation was executed for  $M_T$  moles of propellant, the weight quantity of products of dissociation and ionization comprises  $\mu_T M_T$ , where molecular propellant weight  $\mu_T$  is determined by formulas of Chapter V.

Molar fractions of gaseous components of the mixture can be found by formula

$$x_q = \frac{n_q}{N} = \frac{p_q}{p}. \quad (6.31)$$

The content of condensed substances in the mixture is more conveniently characterized not by numbers of moles  $n_{qz}$ , obtained in calculation, but by weight fractions  $z_{qz}$ , which are calculated so:

$$z_{qz} = \frac{n_{qz} \mu_q}{\mu_T M_T}, \quad (6.32)$$

where  $\mu_q$  - molecular (atomic) weight of q-th condensed substance.

Total weight fraction of condensate in the mixture comprises

$$z_z = \sum_{(qz)} z_{qz}.$$

Quantities  $x_q$ ,  $z_{qz}$  are one of the varieties of writing the composition in relative form.

For many reasons the quantity of mean molecular weight is necessary. It can be determined in the following manner. During calculation on  $\mu_T M_T$  kg of propellant the total number of moles of gaseous products is equal to overall pressure  $p$ . Consequently, mean molecular weight of the mixture, which is the relationship of total weight of products to the number of moles of only the gas phase, comprises

$$\mu = \frac{\mu_T M_T}{p} \frac{\text{kg}}{\text{mole}}. \quad (6.33)$$

Mean molecular weight of gas phase of heterogeneous mixture can be determined by formula

$$\mu_z = \frac{(1 - z_z) \mu_T M_T}{p}$$

or

$$\mu_z = (1 - z_z) \mu. \quad (6.34)$$

### 6.5. Determination of Partial Derivatives of Equilibrium Composition

Partial derivatives must characterize the dissociated mixture in the state of chemical equilibrium. Therefore, they should be found from a system of equations of chemical equilibrium with values of  $p$  and  $T$ , determining this equilibrium. This system for most general case of heterogeneous mixture consists of equations (6.3), (6.11), (6.8) and (6.12). By differentiating the shown system with respect to logarithm of temperature when  $p = \text{const}$  or logarithm of pressure when  $T = \text{const}$ , we obtain the corresponding partial derivatives. As earlier, the pressures of saturated vapors of condensed substances are known functions of temperature, therefore, their partial derivatives should be excluded from the number of unknowns.

By differentiating equations (6.3) with respect to  $\ln T$  when  $p = \text{const}$ , we obtain

$$\left(\frac{\partial \ln p_j}{\partial \ln T}\right)_p - \sum_i a_{ij} \left(\frac{\partial \ln p_i}{\partial \ln T}\right)_p + \left(\frac{\partial \ln K_j}{\partial \ln T}\right)_p - a_{sj} \left(\frac{\partial \ln p_s^h}{\partial \ln T}\right)_p = 0, \\ j = 1, 2, 3, \dots, l; j \neq r.$$

Since constants of equilibrium and pressure of saturated vapors of ideal substances depend only on the temperature, their partial derivatives should be replaced by total.

According to expression (6.4) let us write:

$$\frac{d \ln K_j}{d \ln T} = \frac{d}{d \ln T} \left[ \frac{\sum_i a_{ij} S_i^0 - S_j}{R_0} - \frac{\sum_i a_{ij} I_i^0 - I_j^0}{R_0 T} \right].$$

Considering when differentiating that

$$\frac{dS}{d \ln T} = C_p$$

and

$$\frac{dl}{d \ln T} = C_p T,$$

let us receive

$$\frac{d \ln K_j}{d \ln T} = K'_j = \frac{\sum_i a_{ij} l_i^0 - l_j^0}{R_0 T}. \quad (6.35)$$

Similarly from expression (6.10) we obtain:

$$\frac{d \ln p_q^*}{d \ln T} = \frac{d}{d \ln T} \left( \frac{S_{qs}^0 - S_{qs}^0}{R_0} - \frac{l_{qs}^0 - l_{qs}^0}{R_0 T} \right)$$

or

$$\frac{d \ln p_q^*}{d \ln T} = K'_{qs} = \frac{l_{qs}^0 - l_{qs}^0}{R_0 T}. \quad (6.36)$$

Let us introduce a new designation

$$\bar{K}_j = K'_j - a_{sj} K'_{ss} \quad (6.37)$$

and finally let us write:

$$\left( \frac{\partial \ln p_j}{\partial \ln T} \right)_p - \sum_i' a_{ij} \left( \frac{\partial \ln p_i}{\partial \ln T} \right)_p = -\bar{K}_j, \quad j=1, 2, 3, \dots, l; \quad j \neq r. \quad (6.38)$$

By differentiating equations of conservation of substance (6.11), we obtain:

$$\begin{aligned} & \sum_j' a_{ij} n_j \left( \frac{\partial \ln n_j}{\partial \ln T} \right)_p + (1 - \delta_{is}) n_i \left( \frac{\partial \ln n_i}{\partial \ln T} \right)_p + \delta_{is} n_{ss} \left( \frac{\partial \ln n_{ss}}{\partial \ln T} \right)_p + \\ & + a_{ir} n_{rs} \left( \frac{\partial \ln n_{rs}}{\partial \ln T} \right)_p - B_i \left( \frac{\partial \ln M_r}{\partial \ln T} \right)_p + \delta_{is} p_i K'_{ss} + a_{ir} p_r K'_{rs} = 0, \\ & i = 1, 2, 3, \dots, m. \end{aligned}$$



By introducing new designation

$$\delta_{is} p_i^* K'_{sz} + a_{ir} p_i^* K'_{rz} = \bar{K}_i, \quad (6.39)$$

finally let us write:

$$\sum' a_{ij} n_j \left( \frac{\partial \ln n_j}{\partial \ln T} \right)_p + (1 - \delta_{is}) n_i \left( \frac{\partial \ln n_i}{\partial \ln T} \right)_p + \delta_{is} n_{sz} \left( \frac{\partial \ln n_{sz}}{\partial \ln T} \right)_p + a_{ir} n_{rz} \left( \frac{\partial \ln n_{rz}}{\partial \ln T} \right)_p - B_i \left( \frac{\partial \ln M_r}{\partial \ln T} \right)_p = -\bar{K}_i, \quad i = 1, 2, 3, \dots m. \quad (6.40)$$

For equation of Dalton law (6.8) we obtain:

$$\sum' p_q \left( \frac{\partial \ln p_q}{\partial \ln T} \right)_p + p_i^* K'_{sz} + p_r^* K'_{rz} = 0.$$

Having designated

$$\bar{K}_p = p_i^* K'_{sz} + p_r^* K'_{rz}, \quad (6.41)$$

let us write

$$\sum' p_q \left( \frac{\partial \ln p_q}{\partial \ln T} \right)_p = -\bar{K}_p. \quad (6.42)$$

Finally, for equation of dissociation of gas phase of condensed substance (6.12), we obtain:

$$-\sum' a_{ir} \left( \frac{\partial \ln p_i}{\partial \ln T} \right)_p - a_{sz} K'_{sz} + K'_r + K'_{rz} = 0.$$

By introducing new designation

$$\bar{K}_{rz} = \bar{K}_r + K'_{rz} - a_{sz} K'_{sz}, \quad (6.43)$$

let us finally write

$$\sum_i' a_{ir} \left( \frac{\partial \ln p_i}{\partial \ln T} \right)_p = \bar{K}_{rz}. \quad (6.44)$$

Thus, from equations (6.3), (6.8), (6.11) and (6.12) by differentiation with respect to  $\ln T$  when  $p = \text{const}$  equations (6.38), (6.40), (6.42) and (6.44) have been obtained. The new system of equations is linear relative to derivatives of type  $(\partial \ln f / \partial \ln T)_p$ . Coefficients with derivatives and absolute terms of equations can be represented in the augmented matrix (see page 126).

For determination of derivatives of type  $(\partial \ln f / \partial \ln p)_T$ , the system of equations (6.3), (6.11), (6.8), (6.12) must be differentiated with respect to  $\ln p$  when  $T = \text{const}$ . Bearing in mind that at constant temperature  $\ln p_q^H$  and  $\ln K_j$  do not depend on pressure, we obtain:

$$\begin{aligned} \left( \frac{\partial \ln p_j}{\partial \ln p} \right)_T - \sum_i' a_{ij} \left( \frac{\partial \ln p_i}{\partial \ln p} \right)_T &= 0, \quad j=1, 2, 3, \dots, l, \quad j \neq r; \\ \sum_j' a_{ij} n_j \left( \frac{\partial \ln n_j}{\partial \ln p} \right)_T + (1 - \delta_{is}) n_i \left( \frac{\partial \ln n_i}{\partial \ln p} \right)_T + \delta_{is} n_{ss} \left( \frac{\partial \ln n_{ss}}{\partial \ln p} \right)_T + \\ + a_{ir} n_{rs} \left( \frac{\partial \ln n_{rs}}{\partial \ln p} \right)_T - B_i \left( \frac{\partial \ln M_r}{\partial \ln p} \right)_T &= 0; \quad i=1, 2, 3, \dots, m; \end{aligned} \quad (6.46)$$

$$\sum_q' p_q \left( \frac{\partial \ln p_q}{\partial \ln p} \right)_T = p_s; \quad (6.47)$$

$$\sum_i' a_{ir} \left( \frac{\partial \ln p_i}{\partial \ln p} \right)_T = 0. \quad (6.48)$$

Equations (6.45)-(6.48) will form a system of equations, linear relative to derivatives of type  $(\partial \ln f / \partial \ln p)_T$ . The augmented matrix of this system differs from the matrix for calculations of derivatives with respect to temperature only in the column of absolute terms. A variant of such a matrix is also represented on page 126.

Solution of the system of equations represented by the matrix on page 126 gives values of all derivatives of reacting mixture in the state of equilibrium. It should be noted that the earlier used algorithm of the solution is retained. Furthermore, the almost total identity of matrices substantially reduces the labor input of calculation.

For homogenous working medium it is easy to obtain particular case of system of equations (6.45)-(6.48). Inasmuch as there are no condensed components of the mixture, their corresponding partial derivatives are absent, i.e.,

$$\left(\frac{\partial \ln n_{qj}}{\partial \ln T}\right)_p = \left(\frac{\partial \ln n_{qj}}{\partial \ln p}\right)_T = 0.$$

Summation in equations (6.45)-(6.48) must be total, and quantities  $\bar{K}_j, \bar{K}_i, \bar{K}_p$  respectively are equal to

$$\begin{aligned}\bar{K}_j &= K'_j, \\ \bar{K}_i &= \bar{K}_p = 0.\end{aligned}$$

Variant of augmented matrix for homogenous working medium is represented on page 120.

In conclusion let us establish the connection between derivatives of quantity  $M_T$ :  $(\partial \ln M_T / \partial \ln T)_p$ ,  $(\partial \ln M_T / \partial \ln p)_T$  and corresponding logarithmic derivatives of molecular weight. For this let us differentiate equation (6.31). As a result we obtain:

$$\left(\frac{\partial \ln M_T}{\partial \ln T}\right)_p = \left(\frac{\partial \ln u}{\partial \ln T}\right)_p; \quad (6.49)$$

$$\left(\frac{\partial \ln M_T}{\partial \ln p}\right)_T = 1 + \left(\frac{\partial \ln u}{\partial \ln p}\right)_T. \quad (6.50)$$

For nonreacting mixture  $\mu = \text{const}$ , consequently:

$$\left(\frac{\partial \ln M_r}{\partial \ln T}\right)_p = 0,$$

$$\left(\frac{\partial \ln M_r}{\partial \ln p}\right)_T = 1.$$

Partial derivatives of composition and quantity  $M_r$  are necessary for calculation of equilibrium properties of the mixture: thermal coefficients, thermal capacities, speed of sound and others.

With determination of the composition and its partial derivatives we used the following system of units: pressure and partial pressure - phys. at.; enthalpy - cal/mole; entropy - cal/mole·deg,

$R_0 = 1.98726 \text{ cal/mole} \cdot \text{deg}.$

#### Bibliography

1. Alemasov V. Ye., Tishin A. P., IVUZ, ser. "Aviatsionnaya tekhnika", 1958, vyp. 2.
2. Alemasov V. Ye., Dregalin A. F., Teplo- and massoperenos (Heat and mass transfer), t. VII, izd-vo "Nauka and tekhnika", Minsk, 1968.
3. Vanichev A. P., Termodinamicheskiy raschet gorennya i istecheniya v oblasti vysokikh temperatur (Thermodynamic calculation of combustion and outflow in the high-temperature range). BNT, 1947.
4. Gurvch L. V. and others., Termodinamicheskiye svoystva individual'nykh veshchestv (Thermodynamic properties of individual substances), AN SSSR, 1962.
5. Huff V. N., Gordon S., Morrell V. E., Report NACA, 1951, No. 1037.

## CHAPTER VII

### THERMODYNAMIC PROPERTIES AND PROPERTIES OF TRANSFER OF COMBUSTION PRODUCTS

For calculation and investigation of gas-dynamic and heat-exchange processes the thermodynamic and thermophysical properties of combustion products must be known. As the basis of calculation of these properties serve general thermodynamic relationships and molecular-kinetic theory of gases.

It has been accepted to call electrical conductivity and emissivity of combustion products the thermophysical properties or properties transfer. However, the electrical conductivity and emissivity have a physical nature similar to other properties and are important characteristics of combustion products. Therefore, theoretical determination of the electrical conductivity and emissivities is also considered in this chapter.

#### 7.1. Thermodynamic Functions of the Mixture

The mixture of gases located in the state of chemical equilibrium is reacting, inasmuch as in it proceed reversible reactions of dissociation and ionization. Let us assume the equilibrium composition of such a mixture at certain temperature  $T$  and pressure  $p$  is specified in the following manner: the combustion products contain  $q = l + m$  components, each in a quantity of  $n_i$  moles ( $i = 1, 2, 3, \dots, l + m$ ). In this case some components are in condensed phase with number of moles  $n_{iz}$ . These data, obtained, for example, by the

method given in the previous chapter, permit determining the thermodynamic functions of the mixture.

Since calculation is performed on  $M_T$  moles of propellant, the weight quantity of products of dissociation and ionization constitutes  $\mu_T M_T$ , where molecular propellant weight is determined by formulas of Chapter V.

### Thermodynamic Functions of the Mixture

In the calculation for 1 kilogram of mixture one can determine thermodynamic functions in the following manner.

Total enthalpy

$$I = \frac{\sum_{i=1}^q n_i I_i^0 + \sum_{i=1}^q n_{iz} I_{iz}^0}{\mu_T M_T} \quad \frac{\text{kJ}}{\text{kg}}, \quad (7.1)$$

if  $I_1^0, I_{1z}^0$  in kJ/kmole.

Internal energy

$$E = \frac{\sum_{i=1}^q n_i E_i^0 + \sum_{i=1}^q n_{iz} E_{iz}^0}{\mu_T M_T} \quad \frac{\text{kJ}}{\text{kg}}, \quad (7.2)$$

if  $E_1^0, E_{1z}^0$  in kJ/kmole.

For ideal gases

$$E_i^0 = I_i^0 - R_0 T,$$

for condensed substances

$$E_{iz}^0 = I_{iz}^0.$$

Entropy

$$S = \sum_{i=1}^n n_i S_i^0 + \frac{R \ln \prod_{i=1}^n n_i}{\mu_i M_i} + \sum_{i=1}^n n_i S_{i1}^0 \quad \frac{\text{kJ}}{\text{kg} \cdot \text{deg}}, \quad (7.3)$$

if  $S_i^0, S_{i1}^0$  kJ/kmole·deg.

In the above-listed formulas the values with subscript "z" pertain to substances in condensed state, symbols  $I_1^0, E_1^0, S_1^0$  designate total enthalpy, internal energy and entropy of i-th component at temperature T and pressure in 1.02 bar (standard state). For simplicity of writing in the above-listed and subsequent formulas summation in the second sum is spread to all components, although in actuality one should summarize only with respect to indices of substances in condensed state.

The remaining thermodynamic functions (thermodynamic potential, Helmholtz free energy and others) are determined according to usual thermodynamic relationships with the aid of values of I, S and T.

#### The Form of Representation of Thermodynamic Functions of Individual Components

Experimental determination in wide scales of thermodynamic functions (properties) of individual gaseous substances at high temperatures (above 1000°K) is a complex assignment, practically impracticable at present. However, the thermodynamic functions of any gas can be calculated theoretically if the statistical sum also states of molecules (atoms) is known.

Thermodynamic functions of substances in condensed state, in contrast to gases, are determined on the basis of results of calorimetric measurements of thermal capacity or change in enthalpy, and also measurement of heat of phase and polymorphic transformations.

The most complete publication, containing information about methods of determination of thermodynamic functions of substances, necessary molecular constants, and also tables of properties of

335 individual substances, in the reference book "Thermodynamic Properties of Individual Substances."

In the reference book there have been placed values of reduced thermodynamic potential  $\Phi_r^0$ , entropy  $S_T^0$  changes in enthalpy  $H_T^0 - H_0^0$  and total enthalpy  $I_T^0$ , and also  $\lg K_p$  and  $K_p$ . Values of the shown thermodynamic properties are presented by tables for temperatures 293.15°K, 298.15°K, 400° and further every 100° up to 6000°K. For certain substances the tables have been expanded to 20,000°K. In tables of thermodynamic properties of substances in condensed states there are additionally listed values of thermal capacity  $C$  and quantities  $\lg p^H$ ,  $p^H$ .

In view of the large labor input the calculations of equilibrium compositions of compound mixtures are usually fulfilled on electronic computers (EVM). For a number of reasons the utilization of thermodynamic functions of individual components in tabular form during calculations on an electronic computer seems inconvenient, therefore the tables are approximated by multinomials. In this case there is usually approximated one function (for example, entropy or enthalpy), and for determination of remaining functions there are used thermodynamic relationships.

For example, in the reference book mentioned above there have been approximated tabular values of entropy by multinomials of type

$$S_T^0 = S \ln x + \sum_{n=2}^{n=7} S_n x^n, \quad (7.4)$$

where  $x = T \cdot 10^{-3}$ ;  $S$ ,  $S_n$  - coefficients of polynomial.

In the practice of thermodynamic calculations with sufficient accuracy we can use polynomials of type

$$I_T^0 = \sum_{i=0}^{i=7} a_i x^i. \quad (7.5)$$



## 7.2. Thermal Coefficients

In many calculations thermal coefficients are used namely:  
isobaric coefficient of expansion

$$\alpha_p = \frac{1}{v} \left( \frac{\partial v}{\partial T} \right)_p; \quad (7.6)$$

isothermal coefficient of compression

$$\beta_T = -\frac{1}{v} \left( \frac{\partial v}{\partial p} \right)_T; \quad (7.7)$$

temperature coefficient of pressure

$$\gamma = \frac{1}{p} \left( \frac{\partial p}{\partial T} \right)_v. \quad (7.8)$$

The latter can be expressed through the previous:

$$\gamma = \frac{1}{p} \frac{\alpha_p}{\beta_T}; \quad (7.9)$$

therefore it is sufficient to determine the most commonly used coefficients  $\alpha_p$  and  $\beta_T$ . By knowing these two coefficients, any thermodynamic derivatives can be calculated.

Let us represent thermal coefficients in the following manner:

$$\alpha_p = \frac{1}{T} \left( \frac{\partial \ln v}{\partial \ln T} \right)_p; \\ \beta_T = -\frac{1}{p} \left( \frac{\partial \ln v}{\partial \ln p} \right)_T$$

and use equation of state in the form

$$v = \frac{R_0 T}{p \mu}$$

Bearing in mind that

$$p \mu = \mu_T M_T,$$

let us represent the logarithmic form of equation:

$$\ln v = \ln R_0 + \ln T - \ln M_T - \ln \mu_T.$$

Hence

$$\begin{aligned} \left( \frac{\partial \ln v}{\partial \ln T} \right)_p &= 1 - \left( \frac{\partial \ln M_T}{\partial \ln T} \right)_p; \\ \left( \frac{\partial \ln v}{\partial \ln p} \right)_T &= - \left( \frac{\partial \ln M_T}{\partial \ln p} \right)_T. \end{aligned}$$

Ultimately we obtain

$$\alpha_p = \frac{1}{T} \left[ 1 - \left( \frac{\partial \ln M_T}{\partial \ln T} \right)_p \right]; \quad (7.10)$$

$$\beta_T = \frac{1}{p} \left( \frac{\partial \ln M_T}{\partial \ln p} \right)_T, \quad (7.11)$$

where logarithmic derivatives of quantity  $M_T$  are determined by the methods described in the previous chapter.

### 7.3. Heat Capacity

If during some process the multicomponent working medium is in the state of chemical equilibrium, then the effective heat capacity of the working medium must be determined with allowance for heat of equilibrium chemical reactions. Such heat capacity is called equilibrium.

According to the definition, heat capacity at constant pressure must be written so:

$$c_p = \left( \frac{\partial I}{\partial T} \right)_p$$

If we apply this formula to a reacting mixture, we obtain equilibrium heat capacity  $c_{p,p}$ , considering the change in composition depending on the temperature. Bearing in mind that quantity  $I$  has been represented by formula (7.1), let us write:

$$c_{p,p} = \frac{\partial}{\partial T} \left( \frac{\sum_{i=1}^q n_i I_i^0 + \sum_{i=1}^q n_{iz} I_{iz}^0}{\mu_r M_r} \right)$$

After differentiation we obtain

$$c_{p,p} = \frac{\sum_{i=1}^q n_i C_{pi} + \sum_{i=1}^q n_{iz} C_{iz}}{\mu_r M_r} + \frac{1}{\mu_r M_r T} \left[ \sum_{i=1}^q n_i \left( \frac{\partial \ln n_i}{\partial \ln T} \right)_p I_i^0 + \sum_{i=1}^q n_{iz} \left( \frac{\partial \ln n_{iz}}{\partial \ln T} \right)_p I_{iz}^0 \right] - \frac{I}{T} \left( \frac{\partial \ln M_r}{\partial \ln T} \right)_p \quad (7.12)$$

The first term of expression (7.12) is heat, heading for change in temperature of the mixture of constant composition. This is usual "frozen" heat capacity

$$c_{p,0} = \frac{\sum_{i=1}^q n_i C_{pi} + \sum_{i=1}^q n_{iz} C_{iz}}{\mu_r M_r}, \quad (7.13)$$

inasmuch as for nonreacting mixture of constant composition derivatives

$$\left( \frac{\partial \ln n_i}{\partial \ln T} \right)_p, \left( \frac{\partial \ln n_{iz}}{\partial \ln T} \right)_p, \left( \frac{\partial \ln M_r}{\partial \ln T} \right)_p$$

become zero. One should emphasize that although the mixture

composition when determining frozen heat capacity is considered constant, it is equilibrium and it corresponds to given temperature and pressure.

The second and third terms in expression (7.12) - heat proceeding to change in the composition of equilibrium mixture. Corresponding partial derivatives are determined by equations of the previous chapter.

Figure 7.1 shows values of equilibrium and frozen heat capacity of combustion products of kerosene type fuel +  $O_{2x}$ . Solid lines pertain to pressure 20 bar, broken - to pressure 200 bar. As can be seen the quantity of frozen heat capacity does not practically depend on pressure, whereas the value of equilibrium heat capacity depends noticeably. With increase in the pressure, suppressing dissociation, the equilibrium heat capacity is diminished and differs from frozen to a lesser degree. With small and large  $\alpha$ , i.e., at low temperatures when dissociation weakens, the difference between equilibrium and frozen heat capacities is diminished.

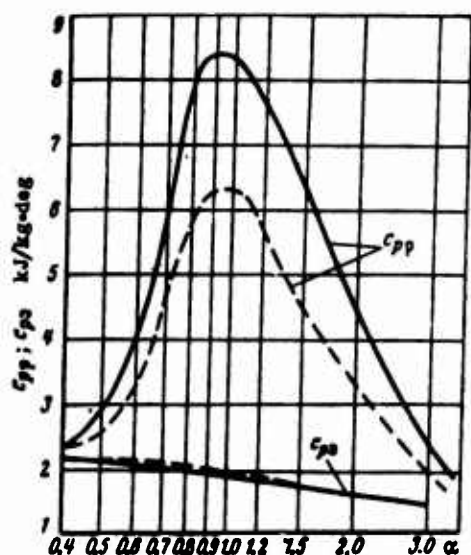


Fig. 7.1. Values of equilibrium and frozen heat capacities at different pressures: kerosene type fuel +  $O_{2x}$ .

Heat capacity with constant volume is determined by expression

$$c_v = \left( \frac{\partial E}{\partial T} \right)_v.$$

It can be obtained from general thermodynamic relationship

$$c_p - c_v = T \left( \frac{\partial T}{\partial p} \right)_v \left( \frac{\partial v}{\partial T} \right)_p.$$

With allowance for expressions (7.6), (7.8), (7.9) and application to reacting mixture we obtain:

$$c_{vp} = c_{pp} - \frac{\alpha_p^2}{\beta_T} vT.$$

By using formulas (7.10) and (7.11), we finally obtain

$$c_{vp} = c_{pp} - \frac{R \left[ 1 - \left( \frac{\partial \ln M_T}{\partial \ln T} \right)_p \right]^2}{\left( \frac{\partial \ln M_T}{\partial \ln p} \right)_T}. \quad (7.14)$$

In the previous chapter it was shown that for nonreacting mixture

$$\left( \frac{\partial \ln M_T}{\partial \ln T} \right)_p = 0, \quad \left( \frac{\partial \ln M_T}{\partial \ln p} \right)_T = 1.$$

Consequently, from formula (7.14) there is obtained, as a particular case, the usual relationship for frozen heat capacities:

$$c_{v3} = c_{p3} - R. \quad (7.15)$$

According to known values of heat capacities there are determined their ratios of equilibrium heat capacities:

$$k_p = \frac{c_{pp}}{c_{vp}} \quad (7.16)$$

and frozen heat capacities:

$$k_s = \frac{c_p}{c_v} \quad (7.17)$$

#### 7.4. Speed of Sound

The speed of sound is determined by general expression

$$a^2 = \left( \frac{\partial p}{\partial \rho} \right)_s$$

in which the derivative is taken under conditions taking place in a sound wave. In case of energy insulation and absence of relaxation phenomena the processes of compression and rarefaction in a sound wave are isentropic, and consequently:

$$a^2 = \left( \frac{\partial p}{\partial \rho} \right)_s = -v^2 \left( \frac{\partial p}{\partial v} \right)_s \quad (7.18)$$

With propagation of sound oscillations in a reacting medium the process in the sound wave will be isentropic if:

1) the frequency of oscillations is great, and the rates of chemical and phase transformations are small, as a result of which the mixture composition is not changed with passage through sound wave, particles of condensate remain fixed and have constant temperature; the process in the wave proceeds as in a nonreacting mixture; in this instant the speed of sound is called frozen;

2) the rate of chemical and phase transformations are great, and frequency of oscillations is insignificant. With compression and rarefaction in a sound wave the mixture composition is changed in accordance with change of temperature and pressure. With passage through wave the chemical and phase equilibrium are retained; particles of condensate have parameters equal to the parameters of

gas. In these conditions the speed of sound is called equilibrium.

Let us determine derivative  $(\partial p / \partial v)_s$ . For this let us use tables of differential thermodynamic relationships 7.1 [7].

Table 7.1. Certain differential thermodynamic relationships.

	$p = \text{const}$	$T = \text{const}$	$v = \text{const}$	$s = \text{const}$	$E = \text{const}$	$I = \text{const}$
$(dp)$	—	$-1$	$-a_p v$	$-\frac{c_p}{T}$	$a_p p v - c_p$	$-c_p$
$(dT)$	$1$	—	$-\beta_T v$	$-a_p v$	$(\beta_T p - a_p T) v$	$(1 - a_p T) v$
$(dv)$	$a_p v$	$\beta_T v$	—	$c_v \beta_T \frac{v}{T}$	$c_v \beta_T v$	$(c_v \beta_T + a_p v) v$
$(ds)$	$\frac{c_p}{T}$	$a_p v$	$-c_v \beta_T \frac{v}{T}$	—	$c_v \beta_T \frac{p v}{T}$	$c_p \frac{v}{T}$
$(dE)$	$c_p - a_p p v$	$(a_p T - \beta_T p) v$	$-c_v \beta_T v$	$-c_v \beta_T \frac{p v}{T}$	—	$(c_p - a_p p v) v -$ $-c_v \beta_T p v$
$(dI)$	$c_p$	$(a_p T - 1) v$	$-(c_v \beta_T + a_p v) v$	$-c_p \frac{v}{T}$	$c_v \beta_T p v -$ $-(c_p - a_p p v) v$	—

**Note:** Derivative of type  $(\partial y / \partial x)_z$  is a result of division of quantity  $(\partial y)$ , taken at intersection of line  $(\partial x)$  and column  $z$ , by quantity  $\partial x$  (intersection of line  $(\partial x)$  and column  $z$ ). For example:  
 $(\partial s / \partial v)_T = a_p v / \beta_T v = a_p / \beta_T$ .

As a result we have

$$\left(\frac{\partial p}{\partial v}\right)_s = -\frac{c_p}{c_v} \frac{1}{\beta_T v} = -\frac{k_0}{\beta_T}.$$

By placing derivative  $(\partial p / \partial v)_s$  in expression (7.18) and considering the equation of state and formula for  $\beta_T$ , we obtain for equilibrium speed of sound:

$$a_p^2 = \frac{k_p R T}{\left(\frac{\partial \ln M_T}{\partial \ln p}\right)_T}. \quad (7.19)$$

For a nonreacting mixture derivative  $(\partial \ln M_T / \partial \ln p)_T$  is equal to one, and the relationship of frozen heat capacities is equal to  $k_3$ . From equality (7.19), as a particular case, we have the speed of sound in working medium of constant composition (frozen speed of sound):

$$a_1^2 = k_3 RT. \quad (7.20)$$

Figure 7.2 as an example shows composition of equilibrium and frozen properties of combustion products of propellant  $C_2H_8N_2 + N_2O_4$  ( $\alpha = 0.8$ ) at various temperatures. As can be seen, the difference between equilibrium and frozen parameters is substantial and certainly must be considered. This difference is the most considerable in the range of maximum dissociation and unessential at conditions when the working medium does not dissociate.

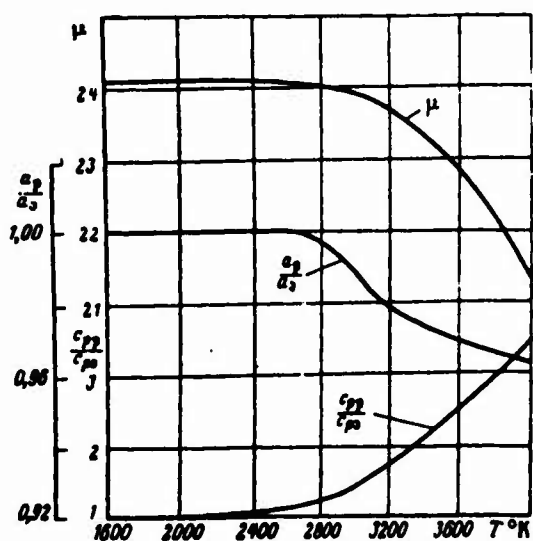


Fig. 7.2. Comparison of equilibrium and frozen thermodynamic properties of combustion products of propellant  $C_2H_8N_2 + N_2O_4$  ( $\alpha = 0.8$ ) at various temperatures ( $p_K^* = 100$  bar).

[Translator's note: in a previous paragraph the fuel was represented as  $C_2H_8N_2 + N_2O_4$ .]

For two-phase medium an important characteristic is the rate of propagation of sound in gas phase. General expression for this speed of sound can be written so:

$$a_{p,1}^2 = \frac{k_{p,1} RT}{(i - z) \left( \frac{\partial \ln M_T}{\partial \ln p} \right)_T},$$



qual  
where relationship of heat capacities and derivative  $(\partial \ln M_T / \partial \ln p)_T$  are determined with condition  $z = \text{const.}$  With propagation of sound the particles remain fixed, their temperature is constant, phase transitions are absent.

0)  
d  
204  
er-  
7.5. Transfer Coefficients (Diffusion, Viscosity, Thermal Conductivity)

Phenomena of diffusion, viscosity and thermal conductivity are physically similar. They assume the transfer (transport) of some physical properties through liquid or gas. Usual diffusion is transfer of mass from one region to another as a result of gradient of velocity; thermal conductivity is transfer of heat as a result of temperature gradient.

um  
s  
nt  
Therefore, the enumerated physical phenomena received the general name - transfer phenomena, and thermophysical coefficients of diffusion, viscosity and thermal conductivity corresponding to them, - transfer coefficients (transport coefficients).

The kinetic theory of gases [6], developed permits theoretically determining the thermophysical coefficients of gases and their mixtures. One of the results of theory is the fact that it turned out to be possible to write down all transfer coefficients through a system of integrals  $\Omega^{(i,j)}$ , considering dynamics of collisions of molecules. The latter is determined by intermolecular function of interaction - potential.

of  
Numerous theoretical and experimental works confirmed the applicability of the kinetic theory of gases for practical purposes.

Thermophysical Properties of Individual Components

Molecular-kinetic theory of gases gives the following expressions for transfer coefficients.

Diffusion coefficient of component  $i$  in a binary mixture of  $i$  and  $j$  gases is equal to

$$D_{ij} = 0,26 \cdot 10^{-6} \sqrt{\frac{T^3 (\mu_i + \mu_j)}{2 \mu_i \mu_j}} \frac{1}{p \sigma_{ij}^2 \Omega_{ij}^{1,1*}} \frac{\text{m}^2}{\text{s}}, \quad (7.21)$$

where  $p$  - pressure in bar;  $\Omega_{ij}^{1,1*}$  - reduced integral of collisions (general writing  $\Omega^{(s,s*)}$ ) - function of reduced temperature

$$T^* = \frac{T}{(\epsilon/k)_{ij}}, \quad (7.22)$$

$\sigma_{ij}$ ,  $(\epsilon/k)_{ij}$  - parameters of potential function of interaction of molecules (atoms) of types  $i$  and  $j$ ;  $\mu_i$ ,  $\mu_j$  - molecular weights of components  $i$  and  $j$ .

In case of equality  $i = j$  (single-component gas) from formula (7.21) a calculated expression is obtained for self-diffusion coefficient.

Viscosity coefficient is equal to

$$\eta_i = 26,7 \cdot 10^{-7} \sqrt{\frac{\mu_i T}{\sigma_i^2 \Omega_i^{2,2*}}} \frac{\text{N} \cdot \text{s}}{\text{m}^2}. \quad (7.23)$$

Coefficient of thermal conductivity for single-component gas is determined as

$$\lambda_i = \frac{15}{4} \frac{R_0}{\mu_i} \eta_i = 0,832 \cdot 10^{-1} \sqrt{\frac{T}{\sigma_i^2 \Omega_i^{2,2*}}} \frac{\text{W}}{\text{m} \cdot \text{deg}}. \quad (7.24)$$

The formula written above is valid for components of a mixture, molecules of which do not have internal degrees of freedom, i.e., for monatomic molecules. For polyatomic molecules at high temperatures the transfer of energy of internal degrees of freedom must be considered. The component of thermal conductivity, caused by

energy exchange between forward and internal degrees of freedom, is calculated with the aid of Eucken correction:

$$\lambda_i' = 0,885 \left( 0,4 \frac{C_{pi}}{R_0} - 1 \right) \lambda_i, \quad (7.25)$$

where  $C_{pi}$  - molar thermal capacity of i-th component at constant pressure in J/mole·deg.

Thus, general coefficient of thermal conductivity of i-th component is equal to:

$$\lambda_i = \lambda_i' + \lambda_i^*, \quad (7.26)$$

#### Thermophysical Properties of the Mixture

Calculated expressions for determination of viscosity and thermal conductivity coefficients of a multicomponent mixture of  $l$  molecules and  $m$  atoms are written as the relationship of determinants on the order of  $l + m + 1$  and  $l + m$ . Into formulas for elements of these determinants enter coefficients of viscosity, thermal conductivity and diffusion of binary systems  $i-j$  for all combinations of components. In view of the indeterminacy connected with the incompleteness of contemporary data about the interaction of mixture components at high temperatures, in calculations of viscosity coefficients and thermal conductivity of combustion products of rocket propellants it is expedient use approximate formulas.

Viscosity coefficient of the mixture can be determined by Budenberg-Wilki formula [6]:

$$\eta_{cm} = \sum_{i=1}^q \frac{x_i^2}{\frac{x_i^2}{\eta_i} + 1,385 \frac{R_0 T}{p} \frac{x_i}{\mu_i} \sum_{j=1}^q \frac{x_j}{D_{ij}}} \quad (7.27)$$

where  $x_i$  - molar fraction of i-th component,

$R_0$  in J/mole·deg;  $p$  in N/m<sup>2</sup>;  $D_0$  in m<sup>2</sup>/sec;  $n$  in mole/m<sup>3</sup>.

Other formulas for the viscosity coefficient of mixtures are widespread, enabling considerably simpler execution of estimation calculations. For example, there is widely used an empirical formula of type

$$\eta_{cu} = \frac{\mu}{\sum \frac{\mu_i x_i}{\eta_i}} \quad (7.28)$$

error of which as compared to strict formulas of kinetic theory comprises approximately 10-15%.

The coefficient of thermal conductivity of a mixture of nonreacting gases, molecules of which do not possess internal degrees of freedom (frozen mixture of nonatomic gases), is determined so [19]:

$$\lambda_{cu} = \sum_{i=1}^n \frac{\lambda_i x_i}{\sum_{j=1}^n \phi_{ij} x_j} \frac{W}{m \cdot \text{deg}}, \quad (7.29)$$

where

$$\phi_{ij} = \eta_{ij} \left[ 1 + \frac{2.41 (\mu_i - \mu_j) (\mu_i - 0.142 \mu_j)}{(\mu_i + \mu_j)^2} \right],$$

$$\eta_{ij} = \frac{\left[ 1 + \left( \frac{\eta_i}{\eta_j} \right)^{0.5} \left( \frac{\mu_j}{\mu_i} \right)^{0.25} \right]^2}{2 \sqrt{2} \left( 1 + \frac{\mu_i}{\mu_j} \right)^{0.5}}$$

The component of the coefficient of thermal conductivity of the mixture, caused by transfer of energy of internal degrees of freedom, can be found by empirical formula

$$\lambda_{cm} = \sum_{l=1}^q \frac{\gamma_l \gamma_l}{\sum_{s=1}^r \frac{D_{ll} x_s}{D_{ls}}} \quad (7.30)$$

Thus, the coefficient of thermal conductivity of frozen mixture

$$\lambda_{fcm} = \lambda'_{cm} + \lambda''_{cm} \quad (7.31)$$

Estimation values of transfer coefficients  $\eta_{cm}$ ,  $\lambda_{fcm}$  can be obtained on the basis of conditional empirical model of "single-component" gas with parameters  $\mu$ ,  $c_{p3}$ ,  $\sigma_{cm}$ ,  $(\epsilon/k)_{cm}$ . Potential parameters of single-component gas are determined by formula [22]:

$$\left. \begin{aligned} \sigma_{cm} &= \sum_i x_i \sigma_i; \\ (\epsilon/k)_{cm} &= \frac{\sum_i x_i (\epsilon/k)_i \sigma_i^3}{\sigma_{cm}^3} \end{aligned} \right\} \quad (7.32)$$

For calculation of the viscosity coefficient of the mixture  $\eta_{cm}$  a formula of type (7.23) is used:

$$\eta_{cm} = 26,7 \cdot 10^{-7} \frac{\sqrt{\mu T}}{\sigma_{cm}^2 \rho_{cm}^{2,2\star}},$$

and coefficient of thermal conductivity  $\lambda_{fcm}$  is determined on the basis of formulas (7.24)-(7.26) for "single-component" gas:

$$\lambda_{fcm} = 1317 \eta_{cm} \left( \frac{3,54}{\mu} + c_{p3} \right), \quad (7.33)$$

where  $c_{p3}$  is in kJ/kg·deg.

Effective coefficient of thermal conductivity of the mixture  $\lambda_e$  involves the effect of chemical reactions. Mechanism of heat transfer of chemical reactions is the following. If in the reacting mixture of gases there exists a temperature gradient, in the

range of elevated temperatures the mixture is dissociated more intensely. As a result of concentration gradient appearing in this case, products of dissociation are diffused into a range of lower temperatures, where recombination occurs and heat of chemical reactions is separated. General method of determination of thermal conductivity component  $\lambda_R$ , which considers this effect, has been proposed by Butler and Brock [12]. Working formulas for  $\lambda_R$ , obtained under the assumption of local chemical equilibrium, are very bulky and are not listed here. To get estimate values of the effect coefficient of thermal conductivity use can be made of approximate formula [12]:

$$\lambda_e = \lambda_{fcm} \frac{c_{p p}}{c_{p s}}. \quad (7.34)$$

Formula (7.34) is obtained on the assumption that all coefficients of diffusion in the mixture are equal to each other and Lewis number is equal to one:

$$\frac{Q_{D1} c_{p s}}{\lambda_{fcm}} = 1.$$

Figures 7.3 and 7.4 show the character of change of quantities  $\lambda_f$ ,  $\eta_{cm}$ ,  $\lambda_c/\lambda_{fcm}$  from temperature at various pressures. Calculations are done for combustion products of propellant  $C_2H_8N_2 + N_2O_4$  when  $\alpha = 0.8$ ; in this case the values of  $\lambda_e$  are determined by exact formulas [12]. Values of  $c_{p p}/c_{p s}$  are applied there, which give the possibility of evaluating the accuracy of formula (7.34). As can be seen, chemical reactions substantially affect  $\lambda_e$ , in this case the maximum values of  $\lambda_e/\lambda_f$ ,  $c_{p p}/c_{p s}$  are attained when the rate of change of dissociation with respect to temperature is maximum.

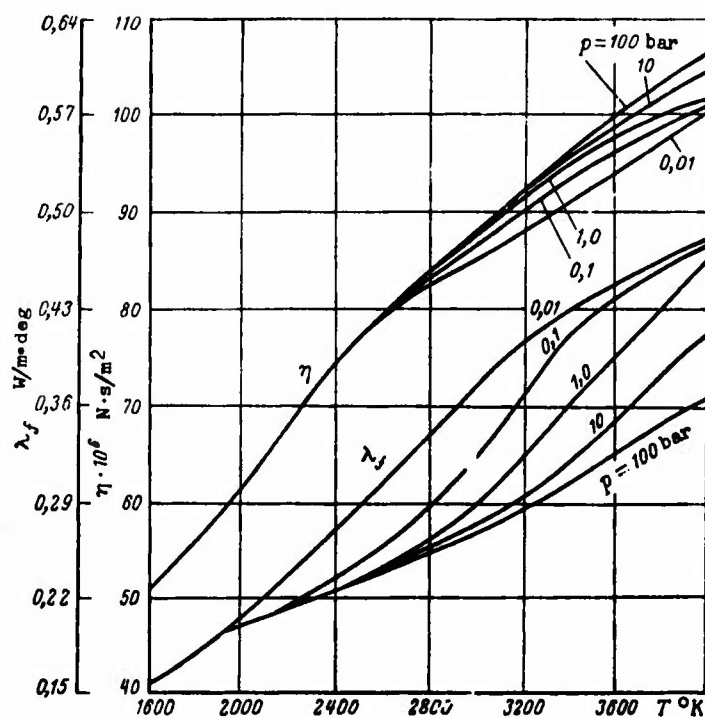


Fig. 7.3. Some thermophysical properties of combustion products at various temperatures and pressures.

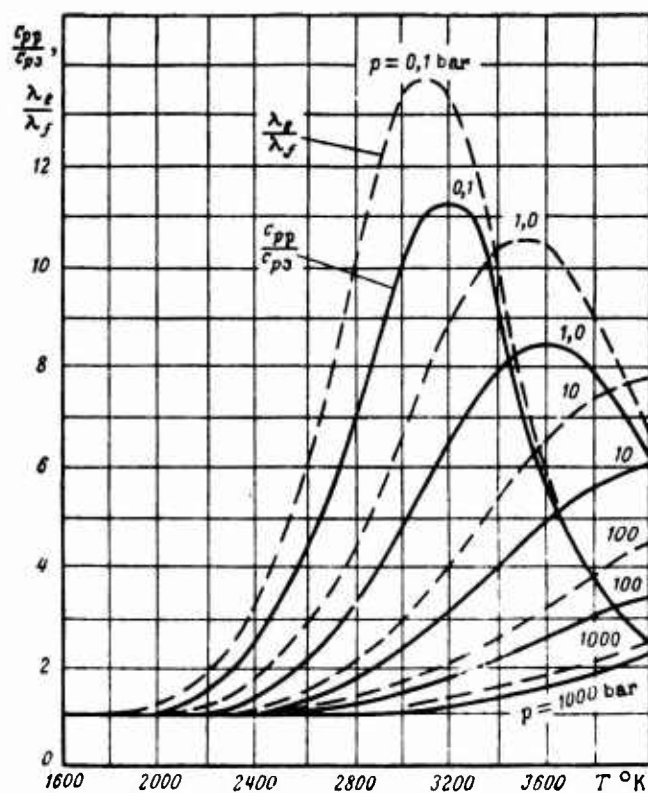


Fig. 7.4. Quantities of relations  $c_{p2}/c_{p1}$  and  $\lambda_e/\lambda_f$  at various temperatures and pressures.

## Interaction Potentials Between Molecules

Transfer coefficients depend on the potential energy of interaction of molecules with their collision. Generally this interaction cannot be described by analytical function of distance, however for calculation purposes many different functional relationships were suggested. These relationships, which approximate the actual behavior of molecules (atoms) at collision, enter the working formulas for transfer coefficients in the form of integrals  $\Omega^{1,1*}$ , considering the dynamics of collision. Selection of some model of interaction (potential) for practical calculations is determined by the nature of the substance, temperature range, the presence of reliable data on parameters of the potential.

Most often in heat engineering calculations there is used Lennard-Jones potential (12-6), inasmuch as it describes collisions of molecules in both low and moderately high temperature ranges. This permits using experimental data for determination of corresponding constants of potential, first of all, and making more or less validated extrapolation, secondly. Furthermore, constants of potential (12-6) can be evaluated by certain physical properties in the absence of immediate experimental data.

Constants of Lennard-Jones potential  $\sigma$  and  $\epsilon/k$  for certain combustion products of rocket propellants have been listed in Table 7.2 [19].

Coefficients  $D_{11}$ ,  $\lambda_1$ ,  $\eta_1$  of individual components are computed so:

a) reduced temperature  $T_1^* = T(\epsilon/k)_1$  is determined and by it from Table 7.3 there is taken the corresponding integral of collisions  $\Omega^{1,1*}$  or  $\Omega^{2,2*}$ ;

b) by using collision diameter of component  $\sigma_1$  the corresponding value of  $\lambda_1$ ,  $\eta_1$ ,  $D_{11}$  is determined;



c) potential parameters  $\sigma_{ij}$ ,  $(\epsilon/k)_{ij}$ , necessary for determination of coefficient of binary diffusion  $D_{ij}$ , are determined according to rules of combination:

$$\sigma_{ij} = 0,5(\sigma_i + \sigma_j); \quad (7.35)$$

$$(\epsilon/k)_{ij} = \sqrt{(\epsilon/k)_i (\epsilon/k)_j}, \quad (7.36)$$

and then temperatures and  $T_{ij}^*$  and  $\Omega_{ij}^{1,2*}$  are already found.

Table 7.2. Parameters of potential (12-6) for certain substances [19].

Substance	$\sigma, \text{\AA}$	$(\epsilon/k), ^\circ\text{K}$	Substance	$\sigma, \text{\AA}$	$(\epsilon/k), ^\circ\text{K}$
CH	2,610	52,6	H <sub>2</sub>	2,827	59,7
CH <sub>2</sub>	3,024	84,1	OH	2,550	79,8
CH <sub>3</sub>	3,371	115,2	H <sub>2</sub> O	2,710	506,0
CH <sub>4</sub>	3,758	148,6	HN	2,330	107,0
HCO	3,460	187,0	HF	2,780	86,0
HCN	3,630	569,1	F <sub>2</sub>	3,357	112,6
CN	3,770	456,0	FO	2,960	137,0
CO	3,585	109,9	O <sub>2</sub>	3,467	106,7
CO <sub>2</sub>	3,941	195,2	N <sub>2</sub>	3,798	71,4
C <sub>2</sub> H <sub>2</sub>	4,033	231,8	NO	3,508	112,4
C <sub>2</sub> H <sub>4</sub>	4,163	224,7	NO <sub>2</sub>	3,900	230,0

Table 7.3. Values of integrals  $\Omega_{ij}^{1,2*}$  for potential (12-6) [6].

$T^*$	$\Omega_{1,1}^{1*}$	$\Omega_{2,2}^{1*}$	$T^*$	$\Omega_{1,1}^{1*}$	$\Omega_{2,2}^{1*}$
0,5	2,066	2,257	4,0	0,8836	0,9700
0,6	1,877	2,065	4,5	0,8610	0,9464
0,7	1,729	1,908	5,0	0,8422	0,9269
0,8	1,612	1,780	6,0	0,8124	0,8963
0,9	1,517	1,675	7,0	0,7896	0,8727
1,0	1,439	1,587	8,0	0,7712	0,8538
1,5	1,198	1,314	9,0	0,7556	0,8379
2,0	1,075	1,175	10	0,7424	0,8242
2,5	0,9996	1,093	20	0,6640	0,7432
3,0	0,9490	1,039	30	0,6232	0,7005
3,5	0,9120	0,9999	40	0,5960	0,6718

In practical calculations with use of the values of thermophysical coefficients  $\eta$ ,  $\lambda$ ,  $D$ , obtained by formulas of this paragraph, it is necessary to bear in mind the following. Most of the known values of potential parameters  $\sigma$ ,  $\epsilon/k$  are determined from experiments on compressibility, viscosity, thermal conductivity and diffusion under low temperature conditions, because of this their application in calculations at high temperatures it is not well-grounded. Furthermore, for a number of substances experimental values of  $\sigma$ ,  $\epsilon/k$  are generally absent and rough empirical formulas are used for their estimation. Therefore, calculated values of thermophysical coefficients  $\eta$ ,  $\lambda$ ,  $D$  as yet have an estimated character.

#### 7.6. Electrical Conductivity

The basic quantity, characterizing electrical properties of ionized working medium, is the specific conductivity of gas. It represents the conductivity of a conductor with length 1 m and section 1 m<sup>2</sup>. The coefficient of specific conductivity (subsequently called electrical conductivity) is a magnitude opposite specific resistance, and has dimension  $(\Omega \cdot m)^{-1}$  or, which is the same, S/m.

By determining scalar electrical conductivity  $\sigma$  from Ohm's law, it is possible to write:

$$\sigma = \frac{j}{E}, \quad (7.37)$$

where  $j$  - current density (A/m<sup>2</sup>);  $E$  - intensity of electrical field (V/m).

By the degree of ionization, which is the ratio of concentration (number of particles in a unit of volume) of electrons to the sum of concentrations of neutral particles and ions, we distinguish slightly, partially and completely ionized gas.

Slightly ionized gas (degree of ionization less than 1%) can

be represented in the form of a mixture of neutral particles and electrons, disregarding the effect of ions. The electrical conductivity of such a gas is determined by expression:

$$\sigma_n = \frac{4\pi e^2 c_e}{3m_e} \int_0^\infty F(v) \frac{d}{dv} \left( \frac{v^3}{v_{en}} \right) dv, \quad (7.38)$$

where  $m_e$ ,  $v$ ,  $e$  - mass, velocity and charge of electron respectively;  $F(v)$  - function of distribution of electron velocities;  $v_{en} = \sum_n v c_n Q_{en}$  - frequency of elastic collisions of electrons with neutral components of gas mixture;  $Q_{en}$  - effective section of collision of electron with neutral component;  $c_e$ ,  $c_n$  - concentrations of electrons and neutral components respectively.

To get the estimate values of electrical conductivity one can use the expression obtained with application of the method of kinetic theory of free path. The basis of the method of the assumption of transfer of current only by electrons and of short time of collision of electron with components of gas mixture as compared to the time between collision. The formula has the form

$$\sigma_n = 0,532 \frac{c_e e^2}{(m_e k T)^{0.5}} \frac{1}{\sum_n c_n Q_{en}} (\Omega \cdot \text{cm})^{-1} \quad (7.39)$$

where  $k$  - Boltzmann constant  $1.38044 \cdot 10^{-23}$  J/deg;  $e = 1.60206 \cdot 10^{-19}$  k;  $m_e = 9.1083 \cdot 10^{-31}$  kg.

The electrical conductivity of completely singly-ionized gas  $\sigma_{ei}$  with allowance for electron-electron and electron-ion interactions is equal to

$$\sigma_{ei} = 0,591 \frac{(kT)^{3/2}}{m_e^{1/2} e^2} \frac{1}{\ln \left( \frac{d}{b_0} \right)}, \quad (7.40)$$

where  $b_0 = \frac{e^2}{3kT}$  - collision parameters, at which the electron with average energy is deflected in the field of positive ion to angle

$\pi/2$ ;  $d = \frac{4}{3} c_e^{-1/3}$  - measure of average distance between neighboring gas particles.

From formula (7.40) it follows that the electrical conductivity of completely ionized gas slightly depends on the electron concentration (the latter enters logarithmic term) and highly depends on the temperature of gas. Inasmuch as the determining factor during interaction of electron with a charged particle is its charge, and not chemical nature, all ionized molecules or atoms of identical multiplicity factor of ionization can be considered as particles of one type.

Temperatures developed in the combustion chambers of rocket engines operating on chemical propellant cause only slight thermal ionization of combustion products. However, with the presence of impurities of alkaline metals it can become necessary to consider the interaction of electrons with charged particles.

Here, as in the case of slightly ionized gas, expression (7.38) is also valid, but instead of  $v_{en}$  quantity  $v_{en} + v_{ei}$  should be used.

The frequency of collisions of electrons with ions  $v_{ei}$  with allowance for electron-electron interactions is determined by formula

$$v_{ei} = 0,476 \frac{2\pi e_e e^2 \ln \left( \frac{d}{b_0} \right)}{(4\pi)^2} \left( \frac{2e}{m_e} \right)^{1/2} \left( \frac{e}{kT} \right)^{3/2} \eta^{-1}, \quad (7.41)$$

where  $\eta = \frac{eu}{kT}$  - dimensionless energy;  $u$  - energy of electrons in eV.

For calculation of the estimate values of electrical conductivity of partially ionized gas use of formulas (7.39) and (7.40) can be made. By taking the additivity of resistances, which appear as a result of interactions between electrons and neutral particles on the one hand, and between electrons and ions on the other, it is possible to write:

$$\frac{1}{\sigma} = \frac{1}{\sigma_n} + \frac{1}{\sigma_{el}}. \quad (7.42)$$

By using expressions (7.39) and (7.40) for the conductivities of slightly and completely ionized gas, let us present formula (7.42) in such a form:

$$\sigma = 0,385 \cdot 10^{-7} \frac{c_e}{T^{1/2} \left( \sum_n c_n Q_{en} + \sum_i c_i Q_{ei} \right)} (\Omega \cdot m)^{-1} \quad (7.43)$$

where index i pertains to charged components of the gas mixture.

Thus, in order to calculate the conductivity of partially or completely ionized gas, its temperature, composition and effective cross section Q of collisions of all components must be known, which make a contribution to the total probability of electron collision.

Collision cross sections of singly charged particles with electron are determined by formula

$$Q_{ei} = 8,1 b_0^2 \ln \left( \frac{d}{b_0} \right). \quad (7.44)$$

Collision cross sections of electrons with neutral components are found from experiments on diffusion of electrons or with the aid of quantum mechanical calculations. Estimate values of  $Q_{en} = f(T)$  for certain components are listed in Table 7.4.

As illustration Fig. 7.5 lists relationships  $\lg \sigma = f(T)$  for combustion products of propellant kerosene +  $O_{2x}$  with various potassium content, and also for heated hydrogen and air. The temperature of combustion products of propellant is determined from calculation of combustion at prescribed pressure.

Table 7.4. Collision cross sections of electrons with certain components of gas mixture.

Com- bus- tion	$Q \text{ cm}^2$	Range $T$	Com- bus- tion	$Q \text{ cm}^2$	Range $T$
O	$3.87 \cdot 10^{-15} - 0.87 \cdot 10^{-18} T + 0.689 \cdot 10^{-22} T^2$	$2 \cdot 10^3 < T < 5 \cdot 10^3$	N	$3.647 \cdot 10^{-15} - 0.94 \cdot 10^{-18} T + 0.88 \cdot 10^{-22} T^2$	$2 \cdot 10^3 < T < 5 \cdot 10^3$
O <sub>2</sub>	$0.31 \cdot 10^{-15} - 0.31 \cdot 10^{-19} T + 0.139 \cdot 10^{-22} T^2$	$2 \cdot 10^3 < T < 5 \cdot 10^3$	N <sub>2</sub>	$1.66 \cdot 10^{-17} T^{0.5}$	$600 < T < 10^4$
H	$0.63 \cdot 10^{-15} - 1.94 \cdot 10^{-17} T^{0.5}$	$600 < T < 10^4$	NO	$0.3388 \cdot 10^{-15} - 0.25 \cdot 10^{-19} T + 0.25 \cdot 10^{-22} T^2$	$2 \cdot 10^3 < T < 5 \cdot 10^3$
H <sub>2</sub>	$0.9 \cdot 10^{-17} T^{0.5} + 8.9 \cdot 10^{-16}$	$300 < T < 10^4$	NH <sub>3</sub>	$9.58 \cdot 10^{-12} T^{-1}$	$T < 10^4$
OH	$1.41 \cdot 10^{-11} T^{-1}$	$600 < T < 10^4$	CO	$1.29 \cdot 10^{-17} T^{0.5} + 2.46 \cdot 10^{-16}$	$T < 2.5 \cdot 10^4$
H <sub>2</sub> O	$1.53 \cdot 10^{-11} T^{-1}$	$T < 10^4$	CO <sub>2</sub>	$7.56 \cdot 10^{-14} T^{-0.5}$	$T < 10^4$
HCl	$4.79 \cdot 10^{-12} T^{-1}$	$T < 10^4$	K, Cs	$2.57 \cdot 10^{-12} T^{-0.5}$	$600 < T < 10^4$

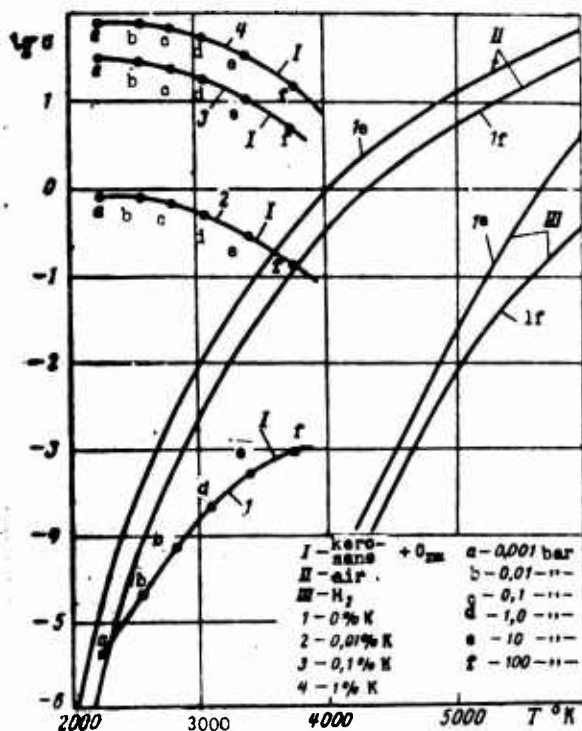


Fig. 7.5. Relationship of electrical conductivity of combustion (heating) products to the temperature at various pressures.

In the case of heterogeneous combustion products the calculation of electrical conductivity is substantially complicated, although the mechanism of electrical conductivity remains the same: electrical conductivity is determined by pulse losses during collisions of

electrons with condensed particles and gas particles. For exact calculation of electrical conductivity of heterogeneous combustion products it is necessary to know the distribution of condensed particles according to sizes, distribution of charges to particle, and also to consider the state of its surface.

### 7.7. Emissivities

At a temperature above absolute zero as a result of oscillations of atoms and of molecules, intensity of which is determined by the temperature, all substances possess the ability to emit radiant energy in the form of so-called quanta. By getting on some substance, the quantum can be reflected from it, but if the surface of the substance is not a "mirror", and the substance is not transparent, then most probably the quantum will be absorbed by some of the atoms (molecules) of the substance.

Let us assume some medium inside an evenly heated shell absorbs all the radiant energy getting on it, not reflecting or admitting anything. With equilibrium inside the shell the radiation of ideal absorber will be equal to the radiant energy getting on it, since otherwise its temperature increases or is decreased as compared to the temperature of neighboring media or walls of the shell. Nonideal absorber reflects or admits (or both) part of the radiant energy getting on it and therefore emits less than the ideal absorber. Consequently, the ideal absorber, called a black body, at assigned temperature in any section of the spectrum in a unit of time emits more energy than any other thermal radiator with the same area.

Radiation, being emitted by nonblack bodies, can be expressed as a certain portion of radiation, which is emitted by geometrically identical black bodies, being at the same temperature. This portion is called total hemispherical emissivity of a nonblack body  $\epsilon$ . Quantity  $\epsilon$  depends on many parameters, including the nature, shape, surface quality of the body being investigated, its temperature, and

also the length or range of wavelengths of the energy being emitted.

In contrast to solids the gas does not radiate heat in the entire range of wavelengths, but selectively - only in definite narrow ranges of the spectrum.

In rocket engines oscillatory-rotatory and purely rotatory bands of molecules of gases  $H_2O$ ,  $CO_2$ ,  $CO$ ,  $NO$ ,  $OH$  and  $HF$  make the basic contribution to radiation of gases; in this case triatomic gases radiate energy more intensively than diatomic.

In the case of thermal equilibrium (Kirchhoff law is assumed valid) total hemispheric emissivity of single-component gas is found by formula

$$\epsilon = \frac{1}{\sigma T^4} \int_0^\infty E(\omega) [1 - \exp\{-K(\omega, T, p, p_i) p_i l\}] d\omega, \quad (7.45)$$

where  $K(\omega, T, p, p_i)$  - attenuation factor of beam, equal to absorption coefficient for absorbing media;  $E(\omega)$  - radiation energy of black body;  $\sigma$  - Stefan-Boltzmann constant;  $l$  - length of path of beam;  $\omega$  - wave number.

As follows from formula (7.45), for theoretical calculation of emissivities of gas it is necessary to determine quantity

$$K(\omega, T, p, p_i)$$

depending on atomic or molecular parameters, and then calculate the integral. Exact solution of this problem with allowance for all factors is very complex. At the temperatures and pressures characteristic for intrachamber processes in contemporary rocket engines (RD), the determination of absorption coefficient of single-component gas, and also the mixture is facilitated by the fact that



1) the spectrum of absorption of molecules of gases consists of many completely overlapping lines;

2) oscillating spectral bands of the mixture of combustion products partially or completely overlap each other.

Total pressure, beginning from which the spectral lines of bands at temperature 290-300°K practically overlap and the emissivity  $\epsilon$  becomes relatively insensitive to total pressure, for  $H_2O \sim 3$  bar, for  $CO_2 \sim 1$  bar and for  $CO \sim 10$  bar [9], and at temperatures  $\sim 3000^\circ K$  in bands of molecule  $H_2O$  - at pressure  $\sim 1$  bar  $CO_2 \sim 0.1$  bar,  $CO \sim 1$  bar,  $HCl \sim 18$  bar,  $NO \sim 13$  bar,  $OH \sim 20$  bar and  $HF \sim 40$  bar [10].

For determination of the emissivity of these gases the analytical method [9] seems useful, involving the fact that each oscillating - rotational band of i-th gas is represented in the form of a rectangle with effective bandwidth  $\Delta\omega_{ij}$  and average index of absorption  $\bar{K}_{ij}(\omega)$ , being determined by molecular parameters at low temperature.

Results of calculations of  $\bar{K}_{ij}(\omega)$  for molecules of certain gases [10] are presented in the form of a summary chart on Fig. 7.6. Values of  $\bar{K}_{ij}(\omega)$  on the chart are determined at partial pressure of components equal to 1 bar.

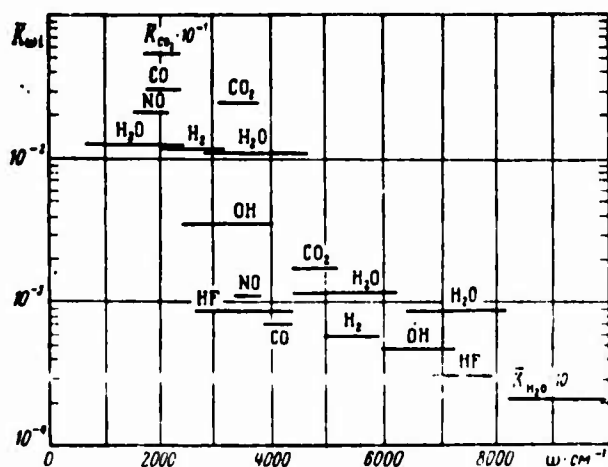


Fig. 7.6. Relationship of absorption  $\bar{K}_{ij}(\omega)$  for certain molecules.

Calculation of the emissivity of gas and mixture using  $\bar{K}_{ij}$  is in such order. Value of  $\bar{K}_{ij}(\omega)$  from the chart is multiplied by partial pressures:

$$\bar{K}_{ij}(\omega, p_i) = \bar{K}_{ij}(\omega) p_i, \quad (7.46)$$

then we correct according to temperature:

$$\bar{K}_{ij}(\omega, p_i, T) = \bar{K}_{ij}(\omega, p_i) \frac{3 \cdot 10^3}{T}. \quad (7.47)$$

The emissivity  $\epsilon$  of mixture of gases for the system of oscillating bands with allowance for their overlap is determined by formula

$$\epsilon = \sum_i \sum_j [1 - \exp[-\bar{K}_{ij}(\omega, p_i, T)] p_i] \frac{E_{\Delta\omega_{ij}} \Delta\omega_{ij}}{\sigma T^4}. \quad (7.48)$$

Here  $\Delta\omega_{ij}$  - interval of wave numbers of  $j$ -th oscillating band of  $i$ -th gas;  $E_{\Delta\omega_{ij}}$  - radiation energy of absolutely black body in the interval of wave numbers  $\Delta\omega_{ij}$ .

For engines which operate on propellants from C, H, O, N-elements the radiation of combustion products is caused primarily by the content of water vapors and carbon dioxide in them.

Taking into account radiation of only  $H_2O$  and  $CO_2$  the emissivity factory of the mixture is

$$\epsilon_r = \epsilon_{H_2O} + \epsilon_{CO_2} - \Delta\epsilon, \quad (7.49)$$

where quantity  $\Delta\epsilon$  considers that the intervals of wavelengths of radiation  $H_2O$  and  $CO_2$  partially coincide, i.e., radiation energy of  $H_2O$  is partially absorbed by  $CO_2$  and vice versa.

At temperatures exceeding  $1000^\circ\text{K}$  correction  $\Delta\epsilon$  in formula (7.49) can be considered as the product of emissivity factors of water vapor and carbon dioxide, i.e.,

$$\Delta\epsilon = \epsilon_{\text{H}_2\text{O}} \epsilon_{\text{CO}_2}. \quad (7.50)$$

Emissivities  $\epsilon_{\text{H}_2\text{O}}$  and  $\epsilon_{\text{CO}_2}$  over the range of temperatures  $2000-4000^\circ\text{K}$  can be determined by the charts of Figs. 7.7, 7.8, calculated while using the idea of effective bandwidth without allowing for the effect of total pressure [10].

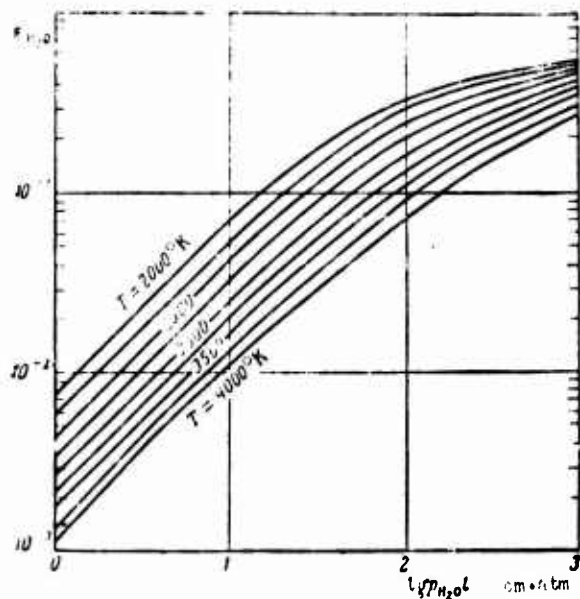


Fig. 7.7. Emissivity of water vapors

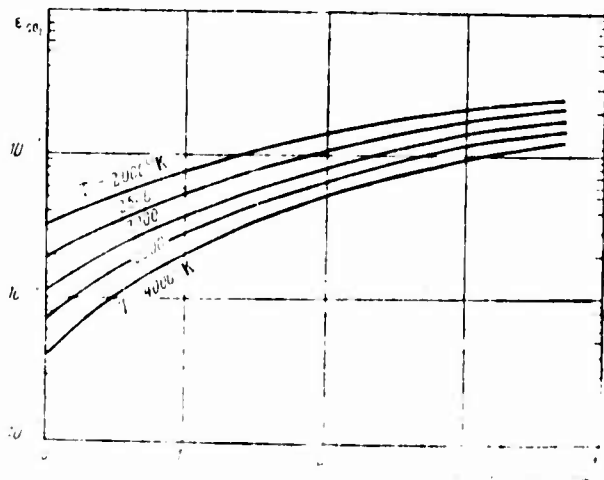


Fig. 7.8. Emissivity of carbon dioxide.

At specified values of  $p_1 l$  the emissivities of gases increase with increase of total pressure. When  $p_1 > 1$  bar they somewhat exceed the quantities obtained by using the accepted values of effective width of bands.

Quantity  $\epsilon_{H_2O}$  over the range of temperatures 1500-3000°K with allowance for the effect of total pressure can be determined by calculations of Ludwig and Ferrizo [20], quantity  $\epsilon_{CO_2}$  in this range - by results of [21].

The effect of surface configuration on  $\epsilon$ , inside which gas is included, i.e., length of beam path  $l$ , is expediently considered according to the method proposed by Khottel'. Khottel' examines radiant heat exchange between hemispherical gas body of radius  $l$  and a section in the center of its base, in this case the total length of each beam is equal to  $l$ . Any other gas body is replaced by equivalent hemispherical body - by hemisphere of radius  $l$ , radiating the same quantity of energy to its center that the real body radiates to the considered element. Values of  $l$  are usually listed in reference books.

In conclusion let us note the features of determination of emissivity of heterogeneous systems. The gas phase of combustion products for thermal radiation is homogeneous or can be assumed homogeneous and, consequently, the passing radiant thermal flow is only absorbed by the gas mixture. Liquid and solid particles of condensate of oxides  $Al_2O_3$ ,  $MgO$  and others, contained in combustion products, can withdraw energy from the flow of radiation both due to absorption and scattering. Thus, from the viewpoint of transfer processes of radiation energy the two-phase products of combustion should be considered as a light-diffusing medium.

As a result of scattering the spectra and angular distribution of radiation energy of two-phase products of combustion depend on a whole series of parameters: sizes of particles, indicatrix of

scattering, scattering and absorption coefficients, thickness of layer, angle of observation, etc.

Scattering includes a combination of effects of reflection, refraction and transfer of radiation by particles.

The scattered radiant energy is spread from the place of scattering just as the emitted energy from the place of radiation, i.e., in all directions in space - forward, to the sides and back, however not in all directions with identical intensity.

In a small volume of combustion products, containing a small quantity of particles, secondary effects of scattering can be disregarded. Radiant energy, scattered by this volume, will be equal to energy, scattered by one particle, multiplied by the number of particles in the volume. Such an effect is called single scattering. However, the energy is scattered two and more times more intensely in proportion to increase in volume, and, consequently, in proportion to increase in quantity of particles. This effect is called multiple scattering and is usually in the assignment of radiant heat exchange in the rocket engine chamber.

Scattering substantially complicates the analysis of transfer of radiation energy. Generally for determination of radiant heat flow from heterogeneous combustion products it is necessary to formulate equation of energy transfer through a small randomly arranged volume:

$$\frac{dI_l}{dl} = -[\alpha(\omega) + \beta(\omega)] I_l(\omega) + \frac{\beta(\omega)}{4\pi} \int_{\Omega} I_r(\omega) S(\vec{l}', \vec{l}) d\omega_r + E(\omega), \quad (7.51)$$

where  $I_l(\omega)$  - intensity of radiation energy in direction  $\vec{l}$ ;  $\alpha(\omega) + \beta(\omega) = K(\omega)$  - attenuation factor including absorption coefficient  $\alpha(\omega)$  and scattering factor  $\beta(\omega)$ ;  $I_{l'}(\omega)$  - intensity of incoming radiation in any direction  $\vec{l}'$ ;  $S(\vec{l}', \vec{l})$  - indicatrix of scattering radiation, representing angular distribution of scattered radiation

in a given place in different directions;  $\vec{r}$  - any direction of beam, from which the scattered radiation passes into the considered direction  $\vec{l}$  of energy transfer;  $\epsilon$  - emissivity of medium.

The physical meaning of transfer equation: change in intensity of radiant thermal flow on the element of length is made up of attenuation, caused by absorption and by scattering, of amplification due to radiation of medium and of amplification due to scattering of energy flows in this direction, which are spread in all other directions.

Solution of equation (7.51) is a complex mathematical task.

For calculation of coefficients of absorption and scattering, which enter equation (7.51) data are necessary on sizes of particles of condensate, and also data on optical properties of material of particles. Optical properties are characterized by complex index of refraction  $m$ :

$$m = n_1 - i n_2 \quad (7.52)$$

where  $n_1$  - index of refraction, and  $n_2$  - index of absorption.

At present the approximate data on optical properties the range of temperatures of interest to the technician are obtained only for particles of  $Al_2O_3$  and some other condensed products.

Investigations of the emissivity of combustion products of aluminumized propellants using approximate solutions of transport equation, and also using experimental data show that quantity  $\epsilon$  in the combustion chamber is within limits of 0.3-0.5.

#### Bibliography

1. Alemasov V. Ye., IVUZ, ser. "Aviatsionnaya tekhnika", 1967, vyp. 40.

2. Alemasov V. Ye., Dregalin A. F., Teplo- i massoperenos (Heat and mass transfer), t. 7, izd-vo "Nauka i tekhnika", Minsk, 1968.
3. Alemasov V. Ye. et al., Teplofizicheskiye svoystva zhidkostey i gazov pri vysokikh temperaturakh i plazmy (Thermophysical properties of liquids and gases at high temperatures and plasma), izd-vo Standartov, 1969.
4. Blokh A. G., Osnovy teploobmena izlucheniym (Fundamentals of heat exchange by radiation), Gosenergoizdat, 1962.
5. Vliyaniye fakela raketnykh dvigateley na radiosvyaz' s raketoy (obzor) (The effect of the flame of rocket engines on radio communication with the rocket (survey)), VRT, 1966, No. 8, 9.
6. Girshfel'der Dzh. et al., Molekulyarnaya teoriya gazov i zhidkostey (Molecular theory of gases and liquids), IIL, 1961.
7. Karapet'yants M. Kh., Khimicheskaya termodinamika (Chemical thermodynamics), Goskhimizdat, 1953.
8. Klabukov V. Ya., Sagadeyev V. I., Teplo- i massoperenoye (Heat and mass transfer), t. 5, izd-vo "Nauka i tekhnika", Minsk, 1968.
9. Penner S. S., Kolichestvennaya molekulyarnaya i izluchatel'naya sposobnost' gazov (Quantitative molecular power and emissivity of gases), IL, 1963.
10. Plastinin Yu. A., Fizicheskaya gazodinamika ionizirovannykh i khimicheskii reagiruyushchikh gazov (Physical gas dynamics of gases and chemically reacting gases), Collection of articles, izd-vo "Nauka", 1968.
11. Polyakov V. I., Rumynskiy A. N., Izv. AN SSSR, Mekhanika zhidkostey i gazov, 1968, No. 3.
12. Problemy dvizheniya golovnoy chasti raket dal'nego deystviya (Problems of motion of the nose section of long-range rockets), Collection of translations., IIL, 1959.
13. Frost L., VRT, 1962, No. 7.
14. Chepman S., Kauling T., Matematicheskaya teoriya neodnorodnykh gazov (Mathematical theory of heterogeneous gases), IL, 1961.
15. Shveyttser, Migner, "Raketnaya tekhnika i kosmonavtika", 1966, No. 6.
16. Sherman A., VRT, 1961, No. 4.

17. Adams J. M., J. Quant., Spectroscopy and Radiative Transfer, 1967, No. 3.
18. Bartky C. D., Bauer E., J. Spacecraft and Rockets, 1966, No. 10.
19. Brokaw R. S., Report NASA, R-81, 1960.
20. Ludwig C. B. et al., Spectroscopy and Radiative Transfer, 1967, No. 1.
21. Malkmus W., J. OSA, 1963, No. 8; 1964, No. 6.
22. Strunk M. R., Pensenfeld G. D., Am. Inst. Chem. Eng. J., 1965, No. 3.



## CHAPTER VIII

### THERMOGAS-DYNAMIC CALCULATION OF PROCESSES IN A CHAMBER

In the chapter are examined methods of thermo gas-dynamics calculation of basic processes in the chamber of an engine operating on chemical propellant: combustion and different variants of isentropic expansion.

The methods can be applied even for calculation of other types of heat rocket engines.

#### 8.1. Problems of Calculation and Basic Assumptions

In the chamber of a rocket engine, operating on chemical propellant, processes of combustion of propellant (section l-k on the diagram of Fig. 8.1) and expansion of combustion products (section k-c) are carried out.

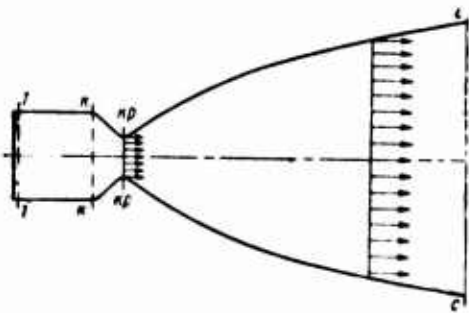


Fig. 8.1. Design diagram of the chamber of a rocket engine.

## Combustion

Calculation of combustion consists of determining the parameters of combustion products at the nozzle inlet. Total enthalpy of propellants and pressure in the combustion chamber are assigned.

It is customary to assume that at the nozzle inlet the state of combustion products is completely equilibrium. In connection with this the basis of calculation of combustion comprises determination of the equilibrium composition of working medium, examined in Chapter VI. In this case all the assumptions introduced into calculation of equilibrium composition are retained. Additional generally accepted assumptions during calculation of combustion are adiabaticity and steadiness of processes and also total heat liberation on the section of the combustion chamber.

Fundamental equation for the described model of the process is equation of conservation of energy, which can be written so:

$$I_k^* - I_T = 0. \quad (8.1)$$

Here  $I_k^*$  - total enthalpy of braked flow at the nozzle inlet;  $I_T$  - total enthalpy of propellant.

Total enthalpy of a unit of mass of propellant is considered as it is shown in Chapter V. For solid propellant quantity  $I_T$  is determined under conditions in the chamber of (PATT) [RDTT] solid-propellant rocket engine before the beginning of combustion, for liquid propellant - under conditions in fuel tanks. The latter not entirely obvious position can be proved by applying the equation of conservation of energy of propellant and of combustion products on the section from fuel tanks to the nozzle inlet (section k-k). Let us consider this section energy isolated, since heat exchange with the surrounding medium can be disregarded, and there are not other forms of energy exchange.

For (ЖРД) [ZhRD] liquid-propellant rocket engine with afterburning of generator gas in the basic chamber the equation of conservation of energy should be written so:

$$I_{OK}G_{OK} + I_{\Gamma}G_{\Gamma} + L_{H,OK}G_{OK} + L_{H,\Gamma}G_{\Gamma} - L_T(G_{OK1} + G_{\Gamma1}) = I_K^*(G_{OK} + G_{\Gamma}).$$

Here  $I_{OK}$ ,  $I_{\Gamma}$  - total enthalpies of fuel components in the tanks;  $G_{OK}$ ,  $G_{\Gamma}$  - total flow rates per second of components;  $G_{OK1}$ ,  $G_{\Gamma1}$  - flow rates per second of components in the first (gas-producing) stage of combustion chamber;  $L_{H,OK}$ ,  $L_{H,\Gamma}$  - energies imparted to components by pumps;  $L_T$  - work of the turbine.

Form energy balance in the turbopump unit it follows that

$$L_{H,OK}G_{OK} + L_{H,\Gamma}G_{\Gamma} = L_T(G_{OK1} + G_{\Gamma1}).$$

Therefore the equation of conservation of energy takes the form:

$$I_{OK}G_{OK} + I_{\Gamma}G_{\Gamma} = I_K^*(G_{OK} + G_{\Gamma}).$$

Having divided this expression by  $G_T = G_{OK} + G_{\Gamma}$  we obtain:

$$I_{OK}g_{OK} + I_{\Gamma}g_{\Gamma} = I_K^*,$$

i.e.,

$$I_T = I_K^*.$$

Analogous reasonings for liquid-propellant rocket engines without afterburning of generator gas lead to relationship

$$I_T + L_H = I_K^*.$$

Quantity  $L_H$  is energy imparted to fuel components in the pumps:

$$L_H = L_{H,OK}G_{OK} + L_{H,\Gamma}G_{\Gamma}.$$

This energy increase the total enthalpy of basic fuel components due to the enthalpy of auxiliary fuel, used in the gas generator. Increase in the enthalpy of basic components, equal to  $L_H$ , is small. Its computation cannot change the specific thrust obtained by calculation by more than tenths of a percent. This is usually disregarded and for liquid-fuel rocket engines without afterburning of generator gas we also take  $I_K^0 = I_T$ .

Two schemes of calculation of the combustion process can be of practical interest.

1. Combustion when  $p = \text{const}$  (isobaric combustion chamber).

Velocity of working medium on section 1-k is taken equal to zero ( $w_1 = w_k = 0$ ). This is responsible for equalities:

$$\left. \begin{aligned} p_1 &= p_i = p_k = p_k^0 \\ T_1 &= T_i^0 \end{aligned} \right\} \quad (8.2)$$

Equation of conservation of energy (8.1) takes particular form:

$$I_K - I_T = 0. \quad (8.3)$$

2. Combustion when  $p \neq \text{const}$  (nonisobaric combustion chamber).

On section 1-k the heat liberation is accompanied by substantial acceleration of the working medium ( $w_k \gg 0$ ) and by a drop of pressure. In connection with this the following relationships are valid:

$$\left. \begin{aligned} p_k &< p_i \\ p_k^0 &< p_i^0 \\ p_k &< p_k^0 \\ T_k &< T_k^0 \end{aligned} \right\} \quad (8.4)$$

Equation of conservation of energy (8.1) can be written:

$$I_0 + \frac{w_0^2}{2} - I_1 = 0. \quad (8.5)$$

### Expansion

The calculation of the expansion process also includes assumptions additionally utilized during calculation of equilibrium composition. The process is considered adiabatic and steady. There is assumed homogeneity of the composition and parameters of mixture along the section and one-dimensional flow, including parallelism of flow at the nozzle exit. For heterogeneous mixture there is assumed temperature equilibrium of gas and condensate ( $T_g = T_c$ ) and also high-speed equilibrium ( $w_g = w_c$ ). The absence of irreversible phenomena is assumed. Along with adiabaticity this assumption causes isentropicity of the expansion process.

The fundamental equation for such a model of the expansion process is equation of constancy of entropy:

$$s - s_0 = 0, \quad (8.6)$$

where  $s_0$  and  $s$  - entropy of unit of mass of combustion products at the nozzle inlet and in any section of the nozzle, respectively.

Different variants of expansion can be considered within the framework of isentropicity.

1. The completeness of equilibrium expansion (subsequently concisely called equilibrium expansion).

The real process of expansion is very frequently close to equilibrium, and that is why the scheme of equilibrium expansion is widely used in the practice of calculations.

2. Chemically "frozen" expansion or expansion with constant composition of working medium (concisely called frozen expansion).

Frozen expansion can occur under conditions when the rates of chemical reactions are small and the time the gas stays in the nozzle is not sufficient for their realization.

Calculation according to the scheme of frozen expansion is usually done in addition to calculation of equilibrium expansion. Results of these two calculations determine the range, inside which indices of the real process are found.

3. Expansion, equilibrium to a certain temperature, and further frozen.

The scheme of calculations with sudden freezing of the composition at a certain temperature can sometimes satisfactorily replace the very complex scheme of the real process with allowance for kinetics of chemical reactions.

#### 8.2. Calculation of Combustion in an Isobaric Chamber

In comparison with calculation of equilibrium composition at  $p, T = \text{const}$  an additional unknown is the combustion temperature  $T_K$ , and additional equation is the equation of conservation of energy (8.3).

The following means of calculation is natural. By the method described in Chapter VI we determine the equilibrium composition of working medium at prescribed pressure  $p_K$  and some value of temperature  $T$ . Values of  $T$  right up to true, satisfying the equation of energy, are improved by the Newton method, applied to equation (8.3). Equation of conservation of energy at arbitrary value of temperature  $T$  has the form:

$$I - I_T = \delta I.$$

By applying the Newton method to it we obtain

$$\left(\frac{\partial I}{\partial T}\right)_p \Delta T = -b_1$$

or

$$\Delta T = -\frac{b_1}{\left(\frac{\partial I}{\partial T}\right)_p} = -\frac{b_1}{c_p} \quad (8.7)$$

Derivative  $(\partial I/\partial T)_p$  may also be determined numerically:

$$\left(\frac{\partial I}{\partial T}\right)_p = \frac{I(T + \Delta T) - I(T)}{\Delta T}.$$

Refinement of temperature is carried out by formula

$$T^{(r+1)} = T^{(r)} + \Delta T^{(r+1)}, \quad (8.8)$$

where  $r$  - number of approximation. Approximations are fulfilled until achievement of the necessary accuracy.

One could use a more general and more economical method of calculation. Let us give this method for a general case of heterogeneous mixture. Initial system of equations consists of equations obtained earlier namely: equation of dissociation of uncondensed substances (6.3), equation of conservation of substance (6.11), equation of Dalton law (6.8), equation of dissociation of gas phase of substances in condensed state (6.12).

Furthermore, the system is supplemented by equation of conservation of energy, being written for  $\mu_T M_T$  kg of propellant and working medium:

$$\sum_q n_q I_q^0 + n_{12} I_{12}^0 + n_{13} I_{13}^0 - \mu_T M_T I_T = 0. \quad (8.9)$$

To closed system of equations (6.3), (6.11), (6.8), (6.12), (8.9) let us apply the Newton method, bearing in mind that a new unknown appeared - temperature, with respect to which differentiation must also be performed.

Appearance of the system after application of the Newton method in this instance is such:

$$\sum_i \left( \frac{\partial f_i}{\partial \ln n_i} \right) \Delta_i + \left( \frac{\partial f_i}{\partial \ln M_i} \right) \Delta_M + \left( \frac{\partial f_i}{\partial \ln T} \right) \Delta_T = -\delta_i, \quad (8.10)$$

where

$$\Delta_T = \Delta \ln T. \quad (8.11)$$

Solution of system of linear equations (8.10) permits finding the corrections to unknowns:  $\Delta_q$ ,  $\Delta_{qz}$ ,  $\Delta_M$ ,  $\Delta_T$ . Refinement of unknowns is performed just as when determining the composition. Thus a joint solution of the equations (6.3), (6.11), (6.8), (6.12), (8.9) permits determining both the equilibrium composition and temperature.

### 8.3. Calculation of Isentropic Equilibrium Expansion

Let us examine the calculation of different variants of equilibrium expansion within the framework of isentropicity.

#### Expansion up to Prescribed Pressure

The most commonly used variant of such calculation is calculation of the process of expansion from conditions in the combustion chamber up to prescribed pressure in the nozzle. The problem of calculation - determine the equilibrium composition of working medium and the temperature at this pressure. By these data one can determine the other necessary parameters.



For general case of heterogeneous system the unknowns are  $\ln n_q$  ( $\ln p_q$ ),  $\ln n_{sz}$ ,  $\ln n_{rz}$ ,  $\ln M_T$ ,  $\ln T$  - ( $l + m + 2$ ) quantities in all.

There are ( $l + m + 1$ ) equations of type (6.3), (6.11), (6.8), (6.12) and additionally - equation of constancy of entropy (8.6), in which quantity  $s_K$  is known after calculation of combustion.

One way of calculation consists of solution of system of equations (6.3), (6.11), (6.8), (6.12) at prescribed pressure  $p$  and assumed value of temperature  $T$ . The temperature is refined by the Newton method, being applied to equation (8.6). This gives:

$$\left( \frac{\partial s}{\partial \ln T} \right)_p \Delta \ln T = -\delta_s,$$

where  $\delta_s = s - s_K$  ( $s$  - entropy at accepted value of  $T$ ) and

$$\Delta \ln T = - \frac{\delta_s}{\left( \frac{\partial s}{\partial \ln T} \right)_p} = - \frac{\delta_s}{c_{pp}}. \quad (8.12)$$

The derivative can also be found numerically.

From approximation ( $r$ ) to approximation ( $r + 1$ ) the temperature is refined by formula

$$(\ln T)^{(r+1)} = (\ln T)^{(r)} + \Delta \ln T^{(r+1)} \quad (8.13)$$

until achievement of the prescribed accuracy.

A more economical method of calculation of expansion is provided by joint solution of system of equations (6.3), (6.11), (6.8), (6.12) and (8.6) and simultaneous determination of the composition and temperature.

### Expansion to Prescribed Temperature

If the temperature of the end of expansion  $T$  has been prescribed, then the pressure of working medium  $p$  corresponding to this temperature becomes unknown.

Analogous to the case of calculation of expansion to prescribed pressure, one means of calculation is to determine the equilibrium composition at prescribed temperature  $T$  and approximate value of pressure  $p$ , and then refine the solution by Newton method, applying it to equation of entropy (8.6).

At assignment of approximate value  $p$  the equation of constancy of entropy is not satisfied:

$$s(\ln p) - s_k = \delta_s.$$

According to the Newton method

$$\Delta \ln p = - \frac{\delta_s}{(\partial s / \partial \ln p)_T}. \quad (8.14)$$

Derivative  $(\partial s / \partial \ln p)_T$  is either determined numerically, or is reduced to the form (see Table 7.1):

$$\left( \frac{\partial s}{\partial \ln p} \right)_T = p \left( \frac{\partial s}{\partial p} \right)_T = - p \left( \frac{\partial v}{\partial T} \right)_p = - p v \alpha_p$$

or

$$\left( \frac{\partial s}{\partial \ln p} \right)_T = - \frac{p v}{T} \left[ 1 - \left( \frac{\partial \ln \mu}{\partial \ln T} \right)_p \right] = - \frac{R_0}{\mu} \left[ 1 - \left( \frac{\partial \ln \mu}{\partial \ln T} \right)_p \right].$$

Then

$$\Delta \ln p = \frac{\delta_s \cdot \mu}{R_0 \left[ 1 - \left( \frac{\partial \ln \mu}{\partial \ln T} \right)_p \right]}. \quad (8.15)$$

Refinement is performed until the prescribed accuracy has been attained.

The second variant of calculation is provided by joint solution of equations of association uncondensed substances, equations of conservation of substance, equations of dissociation of gas phase of substances in condensed state and equation of constancy of entropy. Since the temperature is assigned, corrections  $\Delta_{qp}$  are absent in correction equations.

#### Expansion to Prescribed Number M

A feature of this variant of calculation consists of the fact that both pressure and temperature were earlier unknowns. Let us use the system of equations of the variant of calculation to prescribed pressure, with the exception of equation of Dalton law. It consists of  $(l + m + 1)$  equations of type (6.3), (6.11), (6.12), (8.6). Number of unknowns is  $l + m + 2$ .

The equation closing the system in the equation of conservation of energy, being written for 1 kg of mixture in the form

$$I + \frac{w^2}{2} - I_r = 0.$$

Having multiplied and divided the second term by the square of equilibrium speed of sound, we obtain

$$I + M^2 \frac{a_p^2}{2} - I_r = 0.$$

Having returned to expression (7.19), let us write

$$I + M^2 \frac{k_p R_p T}{2\mu \left[ 1 + \left( \frac{\partial \ln \mu}{\partial \ln p} \right)_T \right]} - I_r = 0. \quad (8.16)$$

Common solution of system of equations (6.3), (6.11), (6.12), (8.6) and (8.16) by Newton method allows determining the equilibrium composition and temperature. Pressure is determined by equation of Dalton law.

### Expansion to Local Speed of Sound ( $M = 1$ )

Calculation of expansion to local speed of sound is necessary for accurate determination of flow parameters in the nozzle throat.

It is obvious that this calculation can be performed as a particular case of the previous variant when  $M = 1$ .

Let us give an additional means of determination of parameters in the nozzle throat. It is known that pressure in this section is approximately  $(0.53-0.57) p_K^*$ . Having prescribed the value of  $p_{kp}$  from this range, by the method examined earlier it is possible to calculate equilibrium expansion to prescribed pressure and find approximate value of  $T_{kp}$  and other parameters. Further refinement of the amount of pressure is performed with the aid of equation (8.16), to which the Newton method is applied. Equation (8.16) in general form can be written so:

$$\varphi(p, s) = 0.$$

By applying the Newton method and considering that as a result of isentropicity  $ds = 0$ , let us write:

$$\Delta p = - \frac{\varphi(p, s)}{\left(\frac{\partial \varphi}{\partial p}\right)_s}. \quad (8.17)$$

The denominator of equation (8.17) can be found with the aid of Table 7.1, in this case in the interval of change of pressure  $\Delta p$  quantities  $k_p$ ,  $\mu$ ,  $(\partial \ln \mu / \partial \ln p)_T$  can be considered constants. As a result we obtain the calculation expression for  $\Delta p$ :

$$\Delta p = \frac{p \nu}{R_0 T} \frac{I_T - I - \frac{a_p^2}{2}}{1 + \frac{a_p a_p^2}{2 c_{pp}}}. \quad (8.18)$$

Pressure is refined by formula

$$p^{(r+1)} = p^{(r)} + \Delta p^{(r+1)},$$

after which calculation of isentropic expansion to prescribed pressure  $p^{(r+1)}$  is repeated. The entire calculation is finished after obtaining the prescribed accuracy with respect to pressure:

$$\Delta p < \omega,$$

where  $\omega$  - permissible error of calculation prescribed in advance.

#### Expansion to Prescribed Relative Area

Characteristic quantities of any section of the chamber passage are: relative area of section (for nozzle - geometrical expansion ratio of nozzle)

$$f = \frac{F}{F_{kp}}; \quad (8.19)$$

[Translator's note:  $kp$  = throat]

specific area of section

$$F_{ya} = \frac{F}{G}. \quad (8.20)$$

[Translator's note:  $ya$  = specific]

It is obvious that

$$f = \frac{F_{ya}}{F_{ya,kp}},$$

and on the basis of continuity equation

$$f = \frac{(Qw)_{kp}}{Qw}. \quad (8.21)$$

The considered variant of calculation allows determining flow parameters in the nozzle section with prescribed quantities  $f^0$  or  $F_{y\lambda}^0$ .

It is necessary to solve equation

$$f = f^0$$

or

$$F_{y\lambda} = F_{y\lambda}^0, \quad (8.22)$$

since at prescribed pressure in the combustion chamber quantity  $F_{y\lambda, \text{кр}}$  is constant. The value of  $F_{y\lambda}^0$  is determined according to prescribed relative area  $f^0$  and quantity  $F_{y\lambda, \text{кр}}$ , which is known after calculation of expansion to  $M = 1$ :

$$F_{y\lambda}^0 = \frac{f^0}{(q\psi)_{\lambda p}}, \quad (8.23)$$

Specific area  $F_{y\lambda}$  depends on the pressure and temperature in the given nozzle section; equation of state and general thermodynamic relationships allow use of other quantities as arguments.

Relationship

$$\ln F_{y\lambda} = \varphi(\ln p, s)$$

is close to linear, therefore equation (8.22) is expediently represented in the form

$$\varphi(\ln p, s) = \ln F_{y\lambda} - \ln F_{y\lambda}^0. \quad (8.24)$$

By applying the Newton method and taking into account that as a result of isentropicity  $ds = 0$ , let us write

$$\Delta \ln p = \frac{\ln F_{y\lambda}^0 - \ln F_{y\lambda}}{(\partial \ln F_{y\lambda} / \partial \ln p)_s}.$$

Derivative  $(\partial \ln F_{yA} / \partial \ln p)_s$  can be determined numerically or with the aid of thermodynamic relationships. The last way is preferable. By using equation of conservation of energy in the form

$$I + \frac{w^2}{2} - I_T = 0,$$

let us represent  $\ln F_{yA}$  so:

$$\ln F_{yA} = -\ln q - \ln \sqrt{2(I_T - I)}.$$

Now with the aid of Table 7.1 it is possible to write

$$\left( \frac{\partial \ln F_{yA}}{\partial \ln p} \right)_s = \frac{R_0 T}{\mu} \left( \frac{1}{w^2} - \frac{1}{a_p^2} \right),$$

and the final expression for  $\Delta \ln p$  takes the form:

$$\Delta \ln p = \frac{\ln F_{yA}^0 - \ln F_{yA}}{\frac{R_0 T}{\mu} \left( \frac{1}{w^2} - \frac{1}{a_p^2} \right)}. \quad (8.25)$$

Calculation of expansion to prescribed relative area  $f^0$  can be completed in such a sequence. Let us designate the assumed value of  $p^{(0)}$  (for example, with the aid of tables of gas-dynamic functions) and let us calculate expansion to prescribed pressure. As a result let us determine all the thermodynamic characteristics and properties at pressure  $p^{(0)}$ . By formula (8.25) let us compute logarithmic correction  $\Delta \ln p$  and let us refine the quantity of pressure

$$\ln p^{(1)} = \ln p^{(0)} + \Delta \ln p^{(1)}.$$

After this the calculation of expansion to assigned pressure, etc., is repeated until the required accuracy with respect to quantity  $f$  is attained.

#### 8.4. Calculation of Isentropic Frozen Expansion

Chemically frozen expansion is taken as expansion with constant composition of working medium. If we consider frozen expansion from some initial known conditions up to pressure  $p$ , then the constancy of composition can be written in the following manner:

$$\frac{p_{q \text{ нач}}}{p_q} = \frac{p_{\text{нач}}}{p} = \frac{M_{T, \text{нач}}}{M_T} = \pi, \quad (8.26)$$

$$\frac{n_{rz \text{ нач}}}{n_{rz}} = \frac{n_{sz \text{ нач}}}{n_{sz}} = \pi. \quad (8.27)$$

[Translator's note: нач = initial]

In expressions (8.26) and (8.27)  $\pi$  - assigned quantity. Relationship (8.27) follows from condition

$$z_q = \text{const},$$

where  $z_q$  - weight fraction of  $q$ -th condensed product, determined by expression (6.32).

Inasmuch as the composition of working medium and quantity  $M_T$  are determined by relationships (8.26) and (8.27), there is no need to solve complex system of equations of chemical equilibrium with refinement of temperature or pressure. Unique unknowns are: temperature - during calculation of expansion to prescribed pressure, pressure - during calculation of expansion to prescribed temperature, or temperature and pressure during calculation of expansion to  $M = 1$  and to  $f^0$ . For their determination we use equations (8.12), (8.15), (8.18) and (8.25) respectively.

As the basis for calculation of frozen expansion to various conditions (pressure, temperature, number  $M$  or  $f^0$ ), as in the case of equilibrium expansion, there can be used calculation of expansion to prescribed pressure. Let us examine this variant in more detail.



In accordance with formula (8.12) in case of working medium of constant composition it is possible to write

$$\Delta T = \frac{T(s_{\text{HAY}} - s)}{c_{p3}},$$

where  $s_{\text{HAY}}$  - known quantity of entropy of 1 kg of working medium.

Entropy and frozen thermal capacity of the mixture are determined by formulas (7.3) and (7.13). Let us substitute initial values of  $n_q$  ( $p_q$ ),  $n_{sz}$ ,  $n_{rz}$ ,  $M_T$  in them by formulas (8.26) and (8.27). After simple conversions we obtain:

$$\begin{aligned} \Delta T = & \frac{T \left[ \mu_T (M_1 s)_{\text{HAY}} - \sum_q n_{q \text{ HAY}} S_q^0 - R_0 p_{\text{HAY}} \ln \pi \right]}{\sum_q n_{q \text{ HAY}} C_{pq} + n_{rz \text{ HAY}} C_{rz} + n_{sz \text{ HAY}} C_{sz}} + \\ & + \frac{T \left[ R_0 \sum_q n_{q \text{ HAY}} \ln n_{q \text{ HAY}} - n_{rz} S_{rz}^0 - n_{sz} S_{sz}^0 \right]}{\sum_q n_{q \text{ HAY}} C_{pq} + n_{rz \text{ HAY}} C_{rz} + n_{sz} C_{sz}}, \end{aligned} \quad (8.28)$$

where entropy and thermal capacity of gas ( $S_q^0$ ,  $C_{pq}$ ) and condensed ( $S_{rz}^0$ ,  $S_{sz}^0$ ,  $C_{rz}$ ,  $C_{sz}$ ) phases are calculated at temperature  $T$ .

The temperature is refined until achievement of the prescribed accuracy. In zero approximation the value of  $T$  can be estimated by isentropic equation of type

$$T = \pi^{\frac{1-\gamma}{\gamma}} T_{\text{HAY}},$$

using tentative values of mean isentropic index of expansion.

Conversion of formulas (8.13), (8.18) and (8.25) for calculation of other variants of frozen expansion is performed similar to that described above.

By combining the variants given in this paragraph, other schemes of the process besides the examined can be calculated. Thus, for

instance, the scheme with sudden freezing is described by equilibrium expansion to prescribed temperature or pressure (depending on whether conditions of freezing have been specified) and further by frozen.

#### 8.5. Calculation of Combustion in Nonisobaric Cylindrical Chamber

Nonisobaric, or high-speed, as they are still called, combustion chambers are characterized by small values of relative area of combustion chamber

$$f_k = \frac{F_k}{F_{kp}}. \quad (8.29)$$

[Translator's note:  $k$  = chamber]

Under identical initial conditions in section 1-1 (see Fig. 8.1) the parameters of working medium at nozzle inlet (section  $k-k$ ) will be different depending on values of  $f_k$ . When  $f_k = 1$  the working medium in section  $k-k$  reaches critical velocity.

For calculation of combustion in nonisobaric chamber, besides total enthalpy of propellant  $I_T$  and pressure  $p_1$ , the quantity of relative area of combustion chamber  $f_k$  must be prescribed.

For determination of the equilibrium composition of working medium, its properties and temperature in section  $k-k$  it is possible to write the following equations: equations of dissociation of uncondensed substances (6.3), equations of conservation of substance (6.11), equations of dissociation of gas phase of substances in condensed state (6.12). Equation of Dalton law cannot be used, inasmuch as pressure  $p_k$  is unknown earlier. Let us use the equation of pulses, written for a section of cylindrical pipe between sections 1-1 and  $k-k$ :

$$\rho_1 + \rho_1 w_1^2 = \rho_k + \rho_k w_k^2. \quad (8.30)$$

Having designated known quantities

$$p_1 + \rho_1 w_1^2 = p_F$$

and bearing in mind that

$$p_K = \sum_q p_q$$

Let us write equation of pulses so:

$$\sum_q p_q + \rho_K w_K^2 = p_F. \quad (8.31)$$

Finally, one ought use equation of energy. For nonisobaric combustion chamber it was written in form (8.5). By using expression (7.1) for enthalpy of working medium, we obtain

$$\frac{\sum_q p_q I_q^0 + n_{rz} I_{rz}^0 + n_{sz} I_{sz}^0}{\mu_1 M_1} + \frac{w_K^2}{2} - I_1 = 0$$

or

$$\sum_q p_q I_q^0 + n_{rz} I_{rz}^0 + n_{sz} I_{sz}^0 + \mu_1 M_1 \frac{w_K^2}{2} - \mu_1 M_1 I_1 = 0. \quad (8.32)$$

Thus, there are  $(l + m + 2)$  equations for determination of  $(l + m + 3)$  unknowns: equations (8.31) and (8.32) include an additional unknown - velocity  $w_K$ . The system of equations can be closed by use of equation of continuity, written for section  $K-K$  and throat.

The solution consists of finding the values of  $w_K$  at which the system is valid.

Let us write continuity equation for sections  $K-K$  and  $KP-KP$ :

$$\rho_K w_K F_K = \rho_{KP} w_{KP} F_{KP}$$

or

$$Q_k w_k = \frac{c}{f_k}, \quad (8.33)$$

where

$$c = Q_k w_{kp}. \quad (8.34)$$

According to equation of state and with allowance for relationship (6.33)

$$Q_k = \frac{p_k \mu_k}{R_0 T_k} = \frac{u_T M_T}{R_0 T_k}. \quad (8.35)$$

Let us write equation (8.31) in the form

$$\sum_q p_q + \frac{(Q_k w_k)^2}{Q_k} = p_F.$$

Then with allowance for expressions (8.33) and (8.35), we obtain:<sup>1</sup>

$$\sum_q p_q + d \frac{T}{M_T} = p_F, \quad (8.36)$$

where

$$d = \frac{c^2}{f_k^2} \frac{R_0}{\mu_T}.$$

In logarithmic form the equation of pulses looks like:

$$\ln \left( \sum_q p_q + d \frac{T}{M_T} \right) - \ln p_F = 0. \quad (8.37)$$

Let us also convert equation of energy, using relationships (8.33), (8.35):

---

<sup>1</sup>When writing the equations, which determine composition and temperature of working medium in section κ-κ criterion of the section - index "κ" is dropped here and further.

$$\sum_q p_q I_q^0 + n_{rz} I_{rz}^0 + n_{sz} I_{sz}^0 + R_0 d \frac{T^2}{2M_T} - p_T M_T I_T = 0. \quad (8.38)$$

3) To system of equation (6.3), (6.11), (6.12), (8.37) and (8.38) we can apply the Newton method and obtain equations that are linear relative to corrections:  $\Delta_q$ ,  $\Delta_{rz}$ ,  $\Delta_{sz}$ ,  $\Delta_M$ ,  $\Delta_T$ .

4) Algorithm of the solution of the system is the following.

on- We assigned initial values of unknowns  $p_q$ ,  $n_{rz}$ ,  $n_{sz}$ ,  $M_T$  (randomly) and quantities  $c$ , indirectly characterizing the velocity of working medium  $w_K$ . In zero approximation the value of quantity  $c$ , assigned by formula (8.34), is taken according to calculation of isobaric chamber ( $f_K = \infty$ ). Equilibrium composition and flow parameters at the nozzle inlet are determined.

5) By the found data we calculated the entropy of working medium and calculated equilibrium expansion to local speed of sound. We found new parameters of the throat and, consequently, new value of quantity  $c$ , which is introduced into calculation of the following approximation, etc. Calculation is repeated until in the neighboring approximations the values of control parameter in the nozzle throat coincide with prescribed accuracy. Such a parameter can be temperature, pressure or velocity.

6) After termination of approximations the parameters of working medium at the nozzle inlet are determined by the following formulas:

$$p_K = \sum_q p_{qK}; \quad \mu_K = \frac{\mu_T M_T}{p_K}; \quad Q_K = \frac{p_K \mu_K}{R_0 T_K},$$

$$w_K = \frac{Q_K p_{Kp}}{Q_K f_K} \quad \text{or} \quad w_K = \sqrt{2(I_T - I_K)}.$$

tem- on - It is interesting to determine total head values of working medium at the nozzle inlet. For this the isentropic equilibrium stagnation of working medium to  $w_K = 0$  must be calculated. The

process is described by equations of dissociation and conservation of substance of type (6.3), (6.11), (6.12), by equation of energy of type (8.1) and by equation of constancy of entropy of type (8.6). Solution of the system gives the equilibrium composition of stagnation working medium, quantity  $M_T$  and the value of stagnation temperature  $T_K^*$ . Stagnation pressure is determined by usual formula:

$$p_K^* = \sum_q p_{qK}^*$$

Calculation of high-speed combustion chamber is more general with respect to calculation of isobaric combustion chamber. The latter is obtained as a particular case, if in the calculation of high-speed combustion chamber we assume  $f_K = \infty$ .

After the conditions at the end of the high-speed combustion chamber (at the nozzle inlet) have been determined, it is possible to consider different variants of expansion by usual methods.

#### 8.6. Thermodynamic Calculation with the Aid of Diagrams and Nomograms

Results of completed thermodynamic calculations can be represented not only in particular form for each concrete problem, but also in more general form - in the form of thermodynamic diagrams or nomograms, which are conveniently used with repeated change of initial data.

Each diagram characterizes one particular propellant or working substance. For liquid rocket propellants the diagram corresponds to the determined excess oxidant ratio  $\alpha$ .

Figure 8.2 contains I-s-diagram for combustion products of kerosene with oxygen when  $\alpha = 0.7$ . The calculation course according to the diagram is the following. The point characterizing the state of combustion products in the combustion chamber is determined by

prescribed pressure  $p_K^*$  and by the quantity of total enthalpy of propellant  $I_T$  (for example, point A on the diagram of Fig. 8.2). It gives the value of temperature  $T_K^*$ .

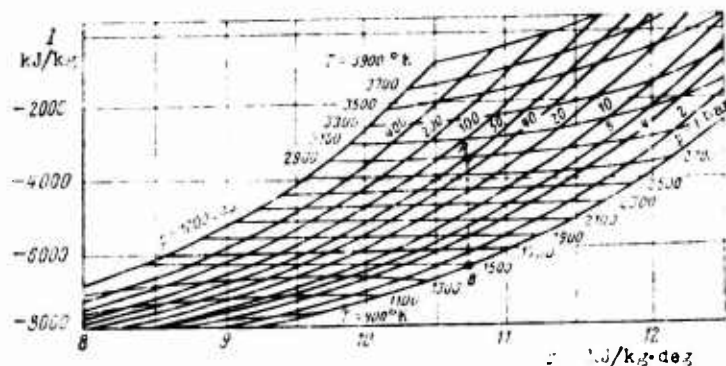


Fig. 8.2. I-s - diagram for combustion products of kerosene with oxygen ( $\alpha = 0.7$ ).

The state of working medium at the nozzle exit ( $I_c$  and  $T_c$ ) is determined by prescribed pressure at the nozzle exit  $p_c$  and by the value of entropy  $s_c = s_K$  (point B on the diagram of Fig. 8.2).

The rate of equilibrium outflow is determined by usual formula, or directly found on a special scale. With the aid of the diagram, the diagram of the exit section of the nozzle and thermal capacity of gas can be rapidly found. All this can be determined at various combinations of pressures  $p_K^*$  and  $p_c$ . The advantage of the diagram also consists in the fact that it allows determining the characteristic parameters with change of initial enthalpy of propellant (its preheating or cooling, refinement of heat of formation, etc.). The main disadvantage is the limitedness of each diagram by some particular composition of propellant. This does not always justify the large expenditures of labor and time for its formulation.

The entropy diagrams for working substances, which were undergoing heating from an independent source of energy (for example, in nuclear engines) have wider value. One such a diagram can

characterize the capabilities of this substance in a very wide pressure and temperature range. Example of such a diagram for hydrogen is on Fig. 8.3 [5]. The diagram contains lines, showing the degree thermal dissociation and ionization of the working medium.

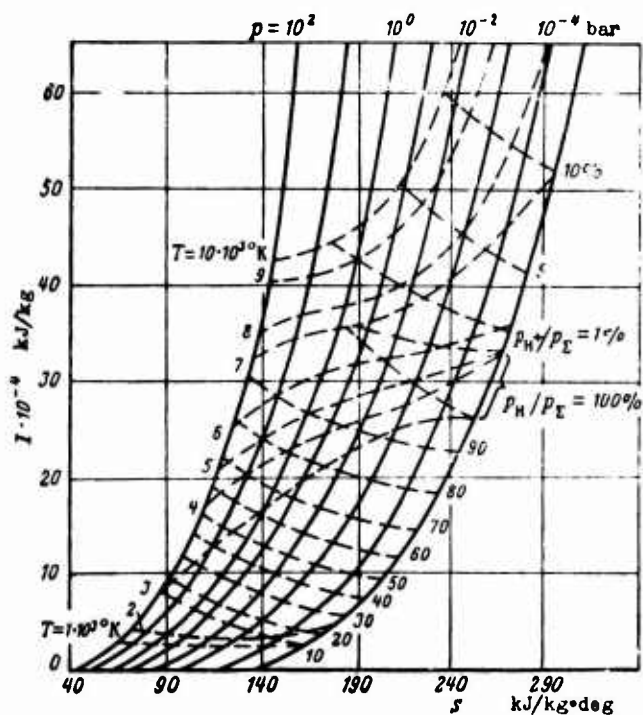


Fig. 8.3. I-s - diagram for hydrogen.

For thermodynamic calculation of a rocket engine use can also be made of nomograms, representing a compact unification of charts of basic relationships for the given propellant or class of propellants. Nomograms have the same disadvantages as thermodynamic diagrams with respect to labor input of formulation and the limitednesses of characteristics being represented.

#### Bibliography

1. Alemasov V. Ye., IVUZ, ser. "Aviatsionnaya tekhnika", 1967, vyp. 40.



2. Alemasov V. Ye., Tishin A. P., IVUZ, ser. "Aviatsionnaya tekhnika", 1958, vyp. 2.

3. Bolgarskiy A. V., Raschet protsessov v kamere sgoraniya i sople zhidkostnogo raketnogo dvigatelya (Calculation of processes in the combustion chamber and nozzle of a liquid-propellant rocket engine), Oborongiz, 1957.

4. Vanichev A. P., Termodinamicheskiy raschet goreniya i istecheniya v oblasti vysokikh temperatur (Thermodynamic calculation of combustion and outflow in the high-temperature range), BNT, 1947.

5. Zenger-Bredt I., Nekotoryye svoystva vodoroda i vodyanogo para - vozmozhnykh rabochikh tel raket (Some properties of hydrogen and water vapor - possible working media of rockets), IIL, 1962.

6. Mel'nikov M. V., Vliyaniye formy kamery sgoraniya i sople na gyagu ZhRD (Effect of the shape of combustion chamber and nozzle on liquid-propellant rocket engine thrust), BNT, 1946.

## CHAPTER IX

### DETERMINATION OF THERMODYNAMIC CHARACTERISTICS

1f

In the chapter are listed working formulas for determining thermodynamic characteristics, methods of their extrapolation and interpolation are given. Initial data are results of thermodynamic calculation of processes in the chamber.

#### 9.1. Determination of Thermodynamic Characteristics in Terms of Data of Detailed Calculation

After fulfillment of thermogas-dynamic calculation under prescribed conditions in any section of the chamber the flow parameters  $p$ ,  $T$ ,  $\rho$ ,  $v$ ,  $I$ , and also the composition and other properties on the working medium are known. With the aid of these quantities one can determine the thermodynamic characteristics.

Velocity of combustion products in an arbitrary section

$$w = \sqrt{2(I_1 - I)} \text{ m/s}, \quad (9.1)$$

if  $I$  is in J/kg.

Specific chamber section area

$$F_{y1} = \frac{F}{G} = \frac{1}{w\rho} = \frac{R_0 T}{w p} \text{ m}^2 \cdot \text{s/kg}, \quad (9.2)$$

if  $R_0$  is in J/mole·deg;  $w$  is m/s,  $p$  is in N/m<sup>2</sup>.

Relative chamber area

$$f = \frac{F}{F_{xp}} = \frac{F_{ya}}{F_{ya, xp}} \quad (9.3)$$

Specific thrust in a void

$$P_{ya, u} = w_c + F_{ya, c} \cdot p_c \quad \text{N} \cdot \text{s/kg} \quad (9.4)$$

if

$$w_c \text{ is in m/s; } F_{ya, c} \text{ is in m}^2 \text{ s/kg; } p_c \text{ is N/m}^2.$$

Specific thrust at altitude h

$$P_{ya, h} = P_{ya, u} - F_{ya, c} p_h \quad (9.5)$$

Specific thrust at condition  $p_c = p_h$

$$P_{ya} = P_{ya, u} - F_{ya, c} p_c \quad (9.6)$$

Specific pulse of pressure in the chamber (expenditure complex)

$$\beta = \frac{p_c^* F_{xp}}{G} = p_c^* F_{ya, xp} = \frac{p_c^*}{p_{xp}} \frac{R_0 T_{xp}}{w_{xp} \mu_{xp}} \quad \text{N} \cdot \text{s/kg} \quad (9.7)$$

Thrust coefficient

$$K_p = \frac{P_{ya}}{\beta} \quad (9.8)$$

By using formulas (9.4)-(9.6), one can determine the thrust coefficient in a void, at altitude  $h$  and when  $p_c = p_h$ .

The process of equilibrium expansion from pressure  $p_k^*$  to pressure  $p$  is often characterized by mean index of isentrope of expansion  $n$ . The process is conditionally described by equation  $pv^n = \text{const}$ , in connection with which

$$p_k v_k^n = p v^n. \quad (9.9)$$

Mean index of isentrope, being determined according to the connection between pressure and specific volume, in case of a reacting working medium depends not only on pressure and temperature at finite points of the process, but also on molecular weight at these points. With allowance for equations of state quantity  $n$  is determined by formula

$$n = \frac{\ln \frac{p_k^*}{p}}{\ln \frac{p_k^*}{p} \frac{RT}{R_k T_k^*}}. \quad (9.10)$$

When  $p = p_{kp}$  and  $RT = R_{kp} T_{kp}$  we obtain the value of  $n$ , approximating the expansion process on the section of the nozzle before the throat; when  $p = p_c$  and  $RT = R_c T_c$  index  $n$  approximates the expansion process from the nozzle inlet to the section.

#### 9.2. Determination of Thermodynamic Characteristics with Respect to Gas-Dynamic Relationships

Approximate values of parameters, necessary in the precomputation and analysis stage, can be obtained with the aid of mean index of isentrope  $n$ , determined by formula (9.10) for the process of expansion between pressures  $p_k^*$  and  $p$ .

When determining parameters of the subsonic part of the nozzle the best results are obtained with use of  $n$ , calculated by drop of  $p_k^*/p_{kp}$ ; when determining parameters in the supersonic part - by drop of  $p_k^*/p_c$ .

The basis of the formulas is equation (9.9), equation of state and usual gas-dynamic relationships:

$$w = \sqrt{2 \frac{n}{n-1} R_k T_k^* \left[ 1 - \left( \frac{p}{p_k^*} \right)^{\frac{n-1}{n}} \right]}; \quad (9.11)$$

$$\frac{R_{kp} T_{kp}}{R_k T_k^*} = \frac{2}{n+1}; \quad (9.12)$$

$$\frac{p_{kp}}{p_k^*} = \left( \frac{2}{n+1} \right)^{\frac{n}{n-1}}. \quad (9.13)$$

where  $R_k$  is in J/kg·deg.

#### Isobaric Chamber

The velocity of combustion products at the nozzle section is determined by substitution of  $p = p_c$  in equation (9.11). The velocity of gas in the throat with allowance for equations (9.11) and (9.13) is usually written in the form

$$w_{kp} = \sqrt{\frac{2n}{n+1} R_k T_k^*}. \quad (9.14)$$

If instead of pressure at the edge or in any other section of the nozzle relative area  $f$  has been prescribed, then for determination

of ratio  $p/p_n^*$  use can be made of known gas-dynamic relationships [3]:

$$\left. \begin{aligned} f &= \frac{F}{F_{kp}} = \frac{1}{q(\lambda)}; \\ \frac{p}{p_n^*} &= \pi(\lambda), \end{aligned} \right\} \quad (9.15)$$

where  $q(\lambda)$  and  $\pi(\lambda)$  - gas-dynamic functions of reduced velocity  $\lambda$ , determined by tables at prescribed  $n$  and  $f$ .

Gas flow rate per second through the nozzle is equal to

$$G = F_{kp} w_{kp} \rho_{kp}.$$

By applying formulas (9.12)-(9.14), we obtain

$$G = A(n) \frac{p_n^* F_{kp}}{\sqrt{R_k T_k^*}}, \quad (9.16)$$

where

$$A(n) = \left( \frac{2}{n+1} \right)^{\frac{n+1}{2(n-1)}} \sqrt{n}. \quad (9.17)$$

The specific area of nozzle sections can be determined with the aid of formulas (9.2), (9.15) and (9.16). As a result we obtain

$$\begin{aligned} F_{ya, kp} &= \frac{\sqrt{R_k T_k^*}}{A(n) \rho_n^*}; \\ F_{ya} &= \frac{F_{ya, kp}}{q(\lambda)}. \end{aligned}$$

Having values of quantities  $w_c$ ,  $p_c$ ,  $F_{уд.с}$ ,  $F_{уд.кр}$  by formulas (9.4)–(9.8) specific thrusts  $P_{уд.п}$ ,  $P_{уд.н}$ ,  $P_{уд}$ , and also complex  $\beta$  and coefficient of thrust  $K_p$  can be calculated. Basic quantities are written so:

$$\beta = p_c^* F_{уд.кр} = \frac{V R_k T_k^*}{A(n)}; \quad (9.18)$$

$$P_{уд.н} = \sqrt{\frac{2(n+1)}{n} R_k T_k^*} z(\lambda_c), \quad (9.19)$$

where

$$z(\lambda_c) = \frac{G w_c + p_c F_c}{G w_{кр} + p_{кр} F_{кр}} = \frac{1}{2} \left( \lambda_c + \frac{1}{\lambda_c} \right).$$

#### Nonisobaric Chamber

Parameters of the working medium at the nozzle inlet in the case of nonisobaric combustion chamber are determined with the aid of known quantities  $f_k$ ,  $p_1$ ,  $T_{к.изобарн}^*$ ,  $n$  and  $k$ . According to the value of  $f_k$  we calculate gas-dynamic function [Translators Note: изобарн = isobaric]

$$q(\lambda_k) = \frac{1}{f_k},$$

which is then used for determination of  $\lambda_k$  and numbers  $M_k$  at the nozzle inlet, and also functions  $\pi(\lambda)$ ,  $\tau(\lambda)$ ,  $\epsilon(\lambda)$  [3].

Statistical parameters at the nozzle inlet are considered by formulas

$$\frac{p_k}{p_1} = \frac{1}{1 + kM_k^2}; \quad (9.20)$$

$$\frac{T_k}{T_{k, \text{стат.}}} = \frac{1}{1 + \frac{k-1}{2} M_k^2}, \quad (9.21)$$

and stagnation parameters  $p_k^*$ ,  $T_k^*$ ,  $\rho_k^*$  - with the aid of gas-dynamic functions  $\pi(\lambda)$ ,  $\tau(\lambda)$ ,  $\epsilon(\lambda)$  at assigned value of  $n$ :

$$p_k^* = \frac{p_k}{\pi(\lambda)}; \quad T_k^* = \frac{T_k}{\tau(\lambda)}; \quad \rho_k^* = \frac{\rho}{\epsilon(\lambda)}.$$

Quantity  $p_k^*/p_1$ , which is usually designated  $\sigma_f$ , is the coefficient of pressure reduction in a cylindrical combustion chamber so that

$$\sigma_f = \frac{1}{\pi(\lambda)(1 + kM_k^2)}. \quad (9.22)$$

Expenditure complex  $\beta$  and specific thrust  $P_{y.d.n}$  are determined by formulas (9.18) and (9.19). In case of prescribed relative area  $f_c$  gas-dynamic function  $z(\lambda_c)$  is found by known value of  $q(\lambda_c)$  in accordance with expression (9.15). If pressure at nozzle section  $p_c$  is prescribed, then the value of  $z(\lambda_c)$  is determined by gas-dynamic tables with the aid of function  $\pi(\lambda_c)$ , which in this instance looks like [Translators Note:  $c =$  section]:



$$\pi(\lambda_c) = \frac{D_c}{p_1 \sigma_f} \quad (9.23)$$

According to equations (9.18) and (9.19) quantities  $\beta$  and  $P_{y_{д.п}}$  when  $f_c = \text{const}$  do not depend on the value of  $f_H$ , inasmuch as gas-dynamic relationships do not allow determining the change of efficiency of gas caused by dissociation,  $R_H T_H^*$  depends on  $p_H^*(f_H)$ .

It is necessary to pause on the characteristics of calculation of gas-dynamic functions  $q(\lambda)$ ,  $\pi(\lambda)$ ,  $\tau(\lambda)$  and others. Utilization of isentropic in form (9.9) leads to such relationships:

$$\left. \begin{aligned} q(\lambda) &= \left( \frac{n+1}{2} \right)^{\frac{1}{n-1}} \left( 1 - \frac{n-1}{n+1} \lambda^2 \right)^{\frac{1}{n-1}} \lambda; \\ \tau(\lambda) &= 1 + \frac{n-1}{n+1} \lambda^2; \\ \pi(\lambda) &= \left( 1 - \frac{n-1}{n+1} \lambda^2 \right)^{\frac{n}{n-1}}. \end{aligned} \right\} \quad (9.24)$$

The connection between  $M$  number and reduced velocity  $\lambda$  is given by formula:

$$M^2 = \frac{\frac{2}{n+1} \lambda^2}{1 - \frac{n-1}{n+1} \lambda^2} \quad (9.25)$$

With fulfillment of calculations with the aid of tables of gas-dynamic functions, the efficiency ratio  $k$  given in tables is taken equal to  $n$  and tabular values of functions  $q(\lambda)$ ,  $\tau(\lambda)$ ,  $\pi(\lambda)$ . Results of calculations are approximate.

### 9.3. Extrapolation and Interpolation of Thermodynamic Characteristics

Calculation of thermodynamic characteristics at certain values of determining parameters and even over a wide range of their change still does not completely solve the problem of thermodynamic designing of a rocket engine. The point is that in the process of engine designing changes in the values of determining parameters are practically inevitable. By these or other considerations the pressures in the combustion chamber and at the nozzle section, relative to nozzle area can be changed. The value of enthalpy of propellant can be changed in connection with change of its temperature (preliminary nonregenerative preheating or cooling), taking into account heat losses in combustion chamber (nonregenerative cooling, undercombustion). Often the enthalpy of propellant changes in connection with refinement of earlier used values.

In the process of engine operation conditions can be created which differ from nominal when real values of initial temperature and enthalpy of propellant, composition of propellant, pressure in combustion chamber and at the nozzle section do not coincide with those accepted in thermodynamic calculation.

Change of some of the initial parameters can require the fulfillment of new thermodynamic calculations. Ultimately, the labor input of designing increases. In connection with this, the method of rapid and accurate extrapolation or interpolation of all basic thermodynamic characteristics and parameters of the chamber with changes in initial conditions is of practical interest. In this case extrapolation and interpolation must be performed by a limited quantity of data, obtained by detailed calculation of "reference" points.

Below is given the method of extrapolation and interpolation of thermodynamic characteristics [1], [4]. In the method are used results obtained at the previous stages of thermodynamic calculation.

#### Formulas of Extrapolation and Interpolation .

For extrapolation there is used expansion of the function in Taylor series:

$$f(x_i) = f(x_i^0) + \sum_{l=1}^n \left( \frac{\partial f}{\partial x_l} \right)^0 (x_i - x_i^0) + \\ + \frac{1}{2} \sum_{l,j} \left( \frac{\partial^2 f}{\partial x_l \partial x_j} \right)^0 (x_i - x_i^0) (x_j - x_j^0) \dots$$

If the second derivatives of the function are unknown, the expression is used without quadratic term. To get the necessary accuracy of extrapolation such a form of functions and arguments should be specially selected, at which derivatives in the interval of extrapolation are close to constant.

For interpolation there are applied polynomials of type

$$y = A + Bx + Cx^2 + Dx^3 + Ex^4 + Fx^5.$$

Coefficients of polynomial are found from joint solution of equations, including values of the function, its first and second derivatives at two points.

If only the first derivatives are known, then interpolation is performed by polynomials of the third power. However, in this variant the accuracy of interpolation is increased as compared to the case of linear interpolation, when at two points only the values of function, and not its derivatives are known.

Thus, for extrapolation and interpolation of thermodynamic characteristics their partial derivatives must be known.

## First Partial Derivatives of Thermodynamic Functions

All thermodynamic properties of the system with known initial composition can be uniquely expressed through any two thermodynamic functions, for example,  $\alpha$  and  $\beta$ . If the initial state of the system was determined by point  $(\alpha_0, \beta_0)$ , then for determination of its new state at finite point it is necessary to know the character of passage and one of the coordinates of finite points, for example,  $\alpha$ . In this case  $\alpha_0, \beta_0$  and  $\alpha$  are independent variables of the process, and  $\beta$  and all other thermodynamic functions are dependent variables.

The type of passage is often characterized by constancy of some third thermodynamic function  $\psi$ . In this instance it is possible to write:

$$\psi(\alpha_0, \beta_0) = \psi(\alpha, \beta) = \psi(\alpha, \varphi),$$

where  $\psi$  - any dependent thermodynamic variable at finite point of the process of passage. Any change of  $\psi$ , caused by change in the position of initial point  $(\alpha_0, \beta_0)$ , must be equated to change of  $\psi_0$ , i.e.,

$$\left(\frac{\partial \psi_0}{\partial \alpha_0}\right)_{\beta_0} d\alpha_0 + \left(\frac{\partial \psi_0}{\partial \beta_0}\right)_{\alpha_0} d\beta_0 = \left(\frac{\partial \psi}{\partial \alpha}\right)_{\varphi} d\alpha + \left(\frac{\partial \psi}{\partial \varphi}\right)_{\alpha} d\varphi. \quad (9.26)$$

Having made use of usual relationship

$$\left(\frac{\partial \psi}{\partial \alpha}\right)_{\varphi} \left(\frac{\partial \alpha}{\partial \varphi}\right)_{\psi} = -1,$$

from equality (9.26) we obtain expressions for partial derivatives of functions at finite point of the process relative to initial coordinates:

$$\left(\frac{\partial \varphi}{\partial \beta_0}\right)_{\alpha_0} = \frac{\left(\frac{\partial \psi_0}{\partial \beta_0}\right)_{\alpha_0}}{\left(\frac{\partial \psi}{\partial \varphi}\right)_{\alpha}} + \left(\frac{\partial \varphi}{\partial \alpha}\right)_{\psi} \left(\frac{\partial \alpha}{\partial \beta_0}\right)_{\alpha_0}; \quad (9.27)$$

$$\left(\frac{\partial \varphi}{\partial a_0}\right)_{\beta_0} = \frac{\left(\frac{\partial \psi_0}{\partial a_0}\right)_{\beta_0}}{\left(\frac{\partial \psi}{\partial \varphi}\right)_a} + \left(\frac{\partial \varphi}{\partial a}\right)_\psi \left(\frac{\partial a}{\partial a_0}\right)_{\beta_0}. \quad (9.28)$$

In the right sides of expressions (9.27) and (9.28) enter usual first partial derivatives, which can be determined directly, and also derivatives  $(\partial a / \partial \beta_0)_{a_0}$  and  $(\partial a / \partial a_0)_{\beta_0}$ , which can be determined for some concrete relationships  $a(a_0, \beta_0)$ .

If  $a = \text{const}$ , equations (9.27) and (9.28) take such a form:

$$\left(\frac{\partial \varphi}{\partial \beta_0}\right)_{a_0, a} = \frac{\left(\frac{\partial \psi_0}{\partial \beta_0}\right)_{a_0}}{\left(\frac{\partial \psi}{\partial \varphi}\right)_a}; \quad (9.29)$$

$$\left(\frac{\partial \varphi}{\partial a_0}\right)_{\beta_0, a} = \frac{\left(\frac{\partial \psi_0}{\partial a_0}\right)_{\beta_0}}{\left(\frac{\partial \psi}{\partial \varphi}\right)_a}. \quad (9.30)$$

If  $a = \text{const} \cdot a_0$ , we obtain

$$\left(\frac{\partial \varphi}{\partial \beta_0}\right)_{a_0, \frac{a_0}{a}} = \frac{\left(\frac{\partial \psi_0}{\partial \beta_0}\right)_{a_0}}{\left(\frac{\partial \psi}{\partial \varphi}\right)_a}; \quad (9.31)$$

$$\left(\frac{\partial \varphi}{\partial a_0}\right)_{\beta_0, \frac{a_0}{a}} = \frac{\left(\frac{\partial \psi_0}{\partial a_0}\right)_{\beta_0}}{\left(\frac{\partial \psi}{\partial \varphi}\right)_a} + \frac{a}{a_0} \left(\frac{\partial \varphi}{\partial a}\right)_\psi. \quad (9.32)$$

Let us note that the right sides of equations (9.29) and (9.31) are identical.

Let us apply the obtained equations to description of processes in the chamber, including isentropic expansion in the nozzle ( $s = \text{const}$ ). Let us consider the values at the nozzle inlet initial values. In this case in equations (9.29)-(9.32) one should assume:

$$\begin{aligned}\psi &= s, & \psi_0 &= s_K; \\ \alpha &= p, & \alpha_0 &= p_K;^{*)} \\ \beta &= I, & \beta_0 &= I_K.\end{aligned}$$

From equations (9.29) and (9.31) we obtain:

$$\left(\frac{\partial \varphi}{\partial I_K}\right)_{p_K, p} = \left(\frac{\partial \varphi}{\partial I_K}\right)_{p_K, \pi} = \frac{1}{T_K} \left(\frac{\partial \varphi}{\partial s}\right)_p. \quad (9.33)$$

Here and further  $\pi = p_K/p$ . From equation (9.30) follows:

$$\left(\frac{\partial \varphi}{\partial p_K}\right)_{I_K, p} = \frac{\left(\frac{\partial s_K}{\partial p_K}\right)_{I_K}}{\left(\frac{\partial s}{\partial p}\right)_p} = -\frac{v_K}{T_K} \left(\frac{\partial \varphi}{\partial s}\right)_p. \quad (9.34)$$

Finally, from equation (9.32) we have

$$\left(\frac{\partial \varphi}{\partial p_K}\right)_{I_K, \pi} = -\frac{v_K}{T_K} \left(\frac{\partial \varphi}{\partial s}\right)_p + \frac{p}{p_K} \left(\frac{\partial \varphi}{\partial p}\right)_s. \quad (9.35)$$

With the aid of equations (9.33)-(9.35) one can determine the partial derivatives of various functions, the most interesting of which are temperature, enthalpy, density, molecular weight. Table 9.1 contains a summary of the first partial derivatives of these functions. Table 7.1 is used during derivation. For all quantities, except enthalpy, frequently having negative values, the logarithmic form is accepted.

---

<sup>\*)</sup>Relationships listed in this paragraph pertain to isobaric combustion chambers, for which  $p_K = p_K^*$ .

Table 9.1. First partial derivatives of certain thermodynamic functions.

$\varphi$	According to enthalpy of propellant		According to pressure in the combustion chamber		According to parameters of nozzle section	
	$\left(\frac{\partial \ln \varphi}{\partial I_K}\right)_{P_K, P}$	$\left(\frac{\partial \ln \varphi}{\partial \ln P_K}\right)_{I_K, P}$	$\left(\frac{\partial \ln \varphi}{\partial \ln P_K}\right)_{I_K, \mu}$	$\left(\frac{\partial \ln \varphi}{\partial \ln \pi_c}\right)_{I_K, P_K} = -\left(\frac{\partial \ln \varphi}{\partial \ln P_c}\right)_s$	$\left(\frac{\partial \ln \varphi}{\partial \ln f_c}\right)_s$	
$T$	$\frac{1}{c_p T_K}$	$-\frac{R_0}{c_p \mu_K}$	$\frac{R_0}{c_p \mu} \left(a_p T - \frac{\mu}{\mu_K}\right)$	$-\frac{a_p T R_0}{c_p \mu}$	$-\frac{a_p T R_0}{c_p \mu} - \frac{R_0 T}{k_p} - \frac{P_{yK}^2 \mu}{P_{yK}^2}$	
$I$	$\frac{T}{T_K}$	$-\frac{R_0 T}{\mu_K}$	$R_0 T \left(\frac{1}{\mu} - \frac{1}{\mu_K}\right)$	$-\frac{R_0 T}{\mu}$	$-\frac{R_0 T}{\mu} - \frac{R_0 T}{k_p} - \frac{P_{yK}^2 \mu}{P_{yK}^2}$	
$Q$	$-\frac{a_p T}{c_p T_K}$	$\frac{a_p T R_0}{c_p \mu_K}$	$\frac{a_p T R_0}{c_p \mu} + \frac{3 T P}{k_p}$	$-\frac{3 T P}{k_p}$	$-\frac{3 T P}{k_p} - \frac{R_0 T}{k_p} - \frac{P_{yK}^2 \mu}{P_{yK}^2}$	
$\mu$	$\frac{1 - a_p T}{c_p T_K}$	$\frac{R_0 (a_p T - 1)}{c_p \mu_K}$	$\frac{R_0}{c_p \mu} \left(a_p T - \frac{\mu}{\mu_K}\right) + \frac{a_p T R_0}{c_p \mu} + \frac{3 T P}{k_p} - 1$	$\frac{a_p R_0 T}{c_p \mu} (a_p T + 1) - 3 T P + 1$	$\left(\frac{\partial \ln \mu}{\partial \ln \pi_c}\right)_{I_K, P_K} - \frac{3 T P}{k_p} - \frac{R_0 T}{k_p} - \frac{P_{yK}^2 \mu}{P_{yK}^2}$	

Obviously the condition that  $p_K = \text{const}$  and  $I_K = \text{const}$  simultaneously is equivalent to condition  $s_K = s = \text{const}$ . Therefore

$$\left(\frac{\partial \ln \varphi}{\partial \ln \pi}\right)_{I_K, p_K} = -\left(\frac{\partial \ln \varphi}{\partial \ln \pi}\right)_s. \quad (9.36)$$

Furthermore, since

$$\left(\frac{\partial \ln \pi}{\partial \ln \varphi}\right)_{I_K, p_K} = \left(\frac{\partial \ln p_K}{\partial \ln \varphi}\right)_{I_K, p_K} - \left(\frac{\partial \ln p}{\partial \ln \varphi}\right)_{I_K, p_K},$$

then

$$\left(\frac{\partial \ln \varphi}{\partial \ln \pi}\right)_s = -\left(\frac{\partial \ln \varphi}{\partial \ln p}\right)_s. \quad (9.37)$$

Equality (9.37) is presented in the table of derivatives.

Analysis of the table of first partial derivatives of thermodynamic functions shows that for calculation of derivatives it is sufficient to know the quantities of thermal coefficients  $\alpha_p, \beta_T$  and relationship of equilibrium thermal capacities  $k_p$ . These quantities are found when determining thermodynamic properties of the working medium.

#### First Partial Derivatives of Thermodynamic Characteristics

Thermodynamic characteristics are determined by formulas of § 9.1. The first partial derivatives of these characteristics can be obtained analogously, with use of earlier found quantities. Summary of first partial derivatives of this category is listed in Table 9.2. By derivatives of specific thrusts derivatives  $\partial P_{yA}^2 / \partial x$  are easily determined, application of which in extrapolation formulas gives more accurate results.



Table 9.2. First partial derivatives of certain thermodynamic characteristics and parameters.

	According to enthalpy of propellant $p_k, p = \text{const}$
$\lambda$	$\left(\frac{\partial \ln \lambda}{\partial I_k}\right)_{p_k, n} = \left(\frac{\partial \ln \lambda}{\partial I_k}\right)_{p_k, p}$
$P_{ya}$	$\frac{1}{2T_k} \frac{T_k - T}{I_k - I}$
$F_{ya}$	$-\left(\frac{\partial \ln P_{ya}}{\partial I_k}\right)_{p_k, n} - \left(\frac{\partial \ln Q}{\partial I_k}\right)_{p_k, n}$
$f$	$\left(\frac{\partial \ln F_{ya}}{\partial I_k}\right)_{p_k, n} - \left(\frac{\partial \ln F_{ya, \text{np}}}{\partial I_k}\right)_{p_k, n}$
$\beta$	$\left(\frac{\partial \ln F_{ya, \text{np}}}{\partial I_k}\right)_{p_k, n}$
$P_{ya, \text{np}}$	$\frac{1}{P_{ya, \text{np}}} \left[ P_{ya} \left(\frac{\partial \ln P_{ya}}{\partial I_k}\right)_{p_k, n} + p F_{ya} \left(\frac{\partial \ln F_{ya}}{\partial I_k}\right)_{p_k, n} \right]$

Table 9.2 (Cont'd).

According to pressure in combustion chamber $I_k, p = \text{const}$		
$\lambda$	$\left( \frac{\partial \ln \lambda}{\partial \ln p_k} \right)_{I_k, p}$	$\left( \frac{\partial \ln \lambda}{\partial \ln p_k} \right)_{I_k, n}$
$P_{yA}$	$\frac{R_0 T}{2(i_k - 1) \mu_k}$	$\frac{R_0 T}{2(i_k - 1)} \left( \frac{1}{\mu_k} - \frac{1}{\mu} \right)$
$F_{yA}$	$-\left( \frac{\partial \ln P_{yA}}{\partial \ln p_k} \right)_{I_k, p} - \left( \frac{\partial \ln Q}{\partial \ln p_k} \right)_{I_k, p}$	$-\left( \frac{\partial \ln P_{yA}}{\partial \ln p_k} \right)_{I_k, n} - \left( \frac{\partial \ln Q}{\partial \ln p_k} \right)_{I_k, n}$
$f$	$\left( \frac{\partial \ln F_{yA}}{\partial \ln p_k} \right)_{I_k, p} - \left( \frac{\partial \ln F_{yA, \text{exp}}}{\partial \ln p_k} \right)_{I_k, p}$	$\left( \frac{\partial \ln F_{yA}}{\partial \ln p_k} \right)_{I_k, n} - \left( \frac{\partial \ln F_{yA, \text{exp}}}{\partial \ln p_k} \right)_{I_k, n}$
$\beta$	—	$1 + \left( \frac{\partial \ln F_{yA, \text{exp}}}{\partial \ln p_k} \right)_{I_k, n}$
$P_{yA, n}$	$\frac{1}{P_{yA, n}} \left[ P_{yA} \left( \frac{\partial \ln P_{yA}}{\partial \ln p_k} \right)_{I_k, p} + \right. \\ \left. + p F_{yA} \left( \frac{\partial \ln F_{yA}}{\partial \ln p_k} \right)_{I_k, p} \right]$	$\frac{1}{P_{yA, n}} \left\{ P_{yA} \left( \frac{\partial \ln P_{yA}}{\partial \ln p_k} \right)_{I_k, n} + \right. \\ \left. + p F_{yA} \left[ \left( \frac{\partial \ln F_{yA}}{\partial \ln p_k} \right)_{I_k, n} + 1 \right] \right\}$

Table 3.2 (Cont'd).

According to parameters of nozzle section $I_K, p_K = \text{const}$		
$\lambda$	$\left(\frac{\partial \ln \lambda}{\partial \ln \pi}\right)_{I_K, p_K} = -\left(\frac{\partial \ln \lambda}{\partial \ln p}\right)_s$	$\left(\frac{\partial \ln \lambda}{\partial \ln f}\right)_s$
$P_{yA}$	$\frac{R_0 T}{2(I_K - I) \mu}$	$\frac{\left(\frac{\partial \ln P_{yA}}{\partial \ln \pi}\right)_{I_K, p_K}}{\frac{\partial T p}{k_p} - \frac{R_0 T}{P_{yA}^2 \mu}}$
$F_{yA}$	$-\left(\frac{\partial \ln P_{yA}}{\partial \ln \pi}\right)_{I_K, p_K} - \left(\frac{\partial \ln Q}{\partial \ln \pi}\right)_{I_K, p_K}$	$\frac{\left(\frac{\partial \ln F_{yA}}{\partial \ln \pi}\right)_{I_K, p_K}}{\frac{\partial T p}{k_p} - \frac{R_0 T}{P_{yA}^2 \mu}}$
$f$	$\left(\frac{\partial \ln F_{yA}}{\partial \ln \pi}\right)_{I_K, p_K}$	1
$\beta$	—	—
$P_{yA, n}$	$\frac{1}{P_{yA, n}} \left\{ P_{yA} \left(\frac{\partial \ln P_{yA}}{\partial \ln \pi}\right)_{I_K, p_K} + \right.$ $\left. + F_{yA} \left[ \left(\frac{\partial \ln F_{yA}}{\partial \ln \pi}\right)_{I_K, p_K} - 1 \right] \right\}$	$\frac{\left(\frac{\partial \ln P_{yA, n}}{\partial \ln \pi}\right)_{I_K, p_K}}{\frac{\partial T p}{k_p} - \frac{R_0 T}{P_{yA}^2 \mu}}$

In the previous section of the thermodynamic characteristics and parameters of the chamber were considered as functions of enthalpy  $I_n$ , pressure  $p_n$  and degree of reduction of pressure  $\pi$ :

$$\lambda = \lambda(I_n, p_n, \pi),$$

including relative nozzle area

$$f = f(I_n, p_n, \pi). \quad (9.38)$$

By excluding  $\pi$  from these relationships, we obtain

$$\lambda = \lambda(I_n, p_n, f). \quad (9.39)$$

The functional form of the last type is useful when designing. Partial derivatives for this form can be obtained in the following manner. Total differentials of equations (9.37)-(9.39) have the form:

$$d \ln \lambda = \left( \frac{\partial \ln \lambda}{\partial \ln p_n} \right)_{I_n, \pi} d \ln p_n + \left( \frac{\partial \ln \lambda}{\partial \ln I_n} \right)_{p_n, \pi} d \ln I_n + \left( \frac{\partial \ln \lambda}{\partial \ln \pi} \right)_{I_n, p_n} d \ln \pi; \quad (9.40)$$

$$d \ln f = \left( \frac{\partial \ln f}{\partial \ln p_n} \right)_{I_n, \pi} d \ln p_n + \left( \frac{\partial \ln f}{\partial \ln I_n} \right)_{p_n, \pi} d \ln I_n + \left( \frac{\partial \ln f}{\partial \ln \pi} \right)_{I_n, p_n} d \ln \pi, \quad (9.41)$$

$$d \ln \lambda = \left( \frac{\partial \ln \lambda}{\partial \ln p_n} \right)_{I_n, f} d \ln p_n + \left( \frac{\partial \ln \lambda}{\partial \ln I_n} \right)_{p_n, f} d \ln I_n + \left( \frac{\partial \ln \lambda}{\partial \ln f} \right)_{I_n, p_n} d \ln f. \quad (9.42)$$

By excluding  $d \ln f$  from expressions (9.41) and (9.42) and comparing the coefficients at differentials with corresponding

coefficients of equation (9.40), we obtain the following relationships (for I the passage of nonlogarithmic form has been accomplished):

$$\left(\frac{\partial \ln \lambda}{\partial \ln p_k}\right)_{I, f} = \left(\frac{\partial \ln \lambda}{\partial \ln p_k}\right)_{I, \pi} - \left(\frac{\partial \ln \lambda}{\partial \ln \pi}\right)_s \frac{\left(\frac{\partial \ln f}{\partial \ln p_k}\right)_{I, \pi}}{\left(\frac{\partial \ln f}{\partial \ln \pi}\right)_s}; \quad (9.43)$$

$$\left(\frac{\partial \ln \lambda}{\partial I_k}\right)_{p_k, f} = \left(\frac{\partial \ln \lambda}{\partial I_k}\right)_{p_k, \pi} - \left(\frac{\partial \ln \lambda}{\partial \ln \pi}\right)_s \frac{\left(\frac{\partial \ln f}{\partial I_k}\right)_{p_k, \pi}}{\left(\frac{\partial \ln f}{\partial \ln \pi}\right)_s}; \quad (9.44)$$

$$\left(\frac{\partial \ln \lambda}{\partial \ln f}\right)_s = \frac{\left(\frac{\partial \ln \lambda}{\partial \ln \pi}\right)_s}{\left(\frac{\partial \ln f}{\partial \ln \pi}\right)_s}. \quad (9.45)$$

Thus the group of partial derivatives of this type can be obtained from the previous.

Thus, for extrapolation and interpolation of all thermodynamic functions and characteristics there are the necessary partial derivatives. In reference to characteristic sections of the chamber extrapolation formulas for any quantity  $\phi$  have the following form.

Extrapolation of parameters in the combustion chamber:

$$\ln \varphi = \ln \varphi^0 + \left(\frac{\partial \ln \varphi}{\partial I_k}\right)_{p_k, p_c}^0 \Delta I + \left(\frac{\partial \ln \varphi}{\partial \ln p_k}\right)_{I, \pi}^0 \Delta \ln p_k. \quad (9.46)$$

Extrapolation of parameters in the nozzle throat ( $M = 1$ ):

$$\ln \varphi = \ln \varphi^0 + \left(\frac{\partial \ln \varphi}{\partial I_k}\right)_{p_k, p_{kp}}^0 \Delta I + \left(\frac{\partial \ln \varphi}{\partial \ln p_k}\right)_{I, \pi}^0 \Delta \ln p_k. \quad (9.47)$$

Extrapolation of parameters at the nozzle section (independent variables  $I_K, p_K, p_C$ ):

$$\ln \varphi = \ln \varphi^0 + \left( \frac{\partial \ln \varphi}{\partial I_K} \right)_{p_K, p_C}^0 \Delta I + \left( \frac{\partial \ln \varphi}{\partial \ln p_K} \right)_{I_K, p_C}^0 \Delta \ln p_K + \left( \frac{\partial \ln \varphi}{\partial \ln p_C} \right)_{I_K, p_K}^0 \Delta \ln p_C. \quad (9.48)$$

Extrapolation of parameters at the nozzle section (independent variables  $I_K, p_K, f_C$ ):

$$\ln \varphi = \ln \varphi^0 + \left( \frac{\partial \ln \varphi}{\partial I_K} \right)_{p_K, f_C}^0 \Delta I + \left( \frac{\partial \ln \varphi}{\partial \ln p_K} \right)_{I_K, f_C}^0 \Delta \ln p_K + \left( \frac{\partial \ln \varphi}{\partial \ln f_C} \right)_{I_K, p_K}^0 \Delta \ln f_C. \quad (9.49)$$

If some of the determining parameters  $p_K, I_K, p_C$  (or  $f_C$ ) remain constant, then formulas (9.46)-(9.49) are simplified accordingly. For example, change in specific thrust  $P_{yA}$  as a result of change in initial enthalpy of propellant  $\Delta I$  at constant  $p_K$  and  $p_C$  can be determined so:

$$\ln P_{yA} = \ln P_{yA}^0 + \left( \frac{\partial \ln P_{yA}}{\partial I} \right)_{p_K, p_C}^0 \Delta I.$$

Taking into account formulas of Table 9.2 the last expression is converted into known formula

$$\frac{\Delta P_{yA}}{P_{yA}^0} = \frac{\Delta I}{2(I_K - I_C)} \left( 1 - \frac{T_C}{T_K} \right), \quad (9.50)$$

where  $\Delta P_{yA} = P_{yA} - P_{yA}^0$ ;  $P_{yA}^0$  - specific thrust at initial value of enthalpy of propellant.

Tables 9.3 and 9.4 contain comparative appraisal of the accuracy of extrapolation of  $T_K$ ,  $\beta$  and  $P_{yA}$  for propellant  $H_2 + O_2$  with  $\alpha = 0.9$ . Parameters of reference point:  $I_T = -811$  kJ/kg;  $p_K = 30$  bar;  $p_C = 0.1$  bar. In columns "exact" there are listed characteristics according to data of thermodynamic calculation, in columns "extrap" these characteristics obtained by extrapolation from a reference point. As can be seen, the accuracy of extrapolation is entirely acceptable with a small change in determining parameters  $p_K$ ,  $I_T$ ,  $p_C$ .

Table 9.3. Comparative appraisal of the accuracy of extrapolation of temperature in the combustion chamber and complex 8.

$p_K$ bar	Quantity	$I_T = -811$ kJ/kg		$I_T = 0$	
		exact.	extrap.	exact.	extrap.
20	$T_K^\circ K$	3420	3416	3485	3483
80		3609	3609	3688	3680
150		3694	3700	3781	3773
250		3761	3776	3855	3851
20	$\beta$ kg·s/kg	223,2	223,5	227,1	227,8
80		226,6	226,6	231,0	231,1
150		227,8	228,1	232,2	232,5
250		228,9	229,3	233,4	233,8

Table 9.4. Comparative appraisal of the accuracy of extrapolation of specific thrust.

$p_K$ bar	$I_T = -811$ kJ/kg				$I_T = 0$			
	$p_C = 1,0$ bar		$p_C = 0,01$ bar		$p_C = 1,0$ bar		$p_C = 0,01$ bar	
	exact.	extrap.	exact.	extrap.	exact.	extrap.	exact.	extrap.
20	319,7	321,8	450,9	450,6	323,5	327,3	461,7	461,4
80	377,5	378,2	472,3	471,5	385,2	386,2	484,9	484,5
150	398,2	398,3	479,7	478,4	407,0	407,0	492,9	492,2
250	412,8	412,7	484,9	482,7	422,5	422,4	498,5	497,4

At present the composition and properties of combustion products, thermodynamic characteristics and coefficients of extrapolation formulas are calculated on an electronic computer.

#### Bibliography

1. Alemasov V. Ye., IVUZ, ser. "Aviatsionnaya tekhnika", 1967, vyp. 40.
2. Barrer M. and others. Raketnyye dvigateli, (Rocket engines), translated from English), Oborongiz, 1962.
3. Vinogradov B. S., Prikladnaya gazovaya dinamika (Applied gas dynamics), izd-vo Un-ta Druzhby Nar., 1965.
4. Gordon S., Zeleznik F. I., ARS Journal, 1962, No. 8.



## CHAPTER X

### RELATIONSHIPS OF THERMODYNAMIC CHARACTERISTICS TO BASIC FACTORS

In the chapter are examined relationships of thermodynamic characteristics of rocket propellants and working substances to basic factors, which determine the conditions of application of these propellants and substances in the chamber of a heat rocket engine.

#### 10.1. General Information

Thermodynamic characteristics include quantities, characterizing the composition of working medium, and also basic thermodynamic parameters of processes being carried out in the chamber.

Thermodynamic characteristics are determined by means of calculation, by methods discussed in previous chapters. Calculation is performed with some general assumptions, without allowing for characteristics of a particular chamber (such as, for example, carburetion system, nozzle circuit, etc.). In this case the thermodynamic characteristics depend only on the nature of propellant being burned or the substance being heated and on fundamental conditions of the processes in the chamber. These determining conditions are somewhat different for propellants containing a source of energy and source of working medium, and for substances for which heating is carried out during heating from an independent source of energy.

For propellants consisting of fuel and oxidizers, the thermodynamic characteristics depend on the ratio of these components. Component ratios in liquid propellant is characterized by the excess oxidant ratio  $\alpha$ , which can change during engine operation. The composition of solid propellant is characterized usually by weight fractions of components. The necessary component ratios in solid propellant is provided during its manufacture and cannot be changed during engine operation. An idea of thermodynamic characteristics depending on the component ratios is necessary for correct selection of propellant and for analysis of engine operation with variable  $\alpha$ .

Other independent factor for chemical propellants is pressure in combustion chamber  $p_H^*$ . With selected component ratios of propellant pressure  $p_H^*$  uniquely determines the equilibrium composition of working medium, its molecular weight and temperature in the combustion chamber.

Composition and total enthalpy of the working medium at the nozzle exit depend on pressure and temperature in the exit section. Under fixed conditions at the nozzle inlet both these quantities are determined by degree of pressure reduction in the nozzle  $\pi_c = p_H^*/p_c$  (this quantity is also called expansion ratio) or by relative nozzle section area  $f_c$  and also by the character of the expansion process.

If the combustion process is not carried out in an isobaric combustion chamber, the thermodynamic characteristics are affected by relative area of combustion chamber  $f_H$ .

A substance, which is heated from an independent source of energy, has a fixed initial composition. Temperature of working medium, obtained from the given substance, depends on the quantity of heat supplied outside and on pressure in the heating chamber. Degree of pressure decrease in the nozzle  $\pi_c$  or relative nozzle area  $f_c$ , and also the character of expansion process determine the composition and parameter of the working medium at the nozzle exit.

Thus, thermodynamic characteristics of substances, which are heated from an independent source, do not depend on the component ratios, but there appears a specific relationship to total enthalpy or heating temperatures.

A change in such thermodynamic characteristics as temperature, molecular weight (or specific gas constant being uniquely determined by them), pressure (if relative area is assigned) is advisable to know at all points of the chamber passage. The most important thermodynamic characteristics - complex  $\beta$  and specific thrust  $P_{yA}$  are generalized quantities. Most frequently their equilibrium values are used, for specific thrust - values in a void.

The totality of thermodynamic characteristics over a wide range of changes in determining factors is the family of thermodynamic characteristics of the given chemical propellant or working medium. Together with thermodynamic and thermophysical properties of working medium the thermodynamic characteristics are usually represented in tabular form (see Table 9.1).

Below are given primarily graphic relationships, clearly illustrating the effect of basic factors.

#### 10.2. Relationships to Component Ratios of Propellant

For liquid rocket propellants the determining parameter is the excess oxidant ratio  $\alpha$ .

The relationship of equilibrium composition of combustion products to  $\alpha$  has a complex character, specific for definite classes of propellants. As examples there are: on Fig. 10.1 the equilibrium composition in molar fractions (for hard carbon - weight fraction) of combustion products of kerosene +  $O_{2M}$  type propellant on Fig. 10.2 - propellant  $H_{2M} + F_{2M}$ . Charts also show the corresponding values of temperature and average molecular weight  $\mu_M$ . Figure 10.2 shows the effect of pressure in the combustion chamber.

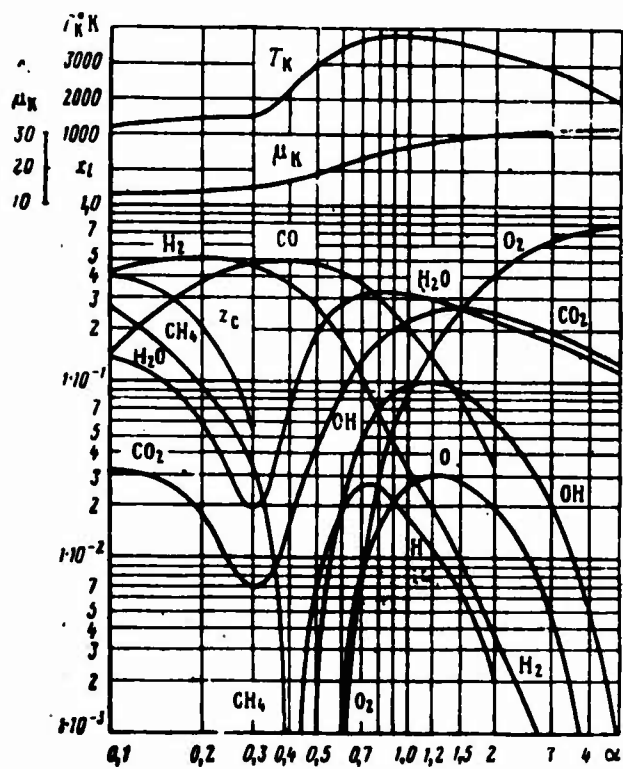


Fig. 10.1. Equilibrium composition of combustion products at different  $\alpha$ : Kerosene +  $O_{2M}$  type propellant;  $p_K = 100$  bar.

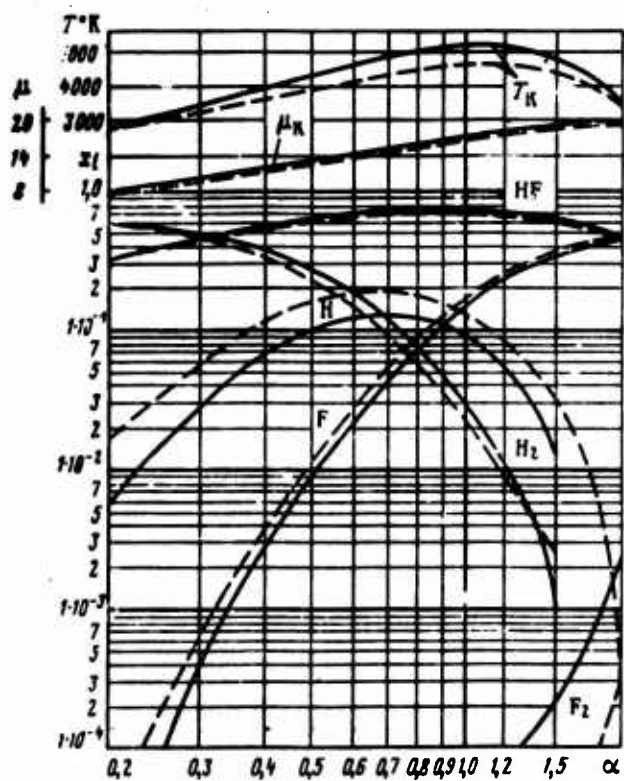


Fig. 10.2. Equilibrium composition of combustion products at different  $\alpha$ : propellant  $H_{2M} + F_{2M}$ ;  $p_K = 20$  bar (dotted line);  $p_K = 200$  bar (solid lines).

On Figs. 10.3 and 10.4 in the function of  $\alpha$  there is shown a change of temperature and molecular weight of combustion products of two mentioned propellants at different pressures. As can be seen, the fundamental character of change of these parameters is identical in both cases. Temperature of equilibrium gas mixture in the combustion chamber  $T_K$  changes with respect to  $\alpha$  with maximum. In the absence of dissociation this maximum must correspond to stoichiometric propellant composition, i.e.,  $\alpha = 1$ . As a result of dissociation this is not observed. As can be seen on Figs. 10.3 and 10.4, maximum  $T_K$  for kerosene +  $O_2$  propellant lies in the range  $\alpha < 1$ , and for propellant  $H_2 + F_2$  - when  $\alpha > 1$ . During comparison with charts 10.1 and 10.2 it can be detected that the maximum of temperature moves from  $\alpha = 1$  into the region of raised content in the working medium of molecules, the most resistant to dissociation. In the combustion products of kerosene +  $O_2$  propellant such molecules are molecules of carbon monoxide CO, in combustion products of propellant  $H_2 + F_2$  - molecules HF. Content of the latter with allowance for dissociation is maximal in the region  $\alpha > 1$ , and content of CO - in region  $\alpha < 1$ . The exact position of maximum is determined for different fuels only by thermodynamic calculation. It is natural that it depends on the pressure, indicating the intensity of dissociation.

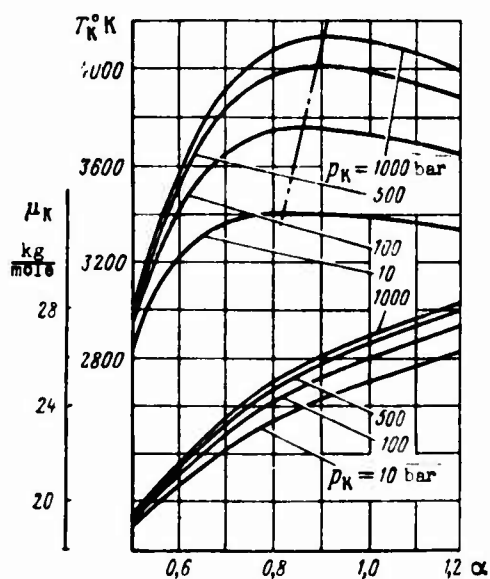


Fig. 103. Relationship of  $T_K$  and  $\mu_K$  to  $\alpha$ : kerosene +  $O_{2H}$  type propellant.

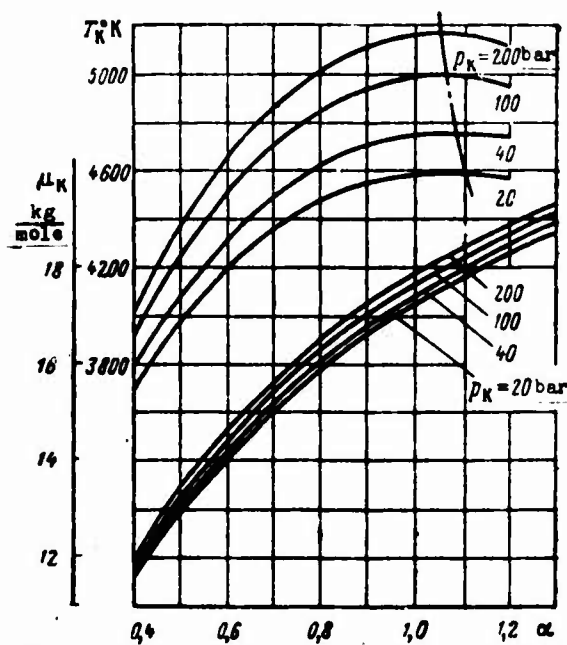


Fig. 10.4. Relationships of  $T_K$  and  $\mu_K$  to  $\alpha$ : propellant  $H_{2H} + F_{2H}$ .

For molecular weight in the combustion chamber  $\mu_K$  a considerable decrease with a decrease of  $\alpha$ , i.e., with increase of light products of incomplete combustion in the working medium is characteristic.

Figure 10.5 contains characteristic relationships of complex  $\beta$  and specific thrust  $P_{y.d.n}$  to  $\alpha$  in case of equilibrium (solid lines) and frozen (dotted line) expansion. As can be seen,  $\beta$  and  $P_{y.d.n}$  are changed with respect to  $\alpha$  with maximum. Coefficients  $\alpha$ , corresponding to maximum values of  $\beta$  and  $P_{y.d.n}$  with frozen expansion are less than with equilibrium.

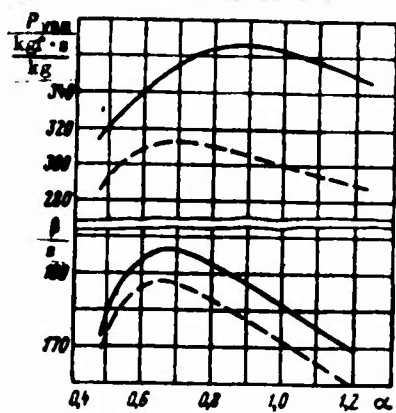


Fig. 10.5. Relationship of complex  $\beta$  and specific thrust in a void to  $\alpha$  with equilibrium and frozen expansion: kerosene +  $O_{2H}$  type propellant;  $p_K = 100$  bar,  $p_c = 1$  bar.

A more or less considerable displacement of maxima of  $\beta$  and  $P_{yA,n}$  into region  $\alpha < 1$  is characteristic for all propellants, in which the weight stoichiometric coefficient of component ratios is more than one ( $\kappa_0 > 1$ ).

Indices of equilibrium expansion are higher than frozen. This is explained by the fact that in case of equilibrium expansion part of the molecules of heat liberated during recombination is converted into kinetic energy and, consequently, increases the outflow velocity and specific thrust.

It is interesting that specific thrust with equilibrium expansion is greater than specific thrust with frozen expansion, whereas the temperature difference is greater in the process of frozen expansion. The point is that specific thrust is determined not by the difference of temperatures, but by the difference of total enthalpies in the process of expansion.

As can be seen on Fig. 10.6, despite the fact that the difference of temperatures is greater with frozen expansion, the difference of total enthalpies is greater with equilibrium. This is explained by the substantial difference of thermal capacities of working medium with equilibrium and frozen expansion ( $c_{pp} > c_{ps}$ ), which was shown in Chapter VII. [Translator's Note:  $p$  = equilibrium;  $s$  = frozen.]

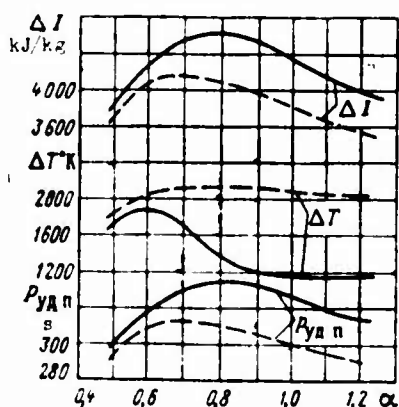


Fig. 10.6. For comparison of specific thrust at equilibrium (solid lines) and frozen (dotted line) expansion (conditions are the same as on Fig. 10.5).

The difference between quantities of equilibrium and frozen specific thrust depends mainly on nature of propellant. For propellants with high combustion temperature it can reach 5-10%.

Figures 10.7 and 10.8 show the change of equilibrium specific thrust in a void with respect  $\alpha$  for two propellants at different values of pressure in the combustion chamber  $p_h^*$  and degree of pressure decrease in the nozzle  $\pi_c$  ( $p_c = 1 \text{ bar} = \text{const}$ ). Characteristic for these and other propellants with increase of  $p_h$  is the approximation of values of  $\alpha$ , corresponding to maxima of temperature and specific thrust, to one. Theoretically when  $p_h^* = \infty$  dissociation is completely suppressed and maximum values of  $P_{y.d.n}$  are reached when  $\alpha = 1$ .

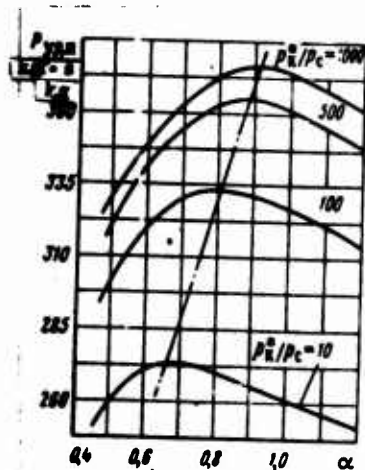


Fig. 10.7. Relationship of  $P_{y.d.n}$  to  $\alpha$  at different values of  $p_h$  and  $\pi_c$  ( $p_c = 1 \text{ bar} = \text{const}$ ): kerosene +  $O_{2M}$  type propellant; equilibrium expansion.

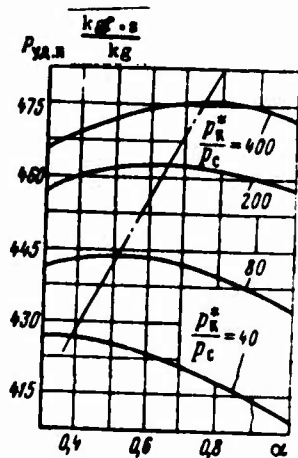


Fig. 10.8. Relationship of  $P_{y.d.n}$  to  $\alpha$  at different values of  $p_h$  and  $\pi_c$  ( $p_c = 0.5 \text{ bar} = \text{const}$ ): fuel  $H_{2M} + F_{2M}$ ; equilibrium expansion.



Dot-dash lines on the charts are lines of maximum values of specific thrust. Values of  $\alpha$ , corresponding to maximum values of  $P_{y\Delta.n}$  can be called thermodynamically optimum. Maxima of relationship  $P_{y\Delta.n} = f(\alpha)$  are often rather mildly sloping.

Relationships of thermodynamic characteristics of solid rocket propellants to the composition (usually to weight fractions of oxidizers in the propellant) in principle are the same as for propellants of liquid-propellant rocket engines.

### 10.3. Relationships to Pressure in the Combustion Chamber

Relationships of temperature and molecular weight of products in the combustion chamber to pressure  $p_H^*$  can be seen on Figs. 10.3 and 10.4. On Fig. 10.9 these relationships are shown in evident form. Their character is uniquely explained by attenuation of dissociation with increase of  $p_H^*$ .

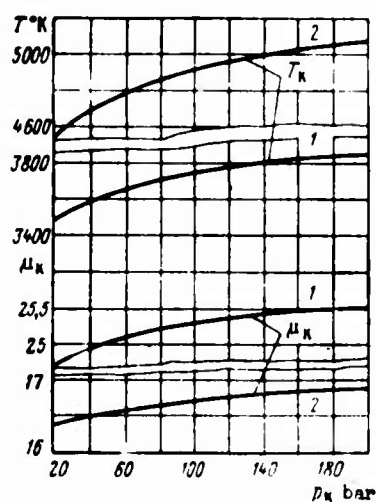


Fig. 10.9.. Relationship of  $T_K$  and  $\mu_K$  to  $p_K$ : propellant: 1 - kerosene +  $O_{2H}$  type; 2 -  $H_{2H} + F_{2H}$ .

Figure 10.10 contains relationships of equilibrium values of  $\beta$  and specific thrust in a void to pressure  $p_H^*$ . Quantity  $P_{y\Delta.n}$  is determined with constant degree of pressure decrease in the

nozzles  $\pi_c$  (different values of  $p_H^*$  in this instance correspond to different nozzles).

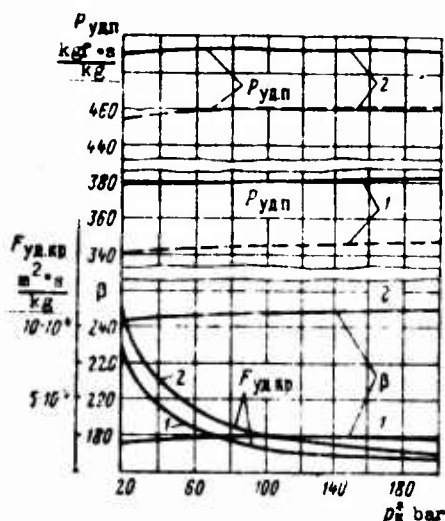


Fig. 10.10. Relationship of complex  $\beta$ , specific thrust in a void and specific throat area to  $p_H^*$  (propellants are the same as on Fig. 10.9): ---  $p_H/p_c = 200$ ; —  $p_H/p_c = 2000$ .

As can be seen, the effect of  $p_H^*$  on complex  $\beta$  is rather weak. It is different for different fuels, somewhat increasing during considerable dissociation. Usually the change of complex  $\beta$  in characteristic range  $p_H^*$  does not exceed 1-2%, in connection with the fact that in preliminary calculations this quantity for the given fuel ( $\alpha = \text{const}$ ) is frequently assumed constant.

Constancy of  $\beta$  explains the decrease in the quantity  $F_{уд.кр}$ , characterizing the handling capacity of the nozzle. According to formula (9.7)

$$F_{уд.кр} = \frac{\beta}{p_H^*}.$$

Decrease of  $F_{уд.кр}$ , i.e., increase in handling capacity of the nozzle with increase of  $p_H^*$ , is physically explained by increase of the density of gas at the nozzle inlet.

The effect of  $p_H^*$  on specific thrust is considerable, especially in the case of highly dissociated combustion or heating products.

This effect is less perceptible with large degrees of pressure decrease in the nozzle  $\pi_c$ .

The character of relationships  $\beta$  and  $P_{y\Delta.\pi}$  to  $p_H^*$  is also explained by the change in intensity of dissociation and recombination accompanying it at various pressure levels.

Of interest is evaluation of the effect of  $p_H^*$  on specific thrust in a void for a chamber with fixed nozzle ( $f_c = \text{const}$ ). Characteristic data are listed in Table 10.1, where results of calculation for the following example are shown: kerosene +  $O_{2H}$  type propellant;  $\alpha = 0.8$ ;  $f_c = 25$ .

Table 10.1. Indices of equilibrium expansion in a chamber with  $f_c = \text{const}$  at different pressures  $p_H^*$ .

$p_H^*$ bar	30	70	150	300
$p_c$ bar	0,1468	0,3315	0,6900	1,346
$M_e$	204,4	211,2	217,4	222,9
$n$	1,128	1,136	1,143	1,149
$P_{y\Delta.\pi}$ kgf./kg	345,9	348,1	349,8	351,2
$\beta$ kgf.s/kg	179,9	181,8	183,3	184,7

As can be seen, with increase of pressure  $p_H^*$  the specific thrust in a void grows noticeably. This is explained by change in the properties of working medium as a result of change in intensity of dissociation, by growth of pressure difference  $\pi_c = p_H^*/p_c$  and, in the final analysis, by increase of drop of total enthalpy in the nozzle.

#### 10.4. Relationship to Degree of Pressure Decrease in the Nozzle or to Relative Nozzle Section Area

This relationship is conveniently analyzed with fixed pressure at the nozzle inlet. For the given working medium the degree of

pressure decrease in the nozzle  $\pi_c$  and relative nozzle section area  $f_c$  are connected together uniquely (Fig. 10.11), therefore it is sufficient to examine one of the forms of relationship. The relationship to  $f_c$  is more graphic.

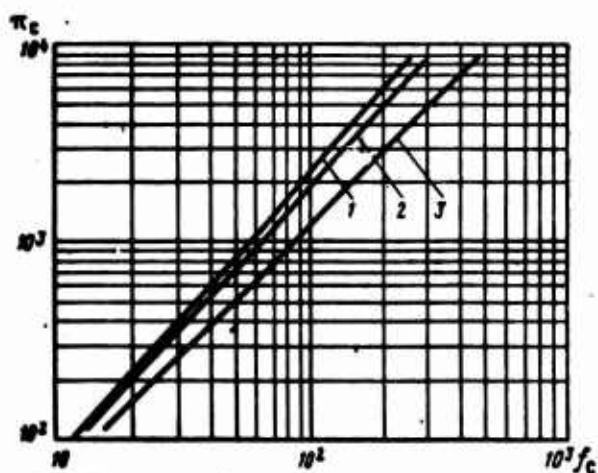


Fig. 10.11. Relationship between  $\pi_c$  and  $f_c$  for various propellants ( $p_h^* = 100$  bar):  
1 -  $H_2 + F_2$  ( $\alpha = 0.6$ ); 2 -  $H_2 + O_2$  ( $\alpha = 0.6$ ); 3 - kerosene +  $O_2$  ( $\alpha = 0.3$ ).

Figure 10.12 shows a change in basic parameters of working medium depending on  $f_c$  with equilibrium and frozen expansion. Specifically, practically the same curve  $\rho = f(f_c)$  is noteworthy.

Figure 10.13 shows the relationship of thrust coefficient  $K_p$  to  $f_c$  during operation of nozzles under various conditions ( $p_h^*/p_h = \text{var}$ ). There is separated the curve of optimum nozzles under these conditions ( $p_c = p_h$ ), and also the boundary of flow separations inside the nozzle under conditions of deep overexpansion. Inasmuch as for the given working medium the quantity of complex  $\beta$  can be considered constant, the relationship of  $K_p$  to  $f_c$  are equivalent to relationships  $P_{yA} = f(f_c)$ .

Fig. 10.12  
nozzle  
kerosene



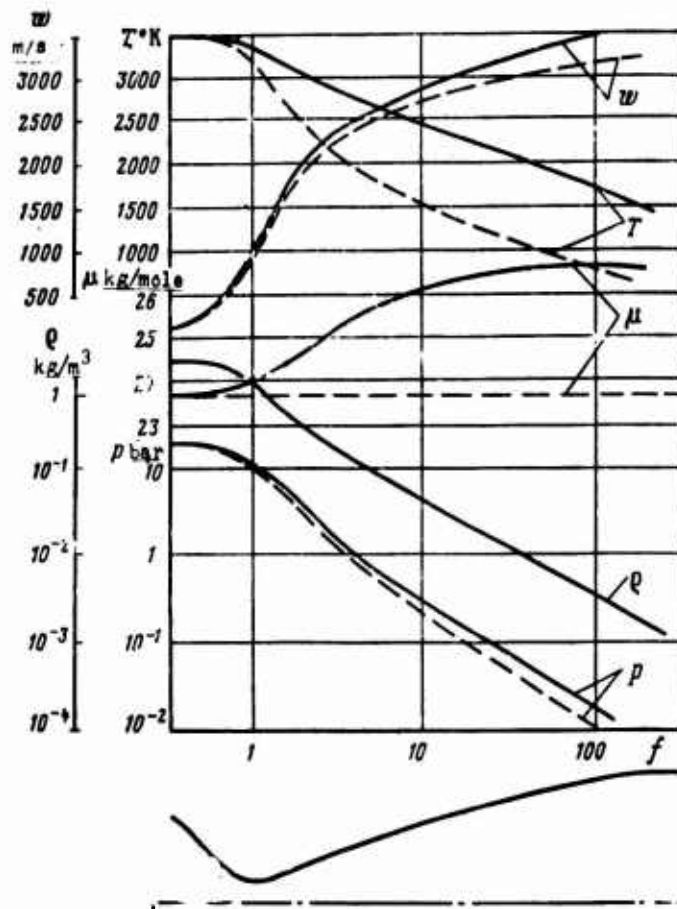


Fig. 10.12. Typical change of parameters of working medium in the nozzle at equilibrium (solid line) and frozen (dotted line) expansion: kerosene +  $O_{2H}$  ( $\alpha = 0.8$ );  $p_H^* = 20$  bar.

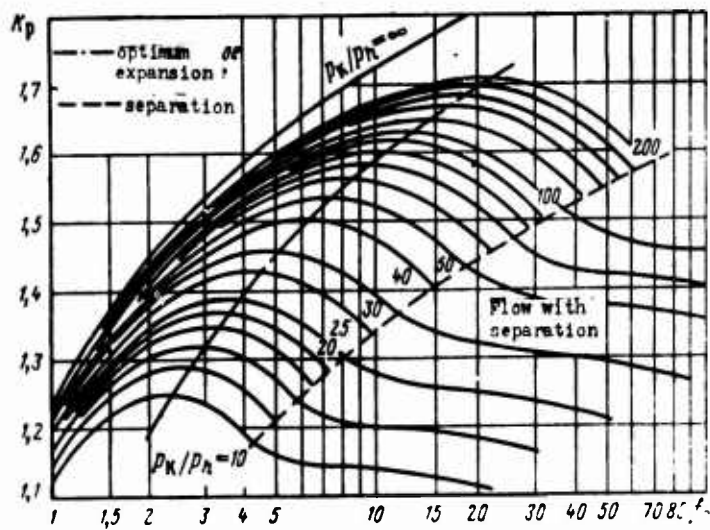


Fig. 10.13. Relationship of thrust coefficient to relative nozzle area.

### 10.5. Relationship to Relative Combustion Chamber Area

As is known, the supply of heat to gas in a cylindrical pipe leads to acceleration of flow, accompanied by a drop not only of static, but also total pressure. Figure 10.14 shows in relative quantities the change of pressures and velocity at different quantities of  $f_K$ .

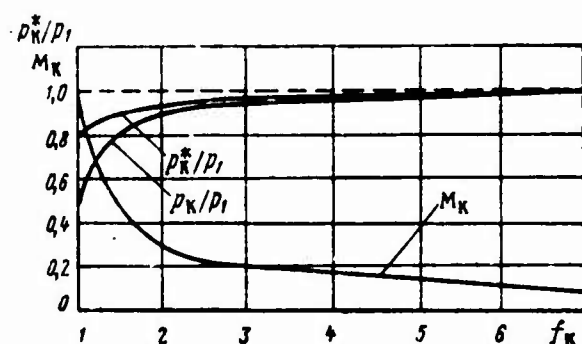


Fig. 10.14. Change in flow parameters depending on the relative combustion chamber area: propellant kerosene +  $O_2$  ( $\alpha = 0.9$ ).

The temperature of flow, statistical and total simultaneously change. Change of the latter in the isenthalpy process is explained by change in the composition of gas and its thermal capacity. Figure 10.15 shows the change in relative quantities

$$\bar{T}_K = \frac{T_K}{(T_K^*)_{\text{изобарн.}}}$$

and

$$\bar{T}_K^* = \frac{T_K^*}{(T_K^*)_{\text{изобарн.}}}$$

There we listed relationship  $\bar{\mu}_K = \frac{\mu_K}{(\mu_K)_{\text{изобарн.}}} = \Phi(f_K)$ , caused by change in intensity of dissociation with change of  $p$  and  $T$ .

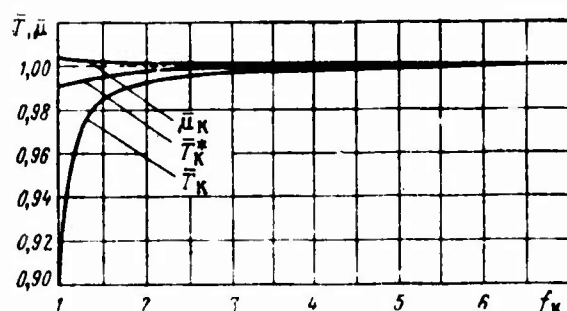


Fig. 10.15. Relationship of relative quantities  $\overline{T}_K^*$ ,  $\overline{T}_K$ ,  $\mu_K$  to  $f_K$  (propellant is the same as on Fig. 10.14).

Decrease of  $f_K$  signifies lowering of total pressure at the nozzle inlet  $p_K^*$ . In the limit, when  $f_K = 1$ , it is lowered approximately to quantity  $0.8p_1$ . Change in intensity of dissociation in this pressure range does not practically affect the quantity of complex  $\beta$ , which therefore can be considered independent of  $f_K$ .

Lowering of  $p_K^*$  leads to decrease in the handling capability of the nozzle throat, i.e., to increase in its specific area:

$$F_{y_{\text{н.т.р}}} = \frac{\beta}{p_K^*}.$$

Concerning the effect of  $f_K$  on specific thrust, it can be evaluated in two cases.

1. If one compares chambers with isobaric and nonisobaric heat supply when  $p_1 = \text{const}$  and  $p_1/p_c = \text{const}$ , then the advantage of the isobaric chamber is revealed. This is explained in the following manner. General drop of pressure can be written as the product of

$$\frac{p_1}{p_c} = \frac{p_1}{p_K^*} \frac{p_K^*}{p_c},$$

in which the first factor is the pressure drop, utilized in a cylindrical combustion chamber (heat nozzle), the second - in geometric nozzle. It is known that the effectiveness of the geometric nozzle is higher than heat. Therefore, with decrease of  $f_K$ , i.e., with increase of  $p_1/p_K^*$ , the specific thrust will diminish. On Fig. 10.16 this position is illustrated quantitatively. Quantity  $\bar{P}_{yд.п}$  is ratio

$$\bar{P}_{yд.п} = \frac{P_{yд.п}}{(P_{yд.п})_{изобар.}}$$

As can be seen, relationship  $\bar{P}_{yд.п} = f(f_K)$  is more substantial at small pressure drops  $p_1/p_c$ .

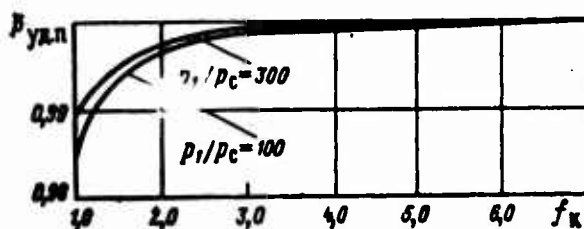


Fig. 10.16. Relationship of relative quantity of  $\bar{P}_{yд.п}$  to  $f_K$  (propellant is the same as on Fig. 10.14).

2. For all practical purposes it is more important to compare the specific thrust of chambers with isobaric and nonisobaric heat release at condition  $p_1 = \text{const}$  and  $f_c = \text{const}$ . In this instance the effect of  $f_K$  on  $P_{yд.п}$  will be indicated only by change in pressure  $p_K^*$ . In the extreme case,  $f_K = 1$ , change of  $p_K^*$  does not exceed approximately 20%. As follows from data of Table 10.1, corresponding change in specific thrust in a void in this case will not exceed tenths of a percent.

On the basis of the typical relationships given on Figs. 10.14-10.16, it may be concluded that the change of separate thermodynamic



characteristics in function  $f_H$  can be disregarded, beginning from certain values of  $f_H$ . Usually the combustion chamber is considered isobaric if quantity  $f_H$  is not less than 5-6.

#### 10.6 Relationship to Temperature or Enthalpy with Independent Heating

Let us examine the relationship of the most important thermodynamic characteristic - specific thrust with fixed degree of pressure decrease in the nozzle  $\pi_c$ .

With increase in the temperature of undissociated working medium the specific thrust increases approximately in proportion to the square root of temperature. Increase in the equilibrium specific thrust in case of reacting working medium at the same temperatures is more considerable. As the temperature increases the difference in specific thrusts is increased.

This is explained by decrease of molecular weight during dissociation and, consequently, by increase in the gas constant. From this it does not follow, however, that dissociation is energetically advantageous. The point is that heating of working medium, being accompanied by dissociation, and its heating to the same temperature without dissociation require substantially different quantities of heat. In the first case the necessary heat supply is considerably more. Dissociation, however, is useful in the fact that it allows the working medium to accumulate a greater quantity of energy at a lower temperature than without dissociation. Recombination, proceeding with equilibrium expansion of the working medium in the nozzle, partially returns the heat spent on dissociation to the working medium. This heat is then converted into kinetic energy of the exhaust stream. However, if expansion of the working medium is frozen, then such return of heat is absent.

Since the intensity of dissociation increases with reduction of pressure, at low pressures in the preheating chamber accumulating power of the working medium at the same temperature is increased. The result can be increased in the specific thrust when  $p_k^*/p_c = \text{const}$  or  $f_c = \text{const}$ .

On Fig. 10.17 according to [2] there are listed values of equilibrium specific thrust at various pressures and temperatures in the heating chamber for two substances - hydrogen (solid lines) and helium (dotted line). Monatomic helium does not dissociate and for all practical purposes does not undergo ionization in the given temperature range. In connection with this, the specific thrust of helium at constant  $p_k^*/p_c$  does not depend on pressure in the heating chamber, but is determined only by the heating temperature. The picture is different for hydrogen. At low temperatures (for example, 2000°K) the reduction of pressure at constant  $p_k^*/p_c$  leads to increase in specific thrust. If the temperature is higher, the maximum of specific thrust is reached at pressures corresponding to practically total dissociation of the working medium. At a temperature of 4000°K this pressure is about 0.1 bar. When the temperature is even higher, maxima of  $P_{yd}$  are reached at pressures in the heating chamber greater than  $p_k^* = 10$  bar.

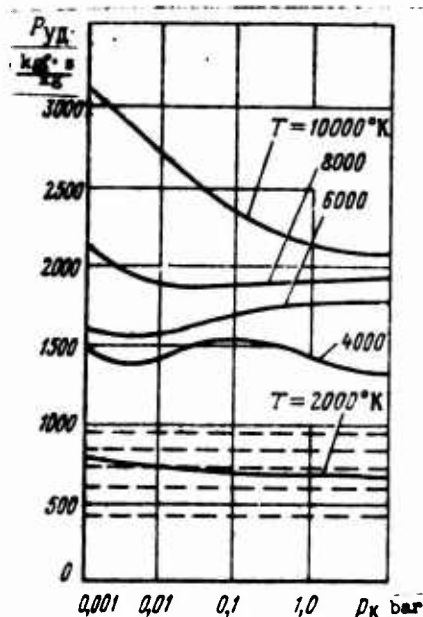


Fig. 10.17. Relationship of specific thrust to pressure and heating temperature:  $p_k^*/p_c = 100 = \text{const}$ ; equilibrium expansion.

At low pressures and high temperatures the tendency of specific thrust to another, higher maximum, caused by thermal ionization of the working medium is clearly evident. Ionization, as dissociation, leads to increase the capability of working medium to accumulate energy from an independent source. In connection with this, in rocket engines using energy of nuclear reactions, we sometimes propose the application of low pressures in the heating chamber and easily dissociating (ionizing) working media. However, the benefits of utilization of low pressures can be completely realized only under the condition of equilibrium of the expansion process in the nozzle, which is not always guaranteed.

Various quantities of supplied energy correspond to values of specific thrust for hydrogen, obtained at the same temperature and different pressures  $p_K^*$ . It is interesting to compare the specific thrusts at various pressures in the heating chamber ( $\pi_c = \text{const}$ ), but identical quantities of supplied energy. Results of such calculations are listed on Fig. 10.18. As was to be expected, in case of identical total enthalpy of 1 kg of working medium large specific thrust is attained at high pressures in the heating chamber, since heat in this case is used energetically more suitably.

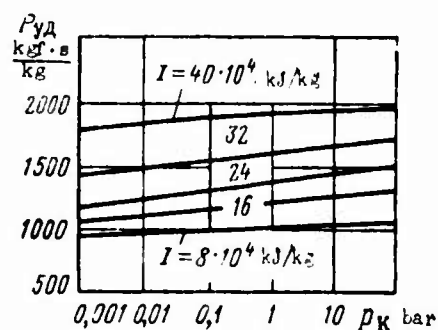


Fig. 10.18. Relationship of specific thrust to pressure and total enthalpy of heating: working medium -  $H_2$ ;  $p_K/p_c = 100 = \text{const}$ , equilibrium expansion.

In rocket engines with heating of the working substance from an independent source of energy the limiting factor will obviously be the heating temperature on which the rate of heat exchange to walls of the chamber depends. Therefore, comparison of the effectiveness of various working substances at identical heating

### Bibliography

1. Alemasov V. Ye. Teoriya raketnykh dvigateley (Theory of rocket engines), Oborongiz, 1962.
2. Zeiger-Bredt I., Nekotoryye svoystva vodoroda i vodyanogo para - vozmozhnykh rabochikh tel raket (Some properties of hydrogen and water vapor - possible working media of rockets), IIL, 1962.
3. Siegel B., Schielder L., Energetics of Propellant Chemistry, New-York, 1964.
4. Wilkins R. L., Theoretical evaluation of Chemical Propellants, Prentice Hall, 1963.

SECOND SECTION

Thermogas-Dynamics of Real Flows and Heat Exchange

## CHAPTER XI

### PROPERTIES OF REAL PROCESSES

In the chapter is examined the effect of some deviations from idealized schemes of calculation for thermodynamic properties and characteristics of combustion products, including specific thrust. The effect of heterogeneity of parameters and incompleteness of combustion, nonideality of working medium, and also nonadiabaticity and chemical nonequilibrium of processes is analyzed.

#### 11.1. Basic Distinctions from Theoretical Schemes

In Chapter VIII the methods of calculation of basic processes in the engine chamber have been examined. The totality of accepted assumptions permitted determining the theoretical thermodynamic characteristics of propellant.

Actual processes in engines proceed with noticeable deviation from idealized schemes of calculation, differ from calculation and properties of combustion products. These differences basically will be reduced to the following.

Limited information about the qualitative composition of combustion products,  $p$ - $v$ - $T$  and other properties of individual components at high temperatures, mechanism and speeds of chemical reactions hampers the obtaining of reliable data on properties of the working medium. Assumptions about the ideality (in the sense

of equation of state) of components, energy and chemical equilibrium of the mixture are valid only in limiting cases ( $p = 0$ ; infinite time of stay). Therefore, known noncoincidence of calculated and actual properties of the working properties can be expected.

Motion of combustion products in the chamber generally is not described by equations of one-dimensional equilibrium isentropic flow. Real flow is not one-dimensional and can be accompanied by nonequilibrium phenomena, for example, energy and chemical nonequilibrium phenomena, for example, energy and chemical nonequilibrium. In two-phase flow high-speed and temperature nonadiabaticity have substantial value. As any real substance, combustion products possess viscosity, thermal conductivity, emissivity. They return part of the heat to the chamber walls.

As can be seen, even with ideal organization of processes in the engine, one should expect some nonconformity of calculated and real thermodynamic characteristics. Real organization of processes can only increase this nonconformity. Incompleteness of combustion, heterogeneity of flow parameters on the cross section of the chamber, nonadiabaticity of flow - all this can introduce noticeable corrections into theoretical values of characteristics.

Some of the properties enumerated above are examined in this chapter, others - in the following chapters of the section.

### 11.2. Nonadiabaticity of Processes

In real conditions the processes in the combustion chamber and nozzle of the engine are always accompanied by heat exchange with the surrounding medium. Two basic cases are possible.

1. Heat is carried off through the chamber walls into the surrounding medium forever. Such, for example, is independent cooling by special liquid, which is not returned to the chamber and takes away removed heat with it. Such removal of heat is observed in chambers cooled by radiation.

2. Heat carried off into cooling liquid is returned together with it to the chamber. This takes place with regenerative cooling of chamber walls by propellant components.

The qualitative effect of adiabaticity of specific thrust is evident. Irreversible heat removal from the working medium doubtlessly reduces specific thrust in comparison with its theoretical quantity during adiabatic processes. Regenerative cooling of chamber walls, on the contrary, can increase the value of specific thrust of the chamber in comparison with theoretical, if in this case we do not consider the expenditures of energy for forcing the liquid through the cooling passage. The benefit from regeneration of heat appears with heat  $Q$  is removed from the working medium at lower pressure than the pressure at which it returns to the chamber. Thus, regeneration of heat on the section of the combustion chamber with constant pressure does not lead to increase of  $P_{y\Delta}$  in comparison with the theoretical value of  $P_{y\Delta t}$ , and regeneration on the nozzle section should bring some benefit. The greater the latter, the more heat that is removed at low pressures, i.e., closer to the nozzle exit.

Let us approximately estimate the effect of nonadiabaticity on specific thrust. Pressures in the combustion chamber and nozzle section are assigned and constant.

#### Effect of Nonadiabaticity with Independent Cooling

Heat  $Q$  carried away from the chamber is the sum of two components: heat  $Q_{\kappa.c}$ , carried away on the section of the combustion chamber, and heat  $Q_c$ , carried away on the nozzle section.

The effect of heat removal in the combustion chamber can be evaluated by extrapolation formulas (see Chapter IX). Assuming in expression (9.50)  $\Delta I = -Q_{\kappa.c}$ , we obtain [Translator's Note:  $\kappa c$  = combustion chamber;  $c$  = nozzle]:



$$\frac{\Delta P_{yA}}{P_{yA}^0} = -\frac{1}{2} \frac{Q_{K.C}}{I_K - I_C} \left(1 - \frac{T_C}{T_K^*}\right), \quad (11.1)$$

where  $\Delta P_{yA} = P_{yA} - P_{yA}^0$ ;  $P_{yA}^0$  is specific thrust under conditions of nonadiabaticity.

As can be seen, all things being equal, losses of specific thrust are proportional to the quantity of removed heat  $Q_{K.C}$ .

Let us determine losses of specific thrust as a result of nonadiabaticity of the expansion process. Let us formulate change in total enthalpy in the process of expansion with heat removal

$$\Delta I_Q = I_K - (I_C + \delta I_C) - Q_C$$

or

$$\Delta I_Q = (I_K - I_C) - \delta I_C - Q_C. \quad (11.2)$$

In expression (11.2)  $I_K$  and  $I_C$  - values of total enthalpy of the working medium in corresponding sections of the chamber during adiabatic process of expansion;  $\delta I_C$  - change in total enthalpy at the nozzle exit caused by heat removal  $Q_C$ .

With  $p_C = \text{const}$  quantity  $\delta I_C$  can be written

$$\delta I_C = T_C \delta S, \quad (11.3)$$

where  $\delta S$  - change in entropy, connected with nonadiabaticity of the process. This quantity is equal to

$$\delta S = - \int_{T_K^*}^{T_C} \frac{dQ}{T} \quad (11.4)$$

(minus sign corresponds to heat removal from the working medium).

For determination of  $\Delta I$  by formula (11.4) it is necessary to know the law of heat removal between temperatures  $T_u^*$  and  $T_c$ , generally speaking, different for different chambers. Expression approximately (11.4) can be written so:

$$\Delta I = -\frac{Q_c}{T},$$

where  $\bar{T}$  - mean temperature on the nozzle section of heat removal.

In the first approximation quantity  $\bar{T}$  can be taken equal to temperature in the nozzle throat  $T_{sp}$ . Then

$$\Delta I = -\frac{Q_c}{T_{sp}}.$$

Since according to approximate gas-dynamic relationships

$$T_{sp} = \frac{2}{n+1} T_u^*,$$

then

$$\Delta I = -\frac{n+1}{2} \frac{Q_c}{T_u^*}.$$

Now expressions (11.3) and, accordingly, (11.2) take the form

$$\begin{aligned} \Delta I_c &= -\frac{n+1}{2} \frac{T_c}{T_u^*} Q_c; \\ \Delta I_Q &= (I_u - I_c) - Q_c \left( 1 - \frac{n+1}{2} \frac{T_c}{T_u^*} \right). \end{aligned} \quad (11.5)$$

Let us compose relative change in specific thrust as a result of nonadiabaticity of the expansion process

$$\frac{P_{\gamma_1}}{P_{\gamma_1}^0} = \sqrt{\frac{\Delta I_Q}{\Delta I}}.$$

where  $\Delta I = I_u - I_c$  is change in total enthalpy during adiabatic expansion.

By using expression (11.5), let us write:

$$\frac{p_{y1}}{p_{y1}^0} = \sqrt[1 - \frac{Q_c}{\Delta I} \left( 1 - \frac{n+1}{2} \frac{T_c}{T_u^*} \right)]{}$$

If  $Q_c \ll \Delta I$ , then according to rules of approximate calculations

$$\frac{p_{y1}}{p_{y1}^0} \approx 1 - \frac{Q_c}{2\Delta I} \left( 1 - \frac{n+1}{2} \frac{T_c}{T_u^*} \right)$$

or

$$\frac{\Delta p_{y1}}{p_{y1}^0} = - \frac{1}{2} \frac{Q_c}{I_u - I_c} \left( 1 - \frac{n+1}{2} \frac{T_c}{T_u^*} \right). \quad (11.6)$$

In the lower part of the chart on Fig. 11.1 are given values of  $\Delta p_{y1}/p_{y1}^0$ , determined by formula (11.6). As can be seen, at the same relative quantity of removed heat  $Q_c/\Delta I$  the specific thrust is lowered more substantially at large values of  $p_u^*/p_c$ . The amount of relative quantity of heat, removed from the working medium in the nozzle, is usually not more than 0.02-0.05 (smaller values pertain to heavy engines). The lowering of specific thrust caused by this is small.

With independent cooling of engines, tested on a stand, a considerable quantity of heat  $Q$  can be removed and decrease of  $\Gamma_{y1}$  can reach 5% for small engines.

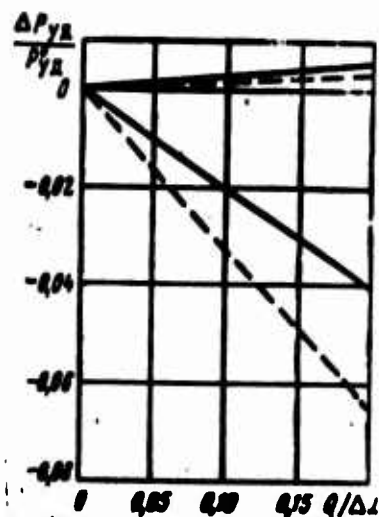


Fig. 11.1. Relationship of  $\Delta P_{yA}/P_{yA}^0$  to relative quantity of removed heat: —  $\eta_c = 100$ ; ---  $\eta_c = 1000$ .

#### Effect of Nonadiabaticity with Regenerative Cooling

With regenerative cooling the same scheme of selection of heat  $Q_c$  in the nozzle throat can be taken. When determining the change in total enthalpy in the nozzle it is necessary to consider that heat  $Q_c$  is completely returned to the combustion chamber. In connection with this, expression (11.2) takes the form

$$\Delta I_Q = (I_x - I_c) - \delta I_c. \quad (11.7)$$

Quantity  $\delta I_c$  can be written, as earlier:

$$\delta I_c = T_c \delta s.$$

Entropy change in the case of regenerative cooling is caused not only by heat removal  $Q_c$  at temperature  $T_{kp}$ , but also by reverse feed of it at temperature  $T_k^*$ , i.e.,

$$\delta s = \delta s_1 + \delta s_2,$$

where

$$\delta s_1 = -\frac{Q_c}{T_{kp}} = -\frac{n+1}{2} \frac{Q_c}{T_k^*}$$

and

$$\delta s_2 = \frac{Q_c}{T_n^*}$$

Consequently:

$$\delta s = -\frac{n-1}{2} \frac{Q_c}{T_n^*}$$

and

$$\delta I_c = -\frac{n-1}{2} \frac{T_c}{T_n^*} Q_c. \quad (11.8)$$

By substituting expression (11.8) in equality (11.7), we obtain:

$$\Delta I_Q = (I_n - I_c) + \frac{n-1}{2} \frac{T_c}{T_n^*} Q_c.$$

By analogy with the previous case

$$\frac{P_{y_n}}{P_{y_n}^0} = \sqrt{1 + \frac{n-1}{2} \frac{T_c}{T_n^*} \frac{Q_c}{\Delta I}}.$$

Approximately

$$\frac{P_{y_n}}{P_{y_n}^0} \approx 1 + \frac{n-1}{4} \frac{Q_c}{\Delta I} \frac{T_c}{T_n^*}$$

or

$$\frac{\Delta P_{y_n}}{P_{y_n}^0} \approx \frac{n-1}{4} \frac{Q_c}{\Delta I} \frac{T_c}{T_n^*}. \quad (11.9)$$

Relationship (11.9) is shown in the upper part of the chart of Fig. 11.1. As can be seen, increase in specific thrust as a

result of regenerative cooling even when  $Q_c/AI = 0.1-0.2$  comprises only fractions of a percent. Actually the relative quantity of heat, circulating in the regenerative cooling system, is even less due to a number of limitations (see Chapter XX).

Thus, regeneration of heat in the cooling passage of the chamber of a liquid-propellant rocket engine is not so substantial a means of increase in specific thrust in comparison with  $P_{yd}$ . However, external regenerative cooling of the chamber walls at least eliminates irreversible heat removal from the working medium and thus averts losses of specific thrust connected with such removal.

### 11.3. Heterogeneity of Parameters and Incomplete Combustion

#### Heterogeneity of Parameters

The method of determination of thermodynamic characteristics examined earlier proposed identical distribution of propellant components along the cross section of the combustion chamber. In actuality the distribution of propellant components is heterogeneous. This heterogeneity can be intentional or can have a random character.

Equilibrium mixing of components in some assigned ratio provides maximum possible liberation of heat under the given conditions. Value of optimum component ratios is selected from conditions of obtaining the best basic indices of the chamber.

However, high values of temperature, at which it is difficult to organize reliable cooling, correspond to the magnitude of optimum component ratios. Therefore, homogeneous distribution can be unacceptable, if it does not provide the necessary life of the chamber.

The low-temperature range near the chamber walls can be organized by various means. This can be, for example, supply of propellant

when  $\kappa \neq \kappa_{\text{opt}}$  or other special liquid, gas (liquid-propellant rocket engines), utilization of special low-temperature propellants or coatings that burn up (PATT) [RDTT = solid-propellant rocket engines] and others. In all such cases the composition and properties of combustion products are heterogeneous along the cross section of the combustion chamber. [Translator's Note:  $\text{opt}$  = optimum.]

The reason for random oscillations of composition and properties of combustion products can be heterogeneity of propellant composition (possible in RDTT), scattering of characteristics of mixing elements (liquid-propellant rocket engines).

Let us determine the basic thermodynamic characteristics of nonuniform flow, consisting of  $i$  propellants of various initial composition (for example, different  $\kappa_i$ ) with relative flow rate  $g_i$ . In addition to earlier accepted assumptions (see Chapter VIII) we will consider that combustion products of separate propellants are isolated from each other, and pressure is constant along the cross section of the chamber. Theoretical characteristics of separate propellants ( $P_{y\Delta i}$ ,  $\beta_i$ ,  $n_i$ ,  $F_{y\Delta i}$  and others) are known by results of thermodynamic calculation.

Continuity equation for combustion products of  $i$ -th propellant

$$\dot{G}_i = \rho_i w_i F_i$$

can be written so:

$$\dot{G}_i = \frac{p_i F_i M_i a_i}{R_i T_i}, \quad (11.10)$$

where  $M_i$  - Mach number.

by using approximate formulas for the speed of sound  $a_i$  and complex  $\beta_i$  in the form

flow) and  $N_2H_4$  (boundary layer) at pressure in the combustion chamber 10.5 bar and general coefficient of component ratios  $\kappa = 1.2$  kg ox/kg fuel. As can be seen, formulas (11.12) and (11.13) give practically coinciding results.

Table 11.1. Comparative appraisal of the accuracy of approximate formula for  $\beta$ .

$N_2H_4$				$N_2H_4 + N_2O_4$				Nonuniform flow	
$g_I$	$\mu$	$n$	$\beta$	$\kappa$	$\mu$	$n$	$\beta$	$\beta_{\text{точн}}$	$\beta_{\text{прибл}}$
0,0				1,2	19,96	1,23	188,4	188,4	188,4
0,085	10,74	1,37	132,3	1,4	20,89	1,23	185,1	181,7	181,68
0,114	10,74	1,37	132,3	1,6	21,60	1,23	181,1	175,6	175,6

[Translator's Note: точн = exact, прибр = approx.]

For determination of specific thrust in a void in case of nonuniformity of flow (pressure at nozzle section  $p_c$  is prescribed) let us use known formula:

$$P_{ya,n} = \frac{1}{G} \left( \sum_i G_i w_i + p_c \sum_i F_i \right). \quad (11.14)$$

By substituting the value of  $F_1$  in formula (11.14), we obtain:

$$P_{ya,n} = \sum_i g_i w_i + p_c \sum_i g_i F_{ya,i} = \sum_i g_i (w_i + p_c F_{ya,i})$$

$$P_{ya,n} = \sum_i g_i P_{ya,n,i}. \quad (11.15)$$



The effect of heterogeneous distribution of components on specific thrust of propellant aerosine-50 +  $H_2O_2$  is shown on Fig. 11.2. Distribution  $\kappa$  along the cross section of chamber, taken as initial data, is shown on Table 11.2 [9].

Table 11.2. Examples of distribution of propellant components.

Variant 1	$\kappa_1$	0,0333	0,2647	0,1453	0,2770	0,1433	0,1354
	$\Delta\kappa\%$	100	-15	10	30	15	12,5
Variant 2	$\kappa_1$	0,0233	0,2500	0,1477	0,2870	0,1453	0,1467
	$\Delta\kappa\%$	-100	0	5	15	10	7

As can be seen, heterogeneous distribution of propellant components in the considered case reduces the specific thrust. Amount of losses  $P_{yд.п}$  is changed depending both on  $\kappa$ , and on relative area of nozzle section.

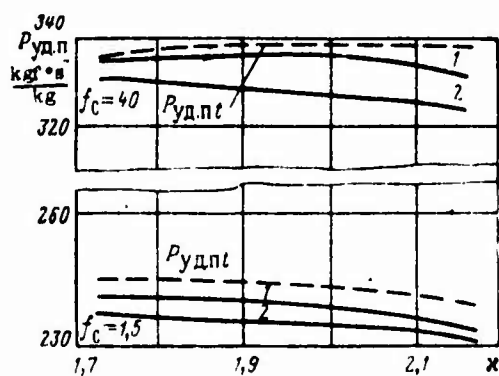


Fig. 11.2. Effect of heterogeneous distribution of propellant components on specific thrust.

Generally the specific thrust of nonuniform flow is always less than the specific thrust of uniform flow at average  $\kappa$ , if relationship  $P_{yд.п} = f(\kappa)$  has been directed concavity downward in the entire range of  $\kappa$ . By levelling the fields of  $\kappa_1$ , accompanying real flow, the effect of nonuniformity of flow diminishes.

## Incomplete Combustion

For evaluation of the effect of incomplete combustion we proposed a number of models. The simplest method consists in the following.

It proposes that as a result of incomplete combustion the temperature in the combustion chamber is lower than calculated; the composition and properties of combustion products correspond to equilibrium values at this temperature. Temperature change  $T_H^*$  can be uniquely connected with change in enthalpy of mixture  $\delta I_T$ , which allows making use of extrapolation formulas.

For simplicity let us examine extrapolation of specific thrust under conditions of equality of pressures  $p_c = p_h$ . Relative change in specific thrust in accordance with formula (9.50) is

$$\delta \bar{P}_{ya} = \frac{P_{ya} - P_{ya}^0}{P_{ya}^0} = \frac{\left(1 - \frac{T_c}{T_k^*}\right) \delta I_T}{(P_{ya}^0)^2}. \quad (11.16)$$

Quantity  $(P_{ya}^0)^2$  is conveniently represented by formula

$$(P_{ya}^0)^2 \approx \frac{2n}{n-1} R_k T_k^* \left(1 - \frac{T_c}{T_k^*}\right).$$

Then expression (11.16) is reduced to

$$\delta \bar{P}_{ya} \approx \frac{n-1}{2n} \frac{\delta I_T}{R_k T_k^*}. \quad (11.17)$$

Change of quantity  $(n-1)/2n$  in range  $f_c = 5-50$  can comprise several percent (increase with increase of  $f_c$ ). Therefore, losses of specific thrust as a result of incompleteness of combustion increase with the increase of  $f_c$ . When  $n = \text{const}$  and at constant pressure in the combustion chamber the losses of specific thrust because of incompleteness of combustion do not depend on  $f_c$ .

#### 11.4. Nonideality of Working Medium

Let us estimate the effect of deviations from equation of state of ideal gas.

Let us examine the state of the system at some prescribed pressure and temperature  $T$ . To it corresponds equilibrium composition, determined by numbers of moles  $n_q$  (molar fractions  $x_q$ ). Let us assume that from state  $p, T$  can change into arbitrary state with invariable chemical composition. Then  $x_q = \text{const}$  and it is simple to establish connection between properties of the mixture at pressure  $p$  and when  $p = 0$  (ideal gas).

Let us determine enthalpy and entropy of the mixture, for which let us integrate the following differential thermodynamic relationships with respect to pressure from prescribed  $p$  to  $p \rightarrow 0$  when  $T = \text{const}$ :

$$dI = \left[ v - T \left( \frac{\partial v}{\partial T} \right)_p \right] dp, \quad (11.18)$$

$$dS = - \left( \frac{\partial v}{\partial T} \right)_p dp. \quad (11.19)$$

As a result we obtain:

$$I = \sum_q n_q I_{q, \text{ideal}}^0 + \int_p^0 \left[ v - T \left( \frac{\partial v}{\partial T} \right)_p \right] dp, \quad (11.20)$$

$$S = \sum_q n_q (S_{q, \text{ideal}}^0 - R_0 \ln p_q) - \int_p^0 \left[ \left( \frac{\partial v}{\partial T} \right)_p - \left( \frac{\partial v}{\partial T} \right)_{p, \text{ideal}} \right] dp. \quad (11.21)$$

[Translator's Note:  $\text{ид} = \text{ideal}.$ ]

The first terms in the right sides of expressions (11.20) and (11.21) - enthalpy and entropy of some fictitious ideal mixture, composition of which (numbers of moles  $n_q$ ) is equal to the composition of mixture of real gases.

For this ideal mixture when  $x_q = \text{const}$  the following relationship is valid

$$x_q = \frac{p_q}{p} = \frac{n_q}{N}. \quad (11.22)$$

Having substituted it in equation (11.21), we obtain:

$$S = \sum_q n_q (S_{q, \text{ia}}^0 - R_0 \ln n_q) - R_0 N \ln p + R_0 N \ln N - \int_0^p \left[ \left( \frac{\partial v}{\partial T} \right)_p - \left( \frac{\partial v}{\partial T} \right)_{p, \text{ia}} \right] dp. \quad (11.23)$$

As earlier, the number of moles of propellant  $M_r$  is taken such, so that the following equality would be fulfilled

$$N = p. \quad (11.24)$$

By using equality (11.24), we obtain:

$$S = \sum_q n_q (S_{q, \text{ia}}^0 - R_0 \ln n_q) - \int_0^p \left[ \left( \frac{\partial v}{\partial T} \right)_p - \left( \frac{\partial v}{\partial T} \right)_{p, \text{ia}} \right] dp. \quad (11.25)$$

In accordance with the formula for chemical potential of the q-th component in a mixture of real gases let us write:

$$\varphi_q = \left[ \frac{\partial (I - TS)}{\partial n_q} \right]_{p, T, n_i} = I_{q, \text{ia}}^0 - T (S_{q, \text{ia}}^0 - R_0 \ln n_q) - \int_0^p \left( \bar{v}_q - \frac{R_0 T}{p} \right) dp, \quad (11.26)$$

where  $\bar{V}_q = (\partial v / \partial n_q)_{p, T, n_i}$  - molar partial volume, determined by equation of state of mixture.

For ideal gas on the basis of formulas (11.22) and (11.24)  $n_q = p_q$ , and molar partial volume is equal to

$$\bar{V}_q = \frac{\partial}{\partial n_q} \left( \sum_q n_q \frac{R_0 T}{p} \right)_{p, T, n_i} = \frac{R_0 T}{p}. \quad (11.27)$$

Taking into account formula (11.27) and equality  $n_q = p_q$  we obtain the expression applied in Chapter VI for chemical potential:

$$\varphi_{q_{\text{на}}} = I_{q_{\text{на}}}^0 - T(S_{q_{\text{на}}}^0 - R_0 \ln p_{q_{\text{на}}}).$$

Equilibrium composition of homogeneous mixture of reacting real gases is found from equations of thermodynamic equilibrium which also were considered in Chapter VI. The original form of equations of chemical equilibrium and conservation of substance remain as previous:

$$\begin{aligned} \sum_i a_{ij} \varphi_i &= \varphi_j; \\ \sum_j a_{ij} n_j + n_i &= M_i b_i, \end{aligned}$$

and instead of equation of Dalton law there is used obvious relationship:

$$\sum_q x_q = 1. \quad (11.28)$$

In the final form for calculations the system of equations appears in the following form:

$$\ln n_j - \sum_i a_{ij} \ln n_i + \ln K_{j_{\text{на}}} - \frac{1}{R_0 T} (\Delta \varphi_j - \sum_i a_{ij} \Delta \varphi_i) = 0; \quad (11.29)$$

$$\ln \left( \sum_i a_i n_i + n_i \right) - \ln M_i - \ln b_i = 0; \quad (11.30)$$

$$\ln \sum_i n_i - \ln p = 0, \quad (11.31)$$

where

$$\Delta \varphi_i = \int_0^p \left( \bar{v}_i - \frac{R_0 T}{p} \right) dp.$$

Technology of solutions of equations (11.29)-(11.31) remains basically as previous, it is necessary only to note the following feature. Generally the last term in equation (11.29) depends on the temperature, pressure and composition. Inasmuch as equilibrium composition of the mixture of real gases was not known earlier, in the first approximation for determination of this term the composition of ideal gas is used. The found composition of real gas is then used for refinement of quantities  $\Delta \phi_q$ , change of which, in turn, leads to the necessity of repeated calculation of composition, etc.

By differentiating system (11.29)-(11.31) with respect to logarithm of pressure or with respect to logarithm of temperature, we obtain values of partial derivatives, necessary for determination of thermodynamic functions and properties of the mixture. The latter are calculated by usual thermodynamic relationships.

An important moment in thermodynamics of real gas is the selection of corresponding equation of state. As criterion of correctness of this selection there is coincidence of calculated and experimental properties of the mixture. As applied to conditions in the chambers of rocket engines the experimental determination of properties of combustion products is difficult and therefore can be performed only with the aid of theoretical equations of state.

Let us take the equation of state for a mixture in virial form [4]:

$$pv = \sum_i n_i R_0 T \left( 1 + \frac{p}{R_0 T} \sum_i \sum_j x_i x_j B_{ij} \right), \quad (11.32)$$

where  $B_{ij}$  - the second virial coefficients.

Selection of equation of state (11.32) is justified by the following considerations:

- a) theoretical validity of equation of state in virial form;
- b) possibility of approximate determination of virial coefficients  $B_{ij}$  in the absence of immediate experimental data;
- c) range of temperatures and pressures ( $T > 700^\circ\text{K}$ ,  $p < 500$  bar) for which it is proposed to use the equation of state.

Values of the second virial coefficients are determined by formulas of molecular-kinetic theory in accordance with the accepted model of interaction (potential):

$$B_{ij} = 1.2615 \sigma_{ij}^3 B_{ij}^* (T_{ij}^*),$$

The tabulated values of functions  $B_{ij}^*$  ( $T_{ij}^*$ ) for the most commonly used potentials are listed in reference book [4].

In Table 11.3 as illustrations there are presented equilibrium properties of combustion products of propellant  $\text{C}_2\text{H}_8\text{N}_2 + \text{N}_2\text{O}_4$  when  $\alpha = 0.8$ , cooled to temperatures 2000, 1200, 800°K at pressures 150 and 300 bar. Units of measurement of thermophysical quantities:  $c_p$ , kJ/kg·deg,  $a_p$ , deg<sup>-1</sup>,  $a_p$ , m/s; upper value - properties of ideal mixture, lower - real [1].

Table 11.3. Equilibrium properties of ideal and real mixtures.

$T$	$p = 150$			$p = 300$		
	$a_p \cdot 10^3$	$c_{pp}$	$a_p$	$a_p \cdot 10^3$	$c_{pp}$	$a_p$
800	1.3594	1.9650	557.3	1.3292	1.8392	558.1
	1.4987	2.0438	566.7	1.6054	2.0011	577.8
1200	0.9002	2.1809	708.7	0.9920	2.5844	702.2
	0.9204	2.2341	726.3	1.0235	2.7108	736.5
2000	0.5002	1.8979	918.2	0.5001	1.9084	918.2
	0.4947	1.9038	935.5	0.4894	1.8960	953.0

As was to be expected, divergences in properties of ideal and real mixtures correspond to known theoretical positions: they are decreased with increase of temperature and with decrease in pressure. From Table 11.3 it is also evident that under conditions ( $p$ ,  $T$ ), analogous to tabular, allowance for deviations in the properties of working medium as a result of nonideality is expedient.

Calculation of processes in the rocket engine chamber with nonideal (in the sense of equation of state) working medium is analogous to calculation listed in Chapter VIII with ideal working medium. In this case the values of composition, enthalpy, entropy and other properties of combustion products must be determined with allowance for a particular equation of state, for example (11.32).

As illustrations Table 11.4 contains relative deviations of real thermodynamic characteristics from ideal for propellant asymmetric dimethylhydrazine +  $N_2O_4$  at values of excess oxidant ratio  $\alpha = 0.5$  and  $0.9$ . As can be seen, in this instance the effect of nonideality is relatively small and cannot be considered in calculations.

Results of fulfilled calculations allow making the following conclusions [2]. In the pressure range 100-500 bar and temperature range 1000-2000°K the reality of gases weakly affects the composition, enthalpy and entropy of the mixture and rather noticeably affects



(5-15.5) thermodynamic properties (thermal capacity, speed of sound).

Table 11.4. Relative change in thermodynamic characteristics of propellant  $C_2H_8 N_2 + N_2O_4$  with utilization of equation of state of ideal and real gas.

$\alpha$	combustion chamber		nozzle throat		nozzle edge $p_c=0.5$	
	$p_k$ bar	$\delta T_k$ %	$\delta p_{kp}$ %	$\delta \beta$ %	$\delta f_c$ %	$\delta p_{y_{1-n}}$ %
0.5	150	0.25	0.39	0.72	0.55	0.05
	250	0.42	0.65	1.19	0.85	0.11
0.9	150	0.02	0.11	0.45	0.27	0.06
	250	0.04	0.21	0.74	0.41	0.09

In connection with the change in thermal capacity under these conditions a change of temperature in the combustion chamber and throat is possible. In gas generators (see Chapter XVII) as a result of low temperatures this change can be substantial (tens of degrees). In the process of gas expansion the effect of reality is diminished rapidly and, most frequently, is not reflected on parameters of the end of expansion.

Since values of virial coefficients  $B_{ii}, B_{ij}$  at elevated temperatures are known only approximately, then the obtained calculation data are estimated.

#### 11.5. Chemical Nonequilibrium

It is known that for establishment of equilibrium in gases finite time is necessary. For gas located in thermal equilibrium, the separate molecules constantly acquire or lose energy as a result of collisions, however the complete change of energy of the system in this case turns out to be equal to zero. Quantity of energy, acquired or lost on one collision (i.e., effectiveness of collisions), under equilibrium conditions turns out to be unessential. However,

if external conditions (for example, temperature and pressure) suddenly change and the gas starts to approach a new state of equilibrium, then the rate of approach to equilibrium (measured usually by time of relaxation) directly depends on the effectiveness of collisions.

With decrease of the temperature in the flow (for example, during flow in the nozzle) various internal balancing processes (energy and chemical relaxation) for their realization require a greater number of collisions between molecules before equilibrium will be attained. If the time of achievement of equilibrium is of the same order as the time of stay, then deviation from equilibrium is possible, which can change the character of flow. These so-called relaxation effects can be observed every time that changes of external conditions with respect to gas occur so rapidly that inside the structure of gas there is no change.

In order that the relaxation process of a separate degree of freedom would affect the flow, two conditions are necessary: time of relaxation must be comparable with the time of stay, and change of energy, connected with the process of relaxation, must comprise a considerable part of the overall change in gas enthalpy. From this viewpoint in the chamber of the engine (time of stay  $10^{-3}$  to  $10^{-4}$  s) the most important relaxation processes are processes of dissociation and recombination, as "slower" and leading to noticeable change of energy in comparison with other types of relaxation. However, in certain cases the nonequilibrium of the process of energy exchange between different types of internal motion of molecules can also show a noticeable effect.

Investigation of processes with allowance for finite rates of reactions requires the inclusions of chemical kinetics - studies about the mechanism and rates of chemical reactions depending on various conditions of the passage of processes.

concer

where  
mixture

S  
partial  
in a u

Th  
particl  
of conc  
connect  
substan

Re  
applied  
assumpt

a)  
monatom  
presence  
improbab

b)  
consider  
and stu

c)  
recomb

The rate of chemical reactions is determined by change in the concentration of reacting substances with time:

$$\omega = \frac{dc_i}{d\tau}, \quad (11.33)$$

where  $\tau$  - time;  $c_i$  - molar concentration of  $i$ -th component of mixture:

$$c_i = \frac{n_i}{V} \frac{\text{mole}}{\text{m}^3}. \quad (11.34)$$

Sometimes as the measure of concentrations we take density or partial pressure of the component, or the number of its molecules in a unit of volume.

The rate of reactions depends on the number of collisions of particles in a unit of time, which is proportional to the product of concentrations of reacting substances. The equation, which connects the rate of the reaction with concentrations of reacting substances, is called kinetic or equation of kinetics.

Relative to rates and mechanism of chemical reactions as applied to processes in rocket engines we usually use the following assumptions:

a) as components of combustion products we consider only monatomic, diatomic and triatomic components of mixtures; the presence of molecules with a large number of atoms is considered improbable;

b) we consider only double and triple collisions, i.e., we consider bimolecular and trimolecular reactions as the more probable and studied in experimental works;

c) we consider, as a rule, generalized reactions of dissociation-recombination with general catalytic particle  $M$ . Such particles

can be any mixture component, consequently, its concentration is equal to

$$c_M = \sum_i c_{Mi}$$

d) when writing equations of kinetics we apply the principle of independence of reactions, i.e., consider that each of them proceeds independently.

As theoretical investigations show, noticeable deviation from equilibrium is more probable in the supersonic part of the nozzle. In the combustion chamber and subsonic part of the nozzle the high-temperature mixture is usually in the state of chemical equilibrium. In gas generators as a result of relatively low temperatures the chemical nonequilibrium is possible. Its effect is evaluated in Chapter XVII.

At present it is not possible to strictly and uniquely select the mechanism of reactions in a multicomponent mixture. This is caused by great difficulties in research on kinetic processes in reacting mixtures.

Nonequilibrium flow of gas in the nozzle in a one-dimensional arrangement is described by such a system of equations: Equation of motion -

$$dp + \rho w dw = 0; \quad (11.35)$$

equation of continuity -

$$F \rho w = \text{const}; \quad (11.36)$$

equation of energy -

$$I + \frac{w^2}{2} = \text{const}; \quad (11.37)$$

equation of state -

$$p = \varrho \frac{R_0 T}{u} \quad (11.32)$$

equations of kinetics -

$$\frac{dc_i}{d\tau} = f_i(c_1, c_2, \dots, c_r, T), \quad i = 1, 2, 3, \dots, r. \quad (11.39)$$

For stationary processes equations (11.39) can be presented in the form:

$$\frac{dc_i}{dx} = \frac{1}{w} f_i(c_1, c_2, \dots, c_r, T), \quad (11.40)$$

Inasmuch as

$$\frac{dc_i}{d\tau} = \frac{dc_i}{dx} \frac{dx}{d\tau} = \frac{dc_i}{dx} w.$$

System (11.35)-(11.38), (11.40) of  $(r + 4)$  equations for determination of  $(r + 5)$  unknowns:  $p, T, w, \rho, F, \{c_i\}$  is open. Therefore, an additional condition is necessary, for example, one of the following: Equation of nozzle profile -

$$F = F(x); \quad (11.41)$$

Distribution of pressure along the nozzle, determined by calculation or experimentally -

$$p = p(x); \quad (11.42)$$

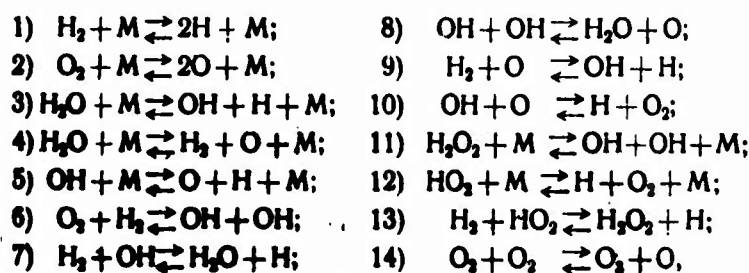
the change in density of working medium in the nozzle, obtained by calculation of equilibrium process -

$$\varrho = \varrho(x). \quad (11.43)$$

As was noted in § 10.4, the chemical nonequilibrium of expansion weakly affects the distribution of density.

System of equations (11.35)-(11.38), (11.40) and one of conditions (11.41)-(11.43) allow completing the calculation for a particular nozzle by numerical methods.

For illustration of the character of calculations of chemically nonequilibrium flows, let us examine one of the probable reaction mechanisms for propellant with the simplest chemical composition  $H_2 + O_2$  [7]. Possible components of combustion products in this case will be:  $H_2$ ,  $O_2$ ,  $H_2O$ ,  $OH$ ,  $HO_2$ ,  $H_2O_2$ ,  $O_3$ ,  $O$ ,  $H$ . Proposed mechanism of reactions are such:



where  $M$  - general catalytic particle - any of the components of combustion products. Mathematically the equation of kinetics is written for each component in the form analogous to that given here for  $H_2O$ :

$$\begin{aligned} \frac{d c_{H_2O}}{dx} = \frac{1}{w} [ & -K_3(T) c_{H_2O} c_M + \bar{K}_3(T) c_{OH} c_H c_M - K_4(T) c_{H_2O} c_M + \\ & + \bar{K}_4 c_{H_2} c_O c_M + K_7(T) c_{H_2} c_{OH} - \bar{K}_7(T) c_{H_2O} c_H + \\ & + K_8(T) c_{OH} c_{OH} - \bar{K}_8(T) c_{H_2O} c_O ]. \end{aligned} \quad (11.44)$$

where  $K_1(T)$ ,  $\bar{K}_1(T)$  - constants of rates of direct and reverse reactions, respectively.

Thus, in case of chemically nonequilibrium expansion in the nozzle the problem is reduced to solution of a complex system of

differential equations, which is feasible only on an (IBM) [IBM = electronic computer].

As illustrations on Figs. 11.3, 11.4 there are some calculation data on temperature, specific thrust and molar fractions for dissociated air [5]. Curves 1, 2, 3 correspond to equilibrium, frozen and chemically nonequilibrium expansion. As can be seen, account of rates of chemical reactions at large values of  $\bar{r} = r/r_{np}$  gives noticeable deviations from results of equilibrium calculation.

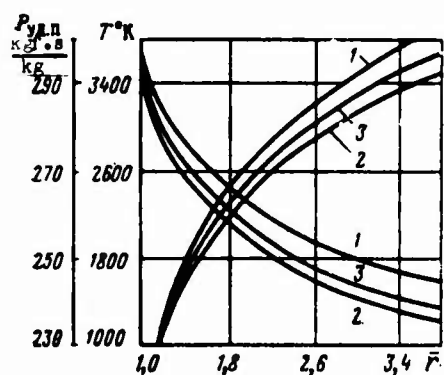


Fig. 11.3. Temperature and specific thrust in a void with expansion of dissociated air in a supersonic nozzle.

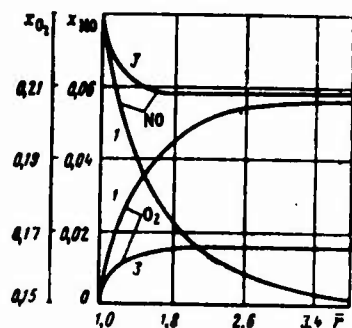


Fig. 11.4. Molar fractions of NO and  $O_2$  with expansion of dissociated air in a supersonic nozzle.

In conclusion the following features of the study and calculation of chemically nonequilibrium flows must be noted.

1. During fulfillment of calculations we encounter difficulties connected with the limited knowledge of true mechanisms of reactions and constants of reaction rates. Many questions of kinetics (theory of chain reactions, theory of combustion, heterogeneous reactions, etc.) have been studied insufficiently for practical utilization and still await comprehensive solution.

2. Calculations are much more bulky than during calculation of equilibrium flow, since we introduced additional variable - space coordinate  $x$  and equations of kinetics - system of differential equations of type (11.40).

3. The character of nonequilibrium flow depends on the physical properties of mixtures, on initial pressure and temperature, on the shape of channel (nozzle). Consequently, calculations do not possess generality of results, it is necessary to perform them for each concrete case.

Comparatively good agreement of obtained calculation and experimental data can be noted. Results of calculations, conducted without allowing for the effect of separate catalytic particles, differ within 5-10% with respect to quantities of molar fractions of components and practically coincide with respect to specific thrust and temperature.

The absence of reliable data about the mechanism and rates of chemical reactions, labor input of accurate calculations frequently force us to resort to approximate methods of analysis of chemically nonequilibrium flows [3]. As an example let us consider the method of "sudden freezing," initially proposed by Bray [3] and modified in other works.

Bray, while studying nonequilibrium flows of diatomic gases in nozzles, revealed that three regions of flow can be conditionally distinguished.

the  
reco  
chan

subs  
one  
and

condi

consi  
of the

flow t  
of fro  
aid of

I:  
to time  
of equi



1. Equilibrium, or almost equilibrium, region, beginning from the combustion chamber, in which the rates of dissociation  $\omega_D$  and recombination  $\omega_R$  are very great in comparison with the rate of change in concentration  $dc_1/d\tau$  necessary for equilibrium flow.

2. Transition region, in which the density and temperature are substantially diminished, and  $dc_1/d\tau$ ,  $\omega_D$ ,  $\omega_R$  become quantities of one order. This causes noticeable deviation from equilibrium, and the process soon after this approaches frozen state.

3. Region of almost frozen flow, in which there is fulfilled condition

$$-\frac{dc_1}{d\tau} \gg \omega_D. \quad (11.45)$$

Approximate solution of the problem can be obtained if we consider that the transitional region is an infinitesimal section of the nozzle, i.e., point during one-dimensional flow.

Consequently, the Bray method proposes calculation of equilibrium flow to the point of instantaneous freezing, and after it - calculation of frozen flow. The position of this point is determined with the aid of Bray criterion, obtained on the basis of equation

$$-\left(\frac{dc_1}{d\tau}\right)_{\text{pash}} = k\omega_D^{\text{pash}}. \quad (11.46)$$

[Translator's Note: pash. = equilibrium]

In equation (11.46) the derivative of concentration with respect to time and the rate of dissociation  $\omega_D$  are determined by results of equilibrium calculation,  $k$  - coefficient of the order of one.

In the following works the Bray method was developed for multicomponent systems. In this instance of all the chemical reactions only those which play a determining role in thermodynamics of the system and mechanism of reactions are considered. In each of these reactions a limited number of components take part. The component, taking part in all reactions, is considered the main. By analogy with Bray criterion in examining a multicomponent system there should be compared the rate of change in concentration of "main" component, required by conditions of equilibrium flow, with its total rate of "compound" reaction. The rate of "compound" reaction is determined by kinetics of all separate reactions, in which the "main" component takes part.

For complex mixtures the rate of "compound" reaction and its freezing point depend on the propellant composition, pressure in the combustion chamber and nozzle shape. Selection of the main component is carried out on the basis of analysis of equations of kinetics, energy contribution of heat of reactions and results of equilibrium calculations.

As calculations of various authors [8], [9] show, losses of specific thrust as a result of chemical nonequilibrium can comprise from fractions of a percent to several percent and even tens of percent. Concrete quantities of losses of specific thrust depend on the propellant, pressure in the combustion chamber, nozzle shape and relative nozzles area  $f_c$ . Some illustrating results are shown on Figs. 11.5-11.7.

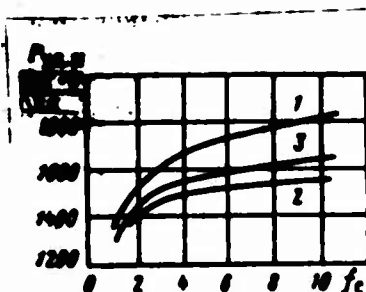


Fig. 11.5. Specific thrust in a void with expansion of hydrogen in a supersonic nozzle:  $p_n = 30$  bar;  $T_n = 6000^\circ\text{K}$ ; 1, 2, 3 - equilibrium, frozen and nonequilibrium expansion respectively.

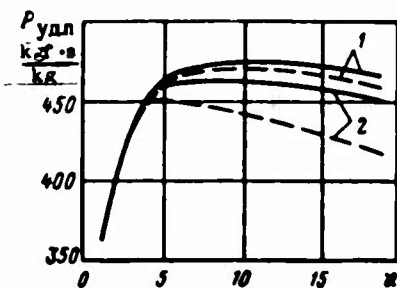


Fig. 11.6.

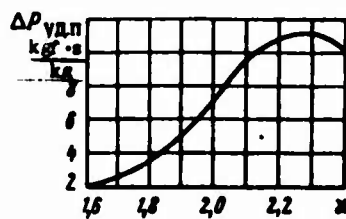


Fig. 11.7.

Fig. 11.6. Relationship of specific thrust in a void to  $\kappa$ : propellant  $H_2 + F_2$ ;  $f_c = 40$ ; —  $p_n = 21$  bar; ---- 4.2 bar; 1 — with equilibrium expansion; 2 — with allowance for kinetics.

Fig. 11.7. Relationship of losses of specific thrust in a void caused by chemical nonequilibrium, to  $\kappa$ : propellant (50%  $C_2H_8N_2 + 50\% N_2H_4$ ) +  $N_2O_4$ ;  $p_n = 7$  bar;  $f_c = 40$ .

#### Bibliography

1. Alemasov V. Ye., *Teplofizicheskiye svoystva zhidkostey i gazov pri vysokikh temperaturakh i plazmy* (Thermophysical properties of liquids and gases at high temperatures and plasma) izd-vo Standartov, 1969.
2. Alemasov V. Ye. and others. *Teplo- i massoperenos, t. 7*, izd-vo "Nauka i tekhnika", Minsk, 1968.
3. *Gazodinamika i teploobmen pri nalichii khimicheskikh reaktsii* (Gas dynamics and heat exchange in the presence of chemical reactions), collection of translations, IIL, 1962.
4. Gurvich L. V. and others. *Termodinamicheskiye svoystva individual'nykh veshchestv*, (Thermodynamic properties of individual substances) Reference book, AN SSSR, 1962.
5. Kamzolov V. N., Pirumov U. G., "Mekhanika zhidkosti i gaza", 1966, No. 6.
6. Kondrat'yev V. N., *Kinetika khimicheskikh gazovykh reaktsiy* (Kinetics of chemical gas reactions), AN SSSR, 1958.
7. Sarli V. and others., VPT, 1966, No. 12.

8. Pieper J. L. et al., J. Spacecraft and Rockets, 1967, No. 5.
9. Valentine R. S. et al., J. Spacecraft and Rockets, 1966, No. 9.
10. Wrobel J. R., J. Spacecraft and Rockets, 1965, No. 6.

## CHAPTER XII

### SINGLE-PHASE FLOW IN THE NOZZLE. FUNDAMENTALS OF PROFILING

In the chapter are examined fundamentals of profiling round and ring nozzles, a system of coefficients considering pulse losses in a real process of expansion is presented. For round nozzles basic principles of selection of optimum supersonic contour are described. Solution of these questions is presented for a single-phase working medium.

#### 12.1. General Information

During flow of a real gas in the nozzle the process of expansion proceeds with noticeable distinction from the idealized scheme of calculation accepted in Chapter VIII. This distinction is caused by internal irreversible processes and due to this has decrease in the outflow velocity and specific thrust. Optimum construction of nozzle profile must guarantee a minimum level of losses of specific thrust at some limiting requirements (overall sizes of nozzle, weight).

Calculation of gas flows in the nozzles and construction of extremal nozzle contours, which satisfy certain specific conditions, are complex problems. Their solution is obtained in [9]-[16].

A contemporary supersonic nozzle consists of three basic parts:

- 1) subsonic part of the nozzle;
- 2) critical section region (nozzle throat);
- 3) supersonic part of the nozzle.

In the subsonic part of the nozzle there occurs acceleration of flow, velocity of which in the throat region reaches local speed of sound. In the supersonic part immediately after the surface of passage through speed of sound there begins a region of preliminary expansion of gas, where flow is accelerated to a certain velocity. Curved wall AA', during flow around which the flow is accelerated, in limiting case can be replaced by break of contour - angular point A (Fig. 12.1). According to [15], during flow around the angular point the flow increases its velocity to prescribed at the shortest length in comparison with any other methods of acceleration of flow due to flow around the wall.

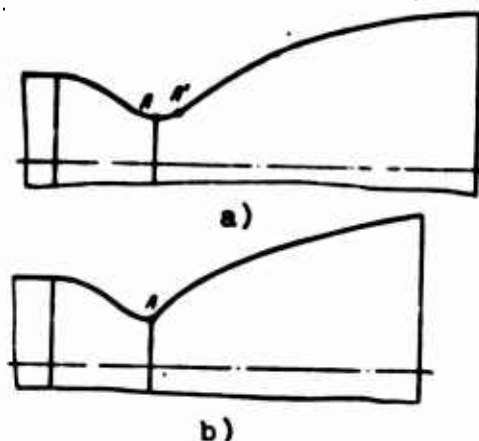


Fig. 12.1. Contour of supersonic part of the nozzle:  
a) without angular point;  
b) with angular point.

After achievement of prescribed value of velocity on the axis of the nozzle by flow, its parameters with further motion are determined by the contour of the supersonic part of the nozzle. Corresponding construction of this contour gives the possibility of obtaining flow uniform and parallel to the axis on the nozzle section.

Profiling of rocket engine nozzles is based on solution of a system of equations of gas dynamics, which for steady irrotational axisymmetrical flow of inviscid and nonheat-conducting gas is written in the following form:

$$\begin{aligned} (w_x^2 - a^2) \frac{\partial w_x}{\partial x} + w_x w_y \left( \frac{\partial w_x}{\partial y} + \frac{\partial w_y}{\partial x} \right) + \\ + (w_y^2 - a^2) \frac{\partial w_y}{\partial y} = \frac{a^2 w_y}{y}, \end{aligned} \quad (12.1)$$

$$\frac{\partial w_x}{\partial y} - \frac{\partial w_y}{\partial x} = 0, \quad (12.2)$$

where  $w_x, w_y$  - projections of flow velocity  $w$  to the axes of coordinates  $x, y$ . Axis  $x$  is directed along the axis of the nozzle, axis  $y$  - perpendicular to it.

System of differential equations (12.1)-(12.2) depending on the flow velocity has different form: elliptic ( $M < 1$ ), parabolic ( $M = 1$ ), hyperbolic ( $M > 1$ ). Accordingly, the methods (basically numerical) of solutions of the system are different. Therefore, questions of profiling the subsonic and supersonic parts of the nozzle are usually considered separately.

## 12.2. Profiling the Subsonic Part of Found Nozzles

Profile of the subsonic part of a nozzle can be found by solution of system of equations (12.1)-(12.2) under concrete boundary

conditions. However, the solution of this system is extremely complex. Complete and accurate calculations of flow in the subsonic part of the nozzle were obtained only recently [11]. Empirical relationships also received wide distribution for profiling the subsonic part of a nozzle; some of them are listed below.

Usually the subsonic part of the nozzle is characterized by the following elements (Fig. 12.2):

$r_{bx}$  - radius of nozzle inlet at the place of conjugation with the contour of the combustion chamber. If the combustion chamber is cylindrical, then  $r_{bx} = r_k$ ; [Translator's Note:  $bx$  = inlet]

$r_1$  - radius of curvature of nozzle inlet.

$\beta_{bx}$  - cant angle of conical section of the nozzle to axis;

$r_2$  - radius of curvature of profile in the nozzle throat;

$r_{kp}$  - radius of throat nozzle.

Contour of the subsonic part must guarantee continuous flow (to avoid burnouts) with uniform and known velocity field in the throat. This gives the possibility of reliably profiling the supersonic part of the nozzle. In accordance with geometrical acoustics the stability of the combustion process must be guaranteed from the viewpoint of high-frequency oscillations. In this case the overall dimensions (and consequently weight and losses on friction) must be minimum. Theoretical construction of the optimum profile of the subsonic part of the nozzle is a complex mathematical problem.

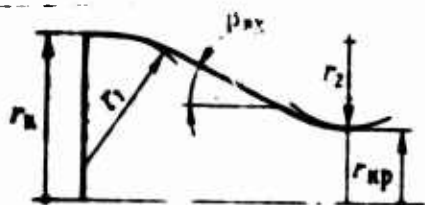


Fig. 12.2. Contour of subsonic part of the nozzle.



If the profile of the subsonic part is selected arbitrarily, then the possibility of shock waves is not excluded in the supersonic part of the nozzle, caused by nonconformity of the subsonic and supersonic parts. The reason for this can be, for example, a too prolonged (gently sloping) profile in the throat region.

As a consequence of the appearance of shock waves, in the nozzle appear disturbances of flow along the entire length of the supersonic part, which leads to decrease in the thrust. Too great a curvature of the wall in the throat region, although it excludes the appearance of shock waves, leads to large nonuniformity of flow in the nozzle throat, as a result of which thrust is also diminished. Optimum magnitude of radius of curvature of the nozzle profile in the throat region is established experimentally; usually it does not exceed  $2r_{np}$ .

The magnitude of entrance angle  $\beta_{bx}$  insignificantly affects the shaping of flow in the nozzle throat, however it strongly affects the intensity of heat output from gas to the wall. It is experimentally shown that increase in angle  $\beta_{bx}$  from  $10^\circ$  to  $35-45^\circ$  diminishes convective heat flow by 40-50% [2]. Furthermore, with increase of  $\beta_{bx}$  the length of the subsonic part of the nozzle is decreased, which favorably affects the weight of the chamber.

Finally the contour of the subsonic part of the nozzle is joined with the contour of the combustion chamber with radius  $r_1$ . Its magnitude affects the character of flow in the region of coupling of combustion chamber and nozzles, where positive pressure gradients are possible. At small values of  $r_1$  ( $r_1 < 0.3r_{bx}$ ) and large values of  $\beta_{bx}$  as a result of large positive pressure gradients boundary layer separation is possible at the wall, which intensifies heat output to walls of the nozzle.

Thus, when designing the subsonic part of the nozzle one can use the following relationships:

$$\left. \begin{aligned} 0 < r_1 < r_{\text{ex}}; \\ \beta_{\text{ex}} \leq 45^\circ; \\ r_{\text{up}} < r_2 < 2r_{\text{up}}. \end{aligned} \right\} \quad (12.3)$$

In certain cases instead of radius subsonic part one can use a conical subsonic part with parameters

$$\left. \begin{aligned} 0 < r_1 < r_{\text{ex}}; \\ \beta_{\text{ex}} \leq 45^\circ; \\ r_2 \approx 0. \end{aligned} \right\} \quad (12.4)$$

Conical subsonic nozzles create noticeable nonuniformity of flow parameters in the throat.

### 12.3. Profiling of the Supersonic Part of Round Nozzles

#### Idea of the Method of Characteristics

The basis of construction of the theoretical profile of the supersonic part of a nozzle is solution of system of differential equations (12.1)-(12.2). Let us examine the fundamental means of solution of this system.

Let us assume that hydrodynamic parameters  $w_x, w_y, a(w_x, w_y)$  are assigned on some line  $F$  and it is required to find their values in the region close to this line. If we could calculate the first and highest derivatives of velocities, then values of  $w_x, w_y$  can be continued outside the curve by expansion into Taylor series:

$$\begin{aligned} w_x &= w_{xP} + \left( \frac{\partial w_x}{\partial x} \right)_P dx + \left( \frac{\partial w_x}{\partial y} \right)_P dy + \dots; \\ w_y &= w_{yP} + \left( \frac{\partial w_y}{\partial x} \right)_P dx + \left( \frac{\partial w_y}{\partial y} \right)_P dy + \dots \end{aligned}$$

For determination of the values of partial derivatives  $(\partial w_x / \partial x), (\partial w_x / \partial y), (\partial w_y / \partial x), (\partial w_y / \partial y)$  let us use equations (12.1)-(12.2) and also the relationships valid along curve  $F$ :

$$dw_x = \left( \frac{\partial w_x}{\partial x} \right) dx + \left( \frac{\partial w_x}{\partial y} \right) dy;$$

$$dw_y = \left( \frac{\partial w_y}{\partial x} \right) dx + \left( \frac{\partial w_y}{\partial y} \right) dy.$$

As a result for determination of the four partial derivatives necessary to us we have a system of four equations:

$$(w_x^2 - a^2) \frac{\partial w_x}{\partial x} + w_x w_y \left( \frac{\partial w_x}{\partial y} + \frac{\partial w_y}{\partial x} \right) + (w_y^2 - a^2) \frac{\partial w_y}{\partial y} = \frac{a^2 w_y}{y};$$

$$\frac{\partial w_x}{\partial y} - \frac{\partial w_y}{\partial x} = 0;$$

$$\frac{\partial w_x}{\partial x} = \frac{dw_x}{dx} - \frac{\partial w_x}{\partial y} \frac{dy}{dx}, \quad (12.5)$$

$$\frac{\partial w_y}{\partial x} = \frac{dw_y}{dx} - \frac{\partial w_y}{\partial y} \frac{dy}{dx}. \quad (12.6)$$

Excluding derivatives  $\partial w_x / \partial x$ ,  $\partial w_y / \partial x$  from equations (12.1) and (12.2) let us write:

$$[w_x w_y - (w_x^2 - a^2) y'] \frac{\partial w_x}{\partial y} + [(w_y^2 - a^2) - w_x w_y y'] \frac{\partial w_y}{\partial y} =$$

$$= \frac{a^2 w_y}{y} - (w_x^2 - a^2) \frac{dw_x}{dx} - w_x w_y \frac{dw_y}{dx},$$

$$\frac{\partial w_x}{\partial y} + y' \frac{\partial w_y}{\partial y} = \frac{dw_y}{dx},$$

where

$$y' = \frac{dy}{dx}.$$

The obtained system of two algebraic equations are concisely rewritten so:

$$a_{11} \frac{\partial w_x}{\partial y} + a_{12} \frac{\partial w_y}{\partial y} = c_1; \quad (12.7)$$

$$a_{21} \frac{\partial w_x}{\partial y} + a_{22} \frac{\partial w_y}{\partial y} = c_2. \quad (12.8)$$

By solving this system of equations, we find:

$$\frac{\partial w_y}{\partial y} = \frac{a_{11}c_2 - a_{21}c_1}{a_{11}a_{22} - a_{21}a_{12}} = \frac{\Delta_1}{\Delta}; \quad (12.9)$$

$$\frac{\partial w_x}{\partial y} = \frac{a_{22}c_1 - a_{12}c_2}{a_{11}a_{22} - a_{21}a_{12}} = \frac{\Delta_2}{\Delta}. \quad (12.10)$$

Let us determine the values of the other two partial derivatives from equations (12.5) and (12.6).

Thus, all derivatives can be found if the following determinant is not equal to zero

$$\Delta = a_{11}a_{22} - a_{21}a_{12} \neq 0.$$

If  $\Delta = 0$ , then system of equations (12.1)-(12.2) can allow only indeterminate solutions. In order that these solutions would remain finite, it is also necessary in this case to require vanishing determinants  $\Delta_1$  and  $\Delta_2$ .

It is clear that determinant  $\Delta$  is not equal to zero on any line  $y(x)$  with tangent of cant angle  $y'$ . Curves, determined from equation  $\Delta = 0$ , are called characteristics of system (12.1)-(12.2). From equation  $\Delta_1 = 0$  (or  $\Delta_2 = 0$ ) we obtain conditions of connection between  $w_x$  and  $w_y$  - differential relationships on characteristics.

Let us introduce Mach  $\alpha$  into examination, determined from relationship

$$\sin \alpha = \frac{a}{w} = \frac{1}{M}, \quad (12.11)$$

and also let us take into account equalities

$$\left. \begin{aligned} w_x &= w \cos \theta, \\ w_y &= w \sin \theta, \end{aligned} \right\} \quad (12.12)$$

where  $\theta$  - angle comprised by velocity vector with axis  $x$ . By solving equations  $\Delta = 0$  and  $\Delta_1 = 0$  relative to  $y'$  and  $dw_x/dw_y$  and considering (12.11), (12.12), after a series of conversions we obtain two solutions:

1) for characteristics of the first family

$$dy = \operatorname{tg}(\theta + \alpha) dx, \quad (12.13)$$

$$\frac{dw}{w \operatorname{tg} \alpha} - d\theta = \frac{\sin \alpha \sin \theta}{y \cos(\theta + \alpha)} dx; \quad (12.14)$$

2) for characteristics of the second family

$$dy = \operatorname{tg}(\theta - \alpha) dx, \quad (12.15)$$

$$\frac{dw}{w \operatorname{tg} \alpha} + d\theta = \frac{\sin \alpha \sin \theta}{y \cos(\theta - \alpha)} dx. \quad (12.16)$$

Equations (12.13), (12.15) assign the directions of characteristics, and equations (12.14) and (12.16) - differential relationships on the characteristics.

Thus, through any point in the region of potential supersonic flow it is possible to draw two lines - characteristics of first and second families (Fig. 12.3), along which the parameters of flow are changed in accordance with differential relationships (12.14), and (12.16). This serves as a basis of numerical methods of solution of corresponding gas-dynamic problems.

During numerical calculation of supersonic flows in the nozzles by method of characteristics four problems can be separated [4].

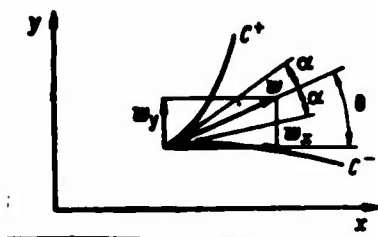


Fig. 12.3. Lines of characteristics:  
 $C^+$  - characteristic of first family;  
 $C^-$  - characteristic of second family.

1. Cauchy problem. Hydrodynamic parameters are assigned on some line AB, not being the characteristic (Fig. 12.4). It is required to determine the values of all flow parameters in region ABC, limited by curve AB and by characteristics of first (BC) and second (AC) families.

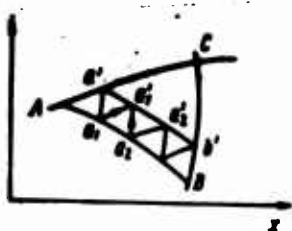


Fig. 12.4. Cauchy problem.

2. Goursat problem (Fig. 12.5). Hydrodynamic parameters are assigned on characteristics AO and OB. It is necessary to determine hydrodynamic parameters in region AOB, where AO' and BO' - characteristics of different families.

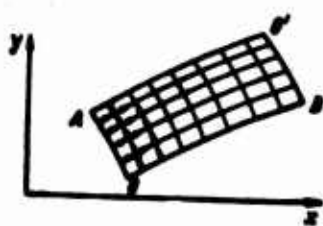


Fig. 12.5. Goursat problem.

3. Hydrodynamic parameters are assigned on the characteristic of one of families AO and solid wall AB is given (Fig. 12.6). Calculate the field of flow in region AOB (BO' - characteristic).

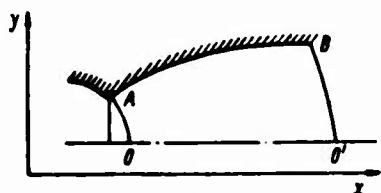


Fig. 12.6. Calculation of field of flow by the method of characteristics.

4. Parameters on the characteristic of the second family and pressure on the free surface are assigned. It is required to determine the shape of free surface and flow parameters.

Design construction of the nozzle profile, determination of flow parameters in a nozzle of prescribed configuration will be reduced to solution one of the enumerated problems, or a combination of them. The technique of numerical solution of these problems has much in common. Let us examine it in the example of Cauchy's problem. Let us divide curve AB (see Fig. 12.4) on which all hydrodynamic parameters are known, by a number of small segments and from points  $a_1$  and  $a_2$  let us draw characteristics of first and second families (let us replace increase of arguments by finite differences):

$$\Delta y_{a_i} = [\operatorname{tg}(\theta + \alpha)]_{a_i} \Delta x_{a_i}; \quad (12.17)$$

$$\Delta y_{a_i} = [\operatorname{tg}(\theta - \alpha)]_{a_i} \Delta x_{a_i}, \quad (12.18)$$

where

$$\begin{aligned} \Delta y_{a_i} &= y_{a_i} - y_{a_{i-1}}, & \Delta x_{a_i} &= x_{a_i} - x_{a_{i-1}}, \\ \Delta y_{a_i} &= y_{a_i} - y_{a_i}, & \Delta x_{a_i} &= x_{a_i} - x_{a_i}. \end{aligned}$$

System of equations (12.17), (12.13) gives the possibility of determining coordinates of point  $a_1'$ :  $x_{a_1'}$ ,  $y_{a_1'}$ . For determination of flow parameters at point  $a_1'$  analogously let us replace differential relationships (12.14) and (12.16) by finite differences:

$$\begin{aligned} \left( \frac{1}{w \operatorname{tg} \alpha} \right)_{a_1} (w_{a_1} - w_{a_2}) - (\theta_{a_1} - \theta_{a_2}) = \\ = \left[ \frac{\sin \alpha \sin \theta}{y \cos (\theta + \alpha)} \right]_{a_1} (x_{a_1} - x_{a_2}); \end{aligned} \quad (12.19)$$

$$\begin{aligned} \left( \frac{1}{w \operatorname{tg} \alpha} \right)_{a_1} (w_{a_1} - w_{a_2}) + (\theta_{a_1} - \theta_{a_2}) = \\ = \left[ \frac{\sin \alpha \sin \theta}{y \cos (\theta - \alpha)} \right]_{a_1} (x_{a_1} - x_{a_2}). \end{aligned} \quad (12.20)$$

Solution of the written system of equations allows determining the values of the velocity  $w$  and angle  $\theta$  at point  $a_1^1$ , and with their aid and quantities of all the remaining parameters. By similar means we find coordinates and parameters of flow also at other points,  $a^1$ ,  $a_2^1$ ,  $a_3^1$ , ...,  $b^1$ , i.e., position of new curve  $a'b^1$  is determined with flow parameters known on it.

When performing practical calculations on an electronic computer system of equations (12.13)-(12.16) is usually reduced to a form more convenient for calculations. Particular working formulas are presented in [8].

#### Construction of Contour of the Supersonic Part of a Nozzle

The most common problem of profiling a nozzle is determination of its contour, providing maximum specific thrust (coefficient of thrust) with minimum weight of the nozzle under assigned conditions. Inasmuch as at prescribed quantity  $f_c = F_c / F_{wp}$  a good measure of nozzle weight is its length or surface, maximum specific thrust should be obtained with minimum length or surface of the nozzle.

The simplest shape of the supersonic part of a nozzle is conical. For conical nozzles the length of supersonic part  $L_{cb}$  at known  $d_c$  and  $d_{wp}$  is uniquely determined by aperture angle of the nozzle:



$$L_{co} = \frac{d_c - d_{up}}{2 \operatorname{tg} \alpha_c}, \quad (12.21)$$

where  $\alpha_c$  - half the aperture angle of a conical nozzle.

Rational selection of angle  $\alpha_c$  can be done on the basis of the following considerations. With increase of  $\alpha_c$  the length of the nozzle and its surface are shortened. In connection with which pulse losses on friction and also weight of the nozzle are diminished. However, dispersion losses simultaneously increase as a result of nonparallelism of outflow. With decrease of angle  $\alpha_c$  dispersion losses drop and the weight of nozzle and friction losses simultaneously increase as a result of increase in the length and surface.

Thus, for each nozzle there exists an optimum value of  $\alpha_c$ , providing a minimum of losses of specific thrust. However, optimum angles  $\alpha_c$  in conical nozzles are rather small ( $\alpha_c \approx 10-15^\circ$ ). Therefore, the length of nozzle and its weight are obtained considerable, especially for chambers which have large values of  $f_c$ . Because of increase of finite weight the characteristics of the apparatus are impaired. Increase of nozzle surface means an increase of heat removal from combustion products, i.e., cooling of nozzle is hampered. Other limitations are possible, for example, complexity of control of swiveling nozzle, etc.

Theoretical and experimental investigations showed that the mentioned deficiencies can be decreased if we replaced the conical nozzle by one specially profiled. Construction of the profile of the supersonic part of a nozzle in this instance is based on the following considerations.

After establishment of critical condition the velocity in nozzle throat becomes equal to the local speed of sound. We will assume that flow is uniform in the nozzle throat. This assumption is generally accepted, which is used when profiling the supersonic part of the nozzle. For determination of the real distribution of parameters in the throat one should calculate flow in the supersonic part.

With uniform flow in the nozzle throat the line of constant velocity, equal to the local speed of sound (transition line), will be straight. On Fig. 12.7 this line is  $AO_1$ . With motion of gas downward along flow from the transition line around angular points A Prandtl-Meyer type flow appears during flow around an external obtuse angle by supersonic flow with the difference that each elementary volume of gas in region  $AO_1O$  takes part in two such motions: on one hand this motion is in a fan of waves of rarefaction, proceeding from point A, on the other hand, - motion in a fan of waves of rarefaction with the center at point A on the opposite side of the nozzle. In this case the flow velocity at point O is parallel to the axis and equal to prescribed. Let us profile the generatrix of nozzle AB so that on the characteristic of the second family OB, proceeding from point O, flow parameters are constant. In this instance the characteristic will be rectilinear, flow velocity at all its points is identical and parallel to the axis, and the nozzle will provide flow that is uniform and parallel to the axis at the exit.

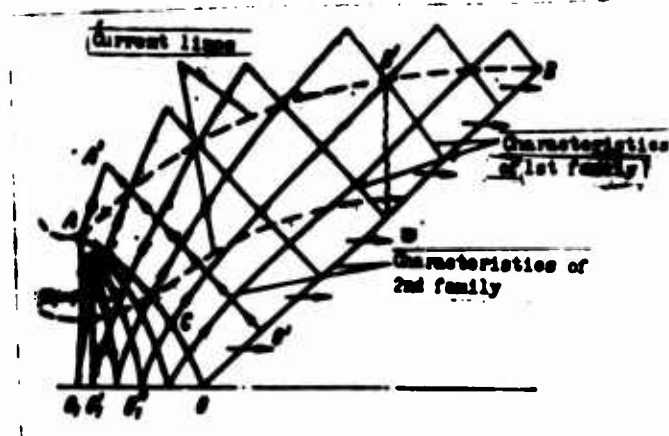


Fig. 12.7. Diagram of construction of supersonic contour.

If there is no angular point, i.e., the nozzle contour in the throat is made, for example, in the shape of an arc of some curve, then analogical reasonings can be made by substituting the arc by a curve with broken line.

Now the scheme of construction of the contour of the supersonic part of a nozzle can be represented so. First there is considered the accelerating section - region  $AO_1O$ . Calculation is performed by the method of characteristics, in this case the last characteristic of accelerating section  $AO$  is constructed from condition of achievement of prescribed velocity or  $M_0$  number by the flow at point  $O$ . The sequence of calculation is shown by pointers on Fig. 12.7. For example, by using the assigned values of hydrodynamic parameters on the characteristic of the first family  $AO_1'$  and solving the Cauchy problem, we find coordinates and distribution of hydrodynamic parameters on characteristic  $AO_1''$ . As a result of calculation of accelerating section  $AO_1O$  we obtain distribution of hydrodynamic parameters on characteristic  $AO$ , in this case at point  $O$  the flow velocity is equal to prescribed.

For construction of nozzle profile  $AB$  it is necessary to calculate flow in the balancing section - in region  $AOB$ . As initial values for this we use the values of hydrodynamic parameters on characteristics  $AO$  and  $OB$ . As already was mentioned, characteristic of the second family  $OB$  must be a straight line and at every point have constant value of velocity and other parameters. Inasmuch as all hydrodynamic parameters after calculation of the accelerating section at point  $O$  are known, consequently, they are also known on characteristic  $OB$ , angle of slope of which is determined according to the prescribed number  $M_0$ :

$$\sin \alpha = \frac{1}{M_0}.$$

Characteristic  $AO$  was constructed above.

Thus, we have known values of flow parameters on two characteristics:  $AO$  and  $OB$ . It is required to find the values of these parameters in region  $AOB$ , i.e., to solve Goursat problem. The sequence of calculation is shown on Fig. 12.7 by pointers, where the construction of the next characteristic  $A'O'$  is shown.

Thus, as a result of completed calculations we have values of all flow parameters in region  $AO_1OB$ . This is sufficient in order to construct current lines, going out from any point of the sound line  $AO_1$ . Each of them can be taken as generatrix of the nozzle, in this case the current line, going out from point A, gives us the contour of the nozzle with break of generatrix (nozzle with angular point), other current lines (intermediate) give a contour without break of generatrix. Inasmuch as contours constructed in this way rest on characteristic OB, they all provide flow that is uniform and parallel to axis.

Tables of supersonic contours for different values of numbers  $M_0$  at the exit and ratios of thermal capacities are listed in a number of works. Usually in tables are listed relative coordinates of contour  $\bar{x} = x/r_{np}$ ,  $\bar{y} = y/r_{np}$ , and also  $\theta$ ,  $\alpha$ , relative side surface and flow rate, projection to axis x affecting the line of current of pressure forces and series of quantities necessary for determination of pulse losses on friction and scattering. As a rule, all calculation of contours are performed for a working medium of constant composition with constant value of ratio of thermal capacities. The effect of variability of properties of working medium with respect to the nozzle on its geometry can be considered with sufficient accuracy with the aid of mean index of isentrope  $n$ , value of which along with number  $M_0$  is used when selecting the contour. As immediate calculations show [13], contours, constructed with allowance for variability of composition and properties of working medium with respect to the nozzle, and contours, constructed according to mean value of  $n$ , practically coincide. The same is valid during calculation determination of pulse losses in the nozzle.

Comparison of conical and profiled nozzles, which have identical relative nozzle section area, shows that while maintaining the constancy of thrust coefficient the profiled nozzle can be 30-50% shorter. Approximately the same figures express decrease in the weight and surface of the nozzle. If the nozzles being compared



have identical length, then the profiled nozzle provides a gain in specific thrust up to 2%.

Methods of profiling the supersonic part of the nozzle, examined here, are not unique. Methods have been developed which provide construction of extremal profile with maximum thrust with certain specified conditions (weight, length, etc.). The starting point of construction of extremal nozzles is the following. As it is known, in the absence of losses maximum thrust is obtained for contours of nozzles, which create flow at the exit parallel to axis. However, the end section of such nozzles barely takes part in the creation of thrust, inasmuch as its surface is practically parallel to the nozzle axis and does not perceive forces directed along the axis. If for such a nozzle the end part is cut off, then with insignificant loss of thrust on scattering substantial economy in weight can be obtained, in this case friction drop losses.

As can be seen (see Fig. 12.7, wavy line) the contour of a shortened nozzle rests on characteristics of different families AC and CB'. Thrust, created by section of nozzle AB', can be determined having examined reference surface OCB'. Generally the distribution of parameters on CB' is not optimum in the sense of obtaining maximum thrust.

Thrust characteristics of the nozzle can be improved, if we specially select distribution of pressure and velocity on OCB', providing maximum thrust. Gas-dynamic feature of the given variational problem is the independence of parameters on characteristic AO and in the region to the left of it from variation (change) of contour AB'. Therefore, the variational problem is solved only about the extremal contour of the supersonic part of the nozzle, passing through two fixed points A and B' and providing the distribution of parameters on characteristic CB' required from condition of maximum thrust.

The problem is solved by methods of calculus of variations [10], [14]-[16]. In this case the following distribution of parameters on characteristic CB' is obtained:

$$\left. \begin{aligned} \frac{\cos(\theta - \alpha)}{\cos \alpha} &= \text{const}_1; \\ r \cos^2 \alpha \cdot \sin^2 \theta &= \text{const}_2. \end{aligned} \right\}$$

Characteristic CB', on which these relationships are fulfilled, they are called variational. If point C coincides with point O, then, as is easy to note, characteristic CB' coincides with uniform characteristic.

Shortened nozzles, contours of which are constructed on the base of variational characteristic, have less friction and scattering losses in comparison with any other nozzle, contour of which passes through the same points A and B'.

Profiles of shortened nozzles, constructed by variational methods, somewhat differ from profiles obtained by simple shortening of the contour of a nozzle profiled for parallel and uniform flow at the exit. However, the corresponding difference in coefficients of pulse losses in this case is relatively small.

#### 12.4. Fundamentals of Profiling Ring Nozzles

In contrast to round nozzles the diagrams of ring nozzles are numerous. The picture of flow in them can have noticeable differences. Figure 12.8 shows some possible diagrams of ring nozzles [5], [12].

In nozzles on Fig. 12.8 (1) the throat is perpendicular to the nozzle axis. They are distinguished by the relative role of the nozzle skirt and inner body in the creation of thrust. In the type (a) nozzle thrust is created simultaneously by the skirt and inner body, and types (b) and (c) - inner body and skirt respectively.

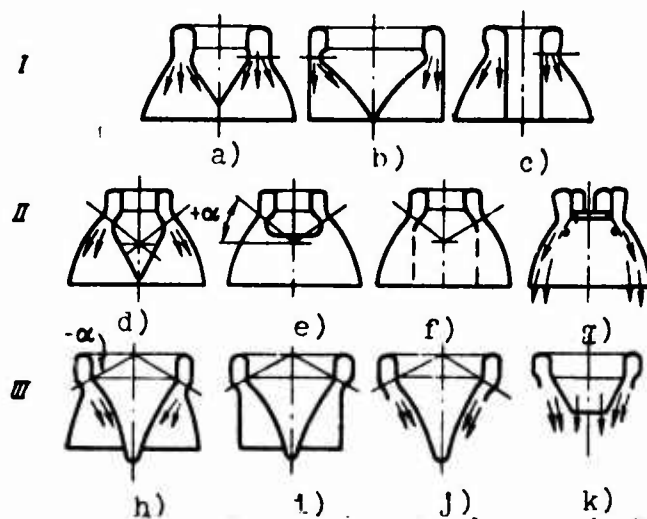


Fig. 12.8. Some diagrams of ring nozzles.

Nozzles of these types are usually calculated by the method of characteristics for uniform and parallel flow at the exit. Immediate calculations of contours of the type on Fig. 12.8, Ia in [12] show that by displacement of lower angular point according to flow it is possible to increase the number  $M$  at the nozzle exit in comparison with number  $M_0$  of ring nozzle with the same dimensions of throat, but with angular points in one plane.

Utilization of a nozzle with displaced lower point allows shortening of the length of ring nozzle two times in comparison with a corresponding round nozzle.

Tables of contours of ring nozzles of the type on Fig. 12.8 Ib when  $n = 1.4$  are contained in [7]. In this type of nozzles the surface of the skirt does not create thrust, however the presence of this surface diminishes the possibility of lowering of thrust because of overexpansion.

In ring nozzles of Fig. 12.8 II the radial plane of the throat is turned to a certain angle  $\alpha$ , in this case the annular throat has conical shape and directs the flow from the engine axis. In

these types of nozzles thrust can be created by the nozzle and inner body, or only by the nozzle skirt. By means of change of the throat angle various distribution of thrust between the inner body and skirt can be obtained. Nozzles are profiled by the method of characteristics. In this case one should bear in mind that the shape of the inner body in any diagram of the given type of nozzles has a relatively small effect on nozzle parameters if all other conditions remain the same.

In the three subsequent types of ring nozzles on Fig. 12.8, III the throat angle provides direction of flow to the nozzle axis. In this case thrust is created either by the nozzle skirt and inner body, or by only the inner body. In all diagrams of these nozzles the preferred role usually leads to the inner body. Sometimes the skirt is replaced by a cylinder, which protects the flow around the inner body from external effects.

Advantage of the nozzle of Fig. 12.8, IIIk (sometimes called aerodynamic) - the possibility of substantial shortening of the inner body. In this case in the end region a small flow rate of the working substance is supplied (for example, products of (TNA) [TNA = turbopump unit] exhaust), increasing the pressure in this zone and lowering the losses because of shortening.

Nozzles of the type on Fig. 12.8, III are calculated also by the method of characteristics. As experiments show, nozzles with radially convergent flow possess poorer parameters in comparison with nozzles of Fig. 12.8, II, inasmuch as the small surface of inner body in the region of flow constraint does not provide it good direction.

As can be seen, the general distinction of nozzles of Fig. 12.8, II and 12.8, III from nozzles of Fig. 12.8, I is turn of the throat, making it possible to noticeably shorten the length of ring nozzle.



Profiles of some diagrams of ring nozzles can be constructed by approximate methods. As an example let us consider profiling a nozzle with inner body (Fig. 12.9).

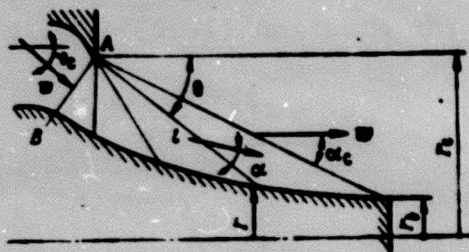


Fig. 12.9. Approximate construction of the profile of inner body.

Let us assume that in the geometrical nozzle throat the flow velocity equal to local speed of sound and is directed at Prandtl-Meyer angle  $\nu_c$  to the nozzle axis, value of which is determined by number  $M_c$ :

$$\nu_c = \left( \frac{n+1}{n-1} \right)^{0.5} \arctg \left[ \frac{n-1}{n+1} (M_c^2 - 1) \right]^{0.5} - \arctg (M_c^2 - 1)^{0.5}. \quad (12.22)$$

Further let us assume that the fan of rarefaction waves in the vicinity of the nozzle edge is the same as in the plane case: characteristics are rectilinear and flow parameters on them are constant.

The current value of passage area for gas is equal to

$$F = 2\pi \frac{r_c + r}{2} \frac{r_c - r}{\sin \theta} \sin \alpha = \frac{\pi(r_c^2 - r^2)}{M \sin \theta}, \quad (12.23)$$

where  $\alpha$  - Mach angle.

Length of any characteristic from the nozzle edge to the surface of inner body will be

$$l = \frac{r_c - r}{\sin \theta}$$

or, with allowance for equation (12.23):

$$l = \frac{r_c - \left( r_c^2 - \frac{M^2 \sin^2 \theta}{\pi} \right)^{0.5}}{\sin \theta}$$

By introducing the value of current relative area  $f = F/F_{np}$  and relative section area  $f_c$  in the last expression, we obtain in dimensionless form:

$$\bar{l} = \frac{l}{r_c} = \frac{1 - \left[ 1 - \frac{f(1 - \eta_b^2) M \sin \theta}{f_c} \right]^{0.5}}{\sin \theta} \quad (12.24)$$

where  $f_c = \frac{r_c^2 - r_b^2}{r_c^2}$ ;  $\eta_b = r_b/r_c$  - dimensionless end radius.

Equation (12.24) together with equation

$$\theta = \gamma_c - \gamma(M) - \alpha(M) \quad (12.25)$$

determines the profile of the inner body.

Thus, for construction of the profile of the inner body by approximate method we should assign the number  $M_c$  at the exit (determined by  $f_c$ ) and value  $\eta_b$  (0-0.5). When selecting quantities  $\eta_b$  one should bear in mind the length of the inner body relatively weakly influences the effectiveness of the nozzle. Thus, for instance, reduction of length of pointed inner body ( $\eta_b = 0$ ) by 20% impairs

the gas-dynamic characteristics of the nozzle by 2-5%. Approximate shapes of contours of the inner body when  $n = 1.4$  and different values of  $M_0$  are listed in [1].

#### 12.5. Estimation of Pulse Losses in the Nozzle

As a result of thermodynamic and gas-dynamic losses the thrust in a void (total pulse of nozzle) is distinguished from the theoretical value obtained in thermodynamic calculation. The following basic features, characterizing real flow in a nozzle can be isolated.

1. Nonparallelism of velocity vector of nozzle axis and nonuniformity of pressure in the nozzle exit section (pulse loss on scattering). These losses can be caused, for example, by shortening of the nozzle, profiled flow that is uniform and parallel to axis.

2. Pulse losses on friction as a result of viscosity of combustion products.

3. Nonuniformity of flow parameters in nozzle throat, can lead to nonuniformity of parameters at the nozzle section, increasing with decrease in the length of the supersonic part of the nozzle.

4. Chemical nonequilibrium of flow, possible in cases when the process of expansion of working medium in the nozzle proceeds so rapidly that the rate of change of flow parameters is balanced with the rates of chemical transformations.

5. Temperature and high-speed nonequilibrium between gas and condensate, possible during passage of two-phase flow in the nozzle.

In all cases the process with nonequilibrium physicochemical phenomena is accompanied by pulse losses.

6. Pulse losses because of the difference of contour of real nozzle from theoretical profile in view of characteristics of technology of production and certain other reasons.

Inasmuch as results of thermodynamic calculation are used when selecting the profile of the nozzle, comparison of real and ideal nozzles should be performed under the following basic conditions:

- a) flow rates per second of both nozzles are identical;
- b) in the throat of the nozzles being compared (with the exception of boundary layer in a real nozzle) the distribution of parameters and properties of flow is identical and corresponds to equilibrium state of the working medium;
- c) real and ideal nozzles have identical nozzle section areas;
- d) real and ideal nozzles have equal values of total nozzle inlet pressure  $p_n^*$ , which when necessary can be averaged with respect to flow-rate:

$$p_n^* = \frac{\int p_{n,i}^* dG}{G} = \frac{(\int p_{n,i}^* dG)_t}{G}$$

Here and further the quantities without indices pertain to real nozzle parameters, with index "t" - to theoretical.

Perfection of the real nozzle is evaluated quantitatively by coefficients characterizing deviations of real processes from ideal. The most important of them are the following.

#### 1. Flow coefficient of nozzle

$$p_t = \frac{G}{G_t} \quad (12.26)$$

when

$$F_{np} = F_{np,t}; (p_{np}^*, s_{np}, l_{np}) = (p_{np,t}^*, s_{np,t}, l_{np,t})$$

## 2. Pulse coefficient of nozzle (nozzle coefficient)

$$\bar{\eta}_c = \frac{P_n}{P_{nt}} \quad (12.27)$$

when

$$G = G_t; \quad F_c = F_{ct}; \quad (p_{up}^*, s_{up}, l_{up}) = (p_{up}^*, s_{up}, l_{up})_t.$$

Theoretical value of total nozzle pulse  $P_{nt}$  must be determined by results of thermodynamic calculation with allowance for losses, caused by imperfection of organization of processes in the combustion chamber.

## 3. Coefficient of pulse losses

$$\xi_c = \frac{P_{nt} - P_n}{P_{nt}} = 1 - \bar{\eta}_c. \quad (12.28)$$

[Translator's Note:  $n$  = total]

In accordance with the reasons enumerated above, causing pulse losses in the real nozzle, coefficient of pulses can be written so:

$$\xi_c = \xi_f + \xi_{fr} + \xi_{np} + \xi_{fn} + \xi_n. \quad (12.29)$$

where  $\xi_f$  - coefficient of pulse losses on scattering;  $\xi_{fr}$  - coefficient of pulse losses on friction;  $\xi_{np}$  - coefficient of pulse losses, caused by nonequilibrium of physicochemical phenomena (chemical and phase nonequilibrium);  $\xi_{fn}$  - coefficient of pulse losses in the nozzle because of distortions of profile in comparison with theoretical as a result of technological and other reasons;  $\xi_n$  - coefficient of pulse losses connected with features of flow of practical gas in the throat.

For determination of coefficients of pulse losses  $\xi_1$  one could use gas-dynamic and thermodynamic relationships. However because of the limitedness of our knowledge relative to a number of phenomena during flow in nozzles not all types of losses can be calculated with sufficient accuracy.

Quantities of pulse losses in the nozzle more or less depend on properties and parameters of the working medium at the nozzle inlet, which determine the mean isentropic index of expansion  $n$ . Therefore, values of thermodynamic characteristics of propellant, serving as basis of determination of real values of indices of the nozzle, must be corrected accordingly due to imperfections of processes in the combustion chamber.

Pulse losses on scattering in a shortened profiled nozzle can be determined with the aid of theorem of momentum. By writing this theorem for volume, limited by throat area, by side surface of the supersonic part and nozzle section area, we obtain

$$P_n = Gw_{sp} + p_{sp}F_{sp} + 2p_n^*F_{n^*} \int \frac{P_r}{P_n^*} \bar{r} d\bar{r},$$

where  $P_n$  - total pulse of real flow at the nozzle section;  $\bar{r}$  - relative radius of the nozzle;  $\bar{P} = \int \frac{P_r}{P_n^*} \bar{r} d\bar{r}$  - projection of pressure forces affecting the current line (usually its quantity is listed in tables of contours).

Let us introduce gas-dynamic function  $z(\lambda)$  into examination, which when  $n = \text{const}$  is determined so:

$$z(\lambda_c) = \frac{Gw_c + p_c F_c}{Gw_{sp} + p_{sp} F_{sp}} = \frac{1}{2} \left( \lambda_c + \frac{1}{\lambda_c} \right).$$

Now the formula for determination of coefficient of pulse losses on scattering can be written in the form

$$\xi_f = \frac{P_{n1} - P_n}{P_{n1}} = \frac{(Gw_{kp} + p_{kp}F_{kp})[z(\lambda_c) - 1] - 2p_n^* F_{kp} \bar{P}}{(Gw_{kp} + p_{kp}F_{kp})z(\lambda_c)}.$$

Let us convert the expression for total pulse of flow in the throat:

$$Gw_{kp} + p_{kp}F_{kp} = p_n^* F_{kp} \left( \frac{q_n^* w_{kp}^2}{p_n^*} \frac{q_{kp}}{q_n^*} + \frac{p_{kp}}{p_n^*} \right) = 2p_n^* F_{kp} \left( \frac{2}{n+1} \right)^{\frac{1}{n-1}}.$$

Having shortened  $p_n^* F_{kp}$  in the formula for  $\xi_f$  and considering the expression for  $Gw_{kp} + p_{kp}F_{kp}$ , we finally obtain

$$\xi_f = \frac{\left( \frac{2}{n+1} \right)^{\frac{1}{n-1}} [z(\lambda_c) - 1] - \bar{P}}{\left( \frac{2}{n+1} \right)^{\frac{1}{n-1}} z(\lambda_c)}. \quad (12.30)$$

Amount of pulse losses on dispersion depends on the relationship of length of the supersonic part of the nozzle  $L_{cb}$  and radius of nozzle section, mean isentropic index of expansion in the nozzle  $n$ . At constant value of radius  $r_c$  quantity  $\xi_f$  is decreased with increase of  $L_{cb}$  as a result of decrease in nonuniformity of flow at the exit. For this reason  $\xi_f$  is decreased with decrease of  $r_c$  when  $L_{cb} = \text{const.}$  Effect of  $n$  on the coefficient of pulse losses is slight.

In case of conical expansion nozzle with half angle  $\alpha_c$  the coefficient of pulse losses on dispersion is usually determined by the formula valid for radial flow:

$$\xi_f = \sin^2 \frac{\alpha_c}{2}. \quad (12.31)$$

In certain cases relationship (12.31) can lead to noticeable errors.

Magnitude of pulse losses on friction  $\Delta P_{\tau p}$  can be found as resultant of friction forces along the entire surface being streamlined

$$\Delta P_{\tau p} = \int_0^{x_c} 2\pi r \tau dx,$$

where  $x_c$  - coordinate of nozzle section. Magnitude of friction stress  $\tau$  is determined from solution of boundary layer equations (see Chapter XIV), or according to empirical relationships through friction coefficient  $C_f$ .

If the solution of boundary layer equations is known, then the thickness of lost pulse  $\delta^{**}$  in any section of the nozzle is usually found. Therefore, quantity  $\Delta P_{\tau p}$  can be written so:

$$\Delta P_{\tau p} = 2\pi r_c \delta^{**} \rho_c w_c^2.$$

In accordance with formula (12.28) the coefficient of pulse losses on friction is equal to

$$\xi_{\tau p} = \frac{\Delta P_{\tau p}}{P_{01}} = \frac{2\pi r_c \delta^{**} \rho_c w_c^2}{G w_c + P_c F_c}.$$

Considering known gas-dynamic relationships

$$\frac{P_c F_c}{G w_c + P_c F_c} = \frac{1}{1 + \kappa M_c^2};$$

$$\frac{\rho_c w_c^2}{P_c} = \kappa M_c^2.$$

we finally obtain

$$\xi_{\tau p} = \frac{2\delta^{**}}{r_c \left(1 + \frac{1}{\kappa M_c^2}\right)}. \quad (12.32)$$



Quantity  $\delta_c^{**}$  can be represented qualitatively by formula

$$\frac{\delta_c^{**}}{r_c} \sim \frac{1}{Re^{0.2} \sqrt{\bar{T}_{cr}}} \Phi(n, M, L_c).$$

[Translator's Note:  $cr$  = wall]

whence, specifically, we see the relationship of friction losses to the wall temperature. All things being equal with increase of  $\bar{T}_{cr}$  the coefficient of pulse losses on friction is diminished.

Quality  $\xi_{rp}$  depends on the length of the nozzle, radius of nozzle section  $r_c$ ,  $n$ , heat exchange factor  $\bar{T}_{cr} = T_{cr}/T_K^*$  and Reynolds number, characterizing flow conditions (laminar or turbulent). At large Re numbers as a result of the effect of wall roughness the coefficient of pulse losses on friction cannot depend on Re. Usually in rocket engine nozzles the flow conditions are turbulent.

Coefficient of pulse losses  $\xi_{rp}$  grows with increase in the nozzle length at  $\bar{T}_{cr}$ ,  $r_c$ ,  $n = \text{const}$  as a result of increase of nozzle surface. With decrease in radius  $r_c$  at  $L_c$ ,  $\bar{T}_{cr}$ ,  $n = \text{const}$ , and also with decrease of  $\bar{T}_{cr}$ ,  $n$  at  $r_c$ ,  $L_c = \text{const}$  coefficient  $\xi_{rp}$  is increased in connection with increase of gas density in the boundary layer.

Reliability of calculation determination of  $\xi_{rp}$  depends on the accuracy of solution of boundary layer equations. According to statistical data  $\xi_{rp} = 0.91-2.65$ .

Coefficient of pulse losses  $\xi_p$  evaluates the effect of nonuniformity of flow parameters in the throat, leading to corresponding nonuniformity of the gas stream at the nozzle exit. Value of  $\xi_p$  is determined by the shape of the throat and the shape of the nozzle exit.

Calculation determination of pulse losses as a result of nonequilibrium of physicochemical phenomena present great difficulties. Basic physicochemical phenomena, leading to decrease in specific thrust, can be considered speed and temperature nonequilibrium in two-phase flows and chemical nonequilibrium of the expansion process (see Chapter XI). Nonequilibrium processes in two-phase flows are considered in the following chapter.

The degree of nonequilibrium ( $\xi_{np}$  increases) with decrease in the time the working medium stays in the nozzle  $\tau_c$

$$\tau_c = \int_0^L \frac{dL}{w}, \quad (12.33)$$

where  $L$  - distance from nozzle entrance;  $w$  - flow velocity.

By graphic integration we can determine  $\tau_c$  and compare it with value  $\tau_c$  for an engine, accepted as a prototype. With equality  $\tau_c$  and pressures in nozzles of comparable engines the corresponding pulse losses on nonequilibrium can be taken close.

As follows from formula (12.30), pulse losses on scattering depend on distribution of flow parameters along the nozzle. As a result of possible deviations of nozzle contour from theoretical for technological and other reasons, distribution of flow parameters along the nozzle can become different, which increases pulse losses on scattering. This is evaluated quantitatively by the introduction of coefficient of pulse losses  $\xi_{fn}$ . Quantity  $\xi_{fn}$  depends on distortion of the nozzle wall angle, distortion of radius and length of the nozzle.

During flow of viscous gas in the vicinities of angular point a number of features appears, caused by viscosity. Corresponding pulse losses can be considered by a special coefficient, quantity of which is usually small.

Nonuniformity of flow in the throat and viscosity of gas, being manifested in the formation of boundary layer, also lead to decrease of flow rate through the nozzle, which is usually evaluated by flow coefficient  $\mu_c$ . Flow coefficient  $\mu_c$  is usually determined experimentally. It can be written so:

$$\mu_c = 1 - \Delta\mu_f - \Delta\mu_{rp}, \quad (12.34)$$

where quantity  $(1 - \Delta\mu_f)$ , considering the nonuniformity of flow parameters, is determined by experimental or calculation relationships (Fig. 12.10), and the effect of friction is considered with the aid of displacement thickness  $\delta^*$  by formula

$$\Delta\mu_{rp} = 2a\delta_{kp}^*/r_{kp}. \quad (12.35)$$

For smooth pipes coefficient  $a$  is equal to one. Magnitude of flow coefficient for rocket engine nozzles comprises  $\mu_c = 0.98-1.0$ .

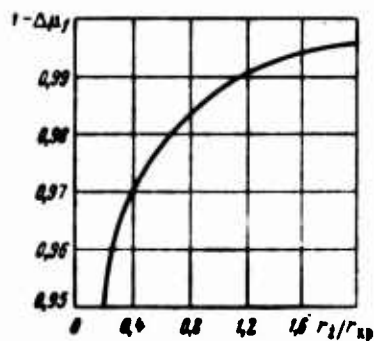


Fig. 12.10. For determination of flow coefficient of the nozzle.

In conclusion let us establish the connection between pulse coefficients  $\phi_1$  and coefficients of pulse losses  $\xi_1$ , considering particular types of losses. According to formulas (12.28) and (12.29)

$$\phi_c = 1 - \sum \xi_i = 1 - \sum (1 - \phi_i). \quad (12.36)$$

When evaluating the particular values of pulse coefficients  $\varphi_i$  it is revealed that they all are close to one. This gives a basis for substituting formula (12.36) by frequently applied approximate formula of type

$$\varphi_c = \varphi_1 \varphi_2 \varphi_3 \dots \varphi_m$$

or

$$\varphi_c = \varphi_f \varphi_{tp} \varphi_a \varphi_{sp} \varphi_f \varphi_n \quad (12.37)$$

Values of coefficient  $\phi_c$  for engines with homogeneous combustion products comprise 0.95-0.98. Pulse losses for two-phase working medium are considered in the following chapter.

#### 12.6. Some Principles of Selection of a Nozzle

Selection of a nozzle for an engine is determined by concrete tactical-technical requirements, imposed on flight vehicles. Nozzle of the engine, as its other elements, must guarantee maximum thrust at the least possible weight. Furthermore, selection of a nozzle can frequently be limited by some additional requirements, for example, by the cooling capability, arrangement of the engine on the flight vehicle.

Solution of practical problems of selection of an extremal nozzle is based on analysis of values of thrust coefficients in a void and at altitude  $H$  ( $K_{p_n}$ ,  $K_{p_h}$ ), determined with allowance for losses in the nozzle. We will consider that combustion chamber with subsonic part of the nozzle are assigned and mean isentropic index of expansion in the nozzle, flow rate of gas and other thermodynamic characteristics are known. For example let us examine the problem of selection of supersonic contour from the family of nozzle contours, providing maximum value of  $K_{p_n}$  under some assigned conditions. Conditional thrust characteristics of the family of nozzle contours with angular point, necessary for solution of the problem, are listed on Fig. 12.11.

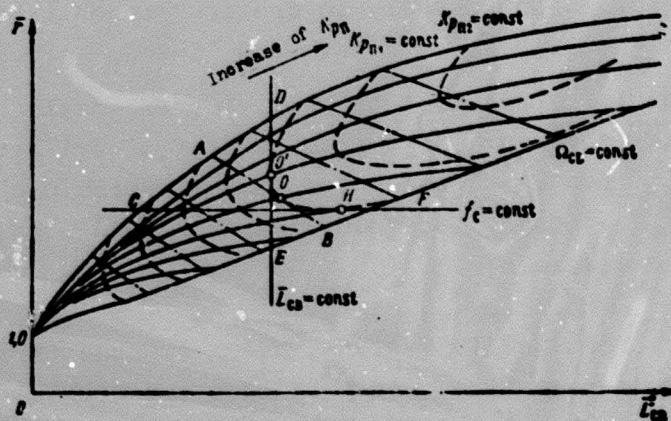


Fig. 12.11. Thrust characteristics of family of nozzle contours when  $n = \text{const}$ ;  $T_{CT} = \text{const}$ : ----- nozzle contours; ----- lines of constant values of  $K_{Pn}$ ; -.-.-.-.- lines of constant side surface of  $Q_{CB} = \text{const}$ .

1. Nozzle with maximum pulse at constant relative side surface of the supersonic part of the nozzle  $\bar{Q}_{CB} = \text{const}$ . Among the family of nozzle contours there are selected shortened contours which have identical side surface  $\bar{Q}_{CB} = Q_{CB}/F_{np}$  (for example, AB). It is obvious that the required properties of maximum pulse when  $\bar{Q}_{CB} = \text{const}$  are possessed by a nozzle, contour of which is terminated at the point of contact of line  $\bar{Q}_{CB} = \text{const}$  with the line of constant value  $K_{Pn} = \text{const}$  (point O).

2. Nozzle with maximum pulse when  $f_c = \text{const}$ . Such a nozzle is located on the point of contact of line CF  $f_c = \text{const}$  with line of constant value  $K_{Pn} = \text{const}$  (Point H). Nozzles with the same value of  $f_c$ , but longer or shorter length, will have greater pulse losses, since with decrease in length the scattering losses strongly increase, and with increase in length the friction losses grow.

3. Nozzle with maximum pulse at constant length  $\bar{L}_{CB} = L_{CB}/r_{np} = \text{const}$ . Selection of such a nozzle from the families of shortened

contours is performed analogously to previous cases. Point of contact of straight line  $\bar{L}_{CB} = \text{const}$  with line  $K_p = \text{const}$  determines the required nozzle (line DE, point O'). Other nozzles of the same length, but with larger or smaller quantity  $f_c$ , have large pulse losses: in the first case dispersion losses, which are not compensated by increase of  $f_c$  strongly increase, in the second - pulse drops as a result of decrease of  $f_c$ .

Above, only certain limitations, being imposed on selection of the nozzle have been examined; in this case the equivalent of weight of the nozzle with respect to thrust was not considered. Combined limitations are possible in principle when, for example quantities  $f_c$  and  $\bar{L}_{CB}$  are assigned. In all cases of selection of nozzles quantities  $\bar{L}_{CB}$ ,  $f_c$  or  $\bar{L}_{CB}$  must be designated with allowance for the effect of external conditions and weight of the nozzle, in this case role of the latter is determined on the basis of ballistic calculations of the flight trajectory.

#### Bibliography

1. Angelino Dzh., "Raketnaya tekhnika i kosmonavtika", 1964, No. 10.
2. Bek L. Kh. and others, "Raketnaya tekhnika i kosmonavtika", 1966, No. 12.
3. Valentayn R. S. and others, VRT, 1967, No. 3.
4. Ginzburg I. P., Aerogazodinamika (Aerodynamics), izd-vo, "Vysshaya shkola", 1966.
5. Ilsen V., VRT, 1963, No. 3.
6. Kamzolov V. N., Pirumov U. G., Zhurnal prikl. mekhaniki i tekh. fiziki, 1967, No. 2.
7. Katskova O. N., "Vychislitel'naya matematika", 1958, No. 3.
8. Katskova O. N. and others, Opyt rascheta ploskikh i osesimmetrichnykh gecheniy gaza metodom kharakteristik (Experience of calculation of two-dimensional and axisymmetric gas flow by the method of characteristics), VTs, AN SSSR, 1961.



9. Krayko A. N. and others "Mekhanika zhidkosti i gaza", 1967, No. 1.
10. Krayko A. I. and others, "Prikladnaya matematika i mekhanika", 1964, vyp. 1.
11. Pirumov U. G., "Mekhanika zhidkosti i gaza", 1967, No. 5.
12. Pirumov U. G., Rubtsov V. A., AN SSSR, "Mekhanika i matematika", 1961, No. 6.
13. Chislennyye metody v gazovoy dinamike (Numerical methods in gas dynamics) collection of articles, VTs MGU, 1962.
14. Shmyglevskiy Yu. D., Nekotoryye variatsionnyye zadachi gazovoy dinamiki (Some variational problems of gas dynamics), VTs, AN SSSR, 1963.
15. Shmyglevskiy Yu. D., Doklady AN SSSR, 122, No. 5, 1958.
16. Shmyglevskiy Yu. D., "Prikladnaya matematika i mekhanika", 1957, vyp 2.

## CHAPTER XIII

### TWO-PHASE FLOW IN A NOZZLE

In the chapter are examined questions of flow of two-phase combustion products in a nozzle. Possible amounts of losses of specific thrust and method of calculation of nonequilibrium two-phase flows is given with allowance for the possibility of collision and fusion of liquid particles of metal oxides.

#### 13.1. Basic Features

Combustion products of metallized propellants in most cases contain a considerable quantity of condensed metal oxides.

Two cases should be separated: the first, when pressure of vapors of oxide at the combustion temperature is insignificantly low, and second, when it comprises a noticeable amount relative to overall pressure. In the first case the gas contains an insignificant quantity of metal oxide, condensation is accomplished during combustion and condensation can not be considered in the process of expansion. Examples of such propellants are fuels with the additions of metals Al, Be, Mg, oxides of which  $\text{Al}_2\text{O}_3$ , BeO, MgO have low pressure of saturated vapors. Weight fraction of these condensed products during expansion, as a rule, is changed insignificantly. Another type of propellant is, for example,  $\text{B}_5\text{H}_9 + \text{H}_2\text{O}_2$ . In the combustion chamber boric oxide  $\text{B}_2\text{O}_3$  can be entirely in gas phase and precipitate into condensate with lowering of temperature in the nozzle.



In the first case the characteristic process of interaction between gas and condensed phases in the nozzle is acceleration of particles and their cooling - transmission of heat to gas. In the second case there is added another process of condensation of oxide vapors.

Assumptions about equilibrium acceleration, heat exchange and condensation with expansion of combustion products in the nozzle, accepted in thermodynamic calculation, are approximate and are needed in refinement for conversion to real characteristics of the engine.

### Basic Characteristics of Condensate

For examination of the interaction between gas and condensate we must know the basic characteristics of both phases. Earlier (Chapter VII) were determined thermodynamic and thermo gas-dynamic properties of gaseous products; from reference books the thermodynamic properties of the most important solid and liquid metal oxides are known. Such properties as density, coefficient of viscosity and surface tension have been studied less. For certain oxides these data are listed on Table 13.1.

Table 13.1. Physical properties of certain oxides.

Oxide	$T_{m}, ^\circ\text{K}$	Density $\rho \cdot 10^{-3} \text{ kg/m}^3$		Coefficients		Heat of melting $\text{kJ/kg}$
		solid	liquid	$\eta, \text{Ns/m}^2$	$\sigma, \text{N/m}$	
$\text{Al}_2\text{O}_3$	2303	3,95	3,05	0,06	0,7	1149,7
$\text{BeO}$	2820	3,01	2,56	—	0,3	2845,3
$\text{MgO}$	3075	3,58	—	—	—	1920,8
$\text{B}_2\text{O}_3$	723	1,82	1,7	0,50 (2100° K)	0,11 (2100° K)	330,63
$\text{Li}_2\text{O}$	1700	2,013	—	—	—	1639,3

Note: Properties of solid oxides are given at normal temperature, liquid - at the melting point.

[Translator's Note: subscript m = melting].

The combustion temperature of propellants, as a rule, is higher than the melting point of oxides, therefore, liquid particles under the action of forces of surface tension assume a spherical shape.

The most important characteristic of condensed phase, which we will also call disperse phase, is the size of its component particles. We distinguish mono and polydisperse systems. The first includes those which consist of particles of identical size; their obtaining is a difficult technical problem.

The particles, which form during combustion of metallized propellants, will form a polydisperse system, i.e., have different sizes. The complete picture of dispersity is characterized by distribution curve of mass of disperse phase according to sizes of particles, example of which is listed on Fig. 13.1.

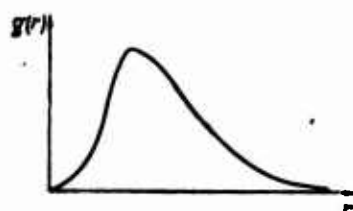


Fig. 13.1. Function of distribution density.

On this curve along the axis of abscissa are plotted values of radii (or diameters) of particles from the smallest to the biggest, and along the axis of ordinates - so-called function of density of distribution

$$g(r) = \frac{1}{M_0} \frac{\Delta M}{\Delta r},$$

where  $M_0$  - overall mass of all particles;  $\Delta M$  - mass of their narrow fraction in the size range from  $r$  to  $r + \Delta r$ .

Polydisperse condensate can be characterized by average sizes of particles. Among them the most important in our case is average

weight radius<sup>1</sup>

$$r_{zm} = \int_0^{\infty} g(r) r dr. \quad (13.1)$$

Here 0 and  $\infty$  conditionally designate the minimum and maximum sizes of particles. According to experimental data the combustion products contain particles with radius from fractions of a micron to tens of microns. During combustion of blended solid propellants with aluminum and beryllium additives particles of oxides with radius  $r_{zm} = 0.5-2 \mu m$  will be formed [12]. Behind the nozzle section, according to experimental data, particles are coarser and their sizes reach  $r_{zm} = 5-8 \mu m$ .

#### Characteristics of Motion of Two-Phase Mixture in a Nozzle

Gas is accelerated in the nozzle as a result of pressure gradient, affecting the volume of gas. Particles can accelerate only under the action of aerodynamic forces, which appear with gas blowing them, i.e., in order to accelerate, they inevitably must move slower, lagging behind gas. Analogously the heat of particles can be transferred to gas only in the presence of a temperature difference. Both these processes are nonequilibrium, are accompanied by energy dissipation in the process of exchange between phases, entropy of the mixture increases and the process of expansion seems less effective in comparison with equilibrium case. In this case the greater the losses the greater the delay of particles with respect to velocity and temperature.

Let us examine which factors in the simplest case determine the lag of particles.

---

<sup>1</sup>In this chapter the following system of designations is used: quantities pertaining to the entire condensate have index "z," to i-th fraction - "i," to a separately considered particle - "p."

Force, affecting the particle of mass  $m$  in the flow of accelerating gas, is equal to the product of mass of the particle by its acceleration:

$$m \frac{dw_p}{d\tau} = \frac{1}{2} C_x \pi r_p^2 |w_s - w_p| (w_s - w_p) \varrho_s. \quad (13.2)$$

In accordance with Stokes law, at small Reynolds numbers

$$Re_p = \frac{2r_p |w_s - w_p| \varrho_s}{\eta_s}$$

the drag coefficient is equal to

$$C_x = \frac{24}{Re_p}.$$

Then, by substituting  $C_x$  in equation (13.2) we obtain

$$w_s - w_p = \frac{2}{9\eta_s} \varrho_p r_p^2 \frac{dw_p}{d\tau}. \quad (13.3)$$

The obtained equation allows revealing the effect of basic factors, which determine losses of specific thrust because of high-speed lag of particles.

Average velocity of motion of a two-phase mixture  $w$  can be written so:

$$w = w_p z + w_s (1 - z) = w_s - (w_s - w_p) z. \quad (13.4)$$

Quantity  $w$  is lowered with increase in lag of condensate. If we do not consider the change in gas velocity, lowering of  $w$  is proportional to the square of radius of particles and to acceleration  $dw_p/d\tau$ . In order to explain the role of acceleration, let us note that comparatively small lags of particles are discussed, then acceleration of condensate in the nozzle is a quantity close to acceleration of gas. If some average velocity in the nozzle is equal to  $w_{cp}$ , then the time of stay in the nozzle with length  $L_c$  comprises

$$\tau = \frac{L_c}{w_{cp}};$$

[Translator's Note: cp = average.]

hence acceleration in order of quantity

$$\frac{dw_p}{d\tau} \approx \frac{dw_i}{d\tau} \sim \frac{w_c}{L_c} w_{cp}.$$

Inasmuch as  $w_c$  and  $w_{cp}$  approximately do not depend on the size of the nozzle, it is evident that acceleration is inversely proportional to the length of the nozzle. Since all nozzles are approximately similar geometrically and  $L_c \sim d_{np}$ , the greater  $d_{np}$ , is the less acceleration and the less the lag of particles. Now it is possible to write

$$w_i - w_p \sim \frac{q_p}{\eta_k} \frac{r_p^2}{d_{np}}. \quad (13.5)$$

The completed analysis is rough, but it correctly reveals basic regularities. From equations (13.4) and (13.5) it follows qualitatively that losses of specific thrust because of high-speed lag of particles increase so:

with increase of weight fractions of condensate - linearly;

with increase in the sizes of particles - proportional to square of radius of particles;

with decrease in the diameter of nozzle thrust - inversely proportional to diameter.

It is possible to show that temperature lag of particles is determined by these factors in the same proportionality.

### 13.2. Thermodynamic Estimation of Maximum Possible Losses

For estimation of the role of deviations of the process of expansion of two-phase mixture from equilibrium it is desirable

examine limiting cases of high-speed and temperature lag of condensate.

Total Equilibrium with Respect to Velocity and  
The Absence of Heat Exchange  
Between Phases

With equilibrium expansion the outflow velocity is determined by formula

$$w_c = \sqrt{2\Delta I},$$

where  $\Delta I = I_k - I_c$  - drop of enthalpy in J/kg. In the absence of heat exchange between phases the temperature and enthalpy of condensate remain constant, due to which the enthalpy of 1 kg of working substance is diminished to quantity

$$\delta I = z(I_k - I_c).$$

Here  $I_{z k}$ ,  $I_{z c}$  - enthalpy of condensate at the combustion chamber exit and the nozzle section during equilibrium expansion.

At the same time, with the absence of heat supply from particles the temperature of gas at the nozzle section is lowered, i.e., drop of enthalpy of gas phase increases. This increase can be evaluated in the following manner.

In the absence of heat exchange between phases and total equilibrium with respect to velocity the process of expansion is isentropic. The entropy of 1 kg of gas phase in this instance will be less than the entropy of gas at the nozzle section in case of equilibrium expansion to quantity

$$\delta s = \frac{z}{1-z} (s_{z k} - s_{z c}),$$

where  $s_{z k}$ ,  $s_{z c}$  - entropy of condensate in the combustion chamber and at the nozzle section with equilibrium expansion.

ite. Hence a decrease of enthalpy of 1 kg of gas at the nozzle section with expansion to the same pressure  $p_c$ , which is also in equilibrium case, approximately comprises

$$\delta I_z = \frac{z}{1-z} (s_{zk} - s_{zc}) T_c,$$

where  $T_c$  - equilibrium temperature at the nozzle section.

Then the overall drop of enthalpy of 1 kg of working substance during expansion with temperature nonequilibrium will be equal to

$$\Delta I_{npT} = \Delta I - z(I_{zk} - I_{zc}) + zT_c(s_{zk} - s_{zc}).$$

ate In accordance with the accepted model of calculation the temperature of condensate in the process of expansion does not change; consequently, if the thermal capacity of liquid phase  $c_z$  is considered constant:

$$\begin{aligned} I_{zk} - I_{zc} &= c_z(T_k - T_c); \\ s_{zk} - s_{zc} &= c_z(\ln T_k - \ln T_c). \end{aligned}$$

Then

$$\frac{\Delta I_{npT}}{\Delta I} = 1 - \frac{zc_z}{\Delta I} (T_k - T_c - T_c \ln T_k + T_c \ln T_c),$$

and specific thrust coefficient, considering temperature nonequilibrium, comprises

$$\begin{aligned} \tau_{npT} &= \sqrt{1 - \frac{2zc_z}{w^2} \left[ T_k - T_c \left( 1 + \ln \frac{T_k}{T_c} \right) \right]} \approx \\ &\approx 1 - \frac{zc_z}{w^2} \left[ T_k - T_c \left( 1 + \ln \frac{T_k}{T_c} \right) \right]. \end{aligned} \quad (13.6)$$

Let us consider for example a typical blended solid propellant, consisting of 70%  $\text{NH}_4\text{ClO}_4$ , 20% binder (polyester) and 10% Al. When  $p_k = 40$  and  $p_c = 1$  bar the propellant has the following equilibrium thermodynamic characteristics:

$$T_k = 3220^\circ \text{K}, T_c = 2050^\circ \text{K}, w_c = 2445 \text{ m/s}, z = 0.19.$$

Thermal capacity of aluminum oxide comprises  $c_p = 1420 \text{ J/kg}\cdot\text{deg}$ .  
By substituting these quantities in formula (13.6) we obtain  
 $\phi_{np} T = 0.988$ .

Thus, maximum loss of outflow velocity, caused by temperature nonequilibrium, under characteristic conditions for solid propellants comprises a quantity on the order of one percent.

#### Total High-Speed Nonequilibrium at Equilibrium Heat Exchange

The considered model is conditional. In this instance the gas does not interact with particles mechanically, does not perform works with respect to their acceleration in the nozzle. Therefore, kinetic energy of particles can be disregarded, however, the weight content of condensate in combustion products (flow rate) in this case remains constant.

By assuming in the first approximation that the temperature at the nozzle section does not change while maintaining a pressure ratio, we obtain that the gas velocity must be increased, since the entire drop of enthalpy is expended on acceleration only of gas:

$$w_{np} = \sqrt{\frac{2\Delta I}{1-z}}. \quad (13.7)$$

Here  $w_{np}$  - gas velocity with total high-speed nonequilibrium

However, the average outflow velocity, determined by formula (13.4), is decreased, since  $w_z = 0$ . On the basis of formulas (13.4) and (13.7) it will comprise

$$w_{np} = (1-z) w_{np} = w \sqrt{1-z}.$$

Specific thrust coefficient, considering high-speed nonequilibrium, when  $w_z \approx 0$  will be equal to

$$\tau_{np} = \sqrt{1-z}$$



or at small values of  $z$  (less than 0.2-0.3):

$$\eta_{sp} \approx 1 - \frac{1}{2} z. \quad (13.8)$$

For the example considered above the quantity of losses, as can be seen from expression (13.8), comprises about 10%.

Thus, the effect of high-speed nonequilibrium is considerably more than temperature, and the amount of possible losses of specific thrust is very considerable.

High-speed nonequilibrium is reflected also on the flow rate of working medium through the nozzle.

For determination of flow rate of two-phase substance with total high-speed nonequilibrium known formula (9.16) can be used:

$$G = A(n) \frac{p_k^* F_{kp}}{\sqrt{R_k T_k^*}}.$$

Here  $A(n)$  - function of mean isentropic index, change of which as a result of nonequilibrium is not considered.

With assigned parameters of working substance at the nozzle inlet ( $p_k^*$  and  $T_k^*$ ) and constants  $F_{kp}$  and  $A(n)$  the flow rate is a function of gas constant, which depends on the character of the expansion process. With equilibrium expansion the gas constant of the mixture is equal to

$$R_k = R_g(1-z)$$

and the flow rate

$$G = A(n) \frac{p_k^* F_{kp}}{\sqrt{R_g(1-z) T_k^*}}.$$

With total high-speed nonequilibrium the gas is expanded without action on the part of condensate (thermal effect is disregarded), as pure gas, and its flow rate is equal to

$$G_{sp} = A(n) \frac{p_u^* F_{sp}}{\sqrt{R_u T_u^*}}.$$

Inasmuch as the relative content of condensate in gas in this case is retained, the total flow rate of working substance comprises

$$G_{sp} = G_e \left( 1 + \frac{z}{1-z} \right) = A(n) \frac{p_u^* F_{sp}}{(1-z) \sqrt{R_u T_u^*}}.$$

Relationship of flow rates at assigned nozzle inlet pressure in cases of total high-speed equilibrium and limiting high-speed nonequilibrium is equal to

$$\frac{n}{n_{sp}} = \sqrt{1-z}.$$

Thus, high-speed lag of particles from gas in the nozzle can lead to considerable increase in the flow rate in comparison with equilibrium, all things being equal. It is interesting that the flow rate increases in the same degree in which the average outflow velocity is lowered.

### 13.3. Nonequilibrium Expansion of Two-Phase Flow

Experimental data attest to the considerable increase of losses of specific thrust in (PDTT) [RDTT - solid-propellant rocket engine] operating on aluminized propellant in comparison with RDTT operating on propellants without metal. The quantity of these additional losses can reach several percent.

The analysis given above shows that "two-phase" losses can be the basic reason for deterioration of the degree of perfection of the process in the engine. In connection with this, in recent years abroad considerable attention has been given to determination of such losses [9].

hout Below is examined the method of calculation of nonequilibrium two-phase flow in a rocket engine nozzle [8].

As obviously follows from § 13.1 the quantity of lag of particles from gas is determined to a decisive degree by their size. Calculations show that particles with diameter less than a micron under typical conditions of natural engines have velocity close to the velocity of gas, and coarse particles move with considerable lag. Ultimately, for example, the velocity of motion of particles 1 and 10  $\mu\text{m}$  in size relative to each other can comprise several hundred m/s. As a result of the relative motion of particles of different fractions collisions can occur between them, and in the case of liquid particles - fusion and coarsening of drops. This phenomenon must be taken into account during calculation of two-phase flow.

With description of processes the following assumptions are taken.

Flow is adiabatic, insulated with respect to mass, one-dimensional and stationary; during expansion the weight fraction, composition and thermal capacity of gas and condensate are constant; pressure, caused by Brownian movement of particles, is negligible; the temperature of condensate particle is identical over its entire volume; the volume of condensate is negligible; heat exchange between particles and gas is only convective; viscosity and thermal conductivity of gas are manifested only during interaction with particles and are functions of temperature; particle concentration is rather small, which allows considering them independent during interaction with gas and not considering the simultaneous collision of three and more particles.

It is assumed that distribution of particles according to their masses is determined by normalized mass function of the density of distribution  $g(m)$ :

$$\int_0^{\infty} g(m) dm = 1,$$
$$dG(m) = G_0 g(m) dm,$$

where  $m$  - mass of particle,  $G_z$  and  $dG(m)$  - flow rate of entire condensate and particles of fraction  $m$ .

Limits of integration 0 and  $\infty$  conditionally designate minimum and maximum masses of particles, being considered in calculation.

As initial data there are prescribed characteristics and properties of gas and condensate, distribution of particles according to sizes at the nozzle inlet and also nozzle profile.

During calculation of nonequilibrium flow in a nozzle of prescribed contour in the region of the throat where the gas velocity is equal to the local speed of sound in gas (number  $M = 1$ ), a specific point is encountered: derivatives necessary for numerical integration must be calculated by a formula of type

$$\frac{dw_i}{dx} = \frac{A}{M-1},$$

where  $A$  - some function.

For passing through point  $M = 1$  it is necessary to specifically select initial data, in order that the numerator would become zero simultaneously with the denominator:  $A(x) = 0$  and  $M = 1$ . This is a very laborious procedure.

It is expedient to solve so-called "inverse" problem. In the prescribed nozzle contour equilibrium flow of two-phase mixture is considered and the relationship is determined, for example, of the density of gas to coordinate along the axis of the nozzle -  $\rho_2(x)$ . Other parameters can be used also, such as pressure  $p(x)$ , velocity -  $w_1(x)$ , etc.

For the found density distribution there is considered non-equilibrium flow: along axis  $x$  all parameters of gas and particles are determined. In this instance, as we shall see below, a specific point does not appear. By knowing in each section the flow rate (equal to equilibrium), the velocity and density of gas, we can find

the area of the nozzle from equation of continuity, i.e., determine the contour of the new nozzle, close to the contour of original. In this nozzle parameters of nonequilibrium flow are known. Calculation of equilibrium flow in the obtained nozzle and comparison of its parameters with nonequilibrium gives the possibility of determining losses of specific thrust.

Thus, we will solve "inverse" problem of nonequilibrium flow, from the beginning without allowing for collisions and fusion of particles (without allowing for coagulation).

With the used assumptions relative to properties of gas and condensate equilibrium two-phase flow can be calculated by usual gas-dynamic relationships.

For description of nonequilibrium flow the entire range of the mass of particles is decomposed into  $n$  parts so that parameters of particles with masses, intermediate between selected  $m_i$  ( $i = 1, 2, \dots, n$ ), could be determined by interpolation.

Let us write equations of motion and heat exchange of particles with mass  $m_i$  in the following form:

$$m_i \frac{dw_i}{dx} = C_{x1} \frac{\rho_s (w_s - w_i) |w_s - w_i|}{2} \frac{\pi d_i^2}{4};$$

$$m_i \frac{dI_i}{dx} = \alpha_i (T_s - T_i) \pi d_i^2,$$

where  $w_i$ ,  $d_i$ ,  $T_i$ ,  $I_i$  - velocity, diameter, temperature, and also specific enthalpy (on 1 kg) of particle of mass  $m_i$ ;  $C_{x1}$ ,  $\alpha_i$  - coefficients of resistance and heat output for this particle. By changing to derivative with respect to  $x$  and taking into account that

$$m_i = \frac{1}{6} \pi d_i^3 \rho_p,$$

$$dI_i = c_x dT_i,$$

we finally obtain

$$\frac{dw_l}{dx} = \frac{3}{4} C_{xl} Q_g \frac{(w_g - w_l)(w_g - w_l)}{w_l Q_g d_l}; \quad (13.9)$$

$$\frac{dT_l}{dx} = \frac{6a_l(T_g - T_l)}{w_l d_l Q_g c_l}. \quad (13.10)$$

Coefficients of resistance and heat exchange can be determined by relationships, considering the effect of inertial forces and rarefaction, when the length of free path of molecules becomes commensurate with the size of the particle.

Resistance coefficient

$$\left. \begin{aligned} C_{xl} &= \frac{C_{xl}^0}{1 + 0.191 C_{xl}^0 M_l}, \\ C_{xl}^0 &= \frac{24}{Re_l} + \frac{4.4}{\sqrt{Re_l}} + 0.42, \end{aligned} \right\} \quad (13.11)$$

where  $Re_l = \frac{Q_g |w_g - w_l| d_l}{\eta_g}$  - Reynolds number,  $M_l = \frac{|w_g - w_l|}{a}$  - Mach number.

Heat output coefficient

$$a_l = \frac{Nu_l \lambda_l}{d_l},$$

where  $Nu_l$  - Nusselt number, determined by formula:

$$\left. \begin{aligned} Nu_l &= \frac{Nu_l^0}{1 + 3.42 \frac{M_l}{Re_l Pr} Nu_l^0}; \\ Nu_l^0 &= 2 + 0.46 Re_l^{0.55} Pr^{0.33}. \end{aligned} \right\} \quad (13.12)$$

Here  $Pr$  - Prandtl number of gas phase.

Quantities designated by index "0" above are determined with allowance for forces of viscosity and inertial forces, without the index - with allowance for even rarefaction.

Continuity equation for gas is written so:

$$Q_g w_g F = (1 - z) G.$$

For condensate let us introduce function  $\rho(m)$ , defining the mass of particles of fraction  $m$  in a unit of volume is the product  $\rho(m)dm$ . From equation of continuity for particles of fraction  $m$

$$\rho(m)w(m)F dm = zQg(m)dm$$

and equation of continuity for gas we obtain the expression for this function:

$$\rho(m) = \frac{z}{1-z} Q \frac{w_z}{w(m)} g(m). \quad (13.13)$$

Equation of motion of gas must be written with allowance for volumetric force, acting on the part of the condensate:

$$Q_z w_z \frac{dw_z}{dx} = - \frac{dp_z}{dx} + P_z.$$

A unit of gas volume on the part of particles of fraction  $m$  is affected by force equal to the product of their mass by acceleration and opposite in sign:

$$dP_z(m) = -\rho(m) \frac{dw(m)}{d\tau} dm$$

or, taking into account expression (13.13):

$$dP_z(m) = - \frac{z}{1-z} Q \frac{w_z}{w(m)} \frac{dw(m)}{d\tau} g(m) dm.$$

Force acting on the part of particles, contained in a unit of volume, comprises

$$P_z = - \frac{z}{1-z} Q_z w_z \int_0^{\infty} \frac{dw(m)}{dx} g(m) dm.$$

Finally the motion of equation of gas assumes the form:

$$Q_z w_z \frac{dw_z}{dx} + \frac{dp_z}{dx} + \frac{z}{1-z} Q_z w_z \int_0^{\infty} \frac{dw(m)}{dx} g(m) dm = 0. \quad (13.14)$$

Equation of conservation of energy of the mixture is obtained from the condition that energy, being carried through any section of the nozzle, remains constant with respect to  $x$ , i.e.,

$$\rho_0 w F \left( I_0 + \frac{w_0^2}{2} \right) + F \int_0^x \rho(m) w(m) \left\{ I(m) + \frac{w(m)^2}{2} \right\} dm = \text{const.}$$

Let us divide the last equation by constant  $\rho_0 w_0 F$  and substitute the value of  $\rho(m)$  from equation (13.13). During differentiation with respect to  $x$  we obtain in final form:

$$(1-z) \left( c_p \frac{dT_0}{dx} + w_0 \frac{dw_0}{dx} \right) + z \int_0^x \left[ c_p \frac{dT(m)}{dx} + w(m) \frac{dw(m)}{dx} \right] g(m) dm = 0. \quad (13.15)$$

Let us write equation of state of gas of constant composition ( $\mu_0 = \text{const}$ )

$$p = \rho_0 R_0 T_0 / \mu_0$$

in differential form

$$\frac{1}{p} \frac{dp}{dx} - \frac{1}{T_0} \frac{dT_0}{dx} - \frac{1}{\rho_0} \frac{d\rho_0}{dx} = 0. \quad (13.16)$$

System of equations (13.9), (13.10), (13.14)-(13.16) is supplemented by the known relationship

$$\rho_0 = f(x). \quad (13.17)$$

Let us introduce designations:

$$\begin{aligned} K_1 &= -\frac{z}{1-z} \rho_0 w_0 \int_0^x \frac{dw(m)}{dx} g(m) dm; \\ K_2 &= -\frac{z}{1-z} \int_0^x \left[ c_p \frac{dT(m)}{dx} + w(m) \frac{dw(m)}{dx} \right] g(m) dm; \\ K_3 &= \frac{1}{\rho_0} \frac{d\rho_0}{dx}. \end{aligned}$$



Then equations (13.14)-(13.16) take the form:

$$\left. \begin{aligned} \varrho_1 w_1 \frac{dw_1}{dx} + \frac{dp}{dx} &= K_1; \\ w_1 \frac{dw_1}{dx} + c_p \frac{dT_1}{dx} &= K_2; \\ \frac{1}{p} \frac{dp}{dx} - \frac{1}{T_1} \frac{dT_1}{dx} &= K_3. \end{aligned} \right\} \quad (13.18)$$

Thus, for determination of  $2n + 3$  unknowns ( $w_1, T_1, w_2, T_2, p$ ) we have  $2n + 3$  equations.

Having solved system of equations (13.18) relative to derivatives, we obtain expressions for them in evident form

$$\left. \begin{aligned} \frac{dw_1}{dx} &= -\frac{K_3 - \frac{K_1}{p} + \frac{K_2}{c_p T_1}}{\frac{w_1}{c_p T_1} - \frac{\varrho_1 w_1}{p}}, \\ \frac{dT_1}{dx} &= \frac{K_2}{c_p} - \frac{w_1}{c_p} \frac{dw_1}{dx}, \\ \frac{dp}{dx} &= K_1 - \varrho_1 w_1 \frac{dw_1}{dx}. \end{aligned} \right\} \quad (13.19)$$

Calculation of parameters of nonequilibrium two-phase flow is accomplished in such a sequence.

It is assumed that in the combustion chamber in section  $x_H$  with a rather large relative area (and, accordingly, low velocity) the gas and condensate are in equilibrium and from this condition there are determined initial data - values of unknown parameters. Flow rate of the mixture and  $\varrho_1 = f(x)$  are determined during calculation of equilibrium flow in a nozzle of prescribed profile.

Parameters of nonequilibrium flow in section  $x_H + \Delta x$  are determined by numerical integration of equations (13.9), (13.10) and (13.19). After  $w_1, T_1$ , and  $w_2$ , are determined as a result of fulfillment of the integration step in section  $x_H + \Delta x$ , gas temperature is

more accurately and simply calculated by finite relationship, obtained from equation of energy in integral form:

$$T_z = T_k - \frac{1}{c_p} \left\{ \frac{w_z^2}{2} + \frac{z}{1-z} \int_0^{\infty} \left[ c_z T(m) - c_z T_k + \frac{w^2(m)}{2} \right] g(m) dm \right\}.$$

It is expedient to determine the pressure in this case from equation of state.

Area of the nozzle after each integration step is found from equation of nonequilibrium by known parameters and flow rate of gas. Repetition of the described procedure gives values of parameters of nonequilibrium flow along the entire nozzle. The shown calculation is rather laborious and is done on an electronic computer.

#### 13.4. Coagulation of Particles of Condensate in the Nozzle

##### Estimation of the Possible Role of Collisions of Particles

As was noted earlier, particles of different sizes move in the nozzle, at different velocity. Figure 13.2 shows typical results of calculation of high-speed lag of particles from gas, obtained by the methods given in the previous paragraph for conditions:  $z = 0.32$ ,  $d_{kp} = 100$  mm and  $p_k = 40$  bar. The nozzle profile is shown on this figure. It is evident that the maximum difference of velocities of gas and condensate takes place after the nozzle throat and for particles 10-20  $\mu$ m in diameter comprises several hundred meters per second. Let us note that at such velocities of blowing of drops, their deformation and splitting are possible.

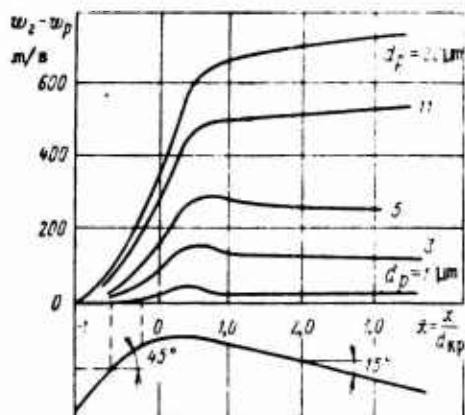


Fig. 13.2. High-speed lag of particles of various sizes in the nozzle.

The velocity of motion of particles relative to each other also reaches considerable quantities. Thus, in the region of the throat and downstream the difference of velocities of particles of unequal sizes comprises about 250 m/s for drops 1 and 5  $\mu\text{m}$  in diameter and reaches 500-700 m/s for particles 1 and 10-20  $\mu\text{m}$  in diameter.

In order to clearly represent the possible role of the process of collision of particles, let us examine such a typical case. In the throat region of the nozzle the density of condensate  $\rho_z$ , i.e., mass of particles in a unit of volume, comprises a quantity of the order of  $\sim 0.5-1.0 \text{ kg/m}^3$ . Let us assume that condensate consists of two fractions having diameters  $d_{p1} = 2 \mu\text{m}$  and  $5 \mu\text{m}$ , weight fractions of which relative to condensate comprise 0.8 and 0.2, respectively.

Having made use of the obvious formula for the number of particles in a unit of volume

$$n_i = \frac{Q_{zi}}{m_i} = \frac{6Q_{zi}}{\pi d_{pi}^3 \rho_p},$$

in the considered case when  $\rho_z = 1.0$  and  $\rho_p = 2.4 \cdot 10^3 \text{ kg/m}^3$  we obtain the following quantities:

$$n_1 = 0.8 \cdot 10^{14} \text{ and } n_2 = 1.2 \cdot 10^{12} \text{ particles/m}^3.$$

The velocity relative to motion of fractions comprises about 200 m/s according to data of Fig. 13.2. Each particle with diameter

5  $\mu\text{m}$ , moving relative to two-micron, in a unit of time should encounter those of them which are contained in volume

$$V' = |w_{p1} - w_{p2}| \pi (r_{p1} + r_{p2})^2, \quad (13.20)$$

i.e., with  $n_1 V'$  particles.

Diagram of this process is shown on Fig. 13.3.

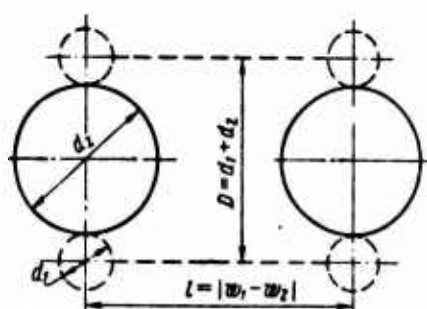


Fig. 13.3. For calculation of the number of collisions of particles.

Substitution of numerical values gives the quantity of collisions of one five-micron drop with two-micron:

$$n_1 V' = 2 \cdot 10^2 \cdot 3,14 (3,5 \cdot 10^{-6})^2 \cdot 0,8 \cdot 10^{14} = 0,6 \cdot 10^6 \text{ s}^{-1}.$$

Let us roughly estimate the number of collisions of one drop during the time of passing a path with length on the order of the throat diameter in the throat region. Assuming that velocity  $w_{z2} \approx 10^3 \text{ m/s}$ , then the time of passage of path  $L = 10^{-1} \text{ m}$  is

$$\tau = \frac{L}{w_{z2}} \approx 10^{-4} \text{ s}.$$

In this time there will occur

$$N = n_1 V' \tau = 0,6 \cdot 10^2 = 60 \text{ collisions}.$$

Thus, a rough estimation shows that a five-micron drop during the time of passage of the throat region will encounter approximately

60 two-micron. If each encounter leads to fusion, then the mass of the particle will increase to

$$m'_2 = m_2 \left[ 1 + 60 \left( \frac{2}{5} \right)^3 \right] = 3.84 m_2,$$

i.e., increases almost 4 times, and the diameter increases  $\sqrt[3]{3.84} \approx 1.6$  times and reaches approximately 8  $\mu\text{m}$ . The relationship of weight fractions of particles of both fractions is changed even more substantially.

However, the assumption about fusion of drops with every encounter is not always valid. During collisions with high velocities, obviously some of the encounters, close to the tangent, will not lead to fusion. Results of investigation of the process of collisions, deformation, splitting of drop by gas flow under various conditions of blowing are contained in special literature. For quantitative evaluation of the role of these processes reliable data are necessary about the physical properties of liquid oxides of metals.

#### Equations for Calculation of Coagulation of Particles in the Nozzle

Let us introduce function  $n(m)$  - calculating distribution density of particles along masses, determining the number of particles of fraction  $m$  in a unit of volume. In accordance with expression (13.13)

$$n(m) = \frac{v(m)}{m} = \frac{z}{1-z} \frac{v_0 w_0}{m w(m)} g(m). \quad (13.21)$$

As before, we will consider the particle trajectories during approach rectilinear and each collision effective, i.e., leading to fusion. Then each particle of fraction  $m_1$  during time  $dt$  will encounter those particles of fraction  $m$ , which are contained in volume  $V'$ , determined by an equation analogous to equation (13.20). The number of these particles of fraction  $m$  comprises

$$\Delta N' = \frac{\pi}{4} [d(m) + d_1]^2 [w(m) - w_1] n(m) dm dt.$$

Evaluations show that in all cases of interest it is sufficient to consider only two-body collisions of particles.

Let us introduce a designation for coagulation constant

$$K(m_1, m) = \frac{\pi}{4} [d(m) + d_1]^2 |w(m) - w_1|. \quad (13.22)$$

The physical meaning of the introduced quantity - amount of collisions occurring in a unit of time between particles  $m_1$  and  $m$  with their concentration along one particle in a unit of volume.

All particles of fraction  $m_1$  during time  $d\tau$  will encounter

$$K(m_1, m)n(m_1)n(m)dm_1dmd\tau$$

particles of fraction  $m$ . However, after the collision the mass of particle  $m_1$  increases and it leaves fraction  $m_1$ . By integrating with respect to  $m$  from 0 to  $\infty$ , we obtain the expression for rate of decrease in the concentration of particles of fraction  $m_1$  because of collisions with all the remaining particles

$$\left[ \frac{\partial}{\partial \tau} n(m_1) dm_1 \right]_{(-)} = -n(m_1) dm_1 \int_0^\infty K(m_1, m) n(m) dm. \quad (13.23)$$

With fusion of two particles there is formed a new, coarser,  $m' = m_1 + m$ , entering fraction  $m'$ . If we continue to consider fraction  $m_1$ , the particles of this mass will be formed with fusion of two finer ones, having masses  $m$  and  $m_1 - m$ .

Just as before, examination gives such an expression for increase of the number of particles of fraction  $m_1$  due to this process:

$$\begin{aligned} & \left[ \frac{\partial}{\partial \tau} n(m_1) dm_1 \right]_{(+)} = \\ & = dm_1 \int_0^{m_1/2} K(m, m_1 - m) n(m) n(m_1 - m) dm. \end{aligned} \quad (13.24)$$

By summing expressions (13.23) and (13.24) and changing to derivative of  $x$ , we obtain integral-differential equation for change of function  $n(m)$  as a result of fusions of particles:

$$\begin{aligned} \frac{\partial n(m_i)}{\partial x} = & -\frac{n(m_i)}{w_i} \int_0^{\infty} K(m_i, m) n(m) dm + \\ & + \frac{1}{w_i} \int_0^{m_i/2} K(m, m_i - m) n(m) n(m_i - m) dm. \end{aligned} \quad (13.25)$$

Numerical solution for  $n$  selection fractions  $n$  of equations (13.25) together with  $(2n + 3)$  equations, examined in the previous paragraph, gives the possibility of determining all the necessary parameters of gas and particles in the nozzle under assigned inlet conditions.

Let us note that as a result of fusion of two particles, the reformed, coarser one will have a higher velocity and lower temperature than particles of its size (mass), but "older age" for example, moving the nozzle inlet. Thus, for instance, when a particle  $5 \mu\text{m}$  in diameter is formed as a result of fusion of two particles with diameters approximately 3 and  $4.5 \mu\text{m}$ , then its velocity can be found from condition of conservation of momentum

$$5^3 \omega_3 = 3^3 \omega_1 + 4.5^3 \omega_2.$$

If we use the data of Fig. 13.2 then it turns out to be approximately 40 m/s higher than the velocity of basic fraction  $d = 5 \mu\text{m}$ .

This can be taken into account in the calculation by corresponding change of average velocity of particles of fraction  $m_i$ . As the basis for determination of the amount of change in velocities of fractions with coagulation we use condition of conservation of momentum: interaction between particles must not change the quantities of motion of the whole condensate. For taking into account analogous temperature shift we use condition of conservation of energy of condensate.

# Some Results of Calculations of Nonequilibrium Two-Phase Flows with Coagulation

Let us cite some results of calculations on an electronic computer, obtained for combustion products of solid propellant, having combustion-chamber temperature  $T_{\text{ch}} = 3100-3200^\circ\text{K}$  and containing in their composition 13-38% condensed aluminum oxide. Nozzle inlet pressure in different cases varied from 10 to 80 bar, diameter of nozzle throat - from 20 to 500 mm.

In all cases we assumed that at the nozzle inlet the particles are distributed according sizes in accordance with logarithmic-normal law with root-mean-square deviation  $\sigma = 1.5$  and average geometric diameter  $d_z = 1 \mu\text{m}$ .

Figure 13.4 shows functions  $g(d)$  obtained by calculation in various sections of the nozzle, geometry of which is shown on this figure, when  $z = 0.28$ ,  $p_{\text{ch}} = 40 \text{ bar}$  and  $d_{\text{kp}} = 100 \text{ mm}$ . As can be seen, the process of coagulation in the nozzle substantially changes the initial function of distribution.

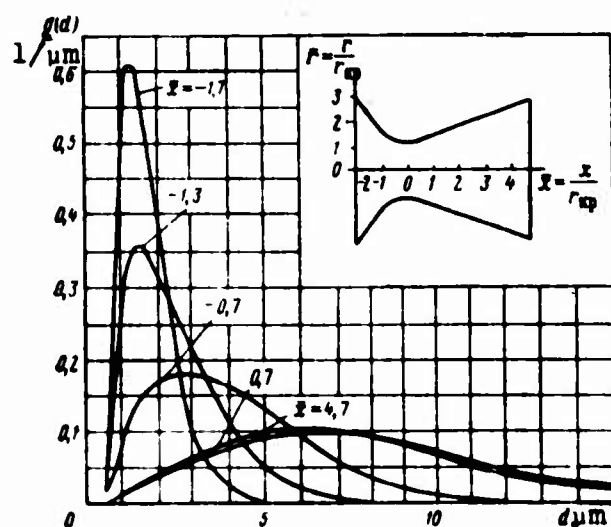


Fig. 13.4. Change in the distribution density as a result of coagulation.



Change of average diameter  $d_{zm}$  along the axis of the nozzle, found under the same conditions, but with different throat diameters, is shown on Fig. 13.5. From the chart it follows that growth of particles is substantially greater with increase of absolute dimensions of the nozzle.

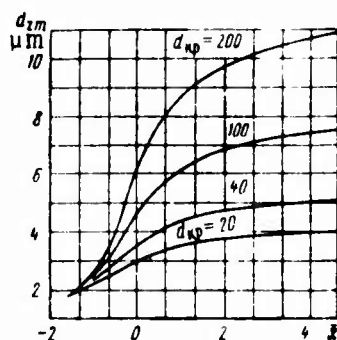


Fig. 13.5. Growth of average diameter of particles in nozzles with various throat diameter.

Analysis shows that such a character of relationship to  $d_{np}$  is a result of the opposition of two processes, which affect coagulation. In larger nozzles the delay of particles and, consequently, the constant of coagulation are diminished (13.22), but time of stay of the mixture in the nozzle increases in proportion to the throat diameter. The effect of the second factor turns out to be considerably greater.

Figure 13.6 shows relationships analogous to previous, obtained when  $d_{np} = 100$  mm and at various contents of condensate. The considerably greater growth of average diameter of particles with increase of their concentration is physically obvious.

According to equation (13.25) the rate of coagulation must be proportional to the square of concentration. Therefore, with increase in pressure in the combustion chamber, all things being equal ( $z = \text{const}$ ,  $d_{np} = \text{const}$ ), the average size of particles increases.

Figure 13.7 shows quantities  $d_{zm}$  at the nozzle section when  $z = 0.25$ ,  $d_{np} = 100$  mm.

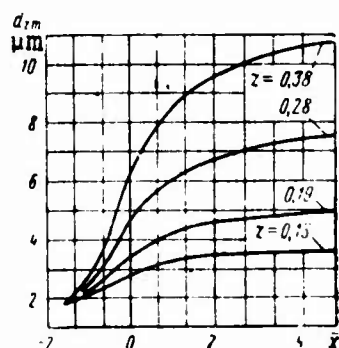


Fig. 13.6.

Fig. 13.6. Growth of average diameter of particles depending on the weight fraction of condensate.

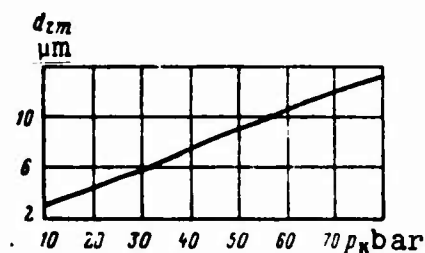


Fig. 13.7.

Fig. 13.7. Change of average diameter of particles depending on pressure in the combustion chamber.

Thus, results of calculations indicate a very substantial growth of particles of condensate during motion in the nozzle. If we consider that losses of specific thrust are determined by the size of particles in the region of the nozzle throat, one should make a conclusion about the determining effect of the process of coagulation on these losses.

This conclusion is illustrated by data of Fig. 13.8, where there are presented values of losses of specific thrust in a void calculated with allowance for and without allowing for coagulation (curves 1 and 2 respectively) with identical initial distribution of particles according to sizes. Quantity  $z$  in calculations is accepted equal to 0.32, and  $f_c = 6.5$ . With throat diameter  $d_{np} = 100-200$  mm and more quantities  $\Delta P_{y.d.n}$  differ 10-15 times. As a result of the considerable growth of particles in the nozzle "two-phase" losses of specific thrust are slightly diminished with increase in the absolute dimensions of the engine.

Decrease of the complex  $\beta$ , connected with nonequilibrium of two-phase flow in the subsonic and supersonic part of the nozzle, as calculations show, is close to the amount of losses of specific thrust:

$$\frac{\Delta \beta}{\beta} = (1.1 - 1.2) \frac{\Delta P_{y.d.n}}{P_{y.d.n}}$$

[Translator's Note:  $\beta$  = loss.]

This decrease of  $\beta$  must be considered when determining through  $\Phi_{\text{pr}}$  measured value of  $\phi_3$  (see Chapter XVI).

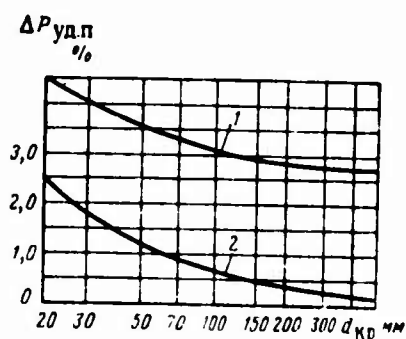


Fig. 13.8. Change of specific thrust in a void depending on throat diameter.

### 13.5. Nonequilibrium of the Crystallization Process of Condensate in the Nozzle

In methods of calculation of theoretical thermodynamic characteristics it is assumed that the process of expansion in the nozzle is equilibrium. For two-phase combustion products this means, specifically, that temperatures and velocities of particles and gas are equal everywhere, and condensate is equilibrium through phase states in proportion to cooling the nozzle. For example, combustion products of blended solid propellant with Al additives contain 15-35% condensed aluminum oxide, having melting point  $2303^{\circ}\text{K}$ . The combustion temperature of these propellants is  $3000-3500^{\circ}\text{K}$ , and the temperature of combustion products at the nozzle section  $1500-2000^{\circ}\text{K}$ . According to equilibrium thermodynamic calculation in the combustion chamber the particles of aluminum oxide are in liquid state. In the course of expansion the temperature of combustion products in some section reaches  $2303^{\circ}\text{K}$  and the expansion process further proceeds isothermally, until heat of crystallization of aluminum oxide is converted into kinetic energy. On this section of the nozzle the condensate gradually, in proportion to output of heat to gas, changes from liquid state to solid. In each section the fraction of hardened condensate is equal to the fraction of removed heat of crystallization.

In a real case the equilibrium course of this process can be limited, first of all, by finite velocity of heat transfer from particles to gas, secondly, by finite velocity of crystallization.

Let us examine the question of the effect of finite velocities of crystallization and heat output on losses of specific thrust as a result of incomplete utilization of heat of phase transition of condensate.

Kinetics of the crystallization process is determined by two basic parameters: number of crystalline nuclei, which appear in a unit of time, and linear velocity of growth of crystals. Probability of formation of a nucleus of new phase in a unit of column on Fol'mer is determined by the following expression:

$$w = A \exp \left[ - \frac{B\sigma^3}{T\Delta T^3} \right],$$

where  $\sigma$ ,  $\Delta T$ ,  $A$ ,  $B$  - interphase surface tension, supercooling of liquid and certain constants respectively.

For metal oxides the process of crystallization was not investigated and constants in this equation are unknown.

Qualitatively the less the probability of formation of at least one center, the smaller the mass of liquid. From investigations in meteorology it is known that small drops of water are supercooled to temperatures several tens of degrees lower than zero. Time necessary for freezing micron drops of water is measured in seconds and in minutes, and submicron - in hours. For water quantity  $\sigma$  comprises about 10 dyn/cm, for aluminum oxide - about 200 dyn/cm. Time of flow of combustion products in the supersonic part of the nozzle, where crystallization should occur, comprises a magnitude on the order of 10  $\mu$ s.

Thus, a number of factors - small sizes of particles (on the order of a micron), considerable magnitude of interphase surface tension between crystalline modification and liquid oxide, and also a very short time, during which hardening of particles must occur, place under doubt the possibility of equilibrium process of crystallization in the nozzle of the engine. Therefore it is not excluded that particles of metal oxide after achievement of melting point and with further cooling are located in liquid, supercooled state.

For calculation of kinetics of possible crystallization at present there are no published data. Limiting case of nonequilibrium, when particles of oxide are located in liquid supercooled state, can be calculated by thermodynamic methods. Results of calculations give an answer to the question of maximum possible effect of the considered process on power engineering of engines.

Approximate thermodynamic estimation of nonequilibrium can be given by proceeding from the following examination. We will consider two-phase combustion products consisting of two subsystems: strictly combustion products with condensate in liquid state and a source of heat.

In equilibrium process, when crystallization takes place, heat from a source is supplied to combustion products at constant temperature, equal to  $T_{пл}$ . If there is no crystallization, heat is not fed from a source to combustion products. In both cases the entropy of the entire system (combustion products and source) remains constant. However, in the process with crystallization the entropy of strictly combustion products will increase.

Let us examine the difference of outflow velocity in these two cases during expansion to prescribed pressure. Equation of energy in the case of absence of crystallization can be written so:

$$\frac{w_{c, \text{нр}}^2}{2} = I_{\kappa} - (I_c + \delta I_c) - Q_{\text{нр}}, \quad (13.26)$$

where  $w_{c.нр}$  - outflow velocity of combustion products in nonequilibrium process without crystallization;  $I_k, I_c$  - enthalpy of combustion chamber and at the nozzle section for flow with crystallization;  $\delta I_c$  - change in enthalpy at the nozzle section with respect to flow crystallization;  $Q_{пл}$  - quantity of heat on 1 kg of working substance, liberating during phase transformation.

Let us rewrite equation (13.26) in the form

$$\frac{w_{c.нр}^2}{2} - (I_k - I_c) = -\delta I_c - Q_{пл}.$$

The second term in the left side of this equation is equal to half the square of outflow velocity in the equilibrium process:

$$I_k - I_c = \frac{w_c^2}{2}.$$

With allowance for this, it is possible to approximately write

$$\Delta w w_c = -\delta I_c - Q_{пл},$$

where

$$\Delta w = w_{c.нр} - w_c.$$

The quantity of heat, which is liberated during phase transformation, is equal to

$$Q_{пл} = z \Delta I_{пл},$$

where  $\Delta I_{пл}$  - heat of melting 1 kg of oxide.

Since the temperature during phase transition is constant, change of entropy of combustion products is equal to

$$\delta S = -\frac{z \Delta I_{пл}}{T_{пл}}.$$

Corresponding change of enthalpy at the nozzle section at constant pressure  $p_c$  comprises

um

$$\delta I_c = - \frac{z \Delta I_{ns} T_c}{T_{nc}},$$

where  $T_c$  - temperature of combustion products at the nozzle section in equilibrium process.

Final expression of relative change of outflow velocity for the process without crystallization has the form:

$$\frac{\Delta w}{w_c} = - \frac{z \Delta I_{ns} (1 - T_c / T_{nc})}{w_c^2}. \quad (13.27)$$

From expression (13.27) it follows that the greater the weight fraction of condensate in combustion products and the lower the temperature at the nozzle section, the greater the effect heat of phase transition has on the outflow velocity.

Table 13.2 shows decrease of outflow velocity in case of the absence of crystallization for two propellants using ammonium perchlorate as base with 7 and 15% aluminum, calculated by formula (13.27).

Table 13.2. Reduction of outflow velocity in the absence of crystallization.

% Al in propellant	$T_c$ °K	$z$	$w_c$ m/s	$\Delta w$ %
7	1740	0.13	2390	0.63
15	2050	0.28	2500	0.56

As can be seen from the table, decrease in the outflow velocity is about 0.6%. In this case for propellant with 7% Al despite a considerably lower content of condensate than for fuel with 15% aluminum, the absence of crystallization leads to a higher decrease of outflow velocity. The determining role here is played by the fact that the temperature at the nozzle section for the first propellant is considerably lower.

The above given approximate estimation of the effect of crystallization on the outflow velocity carries a more qualitative than quantitative character. The process of expansion proceeds with prescribed value of relative nozzle exit section area. In case of the absence of crystallization in the rocket engine nozzle the pressure at the nozzle section, as will be shown below, can considerably differ from design pressure during equilibrium expansion. Therefore, comparison of processes with crystallization and in its absence in a fixed nozzle (at assigned  $f_c$ ), but not under condition of constant exit pressure, is more correct and accurate. Furthermore, comparison of the effectiveness of processes of expansion with respect to outflow velocity can lead to incorrect conclusions. As is known, the addition of heat to supersonic flow slows it down. Consequently, by taking the outflow velocity as criterion, the incorrect conclusion can be made that the process with crystallization is less effective than in its absence. It is more correct to compare with respect to specific thrust in a vacuum.

For estimation of the relative effectiveness of expansion process in a nozzle of prescribed geometry in the absence of crystallization they were conducted special thermodynamic calculations of the above-mentioned solid propellants with 7 and 15% aluminum. Thermodynamic functions of condensed phase when supercooling below the melting point were determined from the condition that the thermal capacity of supercooled liquid is constant and equal to thermal capacity at  $T_{m1}$ .

Figure 13.9 shows temperature change of combustion products in the nozzle at equilibrium and nonequilibrium, in the sense of crystallization, flow for the propellant with 15% Al. As can be seen, curve 1 (with crystallization) and curve 2 (without crystallization) after the section where crystallization occurs during equilibrium process, go practically equidistant. Temperature of combustion products in some section of the nozzle after this section in case of nonequilibrium expansion is approximately 200°K lower. For other propellants the character of curves is analogous,



and decrease of temperature in the nozzle depends on the content of condensate in combustion products, weight fraction of which also determines the extent of the crystallization section. The more condensate in combustion products, the larger the section of crystallization and the more considerable decrease of temperature at the nozzle section in the absence of phase transition.

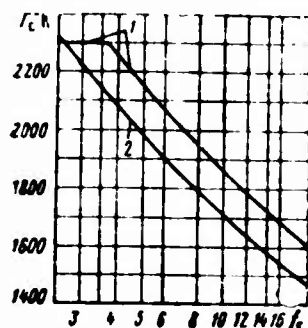


Fig. 13.9. Temperature at the nozzle section with allowance for crystallization (curve 1) and without allowing for it (curve 2).

On Fig. 13.10 for propellants with 7 and 15% Al there is shown the ratio of pressure during flow in the nozzle without crystallization to pressure at equilibrium expansion. On the crystallization section the pressure ratio rapidly drops, and then it begins to increase.

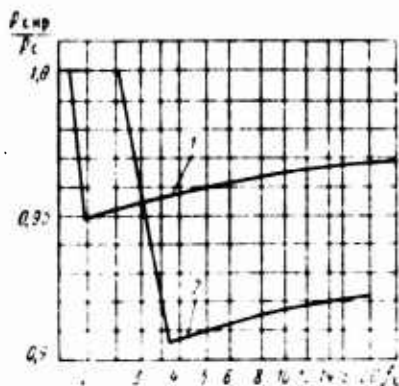


Fig. 13.10. Change of pressure on the nozzle section in the absence of crystallization for various propellants: 1 - 7% Al; 2 - 15% Al.

On Fig. 13.11 for the same propellants there is shown decrease of outflow velocity and specific thrust in a vacuum during expansion without crystallization of liquid phase in percent of values at equilibrium expansion in comparison with equilibrium values. As should have been expected, on the crystallization section the flow

in equilibrium case, when heat of crystallization is supplied, accelerates slower than in nonequilibrium case. However, with respect to the amount of specific thrust in a void the process with crystallization always has advantages. Losses of  $P_{y.d.n}$  because of the absence of crystallization for engines of earth stages reach 1.0 percent and for engines of upper stages - 1.5 percent.

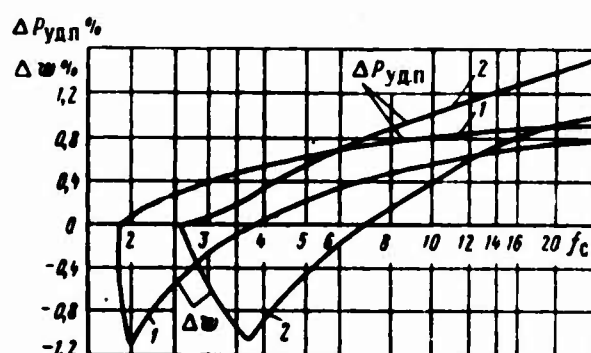


Fig. 13.11. Change of outflow velocity and specific thrust in a vacuum in the absence of crystallization.

Thus, maximum losses of specific thrust in a case when heat of crystallization is not converted during expansion into kinetic energy can be considerable. It is perfectly clear that with finite value of coefficient of heat output for transmission of heat from particles to gas some drop of temperature is necessary, consequently, the temperature of particles is always higher than the gas temperature. Even if crystallization is not retained, the removal of heat separating with it will shift toward lower temperature and pressure than in equilibrium case, and, consequently, it will be less effective. It is possible that under definite conditions the considered process will be limited not by the crystallization rate, but the rate of heat removal from particles.

For research on the role of the process of heat exchange by the methods given in § 13.3, we performed calculations of nonequilibrium flows of two-phase combustion products of blended solid propellant

with 15% aluminum,  $d_{zm} = 5 \mu m$  in a conical nozzle with half angle of aperture  $15^\circ$  and throat diameter 100 mm. Example of the calculation picture of the change in the difference of temperatures of gas and particles along the nozzle is shown on Fig. 13.12. Curve 1 corresponds to nonequilibrium flow in the absence of crystallization, curve 2 - with crystallization taking into account finite rate of heat removal. In the second case on the section of nozzle b-d the temperature difference sharply increases, since before termination of heat removal of phase transition the temperature of condensate remains constant, equal to  $T_{пл}$ , and the gas temperature continues to lower. On this section there is increased, in comparison with the first case, supply of heat to gas, as a result of which the specific thrust in a void increases. However, since section b-d is lower along the nozzle than section a-c, where there is crystallization in equilibrium case, the applied heat is transformed into work of expansion less effectively. With increase in the diameter of particles of condensate section b-d is displaced to the exit section and increase of specific thrust due to liberation of heat of crystallization is diminished.

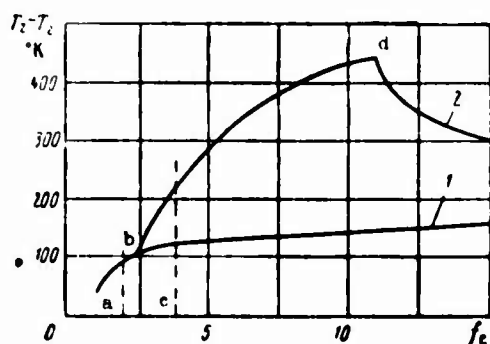


Fig. 13.12. Temperature difference of gas and condensate along the nozzle.

Results of calculations of the above-shown increase of specific thrust in a void at various sizes of particles of condensate are listed on Fig. 13.13. For the selected throat diameter a noticeable fraction of maximum increase of specific thrust (curve  $d_p \rightarrow 0$ ) can be realized under conditions of heat output from particles only with their diameter smaller than  $3-5 \mu m$ . Namely, for fine particles a delay of the process of crystallization is more probable.

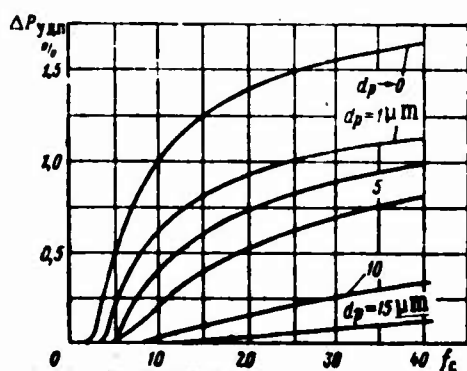


Fig. 13.13. Increase of specific thrust in a void with crystallization.

For particles more than 10-15  $\mu m$  in diameter the increase in specific thrust is negligible under conditions of heat removal. Possible supercooling of liquid oxide of metal reduces this small quantity.

As was noted above, behind the nozzle section of heavy RDTT the average diameter of particles of condensate reaches 10-15  $\mu m$ . In these conditions, according to material presented above, it would be closer to reality to perform thermodynamic calculation without allowing for heat of crystallization of condensate during expansion in the nozzle.

### 13.6. Nonequilibrium of Condensation Process in the Nozzle

If the pressure of saturated vapors of substance, which is in condensed state, is commensurate with pressure in the combustion chamber, the weight fraction of condensate in combustion products according to thermodynamic calculation substantially changes with expansion in the nozzle. An example is propellant pentaborane  $B_5H_9$  with hydrogen peroxide  $H_2O_2$ . In combustion products of this propellant the condensate can generally be absent in the combustion chamber or be contained there in a quantity of several percent. On the nozzle section with deep expansion quantity  $z$  reaches values 0.5-0.7. The process of transition of boric oxide  $B_2O_3$  from gaseous state into liquid is accompanied by liberation of a considerable quantity of heat, which increases the specific thrust. If this

process will proceed with delay or condensation generally does not occur in the nozzle, considerable losses of specific thrust, on the order of 5-10% will take place.

Kinetics of condensation can be limited by the formation of nucleation center, condensation nucleus, and also diffusion of the substance being condensed to centers and removal of heat of condensation from particles.

Obtaining results on kinetics of precipitation of condensate in the nozzle by calculation is hampered by the lack of reliable ideas about the mechanism of the process, and the ignorance of many constants, which determine the rates of other known stages of the process.

Specific difficulties are presented by the description and calculation of the process of homogeneous formation of condensation nuclei. At present there is introduced active theoretical and experimental research of processes of condensation as applied to conditions in rocket engine nozzles. Some results of these investigations can be found, for example, in [1], [6].

### 13.7. Profiling of Nozzles for Two-Phase Combustion Products

The task of profiling an extremal nozzle for two-phase combustion products, as well as for homogeneous, involves seeking a profile providing the greatest thrust from the family of nozzles, which have, for example, identical length, surface or some other parameter. Complication of the problem consists, first of all, in the need to consider a more complex system of equations in comparison with the variant of pure gas, describing nonequilibrium spatial flow of two-phase mixture. Secondly, losses of specific thrust, caused by delay of particles, decisively depend on the geometry of inlet and throat of the nozzle.

The slight dependence of losses of specific thrust on the geometry of nozzle inlet for gaseous products allows, as was shown in Chapter XII, being limited by selection of an extremal supersonic part of the nozzle. On subsonic and supersonic parts in this case there is imposed a number of minimum requirements, revealed experimentally.

In case of two-phase flow the optimization of only the supersonic section with arbitrary fixed geometry of the remaining part is by far an incomplete solution of the problem. Moreover, as will be shown below, for decrease of losses connected with delay of particles of constant size, it is required mainly to change the nozzle throat region.

At present the methods of calculation of nonequilibrium two-phase spatial flows have been developed only for the region of flow where the gas velocity exceeds the local speed of sound in gas. In principle methods of optimization of only the supersonic part of the nozzle have been developed, and this problem can be solved numerically, however, there are no results of such calculations in literature.

In a one-dimensional formulation there can be examined the problem of seeking a nozzle contour, for example, of definite length at prescribed pressures  $p_k$  and  $p_c$ , which provides maximum average outflow velocity of two-phase mixture. Solution of such a problem, obtained by methods of variational calculation in [14] with assumption of small deviation of flow from equilibrium, gives a nozzle contour substantially differing from usual. Figure 13.14 shows a contour of the usual nozzle and by a dotted line - a nozzle contour which provides minimum losses from delay of particles ( $p_k = 70$  bar,  $\tau_c = 60$ ,  $d_p = 5$   $\mu$ m,  $d_{kp} = 150$  mm and  $z = 0.4$ ). A distinctive feature of the optimum nozzle is a highly elongated throat. If for these nozzles we examine typical curves of delay of particles with respect to velocity (Fig. 13.15), then the result of elongation of the throat becomes clear: acceleration of flow (a quantity proportional to delay of particles) becomes close to constant on the nozzle, the section of more rapid dispersal in the throat area of a usual nozzle disappears. Amount of losses of

outflow velocity, caused by delay of particles, for an optimum nozzle in the examined case typical for RDTT can be reduced by approximately one third. Thus, if these losses in the case usual for RDTT comprise a quantity on the order of 3%, then by change of the nozzle contour while maintaining its overall length they can be diminished to approximately 2%. It is entirely obvious that losses from nonparallelism of flow in the nozzle, such as shown on Fig. 13.14, can substantially exceed the indicated 1% gain.



Fig. 13.14.

Fig. 13.14. Comparison of optimum and usual nozzle contours.

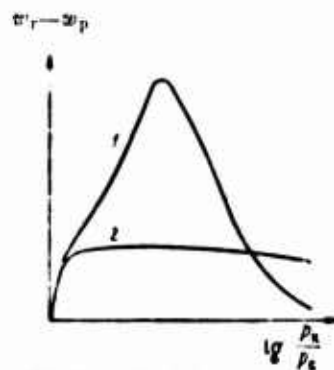


Fig. 13.15.

Fig. 13.15. Character of lag of particles with respect to velocity in usual (1) and optimum (2) nozzles.

In [7] a one-dimensional solution of the problem of selection of extremal nozzle contour with fundamental account of losses on nonparallelism of flow has been examined.

A solution for axisymmetric nonequilibrium flow, as was noted above, can be obtained if we specify the profile of subsonic and supersonic part of the nozzle and initial data of flow on a certain line, where  $M > 1$ . These initial data can be approximately obtained, for example, from one-dimensional calculation or with the aid of calculation of trajectories of particles in a flow of gas, which, in turn, is calculated for equilibrium flow.

Existing methods of calculation of nonequilibrium supersonic two-phase flow allow finding the external profile of the expansion

section of the nozzle by methods of variation calculation. In the latter case, first of all losses connected with heterogeneity of flow on the nozzle section will be reduced to minimum possible, whereas for decrease of delay of particles it is necessary to affect the nozzle throat region remaining constant in this variant of optimization.

No.

It is necessary to note that everything given above pertains to the case when particles do not interact together. In case of calculation of coagulation of particles it can turn out, for example, that it is more advantageous not to lengthen the throat, but shorten it.

No.

The point is that with elongation of the throat region (with preservation of overall length of the nozzle) according to calculations the growth of particles increases as a result of coagulation. This increase in the size of particles can be more substantial than decrease in the gradient velocity, and the amount of losses of specific thrust increases.

Thus, until such complete solutions of the problem of selection of external nozzle profile for two-phase combustion products are developed, we make use of methods of profiling of nozzles for pure gas. In this case the properties of gas are assumed identical with properties of equilibrium two-phase mixture.

#### Bibliography

1. Geterogennoye gorenije (Heterogeneous combustion), Collection of translations, izd-vo "Mir," 1967.
2. Detonatsiya i dvukhfaznoye techeniye (Detonation and two-phase flow), Collection of articles, izd-vo "Mir," 1966.
3. Karlson, Khogland. "Raketnaya tekhnika i kosmonavtika," 1964, No. 11.
4. Kligel', VRT, 1965, No. 10.
5. Krayko A. N., Sternin L. Ye., "Prikladnaya matematika i mekhanika," AN SSSR, 1965, No. 3.



6. Kutrni, "Raketnaya tekhnika," 1961, No. 3, VRT, 1965, No. 11.
7. Sternin L. Ye., "Mekhanika zhidkosti i gaza," 1966, No. 5.
8. Grishin S. D. et al., "Mekhanika zhidkosti i gaza," 1969,  
No. 2.
9. Khogland. "Raketnaya tekhnika," 1962, No. 5.
10. Khoffman, Lorents, "Raketnaya tekhnika i kosmonavtika," 1965,  
No. 1; 1966, No. 1.
11. Khoffman, Thompson, VRT, 1967, No. 3.
12. Brown B., Pyrodynamics, 1965, Vol. 3, p. 221.
13. Carlson D. J., AIAA Paper, No. 66-652.
14. Marble F. E., AIAA Journal, 1963, No. 12.

## CHAPTER XIV

### HEAT OUTPUT TO CHAMBER WALLS

In the chapter are examined methods of calculation of heat output from combustion products to chamber walls. There are listed methods of determination of convective and radiant specific heat flows, their distribution along the chamber passage is analyzed. On the basis of generality of processes transfer in the boundary layer working formulas are given for determination of friction stress.

#### 14.1. Preliminary Information

##### Boundary Layer

As any real liquid, combustion products possess viscosity and thermal conductivity, which leads to formation of a boundary layer directly near the wall.

Depending upon the character of flow, the condition of motion in the boundary layer can be laminar or turbulent. In chambers of rocket engines, as a rule, a turbulent boundary layer is formed, which is caused by high flow velocities. However, in regions directly adjacent to the wall, there is always a viscous (laminar) underlayer, where motion is laminar. Thickness of the viscous underlayer is relatively small in comparison with overall thickness of the boundary layer.

In the boundary layer there occurs change of many parameters and properties of flow. A change of some quantity from the value in external flow (nucleus of flow) to the value at the wall determines the corresponding characteristic thickness of the boundary layer. For example, in dynamic boundary layer with thickness  $\delta$  (Fig. 14.1) is a characteristic quantity there is considered the gas velocity, which is reduced from the value in external flow to zero at the wall. In the thermal boundary layer the characteristic quantity is considered temperature or enthalpy, which is changed from the value on the boundary layer to the value at the wall. Generally, the thicknesses of thermal ( $\delta_T$ ) and dynamic ( $\delta$ ) layers do not coincide ( $\delta > \delta_T$  when  $Pr > 1.0$ ,  $\delta < \delta_T$  when  $Pr < 1.0$ ).

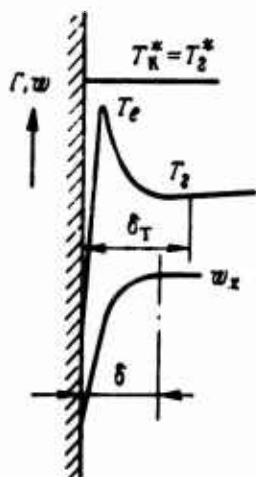


Fig. 14.1. Characteristic temperatures and thicknesses of boundary layer:  $\delta$  - thickness of dynamic boundary layer;  $\delta_T$  - thickness of thermal boundary layer.

It is not possible to clearly determine the external boundary (and thereby the thickness) of boundary layer. Theoretical analysis shows that only at dimensionless distance from the wall are parameters in boundary layer compared with their values for external flow. Therefore, the boundary limit is frequently determined conditionally, for example, for dynamic boundary layer the limit is where the local velocity differs from the velocity of external flow by one percent.

In calculations there are frequently applied conditional boundary layer thicknesses. Usually three conditional thicknesses are used:

$\delta^*$  - displacement thickness,  $\delta^{**}$  - momentum thickness,  $\delta_T^{**}$  - energy thickness. For example, for axisymmetric boundary layer of compressible liquid the conditional thicknesses are determined by formulas

$$\delta^* = \int_0^{\delta} \frac{r - y \cos \alpha}{r} \left( 1 - \frac{Q_{w_x}}{Q_{\infty x}} \right) dy, \quad (14.1)$$

$$\delta^{**} = \int_0^{\delta} \frac{r - y \cos \alpha}{r} \left( 1 - \frac{w_x}{u_{\infty}} \right) \frac{Q_{w_x}}{Q_{\infty x}} dy, \quad (14.2)$$

$$\delta_T^{**} = \int_0^{\delta} \frac{r - y \cos \alpha}{r} \left( 1 - \frac{\Delta I^*}{\Delta I^*} \right) \frac{Q_{w_x}}{Q_{\infty x}} dy. \quad (14.3)$$

Here  $\Delta I^* = I^* - I_{CT}$  - difference of enthalpies at stagnation temperature and wall temperature;  $r$  - radius of nozzle (Fig. 14.2);  $\alpha$  - angle wall to the nozzle axis, symbol  $\sim$  designates parameters in the nucleus of flow.

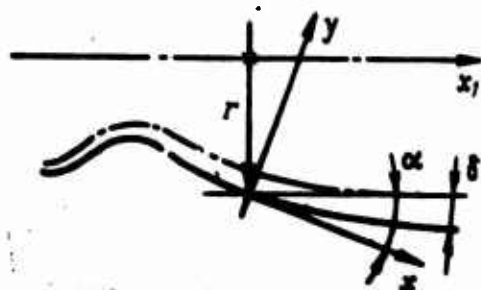


Fig. 14.2. System of coordinates during integration of boundary layer equations.

Conditional thicknesses  $\delta^*$ ,  $\delta^{**}$ ,  $\delta_T^{**}$  have a clear physical meaning [2]. Utilization of  $\delta_T$ ,  $\delta = \delta_T$  as upper limit of integration in formulas (14.1)-(14.3) rids quantities  $\delta^*$ ,  $\delta^{**}$ ,  $\delta_T^{**}$  from uncertainty, connected with conditional selection of boundary layer thicknesses  $\delta$ ,  $\delta_T$ .

During the study of turbulent motion the statistical method is applied. The true value of each flow parameter is represented by the sum of mean  $\bar{\phi}$  and pulsation  $\phi'$  values:

$$\phi = \bar{\phi} + \phi', \quad (14.4)$$

where averaging obeys the following rules:

$$\overline{u+v} = \overline{u} + \overline{v}; \quad (14.5)$$

$$\frac{\partial \overline{u}}{\partial \tau} = \frac{\partial \overline{u}}{\partial \tau}, \quad \frac{\partial \overline{u}}{\partial x} = \frac{\partial \overline{u}}{\partial x}; \quad (14.6)$$

$$\overline{uv} = \overline{u} \overline{v}. \quad (14.7)$$

In accordance with rules (14.5)-(14.7) the average pulsation values of density  $\overline{\delta'}$ , pressure  $\overline{p'}$  and temperature  $\overline{T'}$  are taken equal to zero. Average values of velocity  $\overline{w}$ , temperature  $\overline{T}$ , static enthalpy  $\overline{I}$  and stagnation enthalpy  $\overline{I^*}$  can be determined by formula

$$\overline{\phi \phi} = \overline{\phi \phi}, \quad (14.8)$$

where  $\phi$  - values  $w, T, I, I^*$ .

With the aid of formula (14.8) by direct substitution in it of quantities in the form of expression (14.4) and by subsequent averaging we obtained equalities:

$$\overline{\phi w'} + \overline{\phi' w} = 0; \quad (14.9)$$

$$\overline{\phi T'} + \overline{\phi' T} = 0; \quad (14.10)$$

$$\overline{\phi T''} + \overline{\phi' T''} = 0. \quad (14.11)$$

System of equations for boundary layer is derived from Navier-Stokes equation [6] where values of parameters are substituted in the form (14.4). In this case averaged motion is considered stationary. With averaging of equations of motion and energy the effect of molecular viscosity and thermal conductivity is usually disregarded. After averaging, the terms considering viscosity and thermal conductivity are assigned to obtained equations. In conversions are used formulas (14.9)-(14.11). In this way we can obtain a system of equations that describe turbulent flow of viscous compressible liquid.

In applications to various problems of turbulent flows this system is simplified accordingly. Specifically, for flow in the boundary layer the following simplifying assumptions are used:

$$\begin{aligned} w_y &\ll w_x; \\ \frac{\partial \phi}{\partial x} &\ll \frac{\partial \phi}{\partial y}, \end{aligned}$$

where  $\phi$  - any hydrodynamic quantity. These assumptions are applied when evaluating the possible quantity of each term of equations; terms of higher order of smallness are rejected. As a result, a system of equations is obtained which approximately describes the flow in the boundary layer. For axisymmetric flow characteristic in rocket engine nozzles it has the following form (for simplicity the sign of averaging is preserved only in pulsation components):

$$\frac{\partial}{\partial x}(rQw_x) + \frac{\partial}{\partial y}(rQw_y) = 0, \quad (14.12)$$

$$Qw_x \frac{\partial w_x}{\partial x} + Qw_y \frac{\partial w_x}{\partial y} = -\frac{\partial p}{\partial x} + \frac{1}{r} \frac{\partial}{\partial y}(r\tau); \quad (14.13)$$

$$\frac{\partial p}{\partial y} = 0, \quad (14.14)$$

$$Qw_x \frac{\partial I^*}{\partial x} + Qw_y \frac{\partial I^*}{\partial y} = \frac{1}{r} \frac{\partial}{\partial y}(r q_0); \quad (14.15)$$

$$p = QRT, \quad (14.16)$$

where  $\tau = \eta \frac{\partial w_x}{\partial y} - Q \overline{w'_x w'_y}$  - stress friction; (14.17)

$$q_0 = \frac{\lambda}{c_p} \frac{\partial I^*}{\partial y} - Q \overline{I'^* w'_y} \text{ - heat flow.} \quad (14.18)$$

Boundary conditions for system (14.12)-(14.16) will be the following.

When  $y = 0$ , i.e., directly on the wall:

$$\left. \begin{aligned} w_x = w_y &= 0; \\ T &= T^* = T_{cr}; \\ \tau &= \tau_{cr}; \\ q_0 &= q_{cr} = q_n. \end{aligned} \right\} \quad (14.19)$$

When  $y = \delta$ , i.e., on the limit of dynamic boundary layer with nucleus of flow:

$$\left. \begin{aligned} w_x &= \tilde{w}_x; \\ \tau &= 0. \end{aligned} \right\} \quad (14.20)$$

When  $y = \delta_T$ , i.e., on the limit of thermal boundary layer:

$$\left. \begin{aligned} T^* &= \tilde{T}^*; \\ q &= 0. \end{aligned} \right\} \quad (14.21)$$

Integration of obtained boundary layer equations is connected with great mathematical difficulties in view of their nonlinearity. Therefore, in boundary layer theory approximate methods of solution of equations are used. The basic group of these approximate methods is connected with utilization of integral relationships of pulses and energy.

Integral relationships, which express the law of momentum and law of conservation of energy, can be obtained in integration with respect to  $y$  equations (14.13) and (14.15) using continuity equation (14.12).

In our case the integral relationships are written in such a form [3], [4]:

$$\begin{aligned} & \tilde{w}_x \frac{d}{dx} (\tilde{q} \tilde{w}_x r \delta^{**}) + \\ & + \frac{\tilde{q} \tilde{w}_x r}{1 - \Lambda^2} [\delta^{**} + \delta^* (1 - \bar{T}_{cr}) \delta_T^{**}] \frac{d\tilde{w}_x}{dx} = r \tau_{cr}; \end{aligned} \quad (14.22)$$

$$\frac{d}{dx} (\tilde{q} \tilde{w}_x r \Delta \bar{T}^* \delta_T^{**}) = r q_w, \quad (14.23)$$

where

$$\begin{aligned} \Lambda^2 &= \frac{\tilde{w}_x^2}{2c_{pm} \tilde{T}^*}; \\ \bar{T}_{cr} &= \frac{T_{cr}}{\tilde{T}^*}; \end{aligned} \quad (14.24)$$

[Translator's Note:  $cr$  = wall.]

$c_{pm}$  - average thermal capacity when  $p = \text{const}$  over temperature range  $T-T^*$ .

Thus, from the system of differential equations in partial derivatives we obtained two usual differential equations (14.22) and (14.23), which contain five unknowns -  $\delta^*$ ,  $\delta^{**}$ ,  $\delta_T^{**}$ ,  $\tau_{CT}$ ,  $q_K$ . Together with additional relationships, assigned on the basis of experimental and theoretical data, equations (14.22) and (14.23) allow determining heat flow and friction stress in the boundary layer.

#### Heat Transfer from Combustion Products to Chamber Walls

In a rocket engine chamber there move combustion products which are at high temperature and are highly dissociated. Heat is transferred from combustion products to chamber walls by means of radiation and direct contact with walls (convective heat emission).

Processes of dissociation and recombination in the boundary layer intensifies heat exchange. In the thermal boundary layer a large temperature drop occurs, the level of which is high. Under these conditions turbulent movement of gas volumes from the high-temperature region to low-temperature region near the walls leads not only to transfer of kinetic energy, but also to transfer of heat, which is liberated during reactions of recombination in the zone of lowered temperature. Composition and properties of the working medium across the boundary layer in this case will be variable.

In the viscous sublayer of the turbulent boundary layer as a result of concentration gradient the molecules, which were dissociated in the high-temperature zone, diffused towards the wall. In the low-temperature region there occurs recombination of these molecules and heat liberation. As a result, heat flows increase.



Thus, in contrast to the case of heat exchange in a medium of constant composition, during calculation of convective heat emission from chemically reacting working medium one should take into account the heat transfer of chemical reactions.

On a considerable part of the engine chamber passage there take place high, including supersonic, velocities of motion of compressible medium. As is known in this instance the liberation of heat as a result of friction of gas against the surface must be considered.

Thus, the overall quantity of energy, transferable through the boundary layer by any volume of gas, is equal to the difference of its stagnation enthalpies at extreme points of the path.

Very high thermal head between combustion products and the wall, high pressure in the engine chamber, the possible presence in working medium of condensed luminous particles, and also substantial instability of flows, caused by small relationships of length to diameter of passage, also contribute to increase in the heat emission from combustion products.

The combustion products of certain rocket propellants can contain components, which are in gas phase in the basic flow and are condensed at reduced temperatures at the wall. With a stationary process this can lead to the appearance of a film of condensate. If the surface temperature is sufficiently low, then the existence of solid oxide, covered on top by a liquid film, is possible. From gas to the surface of film in this instance heat is supplied by three types of heat emission: radiation, convective and heat emission connected with heat liberation during condensation.

Calculation of friction and convective heat exchange in the rocket engine chamber is based on solution of boundary layer equations, or on criterial relationships, obtained by generalization of experimental data.

Besides purely systematical features, connected with use of the theory of turbulent flows, large difficulty is involved in reliable determination of properties of the working medium in the boundary layer. It is caused by nonuniformity of flow parameters, its properties and composition along the cross section of the chamber, possible chemical nonequilibrium in the boundary layer.

#### 14.2. Calculation of Convective Heat Exchange and Friction in the Boundary Layer of Reacting Gas (V. M. Iyevlev Method)

Investigations of heat exchange and friction on the basis of boundary-layer calculation are presented in the works of V. M. Iyevlev, V. S. Avduyevskiy, S. S. Kutateladze, M. F. Shirokov and others. Below are listed basic moments of the solution of V. M. Iyevlev [3], [4], frequently utilized in practical calculations.

##### Laws of Friction and Heat Exchange for Incompressible Liquid

For solution of differential equations (14.22), (14.23) additional regularities of friction and heat emission must be obtained. Their derivation is based on the following considerations.

Let us assume, as is usually done in boundary layer theory, that during flow of liquid along the wall the heat flow and friction at each place depend on local values of physical constants,  $\tilde{w}_x$ ,  $\Delta\tilde{T}_0$ , and also on quantities characterizing the development of thermal and dynamic boundary layer: thickness of loss of energy  $\delta_T^{**}$  and thickness of pulse loss  $\delta^{**}$ . In accordance with equations (14.22), (14.23) it is possible to write:

$$q_x = q_x(\rho, \eta, c_p, \lambda, \Delta\tilde{T}_0, \tilde{w}_x, \delta^*, \delta_T^{**});$$

$$\tau_{cx} = \tau_{cx}(\rho, \eta, \tilde{w}_x, \delta^{**});$$

with use of dimensionless quantities

$$\alpha_k = \alpha_k(Re_i, Re_r, Pr); \quad (14.25)$$

$$\alpha = \alpha(Re_i), \quad (14.26)$$

where  $Re_i = \frac{q \tilde{w}_i}{\eta}$ ,  $Re_r = \frac{q \tilde{w}_r}{\eta}$  - characteristic Reynolds numbers;

$\alpha_k = \frac{q_k}{q \tilde{w}_i \Delta T_0}$  - coefficient of convective heat emission;  $\alpha = \frac{\tau_{cr}}{q \tilde{w}_i^2}$  - friction coefficient.

Instead of characteristic Reynolds numbers let us introduce new arguments:

$$z = \frac{Re_i}{\alpha}; \quad z_r = \frac{Re_r}{\alpha_k}. \quad (14.27)$$

In this case, as investigations show,

$$\frac{z}{z_r} \approx \text{const.} \quad (14.28)$$

Considering equalities (14.27), let us now present relationships (14.25) and (14.26) so:

$$\alpha_k = \alpha_k(z, z_r, Pr); \quad \alpha = \alpha(z). \quad (14.29)$$

Laws of friction and heat emission (14.29) are derived in two ways: by utilization of semi-empirical theory of turbulent boundary layer and by utilization of available experimental data. Comparison of regularities obtained in this way allows establishment of some final form of these laws.

For axisymmetric flow with a smooth wall over the range  $z = 10^5 - 10^9$ ;  $Pr = 0.7 - 2000$ ;  $z/z_T = 0.3 - 3.5$  when  $Pr = 1.0$  and  $z/z_T = 10^{-4} - 10^4$  when  $Pr = 1000$ , V. M. Iyevlev obtained the following relationships:

$$\alpha_x = \frac{1}{\left[ 307.8 + 54.8 \lg^2 \left( \frac{Pr}{19.5} \right) \right] Pr^{0.45} z^{0.08} - 650} \left( \frac{z}{z_T} \right)^{0.089 Pr^{-0.56}}; \quad (14.30)$$

$$\alpha = 0.03327 z^{-0.274} + 3.966 \cdot 10^{-4}. \quad (14.31)$$

With satisfactory accuracy expressions (14.30) and (14.31) approximate known experimental data, and also various empirical formulas, obtained for particular bases (for example,  $z = z_T$ ,  $Pr = 1.0$ ).

#### Scheme of Solution of Boundary Layer Equations

Subsonic and supersonic gas flows possess a whole series of features, distinguishing them from flows of incompressible liquid. However, if we consider only the questions of friction, heat exchange and diffusion in the boundary layer without compression shocks, then between flows of incompressible liquid and gas no qualitative differences are discovered. Basic differences are quantitative: for incompressible liquid properties across the boundary layer are constant, and for gas they depend on temperature and pressure. This is valid even for mixtures of gases, including for those dissociated with effective values of temperature and thermal capacity.

It can be expected that the regularities for heat emission and friction on the wall in case of gas flow will be the same as in the case of flow of incompressible liquid, if as physical constants of gas we use certain mean values of them in boundary layer. It is expedient to assume that as the indicated mean values of constants we can take their values at some determining boundary layer temperatures, computed identically for various cases of gas flow.

Selection of corresponding effective temperature for turbulent flow of reacting gases presents definite difficulties. Although the average temperature is determined formally by relationship (14.8), the composition at this temperature cannot correspond

simultaneously to the value of enthalpy in the equation of energy, gas constant in the equation of state and to other properties depending on the composition. The effect of change of composition can be excluded if for the basis we take the composition of undissociated mixture at the same initial conditional formula of propellant. Inasmuch as the quantity of total enthalpy is approximately proportional to product  $RT$ , then

$$I_{\text{нн}} \sim R_{\text{нн}} T_{\text{нн}}; \quad I_{\text{д}} \sim R_{\text{д}} T_{\text{д}},$$

where index "нн" pertains to undissociated mixture, index "д" - to dissociated.

If the following equality is valid

$$I_{\text{нн}} = I_{\text{д}}, \quad (14.32)$$

then

$$R_{\text{д}} T_{\text{д}} \approx R_{\text{нн}} T_{\text{нн}}. \quad (14.33)$$

Value of specific gas constant  $R_{\text{нн}}$  of undissociated gas for all practical purposes does not depend on temperature and pressure, therefore in many instances it is not necessary to solve equation (14.32) for determination of temperature  $T_{\text{нн}}$  and  $R_{\text{нн}}$ . Having completed thermodynamic calculation at prescribed pressure  $p$  and rather low temperature (for hydrocarbon propellants on the order of  $1300^\circ\text{K}$ ), we take the found value of gas constant as  $R_{\text{нн}}$ . Now from equality (14.33) let us determine the static temperature of undissociated gas:

$$T_{\text{нн}} = \frac{R_{\text{д}} T_{\text{д}}}{R_{\text{нн}}}. \quad (14.34)$$

It is obvious that equation (14.32) is satisfied only approximately as a result of inaccuracy of  $R_{\text{нн}}$ . However, the real value of  $T_{\text{нн}}$ , determined from condition (14.32), and  $T_{\text{нн}}$  from equation (14.34) are usually acceptable close to each other.

Magnitude of temperature  $T_{HD}$  corresponds to the value of static enthalpy  $I$ ; to the value of stagnation enthalpy  $I^*$  will correspond stagnation temperature  $T_0$ , - effective gas temperature.

Inasmuch as stagnation enthalpy is usually equal to enthalpy of working medium in the combustion chamber, for calculation of  $T_0$ , the following formula can be recommended:

$$T_0 = \frac{T'_{0s} + T''_{0s}}{2}, \quad (14.35)$$

where

$$T'_{0s} = \frac{R_k^* T_k^*}{R_{HA}}, \quad (14.36)$$

and  $T''_{0s}$  is determined with the aid of equation (14.32) when  $I_{HD} = I_H^*$ .

Analogous to temperatures  $T_{HD}$  and  $T_0$ , it is possible to introduce into examination the effective thermal capacity of undissociated gas, which, as is simple to note, corresponds to usual frozen thermal capacity. Effective thermal capacity is calculated by the composition of undissociated gas, at temperatures  $T_{HD}$  and  $T_0$ . In calculations there is used certain mean value of thermal capacity  $c_{pm}$  over temperature range  $T_{HD}-T_0$ .

When determining the "average" temperature in the boundary layer - determining temperature, the following positions are used. Mean stagnation temperature and velocity of motion in the boundary layer are respectively equal to

$$T_{0m} = \frac{T_{0s} + T_{0\tau}}{2}; \quad (14.37)$$

$$w_m = \frac{\tilde{w}_x}{2}. \quad (14.38)$$

where  
nozz

Then the determining temperature  $T_m$  is

$$T_m = T_{0m} - \frac{w_m^2}{2c_{pm}} = \frac{T_{0s} + T_{0c}}{2} - \frac{w_s^2}{8c_{pm}} \quad (14.39)$$

or taking into account equation (14.24)

$$T_m = T_{0s} \left( \frac{1 + \bar{T}_{cr}}{2} - \frac{\Delta^2}{4} \right). \quad (14.40)$$

Now we can derive laws of friction and heat emission for the case of turbulent gas flow. An important moment in this case is the selection of characteristic quantities of density  $\rho_m$  and  $\eta_m$ . These quantities are calculated when determining the boundary layer temperature  $T_m$ . In this case it turns out that quantities  $z$  and  $z_T$  for gas can be found through values of these quantities for incompressible liquid, for which  $\rho = \rho_x$  and  $\eta = \eta_x$ . Characteristic values of  $\rho_x$ ,  $\eta_x$  can be selected so that values of  $\eta_m$ , and  $\rho_m$  do not enter expressions (14.30) and (14.31), utilized for gas. After a series of conversions and some assumptions V. M. Iyevlev obtained the following formulas for  $\alpha$  and  $\alpha_H$ , valid for compressible liquid:

$$\alpha_r = \frac{\left[ \frac{1 + \bar{T}_{cr}}{2} - \frac{\Delta^2}{4} \right]_{cp}^{0.11} \left[ 1 - 0.21 \frac{1 - Pr}{Pr^{1.33}} \left( \frac{\Delta^2}{1 - \bar{T}_{cr}} \right) \right]^{0.9225}}{\left[ 307.8 + 54.8 \lg^2 \left( \frac{Pr}{19.5} \right) \right] Pr^{0.45} z^{0.08} - 650} \times \left( \frac{z}{z_r} \right)^{0.089 Pr - 0.56} \quad (14.41)$$

$$\alpha = (0.003327 \cdot z^{-0.224} + 3.966 \cdot 10^{-4}) \left[ \frac{1 + \bar{T}_{cr}}{2} - \frac{\Delta^2}{4} \right]_{cp}^{0.11} \quad (14.42)$$

where index  $cp$  pertains to average quantity with respect to the nozzle.

In this case

$$Q_x = \frac{\tilde{p}}{R_{\text{gas}} T_{0x} \left( \frac{3 + \bar{T}_{\text{cr}}}{4} - \frac{9}{16} \Delta^2 \right)^{0.18} \left( \frac{1 + \bar{T}_{\text{cr}}}{2} - \frac{\Delta^2}{4} \right)^{0.82}}; \quad (14.43)$$

$$\eta_x = f(T_{\text{m cp}}); \quad (14.44)$$

$$T_{\text{m cp}} = T_{0x} \left( \frac{1 + \bar{T}_{\text{cr}}}{2} - \frac{\Delta^2}{4} \right)_{\text{cp}}. \quad (14.45)$$

For the purpose of simplicity of integration of differential equations (14.22), (14.23), expressions (14.41) and (14.42) are approximated by power dependences of form

$$\left. \begin{aligned} q_x &= A z \bar{r}^{-n} \text{Pr}^{-m}, \\ \alpha &= A z^{-n}, \end{aligned} \right\} \quad (14.46)$$

where  $A = \text{const}$ ;  $n \approx 0.15$ ;  $m \approx 0.58$ .

Solution of integral relationships (14.22), (14.23) with allowance for a number of simplifications, reliability of which is checked by calculation, gives:

$$z_T = 1,2 \int_0^{x_1} \left[ \frac{1 - \bar{T}_{\text{cr}}(x_1)}{1 - \bar{T}_{\text{cr}}(x)} \right]^{1,2} \left[ \frac{d(x_1)}{d(x)} \right]^{1,2} \frac{q_x(x_1) \tilde{w}_x(x_1) dx_1}{\eta_x \cos \alpha}, \quad (14.47)$$

where coordinate  $x_1$  is counted along the axis, and  $x$  - along the generatrix of the nozzle.

In formula (14.47) the constant of integration is accepted equal to zero, and integration begins from conditional origin  $x_1 = 0$ , starting with which there exists an already developed turbulent boundary layer.

Let us pause in detail on the formulas necessary for calculation of convective heat exchange.

In the case of a rocket engine chamber the integral in expression (14.47) is usually written in the form of the sum of:



$$z_T = \int_0^{x_k} \Phi dx_1 + \int_{x_k}^{x_c} \Phi dx_1; \quad (14.48)$$

in this case the first component pertains strictly to the combustion chamber, the second - to the nozzle.

In many practically important cases during calculation of the first integral in formula (14.48) it is possible to disregard the change in parameters along the length of the combustion chamber, especially as quantity  $z_T$  enters the expression for  $q_k$  in power 0.15. Then for a cylindrical chamber

$$\int_0^{x_k} \Phi dx \approx \frac{Q_x \bar{w}_{xk}}{\eta_x} x_k, \quad (14.49)$$

where quantity  $x_k$  is taken from some conditional origin:

$$x_k = \epsilon L_k. \quad (14.50)$$

For (WPA) [ZhRD - liquid-propellant rocket engines] quantity  $\epsilon$  characterizes the position of flame front and is usually taken equal to 0.75. Calculations show that when  $\epsilon = 0.3, 0.75, 0.9$  the differences in  $q_k$  for the throat comprise only several percent.

#### Sequence of Determination of Specific Convective Heat Flows and Tangential Friction Stress

Let us pause in particular on the determination of separate quantities and the sequence of calculation of specific convective heat flows.

1. The composition of undissociated mixture is determined by methods cited in Chapter VI. Calculation is performed at assigned  $p_k$  and  $T$ ; in this case the temperature of undissociated working medium is designated equal to 1000-1300°K. Composition (number of moles  $n_{HD}$ ) is necessary for determination of the molecular weight of the mixture, gas constant  $R_{HD}$ , thermal capacity  $c_{pm}$ , and coefficient of dynamic viscosity  $\eta_x$ .

2. Effective temperature  $T_{0e}$  is calculated in accordance with formulas (14.35) and (14.36). Temperature  $T_{0e}$  in this case is determined from equation

$$\sum_i n_{i, \infty} / i(T) = I_{\infty} / M_{\infty} \quad (14.51)$$

As calculations show, when  $T_{0e} = 3000-4000^\circ\text{K}$  the values of  $T_{0e}$  and  $T_{0e}'$  practically coincide.

3. Thermophysical coefficients, entering Pr number, are calculated according to the composition of undissociated mixture at the determining temperature in boundary layer  $T_m$  (14.40). For the sake of simplicity of calculations the Pr number can be taken constant and equal to 0.75.

4. Specific convective heat flow  $q_{\mu}$  and tangential friction stress  $\tau_{CT}$  are determined in the following manner. By formulas (14.47) and (14.28) for given value of  $x_1$  we find quantity  $z_T$  also ratio  $z/z_T$ . In this case the wall temperature  $\bar{T}_{CT}$  is considered assigned, and the value of velocity  $\tilde{w}_x$ , necessary for calculation of quantity  $\Lambda$  by formula (14.24), is determined by gas-dynamic relationships. Then by formulas (14.41) and (14.42) we consider quantities  $\alpha_{\mu}$ ,  $\alpha$  and determine  $q_{\mu} = q_{CT}$  and  $\tau_{CT}$ :

$$q_{\mu} = \alpha_{\mu} \rho_{\infty} \tilde{w}_x \Delta T^{\circ}; \tau_{CT} = \alpha \rho_{\infty} \tilde{w}_x^2 \quad (14.52)$$

where

$$\Delta T^{\circ} = T_{0e}' - T_{CT}$$

In all cases the integral, which entered the formula for  $z_T$ , is determined by numerical integration. It is recommended to take ratio  $z/z_T$  equal to

$$\frac{z}{z_T} = \frac{1.25}{\sqrt{1 - \gamma_{CT}}}$$

Some relationships necessary for calculations (propellant kerosene +  $O_{2H}$ ) are listed on Figs. 14.3-14.6.

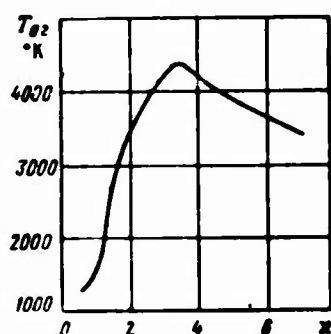


Fig. 14.3. Effective temperature of combustion products of propellant kerosene +  $O_{2H}$ .

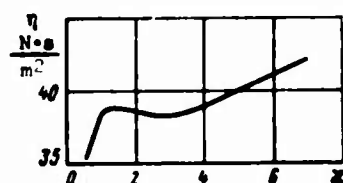


Fig. 14.4. Coefficient of viscosity of combustion products of propellant kerosene +  $O_{2H}$  (multiplied by  $10^6$ ).

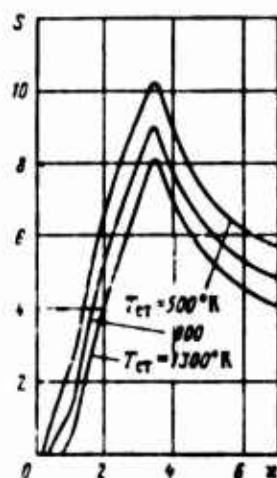


Fig. 14.5. Function  $S$  of combustion products of propellant kerosene +  $O_{2H}$ .

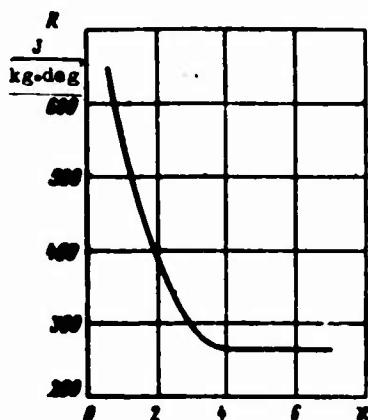


Fig. 14.6. Gas constant of undissociated combustion products of propellant kerosene +  $O_{2H}$ .

#### Conversion of Specific Convective Heat Flows

From analysis of formulas for  $q_k$  it is easy to see the relationship of specific convective heat flow to properties of propellant, pressure in the combustion chamber, wall temperature, and geometry of the chamber. With change of at least one of these factors repetition of laborious calculation of convective heat flows is required. This can be avoided by the following means.

In formula (14.43) for  $\rho_x$  let us disregard quantity  $\Lambda^2$  and let us take the temperatures from under the sign of integral for  $z_T$ , considering them constant. Instead of absolute values of pressure and diameter in the formula for  $z_T$  let us use their relative quantities  $p/p_k$ ,  $d/d_{kp}$ . Let us represent velocity  $\tilde{w}_x$  by approximate formula

$$\tilde{w}_x = \Lambda \sqrt{2c_{pm}T_{0x}} \approx \Lambda \sqrt{\frac{2k}{k-1} R_{0x} T_{0x}}.$$

Then the expression for  $z_T$  takes the form

$$z_T = \frac{1.2 \sqrt{\frac{2k}{k-1}} T_{0x}^{1/2} p_x d_{kp}}{\eta_{0x} R_{0x}^{1/2} \left( \frac{3T_{0x} + T_{cr}}{4} \right)^{0.25} \left( \frac{T_{0x} + T_{cr}}{2} \right)^{0.25}} \int_0^{x_1} \frac{\Lambda}{\cos \alpha} \frac{\tilde{p}}{p_x} \times d\left(\frac{x_1}{d_{kp}}\right). \quad (14.53)$$

In an analogous way by using equation of state and formula (14.46) let us convert the expression for  $q_k$ :

$$q_k = A z_T^{-n} p r^{-m} \frac{p_k \Lambda \sqrt{\frac{2k}{k-1} \frac{\tilde{p}}{p_k} T_{0z}^{1/2} \Delta \tilde{T}^*}}{R_{\mu k}^{1/2} \left( \frac{3T_{0z} + T_{cz}}{4} \right)^{0.18} \left( \frac{T_{0z} + T_{cz}}{2} \right)^{0.82}} \quad (14.54)$$

Let us substitute the value of  $z_T$  from formula (14.53) in expression (14.54) for heat flow  $q_k$  and let us compare the values of  $q_k$  for geometrically similar chambers in sections where  $d/d_{kp} = \text{idem}$ . Inasmuch as in similar sections with identical  $d/d_{kp}$ , the values of  $p/p_k$ ,  $\Lambda$  are also identical, then

$$\left( \frac{q_k}{q_{k0}} \right) = \left( \frac{p_k}{p_{k0}} \right)^{1-n} \left( \frac{d_{kp0}}{d_{kp}} \right)^n \frac{S}{S_0},$$

where

$$S = \frac{\Delta \tilde{T}^* T_{0z}^{0.5(1-n)} \eta_x^n}{R_{\mu k}^{0.5(1-n)} (T_{0z} + T_{cz})^{0.82(1-n)} (3T_{0z} + T_{cz})^{0.18(1-n)}} \cdot \cdot$$

Calculation determination of the viscosity coefficient at high temperatures is an estimate. Therefore, into the formula for  $S$  instead of  $\eta_x$  it is expedient to introduce viscosity coefficient  $\eta_k$  at some normal temperature  $T_k$ , for which experimental data can be known.

Let us use exponential function of form

$$\frac{\eta_x}{\eta_k} \approx \left( \frac{T_{mcp}}{T_k} \right)^{0.7}$$

or taking into account the formula for  $T_{mcp}$  and gas-dynamic relationships

$$\eta_x = \eta_k (T_{0z} : T_{cz})^{0.7} \left\{ \frac{1}{2T_k} \left[ 1 - \frac{k-1}{k+1} - \frac{\Lambda^2}{2(1+\tilde{T}_{cz})} \right] \right\}^{0.7}.$$

During comparison of heat flows for two geometrically similar chambers the expressions in curly brackets will be reduced, inasmuch as they weakly depend on  $\bar{T}_{CT}$  and relationship of thermal capacities  $k$ . With allowance for this and assuming  $n = 0.15$ , we finally obtain the following formula for conversion of convective heat flows:

$$\frac{q_k}{q_{k0}} = \left(\frac{p_k}{p_{k0}}\right)^{0.15} \left(\frac{d_{k0}}{d_k}\right)^{0.15} \frac{S}{S_0}; \quad (14.55)$$

$$S = \frac{\Delta T \cdot T_0^{0.15} \cdot q_{k0}^{0.85}}{R_{k0}^{0.85} (2T_0 + T_{CT})^{0.15} (T_0 + T_{CT})^{0.85}} \quad (15.56)$$

Quantities with index "0" pertain to "standard" chamber, i.e., to a chamber for which calculated or experimental values of specific convective heat flows are known.

Formula (14.55) permits indicating the relationship of  $q_k$  to pressure in the combustion chamber, properties of combustion products and geometry of the passage. The last relationship is weak (power 0.15), therefore with utilization of conversion formula observance of strictly geometrical similarity is optional.

#### 14.3. Utilization of Criterion Relations for Calculation of Convective Heat Exchange

For calculation of convective heat exchange in heat engineering criterion relationships were widely distributed. These relationships, based upon experimental investigation of heat exchange during turbulent flow in long straight pipes, are recommended in a number of works for calculation of heat exchange in a rocket engine chamber.

The value of specific convective heat flow  $q_k$  from gas to the wall in case of high velocities of motion of gas is determined by formula

$$q_k = a_g (T_g - T_{CT}), \quad (14.57)$$

where  $\alpha_c$  - coefficient of convective heat emission from gas to the wall in  $W/m^2 \cdot \text{deg}$ ;  $T_e$  - effective temperature on the outer limit of boundary layer;  $T_{CT,r}$  - temperature of the wall on the part of gas.

The relationship between stagnation temperature in the flow  $T_0$  and  $T_e$  can be established with the aid of temperature recovery factor

$$r = \frac{T_0 - T_i}{T_e - T_i}, \quad (14.58)$$

where  $T_i$  - thermodynamic (static) gas temperature in basic flow.

Value of recovery factor  $r$  is determined experimentally, or by semiempirical formula

$$r = \frac{1}{\sqrt{Pr}}, \quad (14.59)$$

For turbulent boundary layer in a mixture of diatomic and multiatomic gases  $r = 0.89-0.91$ . Magnitude of stagnation temperature in basic flow  $T_0$  and flow velocity are usually known, therefore we have all data available for determination of  $T_e$ .

For calculation of the coefficient of convective heat emission  $\alpha_c$  in case of forced convection we use criterion relationships of type

$$Nu = a Re^m Pr^n,$$

$$\left. \begin{aligned} \text{where } Nu &= \frac{\alpha_c l}{\lambda} - \text{Nusselt number;} \\ Re &= \frac{w_0 l}{\eta} - \text{Reynolds number;} \\ Pr &= \frac{\eta c_p}{\lambda} - \text{Prandtl number;} \end{aligned} \right\} \quad (14.60)$$

$l$  - characteristic length;

$a, m, n$  - constants determined experimentally.

Relationships (14.60) are valid over the range of determining criteria, covered by the experiment. The determining temperature, to which pertained thermophysical parameters of working medium -  $c_p, \eta, \lambda$ , must be specially stipulated. As characteristic length we

usually use equivalent diameter of section  $d_e = \frac{F}{\Pi}$ , where  $F$  - area, and  $\Pi$  - perimeter of section of channel. For round sections quantity  $d_e$  coincides with inside diameter  $d$ .

For conditions similar with conditions in the rocket engine chamber, we recommend assuming  $m = 0.8$ ;  $n = 0.4$  and  $a = 0.025-0.028$ .

Let us take the value of factor  $a$  equal to 0.026, and product  $wp$ , entering the Reynolds number, let us replace by ratio  $G/F$ , equal to it. Then from criterion relationship (14.60) we obtain the calculation formula for  $\alpha$ :

$$\alpha_s = 0.026 c_p \eta^{0.3} \frac{1}{\lambda^{0.3}} Pr^{0.4} \left( \frac{G}{F} \right)^{0.8}. \quad (14.61)$$

Dimension  $\alpha_s$  -  $W/m^2 \cdot \text{deg}$ , if  $c_p$  - in  $J/kg \cdot \text{deg}$ ,  $\eta$  - in  $N \cdot s/m^2$ ,  $d$  - in  $m$ ,  $\lambda$  - in  $W/m \cdot \text{deg}$ ,  $G$  - in  $kg/s$ ,  $F$  - in  $m^2$ .

Thermophysical parameters in equation (14.61) should be determined at mean temperature of boundary layer, equal to

$$\bar{T} = \frac{T_g + T_{cr}}{2}. \quad (14.62)$$

There have been proposed other methods of selection of mean (determining) temperature of boundary layer, aimed at more accurately considering the variability properties of the working medium in boundary layer by empirical means.

For example, Bartz [7] offered relationships, which can be presented in the form

$$q_s = \alpha_s (T_g - T_{cr}); \quad (14.63)$$

$$\alpha_s = 0.026 c_p \eta^{0.3} \frac{1}{\lambda^{0.3}} Pr^{0.4} \left( \frac{G}{F} \right)^{0.8} \left( \frac{d_{sp}}{r} \right)^{0.1}, \quad (14.64)$$

where  $r$  - radius of curvature of wall in the considered section;  $\sigma$  - parameter considering the change of properties of gas across the boundary layer.



It is recommended to calculate quantity  $\sigma$  by formula

$$\sigma = \left( \frac{\rho}{\rho_{T_s}} \right)^{0.8} \left( \frac{\eta}{\eta_{T_s}} \right)^{0.2}, \quad (14.65)$$

where quantities  $\rho$ ,  $\eta$  are calculated at determining temperature

$$\bar{T} = \frac{1}{2} (T_s + T_{cr,r}) + 0.22 Pr^{1/3} (T_s - T_{cr,r}), \quad (14.66)$$

Friction stress on the wall can be found on the basis of hydrodynamic theory of heat exchange, establishing the generality of transfer processes with friction and convective heat transfer. With number  $Pr \sim 0.7$  the calculated expression has the form

$$\tau_{cr} \approx 0.8 \frac{a_{\lambda}}{c_p} a_{kp}, \quad (14.67)$$

where  $a_{kp}$  — critical flow velocity.

All the given formulas far from reflect the specific conditions of heat and mass exchange between gas flow and the rocket engine chamber wall. Therefore, their application for calculation of heat exchange and friction in rocket chambers can give only roughly approximate results.

#### 14.4. Calculation of Radiative Heat Exchange

According to Stefan-Boltzmann law specific radiative heat flow is considered by formula

$$q_r = 5.764 \epsilon_{cr} \left[ \epsilon_g \left( \frac{T_s}{100} \right)^4 - A_g \left( \frac{T_{cr,r}}{100} \right)^4 \right] \frac{W}{m^2}, \quad (14.68)$$

where 5.764 — radiation factor of absolute blackbody;  $\epsilon_{cr}$  — effective emissivity factor of the wall;  $\epsilon_g$  — emissivity of gas at  $T_s$ , °K;  $A_g$  — absorbing power of gas at  $T_{cr,r}$ , °K.

Attention should be drawn to the fact that quantity  $T_s$  is not stagnation, but the thermodynamic temperature of gas.

Inasmuch as the wall temperature in a rocket engine chamber is usually much lower than  $T_1$ , radiation of walls plays a small role. Therefore, by disregarding the second term in formula (14.68), we obtain

$$q_A = 5,764 \epsilon_{cr}' \epsilon_z \left( \frac{T_z}{100} \right)^4. \quad (14.69)$$

The effective emissivity factor of gases is determined by the method discussed in Chapter VII.

In view of the indeterminacy of the state of wall surface its effective emissivity factor  $\epsilon_{cr}'$  is determined as arithmetic mean of the emissivity factor of wall surface  $\epsilon_{cr}$  (absorption of heat with single incidence of beam) and one, corresponding to total absorption of heat with repeated reflections from the inside surface of the chamber:

$$\epsilon_{cr}' \approx 0,5(\epsilon_{cr} + 1). \quad (14.70)$$

Values of emissivity factor  $\epsilon_{cr}$  depend on material and the states of its surface (presence of oxide film, contamination, etc.) and are listed in reference books. The presence of soot on walls sharply increases  $\epsilon_{cr}$ .

One should note that utilization of the discussed methods of calculation of radiative heat exchange is quite justified only when combustion products are uniform along the cross section of the chamber. With the presence, for example, of boundary layer, the composition of which substantially differs from the composition in the nucleus of flow, the picture of phenomena is complicated due to mutual radiative heat exchange between layers.

Calculation of  $q_n$  in such cases must be modified.

#### 14.5. Distribution of Specific Heat Flows Along the Chamber Passage

Total specific heat flow to the chamber walls is made up of convective and radiative heat flows:

$$q = q_k + q_n. \quad (14.71)$$

[Translators note:  $k$  = convective;  $n$  = radiative.]

Let us examine the change of components of heat flow  $q_k$  and  $q_n$  along the chamber passage. Distribution of  $q_k$  can be perceived from analysis of change of quantities, which determine quantity  $q_k$  according to formulas (14.52) and (14.57).

It is simpler to analyze formula (14.57). Change of effective temperature on the external border of boundary layer  $T_e$  scarcely differs from change of  $T'_e$ . These changes are relatively small and for qualitative analysis it is possible to take temperature  $T_e$  constant.

Distribution of wall temperature on the part of gas  $T_{ct,r}$  can be various. With usual relationships between  $T_e$  and  $T_{ct,r}$  the change of  $T_{ct,r}$  by 100-200° leads to change of difference  $(T_e - T_{ct,r})$  by 5-10% in all. Therefore, for qualitative analysis of the distribution of heat flows we will consider difference  $(T_e - T_{ct,r})$  constant.

Thus, change of  $q$  is determined by change in the coefficient of heat emission  $\alpha$ . As follows from formula (14.61), maximum of  $\alpha$ , coincides with maximum of quantity

$$\frac{1}{d^{0.2}} \left( \frac{G}{F} \right)^{0.8} = \frac{(q\alpha)^{0.8}}{d^{0.2}}, \quad (14.72)$$

since quantities  $Pr$ ,  $c_p$ , and  $\eta$ , determined at mean temperature, are close to constant. Complex of quantities (14.72) has maximum in the section with the least area, i.e., in the throat. Specific convective heat flow has analogous character of change, shown in Fig. 14.7.

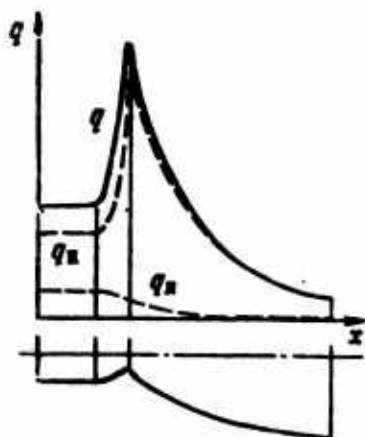


Fig. 14.7. Distribution of specific heat flows along the chamber passage.

Distribution of specific radiative heat flow depends mainly on the change of thermodynamic temperature  $T$ . In connection with this, one should expect an intense drop of  $q_n$  in the nozzle. However, on the section before the nozzle throat the chamber walls quite substantially absorb radiative heat flow from combustion products, which are located in the combustion chamber and have high temperature. Therefore, drop of  $q_n$  on the nozzle section does not begin at once; this drop is very intense in the supercritical part of the nozzle, where beams from the combustion chamber do not fall for all practical purposes.

Considering the degree of approximation of calculation of radiation, it is expedient to compute  $q_n$  only for the combustion chamber. Quantity  $q_n$  in other sections of the chamber can be determined empirically.

1. Starting from the nozzle inlet to a section in the subcritical part of the nozzle with diameter  $d = 1.2 d_{kp}$  radiative heat flow is considered constant and equal to  $q_{n,k}$ , calculated by average gas parameters in the end of the combustion chamber.

2. In the nozzle throat radiative flow is assumed equal to  $0.5 q_{n,k}$ .

3. In the supercritical part of the nozzle there is assumed:

a) in the section with diameter  $d=1,5d_{кр}$ ;  $q_n=0,15q_{н.к}$ ;

b) in the section with diameter  $d=2,5d_{кр}$ ;  $q_n=0,04q_{н.к}$ .

On the section of the combustion chamber of a liquid-propellant rocket engine, beginning from a distance of 50-100 mm from the head, radiative heat flow is constant and equal to  $q_{н.к}$ ; directly near the head -  $0.25 q_{н.к}$ .

Radiative heat flow to the wall of the combustion chamber of RDTT additionally depends on the arrangement of charge in the engine. Typical distribution of  $q_n$  is shown in Fig. 14.7.

Change of total specific heat flow is determined by change of  $q_k$  and  $q_n$ . Small displacement of maximum from the critical section to the subcritical part of the nozzle is characteristic for it.

Thus, in any event the most thermally stressed zone is the critical section of the nozzle, which requires effective protection.

Absolute value of  $q$  depends primarily on the type of propellant being applied and the temperature of its combustion products. For each propellant maximum of  $q$  is obtained with component ratios of propellant corresponding to maximum temperature of combustion products.

The pressure substantially affects the magnitude of specific heat flows. With increase of pressure the density of working medium  $\rho$  and quantity  $\rho w$  increases, on which the specific convective heat flow basically depends. Since quantity  $q_k$  proportional to  $(\rho w)^{0.8}$ , consequently,  $q_k \sim \rho^{0.8}$ . This is evident from stricter formula (14.55). The effect of pressure on specific radiative heat flow is determined mainly by the relationship of emissivity factor of gas to pressure. The effect of pressure on the gas temperature is considerably weaker.

As can be seen from Fig. 14.7, the relationship between convective and radiative heat flows is changed along the length of the chamber. The greatest portion of radiative heat flow will come to the combustion chamber. It increases for combustion products of high-energy propellants, propellants with large content of condensate and for large sized chambers.

Some tentative values of specific heat flows along the length of the nozzle are the following:

$$\text{entrance } q = (1-5) \cdot 10^6 \text{ W/m}^2; q_{\kappa} = (0.7-0.9)q;$$

$$\text{throat } q = (20-80) \cdot 10^6 \text{ W/m}^2, q_{\kappa} = (0.85-0.95)q;$$

$$\text{exit section } q = (0.5-3) \cdot 10^6 \text{ W/m}^2, q_{\kappa} = (0.97-0.99)q.$$

#### Bibliography

1. Avduyevskiy V. S. and others, Osnovy teploperedachi v aviatsionnoy i raketnoy tekhnike (Fundamentals of heat transfer in aviation and rocket technology), Oborongiz, 1960.
2. Vinogradov V. S. Prikladnaya gazovaya dinamika (Applied gas dynamics), Izd-vo Un-ta Druzhby Nar., 1965.
3. Iyevlev V. M., Doklady AN SSSR, 1952, No. 6.
4. Iyevlev V. M., Doklady AN SSSR, 1953, No. 1.
5. Kutateladze S. S., Leont'yev A. I., Turbulentnyy pogranichnyy sloy szhimayemogo gaza (Turbulent boundary layer of compressible gas), Sib. otd. AN SSSR, 1962.
6. Landay L. D., Livshits Ye. M., Mekhanika sploshnykh sred (Mechanics of continuous media), Gostekhizdat, 1953.
7. Bartz D. R., Jet Propulsion, 1957, No. 1.

## CHAPTER XV

### LIQUID ROCKET FUELS

In this chapter the features of liquid substances and their characteristics as components of rocket fuels are examined. The characteristics of a number of typical fuels and oxidizers, and likewise, the basic data on certain used and promising bipropellants (ЖРД) [ZhRD = liquid-propellant rocket engines] are presented.<sup>1</sup>

Liquid unitary fuels, which have low energy characteristics, are used in gas generators and auxiliary engine devices. The specific character in the utilization of these fuels has been briefly examined in Chapter XVII.

#### 15.1. Requirements for Fuels

The requirements for liquid rocket fuels is based on the more general requirement of creating a rocket complex with a minimum of investment over specified and usually short periods.

---

<sup>1</sup>Information on fuels have been borrowed basically, from foreign sources.

Depending on the designed purpose of the rocket complex the requirements for physical, operational, and economic indexes of the fuel will vary. Thus, in a case, where the fuel is selected for an engine of a military rocket, the requirement of high combat readiness permits the use of only those fuels, which allow for fueled-up storage in launching the rocket. The rockets are carriers, designed to insert an artificial earth satellite into orbit; as a rule, they are launched at a prescribed time and their prelaunch preparation must be planned since this requires, specifically, fueling. In this instance there are no obstacles in utilizing cryogenic fuels, i.e., since one or both components are liquified gases.

The great thrust of the engines of heavy rocket-carriers determines the consumption of large quantities of fuel, specifically, with respect to engines during launching pad burn off. Therefore, for example, for the lower stages of rocket-carriers cheap fuels, producible in large quantities, must be used.

The requirement imposed on the fuel components of ZhRD of antiaircraft rockets, which are stored in a fueled-up ready condition out of doors, is that the fuel should be maintained in the liquid state over the range of  $\pm 50^{\circ}\text{C}$ .

From the given examples it is evident that rather varied requirements are imposed on a fuel depending upon the intended purpose of the engine. Among all the fuels it is expedient to separate out the group of so-called long-storage fuels, the components of which consist of high-boiling substances, which can be put in storage in the tanks of rocket or other containers at ordinary temperatures and pressures without substantial losses. This group can be divided into specific subgroups such as fuels whose components have the most desirable physicochemical features and can undergo storage for many years in hermetically sealed containers.



The range of temperatures and pressures, at which the components must be kept stable is, to a certain degree, arbitrary. It proposes, for example, in relation to easily stored fuels that those components whose critical temperatures are higher than  $\sim 70^{\circ}\text{C}$  (they can exist in the liquid state at the maximum ambient temperature), the vapor pressure at  $70^{\circ}\text{C}$  should not exceed 35 bars, and during storage the rate of decomposition should not exceed 1% per annum at a constant temperature of  $50^{\circ}\text{C}$  [10].

The components of fuels for rockets whose tanks are also fueled up and hermetically sealed at the plant, generally should not decompose in storage.

The scope of application of stable fuels is not limited to military rockets. In certain cases engine devices of space equipment will be exposed for a long time under space conditions or on the surface of planets. The utilization of stable fuels in such cases must simply provide for the avoidance of considerable losses during storage.

Thus, based on conditions imposed on the operational characteristics of a rocket complex, all fuels can be divided into two major groups. One group includes the stable fuels, suitable to long storage, the other - everything remaining that does not meet this requirement, specifically, the cryogenic group.

If any group of fuels based on physicochemical features meets the requirements for the operational characteristics of an engine device, further selection can be based on the next most serious requirement for fuels.

1. High energy characteristics, i.e., high values of specific thrust and density of fuels. The sum total of these two parameters must provide for the creation of a rocket of minimum over-all sizes and weight.

2. The possibility of creating an effective and reliable engine device. The fuel used makes it possible to obtain the practical energy characteristics of the engine, close to theoretical, as determined by thermodynamic calculation. This implies, for example, that the process of combustion must be rather complete, must not appear of large losses.

The utilization of self-igniting fuels, i.e., fuels, in which the combustible component and the oxidizer combust upon contact with each other without a supply of energy from the outside, also simplifies the design, and consequently, increases the reliability of the engine. Adequate cooling features, lack of danger of decomposition and of the explosion of components, non-corrosiveness to the structural material all provide for a high degree reliability of the engine with low costs.

Some of the noted features can be improved or have been accomplished as a result of conducting special research. Such research should include the realization of self-ignition by using a special additive with the combustible component or oxidizer, by lowering the corrosiveness, by reducing the tendency toward decomposition, and others.

3. The possibility of safer operational characteristics. It is advisable that the combustible component be less inflammable in order that it will not self-ignite in air. The components of the fuel should have less tendency toward ignition, decomposition and explosion during handling even when in accidental contact with various substances. The utilization of components having low toxicity facilitates handling them safely during the production process, in powering up the engines and in using rocket components with low consumption.

4. Good economic indexes. Fuels, designed for extensive utilization, should take into account their production in a quantity, which meets all the demands of rocket technology. It is advisable, that the components find application in branches of the national

economy, not related to rocket technology. The latter can provide for a substantial expansion of production scales of components and a reduction in their cost. The low cost of 1 kg of fuel is desirable, but first of all analysis of the effect of fuels to the cost of achieving the goal set for the developed rocket complex, is required. In this case without exceptions, the variant with a more expensive fuel will be cheaper.

Such are the basic requirements of liquid rocket fuels. Naturally, there is no fuel, which completely meets all the above examined requirements. In each concrete case there is some characteristic that determines the selection of the combustible component and the oxidizer.

#### 15.2. Physicochemical Features of Components

The melting point, dependence of saturation pressure on temperature and the rate of spontaneous decomposition of the component comprise those physicochemical features, which determine the long storage life or utilization of the component in rockets with plant servicing.

Tables 15.1 and 15.2 and Figs. 15.1-15.3 present the above indicated features of certain fuels and oxidizers together with such characteristics, as density, heat of evaporation and boiling point.

From the presented data it is evident that such fuels, as for example, hydrazine, asymmetrical dimethylhydrazine, monomethylhydrazine, kerosene and pentaborane are stable, and they possess good physical features suitable for long storage. Those possessing properties of oxidizers, are for example, nitric acid, nitrogen tetroxide, chlorine trifluoride and, to a lesser extent, due to chemical instability, hydrogen peroxide and others.

Table 15.1. Certain properties of fuels and oxidizers.

Component	Formula	Melting point, °K	Boiling point, °K	Heat of evaporation, kJ/kg	Density, kg/m <sup>3</sup>	Chemical stability
<b>Fuels</b>						
Hydrogen	H <sub>2</sub>	13.9	20.4	452	0.071	Stable
Ammonia	NH <sub>3</sub>	195.4	239.8	1370	0.68	"
Triethylamine	(C <sub>2</sub> H <sub>5</sub> ) <sub>3</sub> N	158.2	362.5	311	0.728	"
Hydrazine	N <sub>2</sub> H <sub>4</sub>	274.7	386.7	1335	1.01	"
Monomethylhydrazine	H <sub>2</sub> N-NH(CH <sub>3</sub> )	220.8	360.7	877	0.875	"
Asymmetrical dimethylhydrazine	H <sub>2</sub> N-N(CH <sub>3</sub> ) <sub>2</sub>	215.9	336.1	583	0.790	"
Ethylidene	C <sub>6</sub> H <sub>5</sub> (CH <sub>3</sub> ) <sub>2</sub> NH <sub>2</sub>	288.7	490.2	379	0.977	"
Ethyl alcohol	C <sub>2</sub> H <sub>5</sub> OH	158.6	351.7	837	0.789	"
Methane	CH <sub>4</sub>	90.7	111.6	—	0.416	"
Kerosene	C <sub>7.21</sub> H <sub>12.28</sub>	200—220	450	—	0.82—0.85	"
Pentaborane	B <sub>5</sub> H <sub>9</sub>	226.3	331.2	481	0.633	Stable in a hermetically sealed container
Diborane	B <sub>2</sub> H <sub>6</sub>	108.2	181.2	—	0.45	The same
<b>Oxidizers</b>						
Oxygen	O <sub>2</sub>	54.4	90.1	213.5	1.144	Stable
Ozone	O <sub>3</sub>	80.7	161.3	306	1.35	Unstable
Fluorine	F <sub>2</sub>	55.2	85.2	172.5	1.51	Stable
Chlorine trifluoride	CF <sub>3</sub> Cl	190.8	284.9	298.5	1.825	"
Nitrogen trifluoride	NF <sub>3</sub>	56.6	153.2	164	1.55	"
Fluorine perchloride	FCIO <sub>3</sub>	127.0	226.2	188.2	1.7	"
Nitric acid	HNO <sub>3</sub>	231.5	359.0	625	1.52	Unstable
Hydrogen peroxide	H <sub>2</sub> O <sub>2</sub>	273.5	423.7	1520	1.46	"
Nitrogen tetroxide	N <sub>2</sub> O <sub>4</sub>	261.9	294.3	415	1.451	Stable
Bromine pentafluoride	BrF <sub>5</sub>	210.7	313.5	—	2.47	Stable
Perchloric acid	HClO <sub>4</sub>	161.2	383.2	—	1.77	Stable
Oxyfluoride	OF <sub>2</sub>	49.3	128.3	205.5	1.52	Stable

Table 15.2. Physical properties of fuels and oxidizers.

Component	Formula	Viscosity, N/s·m <sup>2</sup>	Thermal conductivity, W/m·degree	Heat capacity J/kg·degree	Surface tension, N/m	Vapor pressure mm Hg	Toxic (maximum permissible concentration in mg/L)
Fuels							
Hydrogen	H <sub>2</sub>	0.13·10 <sup>-4</sup>	—	9420	0.23·10 <sup>-2</sup>	—	Not toxic
Ammonia	NH <sub>3</sub>	0.26·10 <sup>-3</sup>	0.5	4770	0.22·10 <sup>-1</sup>	—	0.02
Triethylamine	(C <sub>2</sub> H <sub>5</sub> ) <sub>3</sub> N	0.35·10 <sup>-3</sup>	0.12	—	0.21·10 <sup>-1</sup>	53	Toxic
Hydrazine	N <sub>2</sub> H <sub>4</sub>	0.97·10 <sup>-3</sup>	—	3070	0.67·10 <sup>-1</sup>	10.6	—
Monomethylhydrazine	H <sub>2</sub> N—NH(CH <sub>3</sub> )	0.78·10 <sup>-3</sup>	—	2940	—	51	—
Symmetric dimethylhydrazine	H <sub>2</sub> N—N(CH <sub>3</sub> ) <sub>2</sub>	0.59·10 <sup>-3</sup>	0.209	2720	0.24·10 <sup>-1</sup>	—	—
Xylidine	C <sub>6</sub> H <sub>4</sub> (CH <sub>3</sub> ) <sub>2</sub> NH <sub>2</sub>	0.49·10 <sup>-2</sup>	—	—	—	—	0.005
Ethyl alcohol	C <sub>2</sub> H <sub>5</sub> OH	0.12·10 <sup>-2</sup>	0.17	2430	0.23·10 <sup>-1</sup>	44	1.0
Methane	CH <sub>4</sub>	0.58·10 <sup>-4</sup>	—	—	—	—	Slightly toxic
Kerosene	C <sub>22</sub> H <sub>44</sub>	0.15·10 <sup>-2</sup>	0.16	—	—	—	0.3
Pentaborane	B <sub>5</sub> H <sub>9</sub>	0.3·10 <sup>-3</sup>	—	2400	—	279	0.00001
Diborane	B <sub>2</sub> H <sub>6</sub>	0.24·10 <sup>-3</sup>	—	—	0.15·10 <sup>-1</sup>	—	Highly toxic

Table 15.2. (Cont'd).

Component	Formula	Viscosity, N/s·m <sup>2</sup>	Thermal conducti- vity, W/m·deg	Heat capacity J/kg·deg	Surface tension, N/m	Vapor pressure mm Hg cm	Toxic (maximum permissible concentration in mg/l)
Oxidizers							
Oxygen	O <sub>2</sub>	0.2·10 <sup>-3</sup>	0.21	1700	0.13·10 <sup>-1</sup>	—	Not toxic
Ozone	O <sub>3</sub>	0.16·10 <sup>-2</sup>	—	795	—	—	0.00003
Fluorine	F <sub>2</sub>	0.26·10 <sup>-3</sup>	—	1505	0.15·10 <sup>-1</sup>	—	0.00003
Chlorine trifluoride	CF <sub>3</sub> Cl	0.48·10 <sup>-3</sup> (285)	—	1270 (278)	0.24·10 <sup>-1</sup>	—	0.00001
Nitrogen trifluoride	NF <sub>3</sub>	—	—	—	—	—	Toxic
Fluorine perchloride	FCIO <sub>3</sub>	0.88·10 <sup>-3</sup>	—	930	0.2·10 <sup>-1</sup>	—	—
Nitric acid	HNO <sub>3</sub>	0.82·10 <sup>-3</sup>	—	1765	0.43·10 <sup>-1</sup> (285)	65	0.005
Hydrogen peroxide	H <sub>2</sub> O <sub>2</sub>	0.13·10 <sup>-3</sup>	—	2430 (273—300)	—	2	0.201
Nitrogen tetroxide	N <sub>2</sub> O <sub>4</sub>	0.44·10 <sup>-3</sup> (288)	0.13	1530	0.3·10 <sup>-1</sup> (275)	—	0.005
Bromine pentafluoride	BrF <sub>5</sub>	—	—	—	—	450	Highly toxic
Perchloric acid	HClO <sub>4</sub>	—	—	—	—	—	Toxic
Oxyfluoride	OF <sub>2</sub>	0.28·10 <sup>-3</sup>	—	—	—	—	0.00001

Notes: 1. Data are expressed for substances at 100% concentration.

2. All values for high-boiling substances are expressed at 293-298°K, for the cryogenic ones - at  $t_{\text{sat}}$  at atmospheric pressure. In certain cases the value of the temperature is expressed in

OK in parentheses.

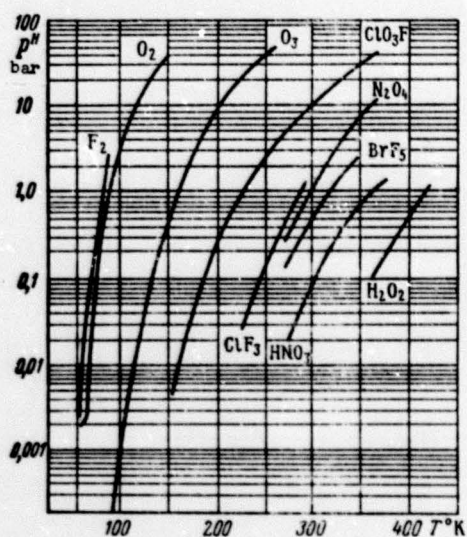


Fig. 15.1. The dependence of saturation pressure on temperature for certain oxidizers.

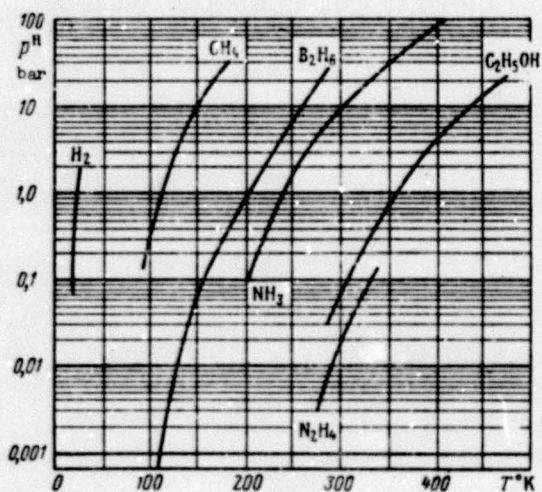


Fig. 15.2. Dependence of saturation pressure on temperature for certain fuels.



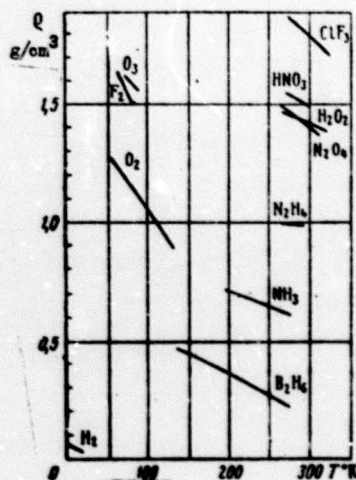


Fig. 15.3. Dependence of density of certain components on temperature.

The density values of the components, given in the table and in Fig. 15.3, show that the high-boiling oxidizers, such as nitrogen tetroxide, hydrogen peroxide, and nitric acid, considerably surpass the widely used cryogenic oxidizer - liquid oxygen according to this index; thus, the weight characteristics of engine devices of rockets using these acidifiers is vastly improved.

Among the fuels - hydrazine for example, has a high density and liquid hydrogen - very low density. It should be noted that the density of one component is not the determining factor. Thus, hydrazine based on density is substantially better than dimethylhydrazine, but when paired with nitrogen tetroxide as a result of larger quantity of oxidizer necessary for the oxidation of the secondary fuel, the density of the fuels seems almost identical in both cases.

For the feasibility of coming up with a reliable engine, the components of the fuel must be effective coolants. This means that their viscosity must be low, in order to provide a high flow rate with low hydraulic losses, and thermal conductivity and heat capacity - with high losses. Such a combination of properties provides good conditions for the transmission of heat from the wall to the coolant.



The viscosity of components should be capable of making a small change with temperature, so that there is no change in conditions of injection and atomization. The dependence of thermophysical coefficients on temperature for a number of the most interesting components of rocket fuels are presented in Figs. 15.4-15.6.

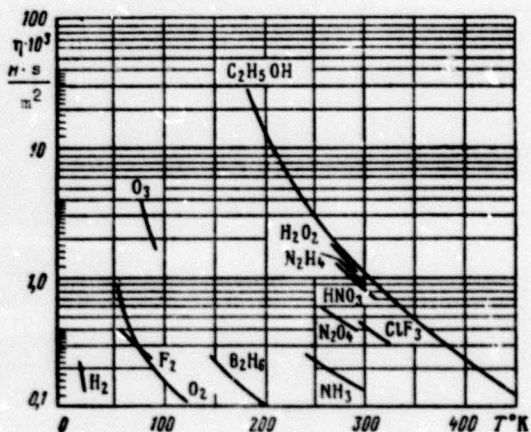


Fig. 15.4. Dependence of the viscosity factor of certain components on temperature.

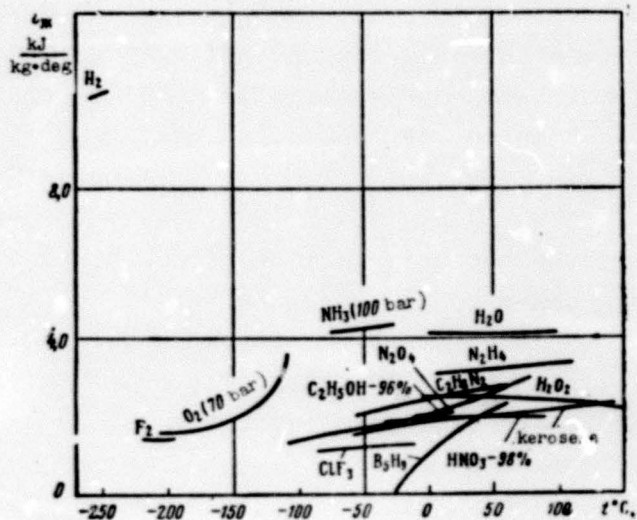


Fig. 15.5. Dependence of heat capacity of certain components on temperature.

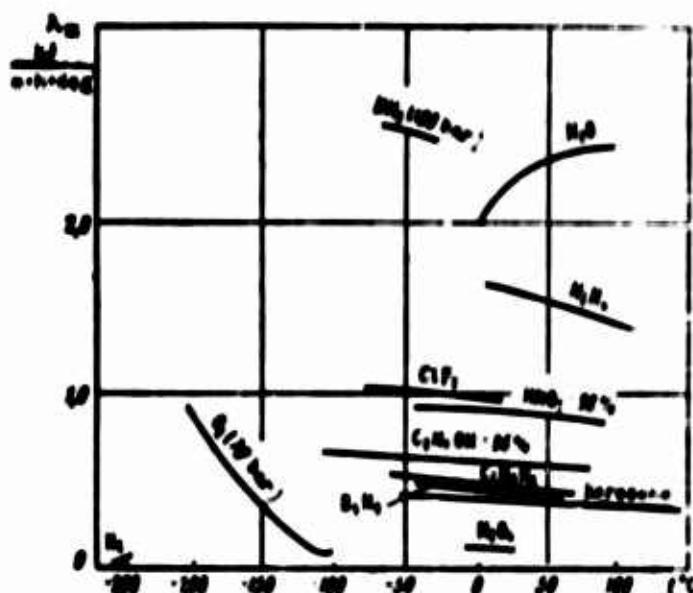


Fig. 15.6. Dependence of thermal conductivity of certain components on temperature.

Cooling components should not decompose and also should not leave deposits on the wall, because this can result in scorching. In order to increase the quantity of heat, which the component can absorb, it is desirable that the component possess a high heat capacity and a low saturation pressure. The latter takes into account the increase in temperature, to which the component in the jacket of the engine can be heated at a prescribed pressure.

A low value of surface tension and a low heat of evaporation are the favorable features, which improve atomization and evaporation of the components during injection in the combustion chamber of the engine or gas generator.

The important feature is the corrosive action of the components. Having high corrosiveness, in order to achieve long periods of storage of the component without the formation of compounds from material of the tank or pipelines the utilization of a select group of resistant, possibly critical and expensive materials may be required. At the same time there are methods of reducing the corrosiveness by means of utilizing a small quantity of an additive, which hardly affects the energy characteristics of the fuel. The

last method requires considerable expense of means and time in the selection of additives and in checking their effectiveness.

The data on substances, which can be used with various components of fuels, are presented in Table 15.3.

Table 15.3. Certain material used in components of rocket fuels.

Component	Structural	Nonmetallic
Oxygen	Copper, aluminum and their alloys; chrome and chrome-nickel steels; alloys of magnesium and titanium.	Teflons, blue asbestoses, paronit, leather
Fluorine Chlorine trifluoride	Alloys of nickel, copper, aluminum and magnesium; stainless steel	Teflons
Nitric acid	Aluminum and its alloy; chrome and chrome-nickel stainless steels; titanium and its alloys	Asbestos, teflons
Hydrogen peroxide	Aluminum and its alloy with a small content of copper; stainless steels	Polyvinyl chloride, teflons
Nitrogen tetroxide	Alloys of aluminum, and of nickel; chrome and chrome-nickel stainless steel; alloys of titanium	Teflons, trifluorochloroethylene polymeric film
Ammonia	Steel, alloys of nickel monel-metal	Teflons, glasses, rubber
kerosene Ethyl alcohol Triethylamine Xylidine Hydrazine	Majority of structural materials	Oil-gasoline resistant grades of rubber
	Aluminum and its alloys; stainless steel	Polyethylene
NIMG*	Alloys with iron and aluminum bases	
Pentaborane	Aluminum, copper and their alloys; lead, soft steel, stainless steel	Asbestos, rubber, polyethylene, teflons
Hydrogen	Aluminum and its alloys; alloys of titanium	

\*NIMG [Translator's note: defined as a asymmetrical dimethylhydrazine].

Table 15.2 presents some of the mentioned properties of a number of components of rocket fuels. Information on toxicity is also presented there.

Prolonged exposure of man in an atmosphere containing the vapor component serves as the characteristic toxicity at maximum permissible concentration. It should be noted that any hazard during the operation of rockets involving toxic components, is substantially diminished where there is plant servicing and hermetic sealing of tanks.

### 15.3. Kinetic Properties of Fuels

The kinetic properties of a fuel are defined by the process of combustion and the process of stationary burning of the fuel.

#### Properties of a Fuel During Ignition

The ignition temperature of the vapors of liquid components is usually not less than 300-500°C. Such a temperature can be attained in various ways.

When using nonsself-ignition components of a fuel, the heat necessary for the vaporization of the mixture and for the development of exothermal preflame reactions in it, are generated from an external source. The self-ignition of the fuel vapors in this instance can be called thermal. Thermal self-ignition is defined as the minimum temperature, at which process of self-ignition is developed, and by the delay period of this process. The latter is defined as the period of time from the moment the flames appear.

The temperature and delay period of thermal self-ignition exist not only for a listed fuel by physical constants inasmuch as these properties on experimental conditions; however, when determined under standard conditions, they are defined as the comparative activity of fuels of ZhRD [4].

Conditions necessary for thermal self-ignition which are variable, are taken into account when the engine is as well as during the steady operation.

Initial ignition includes the creation of a local limited zone of hot gas whose temperature exceeds the temperature of self-ignition of the fuel vapors. This can be facilitated, for example, by a special igniting torch, for which a self-igniting fuel or powder, electrical spark and so forth, are used. Because the heterogeneous and homogeneous mixture is chemically unequal with respect to priming for combustion, initial combustion takes place proceeds in the form of a source whereby the local mixture ratio is close to stoichiometric. The occurrence of even a local area of combustion accelerates processes of fuel preparation for the exothermic reaction and facilitates the ignition of the entire homogeneous mixture.

During the steady operation of the engine, the temperature level of the process in the combustion zone is higher than the temperature of self-ignition of the fuel. In connection with this, the need for special ignition diminishes. However, there is a need for a reliable mechanism for the transfer of heat from the zone of developed combustion to the fresh mixture.

The self-igniting components of the fuel already under ordinary temperature conditions react upon contact in the liquid phase with the release of heat. As a result of the initial energetic warm-up, the fuel mixtures initiate the preflame exothermal reactions, which facilitate the warm-up to the boiling point and higher, leading to the self-ignition of the vapors. This form of self-ignition, which begins in liquid phase and terminates in the gas phase, can be called chemical self-ignition or simply, self-ignition.

The feasibility of self-ignition depends on the chemical affinity of the fuel components. One combustible component with various oxidizers or, conversely, one oxidizer with various fuels



will form various fuel vapors based on activity. Table 15.4 shows the degree of this activity for various fuel compositions.

Table 15.4. Characteristics of combustion of certain fuel compositions.

Oxidizer Fuels							Products of decomposition H <sub>2</sub> O <sub>2</sub>
	ClF <sub>3</sub>	F <sub>2</sub>	O <sub>2</sub>	I <sub>2</sub> NO <sub>2</sub>	H <sub>2</sub> O <sub>2</sub>	H <sub>2</sub> O <sub>2</sub>	
NH <sub>3</sub>	C	C	H	K	K	H	C
C <sub>2</sub> H <sub>5</sub> OH	C	C	H	H	H	K	C
N <sub>2</sub> H <sub>4</sub>	C	C	H	C	C	K	C
Kerosene	C	C	H	H	H	H	C
H <sub>2</sub> A	C	C	H	C	C	H	C
CH <sub>3</sub> N <sub>2</sub> H <sub>2</sub>	C	C	H	C	C	H	C
(CH <sub>3</sub> ) <sub>2</sub> N <sub>2</sub> H <sub>2</sub>	C	C	H	C	C	H	C

Designations: C - self-igniting, N - nonself-igniting, P - in the presence of a catalyst.  
[Translator's notes: subscripts for "liquid" abbreviated to replace W].

Self-ignition of nonself-igniting fuels under ordinary conditions of fuel vapors can be facilitated by a catalytic effect or by introducing an activating additive into one of the components. Thus, for instance, fuel kerosene with nitric acid can be made self-igniting, lead in kerosene by introducing considerable (up to 40%) quantities of asymmetrical dimethylhydrazine or small additions of solid active substances. A suspension of potassium and of lithium or lithium hydride in kerosene provide facilitates self-ignition with a small (up to 2%) content of the active substances. Fuel kerosene with liquid oxygen becomes self-igniting with an addition of small quantities (on the order of hundredths of a percent) of fluoric ozone F<sub>2</sub>O<sub>3</sub> to the oxidizer.

The most important quantitative characteristic of self-ignition is the delay of self-ignition - the time from the moment of contact of the liquid self-igniting components up to the moment of the appearance of flames ( $\tau_3$ ). Naturally, the delay value of self-ignition depends, first of all, on the nature of the fuel. For one

and the same self-igniting vapor (combustible component + oxidizer) the quantity of  $\tau_3$  changes depending on the excess oxidizer ratio,  $\alpha$ , the pressures of medium, and the initial temperature of the components. The effect of the unevenness of injection of the components is demonstrated here. The value  $\tau_3$  can also change with the introduction of an activating or a ballasting additive to the components.

The dependence of the delay of self-ignition of liquid rocket fuels on the various factors and methods of determining this value are examined in special literature [2], [4].

The reliability of starting the engine substantially depends on the value of  $\tau_3$ . The basic requirement for the starting condition is a smooth change in pressure in the combustion chamber and absence of considerable overloading chamber with time is portrayed in Fig. 15.7. A pressure peak  $p_{\text{max}}$  is undesirable or even harmful. The reason for the appearance of such a peak is due to the accumulation in the combustion chamber of a large quantity of fuel components and their subsequent rapid combustion.

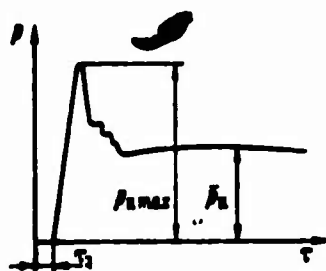


Fig. 15.7. Character of the change in pressure in the combustion chamber when starting.

The value of the average pressure in the combustion chamber under steady engine operation,  $\bar{p}_k$  can be determined according to the relationship

$$\bar{p}_k = \tau_k \bar{G} \frac{R_k T_k}{V_{k,r}}, \quad (15.1)$$

where  $\tau_n$  - time the fuel stays in the combustion chamber;  $\bar{G}$  - fuel consumption in seconds under steady engine operation;  $V_{k.c}$  - volume of the combustion chamber.

When starting the engine over a period of time, equal to the period of delay of self-ignition, the quantity of fuel delivered in the combustion chamber, is equal to

$$\int_0^{\tau_3} \bar{G}_{nyck}(t) dt = \bar{G}_{nyck} \tau_3 \quad (15.2)$$

where  $\bar{G}_{nyck}$  - average value for the starting fuel consumption in seconds.

By assuming that the quantity of fuel  $\bar{G}_{nyck} \tau_3$  burns instantly, it is possible to write:

$$p_{k \max} = \tau_3 \bar{G}_{nyck} \frac{R_k T_k}{V_{k.c}} \quad (15.3)$$

By equating expressions (15.1) and (15.3), we will obtain:

$$\frac{p_{k \max}}{p_k} = \frac{\tau_3}{\tau_n} \frac{\bar{G}_{nyck}}{\bar{G}} \quad (15.4)$$

Thus, the relative increase in pressure when starting is directly proportional to the delay of ignition, and as related to the starting and nominal fuel consumption, it is inversely proportional to the time the fuel stays in the combustion chamber,  $\tau_n$ .

From formula (15.4) it follows: for starting at nominal fuel consumption ( $\bar{G}_{nyck}/\bar{G} = 1$ ) without an overload based on pressure ( $p_{k \max}/\bar{p}_k = 1$ ) it is necessary that  $\tau_3/\tau_n = 1$ .

The time the fuel stays in the combustion chamber  $\tau_n$ , covered in the next chapter, depends on the nature of the fuel, on the geometry of the chamber and on the extent of organization of the processes. For the majority of ZhRD it amounts to several milliseconds.



The assumption that the ignition which has accumulated throughout time  $\tau_3$  of the fuel, occurs instantly, is an extreme and also a poor one; therefore, permissible value  $\tau_3$  can be somewhat larger than  $\tau_n$ . If the value  $\tau_3$  is considerably larger than  $\tau_n$ , the starting fuel consumption should be less than nominal for the proper starting of the engine.

#### Properties of a Fuel During Stationary Combustion

The required property of a fuel should be its capability to burn completely and steadily. The absence of this quality practically precludes the utilization of the fuel. It is known, for example, that the utilization of an additive consisting of finely-dispersed boron to kerosene which increases the theoretical specific thrust, was not actually effective as a result of the low combustion efficiency of boron. The utilization of fuels on the basis nitric acid was limited for a long time due to the unfavorable characteristics of combustion in the sense of resistance.

The conversion process of fuel into products of combustion under steady engine operation involves a complex of physicochemical phenomena. These phenomena are closely interconnected, and it is difficult to demarcate them in reference to time and space.

Furthermore, the conversion process of the fuel is substantially different for engines of ordinary design where both components were fed into the combustion chamber as a liquid, whereas for engines with an afterburner design, one or both components are fed into the combustion chamber in the heated as well as gaseous state. In the second case the contact and conversion of the liquid components is carried out in a gas generator.

It is obvious that the behavior of the fuels, to a considerable extent, is determined by their many characteristics and conditions in the chamber. However, as a result of the complexity of the processes a quantitative relationship between the integral characteristics of combustion (efficiency, resistance) and the

properties of the fuel have still not been achieved analytically. Therefore, in order to determine the kinetic properties of new fuels for the purpose of future design special investigations using model engines and devices are conducted. In order to perfect fuels there are usually statistical data, enabling one to formulate an effective process of carburetion and combustion, and to select the necessary volume of the combustion chamber.

#### 15.4. The Leading Fuels Used

In engine devices of rocket-carriers, for launching space objects, cheap and efficient fuels are widely used based on a cryogenic oxidizer - liquid oxygen. Certain characteristics of these fuels have been presented in Table 15.5.

Table 15.5. Characteristics of certain fuels based on liquid oxygen  $O_{2M}$  at  $p_H/p_C = 70/1$  and with an optimum proportionality of the components.

Combustible component	$\alpha$	$\gamma$ kg/ok	$Q_r \cdot 10^{-3}$ kg/m <sup>3</sup>	$T_K^\circ K$	$T_C^\circ K$	$\beta$ kgf.s/kg	$n$	$P_{Y_1}$ kgf.s/kg	$P_{Y_{1,n}}$ kgf.s/kg	$f_c$
Ethyl alcohol 95%	0.9	1.78	0.99	3411	2306	174	1.124	288	314	10.65
Kerosene	0.8	2.70	1.02	3690	2482	181	1.129	298	325	10.54
NEMG	0.9	1.92	0.99	3524	2487	186	1.124	307	335	10.70
NH <sub>3</sub>	1.0	1.41	0.89	3065	1710	181	1.170	294	328	9.484
H <sub>2M</sub>	0.7	5.56	0.35	3422	1888	239	1.174	386	418	9.375

Oxygen-ethyl alcohol fuel was used in the early stages of the development of rocket technology in German and the USA, and it was replaced by a more effective composition of a fuel of the kerosene type. Here and further on, the name "kerosene" means a special rocket hydrocarbon fuel the aviation kerosene type, derived from petroleum. Such a fuel is widely used both in the USA (for rockets (Atlas), (Titanium), (Saturn-V)), and the USSR (the rocket (Vostok)).

The use of asymmetrical dimethylhydrazine (NDMG) as a fuel made it possible to create an engine in the USSR with the greatest specific thrust with respect to high-boiling fuels. The RD-119 engine working on  $O_{2w} + \text{NDMG}$  fuel is widely used for launching the Cosmos series of satellites. A practical application was found for  $O_{2w} + \text{NH}_{3w}$  fuel; it is used in the engine of X-15 experimental aircraft of the USA. Its efficiency is relatively low.

The  $O_{2w} + H_{2w}$  fuel is classical as one of the most effective fuels in mass application. At present, it is used, for example, in the engines of the second and third stages of the "Saturn-V" rocket. Low density and high volatility of liquid hydrogen are its negative qualities; however, they are overcome as a result of successes achieved in the considerable degree, the realization of main advantage of the fuel - its high specific thrust.

Fuels with a base of high-boiling stable components find application in military rockets and space objects, where the fuel must be stored for a long time in a ready state in the engine. The utilization of high-boiling fuels in the latter case allows for minimum losses of the components without large weight losses to heat insulation.

Energy characteristics of the predominantly used high-boiling fuels are given in Table 15.6.

Fuels with a nitric acid base, feature and whose properties (such as freezing point, density, power engineering, and others) have been improved by an addition of 20-30% of oxides of nitrogen, have comparatively low energy characteristics, but a wide temperature range in the liquid state. These fuels are applied in those cases where the last characteristic is the determining one; for example, for small aviation rockets whose conditions of operation are subjected for a long time to the low or high temperatures of the surrounding medium without constant temperature control.

Table 15.6. Characteristics of certain stable fuels when  $p_H/p_C = 70/1$  and with the optimum proportion of the components.

Oxidizer	Fuel	$\alpha$	$\frac{z}{\text{kg-ox}}$ $\frac{\text{kg-ox}}{\text{kg-fuel}}$	$Q_r \cdot 10^{-3}$ kg/m <sup>3</sup>	$T_r$ °K	$T_c$ °K	$\beta$ kgf.s/kg	$n$	$P_{ya}$ kgf.s/kg	$P_{ya,n}$ kgf.s/kg	$f_c$
HNO <sub>3</sub> + + oxides of nitrogen	Kerosene	0,9	4,76	1,36	3170	1854	161	1,157	263	286	9,719
HNO <sub>3</sub> + + oxides of nitrogen	Mixture of amines	0,9	4,16	1,35	3173	1848	162	1,158	263	286	9,690
HNO <sub>3</sub> + + oxides of nitrogen	NDMG	0,9	3,01	1,27	3165	1771	169	1,169	273	296	9,445
N <sub>2</sub> O <sub>4</sub>	NDMG	1,0	3,06	1,18	3413	2245	172	1,132	283	308	10,47
N <sub>2</sub> O <sub>4</sub>	50% NDMG + + 50% N <sub>2</sub> H <sub>4</sub>	1,0	2,25	1,20	3353	2098	175	1,143	287	312	10,15
90% H <sub>2</sub> O <sub>2</sub>	Kerosene	0,9	7,17	1,27	2773	1479	164	1,177	264	286	9,326

Fuels having an N<sub>2</sub>O<sub>4</sub> base with NDMG, or of a mixture of 50% NDMG + 50% N<sub>2</sub>H<sub>4</sub>, named "aerozine-50", have higher energy characteristics and they are used in ballistic rockets. For example, "aerozine-50" + N<sub>2</sub>O<sub>4</sub> fuel has been used in the Titanium II rocket. It replaced the cryogenic composition of O<sub>2</sub> + kerosene, because it makes it possible for the rocket to be stored for a long time in a ready state for launching. The high melting point of nitrogen tetroxide is not a substantial deficiency, since the launching sites for ballistic rockets provide a narrow range of temperature fluctuations of the surrounding medium.

The comparison data in Tables 15.5 and 15.6 show that better from among the stable fuels the classical cryogenic O<sub>2</sub> + kerosene based on specific thrust are inferior, but have the advantage on density.

The fuel  $N_2O_4$  + "aerazine-50" is also used in the sustainer engine of "Apollo" spaceship in the American space series, intended to land a man on the Moon. The important advantage of this fuel is its spontaneous inflammability.

#### 15.5. Promising Propellants

The search, perfection and introduction of all the more effective fuels - is the invariable trend in rocket technological development. Let us dwell at first on the material which are involved in cryogenic fuels.

Here, one of the basic trends for increasing the efficiency is considered to be the perfection and utilization of liquid fluorine  $F_{2\text{ж}}$ , its compound,  $F_2O$ , and mixtures of liquid fluorine with liquid oxygen. The utilization of an oxidizer, consisting of 30%  $F_2$  and 70%  $O_2$ , was considered as a means of substantially increasing the energy characteristics of the "Atlas" rocket in the USA. When using kerosene as a combustible component, it turned out that an oxidizer, consisting of 70%  $F_2$  and 30%  $O_2$  by weight was optimum for specific thrust. The composition with 30%  $F_2$  was selected for the purpose of facilitating the solution to the problem of the compatibility of structural material with an oxidizer. Except for the increased energy characteristics, the positive quality of this fuel is its spontaneous inflammability.

Table 15.7 presents the characteristics of cryogenic fuels, which, according to published data [3], are being investigated as promising fuels.

Fluorine-hydrogen fuel is most efficient of all known fuels having components which are chemically stable individual substances. Together with high specific thrust this fuel also has a comparatively high density due to the high density of the liquid fluorine and the high value of optimum  $\kappa$ . This fuel is regarded both as a natural development as well as an improvement of the already perfected  $O_{2\text{ж}} + H_{2\text{ж}}$  fuel.

Table 15.7. Characteristics of certain promising cryogenic fuels with  $p_k/p_c = 70/1$  and with an optimum proportion of the components.

Oxidizer	Fuel	$\alpha$	$\frac{x}{y}$ $\frac{\text{kg} \cdot \text{nk}}{\text{kg} \cdot \text{comb}}$	$Q_r \cdot 10^{-3}$ $\text{kg/m}^3$	$T_x$ $^{\circ}\text{K}$	$T_c$ $^{\circ}\text{K}$	$\beta$ $\text{kgf} \cdot \text{s/kg}$	$n$	$P_{ya}$ $\text{kgf} \cdot \text{s/kg}$	$P_{ya,n}$ $\text{kgf} \cdot \text{s/kg}$	$f_c$
$\text{F}_2$	$\text{H}_2$	0.8	15.1	0.67	4762	2791	250	1,179	405	438	9,380
	$\text{NH}_3$	1.0	3.35	1.18	4568	2543	222	1,187	359	388	9,147
	$\text{N}_2\text{H}_4$	1.0	2.37	1.32	4699	2737	225	1,177	364	394	9,416
	Kerosene	0.3	2.40	1.20	3918	2799	187	1,200	313	343	11,09
	Kerosene	0.8	3.26	1.11	3955	2635	191	1,137	314	342	10,40
$30\% \text{F}_2 + 70\% \text{O}_2$											
$\text{OF}_2$	$\text{B}_2\text{H}_6$	0.7	4.10	1.04	4742	3129	226	1,141	370	404	10,30

A combination of  $\text{F}_{2\text{H}} + \text{N}_2\text{H}_4$  has high values of specific thrust and density. The good cooling features of hydrazine diminish the difficulties connected with the high temperature of combustion. According to published data, special additives, which do not affect its power engineering, eliminate the danger of decomposition and of an explosion of hydrazine when it is used for regenerative cooling.

Fluorine monoxide fuel with diborane is of interest when applied in systems where it is stored under space conditions from the several months up to one-two years. By calculation, the physical properties of these cryogenic components (melting point and saturation pressure) enhance storage under space conditions with small losses and small costs involved in heat insulation and thermal control. The high energy characteristics are combined with such unfavorable factors, as low density and the unsuitability of both components for regenerative cooling. It has been considered that an engine, which would operate on this fuel, should be shielded by means of ablating heatproof material.

The combination of  $\text{F}_2\text{O} + \text{kerosene}$  with respect to efficiency, corresponds to a fuel using a mixture of  $(70\% \text{F}_2 + 30\% \text{O}_2)$ .

Promising high-boiling fuels have likewise been comparatively little studied. Published material basically amounts to several compositions, presented in Table 15.8. Accordingly to this data, the most efficient with respect to specific thrust is a fuel having a concentrated hydrogen peroxide base with pentaborane.

Table 15.8. Characteristics of certain promising high-boiling fuels with a  $p_K/p_C = 70/1$  and with an optimum proportion of components.

Oxidizer	Fuel	$\alpha$	$\gamma$ kg ok kg comb	$\rho \cdot 10^{-3}$ kg/m <sup>3</sup>	$T_K$ °K	$T_C$ °K	$g$ kgf·s/kg	$n$	$P_{Y1}$ kgf·s/kg	$P_{Y1,n}$ kgf·s/kg	$f_c$
N <sub>2</sub> O <sub>4</sub>	B <sub>5</sub> H <sub>9</sub>	0,7	3,059	1,08	3917	2682	182	1,121	301	329	10,76
98% H <sub>2</sub> O <sub>2</sub>	B <sub>5</sub> H <sub>9</sub>	0,4	2,64	1,06	3172	2029	190	1,135	309	337	10,47
ClF <sub>3</sub>	N <sub>2</sub> H <sub>4</sub>	1,0	2,89	1,50	3889	1848	184	1,232	292	314	8,349
N <sub>2</sub> H <sub>4</sub>	B <sub>5</sub> H <sub>9</sub>	1,1	3,35	0,88	2092	932	184	1,235	291	313	8,376

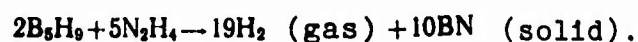
Pentaborane is extremely toxic (see Table 15.2) and self-ignites in air. However, additives have been found, which eliminate the danger of the latter (temperature of self-ignition is raised to 100°C).

Test reports from the USA tell of an engine working on pentaborane having a thrust of more than 20 T. The deficiencies of the investigated fuel include the elevated melting point and the chemical instability of the concentrated hydrogen peroxide. The rate of its decomposition amounts to about 1% per annum at 30°C, as a consequence of which this oxidizer is unsuited for storage in hermetically sealed containers.

The N<sub>2</sub>O<sub>4</sub> + B<sub>5</sub>H<sub>9</sub> fuel has a somewhat poorer theoretical value of specific thrust, but a higher density and excellent stability of both components, suitable for utilization in systems with preliminary servicing and hermetically sealed containers.

A combination of  $\text{ClF}_3 + \text{N}_2\text{H}_4$  has a unique advantage - high density. Interest is generated in this fuel in connection with the need for improving the characteristics of rockets under conditions of limited volume.

There is definite interest in the composition of hydrazine with pentaborane. These components possess excellent characteristics from the viewpoint of stability, and the combination of them has high energy characteristics. The interaction of the components proceeds according to the reaction



Solid boron nitride, which forms as a result of the reaction and consists of 85% by weight of all products of the reaction, is the heat source for hydrogen. The high specific thrust is created at equilibrium exhaust of the two-phase mixture, i.e., when the small particles of boron nitride are carried away by the hydrogen and are ejected from the nozzle practically at the same rate as that of the gas.

#### 15.6. Promising Metalliferous Fuels

Accordingly to thermodynamic calculations the application of an addition of light metals - Al, B, Be and Li can guarantee a substantial increase in the energy characteristics of existing and promising liquid rocket fuels, both of the cryogenic and high-boiling types [8]. Figures 15.8 and 15.9 present the results of calculations of the specific thrust of  $\text{O}_{2\text{w}} + \text{H}_{2\text{w}}$  and  $\text{F}_{2\text{w}} + \text{H}_{2\text{w}}$  fuels with additions of various metals. Along the abscissa the relative content of the metal in the fuel is plotted, along the ordinate - the specific thrust at  $p_{\text{w}}/p_{\text{c}} = 70/1$  and the optimum proportion of the fuel and oxidizer. As can be seen from the presented data, in the case of the oxidizer,  $\text{O}_{2\text{w}}$ , beryllium is the most effective additive, in the case of  $\text{F}_{2\text{w}}$  - lithium.



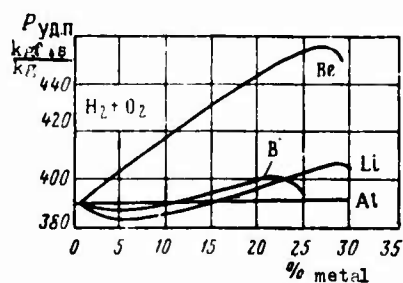


Fig. 15.8. Dependence of specific thrust in a vacuum on the content of metal in the fuel.

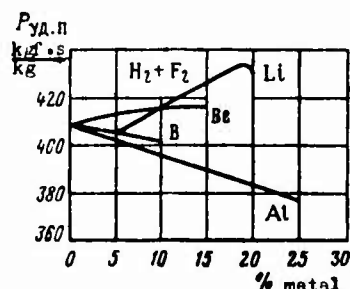


Fig. 15.9. Dependence of specific thrust in a vacuum on the content of metal in the fuel.

The data given in Figs. 15.10 and 15.11, show the feasibility of increasing the characteristics of certain high-boiling fuels by means of utilizing the metallic additive.

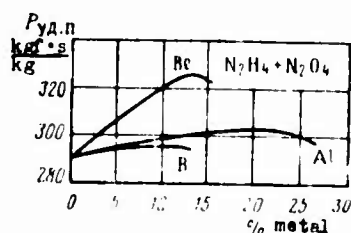


Fig. 15.10. Dependence of specific thrust in a vacuum on the content of metal in the fuel.

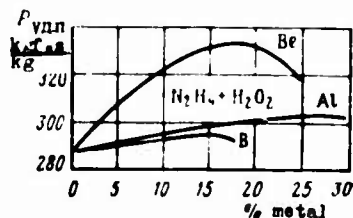


Fig. 15.11. Dependence of specific thrust in a vacuum on the content of metal in the fuel.

The general rule of the efficient utilization of a metallic addition is: the metal in conjunction with the oxidizer should give at combustion the greatest energy release, and the residual products should contain the largest possible quantity of hydrogen. As can be seen from the given results, for beryllium, boron and aluminium the better oxidizer is oxygen, for lithium - fluorine.

The application of a metallic additive to a fuel having a liquid hydrogen base, lowers the density of the fuel; this is associated with a decrease in the quantity of the oxidizer in the fuel and with an increase in the quantity of hydrogen based on optimum proportions. The optimum proportion of all components is approximately such that all of the oxidizer is spent on the stoichiometric oxidation of the metal, and the hydrogen is added to achieve maximum specific thrust.

Dependence of specific thrust on the quantity of hydrogen in the fuel is shown in Fig. 15.12, whereby it is clear that the maximum specific thrust using lithium corresponds to the content of hydrogen, and it is considerably higher than in a fuel without metal (see also Tables 15.5 and 15.7). This the reason for the decrease in the density of the mixture.

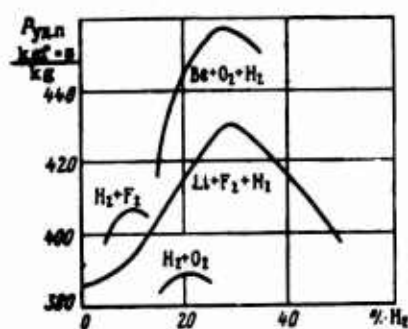


Fig. 15.12. Dependence of specific thrust in a vacuum on the content of hydrogen in the fuel:  $\alpha_F/\alpha_{Li} = 2.74$ ,  $\alpha_O/\alpha_{Be} = 1.8$ .

A reduction in the optimum quantity of an oxidizer with an addition of a metal, is also characteristic for high-boiling fuels; however, in view of considerably higher density of the fuels in comparison with  $H_{2M}$ , the addition of a metal, heavier than both components, increases the density of the fuel. Figure 15.13 as an example demonstrates the dependence of specific thrust on the density of  $N_2O_4 + N_2H_4$  fuel with additions of Al and Be.

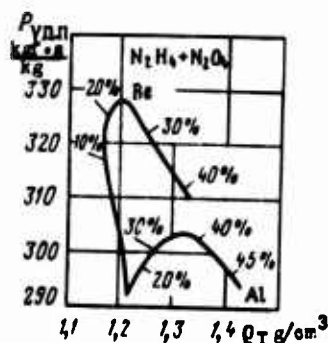


Fig. 15.13. Dependence of specific thrust in a vacuum on the density of the fuel. The figures designate the percentage content of metal in the fuel.

In view of the high theoretical efficiency of metalliferous fuels, various problems in their practical utilization take on a significant role. One of the important problems is that of storage and of supplying metal to the combustion chamber.

Promising solution this problem is considered to be the utilization of the metal suspensions in the fuel, which gelatinize (become like jelly) to prevent the precipitation of the metallic powder. Investigations show [8] that by adding 0.2-0.5% gelatinizing substances to the fuel structures in the fuel will be formed, consisting of long chain molecules, types of polymeric molecules, with transverse bonds between the chains. Under static conditions a gelatinized fuel will not flow and under rather small stresses it shifted similar to a solid body. Under such conditions the suspended particles of the metal do not completely settle out.

Under the action of applied stresses exceeding the limit of fluidity, the failure of the structure of the gel already begins at rather large stresses; for example, by extrusion through the fuel line under pressure, all the bonds are broken and the fuel with

respect to behavior becomes identical with a pure liquid having suspended particles of the metal. After a lapse of a certain time following failure there is again a restoration of the bonds – again a gel forms. Such a feature of a gel whereby it destroys itself by displacement and restores itself again under static conditions is called thixotropy. The example in Table 15.9 demonstrates the properties of pure hydrazine and gelatinized fuel "aluminizin" [Translator's note: This term is not identified in available fuel dictionaries].

Table 15.9. Comparison of the properties of metallized and ordinary fuel.

Properties		Hydrazine	Aluminizin
Composition, %	Hydrazine	100	66,5
	Aluminium	0	33,0
	Gelatinizing additions	0	0,5
Density in g/cm <sup>3</sup>		1,008	1,270
Viscosity in centipoises		0,97	45-10 <sup>3</sup>
Limit of fluidity in g/cm <sup>2</sup>		0	1,7
Melting point in °C		1,5	-2,3

Considering the data given in the table, let us note that the limit of fluidity is rather small, such that the fuel would begin to leak from the tank at a small pressure, but it is sufficient that the particles of the metal should not settle out. The very high viscosity of gel is diminished up to a value, close to the viscosity of pure hydrazine, with the failure of the structure of the gel during the process of flow through the fuel line.

If the problem of storage, of supply and of combustion of metalliferous fuel are to be successfully solved, the realization of a high specific thrust in connection with losses, possibly as a result of the unbalanced flow of a two-phase mixture in the nozzle will remain as the most serious problem. The content of the condensate (oxides of aluminum  $Al_2O_3$ , of beryllium  $BeO$ , and others)

in the products of combustion at a optimum proportion of components amounts to almost 50% by weight. At characteristic pressures in the combustion chamber of a ZhRD up to 100 bars and above, a content of condensate that high can result in a very considerable buildup of particles in the nozzle and can also result in large losses of specific thrust (see Chapter XIII). It is possible that the size of the particles in the area of the nozzle throat by virtue of their considerable buildup does not depend on the dispersiveness of the condensate in the combustion chamber and can be determined merely by the resistance of the drop against atomizing by their gas during blowoff.

To solve problems associated with the losses of specific thrust during the flow of a two-phase mixture in a nozzle, research [5] is being conducted, which affects a very wide range of problems: based on the study of properties of the oxides of metals and of interactions of micron-size drops with gas and among themselves prior to the testing the engines using metallized fuels with an accurate determination of the specific thrust.

#### Bibliography

1. "VRT". 1966, No. 7; 1967, No. 1, No. 4.
2. Zhidkiye i tverdye raketnyye topliva, (Liquid and solid rocket propellants) collection of translation IIL, 1959.
3. Novyye napravleniya kriogennoy tekhniki, (New trends in cryogenic technology) collection Izd-vo "Mir", 1966.
4. Paushkin Ya. M., Khimiya raketnykh topliv, (Chemistry of rocket fuels) AN SSSR, 1962.
5. "Raketnaya i kosmicheskaya tekhnika", 1962, No. 8.
6. Sarner S., Khimiya raketnykh topliv, (Chemistry of rocket fuels) izd-vo "Mir", 1969.
7. Spravochnik khimika, t. 1-3, Goskhimizdat, 1963.
8. Astronautics, 1959, No. 1, 2, 4, 5; 1960, No. 1-8; 1961, No. 1, 2, 6, 7, 11.

9. Chemical Engineering Progress Symposium Series, 1964, No. 7.
10. Fuels and New Propellants, Pergamon Press, 1964.
11. Peters R. L., Design of Liquid, Solid and Hybrid Rockets, New-York, 1965.
12. Siegel B., Schielder L., Energetics of Propellant Chemistry, New-York, 1964.

## CHAPTER XVI

### PROCESSES OF FUEL CONVERSION IN THE COMBUSTION CHAMBER

In this chapter the qualitative description of the conversion processes of fuel in the combustion chamber is given using various diagrams of their layout. The generalized characteristics are presented and methods of evaluating the perfection of the processes are examined.

#### 16.1. Overall Picture of the Phenomena

In the combustion chamber of a (WPD) [ZhRD = liquid-propellant rocket engines] a complex of processes goes on, which should be so organized that it guarantees:

- 1) maximum combustion efficiency;
- 2) rapid release of heat in a chamber of small sizes and weights;
- 3) steady operation of the processes, necessary for reliable and trouble-free work of the engine.

Depending on the phase composition of the components supplied the combustion chamber several schemes of the organization of the working processes can be distinguished.

### "Liquid-Liquid" Scheme

Both components in the liquid phase are injected through jets in the combustion chamber, where the reaction between fuel and the oxidizer should occur. Reaction basically goes on in the gaseous phase. Therefore, conditions should favor the conversion of liquid fuels into the gaseous state. These conditions will be realized in a certain section of the combustion chamber, where there is a complex of processes preparatory to combustion going on: the splitting (atomization) of the liquid components into droplets, their mixing, vaporization and mixing of the vapors, all included in the reaction.

The increase in surface area of the liquid as a result of the splitting into droplets accelerates the process of vaporization. The atomization of the liquid is carried out by jets of various types. Furthermore, with the rapid movement of the droplets in the gas medium they can change their form and under specified conditions can split up which also leads to an acceleration of the process of vaporization.

The criteria of atomization quality are the fineness and homogeneity of the atomization and the flame configuration of the atomization. In order to estimate fineness and homogeneity of atomization one should know the distribution of the liquid, injected through the jet, according to the sizes of the droplets, or so-called spectrum of atomization. A quantitative estimate of sizes of the droplets is necessary in order to calculate the rate of evaporation and motion of the droplets, conditions of mixing, and so forth.

The fineness of the atomization is characterized by a certain average diameter of the droplets. Various researchers have assigned a different meaning to the concept of the average size of the droplets existing in the spectrum of atomization. Frequently, the so-called median diameter is used. The specific gravity of the droplet, whose diameter is less or equal to the median diameter, measures 0.5. The median diameter of a droplet most commonly used in a swirl injector of a ZhRD is usually 25-250  $\mu$ , in a spray injector 200-500  $\mu$ .



The homogeneous distribution of the fuel according to the cross-sectional diameter of the combustion chamber is necessary for steady and efficient combustion, as well as the prescribed proportion of the components  $\kappa$ . These specifications are met in the process of injection and mixing of components (both in the liquid and gas phases). The mixing can be done preliminarily outside the combustion chamber in a two-component emulsion injectors.

Figure 16.1a represents a diagram of the distribution of the fuels components ratio  $\kappa \approx \kappa_{0HT}$  based on the radius of the combustion chamber. By duplicating such a picture at any diameter of the same cross section of the combustion chamber, the distribution of  $\kappa$  in that cross section is ideal in the sense of completeness of the isolation of heat. As was mentioned in Chapter XI, such a distribution of  $\kappa$  is not always acceptable. A diagram of a two-zone distribution of  $\kappa$  is shown in Fig. 16.1b.

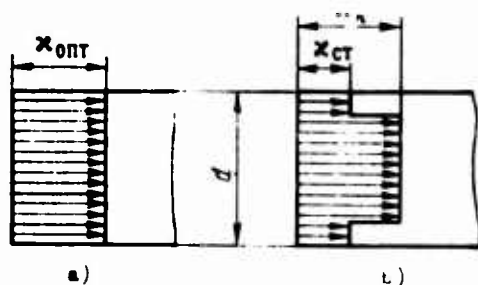


Fig. 16.1. Distribution diagram  $\kappa$  according to the cross section of the combustion chamber: a) without a boundary zone, b) with a boundary zone.

The sum total effect of the processes of atomization, of vaporizations and of mixing of the fuel components insures its preparation for exothermal reactions of combustion.

The pretreatment processes of the fuel prior to combustion and actual combustion processes are closely connected. Exact boundaries between the separate processes exist neither in time, nor in space.

The mixture in the combustion chamber prior to complete combustion of the fuel is two-phase. The interaction of the phases, the heat output from the products of combustion, the strongly developed turbulence of flow and the presence of diffusion processes

all accelerate the pretreatment processes and combustion processes. The overall picture of the entire complex of phenomena is very intricate and depends essentially on the nature of the fuels, on the design of the combustion chamber and on the carburetion system.

Figure 16.2 represents rough diagram of the transformation of the liquid components into products of combustion when self-igniting and nonself-igniting fuels are used.

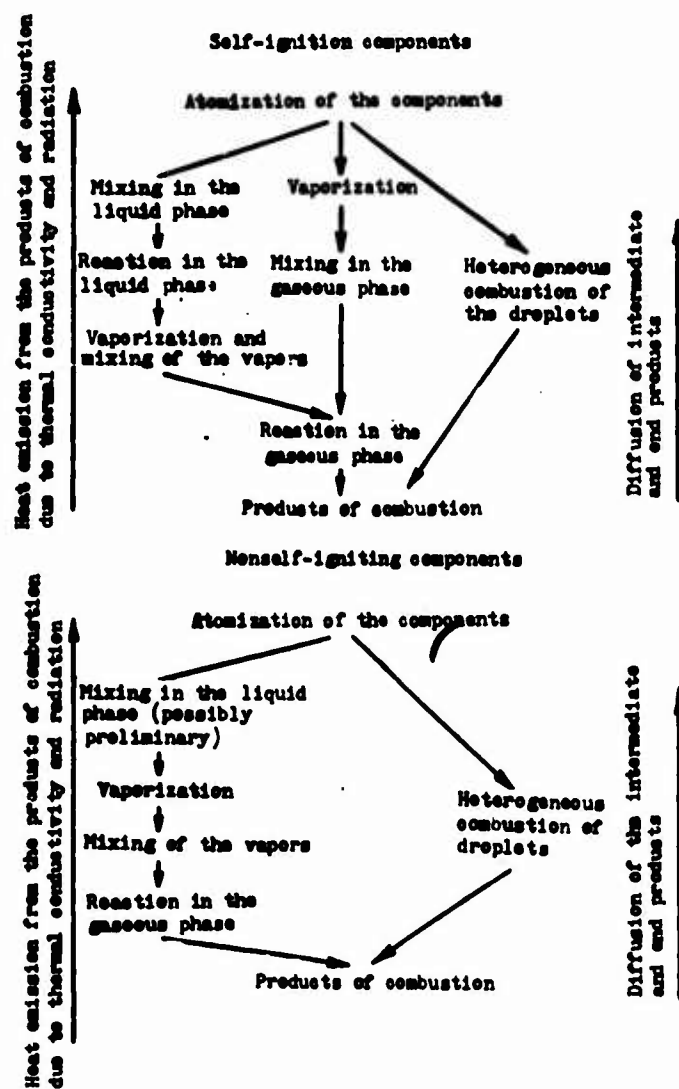


Fig. 16.2. Diagram of the transformation of liquid fuel into products of combustion.

Exothermal reactions in the liquid phase already going on upon contact (mixing) of the droplet of components is characteristic for self-ignition fuels. The energy release of these reactions facilitates the vaporization of the droplets, including those which did not react in the liquid phase, because they did not collide with droplets of another component. After that, the fuel vapors and oxidizer vapors are mixed and chemical gas-phase reactions take place which lead to the formation of the final products of combustion. The combustion of the gaseous fuel and oxidizer is homogeneous.

Whereas in this case the gaseous mixed fuels are not premixed and are heterogeneous, combustion occurs simultaneously with mixed components and with other processes, but the homogeneous combustion of a chemically heterogeneous gas mixture takes place, since in the different sections of the combustion chamber the combustion process can be limited by kinetics of reactions or by diffusion (either this one as well as others), and under certain conditions knocking combustion is also possible.

Heterogeneous combustion, i.e., combustion of liquid droplets of one component in the vapors of another can also occur simultaneously with homogeneous combustion.

This takes place, if one of the components vaporizes considerably faster than the second, and also with considerable nonuniformity in the splitting of the components into droplets (coarse droplets vaporize more slowly than the finer ones).

Figure 16.3 represents a diagram of the combustion of an unpressed drop of fuel in the vapors of an oxidizer. The boiling points of the liquid components are always lower than the temperature of ignition; therefore, the vaporization of the droplets precedes combustion. After the initial ignition of the vapor cloud surrounding the droplet, the combustion undergoes continuous vaporization of the liquid from the surface of the droplet due to the heat supplied from the flames, and also combustion undergoes continuous mixing

(diffusion) of the oxidizer and the fuel vapors. The products of combustion should be removed simultaneously.

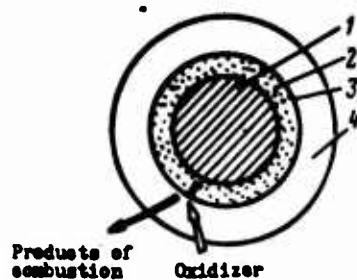


Fig. 16.3. Diagram of the process of combustion of a droplet: 1 - drop of the fuel; 2 - layer of vapors; 3 - flame; 4 - layer of diffusion combustion.

With the necessary condition for the development of homogeneous and heterogeneous combustion which usually accompany each other, there is a supply of heat to the liquid components in order to heat them, vaporize them and ignite them. As has been mentioned, this heat, in part, is released during the reactions of self-igniting components in the liquid phase. Another source for obtaining heat - the products of combustion whereby the heat is returned to the liquid components due to thermal conductivity and radiation, and in addition by means of the convective transfer of heat during the diffusion of intermediate and products of combustion in the direction of the head of combustion chamber.

The decisive role in this phenomenon is played by the so-called "reverse currents." They arise as a result of an injection effect of the liquid from the ejector. The liquid is swept away by side currents of the gas, simultaneously with the reverse currents as well. The reverse currents carry the products of complete and incomplete combustion along with a high temperature, the heat of which is returned to the atomized liquid.

The processes, which occur in case of using nonself-igniting fuels (see Fig. 16.2), are, on the whole, analogous to those mentioned above. Distinction is that the exothermal reactions between the components in the liquid phase do not occur or occur to a very insignificant degree. In connection with this, the supply of heat

takes on the decisive role. For the initial ignition it is carried out by an external source, but for the maintenance of a steady state — by the products of combustion, predominantly due to convection.

As a result of the highly-complex interacting processes described, it is difficult to come up with a general theory, quantitatively evaluating the parameters of the individual processes and their summary indexes. Qualitative investigations of the stationary processes in the combustion chamber make it possible to single out the basic phenomena and reconstruct a simplified model of the processes. According to the theory, which describes such a model, in certain cases rather accurate quantitative results can be obtained, such as presented in [2], [6].

Based on modern opinions the rate of the process of heat emission in the combustion chamber according to the "liquid-liquid" diagram is limited by the rate of vaporization of the liquid drops and by the rate of mixing of the gaseous components. However, the rate of the reactions of combustion under normal conditions of steady work a ZhRD inherently exceeds the rate of the pretreatment processes by several orders.

#### "Gas-Liquid" Diagram

According to the "gas-liquid" diagram one of the fuel components is fed into the combustion chamber in the gaseous state, the second — in the liquid state (Fig. 16.4). This diagram is realized, for example, when the generator gas ( $\alpha \ll 1$  or  $\alpha \gg 1$ ) and the liquid component, which provides the prescribed proportion of  $\kappa$  in the main chamber is delivered to the combustion chamber.

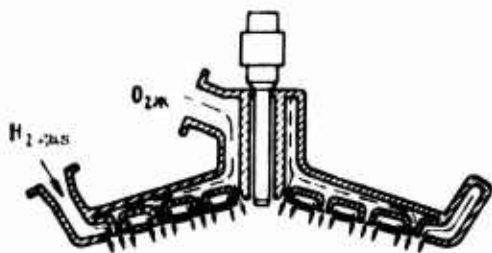


Fig. 16.4. Diagram of an injection head of the "gas-liquid" type (RL-10A ZhRD, USA).

By supplying the components according to the "gas-liquid" diagram, the mixing and the reactions in the liquid phase are absent in the processes of fuel conversion; the remaining picture of the phenomena is analogous to that described above for the "liquid-liquid" diagram.

It is natural that the conversion of the liquid droplet will occur in the shorter section of the combustion chamber in the examined diagram, rather than in "liquid-liquid" diagram and the sizes of the combustion chamber in this case are reduced. A good distribution of the liquid component in the gaseous state and its complete mixing are the necessary conditions. In a number of works [3] it was noted that it was not the vaporization of the components, but their mixing in the gaseous phase that was the determining factor, especially when the process of combustion goes to completion.

#### "Gas-Gas" Diagram

According to this diagram both components of the fuel are delivered to the combustion chamber in the gaseous form. For example, the generator gas from two gas generators enters the combustion chamber, with  $\alpha \ll 1$  in the first generator, and with  $\alpha \gg 1$  in the second.

The examined diagram, obviously, is a better variant in terms of fuel conversion in the products of combustion, because the flow in the combustion chamber is monophasic. The overall diagram of fuel conversion can be formally simplified (the processes of atomization and of vaporization of the liquid components are absent); in this case the determining process is the mixing of the gaseous components or the vapor-gas mixtures.

#### Range of Stable Combustion

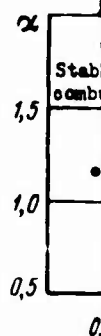
In all the organizational diagrams of the working processes, the sizes of the combustion chamber must be adequate in order to

guarantee  
combustion  
be stable

(vibrations  
in the  
frequency  
(hundreds  
pressure  
superheated  
is possible

in a 2  
approach  
[4], [5]  
are with

The  
of process  
proceeds  
example  
stabilization  
pressure  
As it  
specific  
components



guarantee the thorough burning of the fuel before the products of combustion begin to enter the nozzle; in this case combustion must be stable.

However, during the operation of a ZhRD dangerous unstable (vibratory) combustion can arise. It is accompanied by fluctuations in the pressure of the gas in the combustion chamber. The low-frequency (tens and hundreds of cycle per second) and high-frequency (hundreds and thousands of cycles per second) of fluctuations of pressure in the combustion chamber can be discerned. Mutual superposition of the low-frequency and high-frequency fluctuations is possible. The physical nature of these phenomena is diverse.

A theoretical investigation of the instability of combustion in a ZhRD is one of the most complicated assignments as possible approaches to the solution; these are examined in special literature [4], [5]. Along with theoretical dependences experimental data are widely used.

The results of an experimental investigation of the stability of processes in the combustion chamber frequently follow the procedure analogous to that given in Fig. 16.5, where, as an example, the results of the experimental investigation of the stability of the operation of a ZhRD are given using various  $\alpha$  and pressures in the combustion chamber (fuel - furfuryl alcohol +  $\text{HNO}_3$ ). As it appears, range of stable operation is possible only within a specified pressure range in the combustion chamber and in the fuel components ratio.

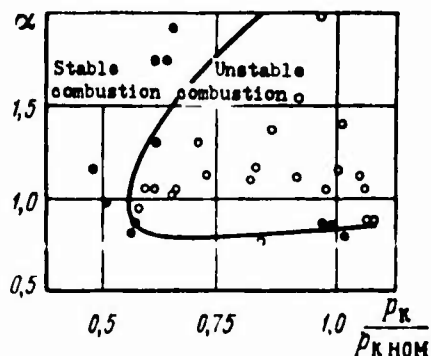


Fig. 16.5. Example of an experimental determination of the range of stable combustion.

## 16.2. Evaluating an Improvement of the Processes

Imperfection in the design of the mixing elements, incomplete mixing and combustion of the fuel components and other losses diminish heat emission and the potential energy of the gas (full inlet pressure in nozzle  $p_n^*$ ), utilized upon expansion of the gas in the nozzle. All this results in the downgrading of the engine characteristics, specifically, a reduction in the specific thrust.

Inasmuch as the magnitude of specific thrust is proportional  $\sqrt{R_n T_n^*}$ , then the degree of distinction of the actual processes in the combustion chamber from the theoretical processes, i.e., the quality index of the actual processes can be evaluated by the quantity

$$\varphi_p = \frac{\sqrt{R_n T_n^*}}{\sqrt{(R_n T_n^*)_t}}, \quad (16.1)$$

where  $\varphi_p$  — ratio of actual to theoretical chamber pressure;  $R_n T_n^*$  and  $(R_n T_n^*)_t$  — actual and theoretical values of the product of the gas constant, and temperature, respectively.

However, an experimental determination of the quantity  $R_n T_n^*$  in the chamber is not yet possible; therefore, another value is taken as criterion of the efficiency of the combustion chamber, depending in many respects on the perfection of processes in the chamber and on that determined experimentally. Such a value is specific impulse pressure in the chamber (complex  $\beta$ ). Degree of distinction of the actual processes from the theoretical processes in the combustion chamber can be represented as:

$$\varphi_\beta = \frac{\beta_g}{\beta_t}, \quad (16.2)$$

where  $\beta_g$  — value of the complex, determined in the experiment;  $\beta_t$  — theoretical value of the complex.



The quantity  $\phi_\beta$  defines in its entirety the complex of processes in the combustion chamber together with the subsonic section of the nozzle. In the absence of irreversible phenomena in the subsonic section of the nozzle  $\phi_\beta$  reliably defines the perfection of the processes in the combustion chamber. Otherwise, high or underrated values of  $\phi_\beta$  can give an incorrect representation of the perfection of work of the combustion chamber.

For example, during the determination of  $\beta_\beta$  under conditions of  $p_{k0}^* = p_{kt}^*$ ,  $F_{kp0} = F_{kpt}$  expenditure of  $G_\beta$  as a result of friction in the subsonic section of the nozzle seems underrated in comparison to the amount necessary to compensate for the lowering of  $p_k^*$  due to incompleteness of combustion. In two-phase flow the high-speed nonequilibrium consumption process results in an increase in expenditure. Thus, in first case the high values of  $\phi_\beta$  can exist even with a low quality of the processes in the combustion chamber, whereas in the second case, the low values of  $\phi_\beta$  - with perfect combustion.

Just as the specific thrust, the specific impulse pressure in the chamber is also proportional  $\sqrt{R_k T_k^*}$ , and consequently, the imperfection of the processes in the combustion chamber can be expressed by  $\beta$  through  $\sqrt{R_k T_k^*}$ . The irreversible phenomena in the subsonic section of the nozzle can be considered with the help of coefficient of consumption  $\mu_c$ . In this way:

$$\varphi_\beta = \frac{\varphi_{p_k}}{\mu_c} \quad (16.3)$$

or

$$\varphi_{p_k} = \mu_c \varphi_\beta \quad (16.4)$$

Coefficients  $\varphi_\beta$  and  $\varphi_{p_k}$  are the most commonly used coefficients, evaluating the perfection of the processes in the combustion chamber. Values of  $\varphi_{p_k}$  usually amount to 0.96-0.99 and are determined by the

fuel (coefficient of excess oxidizer  $\alpha$ ), by the carburetion system, by the pressure in the combustion chamber and its length.

As has been mentioned, the basic reasons for the incomplete heat release are the imperfect mixing of the fuel components and incompleteness of other processes: vaporization "liquid-liquid" diagram, "gas-liquid," diffusion, actual combustion. These two different reasons for losses sometimes can be evaluated based on their nature in the following manner.

In order to estimate the degree of perfection of the mixing of process of the fuel components the values of specific thrust in a vacuum  $P_{уд.п}$ , should be compared, where they have been obtained in case of a prescribed distribution of the fuels component ratio as well as in case of their actual distribution, supplied by the data by the carburetion system (see 11.1).

In the particular case of the heterogeneity of  $\kappa$ , with two-zone distribution, the theoretical value  $P_{уд.п}$  in accordance with formula (11.33) should be defined as:

$$P_{уд.п} = g_n P_{уд.п\ n} + g_{ct} P_{уд.п\ ct},$$

where  $g_n = \frac{G_n}{G}$  and  $g_{ct} = G_{ct}/G$  — relative fractions of the consumption, respectively, in the nucleus as well as in the boundary zone;  $P_{уд.п\ n}$ ,  $P_{уд.п\ ct}$  — theoretical values of specific thrust in a vacuum in these same zones with  $\kappa = \kappa_n$  and  $\kappa = \kappa_{ct}$ ; these values are determined by thermodynamic calculation.

Since  $g_n = 1 - g_{ct}$ , then

$$P_{уд.п} = P_{уд.п\ n} - g_{ct} (P_{уд.п\ n} - P_{уд.п\ ct}). \quad (16.5)$$

In order to determine the values  $P_{y,n,t}$  with actual distribution of the fuel components it is necessary to subdivide the cross section of the combustion chamber into larger possible number of elementary sections with an area  $F_1$  and to determine the values of relative consumption  $g_1$  and fuels component ratio  $\kappa_1$ .

The value of specific thrust in a vacuum  $P_{y,n,t}$  for entire combustion chamber is equal to the sum of values  $P_{y,n,t}$  through all sections (see Chapter XI):

$$P_{y,n,t} = \sum_1^n g_i P_{y,n,t,i}$$

where  $n$  - number of sections, into which the cross section of the combustion chamber has been subdivided.

Thus, the coefficient, determining the quality of mixing of the components, or the coefficient of perfection of the mixing, is equal to

$$\varphi_{cm} = \frac{\sum_1^n g_i P_{y,n,t,i}}{P_{y,n,t}} \quad (16.6)$$

or with two-zone distribution

$$\varphi_{cm} = \frac{\sum_1^n g_i P_{y,n,t,i}}{P_{y,n,t} - g_{ct} (P_{y,n,t} - P_{y,n,t,ct})} \quad (16.7)$$

The value of coefficient  $\phi_{cm}$  is usually less than of unity; however, using a certain curve  $\kappa_1$ , this coefficient can be more than unity. The greater the value  $\phi_{cm}$ , the better organized are the processes of mixing of the fuel components. The authenticity of values of  $\phi_{cm}$  depends on the reliability of the determination of diagrams of the actual distribution of  $\kappa_1$  and  $g_1$ . The determination of such diagrams for an actual head is possible by calculated and experimental methods. Both methods are approximate.

Thus, the losses, governed by the imperfection of the mixing of the fuel components are determined separately. The degree of perfection of the remaining processes in the combustion chamber can be evaluated by a certain coefficient of  $\phi_{\text{rop}}$ .

By setting  $\mu_c \approx \text{const}$ , let us write down:

$$\varphi_{p_k} = \varphi_{\text{cm}} \varphi_{\text{rop}} \quad (16.8)$$

Since  $\varphi_{p_k}$  and  $\varphi_{\text{cm}}$  are known, then

$$\varphi_{\text{rop}} = \frac{\varphi_{p_k}}{\varphi_{\text{cm}}} \quad (16.9)$$

The coefficient  $\phi_{\text{rop}}$  evaluates the quality of the processes of vaporization and of the subsequent mixing in the gas phase (turbulent diffusion) and the combustion itself. The degree of completeness of these processes depends on whether or not the time of stay of the fuel components in the combustion chamber is adequate, i.e., whether or not its sizes are sufficient.

The relative change in the specific thrust as a result of the imperfection of the processes in the combustion chamber are acceptable in order to evaluate the formula

$$\delta P_{y_{k.c}} = \frac{P_{y_{k.c}} - P_{y_{k.c}}}{P_{y_{k.c}}} = 1 - \varphi_{p_k}$$

As it is apparent, using such a means of evaluating estimation the amount of losses of specific thrust,  $\delta P_{y_{k.c}}$  does not depend on the parameters of the process of expansion. However, as the calculations presented in Chapter XI show, the effect of chemical heterogeneity and incompleteness of combustion change depending on the parameters of the expansion process ( $\delta P_{y_{k.c}}$  increases with an increase in the relative area  $f_c$  or  $\eta_c$ ). A more thorough calculation of the dependence of losses  $\delta P_{y_{k.c}} = f(f_c)$  requires reliable data based on the diagram of distribution of  $\kappa_1$  and based on the incompleteness of combustion and even in the absence of these, it is expedient.

### 16.3. Generalized Characteristics of the Processes

The best known generalized characteristics of the processes in the combustion chamber of a ZhRD are as follows.

1. Time of stay. The time of stay  $\tau$ , is called that time during which the fuel components and the products of combustion produced from them are actually in the combustion chamber.

Usually one uses the approximate value of  $\tau_{\Pi}$ , which merely determines the gaseous phase (i.e., vaporized components and products of their combustion) spends the time in the combustion chamber. This quantity is written as:

$$\tau_{\Pi} = \frac{G_{k,c}}{G} = \frac{V_{k,c}\bar{\rho}}{G}, \quad (16.10)$$

where  $G_{k,c}$  - weight of the gas in the combustion chamber;  $G$  - consumption in seconds;  $V_{k,c}$  - volume in the combustion chamber (it is usually defined as the volume in front of the critical section);  $\bar{\rho}$  - average density of the gas in the combustion chamber. It is obvious that for "liquid-liquid" and "gas-liquid" diagram  $\tau_{\Pi} < \tau_{\Pi\Gamma}$ , for "gas-gas" a diagram these quantities coincide.

A further approach amounts to replacing difficulty determinable amount value  $\bar{\rho}$  by the quantity  $\rho_k^*$ , which pertains to exit section of the combustion chamber. Then

$$\tau_{\Pi} = \frac{V_{k,c}\rho_k^*}{G}. \quad (16.11)$$

Since  $\rho_k^* < \bar{\rho}$ , then the value  $\tau_{\Pi}$ , as defined by the formula (16.11), is less real. For a comparative evaluation this is immaterial.

Taking into account the equation of state and the formula for complex  $\beta$  we will obtain:

$$\tau = \frac{V_{k,c}\beta}{I_{sp}R_kT_k^*}$$

or

$$\tau_n = L_{np} \frac{3}{R_k T_k^*}, \quad (16.12)$$

where

$$L_{np} = \frac{V_{k.c}}{F_{kp}} \quad (16.13)$$

the so-called given length of the combustion chamber.

2. The corrected length of the combustion chamber. As can be seen from the formula (16.12), the quantity  $L_{np}$  is proportional to the time of stay of the gases in the combustion chamber and determines to some degree the combustion efficiency of the fuel.

The value  $L_{np}$  depends on the nature of the fuel and on conditions of carburation. For a "liquid-liquid" diagram the order of value in  $L_{np}$  in  $\mu$  is as follows:

Nitric acid-hydrocarbon fuel.....	2.0-3
Nitric acid-NDMG.....	1.5-2
Oxygen-ethyl alcohol.....	2.5-3
Oxygen-kerosene.....	1.5-2.5
Oxygen-hydrogen.....	0.25-0.5
Fluorine-ammonia.....	1.0-1.5
Hydrazine (unitary fuel).....	0.8-3

3. Specific weight flow of the combustion chamber. The specific weight flow is called the consumption of the working medium through a unit area of the combustion chamber per second. It is determined according to the formula

$$G_p = \frac{G}{F_k} = \frac{\rho_k^* F_{kp}}{\rho F_k} = \frac{\rho_k^*}{\rho f_k}. \quad (16.14)$$

Experiments show that with an increase in  $p_{\kappa}^*$ , the working process in the combustion chamber is intensified. Therefore, with an increased  $p_{\kappa}^*$  through the same area of the chamber,  $F_{\kappa}$  can deliver a larger quantity of fuel, i.e., the value  $G_F$  can be increased.

The ratio of the permissible specific weight flow of the combustion chamber of a ZhRD to the pressure in it, can be considered approximately constant and it can be used with calculations making use of such data ( $G_F$  kg/s·m<sup>2</sup>,  $p_{\kappa}^*$  N/m<sup>2</sup>):

Class of engines	$G_F/p_{\kappa}^* \cdot 10^4$
Nitrogen-oxygen	0.8-1.0
Oxygen	1.1-1.3
Fluorine	0.8-0.9

4. Volumetric calorific intensity of the combustion chamber.  
Its value is determined by the formula

$$Q_V = \frac{GH_u}{V_{\kappa,c}}. \quad (16.15)$$

By solving formula for  $\beta$  it is simple to derive the expression (16.15) in the form

$$Q_V = \frac{H_u p_{\kappa}^*}{3L_{np}}. \quad (16.16)$$

As it appears, all things being equal,  $Q_V$  depends on  $p_{\kappa}^*$ .

Frequently instead of  $Q_V$  the given calorific intensity is used, being defined as

$$Q_{V_{np}} = \frac{Q_V}{F_{\kappa}}.$$

Using the expression (16.12), the formula for  $Q_{vnp}$  can be written as:

$$Q_{vnp} = \frac{H_u}{\tau_n R_k T_k^*} \quad (16.17)$$

Since  $R_k T_k^* \sim H_u$ , then  $Q_{vnp} \sim \frac{1}{\tau_n}$  and can be used on an equal basis with  $\tau_n$  or  $L_{np}$ .

Generalized characteristics of the processes  $\tau_n$ ,  $L_{np}$ ,  $G_F/\rho_k^*$  and  $Q_{vnp}$  are interrelated; in this case none of them can be reliably determined by the theoretical method. Nevertheless, these values are necessary for the determination of the sizes of the combustion chamber. The basic source of information on the values  $\tau_n$ ,  $L_{np}$ ,  $G_F/\rho_k^*$  and  $Q_{vnp}$  are statistical data, accumulated in process of testing and perfecting models of the combustion chamber.

#### Bibliography

1. Dvigatel'nyye ustanovki raket na zhidkom toplive (Engine installations of liquid-fuel rockets) Collection of translations, izd-vo "Mir", 1966.
2. Detonatsiya i dvukhfaznoye tekcheniye (Detonation and two-phase flow) Collection of articles, izd-vo "Mir", 1966.
3. Disers et al., VRT, 1966, No. 10.
4. Moshkin Ye. K., Dinamicheskiye protsessy v ZhRD (Dynamic processes in ZhRD) izd-vo "Mashinostroyeniye", 1964.
5. Shaulov Yu. Kh., Lerner M. O., Gorenkiye v zhidkostnykh raketnykh dvigatelyakh (Combustion in liquid-fuel rocket engines) Oborongiz, 1961.
6. Priem P. I., Heidmann M. F., NASA TRR-67, 1960.
7. Reardon F. H., AIAA Reprint, No. 65.



## CHAPTER XVII

### PROCESSES OF GAS GENERATION

In this chapter the processes of gas generation using liquid fuel are examined. The methods of designing gas generators working on unitary and two-component fuels are presented, the methods of producing steam coolant passage are qualitatively described with the assumption that the working process is ideal.

In conclusion, the thermodynamic efficiency of the various methods of gas generation are examined.

#### 17.1. General Information

Auxiliary power units, which utilize the chemical energy of liquid or solid fuel, produce the working medium - the generator gas, which is either directly applied to the pressurized fuel-feed systems and the power supplies of the servomechanisms, or it enters turbine, which drives the necessary units. The processes of gas generation - these are processes of the conversion of the chemical energy of the fuel into a thermal form of energy of the working medium.

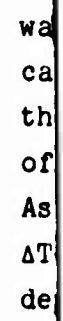
When utilizing liquid fuel the processes of gas generation are similar in principle to the processes performed in the basic combustion chamber of (ЖРД) [ZhRD - liquid-fuel rocket engine]. In principle, the processes are also the generalized characteristics of the processes of gas generation: the time of stay, the given length, and so forth.

of  
fu  
th  
an  
a  
  
of  
in  
ca  
of  
of  
a  
me  
th  
  
wa  
ca  
th  
of  
As  
AT  
de

- wa  
ca  
th  
of  
As  
ΔT  
de

wa  
ca  
th  
of  
As  
ΔT  
de

wa  
ca  
th  
of  
As  
ΔT  
de



wa  
ca  
th  
of  
As  
ΔT  
de

wa  
ca  
th  
of  
As  
ΔT  
de

of passage which becomes commensurable with the time of stay of the fuel in the chamber of the gas generator. The other characteristic, that of the products of combustion, is not ideal (in the sense of an equation of state) and has a noticeable effect which is manifested at low temperatures and high pressures.

The variety of factors, which determine the actual passage of processes in gas generators, the complexity of the experimental investigation in order to confirm these or any other models of calculations do not at present provide for general and strict methods of calculation. Therefore, statistical data are used in the design of a gas generator for perfecting fuel. When utilizing a new fuel, a special investigation is required. For initial evaluation a method of thermodynamic calculation, based upon an assumption about the chemical equilibrium can be used.

The effect of the nonideal nature of the combustion products was examined in Chapter XI; there the methods of thermodynamic calculation were described. Figure 17.2 serves as an example for the comparison of the results of the calculation of the temperature of equilibrium combustion for a fuel of the kerosene +  $O_{2H}$  type. As it appears, with an increase in the pressure, the deviation  $\Delta T = T_{\text{реал}} - T_{\text{ид}}$  increases; in this case, sign of the deviation depends on excess oxidizer ratio.

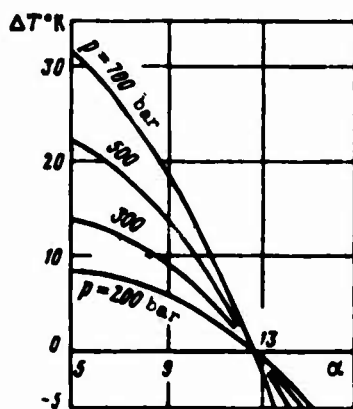


Fig. 17.2. Effect of actual conditions on the equilibrium temperature of combustion.

Let us examine the possible means of obtaining generator gas.

### 17.2. Utilization of Unitary Fuel

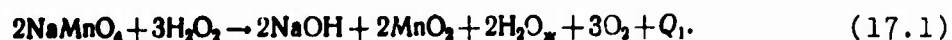
Most widespread and perfected liquid unitary fuel is hydrogen peroxide.

Usually, aqueous solutions of permanganates,  $\text{NaMnO}_4$  and  $\text{Ca}(\text{MnO}_4)_2$  are used as catalysts for the exothermal decomposition of hydrogen peroxide. The contact of hydrogen peroxide and the catalyst can be accomplished using two variations:

1) direct contact of the atomized  $\text{H}_2\text{O}_2$  and the liquid catalyst sprayers;

2) contact of hydrogen peroxide with the surface of a solid catalyst, a granulated substance, saturated in a permanganate solution.

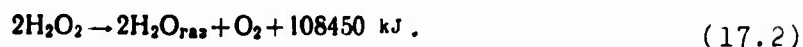
The catalytic actions on hydrogen peroxide does not immediately yield permanganate, but manganese peroxide,  $\text{MnO}_2$ . At a 100% concentration of  $\text{H}_2\text{O}_2$  sodium permanganate reacts to form  $\text{MnO}_2$ , as such:



Only, then after yielding active  $\text{MnO}_2$ , does the second reaction take place - the actual decomposition of hydrogen peroxide:



The quantity of heat being liberating in this reaction allows for the evaporation of all formed water, and in addition, it allows for the heating of the vapor-gas mixture, consisting of steam and oxygen. Taking into account the expenditure of heat to evaporate the water, this reaction can be written as:



gas. Differences in the organization of the decomposition process of hydrogen peroxide with the aid of solid or liquid catalyst can be reduced to the following. When using a liquid catalyst, the products of the first reaction (17.1), including  $\text{MnO}_2$ , are removed from the reaction chamber, is connected with the fact that for the decomposition of new portions of  $\text{H}_2\text{O}_2$  a renewal of the active catalyst,  $\text{MnO}_2$  is required, i.e., a continuous supply of the liquid catalyst.

When using a solid catalyst which has been released in the primary reaction, the manganese peroxide is retained on the surface of the pack of the catalyst. The quantity and activity of the  $\text{MnO}_2$  are sufficient for the decomposition of a considerable quantity of hydrogen peroxide, which is continuously washed over the surface of the pack. Thus, when using a solid catalyst, the specific weight of the primary reaction (17.1) in comparison with the main reaction (17.2) is very small. Therefore, when determining the composition and temperature of the steam gas, it can not be considered the primary reaction. In the case of utilizing a liquid catalyst, the primary reaction has relatively substantial value and should be taken into account in the calculation.

In practice hydrogen peroxide is usually not applied at 100% concentration, but it is an aqueous solution. The concentration of hydrogen peroxide by weight  $c_{\text{H}_2\text{O}_2}$  can be expressed usually in fractions of unity. The calculation of the composition and of the temperature of products of decomposition of hydrogen peroxide can be performed based on described methods in Chapters VI and VIII. As a result of simple composition of vapor gas ( $\text{O}_2$  and  $\text{H}_2\text{O}$ ), the calculation is quite simple.

Figure 17.3 shows the weight (g) and volumetric (r) fractions of  $\text{H}_2\text{O}$  in a vapor-gas mixture, and in addition, the values of the average molecular weight  $\mu$  of the vapor-gas with the decomposition of hydrogen peroxide at various concentrations in presence of a solid catalyst. As it appears, the higher the concentration of  $\text{H}_2\text{O}_2$ , the

smaller the fraction of  $H_2O$  and the larger the fraction of oxygen in the steam gas. Because  $\mu_{O_2} > \mu_{H_2O}$ , the average molecular weight of the steam gas increases with an increase in  $c_{H_2O_2}$ .

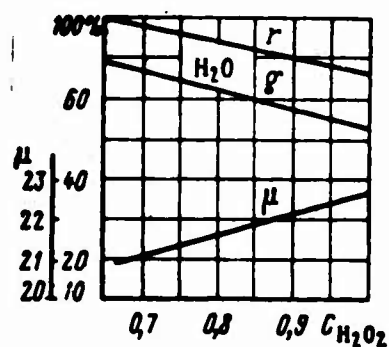


Fig. 17.3. Composition and molecular weight of the decomposition products of hydrogen peroxide at various concentrations.

The temperature of the steam gas depends on the concentration of hydrogen peroxide and should be at a maximum when  $c_{H_2O_2} = 1$ .

Figure 17.4 shows the change in the theoretical temperature of the steam-gas mixture depending on the concentration of the hydrogen peroxide when using a solid catalyst. Also shown on this chart are the values of specific working capacity to steam gas,  $RT$ . The actual heat emission is approximately 0.92-0.95 that of the theoretical.

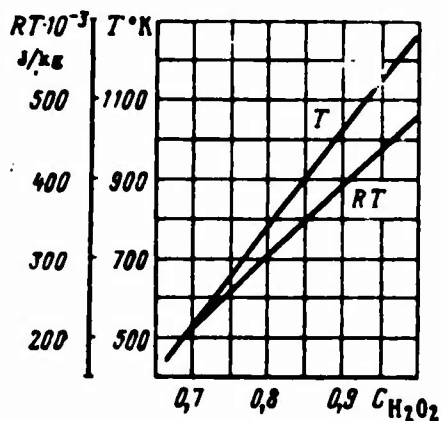


Fig. 17.4. Dependence of  $T$  and  $RT$  of the decomposition products of hydrogen peroxide on its concentration when using a solid catalyst.

The steam gas produced by the decomposition of hydrogen peroxides is usually used for the drive of turbines. The power of the turbine can be regulated by a change in the quantity of hydrogen peroxide applied at a constant temperature of the steam gas.

As can be seen from Fig. 17.4, the concentration of hydrogen peroxide,  $c_{H_2O_2} = 0.8-1.0$ , offers a wide range of temperature for steam gas. The value of  $c_{H_2O_2}$  is selected depending on the permissible temperature in front of the turbine.

Figures 17.5 and 17.7 present the thermodynamic characteristics of other liquid unitary fuels.

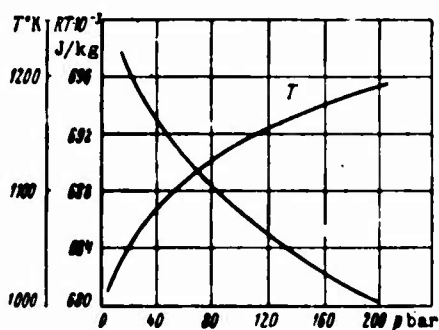


Fig. 17.5. Dependence of T and RT of the decomposition products of asymmetrical dimethylhydrazine, on pressure.

The specific working capacity of the gas RT, of these fuels is higher than by the decomposition of hydrogen peroxide. As a result of complete absence of an oxidizer in the products of decomposition the latter have a low-activity level with respect to the structural material. The generator gas, produced by the decomposition of  $C_2H_8N_2$ , contains solid condensed particles of carbon.

A diagram of a possible design of a gas generator working on monopropellant (for example, hydrazine) is presented in Fig. 17.6. The monopropellant is forced through sprayer 1 in an annular space, formed by cone 2 and cylinder 3. An electric coil 4 is set in the annular space and is heated by a source of current prior to starting. Subsequently, the source of current is turned off and a stable

reaction goes on owing to the heat of the products of decomposition; the coil in this case plays the role of a catalyst. The partially decomposing monopropellant is fed through the system of apertures 5 inside cylinder 3, where the decomposition is completed, and the gas enters pipe 6. Cavity 7 serves to cool sprayer 1, in order to prevent the beginning of decomposition of the fuel in the sprayer.

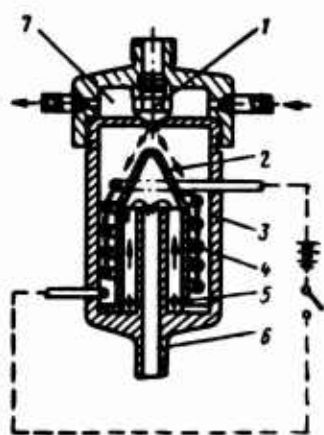


Fig. 17.6. Approximate diagram of a gas generator working on monopropellant (patent USA, No. 3142541, 1961).

Experiments with hydrazine in a sealed bomb, showed that during a thermal decomposition of  $N_2H_4$  there are two successive-stage reactions according to the equations

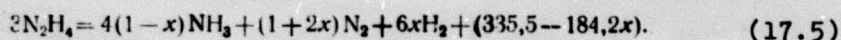


As the results of thermodynamic calculations show based upon chemical equilibrium, at temperatures below  $400^\circ K$  in products of decompositions, according to the reaction (17.3), there are only  $NH_3$  and  $N_2$ . However, if temperature rises significantly above  $400^\circ K$ , then  $NH_3$  decomposes thermally accordingly to equation (17.4), and at a temperature above  $800^\circ K$  the decomposition products of  $N_2H_4$  should not contain ammonia.

In cases where the second reaction (17.4) for some reason does not go to completion, the adiabatic temperature of decomposition is equal  $\sim 1650^\circ K$ ; however, at equilibrium decomposition,  $870^\circ K$ .



The time of stay in the chamber of the gas generator can amount to several milliseconds; therefore, it is natural to expect that only a part of the  $\text{NH}_3$  will decompose depending on the rate of the reaction (17.4). If the reaction (17.3) goes to completion, but the reaction based on equation (17.4) does not go to completion (experiments show that the first reaction goes faster than the second), then the general reaction of decomposition can be represented as a dependence of the molar fractions  $x$  of the dissociated  $\text{NH}_3$  in the following manner:



The molecular weight of the decomposition products accordingly to general reaction (17.5) is equal to:

$$\mu = \frac{96}{5 + 4x}, \quad (17.6)$$

where  $5 + 4x$  - total number of moles of the products of decomposition.

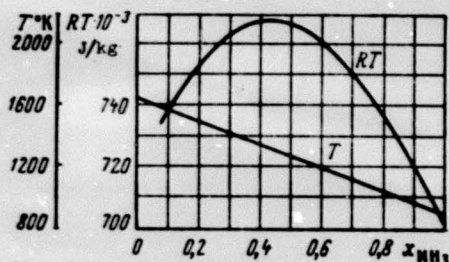


Fig. 17.7. Dependence of  $T$  and  $RT$  of the decomposition products of hydrazine depending on the dissociated fractions of  $\text{NH}_3$ .

The characteristics of hydrazine, applied as a liquid fuel in a gas generator, depend, consequently, on the quantity of dissociated  $\text{NH}_3$ . Figure 17.7 serves as an example of values of  $T$  and  $RT$  depending on  $x$ . It is wise to heed the fact that the values of  $T$  and  $RT$  in interval  $0 < x < 0.8$  change approximately by 5%, despite the fact that  $T$  with an increase in  $x$  substantially diminishes. This is caused by the fact that with the decomposition of  $\text{NH}_3$   $\text{H}_2$  is liberated and the average molecular weight diminishes at approximately the same rate  $T$  diminishes.

Certain action in the decomposition of  $N_2H_4$  can affect the design of a gas generator, enabling it to produce various times of stay.

### 17.3. Utilization of a Bipropellant

Using the same fuel in a gas-producing device and also in the basic chamber is considered the most rational approach. Bipropellant usually applied in rocket engines develop a high temperature of combustion. Its limitation other than that imposed by the basic chambers, are the conditions of the utilization of the fuel itself in the gas generators. It is obvious that the lowering of the temperature of combustion can produce a deviation from those relationships between the oxidizer and fuel whereby a maximum temperature is reached. In other words, one of components by its excess should ballast the mixed fuels and thus depress the temperature of combustion.

Figure 17.8 shows the values of the theoretical temperature of combustion and values of RT for the products of combustion of a fuel of the kerosene +  $O_{2m}$  type over a wide range of the excess oxidizer ratio  $\alpha$ . From the chart it is evident that the lowering of the temperature of the products of combustion is also attained by an excess of oxidizer ( $\alpha > 1$ ), and by an excess of fuel ( $\alpha < 1$ ); however, this lowering is not attained with the same character of change in values of T and RT in these two different ranges of  $\alpha$ .

Accordingly to Fig. 17.8 the same maximum permissible temperature of gas can be produced at a constant pressure of combustion either with small values of the excess oxidizer ratio  $\alpha$ , or with a large  $\alpha$ . In the ranges of small  $\alpha$ , there is a substantially larger specific working capacity of the gas RT, which can be explained by the low molecular weight of the products of incomplete combustion. The gas mixture, produced with a small  $\alpha$ , is a reducing medium, not harmful for the majority of materials, whereas in the composition of the products of combustion, produced with a large  $\alpha$ , there is much free active oxidizer.

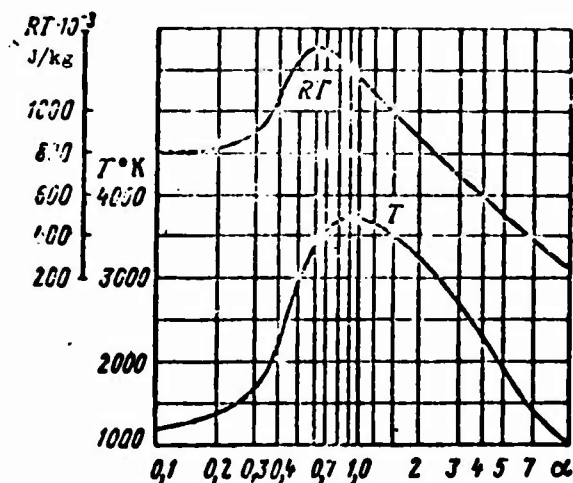


Fig. 17.8. Dependence of  $T$  and  $RT$  of the combustion products of a fuel of the kerosene + liquid oxygen type on  $\alpha$  ( $p_k = 100$  bar).

Because the prescribed proportion of fuel components (excess oxidizer ratio) is held constant only within specified limits when in operation, then with a change in  $\alpha$  fluctuations in the temperature of the gas are possible. These fluctuations can be dangerous for systems, serving as a gas generator, especially for turbine blades, and these fluctuations must be reduced to a minimum. In connection with this, it may be of interest to compare rate of change in the temperature of gas within the ranges of small and large  $\alpha$ . Considering what is specified for that or any other range of tolerance of the regulator, and having the proportion of the fuel components in the form  $\delta\kappa/\kappa = \delta\alpha/\alpha$ , we will obtain that rate of temperature change is  $\partial T/\partial \ln \alpha$ . Figure 17.9 shows the change  $[\partial T/\partial \ln \alpha]$  based on  $\alpha$  for kerosene +  $O_{2M}$  fuel. As it appears, at the same temperature and constant relative tolerance for the proportion of fuel components, the rate of temperature change is different in the range of small and large  $\alpha$ .

From this viewpoint a small  $\alpha$  is more favorable for the specified fuel, where  $[\partial T/\partial \ln \alpha]$  is less than in the range of a larger  $\alpha$ .

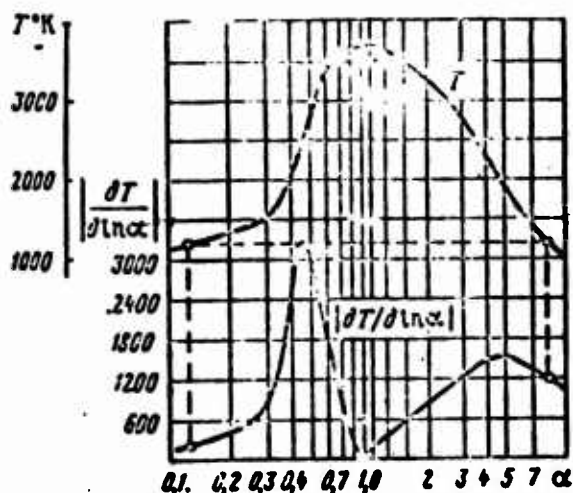


Fig. 17.9. Dependence of the rate of temperature change of the products of combustion of a fuel of the kerosene + liquid oxygen type, on  $\alpha$  ( $p_H = 100$  bar).

Thus, the generator gas produced when  $\alpha \ll 1$ , based on the examined criteria has a decided advantage. However, when selecting an actual variant ( $\alpha_{rr} \ll 1$  or  $\alpha_{rr} \gg 1$ ) it is necessary to also consider other no less important factors: necessary expenditure in schemes with afterburning, possibility of using generator gas for supercharging in both the fuel tanks, and the oxidizer tanks as well as in others.

For two-component gas generators it is better to use self-igniting fuels or make one of the components of the nonself-igniting fuel more active. However, even in this instance the organization of reliable ignition and the ensuing stable combustion with large excess of one of the components of the fuel poses serious difficulties. Therefore, apart from the diagram of direct mixing of the fuel components with the required  $\alpha$  in the zone of the nozzle head, there are other existing purposes for more reliable and more stable work of the chamber. One of possible schemes is a two-zone fuel supply into the chamber (Fig. 17.10). Here, in the zone I the fuel and oxidizer are passed through the head in a proportion reliably facilitating ignition and stable burning, i.e., close to stoichiometric. The excess of one of the components necessary for the corresponding lowering of temperature passes through the auxiliary belt in zone II.



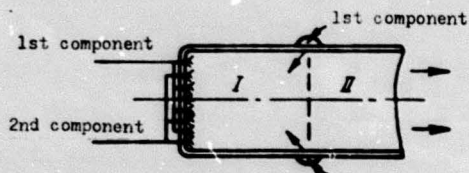


Fig. 17.10. Diagram of a two-stage fuel supply in the chamber of the gas generator.

It should be noted that the thermodynamic indexes of the generated gas using this method will be different from parameters of gas generated using the same general value  $\alpha$  in a single-stage scheme. In order to calculate a diagram with a two-stage fuel feed experimental data is required on the complex process of vaporization and on the partial combustion of the excess component, and in addition, data is required on the degree of balance of the total composition of the gas mixture. A theoretical prediction of the composition and temperature of generator gas using complex hydrocarbon fuels is difficult.

A thermodynamic calculation of the composition and temperature of the generator gas with a two-zone fuel supply in the chamber can be accomplished by assuming the following simplified diagram of the process. Since the heat of evaporation and the heat capacity supplied in the second zone of the component is usually rather great, the products of combustion of the basic fuel after its introduction are sharply cooled. The rates of the chemical reactions with the drop in temperature diminish and at certain temperature  $T_3$ , can be compared to the rate of cooling. At further cooling the composition does not change, and the final composition of generator gas is acquired as a result of the mixing of the products of combustion of the basic fuel and the vaporizing component.

As an example let us examine a possible scheme of calculating a gas generator with an overall value of excess oxidizer ratio  $\alpha_{rr} > 1$ . Pressure in the combustion chamber the value of excess oxidizer ratio in the first zone  $\alpha_1$ , temperatures  $T_3$  and  $T_{rr}$  will be considered given.

1. Based on the results of the thermodynamic calculation at a known pressure  $p_k$  let us determine the value  $\alpha_k$ , at which the equilibrium value of the temperature is equal to  $T_3$  (enthalpy of the fuel in this case is equal to deficiency  $I_{T,3}$ ). The lowering of the temperature of the products of combustion from  $T_k$  to  $T_3$  is caused by heating, evaporation and by the participation of  $v_1$  kg of oxidizer from the total quantity of  $v$  kg, supplied in the second zone. It is obvious that

$$v_1 = (\alpha_2 - \alpha_1) x_0. \quad (17.7)$$

2. In order to lower temperature of the products of combustion of a fixed composition (number of moles  $n_{i,3}$ ) from  $T_3$  up to  $T_{rr}$  for each kilogram of the mixture  $v_2$  kg of oxidizer should be evaporated. At a temperature of  $T_{rr}$  the enthalpy of the mixture amounts to

$$\frac{\sum_i n_{i,3} I_i(T_{rr})}{\sum_i n_{i,3} \mu_i}. \quad (17.8)$$

The reduction of full enthalpy of the mixture in comparison with its value at  $\alpha_2$  is equal to

$$\Delta I = I_{T,3} - \frac{\sum_i n_{i,3} I_i(T_{rr})}{\sum_i n_{i,3} \mu_i}. \quad (17.9)$$

This decrease should be compensated by the increase in complete enthalpy of the evaporated  $v_2$  kg of oxidizer:

$$\Delta I = (I_{\text{ок.газ}} - I_{\text{ок.ж}}) v_2. \quad (17.10)$$

where  $I_{\text{ок.ж}}$  and  $I_{\text{ок.газ}}$  - complete enthalpy of the liquid and evaporated oxidizer at  $T_{rr}$  in kJ/kg.

From the last equation the value  $v_2$  is found:

$$v_2 = \frac{\Delta I}{I_{\text{ок.газ}} - I_{\text{ок.ж}}}. \quad (17.11)$$

In this way, the total quantity of oxidizer, applied in the second zone per 1 kg of fuel, is equal to

$$v = v_1 + v_2(1 + \alpha_3 x_0), \quad (17.12)$$

and the general excess oxidizer ratio in gas generator amounts to

$$\alpha_{rr} = \alpha_1 + \frac{v}{x_0}. \quad (17.13)$$

The gas constant is found in the following manner. The combustion products with a molecular weight of  $\mu_3$  when  $\alpha_3$ , now consists of only a part of the generator gas. Their weight fraction is

$$g_3 = \frac{1}{1 + v_2}. \quad (17.14)$$

The weight fraction of the evaporated (and, possibly, the decomposing) oxidizer with a molecular weight  $\mu_{\text{ок.газ}}$  constitutes

$$g_{\text{ок.газ}} = \frac{v_2}{1 + v_2}. \quad (17.15)$$

The gas constant of the steam-gas mixture is equal to

$$R_{rr} = g_3 R_3 + g_{\text{ок.газ}} R_{\text{ок.газ}}, \quad (17.16)$$

where  $R_3$  - specific gas constant of the products of combustion when  $\alpha_3$ ;  $R_{\text{ок.газ}}$  - specific gas constant of the evaporated oxidizer (molecular weight  $\mu_{\text{ок.газ}}$ ).

In order to calculate a two-zone gas generator when  $\alpha_{rr} < 1$  one could use the same mode of calculation, by changing the corresponding formula (17.7), (17.11).

The deficiency of the examined method of gas generation aside from the complication of design is difficulty of obtaining a uniform field of temperatures at the exit of the chamber of the gas generator; possible local temperature peaks are harmful to the turbine blades and servomechanisms.

Based on information given in the literature for the purposes of gas generation, previously examined bipropellants, such as kerosene, ammonia, liquid hydrogen - with liquid oxygen, dimethylhydrazine, hydrazine, with nitrogen tetroxide and others, were used.

The possible diagram of a gas generator working on bipropellant of the kerosene +  $O_{2M}$  type is presented in Fig. 17.11. An auxiliary supply of kerosene in the zone of the developed combustion through the centrifugal sprayer provides the ballasting of the combustion products with the excess of kerosene.

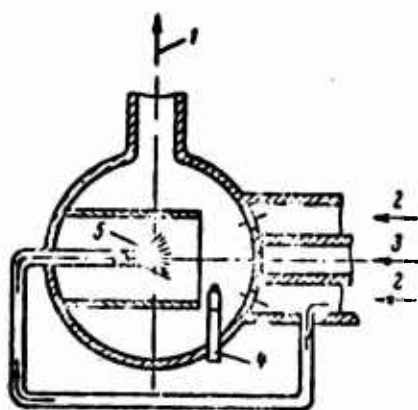


Fig. 17.11. Possible diagram of a bipropellant gas generator: 1 - exit of the gas generator gas; 2 - fuel supply; 3 - supply of oxidizer; 4 - spark plug; 5 - centrifugal sprayer.

The above-examined method of reducing the temperature of the products of combustion of bipropellants consists of ballasting the fuel rising the surplus of one of the components. The same effect of depressing the temperature, in principle, can be achieved by using as ballast the basic fuel and other substances having significant heat of evaporation and a high heat capacity, as for example, water; however, the presence of a third component is undesirable.

#### 17.4. Obtaining Steam in the Coolant Passage of the Chamber

The working medium for a turbine can be produced by the evaporation of the liquid in the coolant passage of the chamber. An open and closed scheme of producing coolant passage are distinguished.



In the closed scheme for example, water can be used. Water is fed through the cooling cavity of the thrust chamber, the water is heated, with the removal of heat from the chamber walls, and the water is converted into steam which enters the turbine. Turbine is equipped with accessories, including a water pump. The consumed steam enters the condenser where it is again converted into water. Thus, by circulating in a closed circuit, the water performs two functions: that of cooling the chamber and that of generating steam for the turbine. Saturated water vapor of the high temperature can be generated in the cooling cavity of the chamber at rather high pressures. Its parameters are determined according to the I-S diagram.

The closed system of producing steam in coolant passage is complex and is characterized by considerable weight and over-all size; possible leakages are very dangerous inasmuch as the water supply is limited. The utilization of such a system can be rational only for engines of large thrust.

Open scheme of producing steam in coolant passage does not provide for the circulation of the same working medium in a closed circuit. Because the ejection consumed steam behind the turbine is too uneconomical, schemes with the supply of steam from turbine into the combustion chamber is proposed. If the steam is produced from the fuel component, then its combustion takes place together with the second component in the combustion chamber. In the latter case, just as in the scheme with after burning, the system is characterized by high economy.

In scheme of the American RL-10A liquid-fuel rocket engine (Fig. 17.12), operating on hydrogen and oxygen, the liquid hydrogen enters the cooling cavity of the chamber 3 at  $T = 20^\circ\text{K}$ , and then following evaporation and preheating, is guided to turbine 2. Behind the turbine,  $\text{H}_2$  is used as a combustible component in the combustion chamber. The turbine in this scheme operates on a gas of a very low temperature ( $\approx 200^\circ\text{K}$ ); however, the adiabatic work of the expansion of the hydrogen is considerable as a result of the large value of the gas constant.

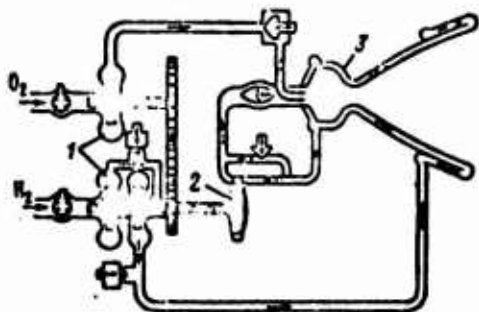


Fig. 17.12. Diagram for generating steam in coolant passage of a RL-10A liquid-fuel rocket engine (USA).

If the power of turbine  $N_m$  which is required for auxiliary systems is not very great, then quantity of heat  $Q$ , which must be removed from the coolant passage, is also insignificant. It turns out, in particular, the less heat need be removed, from walls for the reliable cooling of the chamber.

#### 17.5. Thermodynamic Efficiency of the Various Methods of Gas Generation

The most important indexes of a flight vehicle depend to a large degree on the efficiency of the system of gas generation. For this vehicle a system of gas generation can be considered most effective, which provides the necessary work  $L_z$  while possessing the least weight  $G_{gr}$ . Consequently, the value,  $L_z/G_{gr}$  can be the criterion of the efficiency of the system. Value of the criterion of the efficiency of the various methods of gas generation substantially depends on  $L_{ad}$  and  $(RT)_{gr}$ . The latter can be called the criteria of thermodynamic efficiency. Figure 17.13 presents tentative values of  $(RT)_{gr}$  and  $T_{gr}$  using various methods of gas generation (pressure of 100 bar). These results are produced by thermodynamic design assuming chemical equilibrium.

The following methods of producing generator gas (ordinal numbers correspond to meanings on the charts) are examined.

1. Combustion of the fuel  $H_{2w} + O_{2w}$  with a large  $\alpha = 9.0-7.0$ .
2. Combustion of the fuel,  $H_{2w} + O_{2w}$  with a small  $\alpha = 0.05-0.1$ .

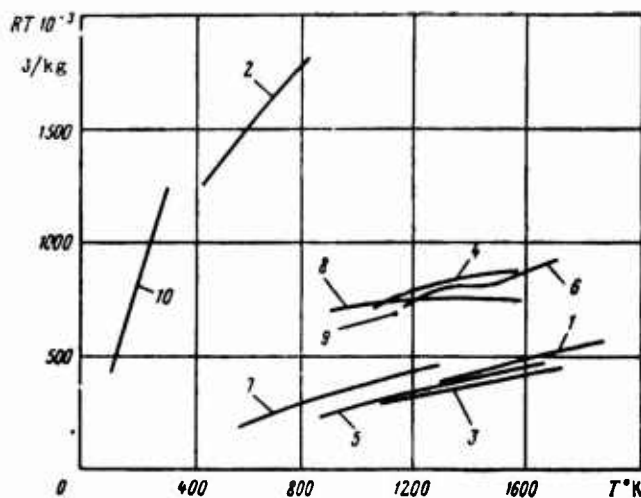


Fig. 17.13. Thermodynamic efficiency of various methods of gas generation.

3. Combustion of the fuel the kerosene +  $O_{2H}$  type with a large  $\alpha = 10-6$ .

4. Combustion of the fuel of the kerosene +  $O_{2H}$  type with a small  $\alpha = 0.05-0.3$ .

5. Combustion of the fuel, asymmetrical dimethylhydrazine + nitrogen tetroxide with a large  $\alpha = 10-4.5$ .

6. Combustion of the fuel, asymmetrical dimethylhydrazine + nitrogen tetroxide with a small  $\alpha = 0.01-0.3$ .

In cases 1-6, the temperature and working capacity of the generator gas change depending on  $\alpha$ .

7. Decomposition of hydrogen peroxide in the presence of a solid catalyst; the range of concentrations 0.7-1.0.

8. Decomposition of hydrazine; the mole fraction of the dissociated ammonia, 0.1-1.0.

9. Decomposition of asymmetrical dimethylhydrazine.

10. Heating and evaporation of hydrogen in coolant passage of the chamber.

It should be noted that the criteria of thermodynamic efficiency do not completely characterize the perfection of the methods of gas generation; however, they are used as a generalized estimate.

#### Bibliography

1. Alemasov V. Ye., IVUZ, ser. "Aviatsionnaya tekhnika", 1965, vyp. 1.
2. Zhidkiye i tverdye raketnyye topliva, (Liquid and hard rocket propellants), collection of translations, IIL, 1959.
3. Protsessy goreniya (Processes of combustion), collection of articles, Fizmatgiz, 1961.
4. Hopmann H., Luftfahrttechnik-Raumfahrttechnik, 1967, No. 6.
5. Space Aeronautics, 1961, No. 1.

## CHAPTER XVIII

### CALCULATION OF THE BASIC PARAMETERS OF AN ENGINE

The procedure for calculating an engine may be formulated, for example, in the following manner: the engine design, which develops a thrust in a vacuum  $P_{\Pi}$  at a pressure at the head of  $p_1$  and on the exit from the nozzle,  $p_c$ . The fuel components, their proportion  $\kappa$  and the theoretical diagram of the distribution  $\kappa$  according to the cross section of the combustion chamber are prescribed.

In this chapter the procedure for determining the specific thrust, fuel consumption sizes of the chamber are considered. For engines with generator gas ejection or with a pressurized supply system losses should be considered, connected with the additional expenditure of the working medium for the supply of components in the thrust chamber. For the case of generator gas afterburning in the basic chamber a scheme is examined for calculating the connection between the pressure in the combustion chamber and the parameters of the channel from the inlet into the pumps to the combustion chamber.

#### 18.1. Determination of Actual Specific Thrust and Second Fuel Expenditure in Seconds

The thermodynamic calculation of a given fuel with several values for the proportion of components  $\kappa_1$  at a specified  $p_1$  and  $p_c$  provides values of  $P_{yд.п 1}$ , complexes of  $\beta_1$  and other required parameters.

After that, the relative area of the combustion chamber  $f_K$  should be determined, and the thermodynamic calculation should again be made, in order to take into account the difference between  $p_K^*$  and  $p_1$ , if  $f_K < 5-6$  (see § 10.5).

Subsequently, we will consider the data of the thermodynamic calculation obtained by the calculation of the pressure drop in the high-speed combustion chamber.

The effect of the heterogeneous distribution of the proportion of components based on the cross section of the combustion chamber, on the theoretical values of specific thrust and of complex  $\beta$  is taken into account according to the formula in Chapter XI:

$$P_{yA.n.t} = \sum_i g_i P_{yA.n.t.i}; \quad \beta_t = \sum_i g_i \beta_{t.i}$$

The actual specific thrust in a vacuum

$$P_{yA.n} = \varphi_{yA} P_{yA.n.t} \quad (18.1)$$

is determined on the basis of specific thrust efficiency  $\phi_{yA}$ , reflected by the imperfection of the processes in the combustion chamber and nozzle, since

$$\varphi_{yA} = \varphi_p \varphi_c \quad (18.2)$$

Coefficient  $\phi_c$ , which takes into account the various types of losses in the nozzle, can be determined by methods given in Chapter XII. Coefficient  $\phi_p$ , which takes into account the imperfection of the process in the combustion chamber, is usually selected on the basis of statistical data obtained during industrial or experimental testing of samples similar to the developed engine.

In the experiment the value,  $\phi_{yA}$ , can be reliably determined. The value  $\phi_p$  can be obtained as

$$\varphi_{p_k} = \frac{\varphi_{v1}}{\varphi_c}, \quad (18.3)$$

where  $\varphi_c$  is determined by a calculated method.

By another method of the experimental determination of the coefficient,  $\varphi_{p_k}$ , a comparison can be made of the expert and theoretical values of complex  $\beta$  (see § 16.2). As has been mentioned, the value of the coefficient of pressure  $\varphi_{p_k}$  amounts to 0.96-0.99.

Thus on the basis of the results of the thermodynamic calculation and experimental-theoretical coefficient of perfection of the processes the actual specific thrust of the chamber of the engine can be determined.

The fuel consumption in seconds, necessary to produce the prescribed thrust, can be found as

$$G = \frac{P_n}{P_{y_{\text{max}}}}. \quad (18.4)$$

## 18.2. Determination of the Chamber Size

### Combustion Chamber

The cylindrical combustion chamber is the most common form. One of the basic advantages is its simplicity of manufacture. Let us examine the determination of the three basic dimensions - diameter  $d_k$ , lengths  $L_k$  and the diameter of the critical cross section of nozzle  $d_{kp}$ .

The volume and diameter of the combustion chambers are determined on the basis of two characteristics - the time of stay and the specific weight flow. The relationship between  $\tau_{\Pi}$  and the given length of the combustion chamber  $L_{\Pi p}$  (16.12) can also be used.

In the expression for complex  $\beta$

$$\beta = \frac{V R_k T_k^*}{A(n)}$$

since the value  $n$  is equal to 1.2, then it is valid for many liquid fuels. Then, from formula (16.12) we will obtain a convenient relationship:

$$\tau_n = 2.4 \frac{L_{np}}{\beta}, \quad (18.5)$$

where  $\beta$  is in m/s.

The volume of the combustion chamber is determined, based on the requirement guaranteeing the time of stay to be sufficient to achieve the necessary completeness of combustion. As was previously mentioned, the optimum value of the time of stay (or given length) depends on the grade of fuel. The value  $L_{np}$  for certain fuels is presented in Chapter XVI.

In order to determine the area of the critical cross section, let us resort to the formula of consumption taking into account the combustion efficiency and the discharge coefficient:

$$G = \frac{p_k F_{kp}}{\beta_k \varphi_k} \mu_c \mu_{\Delta\Phi}, \quad (18.6)$$

where  $\mu_c$  - discharge coefficient which takes into account the displacement of the thickness of the boundary layer and the heterogeneity of the velocity field in critical cross section (see § 12.5);  $\mu_{\Delta\Phi}$  - discharge coefficient which takes into account the delay of the condensate according to the rate and temperature with acceleration of the two-phase products of combustion.

For the homogeneous products of combustion,  $\mu_{\Delta\Phi} = 1$ ; in the case of two-phase products this coefficient is greater than unity and can be determined, as shown in § 13.2.



Thus, from the expression (18.6) taking into account the earlier given formula we will obtain a value of the area of critical cross section of the nozzle

$$F_{kp} = \frac{P_{c3t}}{\mu_c \mu_{\Delta\phi} P_{\kappa}^* P_{\gamma \Delta, n} t \Psi_c}. \quad (18.7)$$

From formula (18.7) it is evident that the increase in losses in the nozzle requires an enlargement in the area of critical cross section in order to pass on the additional consumption compensating for the reduction in the specific thrust. The losses in the combustion chamber ( $\phi_{p_{\kappa}}$ ) do not affect the value,  $F_{kp}$ .

After the determination of  $L_{np}$  and  $F_{kp}$  the combustion volumes which provide the necessary time of stay are found.

When selecting the diameter of the combustion chamber or  $f_{\kappa}$  one should consider that the decrease in  $f_{\kappa}$  increases the convective heat flux and hampers the cooling of the combustion chamber, diminishes pressure  $p_{\kappa}^*$  and therefore increases the over-all sizes of the nozzle at a prescribed  $p_c$ , hampers the positioning of the sprayer on the head of the combustion chamber as well as the layout of the atomization and the mixing of the components. The positive result of the decrease in  $f_{\kappa}$  is the lowering of the weight of the combustion chamber.

In practice when selecting the diameter of the combustion chamber can be oriented to the values of the specific weight flow, attained while developing prototypes or the experimental engine.

According to expression (16.14) the relative area of the combustion chamber can be written as:

$$f_{\kappa} = \frac{1}{\frac{G_F}{P_{\kappa}}}. \quad (18.8)$$

Thus, for instance, for an oxygen engine with values of complex

$\beta \approx 2 \cdot 10^3$  m/s and  $G_F/p_K^* = 1.3 \cdot 10^{-4}$  kg/N·s, the amount of relative area of the combustion chamber can be accepted as being equal to

$$f_K = \frac{1}{1.3 \cdot 10^{-4} \cdot 2 \cdot 10^3} \approx 4.$$

It is quite clear that the above given estimates can change depending on the accepted scheme of carburetion, and on scheme of the engine. For example, in the scheme with the afterburning of the generator gas in the basic combustion chamber, the process of vaporization and mixing of the components will be substantially different from that in the scheme without the afterburning, when both components enter the combustion chamber as liquid.

Thus, the diameters of the combustion chamber and of the critical cross section are determined. It is easy to determine the length of the combustion chamber based on its known volume, or based on  $L_{np}$  and the diameter.

#### The Nozzle

With known values of the diameters of the combustion chamber and of the critical cross section, the subsonic part of the nozzle can be profiled in accordance with the recommendations in Chapter XII.

The basis for selecting the supersonic part of the nozzle are the thrust characteristics of the nozzle, an example of which was also covered in Chapter XII (see Fig. 12.11).

The rated value  $p_c$  determines the relative area  $f_c$  and radius  $\bar{r}_c$  of the section of the nozzles.

If limitations are not imposed on the over-all sizes and lateral surface (weight) of the supersonic part of the nozzle then a contour which lies at the point of contact of line  $K_{p\pi} = \text{const}$ , and  $\bar{r}_c = \text{const}$ , is derived.

### 18.3. Calculation of an Engine Without the Afterburning of the Generator Gas

In engines built according to the scheme without afterburning of the generator gas, the specific thrust is reduced due to the low efficiency of the expansion of the low-temperature generator gas behind the turbine with a pump supply system, and as a result of the considerable residues of gas in the tanks - with a pressurized system.

The sum total expenditure of auxiliary or basic fuel, necessary to accomplish the sum total of work of supply system  $L_{\Sigma}$ , is equal to

$$G_{a,\tau} = \frac{L_{\Sigma}}{L_{y\Delta}\eta}, \quad (18.9)$$

where  $L_{y\Delta}$  - theoretical specific work, which can produce 1 kilogram of working medium of the supply system, in J/kg;  $\eta$  - efficiency of utilization of the working medium in the system.

Under the condition of constancy of consumption based on the time, the required consumption of auxiliary fuel in seconds amounts to

$$G_a = \frac{G_{a,\tau}}{\tau}, \quad (18.10)$$

where  $\tau$  - time of work of the system of gas generation in s.

The relative consumption of auxiliary fuel is equal to

$$\epsilon = \frac{G_a}{G_i} = \frac{L_{\Sigma}}{L_{y\Delta}\eta\tau G_i}. \quad (18.11)$$

Let us examine the expression for the relative consumption  $\epsilon$  in two typical cases of the utilization of generator gas: turbopump and pressurization systems of fuel supply.

## Turbopump Fuel Supply

The required sum total of work in this instance amounts to

$$L_z = N_r \tau, \quad (18.12)$$

where  $N_r$  - power of the turbine, necessary to drive the pumps and various units, in W.

Theoretical specific work of the generator gas when using it in the turbine is equal to the adiabatic work of expansion

$$L_{zs} = \frac{n}{n-1} (RT)_{rr} \left[ 1 - \left( \frac{p_{BHX}}{p_{BX}} \right)^{\frac{n-1}{n}} \right], \quad (18.13)$$

where  $(RT)_{rr}$  - specific working capacity of the generator gas at the inlet of the turbine, in J/kg,  $p_{BX}$ ,  $p_{BHX}$  - pressures at the inlet and outlet of the turbine.

The sum total consumption of the auxiliary fuel is equal to

$$G_{a,r} = \frac{N_r \tau}{L_{zs} \eta_r}. \quad (18.14)$$

where  $\eta_r$  - overall efficiency of the turbine.

The relative consumption of the auxiliary fuel amounts to

$$\epsilon = \frac{N_r}{GL_{zs} \eta_r}. \quad (18.15)$$

If the turbine drives only the fuel pumps, then its power must be equivalent the sum of the power of the fuel pumps and the oxidizer:

$$N_r = N_{a,r} + N_{a,ox} \quad (18.16)$$

The power of the pumps can be calculated by the formula:

$$\left. \begin{aligned} N_{н.г} &= \frac{G_r \Delta p_{под.г}}{Q_r \eta_{н.г}}, \\ N_{н.ок} &= \frac{G_{ок} \Delta p_{под.ок}}{Q_{ок} \eta_{н.ок}}, \end{aligned} \right\} \quad (18.17)$$

where  $\Delta p_{под} = p_{под} - p_{вх.н}$  - pressure of the pump in  $N/m^2$ ;  $p_{вх.н}$  - pressure at the inlet of the pump.

The required pressure of the feed pump  $p_{под}$  is determined taking into account the losses in pressure in the injection head, in the coolant passage as well as in the main feed lines:

$$p_{под} = p_1 + \Delta p_{\phi} + \Delta p_{ох} + \Delta p_{mag}. \quad (18.18)$$

In order to simply clarify the fundamental dependences, let us take

$$\Delta p_{под.г} = \Delta p_{под.ок} = \Delta p_{под}$$

and

$$\eta_{н.г} = \eta_{н.ок} = \eta_n.$$

Then, equation (18.16) can be presented in the form

$$N_{\tau} = \frac{\Delta p_{под}}{\eta_n} \left( \frac{G_r}{Q_r} + \frac{G_{ок}}{Q_{ок}} \right). \quad (18.19)$$

Since

$$\frac{G_r}{Q_r} + \frac{G_{ок}}{Q_{ок}} = \frac{G}{Q_{\tau}},$$

then, expression (18.19) can be rewritten as:

$$N_{\tau} = \frac{\Delta p_{под} G}{\eta_n Q_{\tau}}. \quad (18.20)$$



By substituting expression (18.20) in the formula (18.15), we will obtain:

$$\epsilon = \frac{\Delta p_{\text{pod}}}{L_{\text{sa}} Q_T \eta_T \eta_H} \quad (18.21)$$

or

$$\epsilon = \frac{\Delta p_{\text{pod}}}{L_{\text{sa}} Q_T \eta_{\text{THA}}}, \quad (18.22)$$

[Translator's note: THA = TNA = turbopump]

where  $\eta_{\text{THA}} = \eta_T \eta_H$  - efficiency of the turbopump unit.

As can be seen from formula (18.22), the relative consumption of the auxiliary fuel increases proportionally to  $\Delta p_{\text{pod}}$  and it diminishes with an increase in the adiabatic work of expansion, density of the fuel and efficiency of the turbopump unit.

The value  $\epsilon$  is used to determine the specific thrust of the engine and it usually amounts to 0.01-0.05. The smaller values belong to engines of greater thrust and less pressure  $p_1$ .

#### Forced Fuel Feed

The work, necessary to displace fuel from the tanks, by volume  $V_0$  at pressure  $p_0$ , amounts to

$$L_s = p_0 V_0. \quad (18.23)$$

The theoretical specific work of 1 kilogram of generator gas or any other gas of specified parameters is equal to

$$L_{\text{TA}} = (pV)_{\text{TA}} = (RT)_{\text{TA}}. \quad (18.24)$$

The sum total consumption of auxiliary fuel, necessary to produce work  $L_{\Sigma}$ , amounts to

$$G_{\text{a.t}} = \frac{p_0 V_0}{(RT)_{\text{TA}} \eta_{\text{sa}}}, \quad (18.25)$$

and consumption in seconds,

$$G = \frac{p_0 V_0}{\tau (RT)_{rr} \eta_{b.n}}, \quad (18.26)$$

where  $\eta_{b.n}$  - coefficient of thermal losses in a forced feed system (in a section of the gas generator or storage battery-tanks).

The value of this coefficient, is equal to

$$\eta_{b.n} = \frac{(RT)_0}{(RT)_{rr}}, \quad (18.27)$$

which one usually determines experimentally. For a preliminary estimate it can be taken as equal to 0.2-0.4.

In accordance with formula (18.11) the relative consumption of the auxiliary fuels can be determined as:

$$\epsilon = \frac{p_0 V_0}{\tau G (RT)_{rr} \eta_{b.n}}.$$

Inasmuch as

$$G\tau = G_r$$

and

$$\frac{G_r}{V_0} = Q_r,$$

then

$$\epsilon = \frac{p_0}{(RT)_{rr} Q_r \eta_{b.n}}. \quad (18.28)$$

A comparison of the dependences, (18.22) and (18.28), shows in principle, the same factors also have an effect on the relative consumption of the auxiliary fuel in the force feed systems and in the turbopump fuel supply. The most important characteristic,



specifically, is the specific work of the gas  $L_{ad}$  or  $(RT)_{rr}$ . The greater this value, the less the consumption of fuel (basic or auxiliary) for supplying the components.

#### 18.4. Calculation of an Engine with Afterburning of the Generator Gas in the Basic Chamber

Schemes for engines with afterburning of the generator gas in the basic chamber are presented in Chapter I.

Let us examine conclusively the variant with an oxidizing gas generator, when all of the oxidizer of the engine device and part of the fuel is passed through it. The proportion of components entering the gas generator, is determined by maximum temperature  $T_{rr}$ , permissible under operating conditions of the blades of the TNA turbine. On the basis of the calculated or experimental data the relationship  $\kappa_{rr}$  is determined, whereby the parameters of the products of gas generation consist of:  $T_{rr}$ ,  $(RT)_{rr}$ ,  $n$ .

If the overall proportion of components in the engine device is equal to  $\kappa$ , then it is easy to show that portion of fuel passing through the gas generator, amounts to

$$g_{rr} = \frac{a_{rr}}{G} = \frac{1 + \frac{1}{\kappa_{rr}}}{1 + \frac{1}{\kappa}}. \quad (18.29)$$

In this case the portion of fuel passing through the gas generator, is equal to  $\kappa/\kappa_{rr}$ .

It is obvious that in the engine with afterburning the losses in specific thrust, associated with the supply of components in the combustion chamber are absent. Therefore, an increase in the pressure in the combustion chamber, resulting in an increase in losses of specific thrust in the scheme without afterburning in accordance with formula (18.18) and (18.22), is not associated with an increase in losses here. The attainable level of pressure  $p_1$  depends on the



power engineering of the generator gas, its temperature and parameters of the engine. Let us determine this dependence.

Let the pressure losses during the motion of components from the pumps to the gas generator (in the cavity of cooling, on the sprayers of the gas generator, in the feed mains) constitute  $\Delta'p_{rr}$ , pressure losses along the way of the gas from the exhaust of the turbine into the combustion chamber (in the flue, in the gas sprayers of the head of the combustion chamber) -  $\Delta''p_{rr}$ .

Let us write down the equation of the balance of power (18.16) taking into account formulas (18.13) and (18.17):

$$G_{rr} \eta_r \frac{n}{n-1} (RT)_{rr} \left[ 1 - \left( \frac{p_{mx}}{p_{bx}} \right)^{\frac{n-1}{n}} \right] = \frac{G_r (p_{noz,r} - p_{bx,r})}{Q_r \eta_{h,r}} + \frac{G_{ok} (p_{noz,ok} - p_{bx,ok})}{Q_{ok} \eta_{h,ok}}. \quad (18.30)$$

Let us assume for simplicity that in this examined case the pressure of the fuel pump and oxidizer pump are also identical, and, in addition, the hydraulic losses from the pump to the gas generator are the same:

$$\Delta'p_{rr,ok} = \Delta'p_{rr,r} = \Delta'p_{rr}, \quad (18.31)$$

inlet pressure in the fuel pump and oxidizer pump are identical:

$$p_{bx,h,ok} = p_{bx,h,r} = p_{bx,h}.$$

Let us also assume that efficiency of the turbine  $\eta_T$  and the pump  $\eta_H = \eta_{H,r} = \eta_{H,ok}$ , the characteristics of the generator gas  $(RT)_{rr}$  and  $n$ , the amounts of losses  $\Delta'p_{rr}$ ,  $\Delta''p_{rr}$  and  $p_{bx,h}$  are constant and do not depend on the parameters of operation of the device. Having noted that

$$p_{mx} = p_1 + \Delta''p_{rr};$$

$$\delta = \frac{p_{\text{ex}}}{p_{\text{max}}} = \frac{p_{rr}}{p_1 + \Delta'' p_{rr}};$$

$$p_{\text{noA}} = p_{rr} + \Delta' p_{rr} = \delta (p_1 + \Delta'' p_{rr}) + \Delta' p_{rr},$$

let us write down the expression (18.30) in the following form:

$$G_{rr} \eta_r \frac{n}{n-1} (RT)_{rr} \left( 1 - \frac{1}{\delta^{\frac{n-1}{n}}} \right) =$$

$$= \frac{G}{Q_r} \frac{\delta (p_1 + \Delta'' p_{rr}) + \Delta' p_{rr} - p_{\text{ex},n}}{\eta_n}. \quad (18.32)$$

Hence, pressure  $p_1$ , attainable at selected parameters  $\kappa_{rr}$ ,  $(RT)_{rr}$ ,  $\delta$ , the hydraulic characteristics of main feed lines and efficiency TNA can be found:

$$p_1 = g_{rr} \eta_{\text{TNA}} Q_r \frac{n}{n-1} (RT)_{rr} \left( 1 - \frac{1}{\delta^{\frac{n-1}{n}}} \right) \frac{1}{\delta} -$$

$$- \Delta'' p_{rr} + \frac{1}{\delta} p_{\text{ex},n} - \frac{1}{\delta} \Delta' p_{rr}. \quad (18.33)$$

The majority of parameters, which influence the value  $p_1$ , are defined as certain maximum permissible parameters. Such a temperature is  $T_{rr}$  and the value  $(RT)_{rr}$  associated with it, and also the losses in pressure and  $\eta_{\text{TNA}}$ . The controlling amount selected by design, is the pressure drop, achieved in the turbine.

Let us examine, as how to select the optimum value  $\delta$ , supplying the maximum pressure in the combustion chamber.

Let us designate

$$B = g_{rr} \eta_{\text{TNA}} Q_r \frac{n}{n-1} (RT)_{rr}$$

and let us rewrite expression (18.33) in the following form:

$$p_1 = (B - \Delta' p_{rr} + p_{\text{ex},n}) \frac{1}{\delta} - \frac{B}{\delta^{\frac{2n-1}{n}}} - \Delta'' p_{rr}. \quad (18.34)$$



In order to determine the greatest possible pressure in the combustion chamber  $p_{1\max}$  let us take the derivative  $dp_1/d\delta$  and let us equate it to zero:

$$\frac{dp_1}{d\delta} = -\frac{(B - \Delta' p_{\Gamma\Gamma} + p_{\text{ex},n})}{\delta^2} + B^{\frac{2n-1}{n}} \frac{1}{\delta^{\frac{2n-1}{n}}} = 0.$$

From this let us find the value of the optimum pressure differential

$$\delta_{\text{opt}} = \left( \frac{B}{B - \Delta' p_{\Gamma\Gamma} + p_{\text{ex},n}} \frac{2n-1}{n} \right)^{\frac{n}{n-1}}. \quad (18.35)$$

By substituting value  $\delta_{\text{opt}}$  in expression (18.34), let us find  $p_{1\max}$ .

Thus, in the engine of the examined scheme a pressure not higher than  $p_{1\max}$  can be realized. The principles for the selection of optimum pressure  $p_1$  taking into account its effect on the parameters of the flight vehicle are covered in Chapter XXI.

### Bibliography

1. Dobrovol'skiy M. V., Krylov Yu. V., Izvestiya VUZov, ser. "Mashinostroyeniye", 1967, No. 4.
2. Dvigatel'nyye ustanovki raket na zhidkom toplive (Rocket engines operating on liquid fuel), collection of translations, izd-vo "Mir", 1966.
3. Peters R. L., Design of Liquid, Solid and Hybrid Rockets, Hayden Book Co, New-York, 1965.

## CHAPTER XIX

### CHARACTERISTICS AND THRUST-VECTOR CONTROL

In this chapter the operational characteristics of a liquid-fuel rocket engine - the altitude performance and consumption are examined, the basic means of thrust-vector control are described.

#### 19.1. Preliminary Information

The dependences of thrust and of specific thrust on the basic changing factors in operation are called the characteristics of a rocket engine, including liquid-fuel rocket engine. The external factors are the pressure of surrounding medium and the velocity of motion of the apparatus, the internal factors - fuel consumption in seconds and the proportion of fuel components.

As was previously noted in Chapter II, deviations diagrammed pressures along external surface of the chamber from value  $p_h$ , which is governed by the change in the velocity of the apparatus, is accepted with reference to its resistance, but not to the thrust of the engine. Therefore, the thrust and specific thrust of a liquid-fuel rocket engine should be considered independent of the velocity of motion of the apparatus.

In Chapter X the dependence of specific thrust on the proportion of the fuel component (excess oxidizer ratio  $\alpha$ ) was examined. However, a change in  $P_{yd}$  and consequently,  $P$  owing to  $\alpha$  usually do not apply in operation, by holding  $\alpha$ , it is difficult to obtain a wide range of adjustment, and secondly, the deviation of  $\alpha$  from



a certain optimum value results in a lowering of the economy.

Thus, the two operational characteristics of a liquid-fuel rocket engine have practical value.

1. Dependences of the thrust and of specific thrust on the pressure of surrounding medium with constants of fuel consumption in seconds  $G$  and excess oxidizer ratio  $\alpha$  (under constant operating conditions of the engine). In the utilization of the engines of flight vehicles, such a characteristic is usually called the altitude performance, inasmuch as the atmospheric pressure is uniquely associated with height.

2. The dependences of thrust and of specific thrust on the fuel consumption in seconds,  $G$ , at constant fuel compositions ( $\alpha$ ) and the pressure of the surrounding medium (height). This characteristic is called consumption.

Strictly speaking, the thrust and specific thrust during the operation of a liquid-fuel rocket engine also depends on other factors. For example, a change in the acceleration of flight and of the inertial forces governed by it is expressed in many parameters of the fuel system and the gas generator and can influence the final indexes:  $P$  and  $P_{y\Delta}$ . The change in temperature of surrounding medium, regularities of emptying the tanks, and so forth hold significances. However, effect of such factors in comparison with the singled out basic factors (consumption in seconds  $G$ , pressure of surrounding medium  $p_h$ ) is secondary, and the complex quantitative estimate of this effect is possible for a real engine and apparatus, when the trajectory of flight, the characteristics of the power supply and control systems and others are known in detail. During the stage of preliminary calculation and design they are usually limited by the aforementioned basic dependences.

The characteristics of the chamber and of the engine can be distinguished. The characteristics of the engine can be distinguished from the characteristics of the chamber, if there is auxiliary fuel

consumption in the system of the gas generator ( $\epsilon > 0$ ). The characteristics of multichamber engines are a sum total of characteristics of the individual chambers, utilized in a specified combination.

The characteristics of the chamber can be calculated according to equations

$$P_{ya} = \varphi_{ya} P_{ya.n.t} - \frac{F_c p_h}{G} \quad (19.1)$$

and

$$P = \varphi_{ya} F_{ya.n.t} G - F_c p_h. \quad (19.2)$$

For a chamber with a constant geometry ( $F_c, f_c = \text{const}$ ) the values of  $P_{ya.n.t}$  and  $\varphi_{ya}$  in these equations are taken as constants under all conditions. This assumption in the calculation, does not result in an error of more than 1-3%.

When calculating the altitude performance of a sole variable in the expressions (19.1) and (19.2) it is  $p_h$ ; when calculating the consumption characteristic, the sole variable -  $G$ . If both variables are varied within possible range, we will obtain a family of characteristics of the given chamber. One of the forms of presenting such a family of characteristics is included in the values presented in Fig. 19.1.

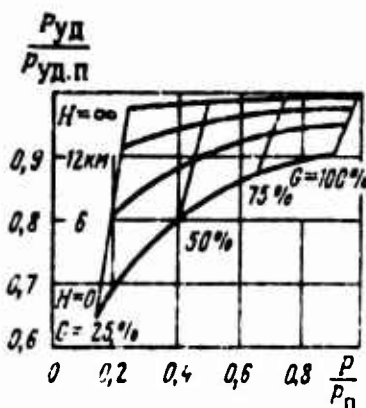


Fig. 19.1. A family of characteristics of a liquid-fuel rocket engine.

## 19.2. Altitude Characteristic

In order to calculate the altitude characteristic the dependence of atmospheric pressure on altitude  $p_h = f(H)$  must be known. It is usually assumed based on the standard atmosphere (SA).

Because the altitude characteristic is calculated with  $G = \text{const}$ , a change in thrust and specific thrust based on  $p_h$  (or based on  $H$ ) has an identical character. If we plot the altitude characteristic in relation to the value  $P_{yA}/P_{yA.n}$ ,  $P/P_n$ , then both dependences are represented as a single straight line in function  $p_h$  or as a single curve in function  $H$ .

Below a form of the characteristic, traditional for engines of flight vehicles is examined.

Figure 9.2 shows the altitude characteristic of two chambers, operating under identical conditions, but having different relative cross-sectional areas of the nozzle  $f_c$  ( $f_{c1} = 10$ ,  $f_{c2} = 50$ ). Chamber 2 at low altitudes operates under conditions of overexpansion with the separation of flow inside of nozzle (point A on curve 2 - beginning of separation, dotted line - hypothetical continuous characteristic). The values of thrust and of specific thrust during the separation of flow are determined according to recommendations in § 2.3.

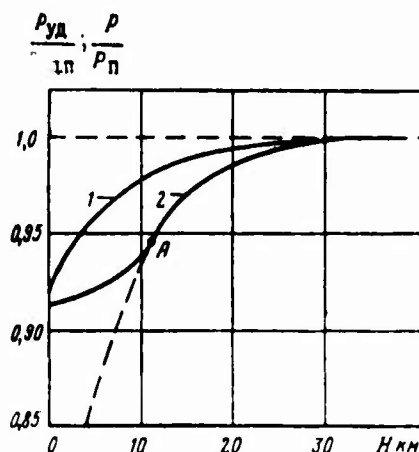


Fig. 9.2. Altitude characteristic of the chambers. The fuel is the kerosene +  $O_{2x}$  type;  $p_k = 100$  bar.

It would be interesting to evaluate the relative increment of thrust, and consequently, the specific thrust within the range of the earth ( $p_h = p_0$ ) - vacuum ( $p_h = 0$ ). This amount constitutes

$$\Delta P = \frac{P_c - P}{P_c} = \frac{f_c P_c}{P_c} = \frac{f_c}{P_c} P_c$$

As it appears in Figs. 19.3 and 19.4, the increment  $\Delta P$  increases for chambers with a large  $f_c$ , and with  $f_c = \text{const}$  - under reduced conditions (small  $p_K^*$  or consumptions).

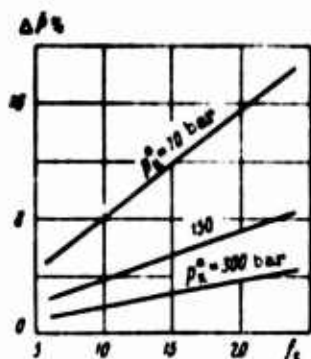


Fig. 19.3.

Fig. 19.3. Dependence of increment  $\Delta P$  on  $f_c$ : fuel  $C_2H_8N_2 + N_2O_4$ ;  $\alpha = 0.8$ .

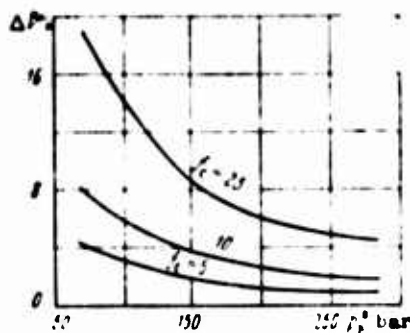


Fig. 19.4.

Fig. 19.4. Dependence of increment  $\Delta P$  on  $p_K^*$ ; the fuel is the same as that in Fig. 19.3.

As is known a nozzle of constant geometry has only one optimum range ( $p_c = p_h$ ): within other ranges its characteristic worsen. In order to maintain the optimum range with an increase in the altitude of the flight area, the cross section of the nozzle should continuously increase. Figure 19.5 shows the altitude characteristic of the chamber with that sort of an ideally adjusted nozzle ( $P_{уд.ид}$ ). The same dependence,  $P_{уд} = f(H)$  is presented for two chambers with various  $f_c$ . Obviously, that the first step to the adjustment by



height  $P_{yd}$  (and consequently,  $P$ ) can be the utilization of the two-position nozzle 2, the cross-sectional area of which changes in steps at the height of  $H_{\text{перекл}}$ . The advantages of a two-position nozzle over nozzle 1 are evident in the range  $H > H_{\text{перекл}}$ , and the advantages over nozzle 3 - in the range  $H < H_{\text{перекл}}$ . There are known attempts to realize a two-position nozzle with the aid of a sliding skirt of the nozzle (for example, the RL-20 American liquid-fuel rocket engine), having removable inserts, and others.

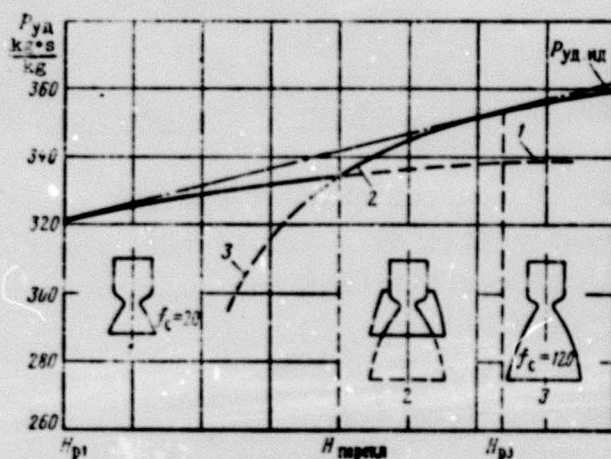


Fig. 19.5. The altitude characteristic of a chamber with a two-position nozzle.

[Translator's note:  $H_{\text{перекл}} = H_{\text{projected}}$ ].

The above presented dependences are with reference to chambers with Laval nozzles. Ring nozzles of external expansion (see Fig. 12.8k) or with a central plate-like body (see Fig. 12.8e) have considerably better characteristic under conditions of over-expansion, including the separation of flow inside the nozzle. Under such conditions these nozzles possess a known degree of self-regulation. The so-called aerodynamic nozzle (see Fig. 12.8l) approaches the ideally adjustable nozzle over a wide range of altitudes. Figure 19.6 as an example is presented for a comparison of the altitude characteristics of chambers with an aerodynamic nozzle (1) and with a fixed area Laval nozzle (2).

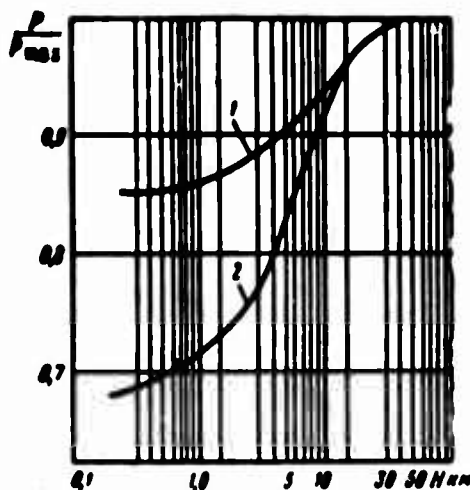


Fig. 19.6. Altitude characteristic of the chambers with various nozzles.

### 19.3. Consumption Characteristic

The throttle or control characteristics are also called the consumption characteristic of a liquid-fuel rocket engine, emphasizing that it reflects capabilities for adjusting the amount of thrust.

According to equations (19.1) and (19.2) the elements of theoretical consumption characteristic of the chamber with constant geometry are:

$P_{y\Delta.\Pi}$  - constant value with assumptions based on an analytical calculation;

$P_{y\Delta h}$  - hyperbola with asymptotes:  $G = \infty$ ,  $P_{y\Delta} = P_{y\Delta.\Pi}$ ,  $G = 0$ ,  $P_{y\Delta} = -\infty$ ;

$P_{\Pi}$  - straight line, passing through the origin of the coordinates;

$p_h$  - straight line, parallel to  $P_{\Pi}$  and lying below it by the value  $F_c p_h$ .

An example of the theoretical consumption characteristic is presented in Fig. 19.7. For each chamber there is a definite range of a realizable characteristic from  $G_{\min}$  to  $G_{\max}$  (Fig. 19.8). The condition  $G_{\max}$  is the maximum permissible forced condition, at which the strength and heat resistance of the chamber have been calculated. Condition  $G_{\min}$  can be governed by threshold of effective and stable work of the chamber, by the overheating of the liquid in the regenerative coolant passage of the chamber (see the next chapter) or by other limitations.

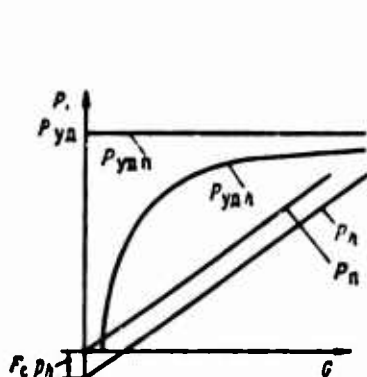


Fig. 19.7.

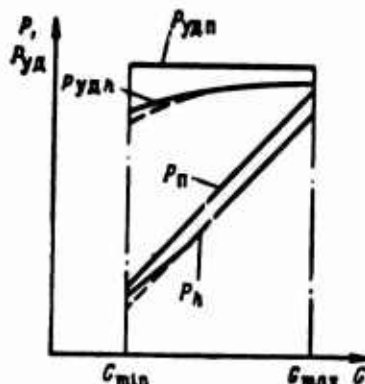


Fig. 19.8.

Fig. 19.7. Consumption characteristic of the chamber.

Fig. 19.8. Operating range of the consumption characteristic of the chamber.

Figure 19.8 shows a segment of the consumption characteristic with a separation of flow inside the nozzle (dotted line - hypothetical continuous flow).

The consumption characteristic can be obtained experimentally on a test stand. In order to determine it measurements of the thrust of second the consumption of fuel in seconds and of pressures of the surrounding medium are required.

A comparison of the results of the calculation and of the experimental determination of the consumption characteristic is shown

In Fig. 19.9. In the defined range of conditions good agreement is discovered; however, with a significant decrease in the consumption the results of the experiment and of the calculation become increasingly more divergent. This can be explained in the following manner. From equation of consumption of the liquid through the injecting devices (sprayers)

$$G = \mu_{\text{spr}} F_{\text{spr}} \sqrt{2 \rho_{\text{a.p}} \Delta p_{\text{a.p}}} \quad (19.3)$$

it follows that the pressure differential on sprayers  $\Delta p_{\text{BPP}}$  with a constant area  $F_{\text{BPP}}$  changes proportionally to the square of the consumption. With a considerable decrease of  $\Delta p_{\text{BPP}}$  the processes of atomization and fuel mixing worsen, and, consequently, the specific thrust efficiency  $\phi_{\text{yD}}$  diminishes (owing to a decrease of  $\phi_{\text{PK}}$ ).

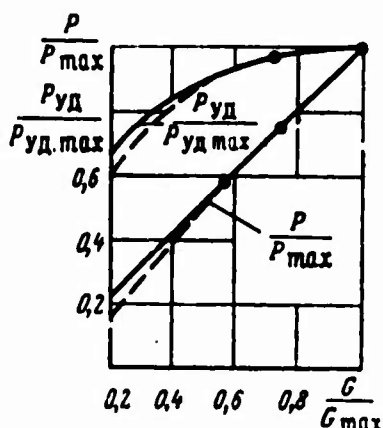


Fig. 19.9. For the comparison of the experimental and calculated consumption characteristics: — calculation; ---- experiment.

The reduction in the specific thrust under all conditions lower than the maximum (when  $p_h \neq 0$ ) is a substantial deficiency in the adjustment of thrust based on the expense characteristic. Basically, this reduction is governed by the lowering of the pressures differential  $p_K^*/p_h$ , and likewise by the worsening of the quality of processes in the combustion chamber.

What is wanted is the regulation of thrust in the chamber, by maintaining the specific thrust constant. Let us analyze how this can be done in principle. For constancy of  $P_{\text{yD}}$  when  $p_h \neq 0$ ,

it is necessary to retain the optimum pressure differential  $p_K^*/p_c = p_K^*/p_c$  and maintain a high quality of the processes. First condition require that the constant  $p_K^*$  and  $p_c$  are held. The only way to maintain  $p_K^*$  at a reduced consumption follows from the expression

$$p_K^* = \frac{G^2}{F_{kp}},$$

a reduction in the area of critical cross section of nozzle  $F_{kp}$  is proportional to the consumption. In order to maintain a constant of pressures  $p_c$ , it is necessary to retain the relative area of the nozzle,  $f_c = F_c/F_{kp}$ , i.e., to change the cross-sectional area  $F_c$  proportional to  $F_{kp}$  and  $G$ .

To preserve the quality of the working processes in the combustion chamber is possible by retaining the pressure differential on sprayers  $\Delta p_{bnp}$  constant. With a reduction in fuel consumption this can be done, as seen from the expression (19.3), by diminishing the area of injection  $F_{bnp}$  proportional to  $G$ .

Thus, in order to control the thrust by fuel consumption at a constant specific thrust it is necessary in general to change  $F_{kp}$ ,  $F_c$  and  $F_{bnp}$  proportional to  $G$ . In a vacuum (when  $p_h = 0$ ) a change in  $F_{kp}$  and  $F_c$  is not required.

Figure 19.10 shows the calculated characteristic 1 of the chamber with changed flow-through sections. For a comparison the consumption characteristic 2 of the chamber without regulated flow-through sections, is shown. Certain technical possibilities of adjusting  $F_c$  were mentioned in the examination of the altitude characteristic; the possible means of changing  $F_{kp}$  and  $F_{bnp}$  will be covered below.

Sometimes, the change in thrusts and specific thrust is represented as a function of the pressure in the combustion chamber  $p_K^*$ , and not as consumption of fuel in seconds. Experimental and



calculated characteristics of this kind are shown in Fig. 19.11. Comparing them with the usual characteristic (see Fig. 19.9) shows that the characteristics are analogous. However, experimental and calculated values of thrust as a function of  $p_K^*$  coincide throughout the range of conditions. The reason is that the worsening of the quality of processes in the combustion chamber at low fuel consumptions has the same effect on pressure  $p_K^*$  and on thrust. With the treatment of the results of bench tests this represents definite conveniences, equal as much as possible to direct control of the parameter - pressure in the combustion chamber. However, characteristics for  $p_K^*$  are less universal, than for fuel consumption. It is inconvenient to use multichamber engines for these parameters, because according to the pressure in each individual chamber one cannot ascertain the thrust of the entire engine.

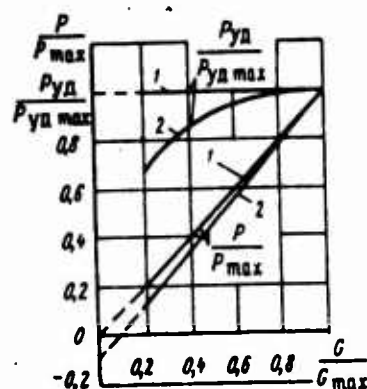


Fig. 19.10.

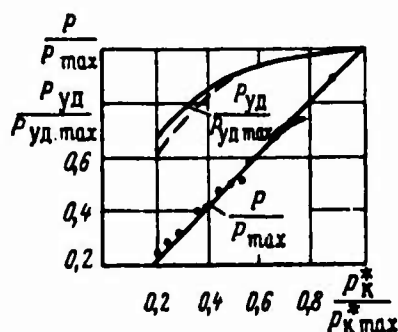


Fig. 19.11.

Fig. 19.10. Two variants of the consumption characteristic of the chamber.

Fig. 19.11. For the comparison of experimental and calculated consumption characteristic.

The consumption characteristic of chambers with ring nozzles and Laval nozzles is identical under conditions of underexpansion. Under conditions of overexpansion, with a large  $p_K^*/p_h$ , consumption characteristic of chambers with ring nozzles is more favorable for the same reasons as that for the altitude characteristic.

A comparison of the consumption characteristics of the chamber and of the engine is shown in Fig. 19.12. In the basic chamber of the engine with the afterburning of generator gas, there is no additional consumption of auxiliary fuel ( $\epsilon = 0$ ) and the characteristics of the chamber and of the engine coincide. The specific thrust of engines without afterburning of generator gas is lower than the specific thrust of the basic chambers. Their differences are more significant the greater  $\epsilon$  is, and the stronger the dependence  $\epsilon = f(p_K^*)$  or  $\epsilon = f(G)$  is.

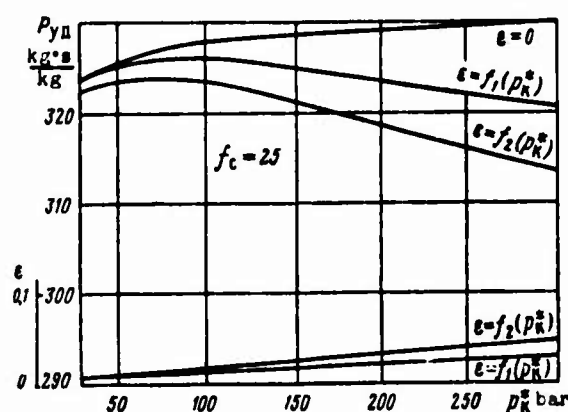


Fig. 19.12. Consumption characteristics of the chamber and of the engine at various dependence of  $\epsilon = f(p_K^*)$ .

#### 19.4. Thrust-Vector Control

In order to fulfill the assigned mission, the rocket must move along a definite trajectory, holding to a specified change-in-thrust pattern while in flight. Under actual conditions random disturbances take place, whose effect can alter after the flight trajectory and the change-in-thrust pattern with time.

Among the external disturbing factors there are, for example, the disturbance upon rocket lift off from the shaft or from the launching rack, sudden wind gusts when travelling in the atmosphere, disturbances at separation of stages, the asymmetry of the aerodynamic

forces, and so forth. These factors affect the rocket, aside from the dependence on the type of engine.

The nature of the effect of the internal factors is associated with type of engine used. For a liquid-fuel rocket engine this is, mainly, the scattering of thrust characteristics of engines of the same type, determined, basically, by the scattering of characteristics of the fuel-feed system - pressure pumps, hydraulic resistances of pipelines and of coolant, and so forth.

As a result errors, in the engine device on the rocket certain asymmetry of the thrust and constant motion can arise in flight, which must be compensated for.

Thus, to facilitate the requiring program of flight it is necessary to control the thrust of the engine according to magnitude and direction, i.e., to control the thrust vector. In this case the necessary range of adjustment is made up of two components. The first one, a specified or calculated value is determined by the character of the trajectory and by the change-in-thrust pattern with time. The second component depends on the random external and internal factors and it is rated, basically, on the data of bench and flying tests.

#### Change in the Amount of Thrust

The basic means of changing the amount of thrust were shown in the previous paragraph. This amounts to a change (throttling) of fuel consumption in seconds while maintaining the characteristic flow-through sections of the channel ( $F_{\text{Bnp}}$ ,  $F_{\text{kp}}$ ,  $F_c$ ) or adjusting them.

The most widely used method, in practice, is that of throttling the fuel consumption per second at a constant geometry of the chamber channel. It is carried out with the aid of special regulators on the fuel mains of the chamber or of the gas generator, and it can



guarantee a smooth change in the thrust. The method is convenient, reliable and also relatively simple. Its limitations and deficiencies were examined above (19.3).

Table 19.1 qualitatively described the diverse variants of change in fuel consumption per second in conjunction with the adjustment of the flow-through sections of the channel.

Table 19.1. Basic methods of changing the amount of thrust of a liquid-fuel rocket engine.

	Method	Parameters of chamber		$p_k$	Specific thrust		Reasons for changing $P_{ya}$
		constant	variable		in a vacuum	in atmosphere	
I	Throttling of fuel consumption with constant flow-through sections of the channel	$F_{Bnp}$ $F_{kp}$ $F_c$	$p_{Bnp}$	Diminishes	Constant	Diminishes	In atmosphere: 1) decrease in $p_k^*/p_n$ ; 2) deviation from optimum range of nozzle 3) lowering of $\varphi_\beta$
II	a) Throttling of fuel consumption with adjustment of the flow-through sections of the channel	$p_{Bnp}$ $F_{kp}$ $F_c$	$F_{Bnp}$	Diminishes	Constant	Diminishes	In atmosphere: 1st and 2nd reasons for method I
	b)	$p_{Bnp}$ $F_{Bnp}$ $F_c$	$F_{kp} \sim G$	Constant	Increase	Diminishes	In atmosphere: 2nd and 3rd reasons for method I In a vacuum: increase in $f_c$
	c)	$p_{Bnp}$ $F_{Bnp}/F_{kp}$ $F_c$	$F_{Bnp}, F_{kp} \sim G$	Constant	Increases	Diminishes	In atmosphere: 2nd reason for method I In a vacuum: increase in $f_c$
	d)	$p_{Bnp}$ $F_{Bnp}/F_{kp}$ $F_c/F_{kp}$	$F_{Bnp}, F_{kp}, F_c \sim G$	Constant	Increases	Constant	In a vacuum: increase in $f_c$ (if $F_c$ is not regulated in a vacuum)
	Turning off and on the chambers of the multichamber engine (step-wise adjustment)	$p_{Bnp}$ $F_{Bnp}$ $F_{kp}$ $F_c$	—	Constant	Constant	Constant	

\*If prior to throttling the nozzle is operated at underexpansion, then it is possible to increase  $P_{ya}$ .

A change in the total flow-through cross-sectional area of sprayer  $F_{\text{Bnp}}$  (var. 11a) is, in principle, attained several ways. It is possible, for example, to turn off separate groups of the sprayer, without changing the optimum condition remaining. It is possible to change the flow-through sections of the sprayer by mechanical means. Both methods are rather difficult to achieve. A way is possible to decrease the density of the fuel which is supplied through the sprayer, by introducing an inert gas (helium, argon) in the liquid component. Small quantities of the inert gas having low molecular weight, and consequently, a high working capacity practically have not effect on the specific thrust. At the same time the introduction of gas provides a wide range of change in consumption at a constant geometry of the sprayer without worsening the quality and resistance of the carburetion processes and combustion.

Changing critical cross section area of the nozzle  $F_{\text{kp}}$  (var. 11b) is possible by mechanical or gas-dynamical means. First, usually it is assumed a movable "needle-shaped" stylus ("bulb") is used, inserted in the critical section; secondly - there is a decrease in the effective flow-through section owing to the injection of the gas. The practical realization of these and any other system poses complex design problems.

The simultaneous adjustment of areas  $F_{\text{Bnp}}$  and  $F_{\text{kp}}$  (var. 11c) and possibly  $F_c$  (var. 11d), although it attracts interest due to its high efficiency, is technically very intricate. It should also be noted that the conditions for the adjustment of  $F_c$  simultaneous with  $F_{\text{kp}}$  in many instances is, probably, superfluous. So when working in a vacuum such an adjustment is not necessary. When working in atmosphere, an adjustment of  $F_c$  is necessary in order to avoid the lowering of  $P_{\text{ya}}$  under conditions of overexpansion. It is possible, however, either to reconcile it without lowering  $P_{\text{ya}}$  very much or to compensate for it by an increase of  $P_{\text{K}}^*$  against the nominal, if this is admissible under reliable working conditions. The utilization of nozzles with external expansion, having a known degree of self-regulation, facilitates this position.

The method of step-wise variation in thrust (var. III) by means of turning off individual chambers while maintaining optimum operating conditions occupies special place. Such a means is free of deficiencies, inherent in other methods. However, its utilization is possible only when a smooth change in thrust is not required.

#### Change in the Direction of Thrust

During the movement of a rocket along a trajectory controlling forces must be produced in the vertical plane (pitch control) as well as in horizontal plane (yaw control), and likewise, a controlling moment relative to the longitudinal axis (roll control). On the basis of experimental design, perfecting and operating rockets a number of general requirements for thrust-vector control systems were developed. Basically, these requirements can be grouped as follows:

- 1) providing sufficient control forces according to magnitude;
- 2) high reliability;
- 3) minimum losses of specific thrust of engine controlled by the presence and operation of a guidance system;
- 4) minimum weight and over-all size;
- 5) simplicity of design and convenience of operation.

In practice it is impossible to produce a system, which satisfies all the enumerated requirements to an equal degree. In accordance with the purpose of the apparatus the defined requirement can be singled out, which, depending on its specifications, can be met in the very best manner, using various methods. In connection with this at the present time it was assumed that a great number of various methods of thrust-vector control has been investigated to some degree.

It is expedient to use two criteria for an estimate and comparison of the various methods:

1) based on a change in the flying range of the rocket as a result of an increase in its final weight and a decrease in specific thrust controlled by system device;

2) according to the degree of reliability of the system.

In order to obtain these criteria conformably to each method it is necessary to construct a working design of the various systems. In this case one should have in mind that at the modern level of knowledge it is difficult to determine quantitatively the reliability of the systems under study.

For the preliminary evaluations of the various methods of changing thrust control such criteria are used:

relative amount of control forces - the ratio of this force to axial thrust of the engine:

$$\bar{P}_y = \frac{P_y}{P_{ya}}; \quad (19.4)$$

relative loss of specific thrust - the ratio of the loss in specific thrust of the engine, caused by the presence of the control system, to the nominal value:

$$\Delta \bar{P}_{ya} = \frac{\Delta P_{ya}}{P_{ya}}; \quad (19.5)$$

quality of the system - the ratio of quantities  $\bar{P}_y$  and  $\Delta \bar{P}_{ya}$ :

$$K_y = \frac{\bar{P}_y}{\Delta \bar{P}_{ya}}. \quad (19.6)$$

The quantities  $\bar{P}_y$  and  $\Delta \bar{P}_{ya}$  are usually expressed in percent.

When developing the rocket complex it is necessary to know not only control force, but rather the moment the relative to the center of gravity of the rocket, being created by this force. It is understandable that one can speak about the value the moment only in case of an actual scheme of a rocket, since different control moments can be produced with the same control force for various assembly schemes. Hence, it is clear that the possibility for comparison with the aid of the shown criteria is rather limited. Nevertheless, for a preliminary analysis they are used extensively.

During the flight of a rocket on a trajectory, the necessary control force changes all the time, attaining at its maximum value at specified moments. Losses in specific thrust also change accordingly. Therefore the system of control must resolve the maximum controlling force according to the amount, and the economy must be characterized by the mean integral amount of loss in specific thrust along the trajectory.

Below, the basic means of thrust-vector control of a liquid-fuel rocket engine are briefly considered. Some of these methods are also applicable for solid propellant rocket engines (RDTT).

Figure 9.13 shows the employment of gas current controls, encountered on in the cross section of the nozzle in jet stream of the combustion products (a) or outside of the jet stream (b). The angle of rotation of the vane is  $\delta = \pm 25^\circ$ . A device with four vanes provides flight control in all planes of stabilization. The control force and resistance (loss in thrust) can be determined according to the conventional formula of aerodynamics:

$$P_y = c_y \frac{\rho w^2}{2} F_p; \quad (19.7)$$

$$P_x = c_x \frac{\rho w^2}{2} F_p. \quad (19.8)$$

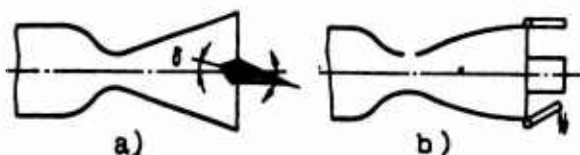


Fig. 19.13. Scheme of gas current controls.

Gas current controls can create great lateral forces ( $\bar{P}_y$  up to 10-15%), truly, at a cost of considerable losses in specific thrust ( $\Delta \bar{P}_{y\Delta} = 2-5\%$ ). The system is simple, reliable, but burdensome. The mounting of the controls in a neutral position outside the jet stream reduces losses in specific thrust, but it requires very large control forces to power the controls.

Annular vanes (deflectors) (Fig. 19.14) are made in the form of spherical bands, cylindrical adapters and their combinations. They are mounted in the cross section of the nozzles in a hinged suspension. With a deviation in the deflector at a certain angle, its edge projects into the supersonic jet stream, in front of the edge an oblique shock wave is created, and a lateral force appears. The system can create large control forces with small losses in specific thrust. In order to determine  $\bar{P}_y$  and  $\Delta \bar{P}_{y\Delta}$  experimental dependences are usually used.



Fig. 19.14. Diagram of annular control.

By structural relationship the system is rather simple, but it has considerable weight and over-all size; in the case of a single nozzle arrangement one can guarantee roll control.

Figure 19.15 shows a diagram of a oblique cross section adapter, from whose exhaust there appears an unbalanced lateral force. A deflection in  $P_y$  is attained by rotating the adapter around the longitudinal axis; the amount of deflection - by axial movement. The characteristics of the oblique cross section adapter can be

determined analytically as well as experimentally. The system produces control forces  $\bar{P}_y = 5-15\%$  with small losses in specific thrust. Roll control with a single nozzle arrangement is infeasible.

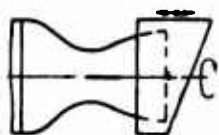


Fig. 19.15. Diagram of an oblique cross section adapter.

The most widely used method of changing the direction of thrust in a liquid-fuel rocket engine is the use of rotary chambers (Fig. 19.16). Both basic and steering (vernier) chambers are used. In case of a single-chamber arrangement without steering engines, the chamber is installed in a cardan suspension and is inclined at an angle,  $\delta = 3-7^\circ$  in two mutually perpendicular planes, providing pitch and yaw control.

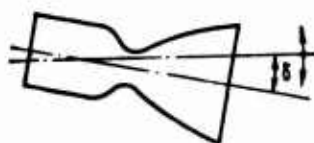


Fig. 19.16. Diagram of a rotary chamber.

During the rotation of the chamber at an angle  $\delta$ , the control force consists of

$$P_y = P_{\text{дв}} \sin \delta, \quad (19.9)$$

the losses in thrust

$$\Delta P_x = P_{\text{дв}} (1 - \cos \delta). \quad (19.10)$$

A system with basic rotary chambers makes it possible to produce large control forces ( $\bar{P}_y$  up to 10-15%) with very small losses in specific thrust ( $\Delta \bar{P}_{y\text{дв}} < 1\%$ ).

In the case of a multichamber engine installation, each of the basic or steering chambers, as a rule, is movable only in one plane. This is sufficient for flight control in all planes of stabilization. There are such steering chambers of RD-107 engine of the first stage of the rocket, Vostok, for example. Their utilization reduces the specific thrust of the engine in a vacuum by only 0.3%.

The reliability of a system with rotary chambers is high; however, the cardan suspension and hinged units have large over-all dimensions and weight.

The control forces can be produced by method of the misalignment thrust of the chambers of the multichamber engine, in a fixed position at a certain angle relative to the axis of the rocket (Fig. 19.17). A difference in thrust is attained by boosting forcing one and by throttling the other chamber by the same amount. The sum total thrust of the engine in this case does not change, but a control moment arises equal to

$$M_y = 2\Delta P(r \cos \delta + L \sin \delta). \quad (19.11)$$

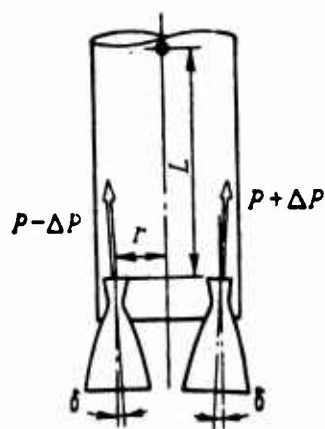


Fig. 19.17. Diagram of the change in thrust of individual chambers of a multichamber engine.

Thrust losses in this case amount to



$$\Delta P_x = 2P \sin \delta.$$

(19.18)

Losses in specific thrust  $\Delta \bar{P}_{y_d}$  usually do not exceed a fraction of a percent.

What has been said can be projected to any numbered pair of chambers in a multichamber device. The advantages of the system - in lieu of any special actuating controls, is the simplicity of convenience of adjustment. With no less than four chambers possible to control the flight in two naturally perpendicular directions. With a corresponding mounting of chambers it is possible to control roll.

Recently, a large amount of attention was devoted to a so-called gas-dynamic method of controlling the direction of thrust. These methods are based on the input of a basic supersonic flow of gas, perpendicular to a liquid or solid obstruction.

If a gas is fed in the supersonic part of the nozzle through an aperture or slot under a specified pressure, as shown in Fig. 19.18, then in front of the jet a cone shock appears or, more accurately, a weakly curved percussion wave with a  $\lambda$ -shaped leg at the base. Simultaneously, a jet stream sweeps through the flow under the action of a dynamic head and at a certain distance from the inlet aperture, it is mixed with this flow. With the main flow across the cone shock, the static pressure in the flow increases and the pressure at the nozzle rises. As a result an unbalanced lateral force arises, consisting of two components: reaction thrust of the ejected gas, and a force governed by the phenomenon of an asymmetrical zone of raised pressure behind the shock relative to the axis of the nozzle. The typical range of raised pressure on the wall of the nozzle in this disturbed zone is shown in Fig. 19.19. The magnitude of the second component may comprise 50-70% of the full lateral force.

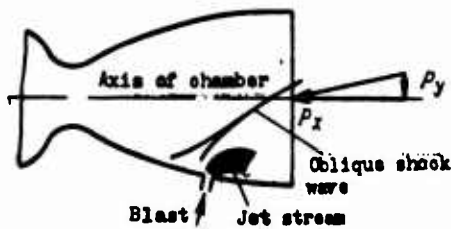


Fig. 19.18.

Fig. 19.18. Diagram of a blast of gas in a supersonic jet.

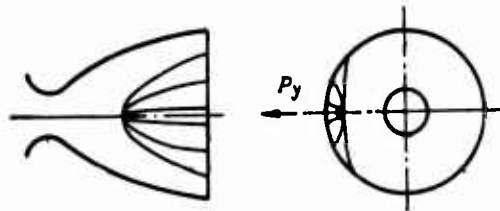


Fig. 19.19.

Fig. 19.19. Area of raised pressure with a blast in the supersonic jet stream.

It should be noted that an increase in the pressure in the disturbed zone increases the thrust of the nozzle somewhat, by increasing the specific thrust, determined according to the expenditure of basic fuel. However, the specific thrust, determined according to total expenditure, is reduced due to the inefficient utilization of part of the fuel (blasted gas). In the calculation one can assume that the blast of gas does not take part in producing the axial thrust of the engine.

Gas for the blast can be removed from the combustion chamber, using a special gas generator or using bottles of compressed gas provided for this purpose. From the viewpoint of efficiency it is most expedient to use high-temperature gas from the combustion chamber for the blasting. However, such a scheme possesses a substantial deficiency of a design nature. It includes the fact that the bypass valve should operate on high-temperature gas, possibly with a content of particles of the condensate. The creation of such a valve is a complex task. The utilization of a relatively low-temperature gas from a special gas generator or cold gas from bottles makes it possible to avoid these difficulties. However, the efficiency of such working media is considerably less, than that of hot gases, and the system, on the whole, is more burdensome.

The utilization of an injection of some kind of liquid from a structural point of view seems more attractive, although based on efficiency such a system is considerably inferior to a system with

a blast of gas. Principle of the creation of a lateral force with the aid of an injection of liquid is practically analogous to a blast of gas. The distinctive feature is that after a blast the liquid is atomized by the flow and either simply vaporizes (if it is chemically neutral with respect to the main flow), or it enters into a chemical reaction. The latter circumstance favorably reflects the efficiency of the system.

When selecting the type of liquid it is necessary to strive for the highest possible density. This makes it possible to reduce the volume of the containers. It must be stable in process of storage and have low toxicity. Low specific heat capacity and low latent heat of evaporation will facilitate an increase in the efficiency of the system. As neutral liquids for injection one can use various freons, and among the reactive liquids, there is nitrogen tetroxide ( $N_2O_4$ ), hydrogen peroxide ( $H_2O_2$ ), chlorine trifluoride ( $ClF_3$ ), and other components of liquid rocket fuels.

Due to the complexity of the phenomena which appear under the interaction of cross streams of gas or by the vaporization of the liquid with the supersonic flow of gas, it is not possible at present to calculate the magnitude of the lateral control force by accurate theoretical methods.

When developing actual systems, experimental dependances are used, produced on models or life-size engines during firing tests. Figure 19.20 presents approximate dependences of the control force relative to the efficiency of various substances during blast (injection).

The important advantage of the examined methods of producing control forces is the absence of any mechanical elements found in a high-temperature jet. The immobility of the chamber and the absence of mobile controls also adds to the positive aspect of this system.

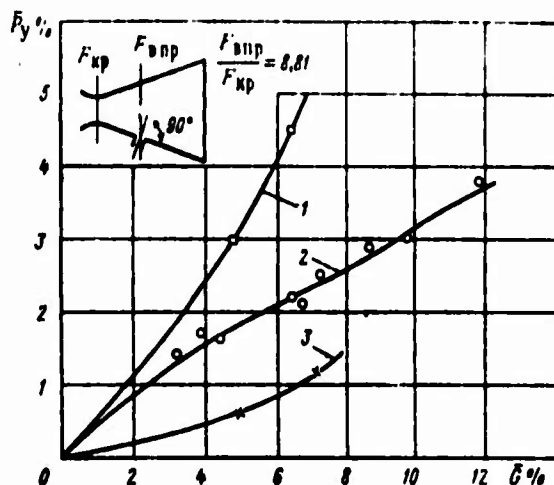


Fig. 19.20. Dependence of the control force on consumption with injection or blasting [3]: 1 - gaseous nitrogen; 2 - freon-12; 3 - water.

The deficiencies can include the difficulty of devising a reliable bypass valve of hot gases, and also the comparatively low economy in the case of injection of liquids. It should be noted that in case of a single-nozzle engine such a system does not facilitate creating control moment relative to the longitudinal axis of the rocket. For these purposes one must provide special devices of the vernier engine types.

To create an asymmetrical redistribution of the pressure in the supersonic part of the nozzle it is possible to introduce a solid obstruction in the form of a rod or a flap (sometimes also called a trimming tab) instead of a gas or a liquid.

If a solid obstruction is introduced between the critical section and the cross section of the nozzle, then the picture of flow is basically similar to that which takes place with blasting or injection. The greatest increase in pressure will take place directly in front of the obstruction. The areas of raised pressure are observed even along the periphery of the disturbed zone. Directly behind the obstruction a stagnant zone will form at a reduced

pressure, as a result of which the magnitude of the lateral side force is somewhat diminished. When positioning a solid obstruction nearer to the critical section relative to its small advancement in the flow, can result in the fact that an oblique shock wave will reach the opposite side of the nozzle, i.e., it will project over the entire section. This sharply reduces the asymmetry of the flow and, accordingly, the magnitude of the lateral force.

With practical realization of such controls, apparently, serious difficulties will arise with the condensation from the break of high-temperature products of combustion in the clearances near the obstruction. The indicated deficiencies make the examined methods of producing control forces not very attractive and they are seldom used.

The majority of the shown deficiencies can be avoided, if a flap is mounted at the cross section of the nozzles. In this instance the zone of rarefaction is absent, thereby diminishing the control force, and the rigid requirements for condensation between the flap and the cross section of the nozzle are raised.

In this case the character of the asymmetrical redistribution of pressure changes somewhat in comparison with the previous case. In front of the flap an  $\lambda$ -shaped shock wave appears, just as shown in Fig. 19.21. Here a typical picture of the distribution of pressure according to the line of symmetry of the disturbed zone is portrayed. From the examination of this diagram it follows that at a certain point in front of the flap there is a break-away of flow from nozzle wall and stagnant or frontal break-away zone will form. At the point of break-away an oblique shock wave appears, which then merges with the curved shock wave arising around the upper edge of the flap. By means of advancing the flap can regulate the size of the area of the disturbed zone and degree of increase in pressure in front of the flap. All this finally results in a change in the control force. Thrust losses using such a method of producing a control force will determine the pressure differential on the front and back surface of the flap.

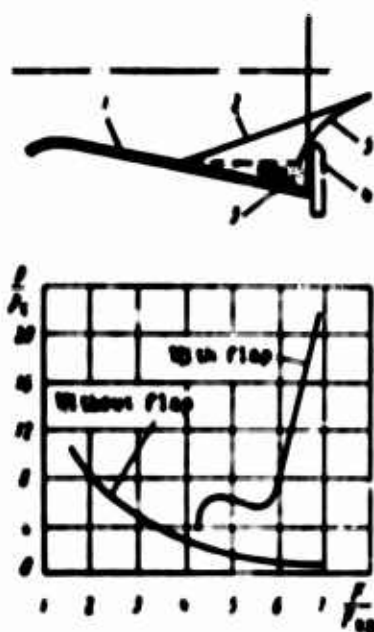


Fig. 19.21. Diagram of the utilization of a flap and character of the pressure distribution in front of it: 1 - nozzle; 2 - oblique wave; 3 - break-away zone; 4 - flap; 5 - percussion wave.

In order to calculate the basic characteristics of such a system it is necessary to determine the size of area of the disturbed zone in front of the flap, to evaluate the degree of increase in pressure in this zone and to find the distribution of pressure according to the front and back surface of the flap. Contemporary methods do not permit one to conduct an accurate calculation of the field of flows in front of the break-away zones. Therefore, during the determination of the basic characteristics of the flaps, just as in the preceding case, experimental data is used.

According to certain data actual values of the coefficient of quality for flaps applied in solid propellant rocket engines (RDTE), they can comprise a quantity, equal to unity or more. A considerable lowering of  $K_g$  takes place due to the pressure of clearance between the flap and the cross section of the nozzle.

The selection of material for flaps and providing for their heat resistance represents a serious problem.

Although the solid propellant rocket engines are regarded as the basic field of application of flaps they are examined here for analogy with methods of blasting of gas and of liquid injection.

### Cutoff of Thrust

A cutoff of thrust or the turning off of the engine is necessary in the following cases: in the first, after achieving the necessary velocity of the state of the rocket or after completing the necessary maneuvers by the space vehicle, in the second, during operation on the test stand after completing a program of tests, or in an emergency situation.

In first case for accurate endurance of the assigned terminal velocity of apparatus, the cutoff of the thrust must be performed sharply, and the pulse of the thrust, acting at the moment and after the cutoff (the so-called pulse after-effect), must be minimum and stable. Stability, i.e., the small scatterings of pulse after-effect with the repeated response of one engine or with the turning off of different engines, offers the possibility of considering it when determining the moment of shutdown.

Shutdown of a liquid-fuel rocket engine is performed by stopping the supply of fuel components upon response of the cutoff valves. The pulse after-effect is caused by the exhaust from the combustion chamber containing products and with afterburning, also components entering the chamber from the spaces between the cutoff valves and the heads. By design of the liquid-fuel rocket engine the attempt is made for these volumes to be as small as possible. Also, the operation of the engine before shutdown at a lowered condition promotes the lowering of the pulse after-effect. It is possible that the last meters of an assigned terminal velocity of the apparatus are attained upon shutdown in a powerful sustainer engine only owing to the work of vernier engines of small thrust (for example, on the "Atlas" rocket) or even owing to the thrust, generated upon exhaust of the working medium of the turbopump unit (TNA).

### Bibliography

1. VRT, 1965, No. 4, No. 6.
2. Issledovaniye raketnykh dvigateley na zhidkom toplive  
(Investigation of rocket engines working on liquid fuel), collection  
of translation, izd-vo "Mir", 1964.
3. Hollstein H. J., J. Spacecraft and Rockets, 1965, No. 6.



## CHAPTER XX

### PROTECTION OF THE CHAMBER WALL

In this chapter the preferred means of protecting the chamber walls of a ZhRD from overheating, oxidation and erosion with the aid of liquid or gaseous coolants are examined. Heat transfer rates from the products of combustion in the walls of the chamber in a specified fuel, for the value  $\kappa$  and  $T_{\text{CT},\Gamma}$  are considered to be known, calculated according to methods in Chapter XIV.

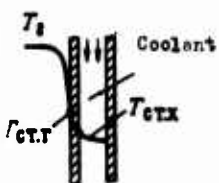
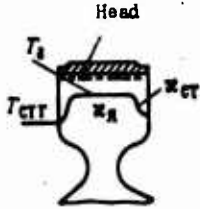
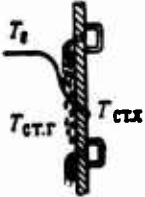
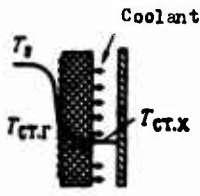
#### 20.1. Basic Methods of Shielding the Wall

Table 20.1 shows the basic methods of shielding the chamber walls using a liquid or gas coolant.

The most extensively used is the external regenerative liquid coolants or gaseous components of the fuel.

The basic idea of internal cooling of the chamber walls is to create a protective layer of liquid or of low-temperature gas (steam) near the fire front. Several variations of internal cooling exist. Thus, a low-temperature near-wall layer can be created with the aid of injection head near the chamber walls, in which the fuels component ratio  $\kappa_{\text{CT}}$  is less than the fuels component ratio in nucleus  $\kappa_{\text{Я}}$ .

Table 20.1. Basic methods of liquid shielding of the wall.

Name	Brief description	Temperature diagram
External regenerative cooling	One or both component of the fuel cool the walls and enter the combustion chamber, returning the removed heat.	
Internal cooling by means of creating a near-wall layer with $\alpha_{\text{near}} \gg \alpha_{\text{core}}$	Near the wall a near-wall layer is created with the aid of an injection head with $\alpha_{\text{ev}}$ , providing a low combustion temperature (usually $\alpha_{\text{ev}} < \alpha_{\text{core}}$ ) and a reducing medium. The low-temperature layer reduces the thermal flow in the wall, and the reducing medium reduces corrosion.	
Internal film cooling	Liquid coolant or gas is fed through a number of bands of curtains	
Internal porous cooling	Liquid coolant or gas penetrates through thin pores in the wall, creates a layer of liquid and vapor and insulates the wall from hot gases, considerably lowering the thermal flow	

[Translator's note:  $\alpha$  = gas;  $ct.x$  = wall gas side;  $ct.r$  = wall, coolant side;  $cr$  = wall;  $\alpha$  = core.]

A variant of internal cooling is film cooling -- a supply of liquid to the inner surface of the wall through special apertures or slots and the creation of a film curtain.

By analogy with a liquid film curtain a gas curtain can be created, if, for example, a low-temperature generator gas is supplied to the inner surface of the wall in an engine with afterburning.

Porous cooling is a development of a method of film cooling. In this variant the liquid coolant is introduced to the fire front through a large number of microscopic ducts in a wall made of porous material.

Frequently, combined systems of wall shielding are employed, i.e., various combinations of the above-mentioned methods, in addition to systems of nonliquid heat shielding (see Chapter XXVI).

In order to cool the chamber reliably and economically, at least one of the components of the fuel must satisfy the following requirements:

- 1) have a significant heat capacity and thermal conductivity;
- 2) have a large latent heat of vaporization (if the component is used for internal cooling);
- 3) does not leave deposits on the cooled wall, which hamper heat removal (scale, coke and so forth);
- 4) does not decompose with the heating of the coolant passage.

## 20.2. External Regenerative Cooling

The physics of the phenomena of heat transfer, examined below, with regenerative and independent cooling of the chamber is identical. Regenerative cooling has its own characteristics governed by, the limited expense of the coolant.

### General Scheme of Heat-Transfer

Figure 20.1 shows a scheme of heat transfer from a gas to a coolant through a separating wall under a stationary condition of external cooling. In the thermal boundary layer of gas having a thickness  $\delta$ , the heat from gas is transferred to the wall and sharply reduces the temperature from  $T_e$  to  $T_{ct,r}$ . The total specific thermal flow from the gas in the wall is equal to the sum of convection and radiant flows

$$q = q_k + q_n,$$

where

$$q_k = \alpha_g (T_e - T_{ct,r}).$$

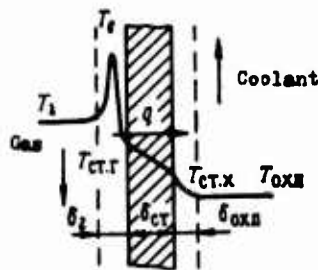


Fig. 20.1. Temperature diagram with external cooling of the chamber.  
[Translator's note: охл = coolant.]

For convenience it is possible to introduce a certain arbitrary value to the heat-transfer coefficient from the gas to wall  $\alpha'_g$ , also taking into account the convection and radiant heat exchange. Then

$$q = \alpha'_g (T_e - T_{ct,r}), \quad (20.1)$$

where

$$\alpha'_g = \alpha_g + \frac{q_n}{T_e - T_{ct,r}}. \quad (20.2)$$

Through the wall of the chamber heat is transferred owing to the thermal conductivity that can be described by the equation

$$q = \frac{\bar{\lambda}_{cr}}{\delta_{cr}} (T_{cr,r} - T_{cr,x}), \quad (20.3)$$

where  $\bar{\lambda}_{cr}$  — mean value of the coefficient of thermal conductivity of the material of the wall, taken at a temperature of

$$T = \frac{T_{cr,r} + T_{cr,x}}{2}.$$

Equation (20.3) is recorded with several assumptions, namely: thermal flow is accepted as one-dimensional, distributed only normal to the wall (to the radius); wall is accepted as a plane, associated with the fact that the difference in the sizes of the internal and external surfaces of the wall are not taken into account, but the quantity  $q$  is accepted as constant. All these assumptions are slightly reflected in the results of the calculation.

In the thermal boundary layer of the coolant with a thickness  $\delta_{охл}$ , heat is transferred from the wall in the coolant and the temperature drops from  $T_{cr,x}$  to  $T_{охл}$ . According to the equation of this process

$$q = \alpha_{охл} (T_{cr,x} - T_{охл}), \quad (20.4)$$

where  $\alpha_{охл}$  — coefficient of convective heat-transfer from the wall to the coolant.

The common solution of equations (20.1), (20.3) and (20.4) provides the following well-known equation of heat transfer from a gas to a coolant through a separated wall:

$$q = \frac{1}{\frac{1}{\alpha_g} + \frac{\delta_{cr}}{\lambda_{cr}} + \frac{1}{\alpha_{охл}}} (T_g - T_{охл}). \quad (20.5)$$

the quantity

$$\frac{1}{\alpha_g} + \frac{\delta_{cr}}{\lambda_{cr}} + \frac{1}{\alpha_{oxl}}$$

is the thermal resistance of the heat transfer from the gas to the coolant. It consists of the thermal resistances of the gas  $1/\alpha_g$ , the wall  $\delta_{cr}/\lambda_{cr}$  and coolant  $1/\alpha_{oxl}$ .

Effect of the various types of thermal resistances is illustrated in Fig. 20.2, where the results of the calculation of external cooling of the chamber under various hypothetical conditions are presented. The line

$$T_{cr,r} = T_{дон}$$

limits the maximum allowable wall temperature on the gas side under conditions of strength and heat resistance.

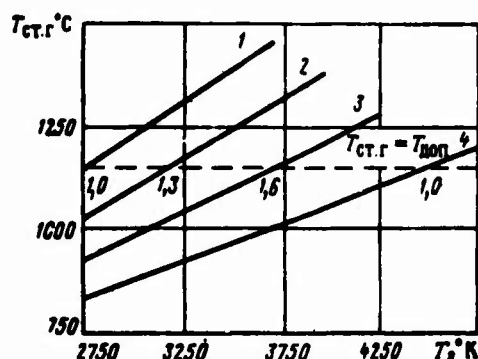


Fig. 20.2. For the analysis of the effect of thermal resistances of the gas, the wall and the coolant. [Translator's note: дон = maximum allowable.]

Line 1 shows the relationship between temperature  $T_{cr,r}$  and the temperature of the gas for several original variants. Line 2 depicts the same relationship at thermal resistance of the coolant, reduced by 5 times that of the original. As it appears, this reduction makes it possible to raise the temperature of the gas  $T_{cr,r}$ . Simultaneously, it increases the thermal flow, transmitted to the coolant (figures at the points signify the relative change in specific thermal flow). Line 3 shows the relationship between  $T_{cr,r}$  and  $T_g$  with a two-fold reduction thermal resistance of the wall and of constant residual resistances. While maintaining  $T_{cr,r}$  the temperature

of the gas can increase even more, but the thermal flow in the coolant sharply increases. Finally, line 4 relates to a case where the thermal resistance of the gas increases two-fold (the remaining quantities are invariable). As it appears, the effect of the thermal resistance of the gas to the permissible temperature of the gas is most significant; moreover, it does not change the specific thermal flow in the coolant.

Questions, connected with heat-transfer from the products of combustion in the wall of the chamber, are examined in Chapter XIV. It is important to also analyze the subsequent stages of the transmission of heat.

#### Heat-Transfer Through the Wall

Heat-transfer equation (20.3) can be solved relative to temperature  $T_{cr,x}$ :

$$T_{cr,x} = T_{cr,r} - q \frac{\delta_{cr}}{\lambda_{cr}}. \quad (20.6)$$

An increase in the thickness of the wall increases its thermal resistance and according to equation (20.5), it somewhat diminishes the specific thermal flow. Simultaneously, temperature of wall on the gas side increases:

$$T_{cr,r} = T_g - \frac{q}{\alpha_g}. \quad (20.7)$$

An increase in the coefficient of thermal conductivity (change of the material) reduces the thermal resistance of the wall and increases the specific thermal flow. Temperature of the wall on the gas side in this case is lowered, and on the coolant side - is elevated.

## Heat-Transfer in the Coolant

Fuels as well as oxidizers are used as coolants for external cooling. The utilization of fuels is preferable, because they usually have more favorable thermal properties and, as a rule, they do not produce an aggressive medium. However, the fuel is always lesser amounts than the oxidizer, and it turns out to be insufficient. Such an oxidizer as  $N_2O_4$  possesses highly favorable coolant properties because of its endothermic dissociation at high temperatures.

In connection with the various properties of coolants and their parameters in the coolant passage different conditions of heat-transfer are possible. In Fig 20.3 these conditions are classified depending on the pressure and the temperature of the coolant with respect to the critical parameter. With pointers in the field of the chart the direction of the change in the parameters of coolant in the coolant passage is shown.

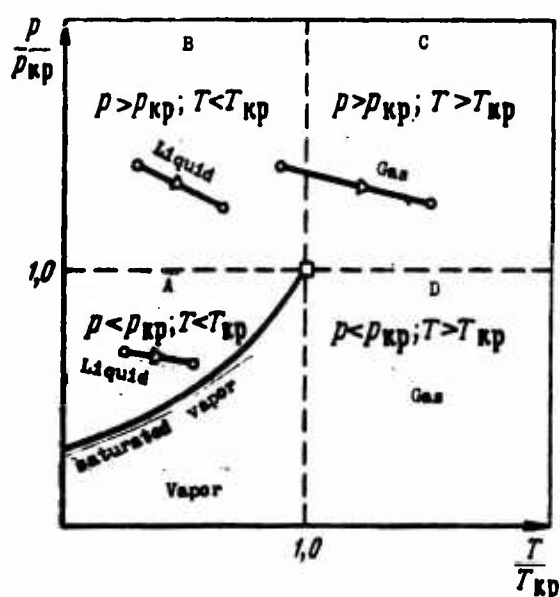


Fig. 20.3. Conditions of heat-transfer in the coolant.

[Translator's note:  $\kappa p$  = critical.]

At a subcritical temperature and pressure (condition A) the coolant can be found in the liquid and vapor phases. The dependence



$p^{\text{н}} = f(T)$  serves as the boundary of these states. A two-phase state of the coolant is also possible. If the wall temperature on the coolant side,  $T_{\text{ст.х}}$  is somewhat (up to 10-50°) elevated to the boiling point of the coolant at a given pressure, then the main mass of flow (nucleus) does not begin to boil, but in the boundary layer little bubbles of vapor appear. The main flow washes the bubbles off the surface of the wall, and they are condensed in the cooler layers of the liquid. The transverse motion of the bubbles intensifies the turbulent transfer of heat from the wall through the boundary layer to the main flow, and consequently, increases the coefficient of heat-transfer from the wall into the coolant. Value  $\alpha_{\text{охл}}$  with bubble boiling can be several times greater, than under a condition without vaporization. However, the increase in  $\alpha_{\text{охл}}$  continues only to a determined value of the overheated wall,  $\Delta T = T_{\text{ст.х}} - T_{\text{кип}}$ , at which numerous bubbles merge into a continuous film of vapor, insulating the coolant from the wall. After this, the coefficient of heat-transfer sharply drops, and temperature  $T_{\text{ст.х}}$  increases. The overall heat-transfer in the coolant is reduced considerably, as a result, it permissibly increases  $T_{\text{ст.г}}$ . The described dependence  $\alpha_{\text{охл}}$  on  $\Delta T$  is shown in Fig. 20.4. Value  $\Delta T$ , corresponding to the maximum  $\alpha_{\text{охл}}$ , is maximum permissible, because when  $\Delta T > \Delta T_{\text{пр}}$  film boiling appears.

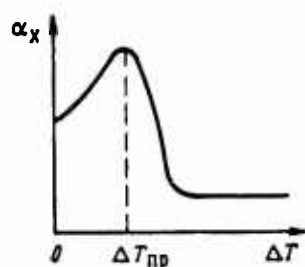


Fig. 20.4. Dependence of  $\alpha_{\text{охл}}$  on  $\Delta T = T_{\text{ст.х}} - T_{\text{кип}}$

[Translator's note: пр = maximum permissible.]

In this way, under condition A, one can use either flow conditions of the liquid without vaporization ( $T_{\text{ст.х}} < T_{\text{кип}}$ ), or conditions of bubble boiling ( $T_{\text{ст.х}} \leq T_{\text{кип}} + \Delta T_{\text{пр}}$ ).

At a supercritical pressure and a subcritical temperature (condition B) the coolant exists as a single-phase drop liquid.

At a supercritical pressure and temperature (condition C) the coolant is in the gaseous state. It is possible as shown in Fig. 20.3 that the liquid component passes into the coolant passage, a supercritical pressure and subcritical temperature; then, it is heated to a supercritical temperature and further on, becomes a gaseous coolant.

Under condition D the coolant is also in the gaseous state.

Table 20.2 shows values of the critical parameters of certain components of liquid fuels.

Table 20.2. Critical parameters of certain coolants

Coolant	Critical pressure, atm	Critical pressure, bar
Fuels		
H <sub>2</sub>	23.2	12.5
NH <sub>3</sub>	405.6	100.2
Kerosene	~600	~22
N <sub>2</sub> H <sub>4</sub>	682	142.3
C <sub>6</sub> H <sub>6</sub> N <sub>2</sub>	322	56
50% N <sub>2</sub> H <sub>4</sub> + + 50% C <sub>6</sub> H <sub>6</sub> N <sub>2</sub> )	~500	~123
Oxidizers		
H <sub>2</sub> O <sub>2</sub>	722	210
N <sub>2</sub> O <sub>4</sub>	431	98
ClF <sub>3</sub>	426	60

Conditions of heat-transfer of the same coolant can be different under the various conditions of a coolant passage. Below are shown the characteristic conditions of heat-transfer in fuel components [7].

Component	Characteristic conditions of heat-transfer
Kerosene	B
Hydrozen	C
Ammonia	A, I
Hydrazine	A
Dimethylhydrazine	A, B
Nitrogen tetroxide	A
Hydrogen peroxide (90-98%)	A

The quantitative laws of heat-transfer under various conditions are different.

1. Liquid single-phase coolant (part of conditions A when  $T_{cr,x} < T_{lim}$ , all of condition B)

The mechanism of heat-transfer - the forced convection during the turbulent motion of the liquid in a channel. In order to calculate one must use the known criterial dependence of M. A. Mikheyev:

$$Nu_{\kappa} = 0,021 Re_{\kappa}^{0,8} Pr_{\kappa}^{0,43} \left( \frac{Pr_{\kappa}}{Pr_{cr}} \right)^{0,25} \quad (20.8)$$

or the dependence close to it

$$Nu_{\kappa} = 0,005 Re_{\kappa}^{0,96} Pr_{\kappa}^{0,4} \quad (20.9)$$

In the criteria with a index " $\kappa$ " the properties of a coolant exhibit a mean liquid temperature with a index "cr" - at a temperature  $T_{cr,x}$ .

The dependence (20.9) is satisfactorily confirmed by experiments with kerosene, hydrazine nitrogen tetroxide and water, and other components. Both dependences, however, require more precise definitions, because they do not reflect the effect of such factors,

as configuration of cross section and curvature of the channel, nonuniformity of heating and so forth.

The critical dependences can solve the relatively heat-transfer coefficient. For example, from the dependence (20.9) let us obtain

$$\alpha_{\kappa} = 0,005 \left( \frac{G_{oxn}}{F_{oxn}} \right)^{0,95} \frac{1}{d^{0,05}} \theta_{\kappa 1} \frac{W}{M^2 \cdot \text{deg}}, \quad (20.10)$$

where  $G_{oxn}$  — consumption of liquid coolant in seconds;  $F_{oxn}$  — cross-sectional area of the coolant passage.

In parameter  $\theta_{\kappa 1}$  the thermal properties are grouped depending for the given liquid only, on the temperature:

$$\theta_{\kappa 1} = \lambda_{\kappa}^{0,6} \frac{c_{\kappa}^{0,4}}{\eta_{\kappa}^{0,55}}.$$

Because

$$\frac{G_{oxn}}{F_{oxn}} = w_{oxn} \rho_{oxn},$$

then, the formula (20.10) can be written so:

$$\alpha_{\kappa} \leq 0,005 \frac{w_{oxn}^{0,95}}{d^{0,05}} \theta_{\kappa 2}. \quad (20.11)$$

Here the density of the liquid, also depending on the temperature, is included in the parameter  $\theta_{\kappa 2}$ :

$$\theta_{\kappa 2} = \theta_{\kappa 1} \rho_{\kappa}^{0,95}.$$

The quantity  $\theta_{\kappa 2}$  is defined as the coolant capacity of the liquid. For drop of liquids it usually increases with an increase in temperature.

2. Liquid coolant with bubble boiling [(part of condition A when  $T_{\text{min}} < T_{\text{ct,x}} (T_{\text{min}} + \Delta T_{\text{np}})$ )]

Mechanism of heat-transfer has been briefly described above. The quantitative determination of the coefficients of heat-transfer is difficult. For each coolant one also experimentally determines such highly important values as  $\Delta T_{\text{np}}$  and  $q_{\text{np}}$  — the maximum heat flow, which can be directed into a liquid without the appearance of film boiling. The quantities  $q_{\text{np}}$  and  $\Delta T_{\text{np}}$  most substantially depend on the rate of the coolant, increasing with an increase in  $w_{\text{oxn}}$ , and also on the difference between the boiling point and the mean temperature in the nucleus of flow, on the pressure in coolant passage as well as on the geometry of the passage.

By way of reducing the quantity  $q_{\text{np}}$  certain coolants rank approximately as follows:  $\text{N}_2\text{H}_4$ ,  $\text{C}_2\text{H}_8\text{N}_2$ ,  $\text{H}_2\text{O}_2$ ,  $\text{NH}_3$ ,  $\text{N}_2\text{O}_4$ .

3. Gaseous coolant (conditions C and D)

Cooling by gas creates great interest, if such efficient coolants as hydrogen or other light gases are used, for example, ammonia. When cooling with hydrogen very large heat removal can be attained as a result of the high heat capacity of the coolant and as a result of the feasibility of considerable preheating. The greater part of the heat removal will occur in gaseous hydrogen.

Information on heat-transfer under conditions, characteristic for a coolant passage in a ZhRD, as yet is scanty. For a developed turbulent motion at steep temperature gradients ( $T_2/T_{\text{cp}} \geq 2$ ) one can use the criterial equation

$$\text{Nu}_2 = 0,025 \text{Re}_2^{0,8} \text{Pr}_2^{0,4} \left( \frac{T_2}{T_{\text{ct,x}}} \right)^{0,55}, \quad (20.12)$$

in which index «2» signifies that the criteria are determined at the average temperature of the coolant gas.

The formula for the heat-transfer coefficient, obtained from equation (20.12), has the form

$$\alpha_s = 0,025 \left( \frac{G_{ox}}{F_{cst}} \right)^{0,8} \frac{1}{d_p^{0,5}} \theta_s \left( \frac{T_s}{T_{ct,x}} \right)^{0,55} \frac{W}{M^2 \cdot deg}, \quad (20.13)$$

where

$$\theta_s = \lambda_s^{0,6} \frac{c_{ps}^{0,4}}{\gamma_s^{0,4}}.$$

• At ratios of temperatures  $T_s/T_{xp} < 2$  the dependences, analogical to the expression (20.12), and not found in the literature.

#### Preheating of the Coolant

The preheating of the coolant in the passage is taken into account in the course of movement of the component. The calculation gives not only the total quantity of preheating, but also the local values of the temperature of the coolant in various sections. For the calculation one usually uses the same lay out of chamber passage in the section, which was used in the determination of specific thermal flows from the gas into the wall. An example of such a layout is presented in Fig. 20.5.

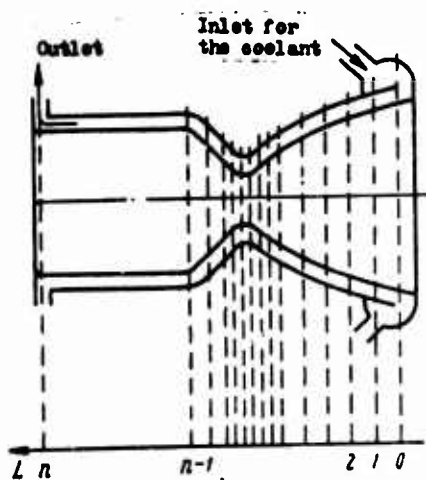


Fig. 20.5. Example of the layout of the chamber passage in the section for the calculation of cooling.

For each of the sections they comprise an equation of heat balance (heat removal in the surrounding medium through the external walls can be ignored):

$$\Delta T_{\text{oxl}} = \frac{Q_l}{G_{\text{oxl}} c_{\text{oxl}}}, \quad (20.14)$$

where  $Q_l$  — quantity of heat, which should be discernible by the coolant in the given section;  $G_{\text{oxl}}$  — consumption of the coolant in seconds;  $c_{\text{oxl}}$  — heat capacity of the coolant at an average of its temperature in the given section.

One determines the value  $Q_l$  by the integration  $q$  in the given section with a length  $L_l$ :

$$Q_l = \int_{L_l}^{L_{l+1}} q \frac{\pi d}{\cos \alpha} dL, \quad (20.15)$$

where  $d$  — inside diameter of the chamber, changing in the section;  $\alpha$  — angle of slope of the forming chamber to its axis. Hence

$$\Delta T_{\text{oxl}} = \frac{1}{c_{\text{oxl}} G_{\text{oxl}}} \int_{L_l}^{L_{l+1}} q \frac{\pi d}{\cos \alpha} dL. \quad (20.16)$$

If the layout to the section is dense, then one can use the means  $q$  and  $d$  for the given section:

$$\Delta T_{\text{oxl}} = \frac{\bar{q}_l \Omega_l}{c_{\text{oxl}} G_{\text{oxl}}}, \quad (20.17)$$

where  $\bar{q}_l$  — average value of specific heat flow in the  $l$ -th section;  $\Omega_l$  — surface of the  $l$ -th section, determined by the formula

$$\Omega_l = \frac{\pi (d_l + d_{l+1})}{2 \cos \alpha} \Delta L_l.$$

Because the value of the temperature on exit from section was unknown earlier, then the average heat capacity of the coolant can be determined by the method of selection.

The temperature of the coolant in the section  $(i + 1)$  comprises

$$T_{\text{oxn}}(i+1) = T_{\text{oxn}} i + \Delta T_{\text{oxn}} i, \quad (20.18)$$

and on exit from the coolant passage -

$$T_{\text{oxn,вых}} = T_{\text{oxn,вх}} + \sum_{i=1}^n \Delta T_{\text{oxn}} i, \quad (20.19)$$

where the value  $\sum_{i=1}^n \Delta T_{\text{oxn}} i$  is the complete preheating of the coolant in the passage.

#### Determination of the Areas of the Coolant Passage

In order to remove the thermal flow  $q$  in the coolant in every section of the chamber a defined value of heat-transfer coefficient from the wall into coolant is required. In general this value is equal to

$$\alpha_{\text{oxn}} = \frac{q}{T_{\text{ct,x}} - T_{\text{oxn}}}. \quad (20.20)$$

Since after the values  $q$ ,  $T_{\text{ct,x}}$  and  $T_{\text{oxn}}$  are defined at the specified consumption of the coolant  $G_{\text{oxn}}$ , it is necessary to assure that there can be  $\alpha_{\text{oxn}}$  only due to the rate of the coolant, which depends on the area of the channel. In case of liquid coolant when the heat-transfer coefficient is determined by the expression (20.10), it is necessary to guarantee

$$\alpha_{\text{oxn}} = 0,005 \left( \frac{G_{\text{oxn}}}{F_{\text{oxn}}} \right)^{0,95} \frac{1}{d_0^{0,05}} \theta_{\text{ж1}},$$

whence the necessary area constitutes

$$F_{\text{oxn}} = G_{\text{oxn}} \left( \frac{0,005 \theta_{\text{ж1}}}{\alpha_{\text{oxn}} d_0^{0,05}} \right)^{1,05}, \quad (20.21)$$



Analogous for a gaseous coolant, using the expression (20.13), we will obtain

$$F_{oxn} = G_{oxn} \left( \frac{0.025 \theta_z}{\alpha_{oxn} d_{\theta}^{0.2}} \right)^{1.25} \left( \frac{T_z}{T_{ct,x}} \right)^{0.687}. \quad (20.22)$$

In order to guarantee the necessary heat removal, area of the flow-through section of the coolant passage must be not more, than that determined by the expressions (20.21) or (20.22).

Based on the accepted values of  $F_{oxn}$  one can calculate rate of movement of the coolant:

$$w_{oxn} = \frac{G_{oxn}}{F_{oxn} \rho_{oxn}}.$$

The rate of liquid coolants attains tens of meters per second, the gaseous - substantially more. For example, in Fig. 20.6 velocities of the liquid are shown, and then gaseous hydrogen in coolant passage of a J-2 ZhRD (USA).

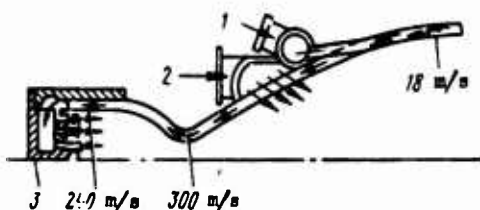


Fig. 20.6. Elements in the diagram of a J-2 ZhRD (USA): 1 - supply of liquid hydrogen; 2 - gases behind the turbine for internal cooling of a part of the nozzle; 3 - injection head of the "gas-liquid" type.

#### Losses in Pressure in the Coolant Passage

Parallel to the calculation of heat-transfers in the coolant passage one can compute the change in pressure in it. In each section the change in pressure can be determined by the change in the quantity of motion ( $Qw\Delta w$ ), by the losses to friction  $\Delta p_{\text{fr}}$  and by the local hydraulic losses  $\Delta p_M$ :

$$\Delta p_{oxn} = Qw\Delta w + \Delta p_{\text{fr}} + \Delta p_M. \quad (20.23)$$

The change in the amount of movement has a value only in case of a gaseous coolant.

Losses to friction for a liquid coolant can be determined according to the usual relationship:

$$\Delta p_{rp} = \xi \frac{\Delta L}{d_s} \frac{\rho_m w_m^2}{2} \quad (20.24)$$

The quantities  $\rho_m, w_m$  and  $d_s$  are taken as average for the given section. The unmeasurable coefficient of friction  $\xi$  can be determined for turbulent fluid flow: when  $Re = 3 \cdot 10^3 - 10^5$

$$\xi = \frac{0.3164}{Re^{0.25}}; \quad (20.25)$$

when  $Re = 10^5 - 10^8$

$$\xi = 0.0032 + \frac{0.221}{Re^{0.237}} \quad (20.26)$$

The reynolds number in the formula for the determination of  $\xi$  can be found based on the average values of the determining parameters, related to the mean temperature of the coolant and hydraulic diameter of the channel.

Losses in pressure due to local resistances (sudden expansion and contraction, rotation, and so forth) are determined by the formula

$$\Delta p_m = \xi_l \frac{\rho_m w^2}{2}, \quad (20.27)$$

where  $\xi_l$  - coefficient of local resistance, adopted from reference books.

Losses in pressure under conditions A with bubble boiling are higher than losses during the movement of the single-phase liquid. An analytical determination of them is difficult.

Losses in pressure under conditions C and D are determined according to the corresponding dependences for gases.

After that the losses in pressure in the section are found; they define the absolute pressure of the coolant

$$p_{i+1} = p_i - \Delta p_{\text{oxn } i},$$

which are necessary for the calculation of the strength and the determinations of the boiling point of the coolant.

Total losses in pressure in the coolant passage are determined by summarizing  $\Delta p_{\text{oxn } i}$  along the entire section:

$$\Delta p_{\text{oxn}} = \sum_{i=1}^n \Delta p_{\text{oxn } i}.$$

This quantity is used in calculating the fuel supply system.

It is interesting to compare the efficiency of heat-transfer in the coolant under a condition of identical losses in pressure in the coolant passage. The difference in the coefficients of heat-transfer in this instance will be governed by the difference in physical properties of the coolants and by the difference of its rates in the passage. By basing on the relationship (20.9) and having in mind that losses in pressure are proportional to the quantity  $qw^2$ , one can obtain the following expression for the comparison of coefficients of heat-transfer of the two coolants under the condition,  $\Delta p_{\text{oxn}} = \text{const}$ :

$$\frac{\alpha_1}{\alpha_2} = \left( \frac{\lambda_{\text{M1}}}{\lambda_{\text{M2}}} \right)^{0.8} \left( \frac{c_{\text{M1}}}{c_{\text{M2}}} \right)^{0.4} \left( \frac{\eta_{\text{M2}}}{\eta_{\text{M1}}} \right)^{0.55} \left( \frac{\rho_{\text{M1}}}{\rho_{\text{M2}}} \right)^{0.475}. \quad (20.28)$$

A comparison of the heat-transfer in different coolants when  $T_{\text{oxn}} = 310^\circ\text{K}$ , performed with the aid of relationship (20.28), is given below. As a standard coolant kerosene was accepted.

Coolant	$\frac{\alpha_H}{\alpha_{\text{kerosene}}}$
---------	---

Fuels

Kerosene .....	1.0
N <sub>2</sub> H <sub>4</sub> .....	4.2
NDMG .....	3.0
50% N <sub>2</sub> H <sub>4</sub> + 50% NDMG.....	2.9

Oxidizers

H <sub>2</sub> O <sub>2</sub> .....	4.8
N <sub>2</sub> O <sub>4</sub> .....	2.7

Limitations of Regenerative Cooling

After the examination of the laws regularities of heat-transfer with regenerative cooling the basic conditions for the reliability and for the rationality of utilizing this type of cooling can be formulated in the following manner:

- 1) the wall temperature on the gas side along its entire length of the chamber must not exceed the temperature, permissible under conditions of strength and heat resistance;
- 2) the wall temperature on the coolant side should nowhere exceed the permissible, excluding conditions of film boiling, thermal and catalytic decomposition, coking;

3) the temperature of the coolant should nowhere exceed the permissible; for example, the boiling point, temperatures of decomposition or cokings depending on the properties of the component;

4) losses in pressure in the coolant tract should be small as possible, in order to reduce the weight of the supply media;

5) coolant passage should be technologically efficient.

It is impossible for all chambers to meet these conditions. With a specified fuel and given maximum thrust there are limitations on the pressure in the combustion chamber, and in this case the fuel and fixed  $p_H$  - based on the amount of thrust.

Limitation on  $p_{K\max}$  is governed by the strength of chamber wall at the maximum permissible  $T_{cr}$ . With an increase in  $p_H$  minimum necessary under conditions of strength of the thickness of the wall from the accepted material  $\delta_{cr,min}$  increases (Fig. 20.7). At the same time, as shown above, for efficient heat-transfer through the wall, the thickness of the wall should be as thin as possible. Its maximum permissible value  $\delta_{cr,max}$  at different  $p_H$  are also shown in Fig. 20.7. The simultaneous meeting of the requirements of strength and of heat-transfer is possible only in the shaded range. As it appears, the range of acceptable values  $\delta_{cr}$  is shortened with an increase in  $p_H$ . The value  $p_{K\max}$  is the maximum permissible for the given material.

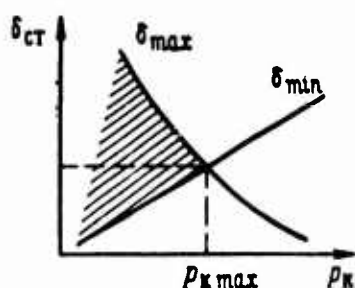


Fig. 20.7. For the analysis of the limitations of regenerative cooling.

Utilization of a connected jacket, when the cold wall of cooling casing carries a power load, of course, will substantially weaken the limitation on  $\Delta_{\text{wall}}$ , and consequently, it expands the range of permissible values of  $p_{\text{H}}$ .

Limitation on  $\Delta_{\text{wall}}$  is governed by the maximum permissible thermal receptivity of the coolant, i.e., by the maximum quantity of heat, which can be transferred to 1 kg of coolant, not overheating it higher than a certain permissible temperature. For the majority of liquids, the limiting temperature of heating should not exceed the boiling point; for some — the temperature of thermal or catalytic decomposition ( $\text{N}_2\text{H}_4$ ,  $\text{H}_2\text{O}_2$ ) or temperature of coking (hydrocarbon fuels).

In the chamber of the adjusted thrust, the lowering of  $p_{\text{H}}$  signifies a proportional decrease in the consumption of the component-coolant. The quantity of heat, which enters the wall and which should be discernible by the coolant, is lowered to a lesser extent, approximately, proportional to  $p_{\text{H}}^{0.5}$ . Per unit of consumption of the coolant a larger quantity of heat is passed, its preheating increases. Moreover, with the lowering of  $p_{\text{H}}$  and consequently, the decrease in pressure of the component coolant lowers its boiling point. As a result, at values of  $p_{\text{H}}$  below a certain  $p_{\text{Hmin}}$ , regenerative cooling with a given component is impracticable as a result of its overheated higher than the permissible temperature. /

The limitation based on the amount of thrust, is realizable in the chamber, we can illustrate by a simple example. Let us operate two chambers of different thrust on the same fuel at identical  $p_{\text{H}}$ . The necessary time of stay of the fuel in the combustion chamber is the same. The volume of the combustion chamber according to the formula (16.10) should change proportionally to the consumption of fuel in seconds, and consequently, the thrust. For a spherical the combustion chamber

$$V_{\text{ch}} = \frac{\pi d_{\text{ch}}^3}{6} = aP.$$

Consequently:

$$d_{h,c} = \sqrt{\frac{16}{\pi}} \sqrt{P} = a_1 P^{1/2}.$$

At the same time the surface of the combustion chamber, receiving the heat, constitutes

$$Q = \pi d_{h,c}^2 = \pi a_1^2 P^{1/2} = a_2 P^{1/2}.$$

Thus, the surface of the heating changes more slowly than thrust and consumption of the coolant component. Under the examined conditions, the specific thermal flow in the walls  $q$  is identical. It means the quantity of heat, transmitted per unit of consumption of the coolant, is more for the chamber of small thrust. At values of thrust lower than a certain amount of  $P_{min}$ , the regenerative cooling of one or even both components is impossible as a result of their overheating.

Figure 20.8 shows the character of change in the temperature of the same liquid coolant in three chambers, designed for different thrusts and operating under variable conditions. By a dotted line limiting boiling point of the coolant depends on the pressure. As it appears, in all the chambers the preheating of the coolant increases with a lowering of  $p_n$ . In chamber No. 1 having the greatest thrust  $P_1$ , this preheating is less significant than in chamber No. 2 with a thrust  $P_2 < P_1$ , but in the second chamber it is less, than in the third with a thrust,  $P_3 < P_2$ . Correspondingly, in chamber No. 1 a wide range of conditions without the overheating of the coolant is possible, whereas in chamber No. 2 it is ascertained, and in chamber No. 3, regenerative cooling is generally impracticable, since the coolant begins to boil even at  $P_{min}$ .

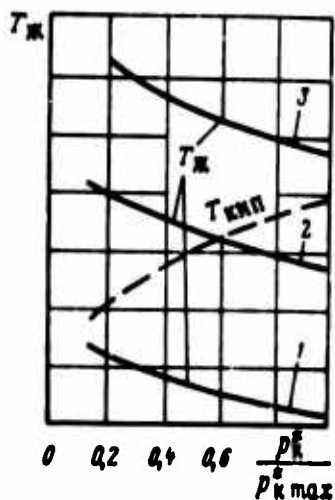


Fig. 20.8. Dependence of the temperature of liquid coolant on pressure  $p_{\text{ж}}^*$  for chambers of various thrusts.

[Translator's note: ж = liquid; кип = boiling].

#### Procedure of the Calculation

The original data for the calculation are:

parameters of the products of combustion, obtained by the thermodynamic calculation;

second the consumption of the coolant and of its properties depending on temperature and pressure;

thicknesses of the chamber walls, specified for conditions of strength and heat resistance;

properties of the material of the wall at various temperatures.

For the chamber with controlled thrust, necessary data are necessary to know the maximum and minimum conditions.

Calculation, in essence, is a check: by assigning a temperature distribution  $T_{\text{cr}} < T_{\text{доп}}$  throughout the entire channel of the chamber, they check, whether or not the reliable regenerative cooling is guaranteed.



The procedure of the calculation is such that:

1. For the condition  $p_{K \max}$  by methods, given in Chapter XIV, the distribution of the specific thermal flows  $q$  for the entire channel is calculated.

One obtains diagram  $q$  at the prescribed fuels component ratio  $\kappa$  in the near-wall layer as far as possible with an allowance for effect of film curtain, if such is anticipated.

If distribution  $q_0$  is known for the channel of a "standard" chamber, geometrically given in detail, then in order to determine  $q$ , one can make use of the formula of conversion (14.55):

$$\left(\frac{q}{q_0}\right) = \left(\frac{p_K}{p_{K0}}\right)^{0.85} \left(\frac{d_{np0}}{d_{np}}\right)^{0.15} \frac{S}{S_0}.$$

This formula can be applied for the conversion  $q$  with a variable  $p_K$ .

2. For a condition  $p_{K \min}$  the preheating of the coolant is checked. If temperature  $T_{\text{cool max}}$  is lower than a certain maximum permissible, then the cooling of the chamber can be, in principle, the component under considerations.

3. According to formula (20.6) the values of temperature of the wall on the coolant side can be determined:

$$T_{\text{ctr}} = T_{\text{ctf}} - q \frac{\delta_{\text{ct}}}{\lambda_{\text{ct}}}.$$

One checks whether or not  $T_{\text{ctr}}$  exceeds the permissible wall temperature. When  $T_{\text{ctr}} > T_{\text{ctr don}}$  or, conversely, with an underrated value of  $T_{\text{ctr}}$ , if possible, the quantities  $\delta_{\text{ct}}$  and  $\lambda_{\text{ct}}$  are varied. With a small deviation of them from the initial values one cannot make the conversion of  $q$  and  $T_{\text{ctr}}$ .

4. The required dimensions of the flow-through sections of the coolant tract is calculated according to formula (20.21) or (20.22). The possibility of the design and technological fulfillment of such a channel are determined, and if necessary, corrections are introduced. The rates of the coolant are determined.

5. After the shaping of the channel taking into account the structural and technological requirements the accepted values are checked. To do this, the values  $\alpha_m$  and  $\alpha_s$  are determined according to formula (20.11) or (20.13) — the values  $\alpha_{sp}$  and  $q_{sp}$  — based on experimental data and then the temperatures of the wall on the coolant side:

$$\begin{aligned} T_{cr,1} &= T_m + \frac{q_{sp}}{\alpha_{sp}} - \text{(condition A, bubble boiling);} \\ T_{cr,2} &= T_m + \frac{q}{\alpha_m} - \text{(part of conditions A, condition B);} \\ T_{cr,3} &= T_s + \frac{q}{\alpha_s} - \text{(conditions C and D).} \end{aligned}$$

Further on, the temperature of the wall on the gas side is calculated

$$T_{cr,4} = T_{cr,3} + \frac{\lambda_{cr}}{\lambda_{gr}} q$$

Usually, there is adequate agreement of the prescribed and obtained values to within several percent. With large discrepancies a conversion is made.

6. The losses in pressure in the coolant tract are determined and their acceptability is evaluated.

If under any conditions of reliability, the external regenerative cooling is not performed using all the possible variants of the scheme, then this is proof of its inadequacy and need for the utilization of additional internal cooling or other means of heat shielding.

### 20.3. Internal Cooling

Let us briefly describe the methods of internal cooling of chamber walls presented in Table 20.1.

#### Creation of the Near-Wall Layer

The near-wall layer, consisting of low-temperature combustion products, can be created with the aid of head whose peripheral sprayers provide a substantial surplus of one of the components, for example, the fuel near the chamber walls. The boundary layer becomes much colder than with the uniform distribution of the fuel components with  $\kappa = \kappa_n$ . As a result, the specific thermal flows, which should be determined according to methods, described in Chapter XIV when  $\kappa = \kappa_{CT}$ , are reduced. The shielding action of the near-wall layer in case of fuel excess amounts to, furthermore, the creation of a reducing medium at the chamber walls.

In connection with this the processes of radial mixing of the fuel components proceeds relatively slowly, and with the proper alignment of the near-wall layer, its shielding action can be maintained up to the critical cross section of the nozzle.

The creation of the near-wall layer with  $\kappa = \kappa_{CT}$  somewhat lowers the specific thrust as compared to the case where all of the fuel is used when  $\kappa = \kappa_n$ . This decrease can be evaluated, using a model of two-layered flow (§ 11.3). Based on formula (11.33) the specific thrust in a vacuum for the diagram  $\kappa$  with a near-wall layer amounts to

$$P_{ya.2} = P_{ya.1} - g_{CT}(P_{ya.1} - P_{ya.1CT})$$

(by index 2 it is noted that the quantity relates to a case of a two-zone diagram  $\kappa$ ). If the near-wall layer is not produced, then value  $P_{ya.1}$  is equal to  $P_{ya.1CT}$

Assuming that the perfection of the remaining processes in both cases is the same it is possible to write the coefficient of losses as

$$\xi_{\text{ст}} = \frac{\delta P_{\text{уд}}}{P_{\text{уд.н.н}}} = g_{\text{ст}} \left( 1 - \frac{P_{\text{уд.н.ст}}}{P_{\text{уд.н.н}}} \right), \quad (20.29)$$

where  $\delta P_{\text{уд}} = P_{\text{уд.н.н}} - P_{\text{уд.н.ст}}$  — decrease in the specific thrust in a vacuum with two-zone distribution of the fuel components (nucleus and near-wall layer).

The dependence (20.29) is depicted in Fig. 20.9. As it appears, the lowering of specific thrust, governed by the alignment of the near-wall layer, depends on the value of relative fuel consumption in the near-wall layer  $g_{\text{ст}}$  and the quantities  $P_{\text{уд.н.ст}}/P_{\text{уд.н.н}}$ . The latter one is determined by the relationship of excess oxidizer ratio in the near-wall layer as well as in the nucleus of flow. The reduction of  $P_{\text{уд.н}}$  can amount to several percent. This is the price of shielding the chamber walls by the method of an aligned near-wall layer with the aid of peripheral sprayers. The lowering of  $P_{\text{уд.н}}$  is especially significant for engines of small thrust, which, as shown in the previous paragraph, is not sufficient for external regenerative cooling.

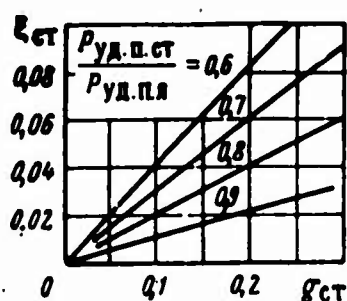


Fig. 20.9. Losses in specific thrust with the creation of a near-wall layer.  
[Translator's note: ст = wall; уд.н.ст = specific flow at the wall; уд.н.н = specific flow of nucleus.]

#### Film Cooling

With this method of shielding the attempt is made to create a stable film of coolant on the fire side of the chamber wall evenly around the perimeter. In order to increase the stability of the

oth  
s  
film, a centrifugal (tangential) feed of the coolant is supplied through special slots or apertures in the cooling zone. The zones can be located in the various sections.

By film cooling with a liquid coolant using a subcritical pressure, a part of the heat from working medium is expended to increase the temperature of the coolant higher than the critical and its subsequent vaporization. As a result of vaporization the film gradually is reduced, and then it disappears. At a certain distance after complete vaporization a layer of vapor of the coolant is retained. As a coolant one could use a fuel component (usually, a combustible component) or a special liquid with favorable properties. The shielding action of the film cooling consists of the lowering of the specific convective thermal flow owing to the reduction in the difference of temperatures in the boundary layer, in the lowering of specific radiant heat flow (the liquid film is a good insulator against thermal radiation) and also in the creation of a wall of reducing or neutral medium. Furthermore, the film protects the walls against erosion pressure of the gas flow.

rs,  
10  
of  
The shielding effect of the liquid film is manifested even at very small thicknesses. An excessive increase in the thickness of the film leads to an appearance of waves on the surface of the film, and then, possibility of break-away of the particles of the liquid ("drop removal" from the surface). The consequence of this is the useless consumption of liquid and even an increase in the overall heat flows to the film due to the increase in its surface.

The consumption of the coolant for film cooling can constitute from 0.5 to 5% of the overall consumption of the fuel. With such small consumptions it is difficult to guarantee a uniform stable protective film of the necessary length around the perimeter. As yet, the necessary length of the protective film is determined experimentally, by varying the injection pressure, the sizes and arrangement of the apertures in the zones or slots of fuel feed, and so forth.

Degree of lowering the specific thermal flows in sections of film cooling can attain 50-70%. Characteristic is the stabilization of heat flows, beginning from a certain value of relative liquid consumption, introduced to create the film:

$$\varepsilon_{na} = \frac{G_{na}}{G_s},$$

where  $G_{na}$  and  $G_s$  — consumptions in seconds through zones of film cooling and the sum total (through the head and zone), respectively, i.e.:

$$G_s = G_{roa} + G_{na}.$$

Fundamental deficiency of film cooling is the loss in specific thrust, in association with ineffectual (in the sense of creating thrust) by utilization of the coolant.

The quantitative evaluation of the losses of specific thrust, associated with film cooling presents considerable difficulties. Noted below are methods, providing only a rough evaluation of the limiting values of losses of specific thrust using film cooling.

1. The substance of the film does not interact with the basic flow and does not participate in the creation of thrust.

The ratio of values of specific thrusts in a vacuum in this instance can be written so:

$$\frac{P_{ya,n}}{P_{ya,0}} = \frac{P_n(G_{roa} + G_{na})}{P_n G_{roa}} = 1 - \varepsilon_{na},$$

where  $P_{ya,0}$  — quantity of specific thrust in the absence of film cooling.

The coefficient of the lowering of specific thrust amounts to

$$\xi_{na} = \frac{P_{ya, n0} - P_{ya, n}}{P_{ya, n0}} = g_{na}. \quad (20.30)$$

2. The substance of the film absorbs heat  $Q_{nn}$  from the basic flow and takes part in the creation of thrust. In the nozzle there is two-layered flow.

In accordance with formula (of 20.29) the coefficient of the lowering of specific thrust in this instance amounts to

$$\xi_{na} = g_{na} \left( 1 - \frac{P_{ya, na}}{P_{ya, n0}} \right). \quad (20.31)$$

The amount of specific thrust in a vacuum  $P_{yd, n, n0}$  for the substance of the film is determined by thermodynamic design using known amounts of  $p_k^*, p_k^*/p_c$ . The value of full enthalpy of the film in this case is equal to

$$I'_{na} = I_{na} + Q_{na}, \quad (20.32)$$

where  $I_{nn}$  — full enthalpy of the film under conditions of supply;  $Q_{nn}$  — quantity of heat, absorbed by the film from the basic flow.

In an analogous way the specific thrust in a vacuum of the basic fuel is determined. The change value of its full enthalpy is equal to:

$$I'_r = I_r - Q_{na} \frac{g_{na}}{1 - g_{na}}. \quad (20.33)$$

The effect of the change in full enthalpy of the film and of fuels for quantities of specific thrusts in a vacuum  $P_{yd, n, n0}$  and  $P_{yd, n0}$  can be also evaluated according to the formula of extrapolation.

3. The substance of the film completely mixes with the nucleus of flow.

The changing composition of fuel is determined by the formula in Chapter V, and the new value of enthalpy of the fuel in this instance is equal to

$$I'_T = (1 - g_{na}) I_T + g_{na} I'_{na}$$

The thermodynamic calculation, made at known values of  $I'_T$ ,  $p_K^*$ ,  $p_K^*/p_c$ , allows one to find the changed value of specific thrust in a vacuum, and consequently, the coefficient  $\xi_{na}$ .

If we ignore the change in composition of the fuel, then one can use the formula of extrapolation.

Then, the change in full enthalpy of the fuel amounts to

$$\delta I_T = \delta I_K = g_{na} (I_{na} - I_K). \quad (20.34)$$

By extrapolating approximately according to formula (9.50), we will obtain:

$$\frac{P_{yK}}{P_{yK0}} = 1 + \frac{\left(1 - \frac{T_c}{T_K}\right) \delta I_K}{2(I_K - I_c)}$$

or, by substituting the expression (20.34):

$$\frac{P_{yK}}{P_{yK0}} \approx 1 + \frac{g_{na} (I_{na} - I_K) \left(1 - \frac{T_c}{T_K}\right)}{2(I_K - I_c)}.$$

Here,  $P_{yK}$  and  $P_{yK0}$  — theoretical values of specific thrust in the presence of film cooling and without one.

The coefficient of the lowering of specific thrust amounts to

$$\xi_{na} = \frac{g_{na}}{2} \left(1 - \frac{T_c}{T_K}\right) \frac{I_K - I_{na}}{I_K - I_c}. \quad (20.35)$$



Coefficient of specific thrust efficiency is determined according to the usual formula

$$\varphi_{\text{пл}} = 1 - \xi_{\text{пл}}.$$

When calculating the chamber value of the coefficient  $\varphi_{\text{пл}}$  one must introduce the overall specific thrust efficiency  $\varphi_{\text{уд}}$ .

When deriving formulas (20.30) and (20.35), it was assumed that the products of vaporization of the film take part in the process of expansion with maximum possible degree of reduction of pressure  $p_{\text{к}}^*/p_{\text{с}}$ . This corresponds to a case of introducing the film in the combustion chamber. Frequently, however, the film is introduced in front of the critical section of the nozzle, highly demanded in heat shielding. In this case the work of expansion of the vapors of the coolant is reduced, and the losses in specific thrust increased.

With identical parameters of the working processes, the loss in specific thrust as a result of film cooling, should be more significant in the chambers of small thrusts. Surface of the chamber is reduced more slowly, than the thrust; therefore, in order to create film cooling of equal efficiency in small chamber the largest relative liquid consumption  $g_{\text{пл}}$  will be required.

In Fig. 20.10 a continuous line shows the calculated dependence of losses in specific thrust using film cooling, on the relative consumption  $g_{\text{пл}}$ . The value  $\xi_{\text{пл}}$  was calculated according to formula (20.30). There, the plotted experimental data was obtained using film cooling of the chamber of the engine with various coolants. As it appears, the dependence (20.30) satisfactorily agrees in this instance with the results of the experiment [6].

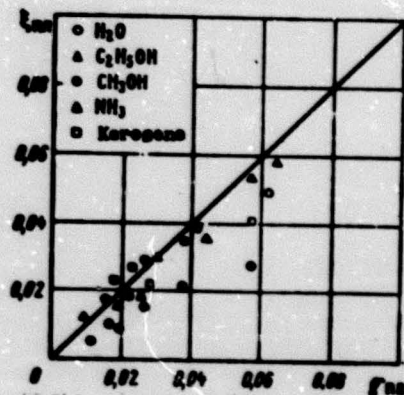


Fig. 20.10. Dependence of the losses of specific thrust on the relative consumption for film cooling.

[Translator's note:  $\pi\pi$  = film.]

### Porous Cooling

Porous cooling is developed using a film. Using this method of heat shielding the internal wall of chamber or part of it, if porous cooling is applied in a specified section of the chamber, is made of fine porous material whose pores have a diameter of several tens of microns. The porous material is usually obtained by sintering the powders of metals, or by pressing metallic mesh. In this case, one strives to obtain a material whose micropores are evenly distributed, and whose quantity per unit area is large.

The shielding action of porous cooling is analogous to a film. The liquid coolant in the pores are forced out at a low velocity to the fire surface of the wall, create a shielding protective film, reducing the specific thermal flow in the wall.

At a certain critical value of consumption of the liquid coolant, the temperature of the wall ceases to be equal to the boiling point of the liquid at the given pressure. Under a condition of critical consumption, the internal wall protects itself by a continuous film of the liquid. With the lowering of the consumption, the liquid partially vaporizes. In connection with less efficient protection by the vapor film, the temperature of wall rises; however, it remains below the permissible.

In principle, it is feasible, and when using coolants as  $H_2$  and  $NH_3$  it is also rational to vaporize the liquid coolant on the external surface of the wall and to blast the cooled vapor into the boundary layer along the internal wall. This provides large uniformity for cooling the surface.

Quantitative relationships between consumption of the coolant and the lowering of specific heat flows depend on the properties of the coolant, on the material of the wall and on the parameters of gas flow. In general, consumption of the coolant using porous cooling is 3-5 times less, than using a film that it is governed by low input rates of the coolant and by uniform cooling of the surface. Economic benefits of porous cooling increase with a steep temperature gradient ( $T_e - T_{cr,f}$ ).

However, when using porous cooling, there are a number of difficulties. Thus, the diameter of the microscopic pores are unequal and with insignificant changes in pressure, the flow of coolant becomes uneven, because the pores are easily plugged up. Wall on the coolant side is cold, and on the fire side, is heated to a high temperature; as a result of this, considerable thermal stresses arise in the wall.

Despite these mentioned difficulties, porous coolings is the most promising and is also almost singularly suitable for cooling engines with very high specific thermal flows in the wall chambers. In the future this method can be applied to heavy single-chamber ZhRDs on high energy fuels with a high pressure  $p_k$ , and likewise in thermal nuclear rocket engines.

#### 20.4. Combined Systems of Wall Shielding

In the chambers of modern ZhRDs, very frequently there are combined systems of wall shielding, which are represented by a combination two or more methods of heat shielding. Combined systems are used in those cases when neither of the examined systems individually provides the necessary resource for the chamber, or if



it causes excessive high cost in weight and complications of the system or causes a substantial lowering of the economy.

Most extensively used is the combination of external regenerative cooling with internal cooling. The latter is used in the form of a shielding zone, created by the head, or in the form of film cooling. Separately in heavy chambers based on the thermal intensity of the variants both mentioned types of internal cooling can be applied simultaneously.

In the presence of well treated porous material it is expedient to apply porous inserts in sections of the maximum thermal flows.

In engines of small thrust even the utilization of both components may not guarantee the necessary cooling. In this instance it is in the best interest to utilize the combined system of film and radiation cooling (see Chapter XXVI).

For engines, which have a large degree of pressure reduction in the nozzle, the part of the nozzle with low temperatures of the gas can be left without liquid cooling, restricting the radiant heat-transfer into the surrounding medium. Figure 20.11 presents the dependence of minimum relative area of a molybdenum nozzle, at the start of which, the enlarging section of the nozzle can cool only due to radiation (thrust of engine - 4.5 T, radiating capacity of the wall -  $\epsilon = 0.9$ ).

There is application for a combination of external cooling with shielding of the fire surface by thermoresistant coatings, as well as by ablating coatings.

The combination of film cooling with ablating coatings reduces the rate of phase transformations in the surfacial layer of the coatings, and correspondingly, reduces the rate of the removal of the coating material.

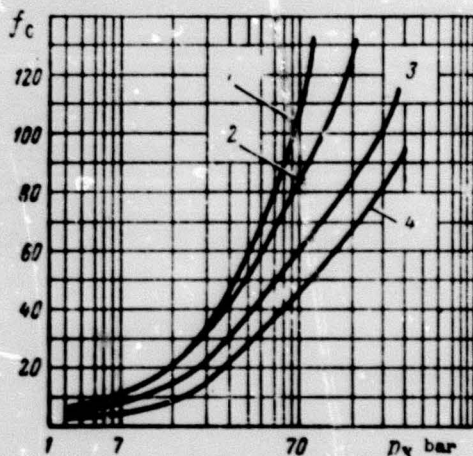


Fig. 20.11. Lower limit of values of the relative area of a molybdenum nozzle, at the start of which there is sufficient radiant cooling of the surface [8]: fuel 1— $H_2 + F_2$ ; 2— $B_2H_6 + OF_2$ ; 3— $H_2 + O_2$ ; 4— (50%  $N_2H_4$  + 50% NDMG) +  $N_2O_4$ .

The utilization of new high calorie fuels and need for increasing the resource of ZhRDs pose new raised requirements for systems of shielding chamber walls. The perfection of these systems goes hand in hand with the search for new high-quality material and expedient structural schemes of external and internal cooling.

### Bibliography

1. Avduyevskiy V. S. et al. Osnovy teploperedachi v aviatsionnoy i raketnoy tekhnike (Bases of heat transfer in aviation and rocket technology) Oborongiz, 1960.
2. Melik-Pashayev N. I., "Teplofizika vysokikh temperatur", 1966, No. 6.
3. Mikheyev M. A., Osnovy teploperedachi (Bases of heat transfer) GEI, 1956.
4. Khendriks, "Raketnaya tekhnika", 1962, No. 2.
5. Bartz D. R., Jet Propulsion, 1958, No. 1.
6. Coulbert C. D., J. of Spacecraft and Rockets, 1964, No. 2.
7. Seader J. D., Wagner W. R., Chemical Engineering Progress Symposium Series, 1964, No. 52.
8. Sutton G. P., Wagner W. R., Astronautics and Aeronautics, 1966, No. T-1.

## CHAPTER XXI

### SELECTION OF OPTIMUM PARAMETERS

In this chapter the bases of the rational selection of a fuel, of sizes and of parameters of the combustion chamber and of nozzles for liquid-fuel rocket engine are examined.

#### 21.1. Criterion of the Selection of Optimum Parameters

Rocket engines, specifically liquid-fuel rocket engines, in many instances are projected from an actual device. This means allows for the maximum correlation of the parameters of the engine and of the apparatus, there by obtaining the overall optimum solution for the entire device. As optimum parameters of the engine one should take into account those values, which provide the best technical-economic indexes of the developed complex.

For the sake of simplicity of an analysis let us assume that the optimization of these indexes is equivalent to the optimization of the most important index of the apparatus - the velocity, attained at the moment of termination of engine operation.

The terminal velocity of the apparatus can be determined by the equation

$$V_{\Sigma} = V_{\Sigma 0} - \Delta V_{1,1} - \Delta V_{1,2} \quad (21.1)$$

in which

$$V_{0.1} = \bar{P}_{yA.AB} \ln A_{0.1}$$

Here  $\bar{P}_{yA.AB}$  - specific thrust of the engine, the average for the trajectory of the flight.

The decrease in velocity of flight owing to gravitation amounts to

$$\Delta V_{g.1} = \int_0^{t_{0.1}} \sin \theta g dt. \quad (21.2)$$

where  $\theta$  - angle of the slope of the trajectory of flight to the horizon;  $g$  - acceleration of the force of gravity, changing with the altitude of the flight.

Value  $g$  at various altitudes is determined according to the equation

$$g = g_0 \left( \frac{R_0}{R_0 + H} \right)^2. \quad (21.3)$$

where  $g_0 = 9.81 \text{ m/s}^2$  - acceleration of the force of gravity on the earth's surface;  $R_0 = 6371 \text{ km}$  - radius of the earth;  $H$  - altitude of the flight in km.

For vertical flight one can write

$$\Delta V_{d.1} = \bar{g} \tau_{akt.1} \quad (21.4)$$

where  $\bar{g}$  - acceleration of the force of gravity, average over time  $\tau_{akt.1}$ .

The deceleration as governed by the resistance of the medium, is determined by the aerodynamic calculation.

As shown from the calculation, the relative values of the decrease in velocity of flight,  $\delta V_{z.T}/V_{HA}$  and  $\delta V_{a.c}/V_{HA}$  as a first approximation, depend only on the initial thrust-weight ratio of the apparatus

$$A_0 = \frac{P_0}{G_0}. \quad (21.5)$$

where  $P_0$  - starting thrust, and  $G_0$  - starting weight of the apparatus.

Figure 21.1 shows the typical character of the dependence of the relative losses of velocity on the initial thrust-weight ratio. The effect of the aerodynamic resistance for heavy rockets is small in comparison to the effect of the weight.

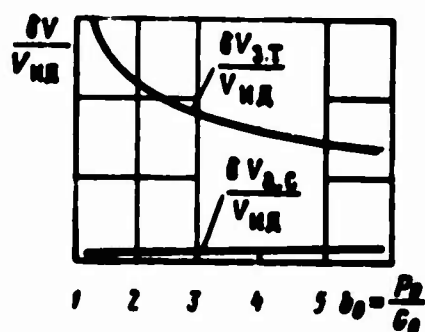


Fig. 21.1. Dependence of the relative losses in velocity on the initial thrust-weight ratio.

If

$$\frac{\delta V_{z.T}}{V_{HA}} = c_{z.T} = f_1(b_0)$$

and

$$\frac{\delta V_{a.c}}{V_{HA}} = c_{a.c} = f_2(b_0),$$

then the terminal velocity can be written in the following manner:

$$V_K = V_{HA} - c_{z.T} V_{HA} - c_{a.c} V_{HA} = (1 - c_{z.T} - c_{a.c}) V_{HA}. \quad (21.6)$$



With the comparative evaluation of the various designed variants of the apparatus of a specific purpose with an assigned value  $b_0$ , it is possible to consider  $c_{3.T} = \text{const}$  and  $c_{a.c} = \text{const}$ . Then, on the basis of equation (21.6), the ratio of the terminal velocities of the apparatus compared to variant 1 and 2 will be equal to the ratio of ideal velocities

$$\frac{V_{\kappa 1}}{V_{\kappa 2}} = \frac{V_{ид 1}}{V_{ид 2}}. \quad (21.7)$$

Consequently, the best variant of the apparatus can be preliminarily selected, by comparing not the terminal velocities of flight, but more simply, the determined ideal velocities.

As criterion of the efficiency of rocket apparatuses one could likewise use the ratio of sum total pulse to the starting weight of the apparatus  $I_{\Sigma}/G_0$ . Let us show that the use of this value as the criterion of efficiency is equal to the use  $V_{ид}$ . Since

$$I_{\Sigma} = \bar{P}_{ya.ab} G_T,$$

then

$$\frac{I_{\Sigma}}{G_0} = \bar{P}_{ya.ab} \frac{G_T}{G_0} \quad (21.8)$$

or, to convert to the mass number of the rocket apparatus  $\mu_K$ :

$$\frac{I_{\Sigma}}{G_0} = \bar{P}_{ya.ab} \left(1 - \frac{1}{\mu_K}\right). \quad (21.9)$$

By comparing expressions (21.1) and (21.9), we are convinced that the quantities  $V_{ид}$  and  $I_{\Sigma}/G_0$  can determine the same factors ( $\bar{P}_{уд.дв}$  and  $\mu_K$ ) and they depend on them equally (they increase with an increase in  $\bar{P}_{уд.дв}$  and  $\mu_K$ ). Consequently,  $V_{ид}$  and  $I_{\Sigma}/G_0$  can be used as criteria of efficiency of rocket systems with equal reason.

As can be seen from equation (21.9), when  $\mu_K \rightarrow \infty$ ,  $I_\Sigma/G_0 \rightarrow \bar{P}_{уд.дв}$ . Consequently, with the theoretical limit  $I_\Sigma/G_0$  using the prescribed fuel there is an average specific thrust of the engine  $\bar{P}_{уд.дв}$ . Degree of the approximation  $I_\Sigma/G_0$  to  $\bar{P}_{уд.дв}$  defines the effectiveness of the specified rocket apparatus.

In the design of the engine it is important to select fuel components and the ratio between them, the pressure in the combustion chamber even on exit from the nozzle. In the selection we will consider the fuel and the mentioned parameters of the engine as optimum, if they provide maximum values of  $V_{ид}$  or  $I_\Sigma/G_0$  to an apparatus of a definite type.

## 21.2. Selection of the Fuel and the Excess Oxidizer Ratio

The most efficient fuel of the several that are suitable, let us say, based on operational characteristics, can be selected by applying the method of evaluation of the fuel on  $V_{ид}$ , presented in Chapter IV.

For every fuel vapor (combustible + oxidizer) it is necessary to evaluate the change of  $V_{ид}$  depending on the excess oxidizer ratio  $\alpha$ . This is done with the aid of equation (4.16), in which  $P_{уд}$  and  $\rho_T$  depend on  $\alpha$ , and quantity  $\sigma_K$  can be considered constant.

Figure 21.2 shows density variation in certain fuels depending on  $\alpha$ , calculated in formula (5.22). Usually  $\rho_{ок} > \rho_T$ ; therefore, with an increase of  $\alpha$ , the density of the fuel increases. The dependence of specific thrust on  $\alpha$  is presented in Fig. 21.3 for these fuels. Using the dependence  $P_{уд.п} = f(\alpha)$  and  $\rho_T = f(\alpha)$ , we will obtain the change  $V_{ид}$  for  $\alpha$  (Fig. 21.4).

From the comparison of graphs 21.3 and 21.4, the following conclusions can be made. Maxima of  $V_{ид}$  are observed for all fuels at values of  $\alpha$ , greater than those, at which the maximum specific

thrust is attained. The difference between  $\alpha$  ( $V_{ид \max}$ ) and  $\alpha$  ( $P_{уд.п \max}$ ) is caused by the character of change  $\rho_T$  based on  $\alpha$ . This difference is greater, the greater the difference between  $\rho_{ок}$  and  $\rho_T$  is. The comparative evaluation of the fuel based on  $V_{ид}$  can give, as this is evident, substantially different results than the evaluation for specific thrust

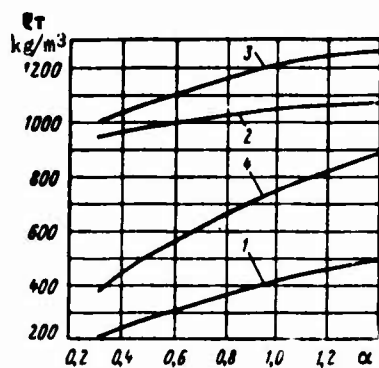


Fig. 21.2.

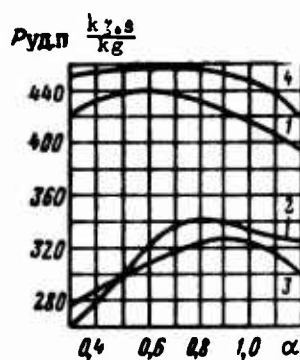


Fig. 21.3.

Fig. 21.2. Dependence of the density of the fuel on  $\alpha$ : 1 - liquid hydrogen + liquid oxygen; 2 - kerosene + liquid oxygen; 3 - asymmetrical dimethylhydrazine + nitrogen tetroxide; 4 - liquid hydrogen + liquid fluorine.

Fig. 21.3. Dependence of the specific thrust in a vacuum on  $\alpha$  (designation for Fig. 21.2):  $p_K^*/p_c = 160$ .

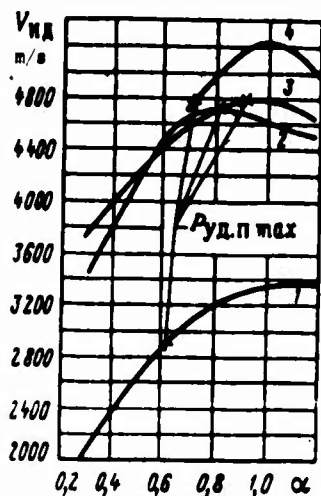


Fig. 21.4. Dependence of the ideal velocity on  $\alpha$  (designations in Fig. 21.2).

As was shown in Chapter IV the value  $V_{ид}$  is proportional to work  $P_{уд} \cdot \rho_T^c$  in which the index  $c$  is determined depending on the variant of the design according to formula (4.23) or (4.32). The selection of an optimum fuel and an optimum  $\alpha$  is conveniently done on charts with coordinates  $\ln P_{уд.п}$  and  $\ln \rho_T$  (Figs. 21.5 and 21.6). In them the lines of constant values  $P_{уд.п} \cdot \rho_T^c$  are straight lines, the slope of which is determined by angular coefficient  $c$ . For each value of  $c$ , it is possible to construct a family of parallel lines (the slope of the straight lines at various  $c$  is shown on the graphs). The displacement of the straight line to the right, to the side of larger  $\rho_T$ , signifies an increase in the quantity  $P_{уд.п} \cdot \rho_T^c$  and consequently, an increase in the ideal velocity. In this way the maximum for the specified fuel corresponds to value  $V_{ид}$  tangent to curve  $\ln P_{уд.п} = f(\ln \rho_T)$ . The point of contact determines the optimum value  $\kappa(\alpha)$ . by comparing the maximum values of  $V_{ид}$  for different fuels, the most effective fuel can be selected.

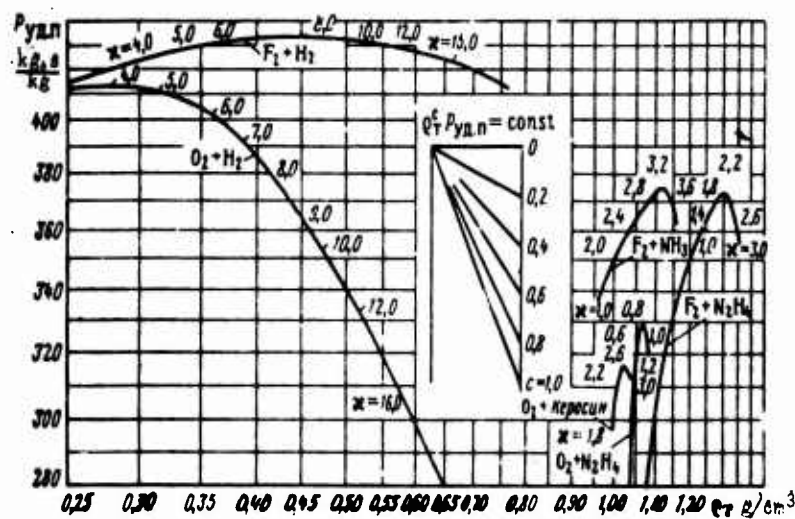


Fig. 21.5. Diagram  $P_{уд.п} = f(\rho_T)$  for low-boiling fuels:  $p_K^* = 3.5$  bar for  $N_2H_4 + F_2$  fuel;  $P = 21$  bar for  $NH_3 + F_2$  and  $H_2 + O_2$ ;  $p_K^* =$  bar for the remaining ones;  $f_c = 10$ . [Translator's note: Керосин = Kerosene].



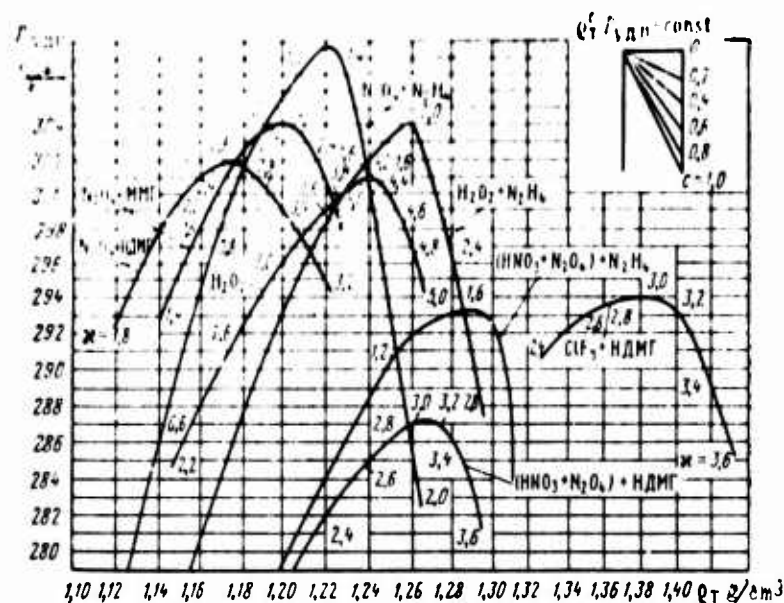


Fig. 21.6. Diagram  $P_{уд.п} = f(\rho_T)$  for stable fuels:  $p_K^* = 35$  bar;  $f_c = 10$ .

[Translator's note: НДМГ = NDMG = asymmetrical dimethylhydrazine].

It is necessary to note that the presented analysis allows one to compare fuels only based on one index. In a practical case, in order to select a fuel one must consider the economic factors. They are determined by the cost of the fuel, by cost of the development of the engines on which this or some other fuel runs, by the cost of the transport of the fuel, of the operation of the rocket complex on which this or some other fuel operates, the starting procedure, and so forth. The reliability and capability of creating a rocket complex over suitable periods of time likewise will depend upon the fuel, and doubtlessly, when selecting the fuel one must consider such factors, as improving the fuels, presence and scales of its production, experimental work with the fuel, and others.

### 21.3. Selection of Pressure in the Combustion Chamber

When selecting the pressure in the combustion chamber as criterion of the optimum, one can use the parameter  $I_\Sigma/G_0$ . The optimum pressure,  $p_{K.онт}^*$  corresponds to maximum  $I_\Sigma/G_0$ . Let us write

down the last quantity in the form

$$\frac{I_3}{G_0} = \bar{P}_{ya} \frac{G_2}{G_0}.$$

The specific thrust of the engine, in general, can be written:

$$\bar{P}_{ya} = \frac{\bar{P}_{ya}}{1 + \epsilon},$$

where  $\bar{P}_{ya}$  - specific thrust of the chamber;  $\epsilon$  - relative consumption of the fuel, spent in the auxiliary systems sometimes  $\epsilon = 0$ ).

The weight of the fuel aboard the apparatus amounts to

$$G_r = G_0 - G_{k1} - G_{k2}, \quad (21.10)$$

where  $G_0$  - complete weight of the apparatus;  $G_{k1}$  - part of the final weight of apparatus, independent of pressure  $p_K^*$  (including, useful load);  $G_{k2}$  - part of the final weight of the apparatus, depending on pressure  $p_K^*$ . Hence

$$\frac{I_3}{G_0} = \frac{\bar{P}_{ya}}{1 + \epsilon} \left( 1 - \frac{G_{k1}}{G_0} - \frac{G_{k2}}{G_0} \right). \quad (21.11)$$

Let us designate

$$\left. \begin{aligned} \bar{P}_{ya} &= f_1(p_K^*); \quad \epsilon = f_2(p_K^*); \\ \frac{G_{k1}}{G_0} &\neq f(p_K^*) = \text{const}, \quad \frac{G_{k2}}{G_0} = f_3(p_K^*), \end{aligned} \right\} \quad (21.12)$$

whereupon

$$\frac{I_3}{G_0} = \frac{f_1(p_K^*)}{1 + f_2(p_K^*)} [1 - \text{const} - f_3(p_K^*)]. \quad (21.13)$$

If the dependence (21.12) is provided analytically (for standard projects semi-empirical relationships are used), then expression (21.13) can be differentiated according to  $p_K^*$  for detecting the maximum  $I_\Sigma/G_0$ .

The dependence  $P_{yA}$  on  $p_K^*$  is determined by the type of basic fuel; the dependence  $\epsilon = f_2(p_K^*)$  - by the type of auxiliary fuel, and likewise, by the type and by the degree of perfection of system of gas generation or fuel-supply of the working system medium from the storage battery potential. The dependence of weight  $G_{K2}$  is determined, mainly, by the structural scheme of the engine device and material used. Basic portion of the weight of  $G_{K2}$  constitutes the weight of the means of fuel supply, including the tanks. Dependence of the weight of the means of fuel supply on  $p_K^*$  is different for a turbo-pump and pressurized fuel supply. For the latter, the weight of the gas generator or of storage battery potential, of loaded fuel tanks and main fuel lines increases with an increase in  $p_K^*$  much more intensively than in the case of pump feed.

The weight of the chamber of the engine included in the value  $G_{K2}$  changes only slightly. With a constant weight of elements of steel framework of the chamber, the weight of the combustion chamber is reduced somewhat with an increase in  $p_K^*$ , mainly, owing to the reduction in the weight of the head (diameter of the combustion chamber with a specified thrust  $P$  and with an increase in  $p_K^*$  is reduced, but the walls are thickened).

In all cases the weight increase in  $G_{K2}$  results in a reduction in the relative content fuel  $G_T/G_0$ , and consequently, in a reduction in the sum total pulse  $I_\Sigma$  with a fixed initial weight of the apparatus. So, the relative consumption of fuel  $\epsilon$  in the auxiliary systems affects  $I_\Sigma$ . The increase in specific thrust with an increase in  $p_K^*$  results in an increase in  $I_\Sigma$ . Ultimately, at a certain value of  $p_K^*$  the maximum  $I_\Sigma/G_0$  (Fig. 21.7) is discovered. According to the degree of improvement of the weight characteristics (var. 2 is better based on weight characteristics than var. 1) the position of

maximum  $I_{\Sigma}/G_0$  shifts to the side of higher  $p_{K}^*$ . This promotes a reduction in the relative fuel consumption in the auxiliary systems. Optimum values  $p_{K}^*$  for engines with a turbopump fuel supply are higher than for engines with a pressurized supply, and the maxima of the dependence of  $I_{\Sigma}/G_0 = f(p_{K}^*)$  are more gently sloping.

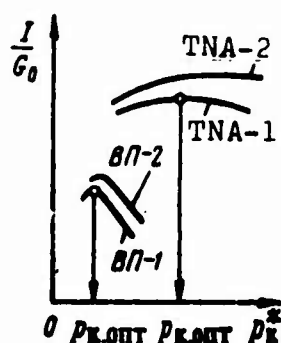


Fig. 21.7. Dependence of the criterion  $I_{\Sigma}/G_0$  on the pressure in the combustion chamber using pressurized and turbopump fuel supply.

In the case of using a turbopump fuel-supply system with afterburning of the working medium quantity  $\epsilon$  is equal to zero and it follows qualitatively from formula (21.13), the maximum  $I_{\Sigma}/G_0$  should be displaced in range of higher pressures as compared to the case of the ejection of working medium of the turbine. An example of the results of a test by the choice of the optimum pressure for two noted variants is shown in Fig. 21.8, where the relative net load  $\bar{G}_{rp}$  included in the orbit of an artificial earth satellite is accepted as criterion.

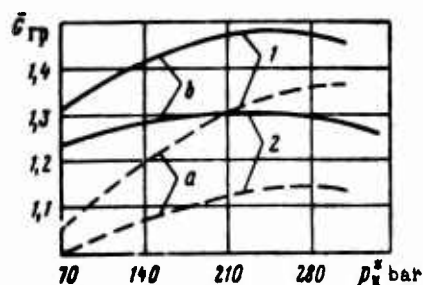


Fig. 21.8. Dependence of relative net load, carried in orbit by the artificial earth satellite at an altitude of 550 km, on the pressure in the combustion chamber: 1 - liquid-fuel rocket engine with afterburning of the generator gas; 2 - liquid-fuel rocket engine without afterburning: a) nonadjustable nozzle; b) adjustable according to the height of the nozzle.

Based on information from foreign correspondence, the value of  $p_{K,OPT}^*$  comprise: with turbopump fuel supply about 70-100 bar for



an open scheme, and more than 200 bar for engines with after-burning of the generator gas; with a pressurized fuel supply - approximately 20-30 bar.

In practice, frequently a selection of values of  $p_k^* < p_{k.ont}^*$  is made such, in order that it is possible to guarantee the reliable cooling of the chamber. Furthermore, when selecting pressures in the combustion chamber of a designed engine one takes into consideration, of course, as far as possible the produced  $p_{k.ont}^*$  to the improved pressure level in modern engines. With too great departure the time and cost of perfecting the engine with a high reliability are lengthened.

Sometimes the ratio of the sum total pulse to the weight of the pulse is used as criterion of the perfection of the engine system, i.e., excluding the fuel weight and net load. One can consider the following values of this criterion as attainable:

	$\frac{I_\Sigma}{G_k - G_{rp}}$
Engine device.....	1300-2100
prolong storage of the fuel.....	5000-9000
one of fuel components being low boiling.....	3000-4000
both fuel components being low-boiling.....	2000-2300
solid fuel.....	

21.4. Selection of Parameters of the Cross-Section of the Nozzles

The selection of parameters of the cross-section of the nozzles means the selection of the optimum outlet pressure from nozzle  $p_{c.ont}$  which can provide the maximum terminal or ideal velocity of apparatus under other specified conditions.

A change in  $p_c$  causes a change in the sizes of the nozzle: with a reduction in  $p_c$  outlet area  $f_c$  increases, and at a constant angle of expansion - and length of the nozzle. Ultimately, the weight of

the nozzle constitutes a small fraction of the final weight of the apparatus, then an increase in this weight can be, as a first approximation, ignored and the final weight of the apparatus  $G_K$  can be considered as constant with various variants of nozzles. With a prescribed  $G_0 = \text{const}$ , consequently, the constant and the quantity  $G_0/G_K$  are maintained. Then, maximum ideal velocity  $V_{ид}$  will correspond to the maximum average specific thrust  $\bar{P}_{yd}$ .

Hence, at a prescribed value of pressure  $p_K^*$  in the combustion chamber one should select such a value of  $p_c$ , which will provide  $\bar{P}_{yd \text{ max}}$ . For nozzles with different degrees of pressure differential  $\pi_c = p_K^*/p_c$ , the value  $\bar{P}_{yd}$  will be different as a result of the different value of losses of specific thrust under uncalculated conditions of the nozzle. The minimum losses in specific thrust for the time of engine operation  $\tau_{акт}$  will correspond to the maximum  $\bar{P}_{yd}$ .

It is possible to show that the maximum  $\bar{P}_{yd}$  is attained when

$$\left(\frac{p_c}{p_K^*}\right)_{\text{опт}} = \frac{\int_0^{\tau_{акт}} \left(\frac{p_h}{p_K^*}\right) d\tau}{\tau_{акт}}. \quad (21.14)$$

In this way, the determination of the optimum for the given trajectory of the degree of pressure differential  $\pi_{c.опт} = (p_K^*/p_c)_{\text{опт}}$ , requires the dependences  $H = f(\tau)$  and  $p_K^* = f(\tau)$  over the powered segment of the flight of the apparatus.

In the particular case of a constant pressure in the combustion chamber we obtain from expression (21.14)

$$p_{c.опт} = \frac{\int_0^{\tau_{акт}} p_h d\tau}{\tau_{акт}}, \quad (21.15)$$

where the value  $\int_0^{\tau_{акт}} p_h d\tau / \tau_{акт} = \bar{p}_h$  is the average atmospheric pressure for

the trajectory of the powered segment of the flight based on the time.

For aircraft engines the continuous functions  $H = f(\tau)$  and  $p_k^* = f(\tau)$  are lacking in connection with relative indeterminate program of flight. The optimum values of  $\pi_c$  for these engines must be selected on the basis of information of certain characteristic values  $H$  and  $p_k^*$  and time of engine operation under these conditions. The calculation in this instance can be the simplified formula (21.14):

$$\left(\frac{p_c}{p_k^*}\right)_{opt} = \sum_{i=1}^n \left(\frac{p_h}{p_k^*}\right)_i \frac{\tau_i}{\tau_{akt}}, \quad (21.16)$$

where  $(p_h/p_k^*)_i$  - the ratio of pressures to the  $i$ -th characteristic condition of engine operation;  $\tau_i/\tau_{akt}$  - relative time of operation to the  $i$ -th condition.

It is natural that

$$\sum_{i=1}^n \frac{\tau_i}{\tau_{akt}} = 1.$$

Above, the methods of the selection of  $p_{c,opt}$  in a simplified case of the absence of forces of gravity weight and of aerodynamic resistance are examined. The calculation of these forces, in principle does not change the methods, but it makes the calculations more laborous. A comparative picture of the efficiency of different nozzles changes little. Utilization of the simplified methods is valid even when allowing for the fact that the found values of  $p_{c,opt}$  out of theoretical considerations more frequently include corrections. Usually, they amount to a certain increase in the calculated value  $p_{c,opt}$  in connection with the following considerations. An increase in  $p_c$  corresponds to a lowering of the weight of the nozzle and a reduction in its sizes. With a reduction in the surface of the nozzle the function of cooling it is facilitated, and hydraulic resistance of the coolant passage is reduced. In the nozzles of

smaller sizes it is simpler to provide the necessary strength and rigidity. The maximum of the dependence of the average specific thrust for  $p_c$  is somewhat gently sloping; therefore, a certain increase in  $p_c$  as opposed to  $p_{c.онт}$  reduces the economy only slightly.

It is necessary to also note that the selection of the optimum pressure at the cross section of the nozzle, i.e., the selection of the area of its outlet section, should correlate with the arrangement of the stern part of flying apparatus. Investigations show that the conditions of interaction of a jet stream and external flow are substantially reflected in the amount of ground resistance of the apparatus. The problem of selecting the optimum nozzle for the chamber whose operation always goes on in a vacuum, stands somewhat apart. This relates to the chambers of the last stages of multistage rockets. The absence of forces of aerodynamic resistance for such rockets is no longer an assumption; the assumption of the absence of the forces of gravity during the analysis, however, holds.

An increase in the velocity to the  $i$ -th degree of a rocket stage can be written as such:

$$V_{ki} - V_{k(i-1)} = \Delta V_k = P_{yд.п} \ln \frac{G_0}{G_k} \quad (21.17)$$

The value  $P_{yд.п}$  for the chamber with a nonregulated nozzle does not change over the time of flight. It is obvious that the lowering of pressure  $p_c$  at the outlet of the nozzle results in a counter pressure by  $\Delta V_k$ , namely: specific thrust increases due to increase in  $p_k^*/p_c$ , but the ratio of  $G_0/G_k$  decreases due to increase in the weight of the nozzle. Ultimately, at a specified value of  $p_{c.онт}$  a maximum  $\Delta V_k$  must exist. If we express the specific thrust in a vacuum as  $P_{yд.п} = \beta K_{pн}$ , then expression (21.17) can be converted in the following way:

$$\frac{\Delta V_k}{\beta} = K_{pн} \ln \frac{G_0}{G_k} \quad (21.18)$$

A variable, depending on  $p_c$ , is left on the right side. The maximum  $\Delta V_K/B$  is sought in function from  $p_K^*/p_c$ , or the relative area of the cross section of the nozzle  $f_c$ . The values  $f_c$ ,  $p_K^*/p_c$  and  $K_{p_n}$  are interrelated.

A change in the weight of the nozzle with a reduction of  $p_c$  can be approximately estimated even during the design stage. Considering the variable component of weight, only the weight of the enlarging part of the nozzle,  $\Delta G_c$  can be written (Fig. 21.19):

$$\Delta G_c = (F_c - F_{np}) \delta_{np} \rho_M \frac{1}{\sin \alpha}$$

or

$$\Delta G_c = (f_c - 1) \frac{F_{np} \delta_{np} \rho_M}{\sin \alpha}, \quad (21.19)$$

where  $\delta_{np}$  - given wall thickness (with the allowance for the jacket of coolant passage);  $\rho_M$  - density of the wall material.

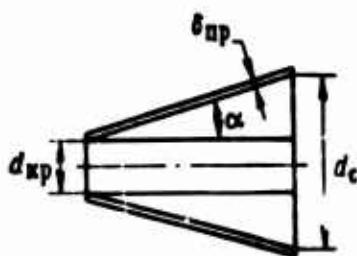


Fig. 21.19. For the determination of the weight of the enlarging section of the nozzle.

From value  $f_{c.опт}$  it is easy to convert to  $p_{c.опт}$ . The found value,  $p_{c.опт}$ , can be increased based on the same considerations as that for rockets, passing through dense layers of atmosphere.

During the examination of the basic principles of selecting the optimum parameters of a liquid-fuel rocket engine it was assumed that such questions as the determination of the amount of thrust of one chamber, the selection of a scheme of the nozzle (of internal or

external expansion) were already solved. However, their solution is an independent and very complex problem. Thus, when selecting the level of thrust of one chamber, one takes into account the earlier attained values, completed experiments, the existence of bench test data, available time, and many other factors. In a number of cases it can be more expedient to create a multichamber engine instead of perfecting a chamber of large thrust. The four-chamber engine of the "Vostok" rocket can serve as an example.

#### 21.5. Trends in the Development of Liquid-Fuel Rocket Engine

The basic trends in the development of a liquid-fuel rocket engine are derived from the general requirements of time reduction and cost of development, operation and the increase in the reliability of the rocket systems. With the expansion of scales in using a liquid-fuel rocket engine in military and rocket-space technology, the role of these factors increases all the more.

On the basis of published data [2], [4] the following basic trends in the development of liquid-fuel rocket engines can be pointed out, reflecting, to a known degree, the effect of the mentioned general requirements.

Independent of purpose, type and sizes of the engine, the invariable trend in the development is for the perfection and introduction of new, all the more efficient fuels, admissible, accordingly, by conditions of the operation of the rocket complex. Resources in this trend, at present, are far from exhausted. Thus, for engines of rocket-carriers of space objects as a result of mastering very efficient oxygen-hydrogen fuel provides the task for perfecting the even more efficient fluorine-hydrogen fuel. Future prospects may be the perfection and utilization of three-component metalliferous fuels. For engine devices of military rockets there is a substantial limitation of a number of possible fuels - they should allow for prolonged storage of the rockets in a ready state.

Operation for the creation and perfection of metalliferous fuels, typical among which is gelled hydrazine with aluminum powder as a fuel, and highly concentrated hydrogen peroxide or nitrogen tetroxide as an oxidizer, can lead to a substantial improvement of energy and weight characteristics of engine devices working on high-boiling fuels.

The second most important trend in the development of liquid-fuel rocket engines is utilization of the resources in the optimization of the basic parameters of the engine: pressure in the combustion chamber, the degree of expansion of the nozzle, the schemes of the engine and others.

The selection of these parameters is intimately connected with the achievements in the structural perfection of the engines, with level of thrust, the purpose, operation time, and other factors, the combined calculations of which must guarantee the selection of the optimum parameters of the working process.

At the present time, apparently, the optimum values of the pressure in the combustion chamber have not been attained. Utilization of a scheme of engines with preignition of the working medium of a turbine in the turbopump unit (TNA) makes it expedient [5] to increase the pressure in the combustion chamber up to 200 bar and higher (in a gas generator, more than 300-400). It is characteristic that the trend to increase the pressure is observed not only in engines of the lower stages of rockets which operate in the dense layers of the atmosphere, but also in space engines. In the latter case a higher degree of expansion in the nozzle can be attained even at low pressures in the combustion chamber. However, an increase in pressure results in a reduction in the over-all sizes, and in a number of cases, in the lowering of the weight of engine. Furthermore, an increase in the absolute pressure make it possible to increase the expansion ratio of the nozzle without fear excessive friction loss in the boundary layer.

Expansion ratios of the nozzle in the developed engines attain very large values - 100 and even 200 (RL-20 engine). In this respect the possibility of a further increase in the specific thrust to a certain extent has been exhausted.

At present there is no final clarity of the problem of the maximum level of thrust of a single-chamber of a liquid-fuel rocket engine. According to the degree of completion of the experiment and of advances of new problems ahead of space technology, the level of thrust of a single-chamber liquid-fuel rocket engine constantly rose. The thrust of the heaviest modern F-1 engine reaches 680 t. Expedient level of thrust in one chamber should be determined by the cost, by the reliability and by the time for development of an engine installation of future more powerful rocket-carriers. In some foreign research works they consider that engines with a thrust of several thousands and tens of thousands of tons should have a scheme different from schemes of existing liquid-fuel rocket engines. For example, frequently a scheme with an annular combustion chamber (or with many chambers, arranged on a ring) and with a nozzle of external expansion are considered.

The important trend in the development of a liquid-fuel rocket engine is the increase in the structural perfection. The basic of this trend is the improvement in the scheme of the engine, the utilization of new, better structural material and techniques in the manufacture of the engines, the improvement in the design of aggregates and units. For example, the introduction of schemes with afterburning of the working medium of the turbine allows one to raise the level of optimum pressure in the chamber of combustion and increase the specific thrust. The perfection of the design, the increase in the economy of the turbine and pumps of the turbopump unit (TNA) allows one to reduce the weight of these units and raise the parameters of the engine. As a result, engines become lighter, more reliable, and their over-all sizes are reduced. On the basis of achievement in the organization of the procedure and technology of the manufacture of the engines, highly efficient engines with resources, measured in



hundreds of seconds are able to be produced. For example, duration of the engine operation of AJ 10-137 (sustainer engine of the "Apollo" spaceship, thrust of 10 t) constitutes 780 s. The need of the repeated turning on of the engine always complicates the problem of obtaining a large resource.

The basis of the development of the liquid-fuel rocket engine is the more profound research on the complex working processes, which go on in the engine. The creation of a reliable boosted and economic engine is unthinkable without a detailed analysis of the basic processes. The constant trend is for all the more exacting and more complete quantitative description of the phenomena occurring in the supply system, in the combustion chamber, in the nozzle of the engine, a more accurate calculation of the dynamics of the processes of engine exhaust under operating conditions and stationary work. The most important problem is the research on the nature of the unstable combustion in a liquid-fuel rocket engine and the development of methods of excluding or of limiting this phenomenon. In connection with this, serious attention should be given to the development of the theory of models of liquid-fuel rocket engines which would permit one to determine the basic indexes of the chamber of large thrust based on the results of testing models with a small chamber. The degree of perfection of the working processes in the combustion chamber and in the nozzle (coefficients  $\phi_{p_k}$  and  $\phi_c$ ) are included among these indexes, boundaries of unstable combustion, the distribution of heat flows, and so forth. Along with simulation, important attention is being given to the development of methods of reliable generalization of the results of investigation of life-size engine. The reduction in the number of tests, based on the determination of such parameters, for example, as the efficiency of the processes and the reliability of the engine using a small number of tests is the goal.

Design of engines with more complete and accurate methods of calculating the basic processes at hand allows for a substantial time reduction and cut in the cost of the development of liquid-fuel

rocket engine, and raise its reliability. The needs of rocket-space technology stimulate the development of allied sciences, associated with the creation of a theoretical bases of calculating and designing of liquid-fuel rocket engines.

#### Bibliography

1. Issledovaniye raketnykh dvigateley na zhidkom toplive (Investigation of rocket engines working on liquid fuel), collection of translations, izd-vo "Mir", 1964.
2. Fridenson Ye. S., Budushcheye raketnykh dvigateley (Rocket engines of the future), Voenizdat, 1965.
3. Cardullo M. W., J. of Spacecraft and Rockets, 1965, No. 1.
4. Space Aeronautics, 1964, No. 4.
5. J. Spacecraft and Rockets, 1967, No. 12.

P A R T IV

ROCKET ENGINES ON SOLID PROPELLANT

## CHAPTER XXII

### SOLID ROCKET PROPELLANTS

In this chapter an analysis is made of the basic requirements for unitary solid fuels, data about their composition, physicochemical properties, energy characteristics, and regularities of combustion.<sup>1</sup>

#### 22.1. Basic Requirements for Propellants

Solid propellant, including in its composition a combustible and an oxidizer (monopropellant solid propellant), is placed in the combustion chamber in the form of one or several units called a charge. A charge can be rigidly fastened to the walls of the chamber or inserted freely. In the second case it is retained in the chamber by special devices.

The absence of liquid components and systems for feeding of fuel substantially simplifies the design of an engine installation operating on solid propellant and creates the prerequisites for development of units of very high reliability and operational readiness. Realization of these features of an (PDTT) - [RDTT - solid-propellant rocket engine] led to their wide utilization in technology - from small rocket projectiles to intercontinental ballistic missiles operating on solid propellant.

---

<sup>1</sup>Information about propellants has been taken basically from foreign sources.

Solid propellants are subject to requirements which stem from the need for development of a rocket with high reliability and minimum launch weight.

The solid-propellant charge is the most important element of a RDTT. The mechanical properties of the fuel should guarantee the possibility of development of a charge of the necessary configuration and achievement of stability of its characteristics in the process of storage, ignition, and combustion. Propellants utilized for charges which are fastened to the engine housing should be sufficiently elastic in order to avoid failure of the charge under the action of thermal stresses or deformation under the action of pressures in process of ignition and operation. "Rigid" propellants are used for deposit charges. The required physical features should be preserved in all temperature ranges of operation of the engine installation and should not change during prolonged storage.

Another group of requirements demanded of a solid propellant concerns its intraballistic properties. Rate of combustion at nominal pressure in each case must be sufficient for achievement of the necessary characteristics of the engine installation. For example, in certain cases high thrust for a short time at very large overloads can be demanded from the booster. The latter based on considerations of strength does not allow the using of a multigrain charge with a very large combustion surface. An acceptable solution is utilization of a charge fastened to the housing, but in this instance the increased combustion rate has to guarantee the necessary consumption with a limited combustion surface. Opposite cases are also possible, when it is necessary to have as low a combustion rate as possible. Change in the combustion rate of propellant depending on pressure and temperature of the charge, and also on rate of flow of gases along the combustion surface, in most cases should be as low as possible.

The most serious requirement demanded of fuel is providing high energy effectiveness of the engine installation. This means the necessity of obtaining high specific thrust with a high density of propellant. The tendency to increase specific thrust determines the basic trends in the development of new solid propellants. In this

case an important limiting condition is the need for the simultaneous obtaining of specific high mechanical features, stability, rate of combustion, and so forth. Placing of propellant in a combustion chamber of an RDTT which is under high pressure substantially increases the influence of propellant density on the characteristics of the rocket. Higher propellant density makes it possible to reduce the combustion chamber volume, to reduce the weight of the structure with a constant weight of propellant, and to improve the characteristics of the rocket.

In addition to the basic requirements enumerated above there is importance in economic characteristics: propellant components should not be scarce and should be inexpensive and accessible for utilization on the required scale. The technology of propellant production must ensure good reproducibility of characteristics, i.e., little variance from one charge to another.

## 22.2. Composition of Solid Propellants

The composition of certain typical solid propellants and their basic characteristics, which are considered below, are given in Table 22.1. In physical structure solid rocket propellants can be divided into two basic classes.

### Double-Base Propellants

These are solid solutions of organic substances, the molecules of which contain combustibles and oxidizing elements. These fuels are also called powders, colloidal propellants. One of their bases is nitrocellulose with a various content of nitrogen. The general formula of nitrocellulose is  $C_6H_7(OH)_{3-x}(ONO_2)_x$ , where  $x = 1, 2, 3$  - number of groups of  $ONO_2$  obtained under various conditions of nitration of cellulose. The second base are substances of the type of

Table 22.1. Characteristics of some solid rocket propellants.

Brand of propellant	Composition in % by weight	$\rho$ , g/cm <sup>3</sup>	$\dot{m}_0$ , cm/s	$\gamma$	$\frac{1}{\rho_0}$ in g/dm <sup>3</sup>	$T_{ch}$ , °K	$\mu$	$n$	$P_{ch}$ , kgf./cm <sup>2</sup>	Operational range		Area of utilization
										$P$ , bar	$t$ , °C	
Double-base powders	Ballistite JFW	1.61	1.63	0.19	0.9-2.3	3200	28	1.21	200-220	>35	-30 - +10	Main engines
	Cordite SC	1.60	0.74	0.09	—	3540	—	—	190	70-210	0 - +10	—
	WASVO DEGN	—	0.7-2.5	0.73	0.6	—	—	—	180-200	10-260	—	Auxiliary engines
	.H*	—	0.73	0.10	1.25	2550	—	—	200-225	>40	-30 - +50	Engines and gas generators
Composite solid propellants	On a base of $\text{KClO}_4$	1.65-1.94	1.35-3.0	0.7-1.0	0.3-2.0	1800-3100	25-35	1.24-1.27	155-210	28-480	-50 - +75	Starting engines
	On a base of $\text{NH}_4\text{ClO}_4$	1.7	1.2	0.24	—	3300	20	1.15	245	>1	—	Main engines
	On a base of $\text{NH}_4\text{NO}_3$	1.68	0.56	0.65	—	3400	—	—	245	>1	—	—
	On a base of $\text{NH}_4\text{NO}_3$	1.63	0.367	0.32	—	1500	—	—	200-220	2-100	-20 - +70	Gas generators
	On a base of $\text{NH}_4\text{NO}_3$	1.55	0.25	0.4	0.3	1800	22	1.26	170-210	7-210	-45 - +70	—
Black powder	KNO <sub>3</sub> 57-60 Coal 18-20 Sulphur 8-22	1.3-2.1	0.55-1.25	0.5-0.8	—	2200-3000	—	—	50-140	7-70	-10 - +50	Igniters

Note: 1. The arbitrary formula  $(C_2H_5O)_n$  notes the typical composition of combustible in composite propellants.

2. Values of combustion rate  $\dot{m}_0$  are given at  $p = 70$  bar,  $t_{ch} = 20^\circ\text{C}$  and  $\epsilon = 1$ .

3. Values of  $P_{ch}$  are given the range  $p/p_0 = 20-100$ .

$\text{CH}_2(\text{ONO}_2)\text{CH}(\text{ONO}_2)\text{CH}_2(\text{ONO}_2)$ , diglycoldinitrate  $\text{CH}_2(\text{ONO}_2)\text{CH}_2\text{OCH}_2\text{CH}_2(\text{ONO}_2)$  and others, which are called solvents. With nitrocellulose they form colloidal systems. The carrier of surplus oxygen (relative to stoichiometry) from fuel components is nitroglycerin. The limiting quantity of it which can be introduced into a fuel under conditions of obtaining the required mechanical properties is substantially less than that necessary for achievement of stoichiometric propellant composition. For example, the stoichiometric relationship  $\kappa_0$  of nitrocellulose (13.25%  $\text{N}_2$ ) and nitroglycerin comprises 8.57. However, for technological reasons it is difficult to introduce more than 43% nitroglycerin in the fuel, i.e., the maximum magnitude of  $\kappa$  comprises around 0.75. In this case the coefficient of surplus of oxidizing elements  $\alpha_3$  in the propellant can reach a magnitude of 0.75-0.8, although the coefficient of surplus of oxidizer, as it appears,  $\alpha = \frac{\kappa}{\kappa_0} < 0.1$ .

Small quantities of certain additives are usually included in the powders: stabilizers are substances which increase the chemical stability of the propellant in the period of storage; plastifiers or cementers are substances which give to the fuel the necessary mechanical properties, and others.

Of the propellants containing nitroglycerin the most widespread in rocket technology are ballistic (on the basis of nitrocellulose with a low content of nitrogen). Based on mechanical features these propellants are rigid and cannot be used for the preparation of charges which are fastened to the chamber walls.

#### Composite Propellants

These are mechanical mixtures of fuel and an oxidizer. The utilization of three basic components is characteristic for the majority of contemporary fuels: a polymeric fuel - a bonding agent, a crystalline oxidizer, and a metallic additive. Many substances can be used as the bonding agent, beginning with asphalt and ending with contemporary polymers, such as polyether and epoxy resins and rubbers - polyurethane, polybutadiene, and others. In the process of preparation



of the propellant disintegrated crystals of oxidizer, metal powder, and other additives are added to the liquid combustible - bonding agent, they are thoroughly mixed, and having pumped out the air from the engine housing or special form, the resulting mixture is poured or squeezed out directly into them. Under the action of the catalysts introduced during mixing at polymerization of the bonding agent takes place at a controlled temperature and the propellant turns into a resin-like mass.

Most frequently ammonium perchlorate  $\text{NH}_4\text{ClO}_4$  is used as the oxidizer. Such substances as ammonium nitrate  $\text{NH}_4\text{NO}_3$ , potassium perchlorate  $\text{KClO}_4$ , lithium perchlorate  $\text{LiClO}_4$ , and others were used or are considered as possible oxidizers. Before mixing with the bonding agent the crystalline oxidizer is ground to particles with a size of an order of tens - hundreds of microns. Sometimes a mixture of various fractions of oxidizers is introduced, for example, particles with a size of 25 and 100 microns. In this manner it is possible to reduce the viscosity of the mixture.

Energy characteristics of composite propellants, just as for liquid, depend on the ratio of components. Figure 22.1 shows the dependence of specific thrust and combustion temperature for a typical propellant: bonding agent - polyester with ammonium perchlorate.

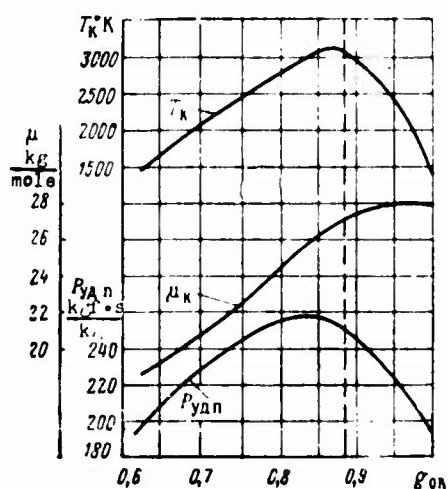


Fig. 22.1. Dependence of basic thermodynamic characteristics on weight fractions of oxidizer in a composite TRT:  
 $p_K^* p_i = 70/1$ , ----- stoichiometric propellant composition [Translators note: TRT - solid rocket propellant].

The utilization of aluminum additive makes it possible to substantially raise the energy characteristics of composite propellants, to increase its density, and to stabilize the combustion process. Usually the content of bonding agent in a propellant for providing the necessary elasticity and strength should be no less, for example, than 15-20%. The remaining 80-85% is distributed between ammonium perchlorate and aluminum. Figure 22.2 shows the results of thermodynamic calculations, indicating, for example that with 17-20% bonding agent the replacement of 15% ammonium perchlorate by aluminium gives an increase of specific thrust by 10-12 kgf·s/kg. For contemporary composite solid propellants, based on American data, a 10-20% content of aluminium is typical.

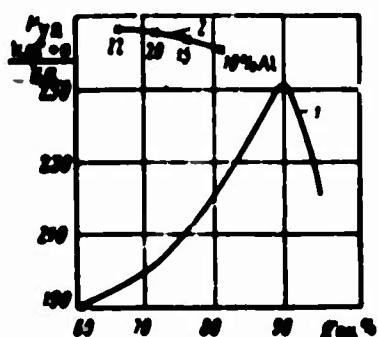


Fig. 22.2. Dependence of specific thrust on content of aluminium in the propellant: 1 - propellant without aluminium; 2 - propellant with aluminium.

### Promising Solid Propellants

According to data in the foreign press, the development of new solid propellants is proceeding along the path of replacement of basic components by more effective ones.

Among the promising oxidizers they include nitronium perchlorate  $\text{NO}_2\text{ClO}_4$ , nitrosyl perchlorate  $\text{NOClO}_4$ , hexanitroethane  $\text{C}_2(\text{NO}_2)_6$ , and others. However, a basic feature of these more effective oxidizers is their instability, explosiveness, and poor compatibility with existing binders.

Greater attention is also given to the development of propellants containing additives which are more effective than aluminium, such as beryllium, hydrides of metals, bimetallic additives, metalorganic compounds, and so forth. For example, the use of beryllium can increase theoretical specific thrust by 20-30 kgf·s/kg, and a bimetallic additive of lithium with beryllium instead of pure beryllium, can increase specific thrust by 6 kgf·s/kg more, inasmuch as the heat of formation of lithium chloride is greater than that of beryllium chloride.

The characteristics of double-base powders can also be improved by introduction of additives into them, for example, crystalline perchlorate of ammonium or of metals.

### 22.3. Mechanism of Combustion

#### General Positions

By pressing or casting double-base and composite propellants in the housing, charges of various configuration are prepared. Two basic types of charges are distinguished: with frontal (end) combustion and with tubular combustion. When using grain which burns from the end its side surface is protected from combustion by a special composition - it is restricted (Fig. 22.3). In the case when the ends of the grain are restricted combustion proceeds along external or internal surfaces or along both simultaneously. Surfaces can be cylindrical or specially profiled. Examples of such charges are shown in Fig. 22.4. Simultaneous combustion on the ends and side surfaces and other variants are possible.

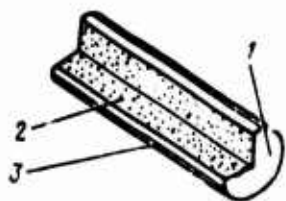


Fig. 22.3. Charge with front combustion: 1 - combustion surface; 2 - propellant; 3 - inhibitor.

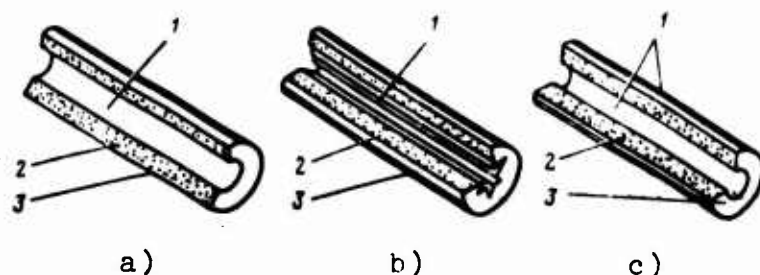


Fig. 22.4. Charges with tubular combustion:  
a) combustion along inner cylindrical surface; b) combustion along inner profiled surface; c) combustion along outer and inner surfaces; 1 - combustion surface; 2 - propellant; 3 - inhibitor.

If the physical conditions at all points of the burning surface are identical and the propellant is uniform, then combustion proceeds evenly, in parallel layers (Fig. 22.5).

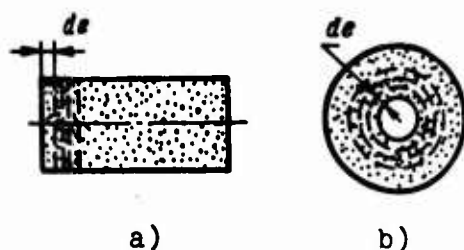


Fig. 22.5. Diagram of shifting of combustion surfaces: a) during frontal combustion; b) during channel combustion.

The basic characteristic of the combustion process is its rate. It is broken down into linear and mass combustion rate. Linear rate of combustion  $u$ , usually called simply combustion rate, is the rate of displacement of combustion surface:

$$u = \frac{de}{d\tau} \text{ cm/s.} \quad (22.1)$$

Mass combustion rate is the mass of propellant which burned down from a unit of burning surface in one second. By definition it is equal to

$$u_m = q_r \frac{de}{d\tau} \quad (22.2)$$

or

$$u_m = u_{\tau} \text{ gf/cm}^2 \cdot \text{s}, \quad (22.3)$$

where  $\rho_T$  - density of propellant in  $\text{g/cm}^3$ .

Initial ignition of a solid propellant is caused by a thermal pulse usually with the help of a special igniter. With the warming up of a specific layer of surface and with the temperature of the surface higher than a certain critical value, which was initially achieved with the help of an igniter, self-accelerating chemical transformations of the propellant begin. These transformations are exothermal and they lead to warming up of reaction products. Heat exchange takes place between the products of combustion and nonreacting fuel and this ensures the further flow of the process without participation of an igniter.

Combustion itself is the process of distribution of a reaction from the surface layers deep into the charge. The mechanism of this process is somewhat different for double-base and composite propellants.

#### Stationary Combustion

Combustion of a double-base propellant can be presented schematically as flowing in three stages. Heat output from combustion products leads to warming up of the surface layer of the propellant (Fig. 22.6, zone 1), in which melting and decomposition of the solid phase begins. Reactions of decomposition are exothermal and accelerate the process gasification of solid propellant.

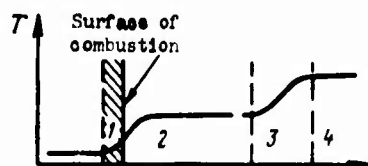


Fig. 22.6. Diagram of combustion of solid rocket propellant.

As a result of the poor thermal conductivity of solid rocket propellants the surface layer which is undergoing warming up ("thoroughly warmed layer") is very thin. Figure of 22.7 shows

the temperature distribution of a solid propellant at various distances  $r$  from the combustion surface. As can be seen, with an increase in the linear rate of combustion the thickness of the warmed layer is rapidly diminished, in connection with which the role of exothermal reactions in this layer is reduced.

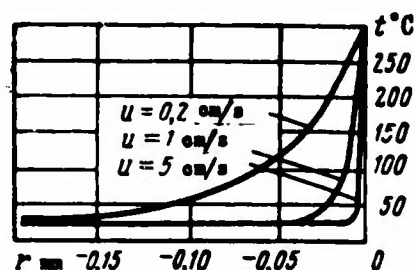


Fig. 22.7. Distribution of temperature in the surface layer of propellant at various rates of combustion.

Gasified decomposition products of the solid propellant at a certain distance from the surface enter into exothermal preflame reactions, which lead to products of incomplete combustion (see Fig. 22.6, zone 2). Finally, in zone 3 there are natural flame reactions between products of incomplete combustion. As a result of these reactions final products of combustion are formed and chemical equilibrium is established (zone 4). Reactions in the gas phase are subordinate to the usual regularities of homogenous combustion. Figure 22.8 shows the characteristic temperature distribution of gas near the burning surface of powder.

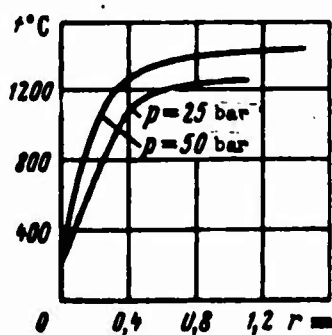


Fig. 22.8. Temperature distribution of gas near the burning surface.

The mechanism of combustion of composite propellants has been studied less than that of double-base. Thermal decomposition of components of a composite propellant in the surface layer is probably not an exothermal, but an endothermal process. Therefore

the need for heat supply from the zone of developed combustion increases. Decomposition and gasification of the fuel and oxidizer flow in a general case at various rates and depend on the nature of the components. The reactions between gasified fuel and oxidizer can be determined by the process of diffusion and of mixing or by the kinetics of chemical reactions, or by both depending on pressure, temperature, sizes of grain of oxidizer, and other factors. In the presence of aluminum interest lies in the process of combustion of particles of metal. Investigations show that on the surface of a burning propellant particles of aluminum are melted and are merged into larger ones. Ignition and combustion take place within the limits of zone considerably exceeding the zone of combustion of a propellant which does not contain metal (extent of the latter is tenths of a millimeter).

In this way a specific stage of combustion of these and other fuels is the process of decomposition and gasification of the solid phase. This process depends substantially on the intensity of heat transfer to the surface of the solid propellant. All factors which increase heat transfer accelerate the decomposition and gasification of the surface layer.

Acceleration of processes in the surface layer as well as in the gas phase means an increase in the linear rate of combustion of solid propellant. From the cited arrangements of processes it may be concluded that rate of combustion should depend on the nature of the propellant, pressures at which combustion is carried out, temperatures of the propellant, of rate of movement of gas along the combustion surface, and of other factors which influence rate of reactions in the condensed or gas phase.

In most cases the theory of combustion only explains, but does not predict analytically these dependences, the quantitative description of which still is based on test data.

## Nonstationary Combustion

Each rate of combustion of a propellant has its corresponding nature of distribution of temperature in the warmed layer. With a rapid change in pressure, taking place, for example, when the engine approaches operating conditions, during cut-off, or for any other reason, the rate of combustion changes but the warmed layer cannot be reconstructed. During this time the rate of combustion is determined by the instantaneous value of pressure and by the magnitude of temperature gradient at the surface of the warmed layer. With a rapid increase in the pressure, for example, the warmed layer turns out to be thicker than the layer corresponding to stationary combustion at this pressure. With a rapid drop in pressure the warmed layer turns out to be very thin and a thicker heated layer, corresponding to stationary pressure, may not be formed. In this case extinguishing of the charge takes place.

The appearance of nonstationary conditions of combustion depends on the free volume of the combustion chamber. In engines with a small free volume the time for gaining stationary condition can be commensurable with the time of formation of the warmed layer. In this case nonstationary phenomena can appear which must be considered during a calculation of processes in the engine.

### 22.4. Dependence of Combustion Rate on Basic Factors

#### Dependence on Pressure

The pressure at which the process of combustion flows is the most serious factor which influences the rate combustion of solid propellant. For the majority of propellants an increase is observed in the rate of combustion with an increase in pressure. This is explained by an increase in the density of current and by the corresponding intensification of heat output to the surface of the propellant. The rate of reactions which proceed in the condensed



phase increases in this case. Simultaneously the increase in the concentration of gaseous reactive substances leads to an increase in the rate of exothermal gas-phase reactions. The high-temperature zone of flames approaches the surface of a solid propellant.

The role of heterogeneous and homogenous reactions in the whole complex of combustion phenomena is diverse at various pressures. In connection with this one cannot expect the same law of change in combustion rate over a wide range of pressure. Treatment of the results of experiments gives various dependences  $u = f(p)$  in different intervals of pressure. These dependences usually have the form

$$u = Bp^v \quad (22.4)$$

or

$$u = A + B_1 p. \quad (22.5)$$

In relationships (22.4) and (22.5)  $A$ ,  $B$  and  $B_1$  - constants, depending on the nature of the propellant and initial temperature of the charge; index  $v$  depends on the nature of the propellant. In the specific range of pressures the magnitudes mentioned do not depend on  $p$ .

For the majority of solid rocket propellants formulas (22.4) and (22.5) in the range of change in pressure which is of practical interest equally accurately reflect the results of experiments. Preference is usually given to dependences of type (22.4). An example of such a dependence, conveniently depicted in a logarithmic coordinate grid, is shown in Fig. 22.9.

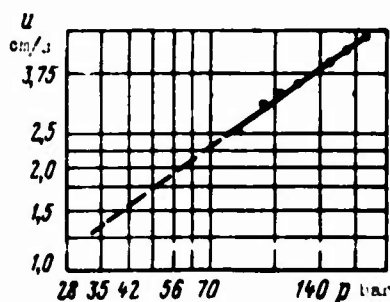


Fig. 22.9. Typical dependence of linear rate of combustion on pressure.

For composite propellants, on the strength of the presence of kinetic and diffusion zones of combustion of products of gasification, Sammerfield obtained the formula

$$\frac{1}{u} = \frac{a}{p} + \frac{b}{\sqrt{p}} \quad (22.6)$$

where coefficient  $a$  is determined by kinetic factors, and  $b$  - by diffusion. This formula during experimental determination of constants  $a$  and  $b$  from measurements of combustion rate very successfully describes experimental data over a wide range of pressure.

The combustion rate of some powders in a specific interval of pressure may not depend on pressure ( $v = 0$ ). Figure 22.10 shows such a dependence of combustion rate on pressure having a sector of constant  $u$ . Also evident there is the effect of initial temperature of the charge.

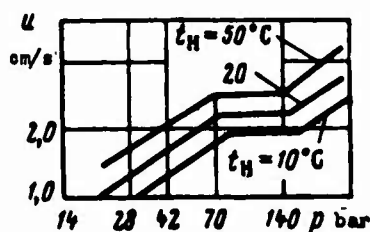


Fig. 22.10. Example of various change in rate of combustion in various intervals of pressure. [Translator's note: subscript  $H$  = initial.]

#### Dependence on Initial Temperature of Charge

The influence of initial propellant temperature on rate of combustion is explained by the dependence of the rate of homogenous and especially of heterogeneous chemical reactions on temperature. As was mentioned, as a result of poor thermal conductivity the temperature of solid propellant changes sharply in a thin layer and already at a distance of tenths of a millimeter from the surface is equal to the initial temperature which the charge had before ignition. As a result of the relative short time of combustion this temperature practically does not change during operation of the engine.

Experiments reveal a noticeably higher rate of combustion at increased initial temperature  $t_H$ . The nature of change in the rate of combustion is not the same in various ranges of change in initial temperature and also depends on pressure. Figure 22.11 shows the dependence of temperature coefficient of combustion rate  $u_{t_2}/u_{t_1}$  on

pressure of nitroglycerin powder in various intervals of change in initial temperature. The temperature coefficient of combustion rate is the relationship of combustion rate at the two initial temperatures being compared and  $p = \text{const}$ . As can be seen from the chart, at increased pressures this coefficient drops, striving for a certain constant value for the given interval of temperatures. A constant value for it is reached earlier for a higher temperature interval. Absolute value in the range of increased pressures is higher for high temperatures.

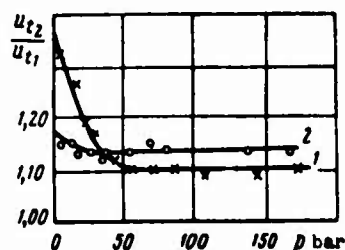


Fig. 22.11. Dependence of temperature coefficient of combustion rate of nitroglycerin powder on pressure:

1 -  $\frac{25^\circ\text{C}}{40^\circ\text{C}}$ , 2 -  $\frac{50^\circ\text{C}}{25^\circ\text{C}}$ .

It can be considered that under conditions characteristic for a RDTT the values of temperature coefficient of combustion rate do not depend on pressure and differ little from one another in various intervals of working temperatures. This creates a base in preliminary calculations to use dependences of the type

$$u_{t_2} = u_{t_1} [1 + \pi_u (t_2 - t_1)], \quad (22.7)$$

where coefficient  $\pi_u$  with dimensionality of 1/degree characterizes the relative change in combustion rate of the given solid propellant with a change in initial temperature of the charge by one degree. For various solid propellants  $\pi_u$  comprises 0.002-0.005.

Usually the dependences of combustion rate on initial temperature are used. These can be written as the dependences of constant  $B$ , entering into formula (22.4), on  $t_H$ .

Figure 22.12 shows the dependence of combustion rate on pressure and initial temperature for several solid propellants.

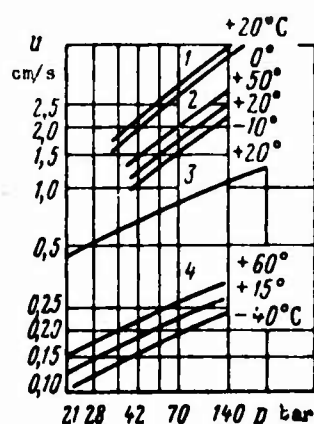


Fig. 22.12. Dependence of combustion rate on pressure and initial temperature for several solid propellants: 1 - on a base of  $KClO_4$ ; 2 - JPN colloidal powder; 3 - on a base of  $NH_4ClO_4$ ; 4 - on a base of  $NH_4NO_3$ .

#### Dependence on Rate of Ventilation of Combustion Surface

The above cases of dependences of combustion rate on pressure and initial temperature of charge relate to a case when the combustion surface is not subject to ventilation. When using a charge with channel combustion the combustion products move along its outer or inner surface (Fig. 22.13). As a measure of removal from the front end of the charge I-I and approach to the nozzle the consumption of gas through the free section of the chamber increases (gas formation proceeds from all the more surface). Therefore the rate  $w$ , of gas flow washing the charge increases towards the nozzle and can at the limit reach the critical rate  $w_{kp}$ .

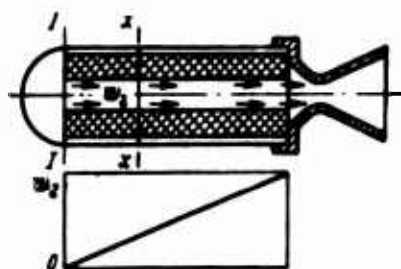


Fig. 22.13. Change in the rate of gas flow in the combustion chamber of an RDTT.

Combustion rate of one and the same fuel under identical conditions ( $p = \text{idem}$  and  $t_H = \text{idem}$ ) increases, if the combustion surface is subjected to ventilation. The basic reason for this phenomenon is that during the washing of the surface of the charge by the hot combustion products the transfer of heat to unreacted propellant increases. This proceeds as a result of an increase of convective thermal flow, which is increased with an increase in the rate of movement of gas along the surface of charge and with an increase in the turbulence of flow. The intensified feeding of heat to the propellant intensifies the chemical reactions, thanks to which there should be an increase in the combustion rate.

Experiment confirms such a dependence of combustion rate on the rate of ventilation of the surface. Figure 22.14 shows the results of determining the relative increase in the combustion rate from the velocity of gas  $w$ , for two types of nitroglycerin powders. The value  $u_0$  is the rate of combustion in the absence of ventilation,  $u$  — rate of combustion at a specific velocity of gas. The values of rates  $u$  and  $u_0$  being compared relate to the same conditions of combustion (pressure and initial temperature of charge). In this investigation a stronger dependence has been revealed for the relative increase of combustion rate in the case of ventilation of the surface of slowly burning propellants ( $u_{02} < u_{01}$ ). At the same time what effects the chemical composition of gases which are washing the surface have not been fixed.

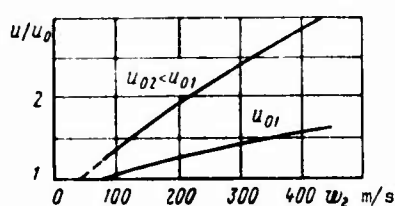


Fig. 22.14. Dependence of relative increase of combustion rate on the velocity of ventilation of the combustion surface.

The phenomenon of an increase in combustion rate in the case of ventilation of the surface of a charge is frequently called the effect of "blowing," and the combustion accompanied by this effect — erosion combustion.

Some researchers propose to describe the dependence of relative increase of combustion rate not in a function of linear velocity of gas flow  $w$ , but in the function of its mass velocity. Such a dependence has the form shown in Fig. 22.15, where along the axis of ordinates the so-called erosion ratio  $\epsilon = u/u_0$  is plotted, and along the axis of abscissa - reduced mass velocity of gas flow  $\delta$ . The reduced mass velocity is the relationship of the given mass velocity of gas to the critical mass velocity which can be attained in the section of a cylindrical channel, where the M number of flow is equal to a unit:

$$\delta = \frac{gw}{(gw)_{cr}}. \quad (22.8)$$

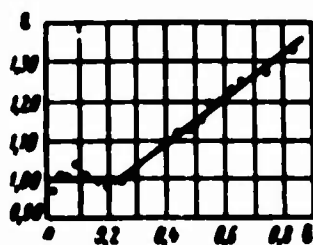


Fig. 22.15. Dependence of erosion ratio on reduced mass velocity.

In connection with the fact that intensity of convective heat exchange depends basically on mass velocity  $gw$ , such a characteristic of erosion combustion is more universal in comparison with a characteristic of the type shown in Fig. 22.14.

It is recommended to determine value  $\epsilon$  according to formula

$$\epsilon = 1 + c\delta, \quad (22.9)$$

where  $c$  - constant of erosion combustion, depending on the nature of the propellant. Value  $c$  increases for slowly burning propellants. Its dependence on rate of combustion of the propellant in the absence of ventilation  $u_0$  and at  $t_w = 15^\circ\text{C}$  is given in a double logarithmic grid in Fig. 22.16.

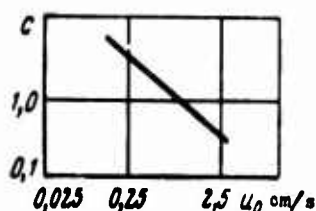


Fig. 22.16. Dependence of constant of erosion combustion of heterogeneous propellants on the combustion rate of propellant in the absence of ventilation.

Experiments did not reveal changes in the characteristics of erosion combustion of the same fuel with a change in the initial temperature of the charge and of pressure. Therefore it is possible to consider  $\epsilon$  independent of  $p$  and  $t_H$ . Then the most widespread formula for rate of combustion (22.4) is generalized for a case of erosion combustion in the following manner:

$$u = \epsilon u_0 = \epsilon B p^* \quad (22.10)$$

It is necessary to note that the effect of erosion combustion is not manifested at any ventilation of the surface of a charge, but, as is evident in Figs. 22.14 and 22.15, only beginning with specific values of linear or reduced mass velocity of the gas. The presence of the threshold velocity may be connected with transition of the laminar boundary layer into turbulent. The effect of flow, running along the burning surface, begins to be expressed only from that moment, when the turbulence which just appeared spreads itself to the zone of preflame reactions. The position of the "threshold" of erosion combustion depends on the nature of the propellant and is determined experimentally. Obviously it also should be determined by the conditions of entrance of flow into the channel of the charge, by the disturbances which promote the transition of the laminar boundary layer into turbulent.

#### Dependence on Other Factors

Under fixed external conditions (pressure and initial temperature) and a specific erosion ratio  $\epsilon$  the rate of combustion of a solid propellant also depends on a number of factors, the effect of which usually is not subject to a strict analytical calculation. These

additional factors are somewhat different for double-base and composite propellants.

Pressed double-base powders usually have an anisotropic structure. In connection with this the rate of combustion of such propellants in a direction parallel to the direction of pressing is 10-15% higher than in a perpendicular direction. A dependence on pressure of pressing and quality of plastification, i.e., on the technology of manufacture of the charge, has also been revealed.

The rate of combustion of composite propellants depends on the average size of a grain of oxidizer. By experimental means it has been found [1] that with a constant composition of a composite propellant and identical external conditions a decrease in the average size of a grain of oxidizer leads to an increase in the rate of combustion (Fig. 22.17).

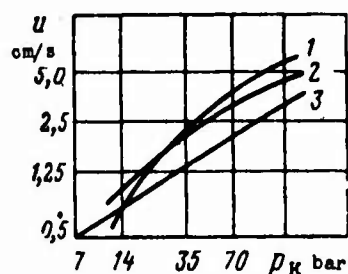


Fig. 22.17. Influence of size of particles of oxidizer on the rate of combustion of a composite propellant: size of particles: 1 - 1-2 microns; 2 - 12 microns; 3 - 35 microns.

A substantial influence is exerted on the characteristics of composite propellants by the quality of mixing of fuel and oxidizer, which again depends on the technology of production of the charge.

In this way the most important characteristic of a solid propellant, the rate of combustion, depends on the conditions of production of the propellant and the charge. In connection with this the characteristics of various lots of one and the same propellant can differ from one another. The stability feature of solid rocket propellants is guaranteed less than for liquid propellants, and this is their substantial deficiency.



An increase of weight fraction of inert additives (stabilizers, plastifiers, and others) always lowers the rate of combustion. At the same time by introduction of small amounts of catalysts into the basic propellant composition it is possible to noticeably increase the rate of combustion.

## 22.5. Limits of Stable Combustion

Normal stable combustion is characterized by invariability in the rate of combustion in time, or by its smooth change according to an assigned law. The stability of combustion can be judged based on the diagram pressure in the combustion chamber - time (Fig. 22.18). As it appears, only in the initial period of ignition of the charge can there be a peak of pressure, then the pressure changes according to the necessary law without any fluctuations. However, normal stable combustion of a charge of solid propellant is not observed always, but is limited by certain limits based on pressure in the combustion chamber, initial temperature of the charge, and other parameters.



Fig. 22.18. Nature of the diagram pressure - time during normal combustion.

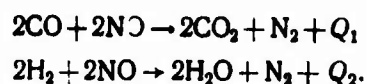
One of the characteristic inadmissible conditions of combustion is anomalous combustion - discontinuous, consisting of several flashes with an interval between them from fractions of a second up to several seconds. The pressure - time diagram under such conditions has the form shown in Fig. 22.19.



Fig. 22.19. Nature of the diagram pressure - time during anomalous combustion.

The reason for the appearance of anomalous combustion lies in a decrease in the supply of heat to unreacting propellant. When the amount of heat supplied becomes inadequate for the normal course of exothermal reactions, combustion is ceased. Then the charge can again be ignited and burn a certain time, then be extinguished, and so forth. There is a certain value in this mechanism in the transfer of heat to fuel from heated elements in the design of the chamber.

All the factors which promote a decrease in the feeding of heat to unreacting fuel increase the possibility of appearance of anomalous combustion. It is most important that it appears with a decrease in pressure lower than a certain limiting one for the given powder. This is explained by the fact that at low pressures exothermal reactions of the following type are strongly inhibited:



This leads to a decrease in the preheating of the propellant and to the stopping of combustion.

Conditions of anomalous combustion can also appear even at high pressures, if the combustion surface is washed by a gas flow of high velocity. In this instance normal heat supply to the propellant is disrupted due to the fact that exothermal reactions do not succeed in flowing completely. The probability of anomalous combustion is increased for long charges, the velocity of ventilation of surface of which is great. Lowering of the initial temperature of the charge also increases the probability of appearance of anomalous combustion.

It is obvious that conditions of anomalous combustion cannot be operational and should be prevented. This imposes specific limitations on the lower limit of pressure in the combustion chamber and on the size and configuration of the charge. It is advisable to use propellants which have low values of a limiting pressure which is a guarantee against anomalous conditions. In this respect there

is an advantage in composite propellants for which  $p_{\min} \leq 1-15$  bar. Double-base powders have higher values of  $p_{\min}$  (usually  $\geq 35$  bar).

Stability of combustion can be disrupted in the range of operating conditions of an RDTT as a result of a nonuniformity of combustion which appears sometimes. Uneven combustion is characterized by the appearance of secondary peaks of pressure (by Fig. 22.20). The reason for such a phenomenon can be, for example, a local increase in the surface of combustion - a crack or partial failure of charge. The appearance of cracks and a reduction in the strength of a charge promote, for example, a low initial temperature of charge, making the charge brittle. As a result of high initial temperature excessive plasticity of the charge and reduced strength appear. This is undesirable from the point of view of stability of combustion and to a known extent limits operational range of temperature for the charge.

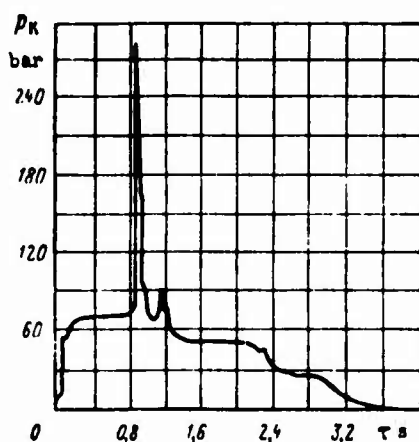


Fig. 22.20. Nature of the pressure - time diagram in the presence of secondary peaks.

The appearance of secondary peaks of pressure can lead to resonant combustion. The resonant effect appears between variations of pressure in the combustion chamber and the rate of combustion depending on  $p$ . The result is low-frequency variations of pressure with a high amplitude. The nature of these variations, just as variations in the chamber of a liquid-fuel rocket engine, is connected with the final time of conversion of the propellant into products of combustion ( $\tau_{np}$ ).

As a result of experimental investigations certain qualitative regularities have been exposed in the uneven combustion of composite rocket propellants.

The index of the tendency of a solid propellant for uneven combustion is the magnitude of the rate of liberation of energy, equal to the product of the mass rate of combustion by the calorific value of the propellant  $u_0 H_u$ . The greater the rate of liberation of energy, the greater the tendency of the propellant for unstable combustion, to the appearance of secondary peaks of pressure. The tendency of a propellant for unstable combustion increases with decrease in the average size of a grain of oxidizer. Nonuniformity of distribution of the oxidizer in the propellant also increases the probability of unstable combustion.

Negative consequences of variations of pressure during unstable combustion are dangerous overload on the structure, harmful vibrations of the vehicle and an increase in heat transfer to the walls.

For dealing with phenomena of unstable combustion semiempirical methods are usually proposed. These include selection of geometry of charge, preventing resonant acoustic oscillations; damping of oscillations with the help of an increase in turbulent viscous friction, for which radial openings are made in the charge or additional rods are introduced in the free volume of the combustion chamber. Numerous experiments confirmed the favorable effect on stability of the combustion of additives of aluminium, magnesium, and other metals included in the propellant in the form of a fine powder [1].

Utilization of aluminium in composite propellants as an energy additive simultaneously solves the problem of preventing acoustic oscillations in the combustion chamber of an RDTT. The mechanism of extinguishing oscillations consists of the dissipation of acoustic energy as a result of lagging of particles of condensate from the gas which form as a result of the combustion of aluminium.

The phenomena of unstable combustion in principle can develop into detonation, connected with a spasmodic increase of pressure, temperatures, and density of gas. The spontaneous transition of combustion into detonation can take place as a result of the appearance of a strong shock wave, which initiates the explosive transformation of propellant in the layer subjected to compression. If the intensity of the shock wave, which appeared during detonation of a layer of substance, is sufficient to cause such a process in the neighboring layer, then detonation will be stationary.

According to the theory of Yu. B. Khariton detonation in a condensed system can proceed steadily if the duration of the chemical reaction in the front of the detonation wave is less than the time in which the pressure in the front of the same wave is able to scatter the reactive substance. Therefore all the factors increasing the time of scattering, for example an increase in the diameter of the charge, facilitate the distribution of detonation. After exceeding a certain diameter of the charge which is critical for the particular propellant combustion can convert into detonation.

Critical factors for composite propellants are the nature of the components and their relationship. The tendency of such propellants for detonation increases with an increase in the content of oxidizer, with an increase in pressure, and with a decrease in the size of crystalline particles of the oxidizer. Conditions, at which spontaneous development of detonation from normal combustion is possible, are usually determined by experimental data.

#### Bibliography

1. Zhidkiye i tverdye raketnyye topliva (Liquid and solid rocket propellants), collection of translations, IIL, 1959.
2. Paushkin Ya. M., Khimiya reaktivnykh topliv (Chemistry of reactive propellants), AN SSSR, 1962.
3. Silant'yev A. I., Tverdye raketnyye topliva (Solid rocket propellants), Voenizdat, 1964.
4. Golub G., J. of Spacecraft and Rockets, 1965, No. 4.

## C H A P T E R   XXIII

### INTERIOR BALLISTICS OF A CHAMBER

In this chapter an analysis is made of the theoretical bases for calculating the parameters of the mass carrier in the combustion chamber of an (PДТТ) [RДТТ - solid propellant rocket engine]. It is assumed that the necessary information about the solid propellant (original composition, complete enthalpy, and law of rate of combustion), geometrical form, and sizes of the charge and engine are assigned.

#### 23.1. Preliminary Information

The historically formed concept of interior ballistics embraces the totality of phenomena taking place during shooting in the barrel of an instrument (weapon) loaded with powder. Relative to rocket engines working on a solid propellant interior ballistics considers the gasdynamics of processes in the chamber of an engine. The basic mission of interior ballistics should be considered the determination of pressure in a combustion chamber and the per second consumption of fuel under the various conditions of engine operation.

The process of change in pressure in a combustion chamber is usually divided into three periods (Fig. 23.1):

a)  $\tau_1$  - period (time) of warm-up, including the time of autonomous combustion of the igniter, time of joint combustion of the igniter and basic charge, and time of stabilization. Duration of the warm-up period is not great and comprises several hundredths or tenths of a seconds;

b)  $\tau_2$  - the basic period of engine operation, which comprises a large share of engine operating time and is approximately equivalent to the time combustion of the charge. The parameters of the mass carrier and the engine during this period are frequently close to constant;

c)  $\tau_3$  - period of aftereffect, setting in after combustion of the basic part of the propellant. During this time there is after-burning of remnants of the charge and emptying of the chamber, and pressure in combustion chamber falls to the pressure of the environment.

For a mathematical description of the change in the parameters in the combustion chamber of an RDTT for all three periods it is possible to use one and the same combination of equations. However, as a result of evident variability the calculation of pressure curve, dependence  $p = f(\tau)$  - for the first and third periods is usually considered specially.

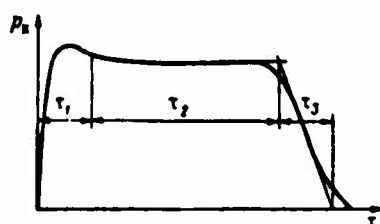


Fig. 23.1. Change in pressure in the combustion chamber of an RDTT.

### 23.2. Pressure and Temperature in a Combustion Chamber

Let us examine in a very simple formulation the problem of calculation of pressure and temperatures in a combustion chamber for

the main period of engine operation. We will consider for the present that pressure and temperature are identical based on volume of the combustion chamber and disregard the kinetic energy of the working medium. Just as before, we will assume that the combustion products are an ideal (in the sense of equation of state) mixture, the composition and properties of which are determined by temperature and pressure.

Pressure in the combustion chamber  $p_k$ , in this case coinciding with stagnation pressure  $p_k^*$ , with a known geometry of charge and engine can be found, having compiled an equation for balance of the working medium:

$$G_k = G_c + \frac{dG}{dt}, \quad (23.1)$$

where  $G_k$  - quantity of combustion products formed in the combustion chamber in 1 s;  $G_c$  - per second expenditure of working medium through nozzle;  $\frac{dG}{dt}$  - increase in the quantity of gas remaining in the chamber (due to filling of volume of solid propellant with burned in 1 s).

The value  $G_k$ , which can also be called rate of gas formation, is equal to

$$G_k = \Omega u \rho_r, \quad (23.2)$$

where  $\Omega$  - complete surface of combustion;  $u$  - linear rate of combustion;  $\rho_r$  - density of solid propellant.

The per second expenditure of working medium through the nozzle can be determined by the formula, valid for a stationary flow with an average index of isentrope  $n$ :

$$G_c = A(n) \frac{\mu_c p_k F_{kp}}{\sqrt{R_k T_k}}. \quad (23.3)$$



Mass of the gas which is found in the combustion chamber can be calculated as:

$$G = \rho_K V_{cb},$$

where  $V_{cb}$  - volume of combustion chamber occupied by products of combustion (volume "free" of propellant);  $\rho_K$  - density of combustion products.

Then

$$\frac{dG}{d\tau} = \rho_K \frac{dV_{cb}}{d\tau} + V_{cb} \frac{d\rho_K}{d\tau}. \quad (2.4)$$

Inasmuch as

$$\frac{dV_{cb}}{d\tau} = Q_u, \quad (23.5)$$

then from equation (23.1) with a calculation of equalities (23.2) and (23.4) we obtain:

$$V_{cb} \frac{d\rho_K}{d\tau} = (\rho_T - \rho_K) Q_u - G_c. \quad (23.6)$$

On the basis of analogical reasonings it is possible to write the law of conservation of energy. Change in enthalpy of gas mass  $\rho_K V_{cb}$  for time  $d\tau$  with a consideration of the function of expansion  $d(p_K V_{cb})$  comprises:

$$d(V_{cb} \rho_K I_K) = (\rho_T I_T Q_u - I_K G_c) d\tau + d(p_K V_{cb}),$$

where  $I_T$ ,  $I_K$  - complete enthalpies of propellant and products of combustion in the chamber respectively.

Differentiating the equation of energy

$$q_v V_{\infty} \frac{dl_v}{d\tau} + l_v V_{\infty} \frac{dq_v}{d\tau} - p_v \Omega u - V_{\infty} \frac{dp_v}{d\tau} = \\ = (q_v l_v - q_v l_v) \Omega u - l_v G_v \quad (23.7)$$

and subtracted from it the product of equation (23.6) by  $l_v$ , we obtain

$$q_v V_{\infty} \frac{dl_v}{d\tau} - V_{\infty} \frac{dp_v}{d\tau} = p_v \Omega u + (l_v - l_v) q_v \Omega u. \quad (23.8)$$

Equations (23.6) and (23.8) make it possible to determine pressure  $p_v$  and temperature  $T_v$  in the combustion chamber. Let us reduce these equations to a form which is more convenient for calculations. With the aid of known thermodynamic relationships (see Table 7.1) it is possible to write:

$$\left. \begin{aligned} \frac{dl}{d\tau} &= \left( \frac{\partial l}{\partial p} \right)_T \frac{dp}{d\tau} + \left( \frac{\partial l}{\partial T} \right)_p \frac{dT}{d\tau} = \frac{1 - \alpha_p T}{\rho} \frac{dp}{d\tau} + c_p \frac{dT}{d\tau}; \\ \frac{dq}{d\tau} &= \left( \frac{\partial q}{\partial p} \right)_T \frac{dp}{d\tau} + \left( \frac{\partial q}{\partial T} \right)_p \frac{dT}{d\tau} = \alpha_p \frac{dp}{d\tau} - c_p \frac{dT}{d\tau}. \end{aligned} \right\} \quad (23.9)$$

Having substituted the last equalities in equations (23.6) and (23.8), inasmuch as  $\phi = \tau$ , we obtain (for simplicity let us omit index "v")

$$\alpha_p \frac{dp}{d\tau} - c_p \frac{dT}{d\tau} = \frac{1}{V_{\infty}} [(q_v - q) \Omega u - G_v]; \\ - \alpha_p T \frac{dp}{d\tau} + c_p \frac{dT}{d\tau} = \frac{1}{V_{\infty}} [(l_v - l) q_v \Omega u + p \Omega u].$$

Let us solve the noted system of equations relative to derivatives  $dp/d\tau$  and  $dT/d\tau$ , using in the conversions the thermodynamic relationship

$$c_p \alpha_p^2 T = \alpha_p^2 T = \frac{c_p}{\alpha_p^2}.$$

where  $a_p$  - equilibrium velocity of sound.

7) Finally we have:

$$\begin{aligned} \frac{dp}{d\tau} = & \frac{a_p^2}{V_{cs}} [(q_r - q) \Omega u - G_c] + \\ & + \frac{a_p^2}{V_{cs} c_p} [(l_r - l) q_r \Omega u + p \Omega u]; \end{aligned} \quad (23.10)$$

$$\begin{aligned} \frac{dT}{d\tau} = & \frac{a_p^2 T}{V_{cs} c_p} [(l_r - l) q_r \Omega u + p \Omega u] + \\ & + \frac{a_p T a_p^2}{V_{cs} q c_p} [(q_r - q) \Omega u - G_c]. \end{aligned} \quad (23.11)$$

In the derivation of equations (23.10) and (23.11) we did not consider the losses of heat in the combustion chamber. For contemporary engines these losses are not great and they also can be disregarded.

With known initial values of temperature  $T_0$  and pressure  $p_0$ , determined in general by a calculation of the period of ignition, the system of equations (23.10) and (23.11) together with equation (23.5) is integrated by numerical methods. As a result we obtain dependences  $p(\tau)$  and  $T(\tau)$  and other parameters of the engine.

#### Pressure and Temperature in the Case of Constant Composition of Combustion Products

For a working medium of constant composition the system of equations (23.10)-(23.11) is substantially simplified. In this instance

$$\begin{aligned} a_p T &= 1; \quad \frac{dp}{p} = 1; \\ c_p &= \frac{kR}{k-1}; \quad c_p = \frac{R}{k-1}; \quad R = \text{const.} \\ l_r - l &= \int \frac{c_p dT}{T} \approx c_p (T_{cr} - T). \end{aligned} \quad (23.12)$$

Using the noted relationships and formula (16.1), we reduce the system of equations (23.10)-(23.11) to such a form:

$$\frac{dp}{d\tau} = \frac{1}{V_{cb}} [kRT_{kt} \varphi_{pk}^2 \Omega_{Q,u} - kRTG_c - p\Omega_u]; \quad (23.13)$$

$$\frac{dT}{d\tau} = \frac{1}{\varphi_{pk} V_{cb}} [(k\varphi_{pk}^2 T_{kt} - T) \Omega_{Q,u} - (k-1)TG_c]. \quad (23.14)$$

Frequently when solving problems of interior ballistics temperature change in the combustion chamber is disregarded. With  $T = \text{const}$  from equation (23.14) it follows that:

$$k\varphi_{pk}^2 T_{kt} \Omega_{Q,u} = T\Omega_{Q,u} + (k-1)TG_c. \quad (23.15)$$

Having substituted in expression (23.12) the equation (23.15) and having taken temperature  $T$  equal to the temperature in the combustion chamber:

$$T = \varphi_{pk}^2 T_{kt},$$

finally we obtain:

$$\frac{dp}{d\tau} = \frac{\varphi_{pk}^2 RT_{kt}}{V_{cb}} \left[ \Omega_{Q,u} - \frac{\Lambda(n) \mu_c F_{kp} p}{\varphi_{pk} \sqrt{RT_{kt}}} - \frac{p\Omega_u}{\varphi_{pk}^2 RT_{kt}} \right]. \quad (23.16)$$

With assigned values of burning surface, rate of combustion  $u(p)$ , coefficient  $\varphi_{pk}$ , initial values  $V_{cb.нач}$ ,  $\Omega_{нач}$ ,  $p_0$ , equations (23.5) and (23.16) are integrated by numeral methods.

#### Equilibrium Stationary Pressure and Temperature at a Constant Burning Surface

In the case of a constant burning surface there is the possibility of steadystate operation the engine, characterized by conditions:

$$\frac{dp}{dx} = 0; \quad \frac{dT}{dx} = 0; \quad G_1 = Q_0 u = Q_0 u \quad (23.17)$$

or

$$T = \text{const}; \quad p = \text{const}. \quad (23.18)$$

Equating the right sides of equation (23.13) and (23.14) to zero and using conditions (23.17) and formula (23.13), we obtain calculation formulas for determination of stationary values of temperature and of pressure:

$$T = \varphi_{p_k}^2 T_{kt}^* + \frac{k-1}{k} \frac{p}{RQ_T}, \quad (23.19)$$

$$\frac{F_{kp}}{Q} = \frac{kR\varphi_{p_k}^2 T_{kt}^* Q_T u - pu}{kA(n)\mu_{cp} + RT}, \quad (23.20)$$

Let us substitute the temperature from equation (23.19) in equation (23.20). Then equation (23.20) at assigned  $F_{kp}$  and  $Q$  will contain one unknown - pressure, which can be found by the method of successive approximations.

With the help of the equation of state we estimate the value of separate component in expressions (23.19) and (23.20):

$$\frac{k-1}{k} \frac{p}{RQ_T} = \frac{k-1}{k} T \frac{Q}{Q_T}; \quad pu = QkTu.$$

Inasmuch as  $Q \ll Q_T$ , then the value of this member can be disregarded in comparison with  $\varphi_{p_k}^2 T_{kt}^*$  and  $k\varphi_{p_k}^2 RT_{kt}^* Q_T u$  respectively. Considering expression (16.1) and

$$u = Bp^n; \quad \varphi_{p_k} \sqrt{RT_{kt}^*} = A(n)^{1/2},$$

from equations (23.19) and (23.20) we finally obtain the value of stationary pressure in the combustion chamber:

$$p = \left( \frac{Q}{F_{np}} B_{0,p} \right)^{\frac{1}{1-\gamma}}. \quad (23.21)$$

The last relationship makes it possible to establish certain fundamental characteristics of interior-ballistic processes in an RDTT.

#### Stability of Pressure in a Combustion Chamber

Pressure  $p_H$ , determined by equation (23.21), answers a case of equality of gas formation and gas discharge through a nozzle. It is possible to show, however, that this pressure is not always steady. In Fig. 23.2 in the function of pressure the dependence is shown for the expenditure of gas through nozzle with  $F_{np} = \text{const}$ , determined by formula (23.3), and gas formation, determined by formula (23.2). Dependence of gas formation on pressure is given in two cases at  $\nu < 1$  and  $\nu > 1$ . In both cases at point A we have equality  $G_H = G_C$ , i.e., an equilibrium condition. At  $\nu < 1$  this condition is steady, because random oscillations of pressure to both sides from  $p_H$  are restored without external pressure. If, for example, state  $p > p_H$  appears, then the expenditure of gas through nozzle will exceed gas formation and pressure again will be brought down to  $p_H$ . If  $p < p_H$ , then equilibrium will be restored because of an excess of gas formation over gas discharge in this range.

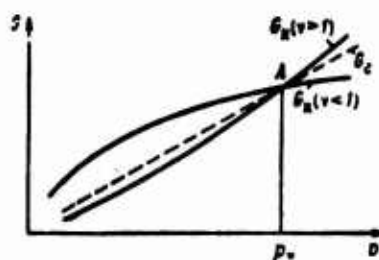


Fig. 23.2. Determination of stability of pressure in a combustion chamber.

At  $\nu > 1$  such self-regulation does not occur, and any random deviation from  $p_k$  increases irreversibly, leading either to cessation of combustion or to failure of the chamber. Equilibrium at point A with  $\nu > 1$  is unstable.

Thus, for stability of pressure in a combustion chamber one equality of gas formation and of gas discharge is insufficient. Stability is determined by the relationship between  $dG_k/dp$  and  $dG_c/dp$ , characterizing the rate of change in gas formation  $G_k$  and gas discharge  $G_c$  with a change in pressure in the combustion chamber. If with equality of  $G_k$  and  $G_c$  gas formation increases with pressure more rapidly than gas discharge, then the condition in the combustion chamber is unstable. Hence it follows that for utilization in an RDTT the only suitable fuels are those which have  $\nu$  less than a unit.

The stability  $p_k$  described here with respect to small random deviations from equilibrium, which is characteristic for fuels with  $\nu < 1$  does not exclude the possibility of the appearance of periodic oscillations during resonant combustion.

The absolute value of equilibrium pressure in a combustion chamber depends, as can be seen from equation (23.21), on the properties of the propellant and on the ratio of combustion surface to the area of critical section. For a given propellant with constant initial temperature of charge the value  $(BQ_0\beta)^{\frac{1}{1-\nu}}$  can be considered constant. Then

$$p_k = \text{const} \left( \frac{Q}{F_{kp}} \right)^{\frac{1}{1-\nu}}. \quad (23.22)$$

In the case when the area of critical section of the nozzle is constant, expression (23.22) shows that the pressure in the combustion chamber is proportional to the combustion surface in the degree  $1/(1 - \nu)$ . Pressure in the combustion chamber, depending on the combustion surface, changes more sharply when propellants with large values of  $\nu$  are used. Thus, for instance, with a change in the combustion

surface by 10% pressure in the combustion chamber changes by 17% for a propellant with  $v = 0.4$  and by 37% for a propellant with  $v = 0.7$ .

#### Dependence of Pressure on the Initial Temperature of the Charge

We will now explain the dependence of pressure in the combustion chamber on the initial temperature of the charge  $t_H$ . It has been accepted to characterize this dependence by the coefficient of temperature sensitivity of pressure in the combustion chamber determined by the formula

$$(\pi_p)_{\Omega/F_{kp}} = \frac{1}{p_k} \left( \frac{\partial p_k}{\partial t_H} \right)_{\Omega/F_{kp}} = \left( \frac{\partial \ln p_k}{\partial t_H} \right)_{\Omega/F_{kp}}. \quad (23.23)$$

Index  $\Omega/F_{kp}$  shows that coefficient of temperature sensitivity of pressure  $\pi_p$  is determined at a constant value of  $\Omega/F_{kp}$ . Coefficient  $(\pi_p)_{\Omega/F_{kp}}$  is measured in percentage of change in pressures for one degree of change in initial temperature. Its order is of fractions of a percent.

Logarithmizing and differentiating equation (23.21), in which  $\alpha$  and  $\beta$  they do not depend on  $t_H$ , we obtain:

$$(\pi_p)_{\Omega/F_{kp}} = \frac{1}{1-v} \left( \frac{\partial \ln B}{\partial t_H} \right)_{\Omega/F_{kp}}, \quad (23.24)$$

from which it follows that sensitivity of pressure in a combustion chamber to initial temperature of charge is higher for propellants with greater values of  $v$ .

The basis of dependence (23.24) is equation (23.21), which was obtained under the assumption  $p = \text{const}$ . Consequently, in this instance we can write:



$$\frac{1}{1-v} \left( \frac{\partial \ln B}{\partial t_n} \right)_{\Omega/F_{kp}} = \frac{1}{1-v} \left( \frac{\partial \ln B}{\partial t_n} \right)_p. \quad (23.25)$$

In Chapter XXII the change in the rate of combustion based on the initial temperature of the charge at a constant pressure was described by the coefficient of temperature sensitivity of combustion rate:

$$(\pi_u)_p = \frac{1}{u} \left( \frac{\partial u}{\partial t_n} \right)_p$$

or with an exponential law of rate of combustion

$$(\pi_u)_p = \frac{1}{B} \left( \frac{\partial B}{\partial t_n} \right)_p = \left( \frac{\partial \ln B}{\partial t_n} \right)_p.$$

From a comparison of the last expression with expression (23.24) it follows that

$$(\pi_p)_{\Omega/F_{kp}} = \frac{1}{1-v} (\pi_u)_p. \quad (23.26)$$

This means that a change in pressure in a combustion chamber with a change of  $t_n$  is greater than a change for this same reason in the rate of combustion at  $p = \text{const}$ . The greater that  $v$  is, the more than  $(\pi_u)_p$  exceeds  $(\pi_p)_{\Omega/F_{kp}}$ . The point is that an increase in the linear rate of combustion with an increase of  $t_n$  leads to an increase in gas formation. At  $\Omega/F_{kp} = \text{const}$  this is accompanied by an increase in pressure, due to which there is an increase in the rate of combustion and rate of gas discharge. A new equilibrium state is established at a higher  $p_k$ . Figure 23.3 shows the change in gas formation and gas discharge at various initial temperatures of charge and the related change of equilibrium pressure in the combustion chamber. Figure 23.4 gives the ratios of pressure  $p_k$  at various values of  $t_n$  to pressure at  $15^\circ\text{C}$ . The value of  $\Omega/F_{kp}$  is constant. Values of index  $v$  for considered propellants 1, 2, 3, and 4 are connected by

the relationship  $v_1 > v_2 > v_3 > v_4$ . As can be seen from these examples, in the ordinary operating range of charge temperatures the change of  $p_H$  can be very considerable, especially at large  $v$ . For obtaining stable characteristics of an RDTT over a wide range of  $t_H$  in accordance with expression (23.26) a low temperature sensitivity of combustion rate is necessary and small values for the index in the law of combustion rate. In this sense it is preferable to have composite propellants.

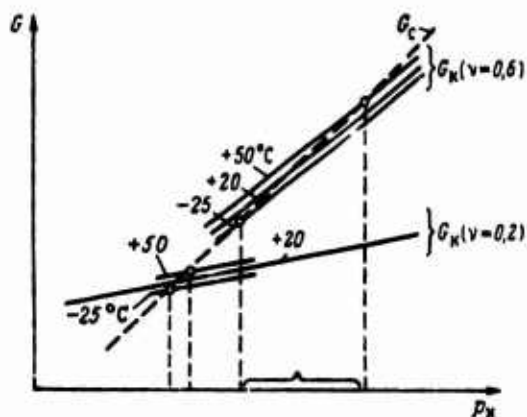


Fig. 23.3. Dependence of pressure in a combustion chamber on the initial temperature of the charge.

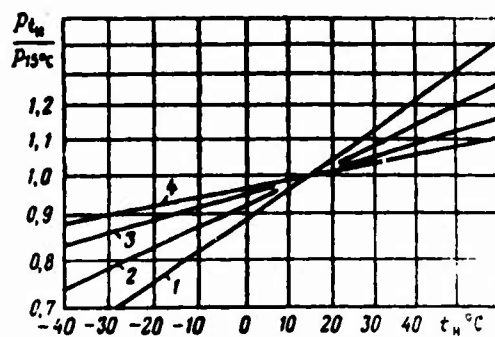


Fig. 23.4. Relative change in pressure in a combustion chamber depending on the  $t_H$  for various propellants.

Equation (23.21) can be solved relative to  $\Omega/F_{kp}$ :

$$\frac{\Omega}{F_{kp}} = \frac{p_k^{1-\gamma}}{\theta_{cr} B} \quad (23.27)$$

The nature of this dependence, which can be obtained experimentally, is shown in Fig. 23.5. Using such a chart, it is possible to find the values  $\Omega/F_{kp}$  which are necessary for achievement of assigned pressure  $p_k$  in the combustion chamber.

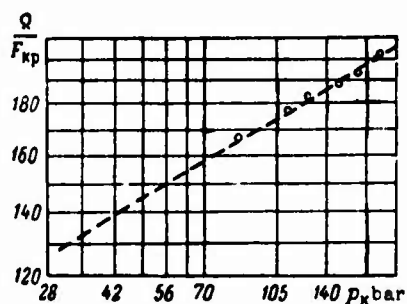


Fig. 23.5. Dependence of ratio  $\Omega/F_{kp}$  on pressure in a combustion chamber ( $t_H = \text{const}$ ).

Although formula (23.21) is valid only for charges with a constant combustion surface  $\Omega$ , the practice of calculations shows that in most cases it gives acceptable accuracy even with a variable combustion surface.

### 23.3. Change in Parameters of Flow Along the Length of a Charge and in Time

#### Model of Calculation

Let us take into account the movement of combustion products, variability of rate of combustion, pressure, and other parameters of flow in a combustion chamber. We will consider movement one-dimensional, and combustion products — a ideal (in the sense of equation of state) working medium.

The velocity of combustion products  $w$  increases in proportion to their advance from the front end of the charge to the nozzle. In connection with this static pressure along the surface of the charge should drop and, consequently, the rate of combustion should diminish. On the other hand, an increase of velocity  $w$  can facilitate an increase in the rate of combustion, i.e., an increase in gas formation. With a constant area of critical section of the nozzle this leads to an increase in pressure. In this way an increase of velocity of flow along the charge has a univalued effect on static pressure and a mutually opposite effect on rate of combustion. In a section at a certain distance from the front end of the charge the static pressure is always less than  $p_1$  (Fig. 23.6), and rate of combustion can be either more or less than in section 1-1, depending on what prevails — a lowering of pressure or erosion combustion.

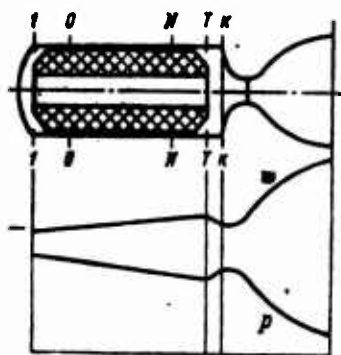


Fig. 23.6. Change in static pressure and velocity of flow lengthwise in a charge.

The section of the nozzle end of the charge T-T in general does not coincide with input section  $\kappa-\kappa$  lattice (diaphragm) retaining the charge can be installed. On sector T- $\kappa$  there is a change in pressure and velocity of combustion initially because of sudden flow expansion, and then — due to its contraction at the entrance to the lattice.

Along with a change in parameters of flow along the charge there is a change in them with time, i.e., in general the processes in the chamber of an RDTT are nonstationary. This is explained by a change

in the combustion surface and the geometry of the flow part as a result of burning out of the charge. For charges with an arbitrary diametrical section with generators parallel to the axis quantity of combustion products which form on the surface  $\Pi \delta x$  in time  $\delta \tau$  is equal to

$$\rho_1 \Pi u \delta x \delta \tau = \rho_2 \frac{\partial F}{\partial \tau} \delta x \delta \tau = \rho_2 \frac{\partial \Omega}{\partial x} u \delta x \delta \tau, \quad (23.28)$$

where  $\Pi$  — perimeter, along which combustion takes place;  $F$  — area of cross section, free for passage of gases.

Total variation of any hydrodynamic quantity  $\phi$  for time  $d\tau$  in the case of one-dimensional nonstationary motion is determined with the help of a substantive derivative

$$\frac{d\phi}{d\tau} = \frac{\partial \phi}{\partial \tau} + w \frac{\partial \phi}{\partial x}, \quad (23.29)$$

Considering not only the local variation in quantity  $\phi$  for time  $d\tau$ , but also its change as a result of a change of position in space.

#### Fundamental Equations

Let us take equations of continuity, movement, and energy for a case of one-dimensional flow of combustion products in the channel of an RDTT charge. For this let us examine the elementary volume  $aabb$  (Fig. 23.7), the position of points  $a$  and  $b$  of which at the moment of time  $\tau$  is equal to  $x$  and  $x + \delta x$ , and at moment of time  $\tau + \delta \tau$  (points  $a'$  and  $b'$ ) respectively  $x + w\delta \tau$  and  $x + \delta x + (w + \frac{\partial w}{\partial x} \delta x) \delta \tau$ . The mass of combustion products in elementary volume  $aabb$  comprises:

at the moment of time  $\tau$  —

$$m(\tau) = \rho F \delta x,$$

at the moment of time  $\tau + \delta\tau$  -

$$m(\tau + \delta\tau) = \left(q + \frac{dq}{d\tau} \delta\tau\right) \left(F + \frac{dF}{d\tau} \delta\tau\right) \left(1 + \frac{\partial w}{\partial x} \delta\tau\right) \delta x,$$

where  $[1 + (\frac{\partial w}{\partial x})\delta\tau]\delta x$  - distance between points  $a'$  and  $b'$  at the moment of time  $\tau + \delta\tau$ .

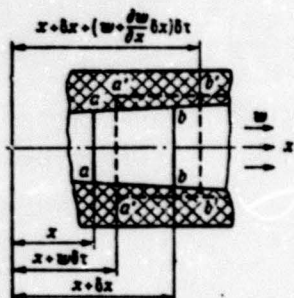


Fig. 23.7. To the derivation of equations of interior ballistics.

The change in the quantity of combustion products in volume  $aabb$  is conditioned by combustion on the surface  $\Pi\delta x$ . Accordingly the continuity equation has the form

$$m(\tau + \delta\tau) - m(\tau) = q_r \frac{\partial F}{\partial \tau} \delta x \delta \tau$$

Or, with allowance for equations (23.28), (23.29), and the formulas for  $m(\tau)$  and  $m(\tau + \delta\tau)$ :

$$\frac{\partial q}{\partial \tau} + w \frac{\partial q}{\partial x} + q \frac{\partial w}{\partial x} + \frac{qw}{F} \frac{\partial F}{\partial x} = \frac{q_r - q}{F} \Pi u. \quad (23.30)$$

The motion equation is derived in the same manner. Change in the quantity of motion  $K(\tau + \delta\tau) - K(\tau)$  for time  $\delta\tau$  comprises:

$$\left(F + \frac{dF}{d\tau} \delta\tau\right) \left(q + \frac{dq}{d\tau} \delta\tau\right) \left(w + \frac{dw}{d\tau} \delta\tau\right) \left(1 + \frac{\partial w}{\partial x} \delta x\right) \delta x - F q w \delta x,$$

and resultant force of pressure and friction is equal to

$$F p - \left(F + \frac{\partial F}{\partial x} \delta x\right) \left(p + \frac{\partial p}{\partial x} \delta x\right) - \Pi_{tp} \tau_{ct} \delta x.$$

Equating the noted expressions and considering equalities (23.28) and (23.29), we obtain:

$$\frac{\partial w}{\partial \tau} + w \frac{\partial w}{\partial x} + \frac{1}{q} \frac{\partial p}{\partial x} = - \frac{q \tau w}{q F} \Pi_{tt} - \frac{1}{q F} \Pi_{tp} \tau_{ct}, \quad (23.31)$$

where  $\Pi_{tp}$  - perimeter of contact of moving gas with the surface (moistened perimeter) section  $x$ .

For derivation of the energy equation we will use the ordinary differential relationship

$$dE^* = \delta Q - \delta A, \quad (23.32)$$

where  $dE^*$  - change in complete energy (internal and kinetic) for time  $\delta\tau$ ;  $\delta Q$  - elementary quantity of heat, entering the system in time  $\delta\tau$ ;  $\delta A$  - elementary quantity of work being accomplished by the system in time  $\delta\tau$ .

Inasmuch as the equation of energy in form (23.32) is valid for systems with constant mass, for such a system we should write it: products of combustion of volume  $aabb$  plus burning solid propellant, the volume of which  $\left(\frac{\partial F}{\partial \tau}\right) \delta x \delta \tau$  - for moment of time  $\tau$ , and products of combustion of volume  $a'a'b'b'$  - for moment of time  $\tau + \delta\tau$ . Accordingly:



complete energy of the system at moment of time  $\tau$  -

$$QFE^*\delta x + Q_\tau \frac{\partial F}{\partial \tau} I_1 \delta x \delta \tau;$$

complete energy of the system at moment of time  $\tau + \delta \tau$  -

$$\left(Q + \frac{dQ}{d\tau} \delta \tau\right) \left(F + \frac{dF}{d\tau} \delta \tau\right) \left(E^* + \frac{dE^*}{d\tau} \delta \tau\right) \left(1 + \frac{\partial w}{\partial x} \delta x\right) \delta x;$$

work of forces of pressure on boundaries of the system -

$$-\delta A = pFw\delta \tau - \left(F + \frac{\partial F}{\partial x} \delta x\right) \left(p + \frac{\partial p}{\partial x} \delta x\right) \left(w + \frac{\partial w}{\partial x} \delta x\right) \delta \tau;$$

heat returned to the chamber walls -

$$\delta Q = -\Pi_q q \delta x \delta \tau,$$

where  $\Pi_q \delta x$  - elementary surface, through which there is heat release.

Let us substitute the noted expressions for complete energy,  $\delta Q$  and  $\delta A$  in equation (23.32). Considering the earlier derived equations and motion, we obtain the equation of energy:

$$\begin{aligned} \frac{dI}{d\tau} = & \frac{Q_\tau}{Q^2} \left( I_\tau - I + \frac{w^2}{2} + \frac{p}{Q_\tau} \right) \Pi u + \frac{w}{QF} \Pi_{\tau p} \tau_{cr} + \\ & + \frac{1}{Q} \frac{\partial p}{\partial \tau} + \frac{w}{Q} \frac{\partial p}{\partial x} - \frac{\Pi_q q}{QF}. \end{aligned} \quad (23.33)$$

In equations (23.30), (23.31), and (23.33) derivatives of several thermodynamic parameters are used:  $p$ ,  $Q$ ,  $T$ ,  $I$ . The equation of state and general thermodynamic relationships make it possible to be limited to derivatives of two functions, for example, pressure and temperature. For this let us use equalities (23.9) ( $\phi$  - coordinate  $x$  or time  $\tau$ ).



Finally we obtain a system of equations for interior ballistics of an RDTT with an allowance for nonstationary motion of combustion products:

$$Q_T^2 \left( \frac{\partial w}{\partial \tau} + w \frac{\partial p}{\partial x} \right) - Q_p \left( \frac{\partial T}{\partial \tau} + w \frac{\partial T}{\partial x} \right) + Q \frac{\partial w}{\partial x} = \frac{Q_T - Q}{F} \Pi u - \frac{Qw}{F} \frac{\partial F}{\partial x}; \quad (23.34)$$

$$\frac{1}{Q} \frac{\partial p}{\partial x} + \frac{\partial w}{\partial \tau} + w \frac{\partial w}{\partial x} = - \frac{Q_T w}{QF} \Pi u - \frac{\Pi_{TP} \tau_{CT}}{QF}; \quad (23.35)$$

$$- \frac{Q_p T}{Q} \left( \frac{\partial p}{\partial \tau} + w \frac{\partial p}{\partial x} \right) + C_p \left( \frac{\partial T}{\partial \tau} + w \frac{\partial T}{\partial x} \right) = \frac{Q_T z}{QF} \Pi u + \frac{\Pi_{TP} \tau_{CT} w}{QF} - \frac{\Pi_Q Q}{QF}, \quad (23.36)$$

where  $z = l_r - l + \frac{w^2}{2} + \frac{p}{Q_T}$ .

The unknowns being determined here are functions  $p(\tau, x)$ ,  $T(\tau, x)$ ,  $w(\tau, x)$ . Their values, in turn, make it possible to find all the remaining quantities: equilibrium composition and properties of combustion products, rate of combustion of solid propellant, and others.

#### Initial and Boundary Conditions

Let us examine the posing of initial and boundary conditions, which must be satisfied by the solution of a system of equations in partial derivatives (23.34)-(23.36). First of all we establish the geometrical boundaries (sections 0-0 and N-N in Fig. 23.6), inside of which the solution is sought. If the face of the charge is not restricted, then in accordance with the recommendations of work [of 3] distance of sections 0-0 and N-N from the ends of the charge should be more than the thickness of the dome. Then with the flow of time sections 0-0 and N-N will remain fixed. Values of variables in these sections we will note respectively by indexes 0 and N.

Let us designate the average values of unknown state parameters for the area left of section 0-0 as  $p_1$ ,  $Q_1$ ,  $T_1$ . If we disregard the

average value of velocity of flow in the zone left of section  $x = x_0$ , then for determination of quantities  $p_1$ ,  $T_1$  it is possible to use the system of equations (23.10)-(23.11). In this case values  $V_{cs}$ ,  $\Omega$ , relate only to the zone left of section  $x = x_0$  and expenditure is equal to

$$G_0 = Q_0 w_0 F_0. \quad (23.37)$$

For determination of parameters in section  $x = x_0$  in addition to equation (23.37) it is necessary to write the equations of pulses and energy

$$p_1 = p_0 + Q_0 w_0^2; \quad (23.38)$$

$$I_1 = I_0 + \frac{w_0^2}{2}. \quad (23.39)$$

In this way the modified system of equations (23.10)-(23.11) together with equations (23.37)-(23.39) establishes the necessary bond between quantities  $p_0$ ,  $T_0$  and  $w$ , i.e., the boundary condition for section  $x = x_0$ .

The boundary condition at the nozzle end of the charge at  $x = x_N$  is reduced to establishment of a bond between parameters of flow at the entrance to the nozzle. However, in the zone between the section  $x = x_N$  and the entrance to the nozzle already it is impossible to use the averaging of parameters based on volume of the zone. As an acceptable assumption within the framework of the one-dimensional theory [3] it is possible to use the condition of quasi-stationary state, i.e., to consider mass, pulse, and energy of working medium in the zone considered as constant, and motion in the nozzle - isentropic and quasi-stationary.

Then the dependence  $M_H = M_H(f_H)$ , and equations of continuity, pulses, and energy in integral form make it possible to establish the boundary conditions for the nozzle end of the charge.

As initial conditions it is recommended to take such a distribution of parameters  $p$ ,  $T$ ,  $w$  lengthwise in the charge at which a critical rate is established in the throat of the nozzle. Such data can be obtained, for example, from calculations of quasi-stationary motion.

Integration of system of equations (23.34)-(23.36) even when using computer equipment is very laborious, therefore in the absence of reliable data on thermodynamic and thermal-physical properties of combustion products and on the combustion rate of a solid propellant calculation of ballistic parameters of an RDTT with allowance for a nonstationary state is hardly justified. The theory of nonstationary processes is used more frequently for studying special questions of RDTT ballistics (wave processes, stability of performance, and others).

#### Calculation of Parameters of Flow for Quasi-Stationary Motion

We will simplify the system of differential equations (23.34)-(23.36). For this we make the following assumptions: motion is quasi-stationary (stationary during interval  $\delta\tau$ ), that is

$$\frac{\partial p}{\partial \tau} = 0; \quad \frac{\partial T}{\partial \tau} = 0; \quad \frac{\partial w}{\partial \tau} = 0; \quad (23.40)$$

composition of the working medium is constant (equalities 23.12 are valid); friction and heat exchange with the walls are absent; the area, free for passage of gases, is constant on the sector between  $x = x_0$  and  $x = x_N$  and is equal to  $F_0$ ; the density of combustion products is negligibly small in comparison with density of propellant, that is

$$\rho_i - \rho \approx \rho_i. \quad (23.41)$$

The totality of the enumerated assumptions makes it possible to write a system of partial differential equations (23.34)-(23.36) in the following form [3]:



$$\frac{d(qw)}{dx} = \frac{q_T u}{F} \frac{d\Omega}{dx}; \quad (23.42)$$

$$\frac{1}{q} \frac{dp}{dx} + w \frac{dw}{dx} = - \frac{q_T w u}{q F} \frac{d\Omega}{dx}; \quad (23.43)$$

$$w \frac{dp}{dx} + k p \frac{dw}{dx} = \left( k R T_{*t} + \frac{k-1}{2} w^2 \right) \frac{q_T u}{F} \frac{d\Omega}{dx}. \quad (23.44)$$

In solving a system of ordinary differential equations (23.42)-(23.44) relative to derivatives  $\frac{dp}{dx}$  and  $\frac{dw}{dx}$ , let us reduce it to the form

$$\frac{dp}{dw} = - \frac{k p w + q w \left( k R T_{*t} + \frac{k-1}{2} w^2 \right)}{k R T_{*t} + \frac{k+1}{2} w^2}; \quad (23.45)$$

$$\frac{d(qw)}{dw} = \frac{k p - q w^2}{k R T_{*t} + \frac{k+1}{2} w^2}; \quad (23.46)$$

We multiply equation (23.46) by  $qw$  and add it termwise to equation (23.45). Adding  $qw$  to both parts of the resulting equation we have

$$\frac{d}{dw} (p + qw^2) = 0.$$

In this way during flow of a gas in the channel of an RDTT charge the ordinary equation of pulses is valid in integral form:

$$p + qw^2 = \text{const} = p_1, \quad (23.47)$$

which is conditioned by the absence of influx or pulse, directed along axis  $x$ .

Now let us substitute value  $p$  from equation of pulses (23.47) in equation (23.46) and perform integration at initial conditions, i.e., at  $x=x_0$ ,  $q=q_0$ ,  $w=w_0$ . As a result we obtain

$$qw = \frac{k p_1 w + c}{k R T_{*t} + \frac{k+1}{2} w^2}, \quad (23.48)$$

and from equation (23.47) with allowance for equality (23.48)

$$p = \frac{p_1 \left( kRT_{kt}^* - \frac{k-1}{2} w^2 \right) - cw}{kRT_{kt}^* + \frac{k+1}{2} w^2}, \quad (23.49)$$

where

$$c = Q_0 w_0 \left( kRT_{kt}^* + \frac{k+1}{2} w_0^2 \right) - k p_1 w_0. \quad (23.50)$$

Equations (23.42) and (23.47) make it possible to write

$$\frac{Q_r u}{F} d\Omega = \frac{kp - Qw^2}{kRT_{kt}^* + \frac{k+1}{2} w^2} dw.$$

Using the found  $Qw$  and  $p$ , finally we obtain:

$$\int_{w_0}^w \frac{1}{u} \frac{k p_1 \left( kRT_{kt}^* - \frac{k+1}{2} w^2 \right) - (k+1) cw}{\left( kRT_{kt}^* + \frac{k+1}{2} w^2 \right)^2} dw = \frac{Q_r}{F} (\Omega_N - \Omega_0), \quad (23.51)$$

where  $\Omega_N$  — complete burning surface between bottom of chamber and section  $x = x_N$ ;  $\Omega_0$  — complete burning surface between bottom of chamber and section  $x = x_0$ .

The values of quantities  $p_0$ ,  $w_0$ ,  $T_0$ , necessary for determination of constant of integration  $c$ , we find from the system of equations (23.37)-(23.39) using the additional relationships:

$$G_0 = Q_0 Q_r u_0; \quad (23.52)$$

$$T_1 = \tau_{p_k}^2 J_{kt}^*, \quad (23.53)$$

where  $u_0 = f(p_1)$  - rate of combustion of propellant in the zone left of section  $x = x_0$ .

As a result we obtain the following calculation expressions:

$$Q_0 w_0 = \frac{Q_0}{F_0} Q_1 u_0; \quad (23.54)$$

$$w_0 = \frac{k p_1 - \sqrt{(k p_1)^2 - 2(k+1) k \gamma_{p_k}^2 R T_{kt}^* (Q_0 w_0)^2}}{(k+1) Q_0 w_0}; \quad (23.55)$$

$$p_0 = \frac{p_1 + \sqrt{(k p_1)^2 - 2(k+1) k \gamma_{p_k}^2 R T_{kt}^* (Q_0 w_0)^2}}{k+1}. \quad (23.56)$$

The bond between parameters in section  $x = x_N$  and the  $M_k$  number at the entrance to the nozzle in the absence of a diaphragm can be obtained from the condition of quasi-stationary state. The calculation relationship, the derivation of which is presented in work [3], has the form:

$$\begin{aligned} \frac{\left( Q_N w_N^2 + \frac{F_N}{F_N} p_N \right)^2}{\left( Q_N w_N + \frac{Q_T}{F_N} u_T Q_T \right) \left( p_N w_N + \frac{k-1}{2k} Q_N w_N^2 + \frac{Q_T}{F_N} u_T Q_T \gamma_{p_k}^2 R T_{kt}^* \right)} = \\ = \frac{(1 + k M_k^2)^2}{k M_k \left( 1 + \frac{k-1}{2} M_k^2 \right)}, \end{aligned} \quad (23.57)$$

where  $Q_T$  - complete burning surface in the zone right of section  $x = x_N$ ;  $u_T$  - average rate of combustion in the zone right of section  $x = x_N$ ;  $F_k$  - area of combustion chamber at entrance to the nozzle.

The magnitude of  $M_k$  is determined with the help of gas-dynamic function  $q(\lambda)$ :

$$\frac{1}{q(\lambda)} = \frac{1}{M_k} \left( \frac{1 + \frac{k-1}{2} M_k^2}{\frac{k+1}{2}} \right)^{\frac{k+1}{2(k-1)}} = \frac{F_k}{\mu c F_{kp}}, \quad (23.58)$$

and the parameters at the entrance to the nozzle according to formulas:

$$p_n = p_N \frac{1 + \frac{\gamma_N}{\gamma_n} M_n^2}{1 + \gamma_n M_n^2}; \quad (23.59)$$

$$M_n = \frac{c_N w_n}{\sqrt{\gamma_n p_n}}; \quad (23.60)$$

$$p_n^* = p_n \left(1 + \frac{\gamma_n - 1}{2} M_n^2\right)^{\frac{\gamma_n}{\gamma_n - 1}}; \quad (23.61)$$

$$T_n^* = T_n \left(1 + \frac{\gamma_n - 1}{2} M_n^2\right); \quad (23.62)$$

$$T_n^* = \frac{c_N w_n^2 T_n^* + c_T w_T^2 T_T^*}{c_N w_n^2 + c_T w_T^2}. \quad (23.63)$$

Now the calculation of ballistic parameters of an RDTT according to the theory of quasi-stationary flow can be presented in the following manner.

a) let us assign, for example, according to formula (23.11) the value of pressure at the front bottom of the chamber  $p_1$  and determine the quantities  $w_0$ ,  $p_0$ ,  $c_0 w_0$ ,  $c$  based on the expressions given above.

b) using the law of combustion rate  $u = u(p, T, w)$ , by a numerical method we seek the values of the integral in expression (23.51). Integration based on rate is continued until the integral does not correspond with the quantity  $c_T(\Omega_N - \Omega_0)$ . The value of the upper limit gives to us the necessary magnitude of rate  $w_N$ .

c) if value  $p_1$  was selected correctly, then it should satisfy equation (23.57). Otherwise it is necessary to change the magnitude of pressure  $p_1$ .

d) in the case of correct selection of pressure at the bottom of the chamber  $p_1$  by the formula (23.59)-(23.63) we determine the parameters at the entrance to the nozzle, and with their help all the

remaining characteristics of the chamber. Using in the right side of expression (23.51) the current value of surface  $S(z)$ , instead of  $S_N$ , we determine the velocity shape of flow and of other parameters lengthwise in the charge on the sector from  $x = x_0$  to  $x = x_N$ .

e) considering now that during the interval  $\delta\tau$  the flow parameters are constant, we determine the change in the geometry of the charge as a result of burning out. After this the calculation is repeated for moment of time  $\tau + \delta\tau$ .

Calculation of the ballistic characteristics of an RDTT with allowance for motion of combustion products is rather laborious and is usually done on an EVM.

#### 23.4. Interior Ballistics of Transitional Processes

Let us examine briefly the characteristics of utilization of equations of interior ballistics for the following transitional processes in an RDTT: ignition and approach of engine to operating condition, outflow from a RDTT chamber after completing of combustion of the charge.

As the basis we will use the methods of work [3].

##### Ignition and Approaching Operating Conditions

In the derivation of equations of interior ballistics for the ignition period it is necessary to consider the difference between ballistic and thermodynamic properties of the igniter (black powder, pyrotechnic composition) and the basic charge. Inasmuch as for a specific period of time the igniter burns simultaneously with the main charge, the equations of interior ballistics have to be written for a combined charge, consisting of several types of propellant.



Assume that in a RDTT chamber (m-1) components are used. Let us designate by  $g_m$  the weight fraction of initial air present in the chamber,  $g_i$  - weight fractions of various kinds of solid propellant (further the properties of these propellants are also noted by index i).

Weight fractions of components satisfy the obvious equalities

$$g_m + \sum_i^{m-1} g_i = 1. \quad (23.64)$$

The equation of interior ballistics for a combined charge can be obtained by generalization of equations (23.1) and (23.7). With consideration of the equation of state they have the form:

$$\frac{d}{d\tau} \left( V_{cn} \frac{p}{RT} \right) = \sum_i \Omega_i \rho_{\tau i} u_i \delta_i - G_c \delta, \quad (23.65)$$

$$\frac{d}{d\tau} \left[ V_{cn} \frac{p}{RT} (I_x - RT) \right] = \sum_i \Omega_i \rho_{\tau i} u_i I_{xi} \delta_i - I_x G_c \delta - \frac{dQ}{d\tau}. \quad (23.66)$$

If we write equation (23.65) for each of the components in the form

$$\frac{d}{d\tau} \left( g_i V_{cn} \frac{p}{RT} \right) = \Omega_i \rho_{\tau i} u_i \delta_i - g_i G_c \delta,$$

then with the help of equation (23.65) it is possible to obtain the dependence of weight fractions on time

$$V_{cn} \frac{p}{RT} \frac{dg_i}{d\tau} = \Omega_i \rho_{\tau i} u_i \delta_i - g_i \sum_i \Omega_i \rho_{\tau i} u_i \delta_i. \quad (23.67)$$

By introduction of coefficients  $\delta_1$  and  $\delta$  it is possible to consider the nonsimultaneous nature of ignitions of individual types of solid propellant (for example, the igniter and the main charge) and delay in onset of discharge. Coefficients  $\delta_1$  and  $\delta$  are determined in the following manner:

$$\delta_1 = \begin{cases} 0 & \text{with } \tau < \tau_{i \text{ наг}} \\ 1 & \text{with } \tau_{i \text{ наг}} \leq \tau \leq \tau_{i \text{ кон}} \\ 0 & \text{with } \tau > \tau_{i \text{ кон}} \end{cases} \quad (23.68)$$

$$\delta = \begin{cases} 0 & \text{with } \tau < \tau_{\text{наг.нст}} \\ 1 & \text{with } \tau > \tau_{\text{наг.нст}} \end{cases} \quad (23.69)$$

Instants  $\tau_{i \text{ наг}}$  of the beginning of ignition of the  $i$ -th charge are determined by achievement certain conditions of ignition which are characteristic for each charge, and which are assumed known on the basis of calculation or experimental data. Coefficient  $\delta$  makes it possible to consider the nonsimultaneous ignitions of components and of discharge. The moment of onset of discharge  $\tau_{\text{наг.нст}}$  can be determined by assigned pressure of failure of nozzle membrane.

The system of equations (23.64)-(23.67) must be supplemented by obvious equation

$$\frac{dV_{\text{сн}}}{d\tau} = \sum_i \Omega_i u_i \delta_i, \quad (23.70)$$

and also by dependences of thermodynamic functions and properties from composition  $g_i$ , pressure  $p$  and temperatures  $T$ , that is.

$$I(g_i, p, T), s(g_i, p, T), a(g_i, p, T), \text{ etc.}$$

Let us dwell in more detail on determination of heat losses  $dQ/d\tau$ . Part of them, conditioned by incomplete mixing and combustion of separate components of combined charge, just as earlier can be

estimated by the coefficient  $\phi_{p_H}$ . Another share of heat loss is caused by expenditures of heat for heating the chamber walls and the inhibitor  $dQ_H/d\tau$ , and also for heating the combustion surfaces of the main charge  $dQ_T/d\tau$ .

According to the theory of heat transfer losses of heat for heating the walls of the engine, the inhibitor, and propellants are expressed by formula:

$$\frac{dQ_H}{d\tau} = \sum \alpha F (T - T_{cr}); \quad (23.71)$$

$$\frac{dQ_T}{d\tau} = \sum \alpha_T F_T (T - T_T), \quad (23.72)$$

where  $F$  — surface of heating;  $\alpha$  — coefficient of heat emission;  $T_{cr}$  — current value of temperatures of wall on the part of heating surface;  $T_T$  — current value of temperature of propellant surface.

In formulas (23.71) and (23.72) summing up is extended to all warmed surfaces. In the case of ignition of a certain surface  $F_T$  the corresponding term should be excluded from the sum in formula (23.72).

For determination of moment of ignition of the propellant it is necessary to solve the problem of its heating up with a consideration of internal sources of heat. In a one-dimensional formulation it is possible to use the equation for thermal conductivity in a solid medium:

$$c_p \rho_p \frac{\partial T(x, \tau)}{\partial \tau} = \frac{\partial}{\partial x} \left[ \lambda_T \frac{\partial T(x, \tau)}{\partial x} \right] + q_v, \quad (23.73)$$

where  $c_p$ ,  $\lambda_T$  — thermal heat capacity and coefficient of thermal conductivity of the propellant;  $q_v$  — average volumetric rate of liberation of energy at a distance  $x$  from the surface at moment of time  $\tau$ .

Volumetric sources of heat  $q_v$  result from exothermal reactions of thermal decomposition of propellant and from the first stages of chemical reactions between products of decomposition. For determination of the magnitude of  $q_v$  it is necessary to have reliable data on the kinetics of complex multistage reactions in solid propellants.

Equation (23.73) is supplemented by boundary and initial conditions, and also by conditions which determine the onset of ignition (surface temperature of charge, quantity of thermally decomposed propellant in the surface layer, and others).

The system of equations (23.64)-(23.67), (23.70) together with equations (23.71)-(23.73) in principle makes it possible to calculate ignition of the charge and the reaching of operating mode by the engine at various initial temperatures of charge, weight, and brands of igniter. However, obtaining of a reliable solution is hampered by the absence of reliable experimental and theoretical data describing the process of combustion and ignition of the propellant. Therefore the weight of the igniter is usually calculated by empirical formulas.

#### Discharge from the Chamber After Completion of Combustion of the Charge

At the moment of termination of combustion of the main charge  $\tau_k$  in the combustion chamber there remains a certain quantity of working medium, the pressure and temperature of which are equal to  $p_{k0H}$ ,  $T_{k0H}$ . We will determine the change in these quantities with time, for which we will use equations (23.13) and (23.14), assuming  $V_{CB} = \text{const}$ ,  $\Omega u = 0$ .

Then

$$V_{CB} \frac{dp}{d\tau} = -kRTG_c, \quad (23.74)$$

$$\frac{V_{CB} p}{T} \frac{dT}{d\tau} = -(k-1)RTG_c. \quad (23.75)$$

Integration of the system of equations (23.74), (23.75) with a consideration of equation (23.3) gives:

$$\left(\frac{p_{\text{кон}}}{p}\right)^{\frac{k-1}{2k}} = 1 + \frac{(k-1)\mu_c F_{\text{кп}} A(n) \sqrt{RT_{\text{кон}}}}{2V_{\text{сн}}} (\tau - \tau_{\text{к}}). \quad (23.76)$$

During the calculation of discharge time  $\tau - \tau_{\text{к}}$  one should be limited to critical drop

$$\left(\frac{p}{p_h}\right) \geq \left(\frac{k+1}{2}\right)^{\frac{k}{k-1}}, \quad (23.77)$$

where  $p_h$  - external pressure (known value).

Having determined from formula (23.77) the pressure  $p$ , from expression (23.76) we find the time of discharge of working medium from the chamber of the engine ( $\tau - \tau_{\text{к}}$ ).

Dependence  $p(\tau)$  for the period of discharge and also the value of  $\tau - \tau_{\text{к}}$  are necessary for determination of the component pulse of aftereffect conditioned by discharge from the chamber after cessation of combustion.

### 23.5. Geometry of Burning Out of Charge

For the solution of problems of interior ballistics of an RDTT it is necessary to know the law of change with time of the geometrical characteristics of a charge: surface of combustion and the free area for the passage of gases. The reason for a change in the geometric dimensions and forms of a charge is its burning out.

Change in the surface of combustion and free area in time is determined by the geometry of the charge. Depending on the nature of change in combustion surface in time there are three basic types of charges.

1. Charges which ensure progressive combustion, i.e., an increase of pressure in the combustion chamber in time. With a constant area of critical nozzle section for this, an increase in the surface of combustion is required. A very simple example of such a charge is a grain which burns on a inner cylindrical surface (see Fig. 22.4a).

2. Charges which ensure regressive combustion, i.e., a lowering of pressure in time due to a decrease in the surface of combustion along with the burning out of the charge. An example of such a charge is a cylindrical grain which burns from the outer surface.

3. Charges which ensure neutral combustion, i.e., invariability of pressure in time, for which a constancy of surface of combustion is required during the entire period of combustion. This takes place, for example, during the simultaneous combustion of a hollow cylindrical grain on the outer and inner surfaces (see Fig. 22.4c) during end combustion. Also close to neutral is combustion of a slit charge with a restricted outer surface (Fig. 23.8).

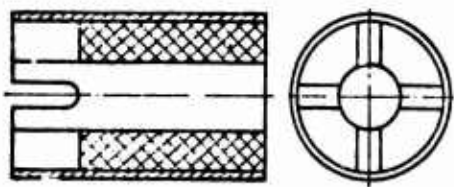


Fig. 23.8. Example of a slit charge.

In addition to a smooth change in the combustion surface, extreme and even spasmodic changes are possible.

The burning time of a charge with an assigned geometry can be various depending on pressure, initial temperature, and physical properties of the propellant. Therefore it is accepted not to connect the change in surface of combustion  $\Omega$  and  $F_{cb}$  directly with the time of combustion, but with the geometrical characteristics of charge, then finding the dependence of these characteristics on the time of combustion.

Let  $\Omega_0$  - initial surface of combustion. Then the change in surface of combustion can be characterized by the relative magnitude of surface  $\Omega/\Omega_0$ . Let us designate this magnitude - characteristic of progressiveness of the charge - as

$$\sigma = \frac{\Omega}{\Omega_0}. \quad (23.78)$$

It can be written:

$$\sigma = \frac{\int_0^L \Pi dx}{\int_0^L \Pi_0 dx}, \quad (23.79)$$

where  $\Pi$  - perimeter, and  $L$  - length of combustion surface.

If the perimeter does not change lengthwise over the combustion surface, then

$$\sigma = \frac{\Pi}{\Pi_0}. \quad (23.80)$$

The last condition proposes a constancy of combustion rate along the length. Strictly speaking, it can be valid for a sector of infinitely small length. However, expression (23.80) can be applied for a sector of finite length, if we determine perimeter  $\Pi$  based on average combustion rate on this sector.

Change in free area  $\Delta F_{CB}$  in sector  $x$  can be written as:

$$\Delta F_{CB} = \int_0^x \Pi dx, \quad (23.81)$$

where  $e$  - thickness of burnt arch.

Then the magnitude of free area at a certain value  $e$  comprises

$$F_{cn} = F_{cn0} + \int_0^e \Pi de, \quad (23.82)$$

where  $F_{cn0}$  - initial value of free area.

Let us designate by

$$\Phi = \frac{F_{cn}}{F_{cn0}}$$

the magnitude of relative free area. According to expression (23.82)

$$\Phi = 1 + \frac{\int_0^e \Pi de}{F_{cn0}}. \quad (23.83)$$

Usually calculated values based on geometrical characteristics of charge  $\sigma$ ,  $\Phi$  are represented in the form of charts or nomograms as a function of relative thickness of the burned arch

$$y = \frac{e}{e_0},$$

where  $e_0$  - initial thickness of arch.

The variety of configurations of charges makes it possible by selection of charge to ensure theoretically any form of dependence  $\sigma(y)$ . However, in actuality the geometry of a charge has specific limitations imposed which are conditioned, for example, by technology of manufacture of charge, its strength, and so forth.

Figure 23.9 gives an example of the sequence of burning out of one of the widespread charges with a star-shaped form (an internal burning), and Fig. 23.10 - dependence  $\sigma(y)$  for this case. By varying the geometry of charges of a star-shaped form it is possible to obtain other regularities of change of  $\sigma$ .



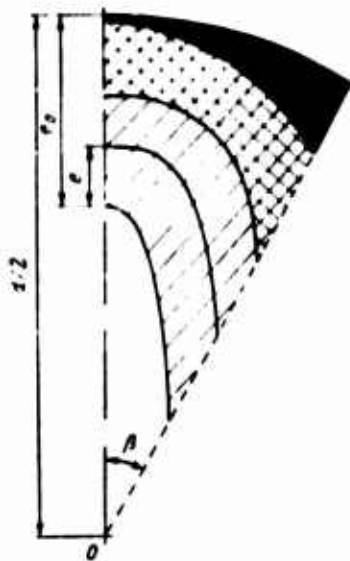


Fig. 23.9. Sequence of burning out of a star-shaped charge.

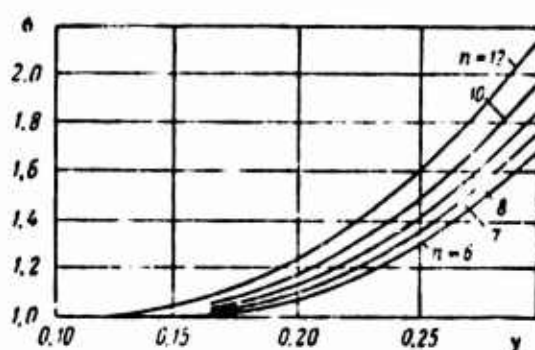


Fig. 23.10. Dependence  $\sigma(y)$  for a star-shaped charge ( $n$  - number of rays).

Calculation of dependences  $\sigma(y)$ ,  $\Phi(y)$  and determination of remainder of unburned fuel for charges of complex configuration is very labour-consuming and is usually done on computers. In the fulfillment of calculations geometrical relationships are used which are specific for concrete types of configurations of charges. In cases when determination of dependences  $\Phi(y)$ ,  $\sigma(y)$  is reduced to calculation of functions  $F_{CB}(y)$  and  $\Pi(y)$  one can use the general method described in the work [1]. Essence of the method is as follows.

The contour of the cross section of a charge of arbitrary form is assigned by equations of its component elements: straight lines and circumferences. As a result of equidistance in the shift of the contour during combustion the equations for its elements are expressed easily as a function of relative thickness of the burned arch. The common solution of these equations determines the coordinates of ends of each element of the contour and the limits of integration during calculation of perimeter and area.

Geometrical characteristics of some widespread forms of charges, dependences of  $\sigma(y)$ ,  $\Phi(y)$ , and the necessary calculation formulas are given in works [2], [4].

#### Bibliography

1. Dregalin A. F., Izvestiya BUZov, ser. "Aviatsionnaya tekhnika," 1964, No. 3.
2. Orlov B. V., Mazing G. Yu., Termodinamicheskiye i ballisticheskkiye osnovy proyektirovaniya raketnykh dvigateley na tverdom toplive (Thermodynamic and ballistic fundamentals for designing rocket engines which run on solid propellant), izd-vo "Mashinostroyeniye," 1964.
3. Sorkin R. Ye., Gazotermodinamika raketnykh dvigateley na tverdom toplive (Gas-thermodynamics of rocket engines which work on solid propellant), izd-vo "Nauka," 1967.
4. Shapiro Ya. M., et al., Teoriya raketnogo dvigatelya na tverdom toplive, (Theory of rocket engines which work on solid propellant), Voenizdat, 1966.
5. Shishkov A. A., Gazodinamika porokhovykh raketnykh dvigateley, (Gas dynamics of powder rocket engines), izd-vo "Mashinostroyeniye," 1968.

## CHAPTER XXIV

### BASES FOR CALCULATION OF CHARGE AND ENGINE

In this chapter we will examine the bases for calculation of a thrust chamber with charges which burn on the side surfaces or on the face, questions of calculation of gas generator, and selection of the igniter.

#### 24.1. Calculation of a Thrust Chamber with a Charge Which Burns on the Lateral Surfaces

In thrust chambers of an RDTT, the mission of which is development of great thrust during a specific time, usually charges are used which burn on side surfaces. A large burning surface, necessary to obtain considerable thrust, is provided in such charges usually due to a large perimeter of combustion and a considerable length of charge.

It is necessary to determine the sizes of the charge and chamber (chambers) which would ensure obtaining the required thrust  $P_h$  with an assigned time of operation  $\tau$  and known initial temperature of the charge.

Initial data for calculation are the characteristics of the assigned propellant, pressure in the combustion chamber  $p_1$  (or  $p_{\kappa}^*$ ) and dependence of pressure on time  $p_1(\tau)$ , and relative area of nozzle exit  $f_c$  (or degree of reduction of pressure in nozzle  $\pi_c$ ). The form of the pressure-time curve  $p_1(\tau)$  is determined by the requirements of external ballistics and the program of thrust  $P_h(\tau)$ .

Characteristics of the propellant can be presented in the following form:

composition, density, thermodynamic characteristics of the propellant;

law of combustion  $u = f(p, T, w)$ ;

minimum pressure in combustion chamber which ensures normal combustion.

In connection with the variability of gas-dynamic parameters of a RDTT lengthwise for the charge and with time it is impossible to determine immediately the necessary indices for the charge and chamber. Calculation is done by successive approximations. The first of them, the zero-dimensional approximation, is performed without allowing for such effects as pressure drop along the charge and erosion combustion. In this case they use certain average values of pressures  $p_{\kappa}^*$ ,  $p_h$  and thrust  $P_h$ .

Thermodynamic calculation, performed by the method given in Chapter VIII, gives theoretical values for temperature of combustion  $T_{\kappa}^* = T_1$ , gas constant of combustion products  $R_1$ , average index of isentrope of expansion  $n$ , specific passage sections of nozzle  $F_{уд.кр}$ ,  $F_{уд.с}$ , and specific thrust in emptiness  $P_{уд.п}$  t. Real specific thrust in emptiness  $P_{уд.п}$  is determined with allowance for deviations from the scheme accepted in thermodynamic calculation:

$$P_{уд.п} = \phi_{уд} P_{уд.п}^* \quad (24.1)$$

where  $\phi_{уд}$  - coefficient of completeness of specific thrust.

Actual specific thrust at altitude  $H$  is found by the known expression

$$P_{уд} = P_{уд.п} - F_{уд.с} \rho_H$$

The nature of losses of specific thrust and methods for their determination for an RDTT are basically the same as that for a liquid-fuel rocket engine. Based on information of the foreign press, actual specific thrust is lower than theoretical by approximately 5% in the case of fuel giving homogenous products of combustion. In engines running on metallized fuels the losses are 2-3% more [3].

Considering that actual specific thrust is equal to its average value during the period of operation of the engine, we determine the necessary per second expenditure of propellant

$$G = \frac{P_k}{P_{ya} h} \quad (24.2)$$

The required reserve of propellant  $G_T$  can be found by the formula

$$G_T = G\tau,$$

where  $\tau$  - assigned time of engine operation.

As was mentioned, many charges do not burn down completely, and regressive combustion of residues of a charge is not always used effectively. It is also possible to use propellant just as ineffectively at the beginning of the launch period. In connection with this the necessary weight of propellant should be increased, determining it according to the formula

$$G_T = aG\tau \quad (24.3)$$

where  $a$  - coefficient, considering the ineffectiveness of utilization of part of the propellant and depending, mainly, on the configuration of the charge.

The required burning surface can be found from the relationship

$$\Omega = \frac{G}{\rho_1 u} \quad (24.4)$$

in this case the combustion rate in the case of average pressure  $p_H^*$  is determined without allowing for erosion.

Thickness of the arch is calculated by the formula

$$e_0 = u\tau, \quad (24.5)$$

if combustion goes along one of the lateral surfaces (external or internal), or

$$e_0 = 2u\tau, \quad (24.6)$$

if combustion is carried out simultaneously on the external and internal surfaces. Based on the resulting values  $\Omega$  and  $e_0$  single-grain or multigrain charges are arranged.

One and the same program of thrust can be provided for with various charge configurations. When selecting a charge from the number of fundamentally possible ones it follows to strive for the most compact placement of propellants in the combustion chamber. At the same time the necessary free area  $F_{cb}$  must be ensured. Small values of  $F_{cb}$  produce a substantial effect of erosion combustion.

Selection of form of charge must ensure the nature of change in pressure and, consequently, of thrust with time in accordance with assigned conditions.

In practice preference is given to charges with combustion on the inner surface, because in this instance the combustion chamber walls, which are screened by propellant with low heat conductivity, operate at low temperature and can be made thinner and lighter. If the charge is poured into the combustion chamber (has been glued to walls), then the volume of the combustion chamber is used more fully. Specifically, it is not necessary to have special adaptations for fixing the charge.

For the accepted charge the law of combustion surface changes  $\sigma = \sigma(y)$  and law of change in free area  $\Phi = \Phi(y)$ .

Nozzle throat area is found by the formula

$$F_{kp} = \frac{Q_1 \Omega u \varphi_p^2 t}{p_h^*} \quad (24.7)$$

Nozzle area at the exit is equal to

$$F_c = f_c F_{kp}$$

where the relative area of nozzle  $f_c$  either is assigned or it is calculated with known  $\pi_c$  and  $n$ .

The subsequent approximation is carried out in more detail with allowance for variability in the geometry of the charge and changes in time parameters and, when indispensable, along the length of the charge. For this the calculation of the planned design of the charge and chamber is done according to the method given in Chapter XXIII. The basic results of the calculation are diagrams  $p_1(\tau)$ ,  $p_h^*(\tau)$ , obtained at assigned value of initial temperature of the charge.

Transition from diagram  $p_h^*(\tau)$  to diagram  $P = f(\tau)$  is carried out in the following manner. Let us write the equation for thrust in the form

$$P = G P_{y.d.n} - F_c p_h$$

Substituting  $P_{y.d.n}$  based on formula (24.1), and  $G$  from the expression for complex  $\beta$ , we obtain

$$P = \frac{p_h^* F_{kp}}{\varphi_p^2 t} \varphi_{y.d} P_{y.d} - F_c p_h$$

Since

$$\frac{P_{y.d} \varphi_{y.d}}{\varphi_p^2 t} = K_{p_{y.d}}$$

then

$$P = p_h^* F_{kp} \frac{\varphi_{y.d}}{\varphi_p^2} K_{p_{y.d}} - F_c p_h \quad (24.8)$$

or

$$P = p_k^* F_{kp} K_{pn} - F_c p_h, \quad (24.9)$$

where

$$K_{pn} = \frac{\varphi_{p1}}{\varphi_p} K_{pni} = \mu_c \varphi_c K_{pni}. \quad (24.10)$$

The quantity  $K_{pn}$  is the real coefficient of thrust in a void.

For a nozzle of constant geometry under the assumption of constancy of coefficients of losses  $K_{pn}$  can be considered constant.

With the aid of equations (24.9) diagram  $P = f(\tau)$  is constructed. Values  $p_k^* = f(\tau)$  are taken based on interior ballistics, and pressure of the surrounding medium - based on assigned dependence  $p_h = f(\tau)$ , which is known from exterior ballistic calculations.

Diagram  $P = f(\tau)$  can have the form shown in Fig. 24.1. On it sectors of ineffective modes are distinguished: part of the period of reaching the operating mode ( $\tau_1$ ) and aftereffect ( $\tau_3$ ).

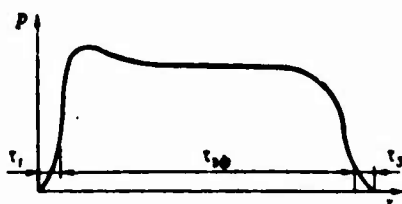


Fig. 24.1. Calculation diagram  $P = f(\tau)$ .

Their boundaries are determined by a certain pressure in the combustion chamber  $p_k^*$ , which ensures high completeness of combustion of propellant and a mode of continuous flow in the nozzle. The necessary value of summary pulse  $I_\Sigma$  in the vacuum should be received during the period of effective combustion  $\tau_{\phi}$ , i.e., for the entire period of combustion less periods  $\tau_1$  and  $\tau_3$ . By subjecting diagram  $P = f(\tau)$  on sector  $\tau_{\phi}$  to two-dimensional geometry we obtain:

$$I_{\Sigma\phi} = \int_{\tau_{\phi}} [P(\tau) + F_c p_h(\tau)] d\tau. \quad (24.11)$$



For determination of specific pulse in a void we use the formula

$$I_{y.d.n} = \frac{I_{z_{\phi}}}{G_r + G_{r3.n} - G_r(\tau_1) - G_r(\tau_3)}, \quad (24.12)$$

where  $G_{r3.n}$  - weight of heatproof coating burned down during the time  $\tau_{z\phi}$  (it is determined during calculation of heat shielding or by weighing of the engine during prototype tests);  $G_r(\tau_1)$ ,  $G_r(\tau_3)$  - weight of propellant which burned ineffectively during periods  $\tau_1$  or  $\tau_3$ .

Value  $t_{z\phi}$  is compared with assigned combustion time, and the magnitude of  $I_{y.d.n}$  with  $P_{y.d.n}$  for the particular fuel - with the same relative nozzle areas  $f_c$ .

Diagrams  $p_k^*(\tau)$  and  $P(\tau)$  can be calculated also with other values of initial temperature of charge  $t_H$  in the possible operational range. Based on minimum static pressure  $p_k$ , determined with the least  $t_H$ , the condition of normal combustion is checked: value  $p_{k \min}$  should be greater than pressure  $\hat{p}_{\min}$ , guaranteeing against anomalous combustion. Maximum value of pressure  $p_1$ , determined at the greatest  $t_H$ , is used in the calculation for strength. Based on dependences  $P = f(t_H)$  and  $\tau = f(t_H)$  it is possible to judge the relative maximum or minimum values of these parameters. An example of these dependences is given in Fig. 24.2. The solid lines show the rated values  $P$  and  $\tau$ , the dotted lines - limits of these quantities as a result of instability of propellant characteristics.

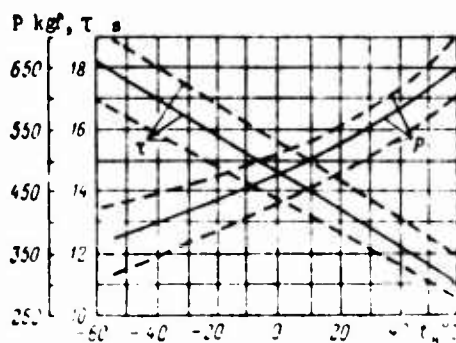


Fig. 24.2. Change in thrust and burning time depending on the initial temperature of the charge.

In case of lack of coincidence of assigned and obtained values the parameters of charge and chamber are corrected and the calculation repeated in the previous sequence. This can be facilitated by utilization of preliminarily composed nomograms.

If assigned thrust is difficult to obtain in one chamber, the engine is designed as a cluster of chambers. Identity of operation of all chambers can be guaranteed by joining them with special lines for equalization of pressure. In the case of rather large sections of lines the simultaneousness of ignition or of stoppings of combustion is reached with an accuracy up to hundredths of a second.

Experimental diagrams  $P = f(\tau)$ , obtained during testing of an engine, were processed in accordance with formulas (24.11) and (24.12). Based on the deviation of magnitude  $I_{y_{d.n}}$  from the value of specific thrust in void  $P_{y_{n.n}}$  it is possible to judge the perfection of the designed engine. In this case  $P_{y_{d.n}}$  must be calculated not for nominal composition of propellant charge, but for an arbitrary propellant, representing a mixture of the main propellant and heatproof coating in a quantity corresponding to its actual burning ~~out~~.

#### 24.2. Calculation of Thrust Chamber with a Charge Burning on the End

The advantages of chambers with charges which use end burning are simplicity of design and of production, high degree of filling the volume of the combustion chamber with propellant, absence of erosion combustion, and less probability of resonant effects. Their deficiencies are difficulty of protecting the chamber walls, which are subjected to the influence of high-temperature flow, and strong displacement of center of gravity of the engine with the burning out of the charge. Utilization of heat-insulating coatings makes it possible to reduce the duration of time of operation of engines with charges burning on the face to tens of minutes. However, the thrust of such engines is limited by the diameter of the charge and the chamber.

The rate of movement of a gas in combustion chambers in charges which burn along the face is usually small, therefore pressure of retarded flow and static pressure can be considered identical and constant in the volume of the combustion chamber. In connection with the constancy of the combustion surface pressure does not change in time (excepting transient conditions). Respectively thrust of the chamber does not change.

Effective summary pulse  $I_{\Sigma \text{ эф}}$  comprises

$$(24.13)$$

The values of  $P$  and  $\tau$  approximately in reverse proportionality to each other with a change in initial temperature of charge and, consequently:

$$I_{\Sigma \text{ эф}} = P_{\max} \tau_{\min} = P_{\min} \tau_{\max}. \quad (24.14)$$

On a mode of least initial temperature of a charge it is necessary to provide minimum pressure in the combustion chamber  $p_{\kappa \min}$ , thus guaranteeing normal combustion, and a certain minimum thrust  $P_{\min}$ . In this case the necessary nozzle throat area should comprise

$$F_{\text{кп}} = \frac{P_{\min}^3}{P_{\text{гг}} \kappa P_{\kappa \min}}$$

or

$$F_{\text{кп}} = \frac{P_{\min} \beta_t^3}{(\varphi_{\text{гг}} P_{\text{гг.н т}} - F_{\text{гг.с}} P_{\text{гг}}) P_{\kappa \min}}. \quad (24.15)$$

Values  $\beta_t$ ,  $P_{\text{гг.н т}}$  and  $F_{\text{гг.с}}$  are obtained in a thermodynamic calculation. From equation (23.21) it is possible to obtain the value  $\Omega/F_{\text{кп}}$ :

$$\frac{\Omega}{F_{\text{кп}}} = \frac{P_{\kappa \min}^{1-\gamma}}{B_{\text{гг}} \varphi_{\text{гг}}^3}, \quad (24.16)$$

from which at a known magnitude of  $F_{kp}$  the necessary combustion surface  $\Omega$  is determined.

In equation (24.16) parameter B corresponds to temperature  $t_{H \min}$ .

The required weight of fuel comprises

$$G_r = a \frac{I_{z_{\text{sp}}}}{P_{yA}}. \quad (24.17)$$

During end combustion the amount of propellant utilized ineffectively in period of attaining operating mode and aftereffect is not great, therefore it can be accepted that  $a \approx 1$ .

If the weight of the charge and surface of combustion are known it is easy to determine the length of the charge

$$L_r = \frac{G_r}{\rho_r \Omega} = \frac{I_{z_{\text{sp}}}}{\rho_r P_{yA} \Omega}. \quad (24.18)$$

Maximum values of pressure in the combustion chamber are determined at the greatest initial temperature of charge  $t_{H \max}$ .

### 24.3 Calculation of Gas Generator

Just as for liquid gas generators, gas generator which operate on solid propellant are included in the composition of auxiliary power units for rocket flight vehicles, and sometimes in vehicles with jet engines. Gas generators working on solid propellant on the whole have the same requirements as liquid (see Chapter XVII). Additional specific requirements are low temperature sensitivity for combustion rate of propellant and little delay of ignition at the lowest temperatures.

Calculation for a gas generator is distinguished from calculation for a thrust chamber by the fact that instead of magnitude of thrust the desired values of gas flow per second, temperature, and pressure of gas are determined. Furthermore the nature of the program  $G = f(\tau)$  are determined.

Pressure in gas generators working on solid propellant fluctuates usually over the range of 35-350 bar. The necessary temperature of gas utilized in auxiliary systems comprises 400-2000°C. The less the time of operation of the system, the higher the maximum permissible temperature. Inasmuch as temperature of combustion of majority of solid rocket propellants exceeds 2000-2500°C, the gas which is received in a gas generator usually has to be cooled. A natural lowering of temperature takes place in the lines and tanks (pressurized supply of propellant). Cooling is applied by the injection of liquid. In order that the working body has a reducing or neutral medium, either fuel or an inert liquid is injected (for example, liquefied nitrogen or helium). Such a method, however, complicates the system. Cooling by sublimation of solid materials is interesting. With this method the gas which is received in the gas generator passes through a porous plastic, which, by gradually sublimating (volatilizing), cools gas flow and simultaneously increases the amount of gas.

The required gas consumption per second  $G$  is assigned on the strength of the value of the summary work which the gas must perform in auxiliary systems. Gas consumption  $G$  is determined by the method given in Chapter XVIII, with allowance for changes in specific efficiency of gas on the way from the gas generator to the place of utilization. The assigned law of change in gas consumption per second in time is ensured by selection of configuration of the charge. More frequently a constant consumption of gas in time is required, in connection with which charges are accepted which burn on the end.

Assigned pressure must be guaranteed with the least initial temperature of the charge; an increase in pressure at  $t_H > t_{H \min}$  should be prevented by a pressure release valve. Assigned time of

operation, conversely, must be ensured at the highest initial temperature  $t_{H \max}$ . At other temperatures the charge will not burn completely.

The necessary burning surface is determined by the formula

$$\Omega = \frac{Q}{u_{\min} \tau}, \quad (24.19)$$

where  $u_{\min}$  - rate of combustion at assigned pressure and  $t_H = t_{H \min}$ .

In the case of end combustion  $\Omega$  is equal to the face area of the charge. The length of the charge in this case should be determined as:

$$L = 1.01 u_{\max} \tau, \quad (24.20)$$

where  $u_{\max}$  - rate of combustion at assigned pressure and  $t_H = t_{H \max}$ ;  $\tau$  - assigned time of operation of gas generator; 1.01 - coefficient of reserve.

Weight of the propellant charge comprises

$$G_r = \Omega L \rho_r. \quad (24.21)$$

In gas generators intended for a small time of operation more frequently they use a propellant with a high rate of combustion. For a long duration of operation, conversely, a slowly burning propellant is necessary. Based on information in the foreign press, fuels have been developed with a rate of combustion exceeding 1 mm/s ( $p \sim$  of 70 bar,  $t_H = 15^\circ\text{C}$ ).

In Fig. 24.3 as an example a gas generator is shown which can be used in pressurization and turbopump systems for the supply of propellant and other auxiliary systems of a rocket vehicle. Depending on the type of propellant and size of charge a gas generator can guarantee various programs  $G = f(\tau)$  over a wide range of pressures (corresponding selection of nozzle is necessary).



Utili  
usually se  
time of op

The p  
the main c  
pressure i  
the normal  
following  
surface up

Trans  
of combust  
convection

For ex  
propellants  
to accurate  
The experim  
energy of  
composite p  
on the pres  
In this cas  
300-600 kW  
a result of  
on pressure  
pressure up

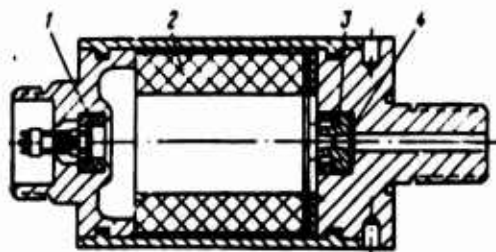


Fig. 24.3. Diagram of a gas generator working on solid propellant: 1 - igniter; 2 - main charge; 3 - nozzle; 4 - explosive membrane.

Utilization of solid propellant for purposes of gas generation usually seems expedient in systems of low power and relatively short time of operation.

#### 24.4 Selection of Igniter

The purpose of an igniter is to thoroughly heat the surface of the main charge up to ignition and in an assigned interval to increase pressure in the combustion chamber up to a pressure of  $p_g$ , ensuring the normal combustion of the main propellant. The charge is ignited following formation of a thoroughly heated layer and heating of surface up to a specific minimum temperature.

Transmission of heat to the surface of the charge from the products of combustion of the igniter is possible by means of radiation, convection, and hot particles settling on the surface of the charge.

For exposure of quantitative indices of inflammability of propellants special sources of heat are used which make it possible to accurately measure the quantity of energy supplied to the charge. The experiments show [2] that minimum energy content (threshold energy of ignition)  $\Delta E$ , ensuring a 50% probability of ignition of composite propellants on the basis of ammonium perchlorate, depends on the pressure and specific thermal flow  $q$  to the surface of the charge. In this case minimum value  $\Delta E$  is equal to  $\sim 4 \text{ J/cm}^2$  at heat fluxes of  $300\text{-}600 \text{ kW/m}^2$  and increases up to  $8\text{-}12 \text{ J/cm}^2$  at  $q = 40\text{-}80 \text{ kW/m}^2$  as a result of decrease in the heat drawn deep into the charge. Depending on pressure, the magnitude of  $\Delta E$  is diminished with an increase of pressure up to 5 bar and further changes insignificantly, remaining

at a level of  $4 \text{ J/cm}^2$ . On the other hand, in order to ensure a time of delay of ignition of the main charge (this time is approximately reversely proportionally to the magnitude of  $q$ ) within the limits of 5-45 ms the average value of specific convective thermal flow must be  $4000-400 \text{ kW/m}^2$ .

On the basis of experiments it can be concluded that the criterion of inflammability should consider not only the surface temperature of the charge, but also the distribution of temperature in the heated surface layer.

In addition to the enumerated factors, inflammability of solid propellants depends also on their composition and initial temperature of the charge (the magnitude of  $\Delta E$  increases linearly with a decrease of  $t_w$ ).

The charge of the igniter is made from a readily combustible and rapidly burning propellant. Black powder is used most widely but it is also possible to use pyrotechnic compositions on the basis of metals (magnesium, aluminium) and mineral oxidizers.

Roughly the weight of the charge of an igniter can be determined by considering that combustion proceeds at a constant volume, equal to the initial free volume of the combustion chamber up to the critical section. This assumption is justified by the fact that for a short time of ignition the emission of gases is negligibly small. Furthermore, frequently the exit from the nozzle is closed by a membrane which is destroyed only upon achievement of an assigned ignition pressure. If the initial free volume of the combustion chamber is equal to  $V_{c80}$ , and the necessary pressure which must be developed by the igniter  $p_8$ , then

$$p_8 V_{c80} = G_8 R_8 T_8,$$



where  $G_B$  - weight of igniter charge;  $R_B$  and  $T_B$  - gas constant and temperature of combustion of igniter, determined at a constant volume.

Hence

$$G_B = \frac{p_B V_{cn} n}{R_B T_B}.$$

This equation, however, does not consider inevitable thermal losses in the walls of the chamber and the charge. In order to compensate these losses, it is necessary to increase the weight of the ignition charge:

$$G_B = \frac{p_B V_{cn} n}{\xi_Q R_B T_B}, \quad (24.22)$$

where  $\xi_Q$  - coefficient of thermal losses in the wall, less than a unit;  $\xi_Q$  is determined by experimental means.

As it appears, the necessary weight of the igniter charge is directly proportional to the pressure developed by the igniter, and to the initial free volume which is proportional to the surface of combustion; consequently, the weight of the igniter charge increases with an increase in the initial surface of combustion.

For a rapid increase in pressure with a low ignition charge weight the gas constant of combustion products of the igniter must be large. At the same time heat emission to the surface of the main charge is increased, i.e., ignition becomes more rapid and reliable, if there are incandescent solid particles in the products of combustion.

The order of magnitude of  $G_B$ , determined by the formula (24.22), comprises several grams per litre of free volume of the combustion chamber.

More physically justified is the model of calculation of weight of an igniter, based on an analysis of heat exchange between products of combustion of the igniter and the main charge. Results of a calculation based on the utilization of such a model satisfactorily coincide with the dependence  $G_B = f(F)$  (Fig. 24.4) for a number of foreign RDTT [4].

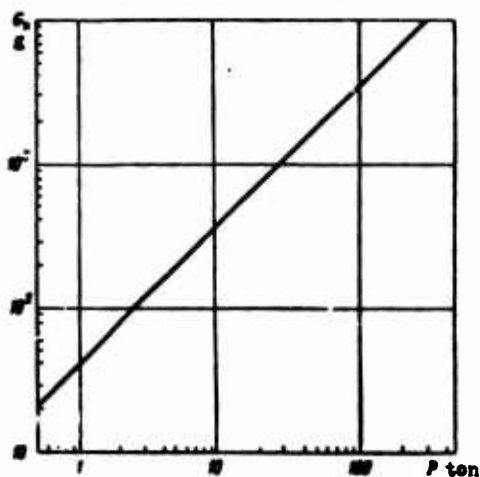


Fig. 24.4. Relationship between weight of the igniter and thrust of the RDTT.

Values of  $G_0$  can change substantially depending on the nature of the propellant of the igniter and the main charge, arrangement of the igniter in the chamber, and other factors. An excessive weight of igniter charge leads to a considerable launching peak of pressure which is dangerous for the design; inadequate igniter weight does not guarantee reliable ignition or slows it down too much.

Ignition of the starting charge does not begin instantly after supply of current to the electric primer, but with a certain delay. Ignition delay depends on the nature of the ignition propellant, its initial temperature, and initial pressure in the combustion chamber. It increases with a lowering of pressure and initial temperature.

#### Bibliography

1. Dolzhanskiy Yu. M., Kurov V. D., Osnovy proyektirovaniya porokhovykh raketnykh snaryadov (Bases of design of powder rocket projectiles), Oborongiz, 1961.
2. Issledovaniye raketnykh dvigateley na tverdom toplive (Investigation of rocket engines working on solid propellants), collection of translations, IIL, 1963.
3. Cheng G., Koen N., "Raketnaya tekhnika i kosmonavtika", 1965, No. 3.
4. Allan D. S., et al., J. Spacecraft and Rockets, 1967, No. 1.

## CHAPTER XXV

### CHARACTERISTICS AND CONTROL OF THRUST VECTOR

In this chapter expenditure and altitude characteristics of an RDTT are described qualitatively, and concepts are given relative to the variance of ballistic parameters. The basic means of control of thrust vector are described.

#### 25.1. Characteristics

In principle a rocket engine working on a solid propellant has the same characteristics as a (ЖРД) - [ZhRD, liquid-propellant rocket engine]; let us note some of their characteristics.

Expenditure characteristic  $P = f(G)$  can be obtained after the dependences  $P = f(\tau)$  and  $G = f(\tau)$  are calculated. However, this characteristic does not have an independent applied value.

The altitude characteristic  $P = f(H)$  can be calculated if we have available the dependences  $P = f(\tau)$  and  $H = f(\tau)$ , obtained at a specific value of initial temperature of charge. Value  $t_H$  does not change with a change in altitude.

When the surface of combustion does not change in time, and the effect of erosion combustion is absent (for example, in the case of end combustion), the altitude characteristic of an RDTT has the same form as the characteristic of a liquid propellant rocket engine (see, for example, Fig. 19.2). A change in initial temperature of the charge displaces the characteristic, while retaining its form.

The altitude characteristic of an RDTT at various initial temperatures of charge has the same form as the characteristic of a chamber of a liquid-propellant rocket engine with various propellant consumption.

If, however, the surface of combustion of a charge changes substantially in time, and, consequently, with flight altitude, then this can have a decisive effect on form of the altitude characteristic. For example, with a considerable decrease in the surface of combustion with altitude the thrust of a rocket engine with a solid propellant will not increase, as this should be at  $G = \text{const}$ , but will decrease. Strictly speaking, with an inconstancy of burning surface the characteristic will cease to be only altitude, since it is determined with two variable factors - altitude and per second consumption of fuel. The form of the characteristic depends on the relationship of the influence of each of the factors.

#### 25.2. Concepts Concerning Variance of Ballistic Parameters of an RDTT

The thrust characteristic of an engine installation with an RDTT changes noticeably with deviations of charge and engine parameters from their calculated values. So in the absence of temperature compensation the rate of combustion of propellant and thrust depend essentially on initial temperature of the charge. For certain fuels used in American rockets a change in initial temperature of charge by  $50^\circ$  leads to a change in engine thrust by 30%. Variations in chemical composition and deviation from procedures for production of the propellant also cause a specific variance of energy characteristics and rate of combustion of propellant in identical types of engines. It is also necessary to consider such random factors as increase in burning surface as a result of the appearance of cracks and pits in the charge, erosion of critical section of the nozzle, and of so forth.

For establishing the bond between deviations in the ballistic parameters (pressure in the combustion chamber, consumption, thrust and specific thrust in a vacuum) and deviations in the characteristics of the charge and engine we will use the following equations:

$$p_k = \left( \frac{2}{F_{kp}} B_{Q_T} \right)^{\frac{1}{1-\nu}} \cdot (G - A(n)) \cdot \frac{p_k F_{kp}}{R_k T_k}; \quad P = P_{\text{ext}} (G - F_c p_h);$$

$$P_{\text{ext}} = \frac{P_0}{G}; \quad \beta = \frac{1}{A(n)} \cdot \frac{R_k T_k}{\dots}$$

Variation, as a possible random deviation of any quantity from its average value under assigned conditions, we will designate by  $\delta$ . In the derivation of calculation dependences, in addition to random deviations in the characteristics of a given batch of propellant  $B, Q_T, R_k T_k$ , it is also necessary to consider the dependence of the latter on initial temperature of the charge. In the first approximation losses as a result of imperfection of processes in engine can be disregarded, complex  $R_k T_k$  can be considered as not depending on pressure, and quantities  $n, \nu$  - constants.

Let us find the relative change of pressure in a combustion chamber depending on the parameters of the charge and engine, for which we will take the logarithm and differentiate the expression for  $p_k$ . Substituting the differentials by variations  $\delta$ , let us write:

$$\frac{\delta p_k}{p_k} = \frac{1}{1-\nu} \left[ \frac{\delta Q}{Q} - \frac{\delta F_{kp}}{F_{kp}} + \frac{\delta Q_T}{Q_T} + \frac{\delta (R_k T_k)}{2 R_k T_k} + \frac{\delta B}{B} + \right.$$

$$\left. + \frac{\partial(Q Q_T)}{\partial t_n} \frac{\delta t_n}{Q Q_T} + \frac{\partial B}{\partial t_n} \frac{\delta t_n}{B} + \frac{\partial (R_k T_k)}{\partial t_n} \frac{\delta t_n}{2 R_k T_k} \right].$$

In accordance with formula of extrapolation (see Table 9.1) the derivative  $\partial(R_k T_k)/\partial t_n$  can be presented as:

$$\frac{\partial(R_k T_k)}{\partial t_n} = \frac{\partial(R_k T_k)}{\partial l} \frac{\partial l}{\partial t_n} = R_k T_k \frac{\partial \ln R_k T_k}{\partial l} c_T = K_k T_k \frac{a_p c_T}{c_p},$$

where  $c_T$  - thermal heat capacity of propellant.

The product  $Q Q_T$  changes inversely proportional to the linear size of the charge, consequently the following equality is valid:

$$\frac{1}{Q Q_T} \frac{\partial(Q Q_T)}{\partial t_n} = -\alpha,$$

where  $\alpha$  - coefficient of linear expansion of propellant.

Let us introduce the designation

$$A_p = \left[ (\pi_n)_p + \frac{a_p c_p}{2c_p} - a \right], \quad (25.1)$$

where  $(\pi_n)_p = \frac{1}{B} \left( \frac{\partial B}{\partial t_n} \right)_p$  - coefficient of temperature sensitivity of rate of combustion. With allowance for designation (25.1) we finally write:

$$\frac{\delta p_n}{p_n} = \frac{1}{1-\nu} \left[ \frac{\delta Q}{Q} - \frac{\nu \delta F_{np}}{F_{np}} + \frac{\delta Q_r}{Q_r} + \frac{\delta B}{B} + \frac{\nu \delta (R_n T_n)}{2R_n T_n} + A_p \delta t_n \right]. \quad (25.2)$$

In the same manner from the equation of G it is possible to determine the variation of consumption:

$$\frac{\delta G}{G} = \frac{1}{1-\nu} \left[ \frac{\delta Q}{Q} - \frac{\nu \delta F_{np}}{F_{np}} + \frac{\delta Q_r}{Q_r} + \frac{\delta B}{B} + \frac{\nu \delta (R_n T_n)}{2R_n T_n} + A_0 \delta t_n \right], \quad (25.3)$$

where

$$A_0 = \left[ (\pi_n)_p + \frac{\nu a_p c_p}{c_p} - a \right]. \quad (25.4)$$

Let us find the variation of thrust. For this the equation of thrust we present in the form:

$$P_n = P + F_c p_n = p_n F_{np} K_{p_n}$$

from which

$$\frac{\delta P_n}{P_n} = \frac{\delta p_n}{p_n} + \frac{\delta F_{np}}{F_{np}} + \frac{1}{K_{p_n}} \frac{\partial K_{p_n}}{\partial f_c} \delta f_c.$$

The last member of this expression can be rewritten as:

$$\frac{1}{K_{p_n}} \left( \frac{\partial K_{p_n}}{\partial f_c} \right) \delta f_c = \frac{\partial \ln K_{p_n}}{\partial \ln f_c} \left( \frac{\delta f_c}{f_c} - \frac{\delta F_{np}}{F_{np}} \right),$$

where derivative  $\partial \ln K_{p_n} / \partial \ln f_c$  is determined with the help of Table 9.2:

$$\frac{\partial \ln K_{p_n}}{\partial \ln f_c} = \frac{\frac{R_0 T_c P_{y_n}}{2(I_n - I_c) \mu_c} + p_c F_{y_n, c} \left[ \left( \frac{\gamma_p}{k} \right)_c - \frac{R_0 T_c}{2(I_n - I_c) \mu_c} - 1 \right]}{P_{y_n, n} \left[ \left( \frac{\gamma_p}{k} \right)_c - \frac{R_0 T_c}{2(I_n - I_c) \mu_c} \right]}. \quad (25.5)$$

Now finally it is possible to write

$$\begin{aligned} \frac{\delta P}{P} = & \left( 1 + \frac{p_c F_c}{P} \right) \left[ \frac{\delta p_n}{p_n} + \left( 1 - \frac{\partial \ln K_{p_n}}{\partial \ln f_c} \right) \frac{\delta F_{np}}{F_{np}} + \frac{\partial \ln K_{p_n}}{\partial \ln f_c} \frac{\delta F_c}{F_c} \right] - \\ & - \frac{p_n F_c}{P} \frac{\delta F_c}{F_c}. \end{aligned} \quad (25.6)$$

Variation of specific thrust in a vacuum is determined through variation of consumption and thrust in a vacuum:

$$\frac{\delta P_{y_n, n}}{P_{y_n, n}} = \frac{\delta P_n}{P_n} - \frac{\delta G}{G}, \quad (25.7)$$

where

$$\frac{\delta P_n}{P_n} = \frac{\delta p_n}{p_n} + \left( 1 - \frac{\partial \ln K_{p_n}}{\partial \ln f_c} \right) \frac{\delta F_{np}}{F_{np}} + \frac{\partial \ln K_{p_n}}{\partial \ln f_c} \frac{\delta F_c}{F_c}, \quad (25.8)$$

and the quantity  $\delta G/G$  is represented by expression (25.3).

Expressions (25.2), (25.3), (25.6) and (25.7) give the dependence of variations of basic ballistic parameters on the characteristics of the charge and engine. With a nonregulated nozzle this dependence can be written in a general form as:

$$\begin{aligned} \frac{\delta \Phi}{\Phi} = & \frac{1}{1 - \nu} \left[ a_1 \frac{\delta \Omega}{\Omega} + a_2 \frac{\delta F_{np}}{F_{np}} + a_3 \frac{\delta F_c}{F_c} + a_4 \frac{\delta Q_T}{Q_T} + \right. \\ & \left. + a_5 \frac{\delta (R_n T_n)}{R_n T_n} + a_6 \frac{\delta B}{B} + a_7 \delta M_n \right], \end{aligned} \quad (25.9)$$

where  $\Phi = p_n, G, P, P_{y.n.}$ , and variations  $\delta\Omega, \delta F_{kp}, \delta F_c, \delta Q_T, \delta(R_n T_n), \delta B, \delta t_n$  should be considered as random values with mathematical expectations equal to zero.

According to the theory of probabilities the limiting values of scatterings of pressure, consumption, thrust, and specific thrust in a vacuum can be found by a general formula of form

$$\frac{\Delta\Phi}{\Phi} = \pm \frac{\sqrt{D_\Phi}}{1-v}, \quad (25.10)$$

where

$$D_\Phi^2 = \left(a_1 \frac{\Delta\Omega}{\Omega}\right)^2 + \left(a_2 \frac{\Delta F_{kp}}{F_{kp}}\right)^2 + \left(a_3 \frac{\Delta F_c}{F_c}\right)^2 + \left(a_4 \frac{\Delta Q_T}{Q_T}\right)^2 + \\ + \left[a_5 \frac{\Delta(R_n T_n)}{R_n T_n}\right]^2 + \left(a_6 \frac{\Delta B}{B}\right)^2 + (a_7 \Delta t_n)^2,$$

and  $\Delta\Omega, \Delta F_{kp}, \Delta F_c, \Delta Q_T, \Delta(R_n T_n), \Delta B, \Delta t_n$  - limiting deviations of values.

Variance of ballistic parameters, determined by formula (25.10), can be reduced by adjustment of critical section of the nozzle.

### 25.3. Control of Thrust Vector

The necessity of adjustment of thrust in an RDTT in flight is caused by external, not depending on the engine, and internal, specific for the given type of engine, random factors. The influence of the latter on thrust characteristics in the absence of adjustment is determined by the general formula (25.10).

The system of controlling the thrust vector must ensure the required flight program. Just as in the case of a liquid-propellant rocket engine, the necessary range of adjustment is made up of two components: the first of them is determined by the assigned law of change of thrust with time, and the second is caused by random internal and external factors.



### Change in the Magnitude of Thrust

The magnitude of thrust of an RDTT in principle can be changed in the same manner as the magnitude of thrust of a liquid-propellant rocket engine. However, in an RDTT this task is complicated by the limited possibility of influencing thrust in the period of operation of the engine and by the strong effect of initial temperature of the charge.

From formulas (25.2) and (25.6) it is evident that at a fixed initial temperature of charge, when  $B = \text{const}$ , two basic ways are possible for changing the magnitude of thrust of an engine which is operating on a specific propellant ( $Q_r = \text{const}$ ,  $\beta = \text{const}$ ).

1. Change of burning surface  $\Omega$  with a constant area of critical nozzle section  $F_{kp}$ .

The nozzle is not regulated, therefore value  $K_{pn}$ , as was shown above, is practically constantly. Consequently:

$$P \propto \Omega^{\frac{1}{1-v}}. \quad (25.11)$$

2. Change in area  $F_{kp}$  with a constant surface of combustion.

The nozzle is regulated. The magnitude of  $K_{pn}$  changes, or remains constant, if simultaneously with  $F_{kp}$  the area of nozzle section  $F_c$  is regulated. In all cases the influence of  $K_{pn}$  on thrust can be considered substantially less in comparison with the influence of  $F_{kp}$ . Then

$$P \propto F_{kp}^{-\frac{v}{1-v}}. \quad (25.12)$$

Because for the propellants being used  $v < 1$ , then it is obvious that the first means of adjustment of thrust makes it possible to change  $P$  in a wider range.

Let us examine briefly the possibilities of these methods of changing the magnitude of thrust. The variety of geometrical forms of charges and the possibility of utilization of components of charges make it possible in planning to select the necessary variant of continuous change or constancy of burning surface in time. This is achieved, however, in a very complex manner and with a limited degree of accuracy.

Still more complex is the task of providing a two-stage program of thrust, which may be desirable for certain rocket vehicles. Such a program can be fulfilled with the help of two different engines which are located on different stages of a multistage rocket. Frequently, however, such a solution is not permissible.

A two-stage program of thrust can be realized by a special shaping of the combustion surface. Figure 25.1 gives an example of such a charge with internal burning. The initial magnitude of this surface 1 is considerable, and, consequently, thrust is considerable (starting mode). After the extensions of the charge burn, the surface of combustion 2 decreases sharply, and then will change very little (march mode). Figure 25.2 shows a charge consisting of two different propellants with different propellants with different rates of combustion. Inner layer 1 with a high rate of combustion ensures the starting stage, and peripheral 2, burning slowly, the march stage.



Fig. 25.1. Example of charge, ensuring two stages of thrust.



Fig. 25.2. Example of component charge.

When using charges which burn from end it is possible to have a tandem arrangement in the chamber of two charges made up of different propellants.

Arrangements for obtaining a two-stage program of thrust in a common chamber with one nozzle usually have the relationship of thrust of the starting and march stages of no more than 5-10; their basic deficiency is an increase in the weight of the structure.

The assigned program of thrust can be maintained more accurately by regulating the area of critical section of the nozzle. However, this is a technically difficult way, especially when for maintenance of value  $K_p$  (for example, preservation of mode of nozzle  $p_c = p_h$ ) simultaneously with a change of  $F_{kp}$  it is also required to change  $F_c$ .

Above it was already noted that the most significant reason, causing a change in the magnitude of thrust of an RDTT, is the dependence of rate of combustion on the initial temperature of the charge. This is one of the main reasons conditioning the necessity for controlling the magnitude of thrust. Inasmuch as the change in temperature of the charge can be controlled then there is always the possibility prior to launching to consider the influence of this change on thrust characteristics and to take the appropriate measures.

In practice this is reduced to the prelaunch adjustment of area of critical section of the nozzle. This can be carried out by two methods:

a) by changing the diameter of critical section (set of launcher adapters),

b) by changing the area of critical section with a constant diameter by means of introduction of a special choke ("bullet") or ("pears").

Tuning of an engine with the help of a mobile choke can be automatic, depending on surrounding temperature.

Adjustment of the area of critical section prior to launching of a rocket is called prelaunch tuning and is used rather extensively for unguided solid propellant rockets. It must be noted that with the help of prelaunch tuning it is possible to compensate for scattering of indices both within a given lot and between various lots of solid propellant charges.

In considering the stated means for adjusting the magnitude of thrust of solid propellant engines it can be noted that tuning with the aid launcher adapters (nozzles) or a choke does not cause any fundamental difficulties. With a set of a rather large number of launcher adapters it is possible to achieve comparatively accurate adjustment. A deficiency of this method is the necessity for carrying out tuning directly before launching, for which a definite expenditure of time is required. This has a negative effect on the combat readiness of the rocket.

For steady adjustment of thrust of an RDTT in flight, just as in the case of a liquid-propellant rocket engine, it is possible to use systems with a mobile choke or gas-dynamic means for changing the area of critical sections. In the latter case in the range of critical section, perpendicular or at a certain angle to the axis of the nozzle, a second gas is blown in and in this way the effective magnitude of the section is reduced.

As an example Fig. 25.3 shows a possible change in thrust and pressures in a combustion chamber depending on change in the area of critical section. As can be seen, from the point of view of adjusting the magnitude of thrust by this method the utilization of propellants with a high index in law of combustion rate is effective.

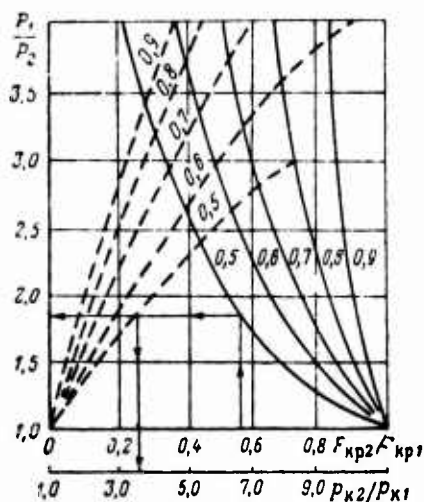


Fig. 25.3. Dependence of thrust (solid lines) and pressure in a combustion chamber on change in the area of critical section.

#### Changing the Orientation of Thrust

For controlling the motion of an RDTT rocket in pitch, course, and rolling systems are necessary which change the direction of the thrust vector. The basic requirements demanded of these systems are the same ones as for systems for controlling the thrust vector of a liquid-propellant rocket engine. Also the same are the criteria for estimating effectiveness in a comparison of various methods of control: relative magnitude of controlling force  $\bar{P}_y$ , relative loss of specific thrust  $\Delta \bar{P}_{yA}$ , quality of system  $K_y$ .

The possible systems for controlling the thrust vector of an RDTT are fundamentally the same as those examined in Chapter XIX for a liquid-propellant rocket engine. These include: a) gas control-vanes in the jet and outside the jet, annular nozzles, obliquely cut adapters; b) gas-dynamic methods (blowing in of gas, injection of liquid, control panels).

Construction features of solid propellant engines do not allow the using of systems of rocking chambers for controlling the vector of thrust, therefore the nozzle or part of it is usually slanted.

Figure 25.4 shows a diagram of a rocking control nozzle. The nozzle joint (break of outline) is made in the subsonic part. The mobile part of the nozzle is attached in hinged suspension and is coupled with the fixed part on a spherical surface; in this case deviation is carried out only in one plane. Such a design ensures rather large controlling forces with small losses of specific thrust and is intended for a multijet arrangement, where it makes it possible to control the flight of a rocket in all three planes of stabilization. In order to use a rocking nozzle in a single-jet design it has to be mounted in a cardan suspension.

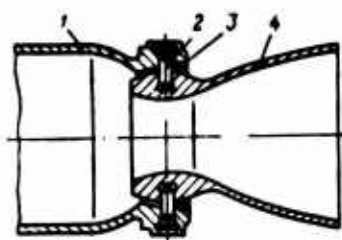


Fig. 25.4. Diagram of a rocking controlling nozzle:  
1 - chamber; 2 - pin;  
3 - annular condensation;  
4 - nozzle.

The basic characteristics - controlling force and losses of specific thrust - are resolved just the same as for the rotary chambers of a liquid-propellant rocket engine.

The practical realization of this arrangement is a complex design mission. High temperatures and pressures and the possibility of condensed particles hitting the spherical surfaces of nozzle joints hamper the development reliably operating sealing on the joint.

The striving to get rid of the deficiencies which were inherent to rocking controlling nozzles led to the investigation and development of the slotted controlling nozzle (Fig. 25.5). In this case the joint (break of outline) is made in the supersonic part, i.e., in the range of comparatively low pressures and temperatures. This considerably facilitates the conditions of work of the seals in the area of the joint. Based on effectiveness and economy this arrangement is not inferior to rocking nozzle, in spite of the break in the outline of supersonic part.

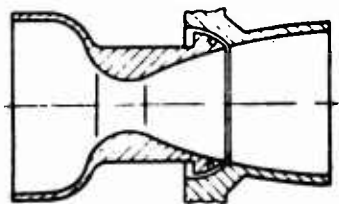


Fig. 25.5. Diagram of slotted controlling nozzle.

Deviation of the thrust vector with a multijet arrangement can be attained not only with a rocking nozzle, but also by means of its rotation relative to the longitudinal axis. A diagram of such a rotating controlling nozzle is shown in Fig. 25.6. The basic characteristics of such organs of control can be calculated, stemming from the kinematics of rotation and geometrical relationships of the structural arrangement of the nozzle.

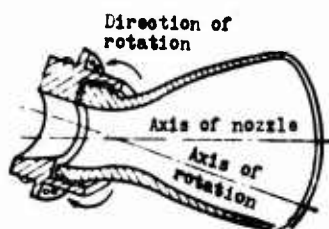


Fig. 25.6. Diagram of a rotating controlling nozzle.

As an illustration Fig. 25.7 shows the comparative characteristics of various methods for controlling the thrust vector of an RDTT. The characteristics are calculated for a conditionally selected three-stage rocket with a useful load of 225 t and altitude of circular orbit of 185 km.

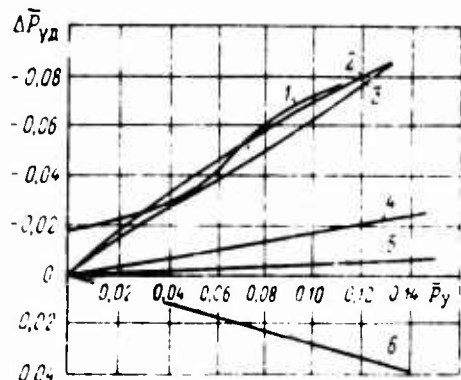


Fig. 25.7. Comparison of effectiveness of different systems for controlling the thrust vector of an RDTT: 1 - gas controls; 2 - gas deflectors; 3 - panels; 4 - nozzle on cardan suspension; 5 - rotating nozzle; 6 - injection of liquid.

## Thrust Cutoff

Thrust cutoff for an RDTT is necessary in the same cases as thrust cutoff in a liquid-propellant rocket engine. It can be attained either by reversing of thrust or by a sharp drop in pressure in the combustion chamber, as a result of which combustion of fuel ceases, or by both simultaneously.

A sharp drop in pressure is usually attained by opening additional apertures with a rather large area. Products flowing out of these openings can be directed into special nozzles, the thrust of which is opposite to the thrust of the main engines. Then together with cutoff there is reverse thrust. In order that following a drop in pressure the fuel ceases to burn the rate of lowering of pressure should be rather high - of an order of several tens of thousands of bar/s. For this the apertures being opened should be of considerable area.

In certain cases a more convenient path for a sharp lowering of pressure in the chamber of an RDTT, thus stopping its operation, are methods based on the injection of water into the combustion chamber or introduction of a powder-like cooling medium.

Following injection of water into a combustion chamber its atomization with a high pressure difference takes place and the evaporating drops remove heat from the products of combustion. The drop in temperature and pressure in the combustion chamber depends on the ratio of mass of injected water to mass of gas. It has been established experimentally that this ratio should be approximately equal to two.

When extinguishing an RDTT by means of introduction of a cooling medium the latter is atomized by blasting a special unit with a hinge-plate, for example, of black powder. For extinguishing an engine ammonium bicarbonate can be used. After blasting the hinge-plates of powder a layer of sublimating small crystals of cooling medium is deposited on the surface of the charge of solid propellants.



### Bibliography

1. Orlov B. V., Mazing G. Yu., Termodinamicheskiye i ballisticheskiye osnovy proyektirovaniya raketnykh dvigateley na tverdom toplive (Thermodynamic and ballistic bases of designing solid propellant rocket engines), izd-vo "Mashinostroyeniye", 1964.
2. Sorkin R. Ye., Gazotermodinamika raketnykh dvigateley na tverdom toplive (Gas-thermodynamics of solid propellant rocket engines), izd-vo "Nauka", 1967.
3. VRT, 1966, No. 3.
4. J. Spacecraft and Rockets, 1967, No. 2.

## CHAPTER XXVI

### PROTECTING THE WALLS OF THE CHAMBER

In this chapter we examine methods for the calculation of the thermal state of chamber walls of an RDTT with various methods for organization of heat shielding: by accumulation of heat in the wall, by utilization of refractory and ablating coatings, and by radiation cooling. Heat transfer rate from products of combustion to the walls of the chamber  $q$ , determined by the formulas in Chapter XIV, depending on local values of thermal-physical constants and parameters of flow, is assumed as known.

These methods of a considerable extent are also valid for an uncooled liquid-fuel rocket engine.

#### 26.1. Means of Liquid-Less Heat Shielding

The process of heat transmission from a working body to the walls of an RDTT chamber are very intensive as a result of high temperature and velocity and pressure of gas flow.

The change in total specific heat flux  $q$  in the chamber of an RDTT in principle is the same as in a liquid-fuel rocket engine during stationary heat emission with a maximum close to the critical section of the nozzle. In chambers of an RDTT with a small relative area  $f_{02}$  heat flows in the prenozzle volume can be very considerable

in the case of a high velocity of gas motion. In an RDTT there is the possibility of nonstationary heat transfer, conditioned by the variability of wall temperature and, in contrast to an uncooled liquid-fuel rocket engine, by variability of parameters of gas flow.

A significant feature of combustion products from composite solid propellants is of condensed particles in them. In conjunction with the high velocities of flow the presence of condensed particles promotes erosion - the washing out of surface material.

In contemporary rocket engines various systems of liquid-less heat shielding are used. The fundamental characteristic of some of them are given in Table 26.1; below they will be examined in detail.

Table 26.1. Means of liquid-less protection of walls.


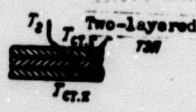




	Designation	Description	Temperature diagram
1	Capacitive cooling	Metallic thick-walled chamber. Thermal equilibrium of the wall is not attained	
2	Use of re-refractory coatings	Heatproof coating [T30] with low thermal conductivity is used for lowering of thermal flow	
3	Use of ablating coatings	On the surface of coating chemical reactions and phase transformations take place. Surface of division 1 separates the condensed phase of material from the gas; surface of division 2 separates the two ranges of the condensed phase	
4	Radiation cooling	Walls of the chamber made from refractory metal are heated to white incandescence and they emit heat by thermal radiation. Thermal equilibrium of the wall is established	

Table 26.1 (Cont'd).

	Designation	Description	Temperature diagram
5	Internal cooling	Porous refractory metallic matrix filled up by vaporizing material, which exudes, passing through the pores to the surface into the gas flow	
		Charge of main solid propellant 1 is supplemented a propellant with a low combustion temperature 2. Low-temperature gas creates a gas curtain between the wall and the main flow of gas.	

Each of the systems of liquid-less protection has inherent advantages and deficiencies. In connection with this frequently combined systems for protection of the walls are used, i.e., various combinations of methods of heat shielding.

Although in this chapter only means of liquid-less heat shielding of an RDTT are considered the utilization of cooling liquids for heat shielding of these engines is not excluded. Passive and active liquid cooling of an RDTT are distinguished.

In both cases cooling is ensured by a cooling medium (metals with low melting and boiling points) enclosed between the nozzle and its surrounding jacket. However, in the first case (passive protection) the walls are cooled by liquid melting circulating in a closed circuit, and in the second case the molten metal is injected through special openings into the inner surface of the wall. A large expenditure of heat for evaporation and protective action ensures reliable cooling.

## 26.2. Accumulation of Heat in the Wall

A characteristic property of heat emission with accumulation of heat in the wall is the variability of the process. After



starting of the engine the elements of chamber design are heated as a result of accumulation of heat (heat withdrawal into the surrounding medium is practically negligible).

Wall temperature, which in the beginning is identical throughout its thickness and is equal to  $T_{cr0}$ , rises rapidly on the inner side and more slowly on the outer (Fig. 26.1).

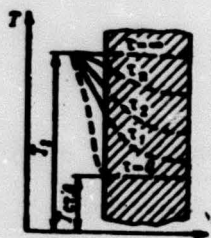


Fig. 26.1. Distribution of temperatures in wall during variable heating.

In connection with the increase of surface temperature on the part of gas specific thermal flow, which depends basically on the difference of temperatures of the wall from the outer side and on the part of the gas  $T_g - T_{cr,r}$ , is diminished, therefore the temperature of the wall increases rapidly at first and then slowly, asymptotically approaching the temperature of the gas and equalizing itself over the thickness of the wall. With achievement of  $T_{cr,r} = T_g$  (theoretically after an infinitely long time) the transfer of heat ceases. Figure 26.2 shows temperature shifts in the wall  $t^\circ$  with time at various distances from the fire surface  $y$  and change in specific thermal flow  $q$ . As it appears, an increase in the temperature of material of the wall in layers which are removed from the fire surface is slowed down.

During the calculation of heating of chamber walls the process of heat transfer is usually assumed unidimensional for the sake of simplicity; heat flow in the surrounding medium is disregarded in comparison with the inner (on the part of gas) flow. With such assumptions for the calculation of variable heat exchange one can use the equation

$$\frac{\partial T}{\partial \tau} = a \frac{\partial^2 T}{\partial y^2} \quad (26.1)$$

with the following boundary and initial conditions:

$$\tau=0; T(y, 0) = T_{cr0} = \text{const}; \quad (26.2)$$

$$y=0, q = -\lambda_{cr} \left( \frac{\partial T}{\partial y} \right)_{y=0}; \quad (26.3)$$

$$y=\delta, \lambda \left( \frac{\partial T}{\partial y} \right)_{y=\delta} \approx 0, \quad (26.4)$$

where  $\delta$  - thickness of wall;  $a = \frac{\lambda_{cr}}{c_{cr} \rho_{cr}}$  - coefficient of thermal conductivity;  $y$  - distance from fire in a direction perpendicular to the wall.

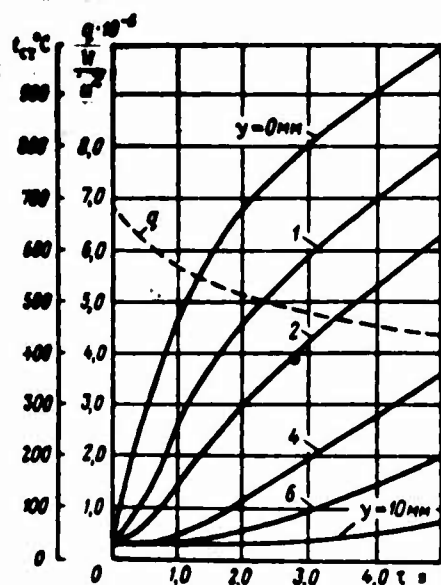


Fig. 26.2. Temperature shift in wall  $t_{cr}$  and specific thermal flow  $q$  in time ( $\alpha = 2900 \text{ W/m}^2 \cdot \text{deg}$ , steel wall).

Equation (26.1) together with boundary conditions (26.2)-(26.4) is valid both for a single-layer and a multilayer wall; in this case for a multilayer wall coefficients  $a$  and  $\lambda$  will have different values for separate layers.

For simplicity of recording the following equations let us present specific heat flux in the form:

$$q = q_k + q_a = \alpha'_e (T_e - T_{cr,r}), \quad (26.5)$$

where  $\alpha'_e$  - arbitrary coefficient of heat emission, considering convective and radiant heat exchange.

An accurate solution of equation (26.1) with allowance for change with time in the value of  $q$  and change from temperature in magnitudes of  $\alpha$  and  $\lambda$  presents known difficulties. Usually the approximate method of elementary balances is used or the numerical method of integration in finite differences.

In the case of using the method of finite differences the wall is divided in thickness into  $m$  layers and private derivatives in equation (26.1) are written with finite differences:

$$\frac{\Delta T}{\Delta \tau} = \frac{T_{n,(k+1)} - T_{n,k}}{\Delta \tau}, \quad (26.6)$$

$$\frac{\Delta^2 T}{\Delta y^2} = \frac{\frac{T_{(n+1),k} - T_{n,k}}{\Delta y} - \frac{T_{n,k} - T_{(n-1),k}}{\Delta y}}{\Delta y}, \quad (26.7)$$

where  $T_{n,(k+1)}, T_{n,k}$  - temperature in  $n$ -th layer at moments of time  $\tau_{k+1}$  and  $\tau_k$ ; indices  $(n-1), (n+1)$  relate to  $(n-1)$  and  $(n+1)$  layers respectively.

Substituting equalities (26.6) and (26.7) in equation (26.1), we obtain the calculation dependence:

$$T_{n,(k+1)} - T_{n,k} = a \frac{\Delta \tau}{\Delta y^2} (T_{(n+1),k} - T_{(n-1),k} - 2T_{n,k}). \quad (26.8)$$

Temperature gradient on the inner surface of the wall is determined with the help of boundary condition (26.3):

$$-\lambda_w \left( \frac{\Delta T}{\Delta y} \right)_{y=0} = q_k + q_{cr}$$

Calculations are simplified if we consider the variability of convective heat flux  $q_k$  with the help of the formula of conversion (14.55). Utilization of this formula makes it possible to consider not only the variability of wall temperature, but also physical constants and parameters of flow with time.

The calculations can be simplified even more, if we make such assumptions:

1) coefficient of heat emission from gases to the wall  $\alpha_g$  is constant in time and is equal to a certain effective value  $\bar{\alpha}_g$ ;

2) thermal-physical constants of the wall ( $\lambda_{cr}$ ,  $c_{cr}$ ,  $q_{cr}$ ) do not depend on temperature.

Then the solution of differential equation (26.1) has form [2]:

$$\eta = \frac{T_g - T_{cr}}{T_g - T_{cr,0}} = \sum_{i=1}^{\infty} \frac{2s_i}{\Phi_i + s_i} \frac{\Phi_i}{c_i \cos \Phi_i} e^{-\Phi_i^2 Fo} \cos \left( \Phi_i \frac{y}{b} \right), \quad (26.9)$$

where  $\Phi_i$  are sequential values of roots ( $i = 1$  to  $\infty$ ) of equation

$$Bi = \Phi_i \operatorname{tg} \Phi_i. \quad (26.10)$$

In expressions (26.9) and (26.10) the following values are used:

$$Bi = \frac{\bar{\alpha}_g b}{\lambda_{cr}} - \text{Biot criterion};$$

$$Fo = \frac{\alpha \tau}{\mu^2} - \text{Fourier criterion}.$$



Dependence (26.9) with consideration of only one root value ( $i = 1$ ) is usually depicted graphically [4] and is applied in the following manner. For each instant  $\tau$  and for various values of  $y$  (usually  $y = 0$ ,  $y = \delta/2$ ,  $y = \delta$ ) Bi and Fo values are determined and based on them the magnitude of  $\theta$ . With the help of this magnitude wall temperatures on the part of gas  $T_{\text{CT},\Gamma}$ , middle and outer are found. In this case values of  $y$  equal zero,  $\delta/2$ , and  $\delta$  respectively.

The average time value  $\bar{a}_\tau$ , which is necessary for determination of the Bi criterion can be calculated by the formula

$$\bar{a}_\tau = \frac{\int_0^\tau a_\tau (T_e - T_{\text{CT},\Gamma}) d\tau}{\int_0^\tau (T_e - T_{\text{CT},\Gamma}) d\tau} \quad (26.11)$$

Inasmuch as preliminarily the dependence  $T_{\text{CT},\Gamma} = f(\tau)$  is unknown, in first approximation one could use the magnitude of  $\bar{a}_\tau$ , determined for the mean temperature of the wall on the part of gas

$$(T_{\text{CT},\Gamma})_{\text{cp}} = \frac{T_{\text{CT}} + T_{\text{CT},\text{out}}}{2},$$

then, after obtaining the dependence  $T_{\text{CT},\Gamma}(\tau)$  repeat the calculation with a refined magnitude for  $\bar{a}_\tau$ .

The accumulation of heat by the walls of a chamber in the process of variable heat exchange with gas is the basis for the method of so-called capacitive cooling of a chamber.

It is obvious, that the time of safe operation of a chamber of this type will be limitedly by the time in which the temperature of the fire surface of the wall  $T_{\text{CT},\Gamma}$  reaches the maximum permissible value. During capacitive cooling this temperature is close to the melting temperature of the material if the deep layers of the wall ensure the necessary strength. The time for achievement of a

temperature which is dangerous in this sense depends on the magnitude of melting (or sublimation) temperature for the given material, its heat capacity, and thermal conductivity.

The higher the heat capacity of the material, the greater the amount of heat which can accumulate in the bulk of the wall, and the slower will be the increase of wall temperature on the part of the gas. An increase in thermal conductivity of a material allows the more rapid draining of heat from the fire surface and slows down the growth of  $T_{cr}$ .

Various materials have different combinations of values of heat capacity and thermal conductivity, therefore under identical conditions the time of safe operation for them is different. Figure 26.3 shows temperature shift in a wall on the part of gas under conditions which are characteristic for rocket engines (initial temperature difference between gas and surface  $3300^\circ\text{K}$ ;  $q = 16 \cdot 10^6 \text{ W/m}^2$ ;  $\bar{\alpha} = 5600 \text{ W/m}^2 \cdot \text{deg}$ ) for three different materials. The curves are brought to melting points.

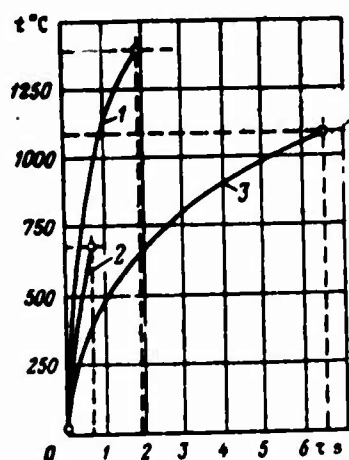


Fig. 26.3. Time of safe performance of a wall made from various materials: 1 - soft steel; 2 - aluminum alloys; 3 - copper.

As it appears the time of safe operation of a copper wall is substantially greater than for steel, despite its lower melting point and approximately identical thermal heat capacity. The reason is the

considerably greater thermal conductivity of copper. This is also confirmed by the graph in Fig. 26.4, where the temperature distribution is shown through the thickness of a wall 2 s after the beginning of heating (conditions the same).

In a steel wall the heat absorbed by the fire surface is led down into the walls at a slower rate than in copper, therefore the temperature of the surface increases very rapidly, whereas neighboring layers of material remain relatively cold. In this way the thermal capacity of a steel wall is used only partially, and the time of safe operation is limited by thermal conductivity. One ought to add that high thermal conductivity is also favorable because it decreases the temperature gradient in the wall, due to which thermal stresses in it are reduced.

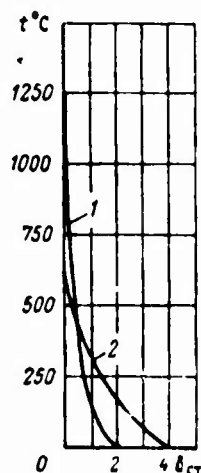


Fig. 26.4. Temperature distribution in copper and steel walls: 1 - soft steel; 2 - copper.

Protection of chamber walls is facilitated by using materials which are more refractory than ordinary structural metals. Such materials are metals of type molybdenum, tungsten, titanitic alloys, various types of ceramics and ceramic metal, graphite, pirographite.

Conditions for heating the wall of an RDTT depend on the change in the initial temperature of the charge. For an illustration of this in Table 26.2 design values are given for the distribution of

temperatures in a 7.1 mm thick steel wall which is washed by gas at various values  $t_{\text{H}}$ . Low initial temperature of the charge corresponds to less pressure in the combustion chamber, and consequently, less value for coefficient of heat emission. Simultaneously there is an increase in combustion time and overall amount of heat imparted to the wall, and its average temperature increases. However, in this instance the heat is distributed more evenly through the thickness of the wall, therefore the most dangerous temperature of the inner surface is lowered, and the temperature of the outer surface and average temperature of the wall increases. Consequently, from the point of view of strength (in calculations usually strength characteristics with  $T_{\text{cr.cp}}$  are used) the conditions of operation at low temperatures of a charge are determining during calculation of elements of construction.

Table 26.2. Influence of initial temperature of charge on heating of the chamber wall of an RDTT.

Initial temperature of charge in °C	-23	+60
Average pressure in combustion chamber in bars	67	134
Time of combustion in s	1.40	0.70
Temperature at end of combustion in °C:		
on the inner surface	1090	1320
on the outer surface	227	149
Average temperature in °C	560	538
Average increase in temperature in °C	583	478
Quantity of heat imparted to wall, in kJ/m <sup>2</sup>	18,450	14,500

As a result of the heavy weight of massive walls and practical absences of protection from erosion the method of accumulation of heat (capacitive cooling) has limited usefulness basically in model engines with small time of operation.

### 26.3. The Use of Refractory Coatings

Refractory material can be used as heat-insulating coatings for insulation of the basic material of wall on the part of the fire

surface. Their protective effect is illustrated schematically in Fig. 26.5. A refractory protective covering is able to withstand a high temperature  $T_{cr,r}$  and therefore reduce heat flow. According to the equation

$$q = \frac{\lambda_1}{\delta_1} (T_{cr,r} - T_1)$$

the highest temperature of the basic material comprises

$$T_1 = T_{cr,r} - q \frac{\delta_1}{\lambda_1}.$$

Since refractory coatings usually have low thermal conductivity, then the temperature of the basic material is considerably lower than the temperature of the fire surface. As is apparent, in this instance low thermal conductivity is not a deficiency (if melting temperature of the coating is rather high).

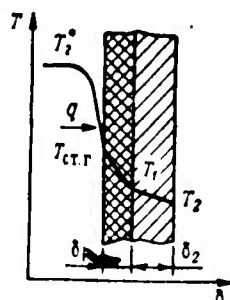


Fig. 26.5. Temperature distribution in a two-layer wall.

Among the requirements which must be satisfied by refractory coatings the most significant are such: reliable protection with minimum weight of coating, good cohesiveness (adhesion) of coating with the basic material with high resistance to erosion, thermal and mechanical shocks, and vibration loads.

The thickness of refractory coatings can comprise from fractions of a millimeter to several millimetric. It is appropriate to note that the propellant charge, secured to the housing of the engine,

as a result of the low thermal conductivity of propellants also plays the role of heatproof coating.

As material for coatings refractory metals (molybdenum, tungsten, tantalum, niobium, and others) or ceramic metals (oxides of aluminum, magnesium, zirconium; carbides, nitrides and borides of certain metals) are recommended. It is possible to use graphite. Characteristics of some of the enumerated material are presented in Table 26.3.

Table 26.3. Characteristics of some refractory materials.

Material	Temperature of melting or decomposition, °C	Density $\rho$ , kg/m <sup>3</sup> · 10 <sup>-3</sup>	Coefficient of linear expansion* $\alpha$ · 10 <sup>6</sup>	Coefficient of thermal conductivity $\lambda$ , W/m · deg	Specific heat capacity $c$ , kJ/kg · deg
Molybdenum	2620	10,2	5,1	140,72	0,252
Tungsten	3370	19,34	4,3	168,63	0,133
Tantalum	3027	16,6	6,5	54,68	
Niobium	1950	8,5	7,06	47,68	0,267
Carbon (graphite)	3550	2,25	7,86	174,45	0,669
Pyrographite	3500	2,22	50/90*	372,37/1,87	0,962
Aluminum oxide	2030	3,96	8,1	2,59	1,13
Beryllium oxide	2548	3,01	8,0	14,96	1,80
Magnesium oxide	2802	3,58	14,3	3,48	0,78
Thorium oxide	2800	9,69	9,4		0,25
Zirconium dioxide	2707	6,27	11,0	0,72	0,70
Boron carbide	2449	2,51	4,5	1,73	
Silicon carbide	2700		25/1200	52,30/4,184	1,25
Titanium carbide	3100		—	7,78	0,88
Boron nitride	2730		0,77/7,51	12,13	0,92

\*For anisotropic materials the characteristics are given separately for longitudinal and transverse directions.

Temperature Distribution in a wall with a refractory coating can be found by solving equations (26.1) with the corresponding change in boundary conditions. The solution is substantially simplified, if along with the previous assumptions concerning the constancy of values  $\alpha'$  and thermal-physical constants of the material of the

coating and walls one were to disregard the temperature gradient in the basic material of the wall. The last assumption is valid in the case when the element of the carrying construction is made from metal (thermal conductivity of the metal is usually considerably greater than the thermal conductivity of the coating), or in the case of a large thickness of coating.

With such assumptions the solution of equation (26.1) can be presented in a form similar to expression (26.9). In this case we introduce the additional criterion [9]:

$$\mu = \frac{1}{Bi} + \frac{Q_{cr} \epsilon_{cr} \delta_{cr}}{Q \epsilon_n \delta_n} \left( 1 + \frac{1}{Bi} \right), \quad (26.12)$$

and the Biot and Fourier criteria are calculated on the characteristics of the coating (index "n"):

$$Bi = \frac{\bar{a}_n y}{\lambda_n}; \quad Fo = \frac{a_n \tau}{y^2}.$$

The solution of equation (26.1) in the form of a functional dependence

$$\theta = \frac{T_e - T_1}{T_e - T_{cr0}} = f(Bi, Fo, \mu) \quad (26.13)$$

for calculation purposes is conveniently approximated by the dependence [8]

$$\lg \theta = 0,0212 - \frac{0,45}{\mu + 0,4} Fo. \quad (26.14)$$

As analysis shows, the accuracy of approximation of solution (26.13) in the range  $\mu = 0.2-20$  it comprises approximately 1-2%; with  $\mu \rightarrow 0$  errors increase, remaining within the limits of 10-12%.

Now the calculation of the thickness of heat-insulating coating  $\delta_n$  made from refractory material, which for an assigned time ensures the temperature of the wall on the boundary with the coating lower than  $T_1$ , can be carried out in such a sequence:

a) we select the material for the coating ( $c_n, \lambda_n, \rho_n$ ) and assign it the thickness  $\delta_{n1}$ ;

b) we determine the Bi and  $\mu$  criterion and magnitude of  $\theta$ ;

c) from equation (26.14) we find the Fo criterion, which gives the new value of thickness  $\delta_{n2}$ .

If value  $\delta_{n2}$  differs substantially from  $\delta_{n1}$ , then the calculation is repeated from point (a), using value  $\delta_{n2}$ .

In an analogous way the assignment concerning determination of wall temperature with a known thickness and properties of coating can be solved.

Table 26.4 gives the calculation values, characterizing the influence of the refractory coating on the distribution of temperatures in the wall. As can be seen, a thin layer of coating with low thermal conductivity sharply lowers the heat flux in a steel wall and considerably improves the conditions of its performance.

Table 26.4. Temperature distribution in the wall of a combustion chamber for an RDTT.

	Without thermal insulation	With thermal insulation
Thickness of wall in mm	3.05	3.30
Thickness of layer of thermal insulation in mm	-	0.25
Temperature at end of combustion in °C:		
on the inner surface of thermal insulation	-	1790
on the inner surface of a steel wall	1180	483
on the outer surface of a steel wall	843	260
Average temperature of steel wall in °C	965	345
Amount of heat imparted to wall, in kJ/m <sup>2</sup>	11,800	3745



#### 26.4. Use of Ablating Coatings

Considered as one of the basic methods for the protection of walls is the use of coatings which undergo ablations. The term (ablation) generalizes the totality of various phenomena, which appear following heating, thermal decomposition, and subsequent removal of substance from surface of a solid body which is washed by a hot gas flow. In this case heat is expended for phase transformations (melting, evaporation, sublimation) and endothermic reactions of pyrolysis (for organic substances) in the surface layer of the coating. Furthermore a protective effect is rendered by gaseous products which are liberated during ablation, since their temperature is usually lower than the temperature in the nucleus of flow. Therefore in contrast to refractory coatings the use of ablating coatings is possible at any temperature of combustion products.

Thermal insulating materials which undergo ablation must satisfy many requirements. Below the basic ones are given.

1. Low thermal conductivity. At small  $\lambda$  the conversion and removal of a substance will proceed only in the surface layer, which will prevent overheating and loss of strength of the basic material.

2. High heat of ablation, i.e., a large quantity of heat being spent in processes of heating and conversion of the carrier surface layer.

3. Extensive gas formation, ensuring the thickening of the boundary layer and lowering of thermal flows into the wall.

4. Satisfactory resistance to thermal and mechanical shocks and erosion.

The optimum combination of enumerated physicochemical characteristics can guarantee the least weight and low relative loss of weight

of the coating during insulation. Materials with a high heat of ablation are not always the best. Thus in pure graphite heat of ablation is evaluated as a quantity, exceeding  $23 \cdot 10^3$  kJ/kg. However, as a result of comparatively high thermal conductivity ( $\lambda \approx 186$  W/m-deg) a considerable quantity of heat is imparted to the wall, leading to an increase in its temperature. If, however, graphite is used in conjunction with a material possessing low thermal conductivity, then in this case the high heat of ablation of graphite will be used effectively.

Among coating materials which undergo ablation there are substances which sublime during heating (coatings made from mineral salts and organic binders), those which melt and evaporate (various types of rubber insulation, quartz), and combinations of them. A distinctive feature of these coatings is the surface removal of a substance without the formation of a charred layer.

A large group of ablating materials are the reinforced plastics on the basis of phenol, silicon-organic, and other resins (heat absorber) with a structure carrier made from quartz fiber and other substances. Such plastics have a high heat of ablation, extensive gas formation, and the porous coke-like residue from the pyrolysis of resins, having a low thermal conductivity, is good protection for the basic material. A distinctive feature of ablating materials of this group is the inner removal of a substance.

An important problem, connected with the ablation of material in nozzles, is the change in sections of a nozzle with time, mainly the critical section. For a small and regular change in nozzle section in time the rate of ablation should be low, constant in time, and identical along the perimeter of the section. In the opinion of some researchers [3], nozzles are possible with admissible erosion of critical section which are made wholly from plastic. At known regularities of ablation change of  $F_{np}$  and programs of thrust can be evaluated by calculation.

A pressure-time diagram typical for a nozzle with a coating which undergoes ablation is shown in Fig. 26.6. As is apparent, an increase of  $F_{kp}$  with time leads to a lowering of pressure in the combustion chamber. The effect of lowering of  $p_k$  is diminished with an increase in critical throat diameter [7]. However, by selection of the configuration of the charge another form of diagram can be obtained. A neutral diagram, for example, can be given by a progressively burning charge in conjunction with increase of  $F_{kp}$  with ablation.

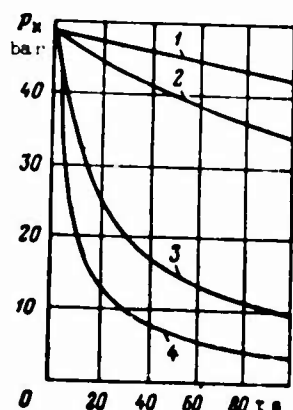


Fig. 26.6. Change of pressure in chamber with erosion of the critical section: 1 -  $d_{kp} = 1575$ ; 2 - 660; 3 - 82; 4 - 32.

#### Calculation of Ablating Coating with Surface Removal of a Substance

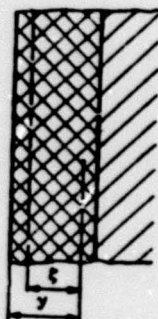
The basic group of ablating coatings of this type is made up of materials which sublime upon heating. Characteristics of some of them are given in Table 26.5.

Let us examine cases of stationary ablation, when the surface of the ablating coating moves into the material at a constant linear rate  $u$ . The distance of any point inside the coating from the sublimating surface  $\xi$  (Fig. 26.7) for any instant  $\tau$  is equal to:

$$\xi = u \tau. \quad (26.15)$$

**Table 26.5. Characteristics of some ablating substances.**

Substance	Density kg/m <sup>3</sup> · 10 <sup>-3</sup>	Temperature of decomposition °C	Heat of sublimation or of dissociation kJ/kg
Mg <sub>3</sub> N <sub>2</sub>		1500 (decomposition)	8912
Si <sub>3</sub> N <sub>4</sub>	3.44	It sublimates	11715
AlN	3.26	2000 (sublimation)	15564
NH <sub>4</sub> F	1.315	It sublimates	5338
NH <sub>4</sub> Cl	1.527	355 (sublimation)	4159
AlF <sub>3</sub>	3.07	1270	3786
SiS <sub>2</sub>		It sublimates	2903
CdO	6.95	900—1000 (decomposition)	2903
ZnO	5.61	1800 (sublimation)	3326



**Fig. 26.7. For the calculation of ablating coating.**

Let us use in the equation of thermal conductivity (26.1), instead of variable  $y$  the quantity  $\zeta$ . Since the process is stationary ( $T = \text{const}$ ,  $u = \text{const}$ ), that from formula (26.15) it follows that

$$\frac{\partial \zeta}{\partial y} = 1; \quad \frac{\partial \zeta}{\partial \tau} = -u; \quad \frac{\partial^2 T}{\partial y^2} = \frac{d^2 T}{d\zeta^2} = \frac{d^2 T}{d\zeta^2}; \quad \frac{\partial T}{\partial \tau} = -u \frac{T}{d\zeta}.$$

and the equation of thermal conductivity (26.1) assumes the form:

$$\lambda_T \frac{d^2 T}{d\zeta^2} = -\frac{dT}{d\zeta}, \quad (26.16)$$

where  $\lambda_T = \frac{a_n}{u}$ .

Equation (26.16) has the general solution:

$$T = -c_1 \delta_T e^{-\zeta \delta_T} + c_2, \quad (26.17)$$

where integration constants  $c_1$  and  $c_2$  can be determined from conditions

$$\begin{aligned} \zeta = \infty, \quad T = T_{cr0}, \quad c_2 = T_{cr0}; \\ \zeta = 0, \quad T = T_s, \quad c_1 = -(T_s - T_{cr0})/\delta_T. \end{aligned}$$

Having substituted the values of constants  $c_1$  and  $c_2$  in equation (26.17), we finally obtain:

$$T - T_{cr0} = (T_s - T_{cr0}) e^{-\zeta \delta_T}, \quad (26.18)$$

where  $T_{cr0} = \text{const}$  - initial temperature of coating;  $T_s = \text{const}$  - surface temperature, equal to temperature of sublimation.

Flow of heat, which is drawn from the surface of the coating into the material of the wall is equal to

$$q_n = -\lambda_n \left( \frac{\partial T}{\partial \zeta} \right)_{\zeta}$$

or in accordance with the formula obtained from expression (26.18) for derivative  $(\partial T / \partial \zeta)_{\zeta}$

$$q_n = \lambda_n \mu_n c_n (T_s - T_{cr0}). \quad (26.19)$$

Thermal flow  $q_1$ , applied to the surface of sublimating coating, should be examined with allowance for absorption of heat by the sublimate which is moving toward it:

$$q_1 = q - \eta_q \alpha u (I^* - I_s), \quad (26.20)$$



where  $q$  - heat flux, determined without allowing for gas formation during sublimation;  $I^0$ ,  $I_s$  - enthalpy of main flow and gaseous sublimate at corresponding temperatures  $T_e$  and  $T_s$ ;  $\eta_q$  - experimental coefficient, equal to  $\sim 0.8$  for laminar flow and  $\sim 0.4$  for turbulent [6],

By compiling the balance of heat in the form

$$q_1 = q_n + Q_s u Q_s, \quad (26.21)$$

where  $Q_s$  - heat of sublimation, we find the rate of stationary sublimation (ablation)

$$u = \frac{q}{Q_n [Q_s + (T_s - T_{cr0}) c_n] + \eta_q (I^0 - I_s)} \quad (26.22)$$

With a known time of operation of the engine  $\tau$  the thickness of the layer which is sublimated in this time is

$$\Delta_s = u \tau, \quad (26.23)$$

and the minimum thickness of coating, ensuring a permissible temperature on boundary of the coating and the carrier construction  $T \leq T_{don}$ , equals

$$\Delta_{min} = u \tau + \zeta_{T-T_{don}} = u \tau - \frac{a_n}{u} \ln \frac{T_{don} - T_{cr0}}{T_s - T_{cr0}} \quad (26.24)$$

A characteristic of calculation of organic coatings, which are decomposed during heating without the formation of a charred layer, is the dependence of mass rate of ablation also on temperature  $T_s$ , which is determined formally by the law of Arrhenius [5]:

$$\dot{m}_s = Q_s u = K e^{-\frac{E}{R_s T_s}}, \quad (26.25)$$

where  $E$  - energy of activation,  $K$  - pre-exponential coefficient.

Substituting in equations (26.19)-(26.21) the value  $\rho_n u$  from expression (26.25), from equation (26.21) by selection it is possible to find the temperature  $T_s$ , and then the rate of ablation  $u$ .

The stationary ablation examined by us is the limit to which the process of ablation approaches asymptotic. However, as calculations show [8], after a short initial period, conditioned by warming up of the coating to the temperature on the surface  $T_s$ , the process of ablation differs practically insignificantly from stationary.

Ablating of this type of coating is used in a number of designs realized. As an example one can name unguided rocket projectile "Honest John" [12] and the engines of the three-stage rocket "Minute-man" [10]. The initial thickness of ablating coatings being applied, depending on the conditions of operation can be from several millimeters to tens of millimeters.

#### Ablating Coatings with Internal Removal of a Substance

An important class of ablation compositions are plastic materials on an organic base. With intensive heating thermal decomposition of the binding substance (filler) takes place; this is known as the reaction of pyrolysis. Under conditions of an engine chamber in the case of an inadequate rate of flow the residues of thermal decomposition can form a porous charred layer reaching several millimeters on the surface.

The basic type of reinforcing fibers for ablating plastics are graphite fibers and fiberglass. Under conditions of large forces of shift graphite fibers, in contrast to fiberglass, do not melt, which makes it possible to avoid melt erosion. For gas flows with a high oxidizing capability in the case of prolonged operation there is substantial interest in fibers made from polycrystalline zirconium dioxide. Besides the increased resistance to oxidation, these fibers have a smaller coefficient of thermal conductivity than graphite fittings.



Effective performance of an ablation thermal shield, including erosion resistance, is possible only if thermal decomposition of resins included in its composition proceeds with the formation of a strongly carbonized layer on the surface. Therefore the greater the expenditure of solid products of the pyrolysis reaction (usually carbon), the better the fittings are maintained and the higher the strength of the carbonized layer. Phenol, phenyl-silane, and epoxy resins as fillers are used.

Calculation of an ablation coating with inner removal of substance can be completed only approximately, for example, based on the dependences given in work [8].

#### 26.5. Radiation Cooling

In the case of radiation cooling thermal flow from high-temperature products of combustion is transmitted to the wall of chamber by convection and by radiation, and from the wall to the surrounding medium - only by radiation.

After starting the engine the initial temperature of the wall increases rapidly and after it reaches a certain equilibrium value  $T_{cr,p}$  practically remains constant and identical throughout the thickness of the wall. In a first approximation this temperature can be determined from equation of balance of heat, transmitted to the wall by combustion products and drawn from it by radiation:

$$q = \alpha_2(T_e - T_{cr,p}) = \epsilon_{cr} \sigma \left( \frac{T_{cr,p}}{100} \right)^4, \quad (26.26)$$

where  $\epsilon_{cr}$  - degree of blackness of the external surface of the chamber.

Emitting power  $\epsilon$  of the surface of a chamber depends on the material and state of its surface. For contemporary metals and coatings data on  $\epsilon$  are limited.



Results from the solution of equation (26.26) can be presented in a form analogous to Fig. 26.8.

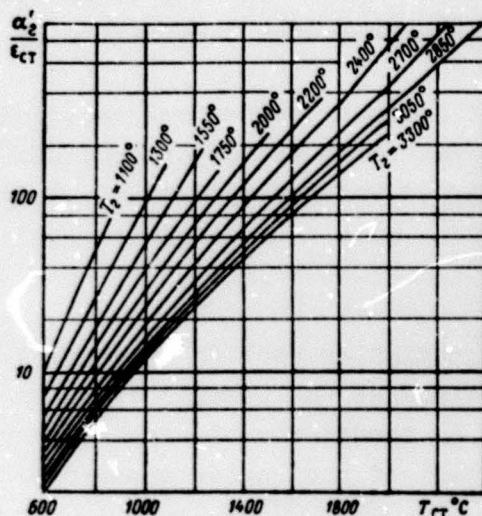


Fig. 26.8. Dependence of wall temperature on temperature of gas flow in the case of radiation cooling.

The change of wall temperature in time up to the moment of achievement of equilibrium temperature  $T_{cr.p}$  is determined from equation

$$\alpha'_2(T_e - T_{cr}) = c_{cr} \rho_{cr} \delta_{cr} \frac{dT_{cr}}{d\tau}, \quad (26.27)$$

where  $T_{cr}$  - temperature of wall at the moment of time  $\tau$ .

The joint solution of equations (26.26) and (26.27) makes it possible approximately to find the temperature  $T_e$  based on experimentally measured values of  $dT_{cr}/d\tau$ ,  $T_{cr}$ ,  $T_{cr.p}$ .

Effective removal of heat from the chamber walls by radiation begins at a temperature  $T_{\text{crit}} \approx 700^\circ\text{K}$ . At this temperature radiation removes about 1% of the heat transmitted to the wall by combustion products. The process of heat withdrawal becomes practically stationary with achievement of a temperature of  $1700\text{--}1800^\circ\text{K}$ .

Utilization of ordinary structural materials contained the development of the radiation method of cooling. Successes in industrial mastering of refractory metals - tungsten, molybdenum, tantalum, and others - made it possible to apply this form of cooling more extensively.

Advantages of radiation cooling over other methods lie in the fact that the structure of the chamber is simple and light, there are no limitations on conditions of heat exchange with a change in mode, and service life of the engine chamber is increased.

However, utilization of the radiation method of cooling has a number of limitations, the most significant of which is the requirement for a comparatively low pressure in the engine chamber. Inasmuch as with the development of large-scale rocket engines the problem of reducing the size and weight is solved to a certain extent by selection of high pressure in the chamber  $p_n$ , then radiation cooling of engines with high thrust can be applied only on sections of the enlarging part of the nozzle.

The second significant deficiency of the method of radiation cooling is the need of positioning the chamber on the flight vehicle in such a way as to guarantee heat removal by radiation, for example, outside the aircraft. A chamber unit inside the flight vehicle is undesirable.

Utilization of the method of radiation cooling is also difficult for other reasons. Refractory metals upon heating to a high temperature and subsequent cooling recrystallize and become brittle, which is undesirable for repeated launchings. At high temperatures

there is intensive oxidation of the chamber surface by products of combustion and the surrounding air. To avoid oxidation it is necessary to apply special coatings. However, a number of contemporary coatings will go out of commission at a temperature of about 1500-1600°C, and scratches on coatings promote a reduction of engine performance. Welding, stamping, and other technological operations with refractory material to a sufficient degree have still not been mastered. Certain refractory metals become brittle under the influence. Inasmuch as hydrogen is formed in the combustion products of many rocket propellants, then this limitation can be decisive.

The radiation method of cooling can find application in low-thrust liquid-fuel rocket engines used for steering on space vehicles and in engines for correction and manoeuvres (with low thrust and pressure in the combustion chamber up to ~3.5 bar). Utilization of the radiation method for cooling the enlarging part of the nozzle of chambers of engines working on liquid and solid propellant is justified if thermal flow from the gas to the wall and local pressure of combustion products on the given section of the nozzles is low, and the nozzle extends beyond the outer casing of the flight vehicle. The combustion chamber and subcritical part of the nozzle in this instance should be cooled by other means.

#### Bibliography

1. Avduyevskiy V. S. and others, Osnovy teploperedachi v aviatsionnoy i raketnoy tekhnike (Bases of heat transfer in aviation and rocket technology), Oborongiz, 1960.
2. Lykov A. V., Tsoriya teploprovodnosti (Theory of thermal conductivity) Gostekhteorizdat, 1952.
3. Makelister L. and others, VRT, 1964, No. 3.
4. Orlov B. V., Mazing G. Yu., Termodinamicheskiye i ballisticheskiye osnovy proyektirovaniya raketnykh dvigateley na tverdom toplive (Thermodynamic and ballistic design fundamentals for rocket engines working on solid propellant) izd-vo "Mashinostroyeniye", 1964.



5. Skala S., Gil'vert L., VRT, 1962, No. 6.
6. Fledderman, VRT, 1960, No. 3.
7. Korcher Kh., Mitchel B., VRT, 1964, No. 3.
8. Shapiro Ya. M. and others, **Teoriya raketnogo dvigatelya na tverdom toplive (Theory of rocket engines working on solid propellant)**. Voenizdat, 1966.
9. Grover I. H., Holter W. H., Jet Propulsion, 1957, No. 12.
10. Missiles and Rockets, 1963, No. 1, 2, 5.
11. Chemical Engineering Progress Symposium Series, 1964, No. 52.
12. Yaffee M., Aviation Week, 1959, No. 23.

## CHAPTER XXVII

### SELECTION OF OPTIMUM PARAMETERS

In this chapter an analysis is made of the bases for rational selection of propellant and the size and parameters of the combustion chamber and nozzle of an RDTT.

#### 27.1. Features in the Selection of Optimum Parameters of an RDTT

Selection of rational values of parameters for an RDTT is intimately connected with optimization of parameters of the rocket. The latter can imply those values which correspond to minimum starting weight when fulfilling operational requirements and sufficient reliability.

Optimum engine parameters - pressure in the combustion chamber and on the nozzle section, thrust, time of operation, dimensions - are closely connected with the parameters of the rocket - number of stages, thrust-weight ratio, distribution of weight by stages, and others. The complete solution of the mission of selection of optimum design parameters of a solid propellant rocket is very complex. It is necessary to solve the mission of finding the values of a large number of parameters, connected with complex dependences, at which a certain function of them, for example, launching weight of a rocket, will have a minimum value.

We will consider a simpler case with minimum limitations imposed on the parameters, when in the task of designing a solid propellant engine installation it is necessary to determine only value of total pulse  $I_E$ . Selection of fuel, geometry of the charge and of the chamber, and pressures in the combustion chamber and the exit from the nozzle can be relatively free.

The principles of selection of optimum values for these parameters are the same as for a liquid-fuel rocket engine, but they also have a specific nature.

Formerly, most commonly used criterion of effectiveness is the relationship of total pulse to complete weight of the vehicle. As is known, it can be written in the form

$$\frac{I_E}{G_0} = \frac{\bar{P}_{ya} G_T}{G_0} = \bar{P}_{ya} \Lambda, \quad (27.1)$$

where  $\Lambda$  - relative content of propellant on the vehicle.

From expression (27.1) it follows that effectiveness of the system is raised with an increase in the mean specific thrust  $\bar{P}_{ya}$  and relative content of propellant  $\Lambda$ .

Structural perfection of an RDTT is determined by the coefficient of weight of construction  $\alpha_K$ , representing the ratio of weight of engine structure (housing, heat shielding, nozzle unit) to the weight of the propellant. This coefficient is connected with  $\Lambda$  by the following evident relationship:

$$\Lambda = \frac{1}{1 + \alpha_K}$$

or

$$\alpha_K = \frac{1 - \Lambda}{\Lambda}.$$

With allowance for the latter, expression (27.1) can be written as:

$$\frac{I_x}{G_0} = \frac{\bar{P}_{yA}}{1 + a_n} \quad (27.2)$$

from which it follows that for increasing the effectiveness of the system it is necessary to have minimum values of coefficient of weight  $a_n$ . The limit, to which  $I_x/G_0$  strives, is mean specific thrust. In good designs the value of  $I_x/G_0$  can reach 0.90-0.95 from the magnitude of specific thrust (i.e.,  $A = 0.90-0.95$ ) which corresponds to  $a_n = 0.11-0.05$ .

Let us write the full weight of the vehicle  $G_0$  in the following manner;

$$G_0 = G_{n1} + G_{n2} + G_T \quad (27.3)$$

where  $G_{n1}$  - weight of engine structure;  $G_{n2}$  - weight of other parts of the vehicle.

Weight of the engine structure consists of weight of the combustion chamber and of the nozzle:

$$G_{n1} = G_{n.c} + G_c \quad (27.4)$$

Now the value of  $I_x/G_0$  can be presented as:

$$\frac{I_x}{G_0} = \bar{P}_{yA} \frac{G_i}{G_0} = \frac{\bar{P}_{yA}}{\frac{G_{n.c}}{G_T} + \frac{G_c}{G_T} + \frac{G_{n2}}{G_T} + 1} \quad (27.5)$$

The weight of the combustion chamber can be considered as consisting of the weight of the cylindrical part and weight of



the two flat end plates. Actually the plates are elliptical or spherical, one of them (in the nozzle end of the charge) is not compact; there are certain fittings for the combustion chamber, however, during qualitative analysis this does not have to be considered.

Weight of the cylindrical part of the combustion chamber is equal to

$$G_n = 2\pi r_{n.c} L_{n.c} \delta \rho_m. \quad (27.6)$$

where  $r_{n.c}$  and  $L_{n.c}$  - radius and length of cylindrical part of combustion chamber;  $\delta$  - thickness of wall;  $\rho_m$  - density of wall material.

Weight of the two flat end plates

$$G_{an} = 2\pi r_{n.c}^2 \delta \rho_m. \quad (27.7)$$

Ultimately the weight of the combustion chamber is

$$G_{n.c} = 2\pi r_{n.c} \delta \rho_m L_{n.c} \left(1 + \frac{r_{n.c}}{L_{n.c}}\right).$$

Wall thickness is determined from conditions of strength:

$$\delta = \frac{p_n r_{n.c}}{\sigma}, \quad (27.8)$$

where  $p_n$  - pressure in the combustion chamber;  $\sigma$  - permissible stress for the given material.

With a calculation of expression (27.8) we obtain

$$G_{n.c} = 2\pi r_{n.c}^2 L_{n.c} \rho_m \frac{p_n}{\sigma} \left(1 + \frac{r_{n.c}}{L_{n.c}}\right). \quad (27.9)$$



Weight of the propellant charge in the combustion chamber can be written in the following manner:

$$G = \Delta \pi r^2 L_{k.c} \rho_{k.c} \quad (27.10)$$

where

$$\Delta = \frac{V_r}{V_{k.c}} \quad (27.11)$$

is the volumetric ratio of propellant to volume of the combustion chamber, called the density of loading.

On the basis of expressions (27.9) and (27.10) let us write

$$\frac{G_{k.c}}{G_r} = 2 \frac{Q_M}{\sigma} \frac{p_K}{Q_r} \frac{1}{\Delta} \left( 1 + \frac{r_{k.c}}{L_{k.c}} \right). \quad (27.12)$$

Substituting this expression in equality (27.5) we obtain

$$\frac{I_z}{G_0} = \frac{\bar{P}_{YA}}{2 \frac{Q_M}{\sigma} \frac{p_K}{Q_r} \frac{1}{\Delta} \left( 1 + \frac{r_{k.c}}{L_{k.c}} \right) + \frac{G_c}{G_r} + \frac{G_{k.c}}{G_r} + 1}. \quad (27.13)$$

An important consequence of analysis of expression (27.13) is the necessity of selecting a material with maximum value  $\sigma/\rho_M$ . Specifically, despite the lower permissible stresses, aluminum alloys and reinforced plastics have greater values of  $\sigma/\rho_M$  than steel. For some bodies of rockets such as, for example, the American "Minuteman" rocket, titanium alloys are used.

The materials should be evaluated at temperatures which are characteristic for the structure with a consideration for a lowering of  $\sigma/\rho_M$  with an increase in temperature.

If we consider the parameters entering in equation (27.13) as independent from one another, then it may be concluded that an increase in effectiveness is also promoted by:

- 1) increase in specific thrust  $\bar{P}_{yA}$ ;
- 2) increase in density of propellant  $\rho_r$ ;
- 3) increase in density of loading  $\Delta$ ;
- 4) decrease in pressure  $p_K$ ;
- 5) decrease in geometrical characteristics of combustion chamber  $r_{K.C}/L_{K.C}$ ;
- 6) decrease in weight of nozzle  $G_c$  and other parts of the structure  $G_{K2}$ .

However, the majority of these parameters are interconnected with each other, therefore a change in one of them is reflected on others, which also must be considered during determination of conditions for ensuring the maximum effectiveness of the engine.

## 27.2. Selection of Propellant

The characteristics of propellant which directly influence the value  $I_E/G_0$  are specific thrust and density of propellant. An optimum propellant should have a combination of  $\bar{P}_{yA}$  and  $\rho_r$ , which provides, with other parameters equal, the maximum effectiveness of the system, i.e., maximum value  $I_E/G_0$ . In this respect selection of propellant for an RDTT is no different from selection of propellant for a liquid-fuel rocket engine. When a change of propellant for any reason causes a change in density of loading  $\Delta$ , then it is necessary to consider  $\bar{P}_{yA}$  and the derivative of  $\rho_r \Delta$ .

Density of loading  $\Delta$  is always less than a unit, because part of the volume of the combustion chamber occupied by the charge inhibitor and by adaptations for fixing it in case of an inserted charge. In chambers with charges which burn along the side surfaces, a free area and volume is left for the movement of gas flow. Therefore for charges with end combustion density of loading is greater than for charges with combustion on side surfaces. In the first case  $\Delta = 0.8-0.97$ , and in the second  $\Delta = 0.25-0.80$ . Lesser values pertain to multigrain charges.

Usually a change of fuel entails a change in the weight characteristics of the engine. The following position is a characteristic. In a number of cases fuels which develop a high specific thrust also have a high temperature of combustion:

$$P_{y1} \propto \sqrt{T_k}.$$

High temperatures in the passage require an increase in weight, mainly due to heatproof coatings and reinforcement of strained elements of structure. The necessary increase in weight is more considerable for engines with a prolonged period of operation. Based on statistical data, for example, the weight of a nozzle is proportional to the magnitude of total pulse:

$$G_c = a I_t \quad (27.14)$$

and consequently:

$$G_c = a \bar{P}_{y1} G_T \propto \sqrt{T_k} \quad (27.15)$$

If with identical  $\rho_T \Delta$  we compare propellants with various specific thrust, conditioned by various temperature  $T_k$ , then, as this is clear from equation (27.13), magnitude of  $I_T/G_0$  should change with the maximum. An increase in specific thrust increases, and a simultaneous increase in the weight of the nozzle  $G_c$  and

the combustion chamber  $G_{n,2}$  (as a result of decrease in permissible stress  $\sigma$ ) decreases  $I_z/G_0$ . Figure 27.1 shows the results of such an analysis with an assigned total pulse  $I_z$ . In this case the maximum of effectiveness of  $I_z/G_0$  corresponds to the minimum of complete weight  $G_0$ , determined by formula (27.3).

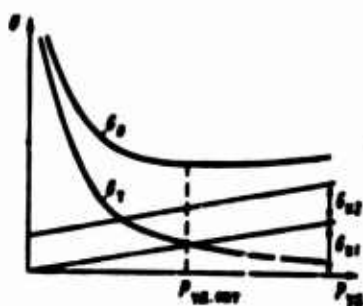


Fig. 27.1. For the selection of optimum fuel.

Some of the weight of the structure  $G_{n1}$  is proportional to specific thrust:

$$G_{n1} = c_1 \bar{P}_{ya},$$

another part  $G_{n2}$  does not depend on it:

$$G_{n2} = \text{const.}$$

Propellant weight  $G_r$  is equal to

$$G_r = \frac{I_z}{\bar{P}_{ya}}$$

and consequently:

$$G_1 = \frac{c_2}{\bar{P}_{ya}}.$$

Ultimately

$$G_0 = c_1 \bar{P}_{ya} + \text{const} + \frac{c_2}{\bar{P}_{ya}}.$$

is a function which is changed by  $\bar{P}_{ya}$  with a minimum.

ible  
ch

Utilization of elastic fuels makes it possible to use charges with central channel fastened with the engine housing. In the case of sufficient elasticity the area of the channel can approximate the area of critical section so that the density of loading reaches the highest possible values. The fact that during the entire time of operation the propellant charge protects the engine housing from the action of high temperatures makes it possible to reduce the weight of heatproof coating, improve the values  $\alpha_n$ , and reduce the effect of increased temperature on the weight of the structure.

Thus the fuel with the greatest effectiveness must be determined with a consideration of the influence of its properties on the weight of the structure.

In ensuring a high effectiveness of the engine system a fuel must satisfy a number of other requirements. Above we clarified the need for low sensitivity of combustion rate to pressure (small  $v$ ) and low temperature sensitivity (small  $\tau_p$ ) in all operational ranges of charge temperatures. It is advisable that the fuel not be inclined to erosion and resonant combustion and have a low threshold of abnormal combustion. Since the charge experiences high stresses, good mechanical features are required of the charge. For composite propellants mechanical features are improved with increase in the propellant of the elastic binder, the role of which is usually played by the combustible. Consequently, for such propellants small values of stoichiometric relationship of oxidizer and propellant are desirable.

Important requirements are those for a low coefficient of thermal expansion of charge and a good bond between it and the housing and the inhibitor. The charge must be chemically inert and stable during prolonged storage. Also very significant are the requirements for a simple and safe technology of production.

### 27.3. Selection of Sizes of Charge and Combustion Chamber

With an assigned value of total pulse  $I_T$  and a selected propellant with specific thrust  $F_{ya}$  the weight of the necessary propellant  $G_T$  and its volume  $V_T$  are determined uniquely. A charge with volume  $V_T$  should be placed in a combustion chamber of the least weight. For an assigned wall material (fixed value  $\sigma/\rho_m$ ) the minimum of weight corresponds to specific values for the radius and of the combustion chamber. Let us show this in an example of the arrangement of a tubular charge with a free area which is constant lengthwise and with initial value  $F_{c0}$  assigned [1].

The weight of the combustion chamber we will present as the weight of the cylindrical part [see (27.6)] and the weight of the two end plates [see (27.7)], less the weight  $F_{c0}\delta\rho_m$  on section of area free for the passage of gases.

Then

$$G_{k,c} = \delta\rho_m (2\pi r_{k,c} L_{k,c} + 2\pi r_{k,c}^2 - F_{c0})$$

or with a consideration of expression (27.8)

$$G_{k,c} = p_k \frac{V_T}{\sigma} (2\pi r_{k,c}^2 L_{k,c} + 2\pi r_{k,c}^3 - F_{c0} r_{k,c}). \quad (27.16)$$

Length of the combustion chamber is

$$L_{k,c} = \frac{V_T}{F_s},$$

where  $F_s$  - area of cross section of charge.

Since

$$F_s = \pi r_{k,c}^2 - F_{c0},$$

then

$$L_{k,c} = \frac{V_T}{\pi r_{k,c}^2 - F_{c0}}. \quad (27.17)$$

Substituting this expression in equality (27.16), we obtain:

$$G_{\kappa.c} = p_{\kappa} \frac{c_M}{a} \left( \frac{2\pi r_{\kappa.c}^2 V_T}{\pi r_{\kappa.c}^2 - F_{c\kappa 0}} + 2\pi r_{\kappa.c}^3 - F_{c\kappa 0} r_{\kappa.c} \right). \quad (27.18)$$

For determination of optimum radius of the combustion chamber expression (27.18) must be differentiated with respect to  $r_{\kappa.c}$  and the derivative equated to zero.

This gives

$$(6\pi r_{\kappa.c}^2 - F_{c\kappa 0})(\pi r_{\kappa.c}^2 - F_{c\kappa 0})^2 = 4\pi r_{\kappa.c} V_T F_{c\kappa 0}. \quad (27.19)$$

The value of  $r_{\kappa.c}$  found from expression (27.19) is optimum. Substitution of it in equation (27.17) determines the optimum value of length of the combustion chamber  $L_{\kappa.c}$ . Deviations from optimum dimensions of a combustion chamber noticeably increase its weight, especially at small lengthenings  $L_{\kappa.c}/r_{\kappa.c}$ .

In the example given an approximate solution is received, the weight of the inhibitor, auxiliary units, and so forth were not considered. The results can be refined without changing the method of analysis.

Since the value of specific thrust depends on pressure in the combustion chamber  $p_{\kappa}$ , then  $V_T$  also depends on  $p_{\kappa}$ . Consequently the optimum dimensions of a combustion chamber depend on pressure.

#### 27.4. Selection of Pressure in a Combustion Chamber

The maximum of value  $I_T/G_0$ , or with an assigned  $I_T$  - a minimum of weight  $G_0$  to optimum pressure in the combustion chamber should correspond.

Consequently the condition of optimality  $p_n$  takes the form

$$\left( \frac{dG_0}{dp_n} \right)_{I_2} = 0. \quad (27.20)$$

Part of the weight  $G_{n2}$  can be considered as not depending on  $p_n$ . The weight of the nozzle  $G_c$ , as was mentioned, is proportional to  $I_2$  (pressure  $p_n$  varies with a constant degree of lowering of pressure in the nozzle  $\pi_c$ ). Then

$$G_0 = \text{const} + G_{n,c} + G_r$$

and equation (27.20) we will write as:

$$\left( \frac{dG_{n,c}}{dp_n} + \frac{dG_r}{dp_n} \right)_{I_2} = 0. \quad (27.21)$$

Since

$$G_r = \frac{I_2}{\bar{P}_{r,1}},$$

then

$$\left( \frac{dG_r}{dp_n} \right)_{I_2} = - \frac{I_2}{\bar{P}_{r,1}^2} \frac{d\bar{P}_{r,1}}{dp_n}. \quad (27.22)$$

Now the condition of optimality  $p_n$  acquires the following form:

$$\frac{1}{G_0} \left( \frac{dG_{n,c}}{dp_n} \right)_{I_2} = \frac{1}{\bar{P}_{r,1}} \frac{d\bar{P}_{r,1}}{dp_n}. \quad (27.23)$$

An analytical solution of this equation is difficult.



Minimum weight  $G_0$  can be determined on charts such as those given in Fig. 27.2 [1]. At assigned values of  $p_n$  the optimum dimensions of a combustion chamber and its weight are determined by the method given in the previous section. Weight of the combustion chamber and, consequently, weight of the entire structure increases with an increase in pressure  $p_n$ . At the same time the weight of the propellant necessary for achieving the assigned  $I_T$  is decreased. This determines the change of  $G_0$  with a minimum, which also corresponds to optimum pressure in the combustion chamber.

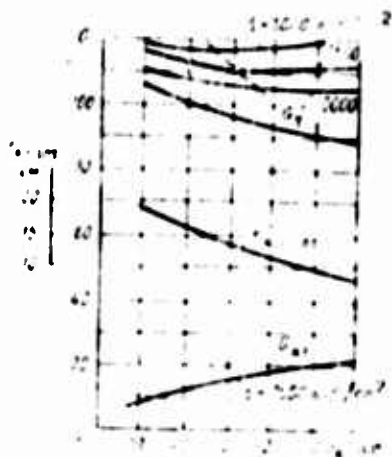


Fig. 27.2. For the selection of optimum pressure in a combustion chamber ( $I_T = 2 \times 10^5$  N·s,  $f_{ca} = 2$ ).

As is apparent, the minimum of  $G_0$  is shifted to the side of larger  $p_n$  with an increase of permissible stress  $\sigma$ . Simultaneously this minimum becomes more sloping. In connection with the last circumstance it is possible to allow a deviation from  $p_{n, opt}$  in order to ensure the other requirements (stability of combustion, heat emission, and so forth). Optimum values of  $p_n$  increase with a decrease in the duration of operation of the engine. According to published data they lie in the range of 35-105 bar.

## 27.5. Selection of Nozzle Dimensions

In the overall weight of an RDTT a considerable portion belongs to the nozzle. The weight of nozzle can constitute more than 30-50%

of the weight of the engine structure. This is explained mainly by the absence of cooling of nozzle walls which are not screened by a layer of propellant.

Selection of optimum outlet pressure from the nozzle, thus influencing the size of the nozzle, amounts to determining the maximum of  $I_E/G_0$ , with an assigned  $I_E$ , a minimum of weight  $G_0$ . The condition optimality appears as follows:

$$\left( \frac{dG_0}{dp_c} \right)_{I_E} = 0. \quad (27.24)$$

In the value

$$G_0 = G_{H.C} + G_c + G_{R2} + G_T$$

the only variables are  $G_c$  and  $G_T$ ; consequently it is possible to write

$$\left( \frac{dG_c}{dp_c} + \frac{dG_T}{dp_c} \right)_{I_E} = 0.$$

Because by analogy with expression (27.22)

$$\left( \frac{dG_T}{dp_c} \right)_{I_E} = - \frac{I_E}{P_{y1}^2} \frac{dP_{y1}}{dp_c}, \quad (27.25)$$

then the condition of optimality  $p_c$  acquires the following form

$$\frac{1}{G_T} \left( \frac{dG_c}{dp_c} \right)_{I_E} = \frac{1}{P_{y1}} \frac{dP_{y1}}{dp_c}. \quad (27.26)$$

For practical purposes a graphic method of solution similar to the previous case can be used.

In connection with the greater weight of the nozzle walls optimum values of pressure  $p_c$  received for an RDTT, all other things being equal, are significantly higher than for a liquid-fuel rocket engine. Furthermore the designer sometimes deviates from optimum values to the side of larger  $p_c$  due to the same considerations as for a liquid-fuel rocket engine. In certain cases the values of  $p_c$  taken exceed the value of atmospheric pressure at the earth.

Constructively a decrease in the weight of the nozzle is achieved by shaping of nozzle, carrying this out just as for liquid-fuel rocket engine, and by using light, mainly nonmetallic materials and coatings. Sometimes replacement of one long nozzle by several short ones can guarantee a gain in weight. It is necessary, however, to keep in mind that the rationality of such a replacement must be evaluated with a consideration of losses of specific thrust in a multijet design. With an increase in the number of nozzles and preservation of overall surface being washed by the gas the Reynolds number of the flow is lowered, and consequently, the coefficient of friction increases as well as the losses of specific thrust to friction conditioned by this. Reduction in the length of nozzles means a decrease in the time of stay of the gas in the nozzle and an increase of losses to thermodynamic nonequilibrium and nonequilibrium of a two-phase flow. For illustration Fig. 27.3 shows the results of a tentative calculation of change in losses of specific thrust with a change in the number of nozzles [4]. The quantities  $\delta P_{yA}$  represent an increase in losses of specific thrust, conditioned by friction ( $\delta P_{yA, \text{TP}}$ ), thermodynamic nonequilibrium ( $\delta P_{yA, \text{T.H}}$ ) and jointly with other effects ( $\delta P_{yA\Sigma}$ ) for a design with 1 nozzles in comparison with a single nozzle design:

$$\delta P_{yA} = \delta P_{yA, \text{TP}} + \delta P_{yA, \text{T.H}} + \delta P_{yA, \text{other}}$$

Thus, during transition to a multijet design a decrease in the weight of the nozzle and a lowering of specific thrust exert an opposite influence on the indices of the vehicle. ( $I_E/G_0$  or  $V_M$ ).

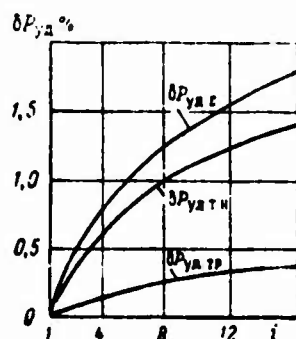


Fig. 27.3. Change in losses of specific thrust depending on number of nozzles ( $P = 9T$ ,  $p_k^*/p_c = 35$ )

## 27.6. Tendencies in the Development of RDTT

On the basis of publications about achievements and promising developments in RDTTs it is possible to examine the basic trends in the development of these engines. A characteristic feature of recent years is the wider introduction of RDTT in those areas of rocket-space technology, where until recently only liquid-fuel rocket engines were used.

Combat rockets of various classes, from tactical to intercontinental ballistic missiles, have engine installations which operate on solid propellant. In the field of carrier rockets for space objects powerful RDTTs are being used as boosters in the first stage as well as highly effective space engines (for example, the braking RDTT of the moon vehicle "Surveyor"). In the future even wider utilization of RDTTs is planned, especially in those areas where engine installations are required which have thrust which is measured in thousands of tons. Thus contemporary RDTTs have a thrust which reaches hundreds of tons, and those being developed - thousands of tons. The period of operation of these engines reaches hundreds of seconds and more. In essence, engines using solid propellant can be used and to a considerable extent are being used for solving practically all missions which are assigned to contemporary rocket technology.

The wider utilization of RDTTs is explained by the successful realization of the basic advantages of this type of engine - simplicity and high reliability, constant readiness for operation, low cost. The last factor becomes especially significant if one considers the relative simplicity of operation.

Achievement of these high qualities in action become possible because of successes in the field of materials and technology of production of housings, propellants, fault detection of charges, and a number of other areas.

Under these conditions one of the important trends in the perfection of RDTTs is improvement of their weight and power characteristics. The utilization of more effective propellants, just as formerly, is considered as a means for a considerable increase in the specific pulse of solid propellant engines. In this case, however, the requirement not only of preserving, but also of improving the physical-mechanical features of charges is significant.

Existing composite fuels, predominantly consisting of polymeric fuel-binding ammonium perchlorate oxidizer and of aluminum powder can be improved by replacement of each of the three basic components. Some possible trends are examined in detail in Chapter XXII.

A considerable reserve of improvement of power characteristics of an RDTT is the increase in the perfection of processes of combustion and discharge. Specifically one of the ways is the lowering of losses connected with velocity nonequilibrium of two-phase flow by means of the appropriate shaping of the nozzles. The utilization of new, is more durable, and lighter structural materials, fiberglass for example, for manufacture of the housing and nozzles more effective heatproof coatings, and also improvement in the design of engines, is one of the basic trends for perfection of weight characteristics of an RDTT. An increase in the coefficient of filling the volume of the engine, which is possible with an increase in the elasticity and strength of charges of the solid

propellant, can also serve this goal. As a rule contemporary engines have a charge which is rigidly fastened to the casing and is obtained by priming with propellant mass directly in the housing. For large-scale engines it is planned to assemble the charge from sections, the sizes of which make it possible to readily produce, transport, and control them. In case of a sectional charge the weight characteristics of the engine turn out to be somewhat lower than in the case of pouring in the housing.

For designs of recent years a characteristic has been the transition from multijet to single-nozzle designs. In this case they usually use designs with a recessed nozzle, which makes it possible to substantially reduce the length of the engines. The use of single-nozzle designs, which have better weight and power characteristics, become possible specifically due to the development and mastering of new means for controlling the thrust vector - such as injection of liquid, blowing in of gas, and others (see Chapter XXV).

Serious attention is given to the solution of problems of regulating RDTT thrust, cutoffs, ignitions, and repeated switching on of engines.

In the investigation of operations and development of methods for reliable calculation of operations problems which are common with liquid-fuel rocket engines can be noted. In most cases these are connected with the movement of the reaching, two-phase working body. The rapid development of reliable and effective RDTTs is possible only on a basis of perfected methods for calculating the strength of the charge and housing, processes of ignition, stationary mode, and engine cutoffs. The missions of theory include a description of combustion processes of the propellant and flows of products in the channel of the charge and the nozzles, heat exchange with walls of the engine housing and the nozzle, and other basic processes. The present wide distribution and great prospects for RDTTs in the future will give particular urgency to missions of development and a more precise definition of methods for the calculation of engines.

### Bibliography

1. Vandengerkkhove Dzh., "VRT", 1960, No. 2.
2. Orlov B. V., Mazing G. Yu. Termodinamicheskiye i ballisticheskieskiye osnovy proyektirovaniya raketnykh dvigateley na tverdom toplive (Thermodynamic and ballistic design fundamentals for rocket engines operating on solid propellant), izd-vo "Mashinostroyeniye", 1964.
3. Fridenson Ye. S. Vudushcheye raketnykh dvigateley (The future of rocket engines), 1965.
4. Dunning J., J. of RAS, 1960, No. 600.
5. Szego G. C., IX International Astronautical Congress, Springer-Verlag, 1959.

P A R T V

COMBINED ENGINES ON CHEMICAL PROPELLANT



## CHAPTER XXVIII

### HYBRID ROCKET ENGINES

This chapter contains a brief consideration of the basic features of operation of hybrid rocket engines. Some information about characteristic propellants is presented.

#### 28.1. General Information

A characteristic property in the organization of operation in a hybrid engine is combustion of the charge of solid propellant of oxidizer with the washing of its surface by a second component in a liquid or gasified state; both components are stored onboard the rockets.

The solid component of a (ГРД) [GRD - hybrid rocket engine] is located in the combustion chamber, into which another component is fed, in such a manner that the solid component burns under the action of the flow of combustion products moving along its surface with a surplus of the second component. Figure 1.13 showed two basic variants of a GRD on a solid-liquid propellant: a "straight" arrangement (solid combustible and liquid oxidizer) and a "reverse" arrangement (solid oxidizer and liquid combustible). According to the nature of operation they are joined by an engine with separate solid charges of fuel and oxidizer (separate loading which is presented in Fig. 28.1. This variant belongs to the (РДТТ) [RDТТ - solid-propellant rocket engine] class, inasmuch as both components of the propellant are solids in the original form.

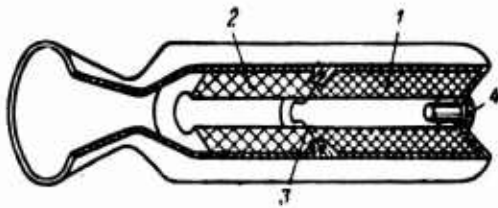


Fig. 28.1. Arrangement of an engine with separate-loading propellant charges: 1 - charge with surplus of oxidizer; 2 - charge with surplus of propellant; 3 - throttle; 4 - igniter.

An engine installation on hybrid propellant occupies a certain "intermediate" position between the (ЖРД) [ZhRD - liquid-propellant rocket engine] and the RDTT. At the same time, in comparison with each of these the GRD can have certain advantages under specific conditions of utilization.

An important feature of hybrid rocket engines is the possibility of using as propellant in them components which cannot be used in engines with other systems. In many instances the maximum power characteristics or greatest densities of propellant can be attained with components which are found in various aggregate states. In a GRD solid components can be used, which based on conditions of compatibility cannot be used in a RDTT, and in those ratios with the oxidizer which are most advantageous.

They are considering [2] hybrid engines on three-component propellants which have very high power characteristics.

In this case it is considered that a GRD can guarantee a number of operational advantages, such as increased reliability and stability of operation, the possibility of adjustment of thrust over a wide range, and also the possibility of realization of a procedure with a number of shutdowns and starts by means stopping or renewal of the supply of the liquid component of the propellant.

The development of hybrid engines which is being carried out in a number of countries pursues two basic goals: an increase in the power characteristics of the rocket engine and achievement of those operational features which are difficult to obtain from a ZhRD or an RDTT.

The advantages of rocket engines using a solid-liquid propellant in comparison with a ZhRD are: simplicity and compactness of the installation; improvement of heat shielding of the combustion chamber in connection with the use of a solid low heat-carrying charge which burns from within; high reliability and safety of operation. Inasmuch as usually it is proposed to use liquids which are suitable for prolonged storage as oxidizers, the complete readiness for launch during a prolonged period is ensured.

In comparison with an RDTT a rocket system on solid-liquid propellant or a propellant with separate loading is distinguished favorably by the possibility of simple adjustment of engine performance, including magnitude of thrust generated by it, due to oxidizer consumption. Sensitivity to initial temperature of propellant is practically excluded. The time of operation can also be substantially increased due to regenerative cooling of the afterburner and nozzle with the liquid oxidizer. Because of the low content or absence of oxidizer in a solid fuel its charge possesses good mechanical features.

In this way hybrid rocket engines can be advantageous for controlled flight crafts which are distinguished by simplicity and reliability and are found in constant readiness for launching. Also being discussed is the possibility of using the GRD for powerful carrier rockets [2]. In the presence of highly effective propellant compositions it can turn out to be expedient to also use the GRD for the upper stages of rockets. The possibility of adjustment and repeated switching on together with a high expected specific thrust can justify the use of a GRD for correction of velocity, orientation, or maneuvering of space crafts.

## 28.2. Propellants for a GRD

### Two-Component Solid-Liquid Propellants

Hybrid propellants of such a type were used for the first time in 1933 in the USSR (see 1.4).

In Germany in 1943 experiments were performed with engines, the combustible of which was perforated carbon grains and the oxidizer was liquid nitrous oxide  $N_2O$ . Propellants being investigated at present for the most part also belong to the group solid combustible + liquid oxidizer. This is connected with the fact that such compositions have been developed better and provide the greatest specific thrust. Furthermore the volume of fuel, as a rule, is less than the volume of oxidizer, as a result of which this scheme requires less dimensions for the combustion chamber, which is found under the influence of high pressure. A significant fact is that a very large number of different substances can be used as effective fuels, while the number of effective solid oxidizers suitable for utilization is small.

As solid propellants, polymer compounds are considered which are also used as propellant-binders for composite solid propellants. For the purpose of increasing the power characteristics metals and hydrides of metals are added to them: aluminium, beryllium, boron, lithium, and others. As oxidizers one considers both the components which are widely utilized in ZhRD, and the new, more effective:  $HNO_3$ ,  $N_2O_4$ ,  $O_2$ ,  $H_2O_2$ ,  $F_2$ ,  $ClF_3$ .

Table 28.1 shows the energy characteristics of hybrid compositions [2], [3], [4]. There for a comparison data are given for the basic composite solid and liquid rocket propellants.

A comparison shows that the already existing hybrid compositions based on theoretical specific thrust substantially surpass solid propellants and are on the level of existing liquid stable propellants, being inferior to the promising stable and cryogenic liquid rocket propellants. Based on density of propellant the hybrid compositions are located between liquid and solid.

compos  
because  
interest  
peroxi  
the mo  
propel

Table 28.1. Values of specific thrust and density of propellants for certain compositions at  $p_k/p_c = 70/1$ .\*

Propellants			$I_{sp}$ k.g.s/kg	$\rho \cdot 10^{-3}$ kg/m <sup>3</sup>
Stable propellants				
Solid	Existing	NH <sub>4</sub> ClO <sub>4</sub> + (Al + polymer)	267	1.7
	Promising	NH <sub>4</sub> ClO <sub>4</sub> + (Li, Be + polymer)	290	1.3
Liquid	Existing	N <sub>2</sub> O <sub>4</sub> + NMG	283	1.18
	Promising	H <sub>2</sub> O <sub>2</sub> + B <sub>2</sub> H <sub>6</sub>	309	1.06
	Existing	H <sub>2</sub> O <sub>2</sub> + (Al + polymer)	289	1.5
		HNO <sub>3</sub> + (Al + polymer)	273	1.52
Hybrid	Being developed	ClF <sub>3</sub> + LiH	293	1.52
		ClF <sub>3</sub> + Li	318	1.16
		N <sub>2</sub> O <sub>4</sub> + BeH <sub>2</sub>	351	1.5
		H <sub>2</sub> O <sub>2</sub> + BeH <sub>2</sub>	375	1.5
		NO <sub>2</sub> ClO <sub>4</sub> + N <sub>2</sub> H <sub>4</sub>	295	1.45
Cryogenic propellants				
Liquid	Existing	O <sub>2m</sub> + kerosene	298	1.02
		O <sub>2m</sub> + H <sub>2m</sub>	386	0.35
	Promising	F <sub>2m</sub> + H <sub>2m</sub>	405	0.67
Hybrid	Existing	O <sub>2m</sub> + polymer	298	1.1
	Being developed	F <sub>2m</sub> + LiH	363	1.3
		F <sub>2m</sub> + BeH <sub>2</sub>	395	1.53
		O <sub>2m</sub> + BeH <sub>2</sub>	371	1.3
		F <sub>2m</sub> + AlH <sub>3</sub>	353	1.55

\*Based on foreign data.

[Translator's Note: the subscript m = 1 (liquid).]

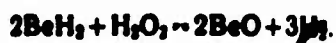
Of the promising hybrid rocket propellants attention is drawn to compositions with propellants - hydrides of metals. Specifically because of the high energy characteristics there is considerable interest in a composition beryllium hydrid BeH<sub>2</sub> with hydrogen peroxide H<sub>2</sub>O<sub>2</sub>. Based on theoretical characteristics this is probably the most effective composition of stable components of rocket propellants. The characteristics of "reverse" hybrid composition,

nitronium perchlorate with hydrazine, are rather high in comparison with existing stable liquid rocket propellants.

All the cited theoretical values of specific thrust of hybrid rocket propellants being developed relate to pure substances. For creation of a practical solid charge with the necessary mechanical characteristics it is necessary to use binders, which as a rule reduce specific thrust.

Practically all existing and promising hybrid rocket propellants contain a considerable quantity of metal. For the development of engines with a high coefficient of completeness of specific thrust it is necessary to ensure thorough burning of the metal and low losses during expansion of two-phase products in the nozzle. The seriousness of the last problem is indicated, for example, by such data.

The propellant beryllium hydride with hydrogen peroxide has a maximum specific thrust at a relationship of components when complete oxidation of beryllium is ensured and the hydrogen remains free. This takes place in the presence of the reaction



In products of combustion the weight fraction of beryllium oxide in this instance comprises

$$z = \frac{2\mu_{\text{BeO}}}{2\mu_{\text{BeO}} + 3\mu_{\text{H}_2}} = \frac{2 \cdot 25.01}{2 \cdot 25.01 + 3 \cdot 2.016} = 0.89.$$

With such a high content of condensate acceleration of products of combustion in nozzle is accompanied by intensive consolidation of particles. According to calculations based on the methods given in Chapter XIII, even with very small particles of BeO in the composition chamber ( $\sim 1 \mu\text{m}$ ) in the area of the throat their average size increases up to tens of  $\mu\text{m}$ . In this case losses of specific thrust can exceed 10%. A substantial role in all aspects of this process should be played by splitting of particles of condensate in the throat area.

### Three-Component Solid-Liquid Propellants

The use of a triple composition in a hybrid engine proposes the placing of a charge contain the solid component in the combustion chamber.

It is considered that such a feasibility to use a third solid component, which is natural for a GRD, gives bases to refer a number of maximally effective triple systems to hybrid.

Three-component fuels have been examined partially in the division on fuels for a ZhRD. It is known that such triple systems as hydrogen + beryllium + liquid oxygen ensure the highest theoretical specific thrusts among known chemical systems. Instead of beryllium sometimes the hydride of beryllium is considered. In the latter case maximum specific thrust is no different from the first variant, but the density of fuel turns out to be higher, inasmuch as less liquid hydrogen is required. According to thermodynamic calculations the use of beryllium or beryllium hydride makes it possible to create systems which exceed by 100 kgf·s/kg based on theoretical specific thrust the propellant hydrogen with oxygen.

However, in the literature data concerning experimental confirmation of the high theoretical characteristics of triple metal-containing systems are lacking.

### Solid Propellants with Separate Loading

In solid propellants with separate loading it is proposed to use highly effective, based on specific pulse, combinations of components, the chemical incompatibility of which does not permit using them in composite RDTT engines.

Being considered as fuels are the hydrides of light metals: aluminum  $\text{AlH}_3$ , beryllium  $\text{BeH}_2$ , and others, and also aluminum hydroxides and boron hydrides  $\text{LiAlH}_4$ ,  $\text{Be}(\text{AlH}_4)_2$ ,  $\text{Be}(\text{BH}_4)_2$ .

Possible oxidizers are perchlorates and nitrates (or their mixture) with additions of small quantities of other substances, which ensure self-combustion of the oxidizer charge.

Based on specific thrust solid propellants with separate loading noticeably surpass RDTT propellants. For example, specific thrust of propellants on the basis of the enumerated propellants with the oxidizer  $\text{NH}_4\text{ClO}_4$  at  $\pi_c = 40$  is found in the range of 270-310 kgf·s/kg.

### 28.3. Some Arrangements for a GRD

Arrangements of engine installations with a GRD can be very diverse. There can be a different arrangement of capacities containing liquid and solid component, organization of supply of liquid component (pressurization, pumping), process of combustion, and so forth. Let us examine some of the possible schemes described in the literature.

Figure 28.2 shows scheme of an experimental rocket engine operating on hydrogen peroxide and polyethylene. The latter is placed in the combustion chamber in the form of two grains, one of which burns on the outer, and the other on the inner surfaces. Hydrogen peroxide is preliminarily decomposed by passing through stem-gas generator with a solid catalyst. This eliminates the possibility of accumulation of liquid  $\text{H}_2\text{O}_2$  in the period of launching and the possibility of its explosion; reaching operating mode becomes steady.

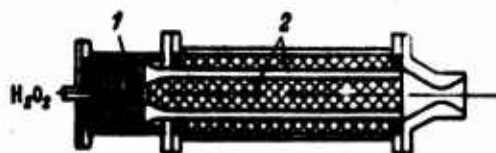


Fig. 28.2. Diagram experimental GRD on polyethylene and hydrogen peroxide: 1 — pack of catalyst; 2 — charge of fuel.

In the presence of a stem-gas generator the process of combustion flows as a reaction between solid (combustible) and gaseous (oxygen-steam mixture) phases. Experiments showed the uniformity and excellent



stability of such a process over a wide range of pressure in the combustion chamber. Linear rate of combustion of the solid phase constituted 0.5-1.0 mm/s. After burning out of the solid charge the engine can operate a certain time as a "cold" ZhRD (catalytic decomposition of  $H_2O_2$ ) with a specific thrust of 120-140 kgf·s/kg, which can be used as the march stage of the general program of operation.

Dependence of temperature in the combustion chamber and specific thrust of the propellant  $(C_2H_2)_n + 90\% H_2O_2$  on the relationship of components is shown in Fig. 28.3. The comparatively weak change in specific thrust with variation in the relationship of these components over the range  $\kappa = 5-11$  makes it possible to easily regulate the thrust of engine without large losses of  $P_{yd}$ .

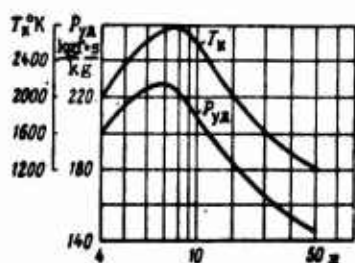


Fig. 28.3. Dependence of specific thrust and temperature of combustion of the propellant polyethylene +  $H_2O_2$  (90% concentration).

In Fig. 28.4 we have another diagram of an engine on a solid-liquid propellant. It is distinguished from the previous scheme by the fact that the process of combustion flows as a reaction between the solid propellant and liquid, and not gaseous, oxidizer, spreading over the whole propellant charge. When using charges containing a self-burning combustible (it can include a metal and a small quantity of oxidizer), engine thrust can be regulated comparatively simply over wide limits with the aid of a change in combustion of liquid oxidizer.

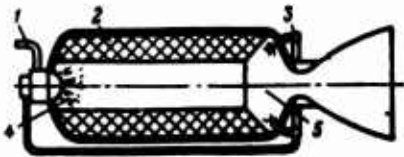


Fig. 28.4. Diagram of a GRD: 1 - supply of oxidizer; 2 - charge of fuel; 3 - jets from afterburner; 4 - sprayers of oxidizer; 5 - afterburner.

In the chamber of the afterburner combustion is carried out with  $\alpha$  close to a unit, which provides high specific thrust.

In experimental investigations of such schemes a specific thrust up to 255-265 kgf·s/kg has been obtained. Stability of combustion is retained to very low pressures ( $p_k$  of an order of 5 bar with overfall pressures on sprayer of about 1 bar). Combustion efficiency reaches 0.90-0.95. The overall arrangement of the system makes it possible to obtain a coefficient of weight perfection in the design of the engine installation  $\alpha_k = 0.1-0.15$ .

#### 28.4. Operating Processes in a Combustion Chamber

The basic problem in designing a rocket engine on hybrid propellant from the viewpoint of its interior ballistics consists of the calculation of consumption of solid component depending on the coordinate along the charge, time and, consumption of liquid component.

In this case there is importance in questions about the flow of the process of decomposition of solid component, dependence of this process on hydrodynamic, physicochemical, and other factors. This process influences the overall sizes of the charge, coefficient of volumetric filling, and the amount of unburned residues.

##### Burning Out of Solid Component

Combustion in a GRD has a heterogeneous nature conforming to the heterogeneous nature of the propellant. The structure of the combustion zone depends on the physical and chemical properties of

propellant components. Figure 28.5 shows variants in the structure of a burning charge. Simplest scheme of the process is for fuel of the plastic type which transforms directly from a solid into a gaseous state (Fig. 28.5a). Figure 28.5b shows a case, when between the original and final phase an intermediate one is formed, and namely: the combustible initially converts into a liquid, and a film of it under the influence of flow moves along the combustion surface.

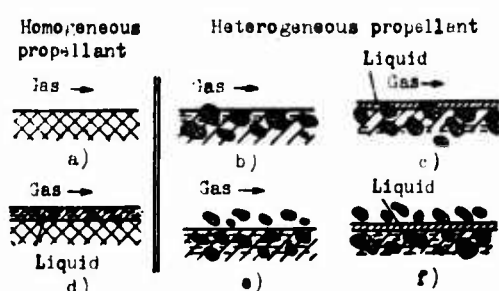


Fig. 28.5. Variants in the structure of a burning charge.

In practice the particles of fuel are placed in plastic substance in order to obtain the necessary mechanical properties of the charge. Depending on rate of decomposition of components the following cases can appear.

If fractions of fuel decompose at the same rate as the binder (Fig. 28.5c, d), then approximately the same picture is obtained as in cases a, b (if the fractions are not too large). If, however, on the contrary, the time of decomposition of fractions is great as compared to the time of decomposition of the binder (Fig. 28.5e, and f), then they can be carried away by the gas flow and their combustion will proceed already in the flow. Fractions of propellant, for example, aluminium, beryllium or lithium, can be carried out of the chamber.

The model of combustion should make it possible to determine if not the magnitude of local rate of burning out, then at least its qualitative dependence on these or other factors. For this purpose an analysis is made of phenomena of heat and mass transfer in the boundary layer with blowing in of chemically active substance from the wall of the channel. Chemical reactions with the participation of this substance basically flow in the boundary layer, as a result of which the area of maximum heat emission is located near the surface.

This area is zone which is washed away by turbulent pulsations and is constantly increasing downward along the channel. Above (normal to the wall) this zone a surplus of products of the core is observed, and below - products of decomposition of wall, although products of the core as a result of turbulent transfer also turn out to be directly at the wall. The fixed consumption of active material from the core of flow and its dilution by combustion products change the composition of products of the core, but the developing boundary layer leads to decrease in the thickness of the core, bringing it to zero at a distance of 20-30 calibers from the entrance to the channel.

The local rate of decomposition the solid component is determined by the amount of heat applied to the wall due to convective and radiant heat flows from the zone of maximum heat emission. The nature of passage of reactions in the combustion zone at high pressures is determined basically by mutual diffusion of chemically active products from the core and from the wall. At low pressures the kinetics of chemical reactions can become the limiting process.

A diagram of the combustion process in a flow of gases which are washing surface of the fuel is presented in Fig. 28.6a. The diffusion flame begins in the boundary layer; it divides it into two parts. The first part is located near the surface of the propellant; it is enriched by fuel and contains gaseous products combustion. The second part, located over the diffusion flame, consists of a gaseous oxidizer and simultaneously contains products

of combustion. Depending on the Reynolds number and disturbances at the entrance to the channel, the boundary layer can be laminar or turbulent. The diffusion flame is located close to surface of the propellant, and removal of it comprises 10-20% from the local thickness of the boundary layer.

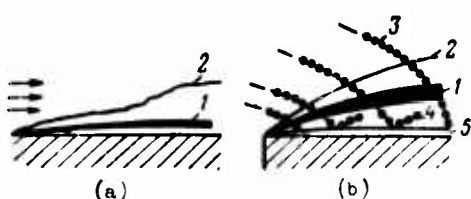


Fig. 28.6. Diagram of combustion of solid propellant in the flow of a gaseous (a) and liquid (b) oxidizer: 1 - diffusion flame; 2 - limit of boundary layer; 3 - trajectory of drops; 4 - zone of heterogeneous combustion; 5 - zone of reaction between drops of oxidizer and solid propellant.

If the oxidizer is brought in a drop form and the drops come in contact with the surface of the charge, then process of combustion is complicated (Fig. 28.6b): upon contact self-ignition proceeds immediately, then an exothermal reaction is developed, as a result of which a certain share of fuel and oxidizer vaporises, so that near the surface of the propellant heterogeneous combustion takes place. Drops of oxidizer partially vaporize already at the intersection of the boundary layer, therefore in addition to heterogeneous combustion near the surface, additionally a diffusion flame will be formed.

Analytical models, worked out for describing the process of burning out of fuel in a GRD, permit only a qualitative clarifying of the dependence of rate of burning out on these or other factors. On this basis it is possible to determine the form of empirical formula for describing experimentally found regularities.

The rate of burning out in a GRD depends on the following basic factors:

- on chemical composition and nature of fuel and oxidizer;
- on mass density of flow of gaseous products over the surface of combustion;

- on pressure in the combustion chamber;
- on the geometry of channel, organization of supply of oxidizer, and the nature of flow in the channel.

Not stopping for a consideration of individual factors, let us note that for a specific propellant with a definite design in most cases the basic influence on rate of burning out is exerted by the mass flux density ( $qw$ ) of products in the channel of the charge. With a weakly changing in the relationship of components as well as with a large value of  $\kappa$  this is equivalent to dependence on consumption of oxidizer. The influence of pressure at rather high  $p_{\kappa}$  is usually minor and is expressed basically through a change in density of the gas, i.e., through  $qw$ .

A certain influence is exerted on the rate of combustion by the temperature of the combustion products. For a specific fuel this means dependence on the relationship of components which is sometimes expressed as the dependence on complex  $\beta$ .

In general the dependence of rate of burning out on the parameters of operation of the engine is written as:

$$u = a \left( \frac{G_{ox}}{F_{\kappa}} \right)^{\nu_1} p_{\kappa}^{\nu_2} \beta^{\nu_3}, \quad (28.1)$$

where  $F_{\kappa}$  - area of charge channel.

Here coefficients  $a$ ,  $\nu_1$ ,  $\nu_2$ ,  $\nu_3$  are determined experimentally.

If dependence on  $p_{\kappa}$  and  $\beta$  is weak, then formula (28.1) acquires the following form:

$$u = G(qw)^{\nu} \quad (28.2)$$

or

$$u = a \left( \frac{G_{ox}}{F_k} \right)^{v_1} \quad (28.3)$$

in the case of an evident registration of considerable increase in consumption along the channel due to the burning out of fuel.

#### Potentialities for Regulating a GRD

The controlling parameter of a GRD is consumption of oxidizer. In the process of engine operation along with the burning out of fuel the area of the channel increases; consequently, with a constant consumption of oxidizer there is a reduction in the magnitude of  $q_w$  and the rate burning out of the solid component. For maintaining a constant, most advantageous relationship of components the combustion surface must be increased by the appropriate means. If index  $v_1$  in the law of velocity of burning out (28.2) is equal 0.5, then the round cylindrical channel ensures maintenance of a constant relationship of components in the case of erosion.

Really, if  $r_k$  - radius of channel, then at  $G_{ox} = \text{const}$  the rate of burning out is proportional to

$$\left( \frac{G_{ox}}{F_k} \right)^{v_1} = \frac{G_{ox}^{v_1}}{\pi^{v_1} r_k^{2v_1}} \quad (28.4)$$

Multiplying the rate of burning out by the surface of combustion

$$\dot{Q}_{top} = L 2\pi r_k \quad (28.5)$$

we obtain the propellant consumption

$$G_r = k_1 r_k^{1-2v_1} \quad (28.6)$$

where  $k_1$  - constant.

In this way with  $v_1 = 0.5$  fuel consumption and the relationship of components remain constants in proportion to erosion of the cylindrical channel. In practice, based on published data, the magnitude of  $v_1 = 0.5-0.8$ , therefore to get a constant relationship of components it is required to have a geometry of charge channel which ensures a more rapid increase in the perimeter than a circular cylinder.

The possibility of easy adjustment of thrust is considered one of the important distinctive features of a GRD. The simplest adjustment is carried out by changing the consumption of oxidizer. In this case it is necessary to guarantee operation of the engine on a relationship of components which is close to optimum. From equation (28.2) it is evident that change in consumption of fuel, proportional to the consumption of oxidizer, can take place only at  $v_1 = 1$ .

In actuality the values of the index in the law of combustion  $v_1$  is less than a unit. Therefore with a decrease in the consumption of oxidizer the expenditure of fuel will diminish more slowly and this will lead to a change in the relationship of components  $\kappa$ . In this way operation of a GRD with adjustment of thrust by a change in consumption of oxidizer must be accompanied by a change in relationship of components, by work on noneptimal mode. The magnitude of change of  $\kappa$  can be judged according to the following example. If  $v_1 = 0.5$ , then lowering of thrust, for example, by four times, can be obtained by the corresponding decrease in the consumption of oxidizer by approximately four times (if we disregard fuel consumption, the portion of which is relative small); in this case consumption of fuel is decreased [see (28.2)] only by two times, i.e., the magnitude of  $\kappa$  is decreased two times. Simultaneously it is possible to reduce specific thrust, and the possibility appears for large residues of one of the components of the fuel in the tank or in the combustion chamber.



Various solutions have been proposed for the solution of this problem. One of such solutions can be considered the scheme for an engine which is shown in Fig. 28.4. Here the oxidizer is injected into the head of the propellant charge in such a quantity that the mixture of gases along the entire length of the charge would have a surplus of fuel. An additional share of oxidizer is injected into the afterburner in a quantity necessary for maintenance of the required relationship of components  $\kappa$ . Another possible solution of the problem of ensuring a constant  $\kappa$  over a wide range of adjustment is increasing the dependence of rate of burning out of fuel on pressure.

In this case it is necessary that the values of indexes in formula (28.1) satisfy the condition  $v_1 + v_2 = 1$ .

The solution of this problem of ensuring operation at optimum for specific thrust will be more effective in case of utilization of propellants, the specific thrust of which changes slightly with considerable deviations in the relationship of components from optimum. An example of such a propellant is the propellant polyethylene with hydrogen peroxide, characteristics of which are given in Fig. 28.3.

The combustion instability has a low frequency of oscillations of pressure. The reasons for this are, basically, design of the chamber and the structure of combustion inside the chamber. Predominantly instability appears with an increase of thrust. In contrast to a ZhRD in a GRD unstable low-frequency oscillations do not appear at low pressures.

#### Bibliography

1. Geterogennoye goren'ye (Heterogeneous combustion), collection of translations, izd-vo "Mir," 1967.
2. Tibridnyye raketnyye dvigateli (obzor) (Hybrid rocket engines (survey)), VRT, 1965, No. 10.

3. Wahlquist A. L., Panelli G. C., J. Spacecraft and Rockets, 1965, No. 3.

4. Moutet A., Luftfahrttechnik - Raumfahrttechnik, 1966, Nr. 1.

## CHAPTER XXIX

### COMBINED ENGINES WHICH USE SURROUNDING MEDIUM

This chapter contains a brief description of schemes and bases of procedure of power units, organically combining the elements of rocket and atmospheric or hydrocket engines.

#### 29.1. General Information

The environment (atmosphere, water) in combined power devices usually is used as an oxidizer or working substance.

The development of combined air-rocket systems is explained by tendency to combine the advantages of a (БРД) [VRD - jet engine] - low expenditure of propellant (fuel), with the advantages of rocket engines - high speed and rate of climb, excellent altitude characteristics. Air-rocket systems have limited upper ceiling of action, which, however, should be higher than for strictly a jet engine. Accordingly achievement of higher flight velocities can also be expected. Utilization of air as an oxidizer on the sector of trajectory passing through the atmosphere of the earth is considered as one of the effective means of increasing the characteristics of rocket systems.

In order to ensure movement of underwater vehicles at a speed greater than 150-170 km/h it is necessary to use reactive principles of movement. Analogous to engines of flight vehicles jet engines

of underwater vehicles make it possible to remove limitations imposed by the propeller (sharp lowering of efficiency at high speeds) and to obtain high frontal thrust. As one of the components of the propellant the use of the surrounding water is being considered.

For jet engines which use the surrounding medium (air, water) in an absolute quantity  $G_n$  kg/s and relative (with respect to consumption of fuel  $G_T$ )

$$x_n = \frac{G_n}{G_T},$$

two variants can be examined for the determination of specific thrust. In the first - thrust refers to total consumption of propellant and surrounding medium:

$$P_{ya.z} = \frac{P}{G_T + G_n}, \quad (29.1)$$

in the second - to consumption of propellant being transported aboard apparatus:

$$P_{ya} = \frac{P}{G_T} = (1 + x_n) P_{ya.z}. \quad (29.2)$$

Subsequently by specific thrust of combined engines  $P_{yA}$  is always understood. Somewhat changed is the concept of propellant, by which subsequently only substances being transported on board the vehicle are implied.

## 29.2 Rocket-Ramjet Engines (RPD)

### Fundamental Arrangements

For a ramjet engine (ПБРД) [PVRD] operating on hydrocarbon fuel, the magnitude of  $P_{yA}$  can comprise 2000-3000 kgf·s/kg. This is almost an order more than the magnitude of specific thrust of rocket engines. In this connection one can understand the interest being given to ramjet engines as the engines for the lower stages of operational rockets and carrier-rockets for space objects, including recoverable stages for repeated utilization.

A significant deficiency of the PVRD is the impossibility of independent starting and low effectiveness at low flight velocities. The utilization rocket engines, most frequently the RDTT, as ratio units which are rejected after depletion of fuel and achievement of the necessary velocity, is one of the solutions of this problem which is being put into practice.

The literature [3], [4] also considers a rocket-ramjet engine variant, the fundamental layout of which is shown in Fig. 29.1. Some constructional layouts are cited in work [3]. The structural difference of an engine with such a layout from a ramjet engine lies in the presence of a primary circuit which functions similar to a rocket engine. It can be either a liquid or solid propellant engine which operates on a propellant with  $\alpha < 1$ . The function of this circuit is to supply the products of incomplete combustion to the chamber of the ramjet engine. In essence this is a gas generator or fuel-feeding system. The latter becomes especially clear when for the purpose of improving the processes of mixing one nozzle of the engine of the first circuit is replaced by a large quantity of small nozzles, in essence an injector.

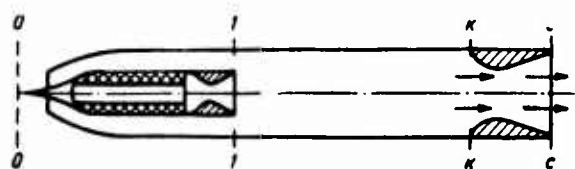


Fig. 29.1. Layout of a rocket-ramjet engine.

The only fundamental difference in procedure in the second circuit of an engine with such a layout from a ramjet engine is the presence of the ejector action of the jet (or jets) of combustion products from the engine of the first circuit. In a classical ramjet engine pressure in section K-K is determined by the dynamic head of incident flow, effectiveness of the diffuser, and losses in the combustion chamber. In an engine of the type shown in Fig. 29.1, the enumerated factors are coupled with the ejector effect of escaping

products of combustion, which increases pressure in section  $\kappa-\kappa$  in comparison with a ramjet engine. This effect leads to a certain improvement of the characteristics of the engine at low velocities – at  $M = 0.5-1.5$ . At higher velocities this difference disappears. Apparently an engine with such a layout, on the strength of its fundamental characteristics, can be called a ramjet-ejector engine.

Also possible is a combination of a rocket engine with a classic ramjet engine based on the layout shown in Fig. 29.2. Air, entering through the diffuser, is mixed up with the products of incomplete (or complete) combustion of one or several rocket engines. After mixing the gases enter the chamber, where, at velocity lower than the speed of sound, injection and afterburning of the additional fuel take place. Then the products are expanded in the nozzle. At high flight velocities the primary rocket circuit can be turned off and the engine operates as an ordinary ramjet engine. A feature of this are the improved, in comparison with a conventional ramjet engine, characteristics at low ( $M \approx 1$ ) flight velocities, a higher specific thrust at operational flight speeds.

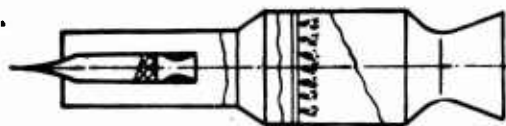


Fig. 29.2. Layout of a rocket-ramjet engine.

Another arrangement of an engine, combining rocket and ramjet circuits in one system, is shown in Fig. 29.3a. Air entering through the diffuser is mixed with products of the primary rocket circuit and simultaneously afterburning and expansion take place in the common nozzle. In this engine, just as in the previous ones, the process of ejection is significant, i.e., the mixing of the high-speed primary jet with air which has less velocity. As a result of mixing there is an acceleration of the secondary flow and an increase in total pressure. This arrangement is distinguished by simplicity and attracts attention, specifically, relative to heavy rockets. The engine installation of such rockets can include a large number of combustion chambers which are arranged around the periphery of the rocket housing, which serves as the central body of the nozzle (Fig. 29.3b).

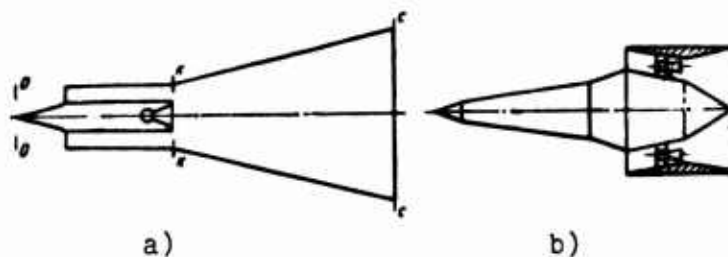


Fig. 29.3. Layouts for a rocket-ramjet engine.

### Thermodynamic Design

The basis of thermodynamic calculation of a rocket-ramjet engine is the calculation of combustion at an assigned pressure. If the rate of flow in the end of the combustion chamber (section  $\kappa-\kappa$ ) is low and static and total pressures differ insignificantly, then calculation is executed in the same manner as calculation for an isobaric combustion chamber.

The original data necessary for such a calculation — pressure  $p_\kappa$ , composition and enthalpy of fuel — are determined in the following manner.

Pressure  $p_\kappa$  is found for each point of the trajectory by calculation of the process in the diffuser and losses during mixing of the primary and secondary flows. Methods for such a calculation are expounded in special literature (see, for example, [4]). Speed of the rocket, atmospheric pressure, and air temperature are known quantities. The upper limit of pressure  $p_\kappa$ , which is not attained in practice, is the pressure of isentropic inhibition of flow from velocity, equal to flight velocity of the rocket, to zero.

Composition, properties and parameters of the jet from the primary engine can be determined by the conventional, previously expounded (Chapter VIII), methods. These data are necessary for calculation of mixing and pressures  $p_\kappa$ .

Propellant composition, corresponding to combustion products in section  $\kappa-\kappa$ , is found as a mixture of 1 kilogram of propellant from the primary circuit and  $\kappa_g$  kilograms of additional oxidizer, in this case air. The composition of air, the basic components of which are oxygen and nitrogen, can be taken based on data of the composition of standard atmosphere. A method for determination of an arbitrary formula for propellant (products of combustion of the primary circuit in a mixture with air) is examined in Chapter V. Enthalpy of products in section  $\kappa-\kappa$  is found as enthalpy of a mixture of propellant for a rocket engine and air. Enthalpy of the latter is defined as enthalpy of free air at the given altitude plus energy of inhibition from flight velocity of the vehicle to zero.

After the calculation of combustion by standard methods it is possible to calculate escape up to an assigned pressure or degree of expansion of the nozzle. It is necessary to note that as a result of low pressures and high temperatures in the chamber combustion, which are characteristic for flight at large Mach numbers at high altitude, the degree of dissociation of products in the chamber is high. As a result of a low pressure level the process of recombination during expansion in the nozzle can deviate from equilibrium.

Thrust of a jet engine, as is known, is determined by the difference in velocities of products which emanate from the nozzle and incident flow. In this case a relatively small change in rate of discharge as a result of chemical nonequilibrium can lead to a considerable change in the difference of velocities, i.e., thrust and specific thrust of the engine. Under these conditions an important role is acquired by calculation of kinetics of the process of recombination during the calculation of expansion in the nozzle. Within the framework of thermodynamic methods, just as earlier, in the case considered it is possible to determine the maximum and minimum values of specific thrust, which are determined during calculation of equilibrium and frozen escape.



Thus on the basis of results of calculation of combustion at an assigned pressure and expansion up to an assigned pressure or relative nozzle area it is possible to determine specifically, such magnitudes as temperature of combustion  $T_H$ , pressure and temperature on a section of nozzle  $p_c$ ,  $T_c$ , and rate of escape  $w_c$ .

Thrust of an engine is found according to the known formula

$$P = G_s w_c - G_a w_a + F_c (p_c - p_a)$$

or

$$P = G_1 [(1 + \alpha_a) w_c - \alpha_a w_a + (1 + \alpha_a) F_{ya,c} (p_c - p_a)], \quad (29.3)$$

where  $w_a$  - velocity of incident flow of air.

Specific thrust of a rocket-ramjet engine according to formula (29.2) is

$$P_{ya} = (1 + \alpha_a) w_c - \alpha_a w_a + (1 + \alpha_a) F_{ya,c} (p_c - p_a). \quad (29.4)$$

In a case when the rate of flow at the entrance into the nozzle is considerable the process of combustion cannot be considered isobaric. If the combustion chamber in this case is cylindrical, then the thermodynamic calculation is similar to the calculation given in Chapter VIII. With a variable area on the sector  $1 - \kappa$ , for the calculation it is necessary to know the distribution of pressure on this sector as determined by the processes of mixing and combustion. Calculation of these processes is difficult, therefore one should use experimental data or approximate dependences of pressure on the coordinate of the sector [5].

#### Propellants

The basic requirements for fuels for rocket-ramjet engines coincide with those requirements which were noted when considering liquid-propellant rocket engines and RDTTs. The requirements for

energy characteristics are specific. With the addition in the second circuit of an optimum, based on specific thrust, amount of air  $\kappa_g$  the specific thrust of an RPD will be greater, the less the coefficient of surplus of propellant oxidizer for the primary circuit. However, the presence of this oxidizer is necessary for organization of the process of combustion in the primary circuit and conveyance of combustion products. Furthermore, during launching or during flight at low speeds the ejector effect leads to a pressure increase in sector  $\kappa-\kappa$  and, consequently, of specific thrust of the RPD. The magnitude of this effect is greater, the higher the rate of discharge from the nozzle of the first circuit, i.e., the closer the propellant composition to stoichiometric. In this way there are two opposite pressures on the composition of propellant in the first circuit. Concrete selection can be made during consideration of the flight program for the vehicle.

The solid, liquid, and hybrid propellants can be used in an RPD. As components of liquid or hybrid propellants it is possible to use the components examined earlier in the appropriate sections.

Figure 29.4 shows the curves for values of specific thrust  $P_{yA}$  for an RPD as determined by the method given above. The calculation is made under the condition of isentropic inhibition of air for an isobaric combustion chamber [1]. In principle for liquid and hybrid propellants the coefficient of surplus of oxidizer  $\alpha$  can be selected as variable based on trajectory of flight. Consumption can also be changed in this way so that in accordance with the characteristics of the diffuser it ensures the most advantageous value of  $\kappa_g$  at every moment of flight.

In case of utilization of solid propellants it is impossible to regulate the relationship of components  $\kappa$ . The magnitude of  $\kappa_g$  can be maintained by a specific geometry of charge in accordance with the required law, if the flight trajectory had been preset during planning.

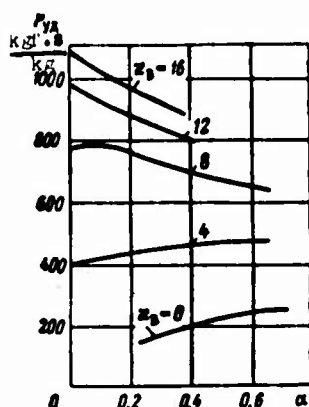


Fig. 29.4. Dependence of specific thrust of an RPD on  $\kappa_B$  at  $H = 0$ ,  $M = 1.5$  and with a different relationship of components  $\alpha$  in the first circuit: propellant: mixture of amines +  $\text{HNO}_3$ .

Solid propellants for an RPD can be ballistite or composite. The most effective fuels are those with a low content of oxidizer. In this respect wider possibilities are being opened with the utilization of composite fuels. Here the lower limit of oxidizer content is determined by the conditions of combustion of the composition in the first circuit. The basic components of such propellants are the same as for propellants for an RDTT. Most frequently the oxidizer is ammonium perchlorate, and the binders - high-molecular organic compounds. Additives of metals or of their compounds can also be used as a component of the propellant. A characteristic for the composition of solid propellant for an RPD is the comparatively low content of ammonium perchlorate - 30-50%, and a high content of metal, most frequently aluminium - 60-40%. The content of binder is selected as the minimum necessary for ensuring the physics - mechanical properties of the propellant - 10-15%.

An important problem is ensuring total combustion of propellant with a minimum length of afterburner chamber. In this respect the use of metals creates difficulties, because the time necessary for combustion of metallic particles is much greater than the time which is required for combustion of gaseous fuel.

#### Ranges of Utilization

In order to evaluate the comparative characteristics of various types of engines and the range of their rational utilization, in Fig. 29.5 we show the results of a tentative calculation of specific

thrust depending on velocity of flight. The propellant includes components which are disposed on the flight vehicle.

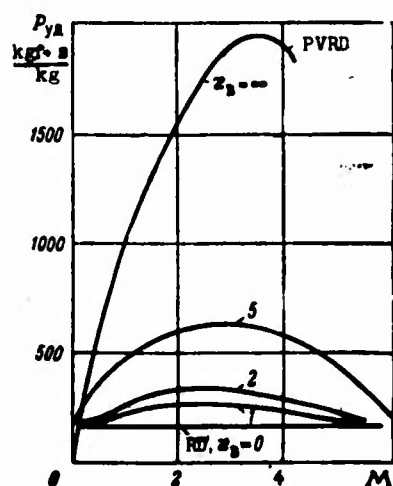


Fig. 29.5. Speed characteristics of an RPD.

As it can be seen, rocket-ramjet engines based on their characteristics occupy an intermediate position between the RD and ramjet engine. The magnitude of specific thrust and, consequently, the economy of engines, which is evaluated by propellant consumption, depends substantially on the magnitude of  $\kappa_g$  and velocity of flight. Achievement of high flight velocities is ensured only with a considerable increase in consumption of propellant which is transported by the vehicle.

It is expected that the utilization of RPDs will noticeably expand the range of accessible velocities and altitudes for an engine in comparison with the ramjet engine and substantially increase its economy in comparison with the RD.

### 29.3. Turbojet Engines

A combination of a turbocompressor jet engine and a rocket engine is put into practice in the form of two independent engines, installed on one vehicle and operating independently of one another. With the utilization of a liquid-propellant rocket engine its fuel pumps can be driven from the shaft of a (TPД) [TRD - jet engine]. However, the characteristics of such combinations can turn out to be less

advantageous than the characteristics of combined devices in which the elements of one or the other engine are organically connected with each other.

An example of such a layout of an engine, which can be called turbojet, is shown in Fig. 29.6. Rocket chamber 2, operating on a monopropellant, is used as a gas generator for turbine 3, which drives the air compressor 1. Air which is forced by the compressor is fed into the afterburner 4, where the gas used in the turbine burns (it usually has a deficiency of oxidizer), and also the combustible is burned additionally, just as in the afterburner of a TRD with afterburning.

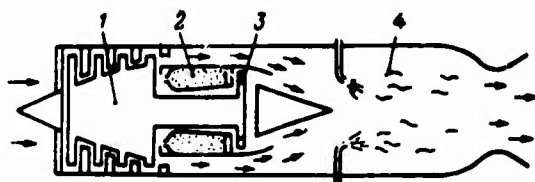


Fig. 29.6. Layout of a turbojet engine.

The advantages of such an arrangement are independence of the power of the turbine on flight altitude and the lowering of limitations connected with high flight velocities. It is conjectured that in a weight ratio the turbojet engine is more advantageous than a simple combination of a TRD and liquid-propellant rocket engine.

Figure 29.7 shows the speed characteristics of a turbojet engine. Specific thrust  $P_{yA}$ , relative to the consumption of gas in the rocket channel, is plotted along the axis of ordinates, and along the axis of abscissas - flight Mach numbers.

The characteristics are obtained by the calculation method with certain average values of parameters (temperature before the turbine  $1400^\circ\text{K}$ , optimum stages of increase in pressure in the compressor, specific thrust of monopropellant  $180 \text{ kgf}\cdot\text{s/kg}$ ).



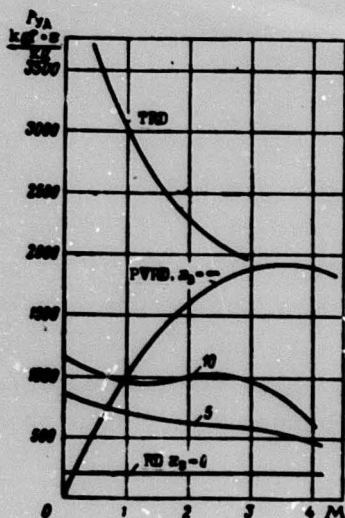


Fig. 29.7. Speed characteristics of a turbojet engine.

As it seems, one of the determining parameters is the relationship  $\kappa_B$  between consumption of gas in the air channel and consumption in the rocket channel. At  $\kappa_B = 0$  (air is not supplied) the engine becomes purely rocket, at  $\kappa_B = \infty$  (monopropellant not supplied, turbo-compressor moved away) the engine turns into a ramjet engine. At  $\kappa_B = 5-10$  the characteristics of the turbojet engine are intermediate between the characteristics rocket and ramjet engines. It can be expected that turbojet engines will provide aircraft with greater capabilities for altitude and rate of climb than a turbocompressor jet engine with an afterburner. The range of accessible velocities and altitudes for such a system probably will be expanded, and operation will become more flexible.

#### 29.4. The Possibility of Using the Atmosphere of Other Planets

In the air-rocket engines cited above oxygen of the air is considered as the natural sources of oxidizer, which is favorably expressed on the weight characteristics of the installation. In the same manner during the investigation of outer space it is possible to

use the atmosphere of other planets. For example, based on data from work [11] the atmosphere of Mars consists basically of  $N_2$ , Ar, and  $CO_2$  and small quantities of  $O_2$ ,  $NO_2$ , CO, and  $H_2O$ . Although the atmospheric pressure at the surface of the planet is not high, the atmosphere is stretched out far from its surface. There is definite interest in an analysis of the thermodynamic characteristics of propellants which use atmospheric nitrogen as the oxidizer.

A number of means of utilization of nitrogen are being considered [9]. The most important of them are:

a) utilization of nitrogen as the oxidizer in turbojet and ramjet engines;

b) liquefaction of nitrogen and feeding it into a chamber similar to the chamber of a rocket engine. In this case nitrogen is used either as the oxidizer or as the working substance, being heated in a chamber, for example, from the products of combustion of the main propellant. Components of the main propellant can be obtained aboard the rocket by using atmospheric nitrogen (for example,  $NH_3$ ,  $N_2H_4$ ,  $HNO_3$ );

c) utilization of nitrogen as the working substance in engines with a nonchemical source of energy.

A combination of the enumerated methods is possible.

Light metals are proposed as possible fuels: boron, aluminium, beryllium, or the hydrides of these metals. Inasmuch as nitrogen is not transported aboard a rocket, that when evaluating the effectiveness of a propellant the magnitude of thrust relative to the per second consumption of fuel,  $P_{y\Delta}$  is more significative. Based on magnitude of  $P_{y\Delta}$  the hydrides of light metals are inferior to the metals.

Inasmuch as the content of Ar, CO<sub>2</sub>, O<sub>2</sub>, and other impurities in atmosphere of a planet is considered low, when evaluating the thermodynamic characteristics of propellants they can be disregarded.

As an example Fig. 29.8 shows the magnitudes of specific thrust relative only to consumption of fuel. Liquid nitrogen is used as an oxidizer (N<sub>2</sub> + B, N<sub>2</sub> + Al, N<sub>2</sub> + Be) and as a working substance (mixture of HNO<sub>3</sub> and N<sub>2</sub>O<sub>4</sub> + Be + N<sub>2</sub>, ratio (HNO<sub>3</sub> + N<sub>2</sub>O<sub>4</sub>)/Be - stoichiometric). Calculations have been made for a case of utilization of nitrogen in a rocket chamber.

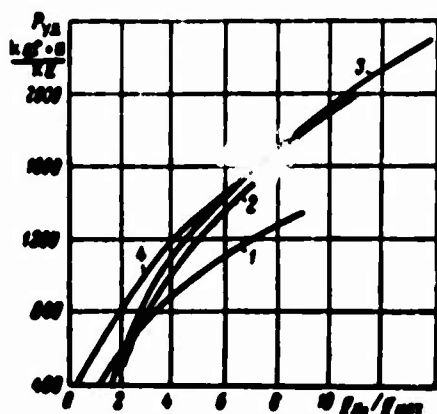


Fig. 29.8. Magnitudes of specific thrust  $P_{yA}$  for certain fuels using nitrogen:  $p_H = 18$  bar,  $f_c = 40$ .  
1 - N<sub>2</sub>/Al; 2 - N<sub>2</sub>/Be;  
3 - N<sub>2</sub>/B; 4 - (HNO<sub>3</sub> + N<sub>2</sub>O<sub>4</sub>) + Be + N<sub>2</sub>.

As it appears, with the utilization of nitrogen as an oxidizer the specific thrust relative to consumption of fuel increases with an increase of weight fraction of nitrogen in the propellant. However, simultaneously the area of fenced devices for the supply of nitrogen increases and the temperature of combustion products drops. For example, for the propellant N<sub>2</sub> + B at  $x = G_N/G_B = 4$ ,  $T_H = 3250^\circ\text{K}$ , and at  $x = 16$  it comprises only  $T_H = 1350^\circ\text{K}$ , which can influence the completeness of the combustion process. Consequently a certain optimum value of  $x$  exists.

#### 29.5. Hydrorocket Engines

In many reactive engines for underwater vehicles the use of the surrounding water is planned and their systems include elements of a rocket engine. Such engines are called hydrorocket.



A number of arrangements of hydrocket of engines are under discussion [7], [8].

#### Hydrodirect-Flow Engine

In the combustion chamber of engine rocket, predominately solid propellant is burned. The surrounding water is fed into the products of combustion under the pressure of dynamic head. Secondary reactions take place, the water vaporizes partially, and polyphase working body is expanded in the jet nozzle.

Similar to the ramjet engine this engine is not capable of independent starting and operation at low velocities. At a constant rate of movement the characteristics of the engine depend on the depth of immersion of the vehicle (the degree of lowering of pressure in the nozzle is decreased with depth).

#### Hydroturbojet Engine

Surrounding water is supplied by pumps which are driven by a turbine. The turbine operates on the combustion products of a rocket propellant (the use of water is also possible).

The engine can accelerate independently and operate at low rates of movement.

#### Engine Operating on Hydrosensitive Propellant

The layout of the engine is similar to a liquid-propellant rocket engine or a (ГРД) [GRD]. One of components of the propellant is the surrounding water, which reacts with the second, liquid or solid component.

The economy of the engine (specific thrust) should be evaluated only on the expended propellant which is transported by the vehicle. A comparison of various propellants is made more correctly based on volumetric specific thrust. The point is that the resistance of the vehicle, which is overcome by the thrust of the engine, depends on

the frontal area and external form, and not on weight, which is compensated by lifting (pushing) force. This imposes limitations on volume, and not on the weight of the propellant which is stored on the vehicle. Moreover the fraction of weight of the propellant in underwater vehicles is considerably less than in rockets (usually less than 50%).

As an illustration Figs. 29.9-29.10 show the theoretical characteristics of some hydoreactive propellants, based on data from work [8]. The greatest attention among the components of such propellants is given to metals.

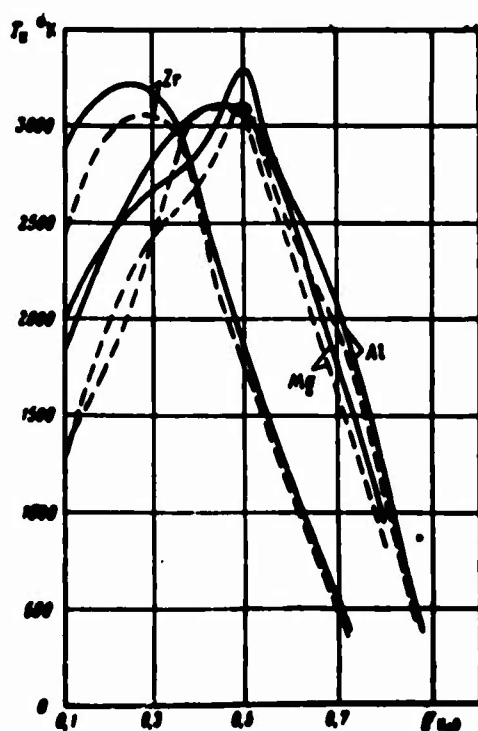


Fig. 29.9. Combustion-chamber temperature for certain metals with water at  $p_k = 70$  bar:

— metal in molten state;  
 ---- in solid state.

. One ought note that power characteristics alone cannot predetermine the selection of propellant. Very important is the problem of organization of an effective and stable procedure under the specific conditions of the particular vehicle.

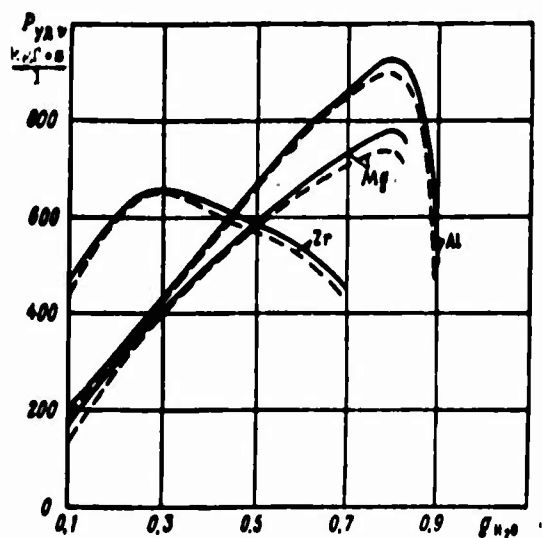


Fig. 29.10. Volumetric specific thrust relative to expenditure of metal:  
 $p_H = 70$  bar;  $p_C = 1.0$  bar.

The following basic means of organization of operating procedure are being considered for these engines [8].

1. In the combustion chamber water reacts with molten metals (Al, Mg, Li) which are fed there in a liquid phase. The source of heat for melting is the combustion chamber or a separate power plant.

2. Metals are fed into the combustion chamber in the form of fine powders or pastes. They react with oxidizers of the type  $HNO_3$ , and  $H_2O_2$ . It is possible that with a very thin grinding of metals it is possible to initiate their reaction with water.

3. In the combustion chamber a reaction is carried out between a charge of solid metallized rocket fuel, containing a combustible and oxidizer, and water.

All these methods of organization of operating procedure are complex and still have not been studied sufficiently. The development of the most important layouts of hydrocket engines depends on successes in their realization.

### Bibliography

1. Allen D., Bern B., "Raketnaya tekhnika i kosmonavtika", 1965, No. 5.
2. Bondaryuk M. M., Il'yashenko S. M. Pryamotochnyye vozdukhoreaktivnyye dvigateli (Ramjet engines), Oborongiz, 1958.
3. Glassmen I., Chermk DZh., Raketno-pryamotochnyye dvigateli (Rocket-ramjet engines), collection "Reaktivnyye dvigateli", Voenizdat, 1962.
4. Orlov B. V. et al., Osnovy proyektirovaniya raketno-pryamotochnykh dvigateley dlya bespilotnykh letatel'nykh apparatov (Bases for designing rocket-ramjet engines for pilotless aircraft), izd-vo "Mashinostroyeniye", 1967.
5. Brevig O. J. Spacecraft and Rockets, 1968, No. 4.
6. Cooper P. J., Spaceflight, 1966, No. 12.
7. Gongwer C., ARS J., 1960, No. 12.
8. Greiner L., ARS J., 1960, No. 12.
9. Perini L. L. and oth., J. Spacecraft and Rockets, 1964, No. 6.
10. Space/Aeronautics, 1967, No. 3.
11. Weber J. Q., Mueller K. H., Chemical Engineering Progress Symp. Series, vol. 60, No. 52.

### Bibliography to Entire Course

Barrer M. et al., Raketnyye dvigateli (Rocket engines), Oborongiz, 1962.

Vasil'yev A. P. et al., Osnovy teorii i rascheta zhidkostnykh raketnykh dvigateley (Bases for the theory and calculation of liquid rocket engines), izd-vo "Vysshaya shkola", 1967.

Dobrovol'skiy M. V., Zhidkostnyye raketnyye dvigateli. Osnovy proyektirovaniya (Liquid rocket engines. Bases of design), izd-vo "Mashinostroyeniye", 1968.

Kvasnikov A. V., Teoriya zhidkostnykh raketnykh dvigateley (Theory of liquid rocket engines), ch. I, Sudpromgiz, 1959.

Kosmonavtika (entsiklopediya) (Cosmonautics (encyclopedia)), izd-vo "Sovetskaya entsiklopediya", 1968.

Mel'kumov T. M. et al., Raketnyye dvigateli (Rocket engines), izd-vo "Mashinostroyeniye", 1968.

Appendix I. Basic data for some liquid-fuel rocket engines.

Firm and make of engine	Country	Purpose	Fuel	Thrust in vacuum, kg	Specific impulse, kg·s/kg	Time of work, min	System for supply of propellant	Cooling	$P_c$ , bar	$f_c$	$\gamma_{\text{ex}}$ kg dry wt./t thrust	Notes
RD-214	USSR	1st stage of "Kosmos"	Mixing of oxygen and kerosene	74	264		TNA + gas generator on $H_2O_2$	Regenerative, by fuel	45	$P_c/P_c = 64$		Serial
RD-119	USSR	2nd stage of "Kosmos"	$O_{2x} + N_2H_4$	11	352				80	100		
RD-107	USSR	1st stage of "Vostok"	$O_{2x} + \text{kerosene}$	102	314		TNA + gas generator on $H_2O_2$	Same	60	19		Same
RD-108	USSR	2nd stage of "Vostok"	$O_{2x} + \text{kerosene}$	96	315		TNA + gas generator on $H_2O_2$	Same	54	$P_c/P_c = 150$		Same
Rocketdyne H-1	USA	1st stage of "Saturn" IB	$O_{2x} + \text{kerosene}$	105	285	160	Same	Same	42	8	7.5	Same
Rocketdyne F-1	USA	1st stage of "Saturn" V	$O_{2x} + \text{kerosene}$	793	300	150	TNA + 2-component gas generator	Regenerative up to $f_c = 10$ further - by exhaust gases of turbine	63	16	10.5	Same
Rolls-Royce	England	Rocket "Blue Streak"	$O_{2x} + \text{kerosene}$	136	289	160	Same	Regenerative, by fuel	38	8	10	
BZ-2	USA	Experimental aircraft X-15	$O_{2x} + N_2H_4$	26.3	264	146	TNA + gas generator on $H_2O_2$	Same	42	10	15	Experimental series
Rocketdyne 1-2	USA	2nd stage of "Saturn" IB and V	$O_{2x} + H_{2x}$	105	422	500	TNA + 2-component gas generator	Same	45	40	18	Serial
Pratt-Whitney RL 1043-3	USA	Stage "Centaur"	$O_{2x} + H_{2x}$	7.7	443	475	TNA turbine operates on $H_2$	Same	28	57	17	Same
Pratt-Whitney RL 201-3	USA		$O_{2x} + H_{2x}$	120	465 ( $f_c = 75$ ) 490 ( $f_c = 100$ ) 440 ( $f_c = 150$ )		Same	Same	210	Pervan-pyrene: 1-75; 2-195	7.5	Experimental
Holl	USA		$F_{2x} + H_{2x}$	13.6		540	TNA + 2-component gas generator	Regenerative by fuel up to $f_c = 22$ further - radiation	21	45		Same
General Electric RL77-A1-5	USA	1st stage ICM "Titan" II	$H_2 + \text{aero-zinc-SO}$	107.4	286	165	Same	Regenerative, by fuel	57	8	7.5	Serial
General Electric RL77-A1-5	USA	2nd stage ICM "Titan" II	$H_2 + \text{aero-zinc-SO}$	45.4	316	180	Same	Same	60	49	11	Same
General Electric RL77-A1-5	USA	Spacejet "Apollo"	$H_2 + \text{aero-zinc-SO}$	10	315	750	Displacement by Helium	Regenerative + ablation	7	62.5	35	Same
Holl RL10-BA-40	USA	Stage "Astra"	$(HNO_3 + H_2O) + N_2H_4$	7.25	300	240	TNA + 2-component gas generator	Regenerative, by oxidizers	36		19	Same
Pratt-Whitney RL10-BA-40	England	Rocket "Black Knight" 3	$H_2 + (95-97\%) \text{ kerosene}$	11.3	265		TNA + gas generator on $H_2O_2$	Same	35		32	Same

[Translating notes: TNA = turbine pump unit]

Appendix II. Basic data on some American serial RDTTs.

Firm and make of engine	Purpose	Propellant	Thrust, T	Specific thrust kgf·s/kg	Time of operation, s
Thiokol M-55	1st stage ICBM "Minute- man"	NH <sub>4</sub> ClO <sub>4</sub> + polibutadiene + + acrylic acid + Al	77	250	60
Aerojet M-56	2nd stage ICBM "Minute- man"	NH <sub>4</sub> ClO <sub>4</sub> + polyurethane + + Al	25	246	60
Hercules Powder	3rd stage ICBM "Minute- man," 2nd stage MRBM "Polaris"	NH <sub>4</sub> ClO <sub>4</sub> + nitroglycerine- - nitrocellulose + Al	16	253	60
Aerojet	1st stage MRBM "Polaris"	NH <sub>4</sub> ClO <sub>4</sub> + polyurethane + + Al	36.3	245-250	-
Aerojet "Algol" 2A	1st stage of "Scout" rocket	NH <sub>4</sub> ClO <sub>4</sub> + polyurethane + Al	52	214	66
Thiokol "Castor"	2nd stage of "Scout" rocket	NH <sub>4</sub> ClO <sub>4</sub> + copolymers polibutadiene and acrylic acid	28	224	27
Allegheny "Antares"	3rd stage of "Scout" rocket	-	10	255	36
United Tech- nology FW-4S	4th stage of "Scout" rocket	NH <sub>4</sub> ClO <sub>4</sub> + polibutadiene + + acrylnitrile + Al	2.7	283 (p <sub>h</sub> = 0)	30
United Tech- nology UA-1205	Booster on "Titan" IIIC rocket	NH <sub>4</sub> ClO <sub>4</sub> + polybutadiene + + acrylnitrile + acrylic acid + Al	450-550	248	100-120

UNCLASSIFIED

Security Classification

DOCUMENT CONTROL DATA - R & D		
(Security classification of title, body of abstract and indexing annotation must be entered when the overall report is classified)		
1. ORIGINATING ACTIVITY (Corporate author) Foreign Technology Division Air Force Systems Command U. S. Air Force		2a. REPORT SECURITY CLASSIFICATION UNCLASSIFIED
		2b. GROUP
3. REPORT TITLE THEORY OF ROCKET ENGINES		
4. DESCRIPTIVE NOTES (Type of report and inclusive dates) Translation		
5. AUTHOR(S) (First name, middle initial, last name)  Alemasov, V. Ye., Dregalin, A. F. and Tishin, A. F.		
6. REPORT DATE 1969	7a. TOTAL NO. OF PAGES 732	7b. NO. OF REFS
8a. CONTRACT OR GRANT NO.  a. PROJECT NO. 6040104  c.  d. DIA Task No. T65-04-18A		8b. ORIGINATOR'S REPORT NUMBER(S)  FTD-MT-24-116-70 8b. OTHER REPORT NO(S) (Any other numbers that may be assigned this report)
10. DISTRIBUTION STATEMENT Distribution of this document is unlimited. It may be released to the Clearinghouse, Department of Commerce, for sale to the general public.		
11. SUPPLEMENTARY NOTES		12. SPONSORING MILITARY ACTIVITY Foreign Technology Division Wright-Patterson AFB, Ohio
13. ABSTRACT  This book treats general questions of the theory and calculation of thermal rocket engines, describes processes of ZhRD and RDTT and considers their characteristics. The necessary information about liquid and solid fuels for RD is given. In the 2nd considerably reworked edition, contemporary methods of thermogas-dynamic design of processes in RD with high-temperature working media have been more fully explained. Results published in recent years of theoretical and experimental investigations to determine thermophysical features of combustion products and characteristics of chemically nonequilibrium processes combustion and expansion are reflected. Considerable attention is given to questions of the specific character of two-phase flows and to schemes of heat- ing shielding. The book is intended for students of aviation institutes of technology and departments and may also be useful to engineers and graduate students, who specialize in rocket technology. Orig. art. has: 36 tables, 257 illustrations, and 178 bibliographies.		

DD FORM 1 NOV 66 1473

733

UNCLASSIFIED

Security Classification



UNCLASSIFIED

Security Classification

14	KEY WORDS	LINK A		LINK B		LINK C	
		ROLE	WT	ROLE	WT	ROLE	WT
	Rocket Engine Liquid Rocket Engine Solid Rocket Engine Rocket Fuel Rocket Engine Thrust Thermodynamic Property Combustion Product						

UNCLASSIFIED

Security Classification

END